Palladium-Catalysed Desulfinative Cross-Coupling Reactions: Leveraging Mechanistic Insights for Reaction Optimisation

Antoine de Gombert



St Hilda's College, University of Oxford

Hilary Term 2021

Supervisor: Prof. Michael C. Willis

A thesis submitted in partial fulfilment of the requirements for the degree of

Doctor of Philosophy in Organic Chemistry

Abstract

In this thesis, the mechanism of the palladium-catalysed desulfinative cross-coupling of aryl bromides and (hetero)aryl sulfinate salts is investigated. The challenges that must be overcome to deliver improved, lower temperature versions of this process are discussed, and optimisation work based on these mechanistic insights is presented.

Chapter 1 is a literature review surveying the use of sulfinate salts in palladium-catalysed cross-coupling reactions. Particular emphasis is placed on the mechanism of these transformations and the structure of palladium sulfinate intermediates.

Chapter 2 describes the mechanistic studies of the palladium-catalysed desulfinative cross-coupling of 1-bromo-4-fluorobenzene and (hetero)aryl sulfinate salts. 2-Pyridyl and carbocyclic sulfinate substrates are compared, and different catalyst resting states and turnover limiting steps are established for the two classes of reagent. The role of the carbonate additive and the reduction of the palladium(II) precatalyst is also investigated.

Chapter 3 demonstrates the significance of the challenges associated with developing lower-temperature desulfinative cross-coupling reactions. A survey of a number of reaction parameters and their influence on the outcome of the reaction is presented.

Chapter 4 focuses on the use of the Xantphos ligand and the synthesis of Xantphos derivatives to promote desulfinative cross-coupling reactions at 100 °C.

Chapter 5 discusses the development of a desulfinamidative cross-coupling reaction using a primary aryl sulfinamide as the nucleophilic coupling partner. The feasibility of this process is demonstrated, and initial optimisation results are presented.

Chapter 6 discusses the conclusion of the research and the potential for future work.

Chapter 7 presents the experimental data.

Declaration

The work described in this thesis is entirely the work of the author except where specifically indicated. This thesis has not been previously submitted for a degree, diploma or any other qualification at the University of Oxford or elsewhere.

Antoine de Gombert

April 2021

Acknowledgements

People often asked me: “How is the PhD life in Oxford?”. ***W***ell, Oxford is great, but with such a nice crew, it could have been in the m***i***ddle of nowhere, all I needed was these people (and ok, maybe a pub).

Firstly, I would ***l***ike to thank Prof. Michael Willis, aka Mike, for his supervision. Thank you for the many “Sounds good. M” which a***l***ways comforted me in my choices when I needed it. Your trust, guidance and support have been instrumental to my development as a chemist. Thanks also to Dr Chris Davis and Dr Katherine Wheelhouse for all the insightful discussions and for providing a perspective on my chemistr***y*** from outside the academic box.

I w***o***uld like to thank Prof. Richard Cooper and Dr Alasdair McKay, who were key to the crystallographic work of this thesis. Special thanks to Richard who took the time to train me and explain the f***u***ndamentals of X-ray crystallography to me. Thanks also to Charlie Prentice for helping me with the super scary X-ray diffractometer. Thanks also to Dr Liana Allen for the high throughput screening work, to Dr Sreenithya Avadakkam and Pro***f***. Rob Paton for the computational chem***i***stry work, and Dr Nader Amin and Prof. Tim Claridge for their help with the NMR spectroscopy experiments. I would also like to thank the Centre for Doctoral Traini***n***g: Synthesis for Biology and Me***d***icine (SBM) for the opportunity to be part of such a unique program, special thanks to Lara, Laura and Maitane.

To ***t***he ancients of the MCW group. Firstly I would like to thank TQD for proofreading my numerous abstracts and helping me with a number applications. I owe you a lot for that. I really don’t hate you anymore ***h***a! To the most ancient of all, RNS the wise, for annoyingly always being right, apart from when you called me a twat. To my favourite ging***e***r, Vincent, for your constant happiness, you made F1 the best environment I could have dreamed of when I joined the group. J’espère que tu gardes la pêche! Also thanks to Qian Wen for being such a great desk and tennis buddy, to Terry, for not often drying your phone in the desiccator***s***, to Rita for your kindness (and your Schlenk line), and to Tim, without whom my project would not have existed.

For proofr***e***ading this looooonng thesis, until the last minute, and under some strong time constraints, I would like to thank Ndi (twice), Damien, Xinlan (twice), Jonny, Charlie and Dan. Without you, this thesis would be full of typos and grammatical nonsense, just like these a***c***knowledgements.

Very special thanks to my arche nemesis, Mich(a)el Tilby, for all the bitching, the banter, the laughs, the tea***r***s, the stirring, the desk, and all the lovely pub dates. For being such a good friend over these last four years and a bit, you definitely have deserved that alpha+ ! Much lov***e***.

Thanks to Xinlan for always keeping up good vibes, and for always filling all the awkward silences; to Dan, you fukken draggo for being the best fu***m***ehood neighbour ever, despite the unacceptable mess; to Jonny for always praising the quality of my favourite Spotify playlist; to Tony, for always going big and not home; and to Jagadeesh, for your great advices.

To the many part two students, for always taking the blame when something goes wrong, because it is obviously always the part two's fault, especially Alvin's (apart from when the lab stinks b***e***cause of someone's "bad technique"). Special thanks to my dear apprentice Hugh, for all the thought challenging conversations, and for making me discover the delicious Hook Nortons, and to Ben (and Dan again) for showing me the amazing Big Lez Show.

To the Council: Ben Jonny, Mix, and Rob, thanks for the***s***e amazing formative years, with all their unforgettable moments: the legendary Tiki Tiki parties, the pub fights, the iron outside the box, the Chri***s***tmas dinners, the Bartlemas whiteboard rules, the betrayal, the trips to Scotland and Lake district, Jersey, the Jenga, the many formal dinners... The list is endless. All this depr***a***vity has probably cost me 5-10 years of life expectancy, worth it though.
A thousand years.

Aux distinctifs et représentatifs Red-Hots, pour votre amitié sans faille, infiniment merci. Special thanks à Anne-Soulaïne qui a traversé la Manche non pas une mais deuuuxxx fooiiiss pour venir me rendre visite, et à Adélounette pour ses nombreux messages d'encoura***g***ements et amitié sans faille. #coeurcoeurniais.

A mon BFF, que dis-j***e***, l'amour de ma vie, Pupu. Vivement l'âge de la retraite à Sisteron, on pourra alors se faire autant de carafes en cristal que l'on désire en écoutant *Heart of Gold*.

A mon couz Dimou, merci pour l'intérêt que tu as porté à ma chimie, et pour avoir écouté mes explications farfelues, armé de cailloux et de bâtons à la lueur des feux d'artifice du 14 juillet.

Enfin, Papa, Maman, Popo (et non pas Paupau), merci pour votre immense soutien. Les photos et discus***s***ions quotidiennes sur *Familia* ont illuminé mes journées pendant ces quatre et quelques dernières années. Grâce à elles, vous n'avez finalement jamais été si loin que ça. Je vous embrasse fort, bbn, edf.

To the dedicated reader, thanks for reading until the end of this page! Just 383 more to go!

Table of Contents

Chapter 1 – Introduction **1**

1.1. Palladium-Catalysed Cross-Couplings 1

1.1.1. Palladium in Catalysis 1

1.1.2. Palladium-Phosphine Binding 1

1.1.3. Cross-Coupling Arylation Reactions 4

1.2. Sulfinate Salts in Palladium-Catalysed Cross-Coupling Arylation Reactions 6

1.2.1. Synthesis of Sulfinate Salts 6

1.2.2. A Note on the Nomenclature 7

1.2.3. Sulfinate Salts as Electrophilic Coupling Partners 8

1.2.4. Sulfinate Salts as Nucleophilic Coupling Partners 9

1.2.5. Homocoupling Reactions 11

1.2.6. C-H Activation Reactions 12

1.3. Mechanistic Insights in Metal-Catalysed Desulfination Reactions 15

1.3.1. Desulfination *vs* Decarboxylation *vs* Desulfonation 15

1.3.2. Palladium Sulfinate Complexes 16

1.3.3. Desulfination at Palladium: Electrophilic Sulfinate 20

1.3.4. Desulfination at Palladium: Nucleophilic Sulfinate 21

1.4. Research Aims 22

Chapter 2 – Mechanistic Studies of the Palladium-Catalysed Desulfinative Cross-Coupling of Aryl Bromides and (Hetero)Aryl Sulfinate Salts **24**

2.1. Model Reactions and Substrates 24

2.2. Formation of the Active Pd(0) Species 25

2.3. Synthesis and Characterisation of Relevant Palladium Complexes 29

2.3.1. Oxidative Addition Complex 29

2.3.2. Aryl Palladium Sulfinate Complexes 30

2.4. Reactivity of Aryl Palladium Sulfinate Complexes 33

2.4.1. At Room Temperature in Presence of Tricyclohexylphosphine 33

2.4.2. Extrusion of SO_2 from Complexes **12** and **14**. 35

2.5. Study of the Transmetalation Step 38

2.5.1. Working Hypothesis 38

2.5.2. Importance of the Sulfinate Counter Cation 39

2.5.3. Impact of the Concentration of PCy_3 on the Rate of Transmetalation 41
2.5.4. Lability of PCy_3 in the Oxidative Addition Complex **9** 44
2.6. Identification of the Resting State Intermediates 45
2.7. Kinetics of the Catalytic Reaction 48
2.7.1. Experimental Procedure: Initial Rates of the Reaction 48
2.7.2. Heterogeneous *vs* Homogeneous Catalysis 50
2.7.3. Order in Aryl Bromide **2** 51
2.7.4. Order in Sulfinate Salts and K_2CO_3 52
2.7.5. Order in Catalyst 52
2.8. SO_2 By-product 54
2.9. Project Summary 57

Chapter 3 –Towards a Lower Temperature Cross-Coupling Reaction 60
3.1. Choice of the Model Substrates 60
3.2. Tetramethylammonium Cation 61
3.3. Silver Salts 62
3.4. Copper Additives 63
3.5. Solubility of the Sulfinate Coupling Partner 64
3.6. Nature of the Aryl Halide 66
3.7. Cationic Phosphine Ligands 67
3.8. Other Phosphine Ligands 70
3.9. Summary of the Screening Strategy 76

Chapter 4 – Xantphos-Like Ligands 78
4.1. Introduction 78
4.1.1. Comparison of the Mechanisms for Sulfone or Biaryl Formation 78
4.1.2. Xantphos Palladium Complexes 80
4.1.3. Palladium-Catalysed Coupling of Aryl (Pseudo)Halides and Aryl Sulfinate Salts 83
4.2. Mechanistic Insights 85
4.2.1. Importance of the Sulfinate Counter Cation 85
4.2.2. Reversibility of the Transmetalation Step 86
4.3. Key Structural Features of the Xantphos Ligand 88
4.3.1. Model System 88

4.3.2. Variations of the Xanthene Backbone 89
4.3.3. Symmetrical Variation of the Diphenylphosphino Groups 93
4.3.4. Chelating Ability of the Ligand 94
4.3.5. Variation of One Diphenylphosphino Group 95
4.4. Conclusion 99

Chapter 5 – Aryl Sulfinamides as Novel Nucleophiles for Palladium-Catalysed Carbon-Carbon Bond-Forming Reactions **102**
5.1. Introduction 102
5.2. Initial Evaluation at 150 °C 104
5.3. Lowering the Reaction Temperature to 100 °C, Base and Solvent Screening 106
5.4. Ligand Screening 108
5.5. Palladium Precatalyst 112
5.6. Additives 113
5.7. Preparative Scale, Isolation 116
5.8. Conclusion and Future Work 117

Chapter 6 – Conclusion **118**

Chapter 7 – Experimental Data and Procedures **121**
A detailed Table of Contents can be found at the beginning of this section 121

8. References **269**

9. NMR Spectra **276**

A detailed Table of Contents can be found at the beginning of this section 276

Abbreviations and Acronyms

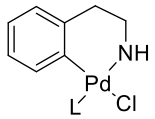
aq.	aqueous
Ac	acetyl
Ar	aryl
BAr_F^4	tetrakis[3,5-bis(trifluoromethyl)phenyl]borate
Bn	benzyl
Boc	*tert*-butyloxycarbonyl
Bz	benzoyl
Bu	butyl
cat.	catalyst *or* catalytic
COD	cyclooctadiene
Cy	cyclohexyl
dba	dibenzylideneacetone
decomp.	decomposition
DFT	density functional theory
DMF	*N*,*N*-dimethylformamide
DMSO	dimethyl sulfoxide
equiv.	equivalents
ESI	electrospray ionisation
h	hour(s)
Het	heteroaryl
HPLC	high performance liquid chromatography
HRMS	high resolution mass spectrometry
HTE	high throughput experimentation
HTS	high throughput screening
Hz	hertz
i	iso
IR	infrared
J	coupling constant
L	ligand *or* litre
LRMS	low resolution mass spectrometry
M	metal *or* molar
Ms	mesylate

MS	molecular sieves
MW	molecular weight *or* microwave
m	milli *or* multiplet
m	*meta*
NMR	nuclear magnetic resonance
o	*ortho*
OA	oxidative addition
p	*para*
Ph	phenyl
ppm	parts per million
pyr	pyridyl
R	generic group/substituent
RSI	resting state intermediate
RE	reductive elimination
rt	room temperature
s	secondary
sat.	saturated
t	tertiary
Tf	trifluoromethanesulfonyl
TBA	tetrabutylammonium
TBAB	tetrabutylammonium bromide
TBPA	*tert*-butyl peroxyacetate
TMA	tetramethylammonium
TFA	trifluoroacetate
THF	tetrahydrofuran
TLC	thin layer chromatography
TLS	turnover limiting step
TM	transmetalation
Tol	tolyl
UV	ultraviolet
X	(pseudo)halide (unless stated otherwise)
XRD	X-Ray diffraction
μ	micro
ν	frequency

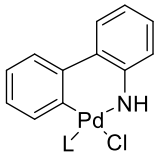
Ligand Structures

Pd GX refers to the generation of the Buchwald palladium precatalysts.
In the structures below, L stands for a generic phosphine ligand.

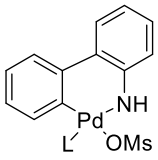
G1:



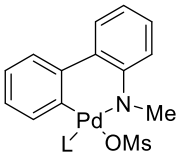
G2:

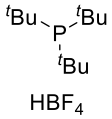


G3:

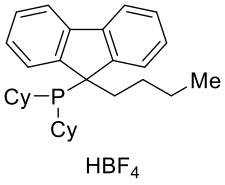


G4:

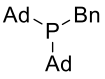




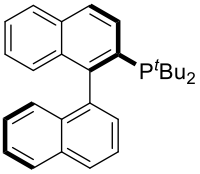
P(^{t}Bu)$_3$•HBF$_4$



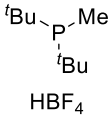
CataCXium FBu



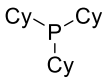
PAd$_2$Bn



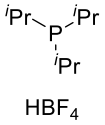
TrixiePhos



P(^{t}Bu)$_2$Me•HBF$_4$



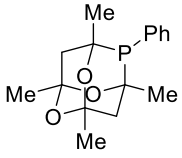
PCy$_3$



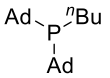
P(^{i}Pr)$_3$•HBF$_4$



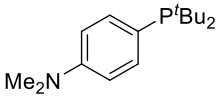
PAd$_2$H



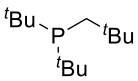
meCgPPh



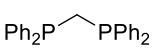
cataCXium A



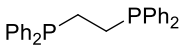
APhos



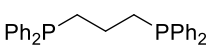
DTBNpP



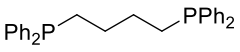
dppm



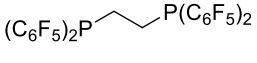
dppe



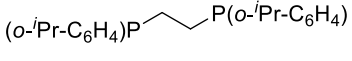
dppp



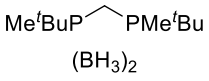
dppb



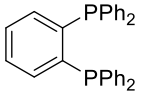
^{F}dppe



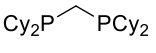
***o*-^{i}Pr-dppe**



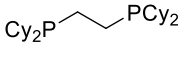
MtBpe



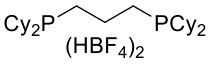
dppbenz



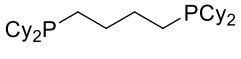
dcpm



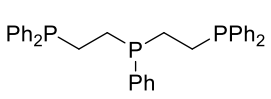
dcpe



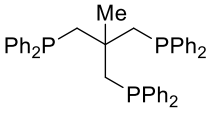
dcpp(HBF$_4$)$_2$



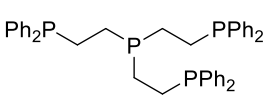
dcpb



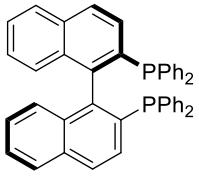
Triphos 1



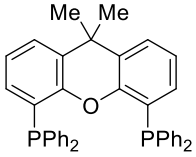
Triphos 2



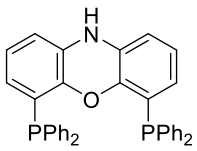
Tetraphos



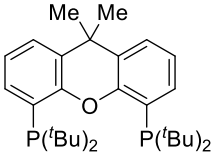
binap



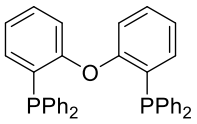
Xantphos



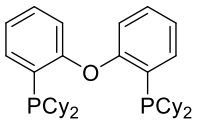
Niantphos



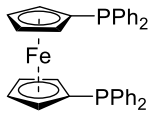
***t*-Bu-Xantphos**



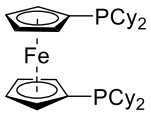
DPEPhos



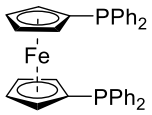
DCEPhos



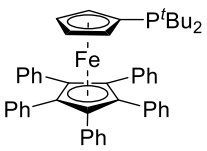
dppf



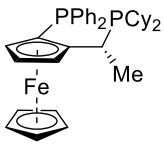
dcpf



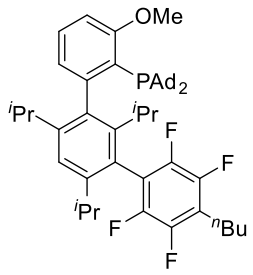
dtbpf



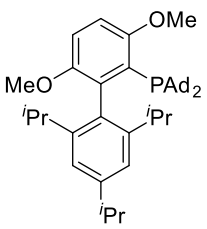
QPhos



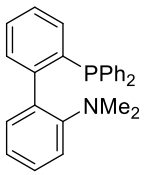
JosiPhos



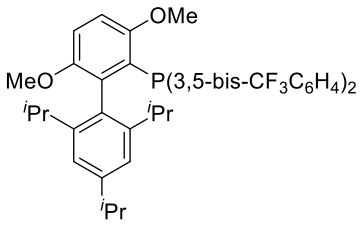
AlPhos



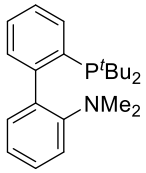
AdBrettPhos



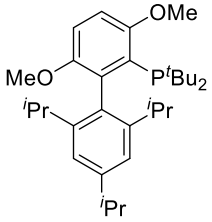
PhDavePhos



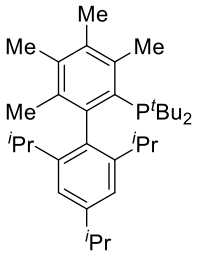
JackiePhos



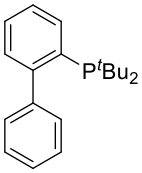
***t*-BuDavePhos**



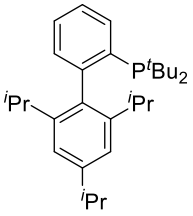
***t*-BuBrettPhos**



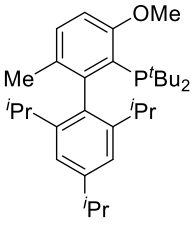
Me$_4$*t*-BuXPhos



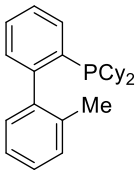
JohnPhos



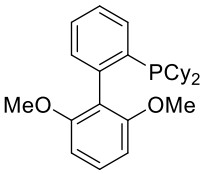
***t*-BuXPhos**



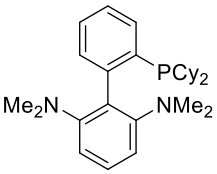
RockPhos



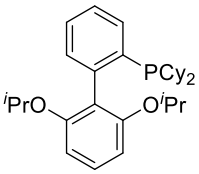
MePhos



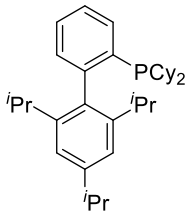
SPhos



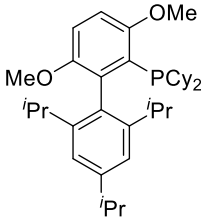
CPhos



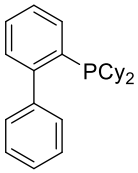
SPhos



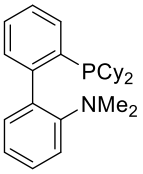
XPhos



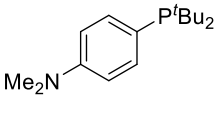
BrettPhos



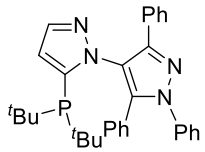
CyJohnPhos



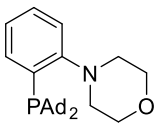
DavePhos



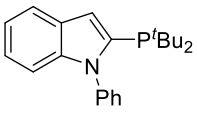
APhos



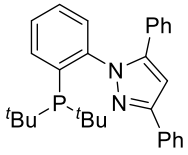
Bippyphos



MorDalphos



***t*-BuPhIndolePhos**



P*t*-Bu$_2$PhPyr

Chapter 1 – Introduction

1.1. Palladium-Catalysed Cross-Couplings

1.1.1. Palladium in Catalysis

Transition-metal-catalysed reactions have undeniably changed the field of organic chemistry. Key carbon-carbon bond formation reactions that were typically achieved *via* the use of stoichiometric reactive nucleophiles or pericyclic reactions, are now routinely performed with the help of transition-metal catalysts, in both academic laboratories and multi-ton production plants.[1] Among all the transition-metals available to synthetic chemists for catalysis, palladium has a special status. Brown and Boström conducted a statistical analysis of the literature using a representative set of papers from the *Journal of Medicinal Chemistry* for screening compounds and from the *Journal of the American Chemical Society* and *Angewandte Chemie, International Edition* for natural products in 2014. In this sample of the literature, the Suzuki-Miyaura reaction represented 19% of all reactions performed, ranking this palladium-catalysed process as first place amongst all other transition-metal-catalysed reactions, closely followed by the Sonogashira and Buchwald-Hartwig coupling reactions.[2] The prevalence of palladium-catalysed processes in organic chemistry was internationally recognised in 2010, with the attribution of the Nobel Prize to Richard Heck, Ei-ichi Negishi and Akira Suzuki "for palladium-catalyzed cross couplings in organic synthesis", acknowledging the extent to which this element had revolutionised the art of synthesis.[3-4]

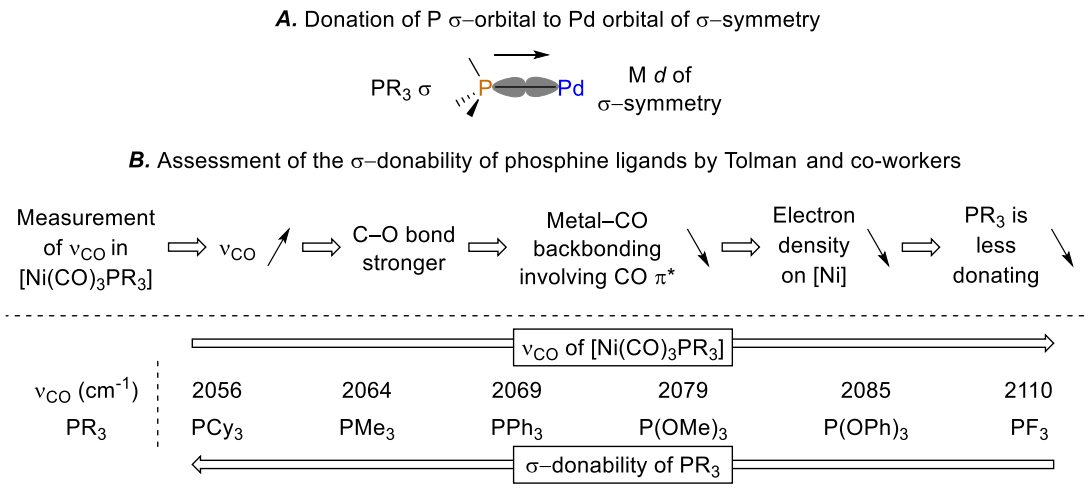
1.1.2. Palladium-Phosphine Binding

Palladium has been extensively used in heterogeneous catalysis,[5] notably for hydrogenation reactions, for example with Pd/C[6] or Lindlar's catalysts.[7] In homogeneous catalysis, the development of ancillary ligands has largely contributed to its success. A wide range of structurally different ligands have been developed, such as NHCs, η^6-arenes, or nitrogen-based

ligands, mainly sp^2 hybridised (bipyridines and imine derivatives) but also sp^3 (TMEDA for example). Nonetheless, phosphine ligands dominate the scene for palladium catalysis.

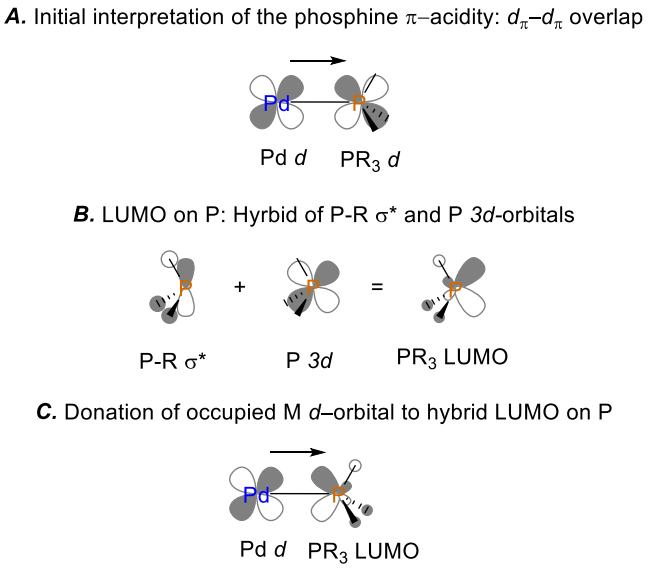
Palladium-phosphine binding is mainly due to Lewis acid-base interactions. Palladium is a d^{10} transition-metal with soft Lewis acid properties, likewise, tertiary phosphines are described in the HSAB theory as soft ligands.[8-10] In contrast, amines are harder Lewis bases, and therefore give rise to weaker bonds with palladium, although in terms of Brønsted basicity, trialkyl phosphines and amines are similar ($pK_a(HNEt_3)$ = 9.0 in DMSO, $pK_a(HPEt_3)$ = 9.1 in DMSO).[11]

Palladium-phosphine binding can be described by two main interactions. Firstly, a σ-component, involving the donation of electrons from the soft and diffuse lone pair of the tertiary phosphine ligand to an empty palladium orbital of σ-pseudosymmetry (***Scheme 1.1.A***). Chadwick, Tolman and DuPont indirectly quantified the donating ability of a range of PR_3 ligands by measuring the ν_{CO} of $[Ni(CO)_3PR_3]$ complexes by infrared spectroscopy.[12-13] These studies showed that among the ligands assessed, PF_3 was the weakest donor, and the donating ability of PR_3 increased from phosphites to phosphines, and from triaryl to trialkyl phosphines (***Scheme 1.1.B***).



Scheme 1.1. Palladium-phosphine binding: σ-component.

In addition to this first σ-component, there is an important π-contribution to the palladium-phosphine binding. The π-acidity of phosphines was first assigned to an interaction between the occupied metal *d*-orbitals and the phosphine "low-lying" and empty *3d*-orbitals (***Scheme 1.2.A***).[14] Later, Orpen and Connelly observed that the P-R bond lengths in [M-PR_3] units decreased on oxidising the metal in 24 transition-metal phosphine and phosphite complexes. This was rationalised by the contribution of P-R σ*-orbitals to the phosphorus LUMO, which is responsible for the π-acid ability of phosphine ligands (***Scheme 1.2.B***).[15-17] These structural observations were consistent with some early *ab initio* molecular orbital calculations on simple phosphine-metal complexes.[18-19] For these reasons, the π-component of the palladium-phosphine binding is better described by the backbonding between the filled palladium *d*-orbitals and a hybrid orbital of the P-R σ* and the phosphorus *d*-orbitals (***Scheme 1.2.C***).



Scheme 1.2. Palladium-phosphine binding: π-component.

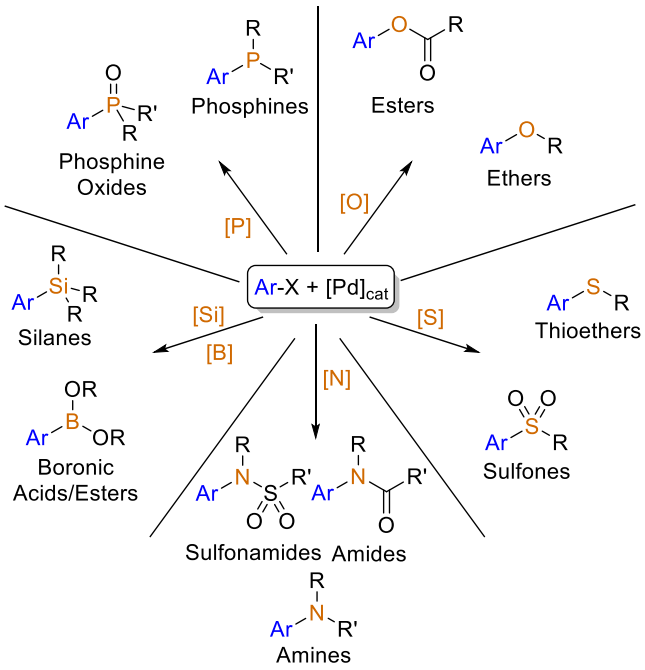
The number of phosphines that have been developed over the last three decades for palladium catalysis is immense. Due to the large size of the phosphorus atom, the presence of bulky ligands on the phosphorus is possible, allowing a large diversity of compounds without weakening the Pd-P binding significantly. This is not the case for the parent alkyl amines for

example, which are more congested and have larger cone angles. These steric effects, together with the hard/soft mis-match between amines and palladium, explain the much larger success of trialkyl phosphine ligands compared to trialkyl amines.[11]

The effects of phosphine steric and electronic properties on the structure and reactivity of palladium complexes has been studied extensively, and the emergence of key phosphine parameters that are simple to predict and apply, such as the cone angle, contributed to the development of highly efficient catalysts.[20] From Tolman steric and electronic parameters reported in the 1970s,[12-13, 20] to more and more elaborate ligand descriptors that are developed with the progress of computational methods and machine learning,[21-24] our understanding of palladium-phosphine binding is constantly increasing together with catalyst performance.

1.1.3. Cross-Coupling Arylation Reactions

A cross-coupling reaction is a process in which a catalyst, usually a transition-metal complex, mediates the assembly of two starting materials to form a new covalent bond. Within this rather general definition, reactions that involve the substitution of an aryl (pseudo)halide by a nucleophile (see **Section 1.2.2** for a note on the terms electrophile/nucleophile in the context of cross-coupling reactions) and follows the mechanistic course of oxidative addition, transmetalation and reductive elimination, represent a major section of cross-coupling reactions.[25] This does not only apply to carbon-carbon bond formation. There is indeed a plethora of heteroatomic nucleophiles that can be combined with aryl (pseudo)halides. The most emblematic are amines, and their coupling is known as the Buchwald-Hartwig cross-coupling reaction.[26] However, oxygen, sulfur, phosphorus, boron and many other heteroatomic nucleophiles have also been arylated using palladium or other transition-metal catalysis (***Scheme 1.3***).[27]



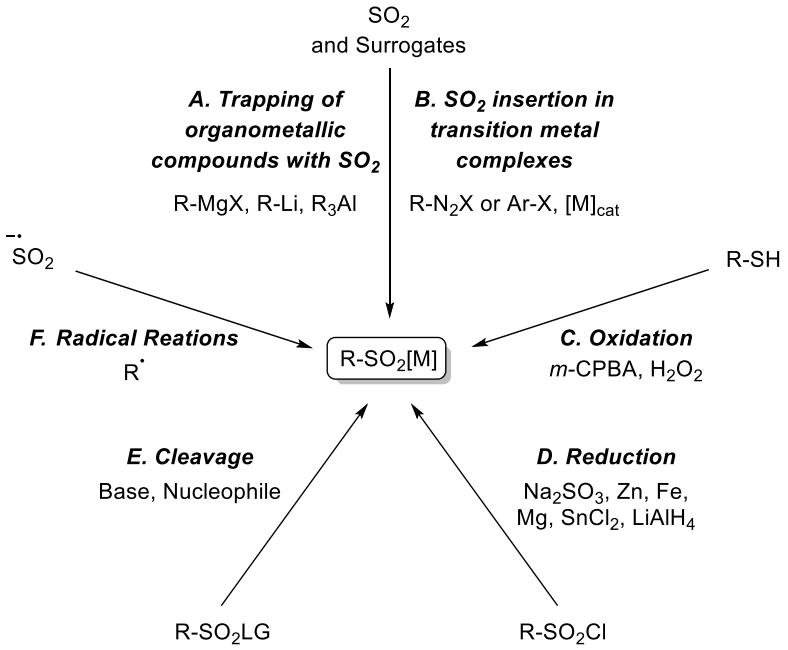
Scheme 1.3. Cross-coupling arylations with heteroatomic nucleophiles.

Nonetheless, palladium catalysed cross-coupling reactions are most famous for carbon-carbon bond formation. Colacot, Snieckus and co-workers traced the origins of metal-mediated carbon-carbon bond forming reactions all the way back to 1869, when Glaser reported the homocoupling of cupric acetylides, in a very interesting historical review.[3, 28] Nowadays, the venerable Suzuki-Miyaura (boron),[29] Kumada-Corriu (magnesium),[30] Negishi (zinc),[31] Stille-Migita (tin),[32] Hiyama-Denmark (silicon),[33] Heck (alkenes),[34] and Sonogashira (alkynes)[35] reactions have become canonical, and are generally referred to with the name of their discoverers rather than the name of the nucleophile. In the 2000s, Goossen demonstrated that carboxylic acids could also be employed as the nucleophilic coupling partner in cross-coupling arylation reactions,[36-37] and more recently, sulfinate salts have also emerged as an efficient alternative in these palladium catalysed carbon-carbon bond formation processes.[38] This is the focus of the next section.

1.2. Sulfinate Salts in Palladium-Catalysed Cross-Coupling Arylation Reactions

1.2.1. Synthesis of Sulfinate Salts

Sulfinate salts, also referred to as sulfinic acid salts, were first reported in 1861.[39] They are usually colourless, odourless, non-corrosive bench-stable solids.[40] Their use as a versatile building block has been reviewed by four different groups in the last three years, showing their prevalence in organic synthesis.[41-43]



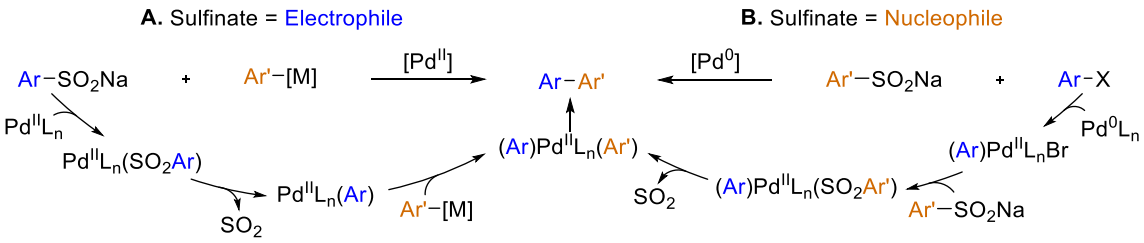
Scheme 1.4. Synthetic Routes to Sulfinate Salts.

Aryl sulfinate salts can be made from five main sulfur sources, as shown in ***Scheme 1.4.*** Trapping of SO_2 gas, or of a SO_2 surrogate, by an organometallic reagent (*Route **A***) is one of the most straightforward methods to prepare sulfinate salts. Similarly, SO_2 gas or surrogates have been utilised in conjunction with transition-metal catalysis (*Route **B***), allowing sulfination under milder and more functional-group-tolerant reaction conditions compared to organometallic reagents. Sulfinate salts can also be obtained from sulfur derivatives at a different oxidation state. Both the oxidation of thiols (*Route **C***) and the reduction of sulfonyl chlorides (*Route **D***) are extremely well documented and established methods. Masked aryl

sulfinate salts can also be released by nucleophilic or base-mediated cleavage of sulfonyl-containing compounds (*Route **E***), such as alkyl sulfones or thiosulfonates. Finally, although under-represented, radical combination with the sulfur dioxide radical anion $SO_2^{\bullet-}$ is another avenue for the synthesis of sulfinate salts (*Route **F***). These methods were reviewed in depth by Manolikakes and co-workers in 2020.[44] It is, however, important to highlight that the isolation of sulfinate salts in their pure form, rather than their direct trapping and functionalisation in a one-pot process, remains a challenge.

1.2.2. A Note on the Nomenclature

Although cross-coupling reactions do not necessarily combine electrophile and nucleophile substrates, it is possible to formally call both coupling partners either electrophilic or nucleophilic depending on their role in the reaction mechanism rather than their intrinsic reactivity. This is perfectly illustrated by homocoupling reactions where the same functional group acts simultaneously as the electrophilic and nucleophilic coupling partner.



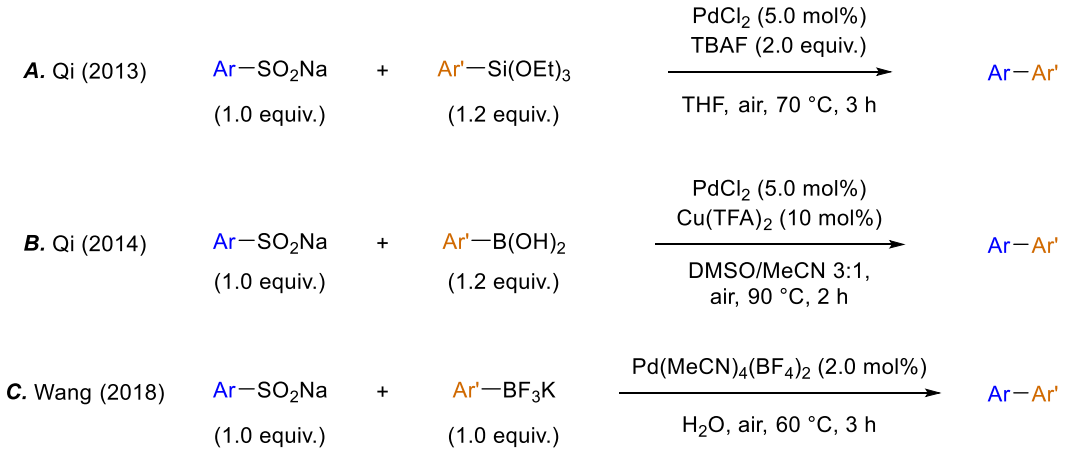
Scheme 1.5. Aryl sulfinate salts as electrophilic or nucleophilic coupling partners.

Sulfinate salts have been used as both nucleophilic and electrophilic coupling partner. When the sulfinate salt is involved in a ligand exchange with the catalyst, followed by extrusion of SO_2 to generate an aryl palladium complex which subsequently undergoes transmetalation, the sulfinate is designated as the electrophilic coupling partner (***Scheme 1.5.A***). This designation is not intuitive as the initial step of this process is essentially a nucleophilic attack of the sulfinate on the palladium salt. After transmetalation and reductive elimination giving the product and a Pd(0) complex, an oxidant is required to oxidise the palladium back to its initial

oxidation state. When the sulfinate is however involved in a transmetalation type step with an aryl palladium halide complex (***Scheme 1.5.B***), the sulfinate is designated as the nucleophilic coupling partner. This second catalytic cycle is redox neutral, and does not require external oxidants. These mechanisms will be explored in more detail in **Section 1.3.**

1.2.3. Sulfinate Salts as Electrophilic Coupling Partners

Mild and efficient Hiyama- or Suzuki-type couplings, using (hetero)arylsulfinates salts as the electrophilic coupling partners, have been reported for the synthesis of biaryls (***Scheme 1.6***).



Scheme 1.6. Hiyama and Suzuki-type cross-coupling reactions.

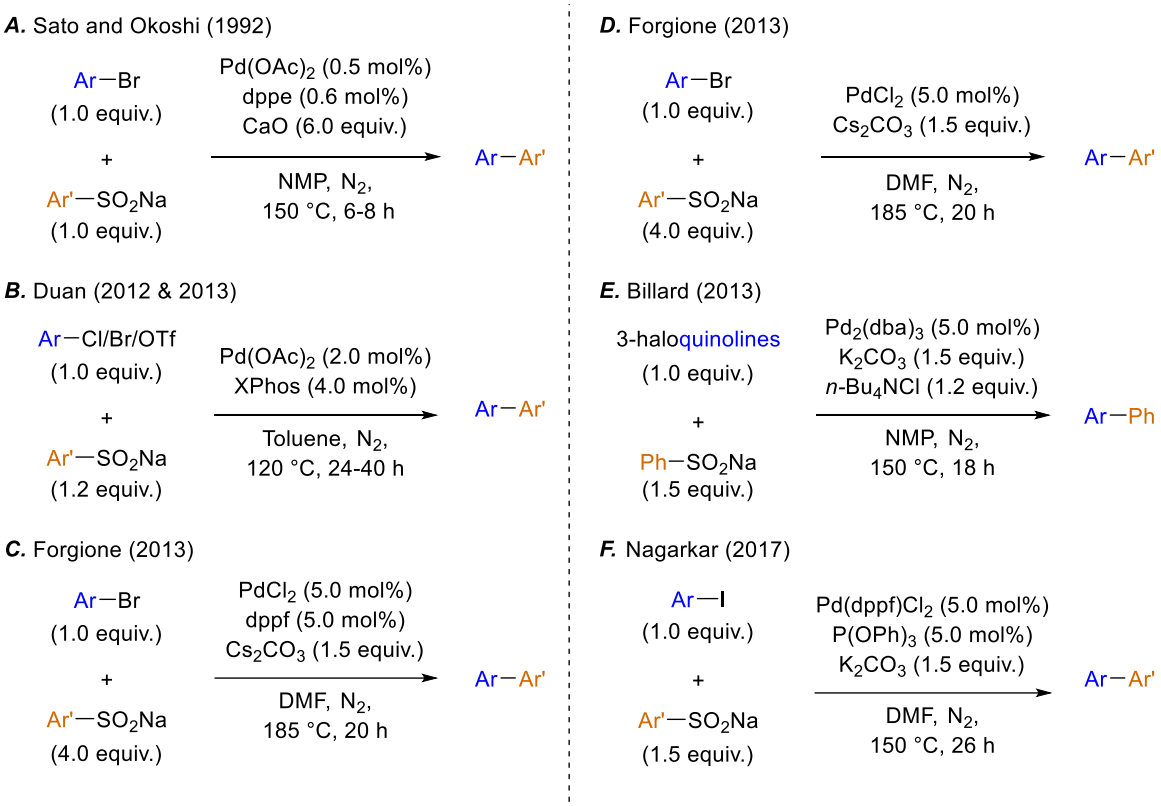
A source of fluoride was necessary to induce the transmetalation for the reaction with triethoxysilanes (***Scheme 1.6.A***),[45] and the reaction proceeded smoothly at 70 °C. Air was the source of oxygen, acting as the stoichiometric oxidant required to regenerate the Pd(0) catalyst after final reductive elimination. In the reaction involving aryl boronic acids as the nucleophilic coupling partners (***Scheme 1.6.B***),[46] the oxygen present in air was also employed as the final oxidant, but this time a copper co-catalyst was used to obtain higher yields, and the temperature had to be slightly raised (90 °C) compared to the silane system. The use of potassium aryl trifluoroborate salts by the Wang group (***Scheme 1.6.C***),[47] was a significant improvement as it allowed the coupling to happen in water and at 60 °C over 3 hours. Once again, air/oxygen was used as the stoichiometric oxidant, and no other additive was required, making this reaction

the greenest process compared to the two others aforementioned. Interestingly, none of these reactions required ancillary phosphine ligands.

1.2.4. Sulfinate Salts as Nucleophilic Coupling Partners

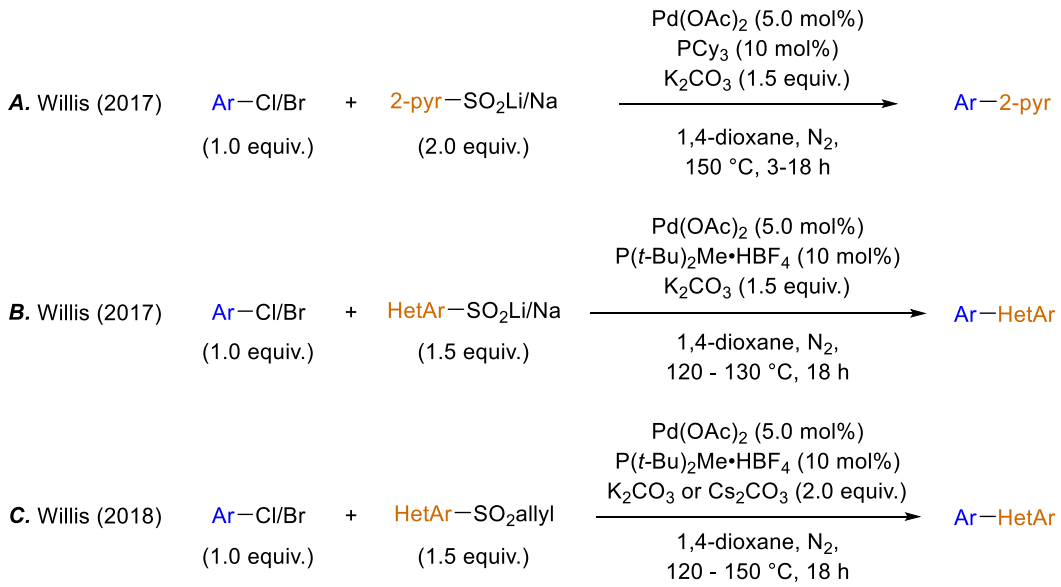
Although the coupling between aryl sulfinate salts and aryl halides was reported as early as 1992 in a seminal patent (***Scheme 1.7.A***),[48] it was not until 2012 that this reactivity was explored again, this time using aryl triflates, by Duan and co-workers (***Scheme 1.7.B***).[49] The same group extended their reaction scope to aryl chlorides and bromides in a subsequent paper using the same reaction conditions.[50] The Forgione lab concurrently reported a catalytic system based on $PdCl_2$ and dppf that required higher reaction temperatures but allowed a broader substrate scope (***Scheme 1.7.C***),[51] then later showed that dppf could be omitted without loss of efficiency (***Scheme 1.7.D***).[52] The scope of the electrophilic coupling partner was extended to 3-haloquinolines by Billard and co-workers using a combination of $Pd_2(dba)_3$ and the DavePhos ligand (***Scheme 1.7.E***),[53] and further broadened by the Nagarkar lab with aryl iodides, using the unusual combination of $Pd(dppf)Cl_2$ and $P(OPh)_3$ (***Scheme 1.7.F***).[54]

The Forgione lab also reported three different catalytic systems ($PdCl_2/PPh_3$, H_2O/DMF, 170 °C; $Pd(P(t\text{-}Bu)_3)_2$, DMF anhydrous, 170 °C; $Pd(acac)_2/PPh_3$, EtOH, 150 °C) for the successful coupling of (benzo)thiophene and (benzo)furan sulfinate salts with aryl bromides or triflates using microwave irradiation.[55-57] Under these conditions, no other additive was required and reactions were completed between 8 minutes and 1 hour.



Scheme 1.7. Desulfinative cross-couplings between aryl halides and aryl sulfinates.

More recently, the Willis group has pioneered the use of 2-pyridyl sulfinate salts in cross-coupling reactions with (hetero)aryl bromides (***Scheme 1.8.A***).[58] These conditions were successfully applied to the synthesis of pyridyl[2.2]paracyclophanes, a useful scaffold in the field of materials chemistry by the Rowlands group.[59] 2-Pyridyl sulfinate salts are particularly interesting because these substrates are easy to prepare and bench stable, and their couplings are generally robust and high yielding, conversely to 2-pyridyl boron nucleophiles.[60] Subsequent work in our group demonstrated that a change of the phosphine alkyl substituents allowed a slight reduction of the reaction temperatures from 150 °C to 120-130 °C using P(*t*-Bu)$_2$Me•HBF$_4$ instead of PCy$_3$ (***Scheme 1.8.B***).[61] In addition to 2-pyridyl substrates, a wide range of 5- and 6- membered heterocyclic sulfinates, bearing multiple heteroatoms, were shown to be effective nucleophilic coupling partners under the same conditions.



Scheme 1.8. Desulfinative cross-couplings between aryl halides and heteroaryl sulfinates.

As previously discussed in **Section 1.2.1**, the purification of sulfinate salts can be problematic. Furthermore, the anionic nature of the sulfinate functional group makes these nucleophiles unsuitable for multistep synthetic sequences. These problems were circumvented with the use of allyl sulfones as latent nucleophiles, releasing the masked sulfinate *in situ* under similar reaction conditions (***Scheme 1.8.C***).[62] Complex heterocyclic molecules and drug analogues were synthesized to demonstrate the power of these latent nucleophiles.

Despite the utility of sulfinate salts as nucleophilic coupling partners, especially in the context of the "2-pyridyl organometallic cross-coupling problem",[60, 63] their use is plagued with the requirement of harsh reaction conditions, with temperatures ranging from 120 °C to 185 °C. It is important to highlight that this is not the case when sulfinate salts are used as the electrophilic coupling partners, as shown in **Section 1.2.3.**

1.2.5. Homocoupling Reactions

The homocoupling of sodium 4-methylbenzene sodium sulfinate to form 4,4'-dimethylbiphenyl was first reported by Garves in 1970.[64] The biaryl product was obtained in 35% yield using stoichiometric Na_2PdCl_4. This yield doubled when HgCl was used as a catalyst. Since this

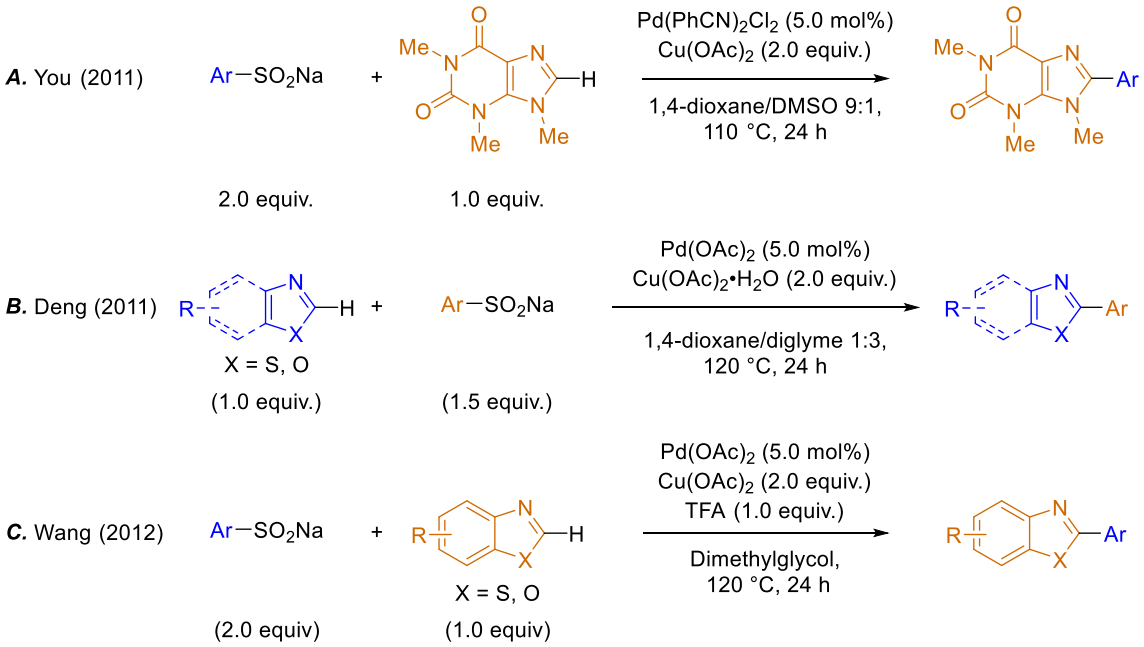
seminal report, greener approaches to symmetrical biaryls have been developed by the groups of Luo[65] and Forgione.[66] Both methods used a palladium catalyst and oxygen as the terminal oxidant, with either copper oxide or TEMPO as a co-catalyst.

1.2.6. C-H Activation Reactions

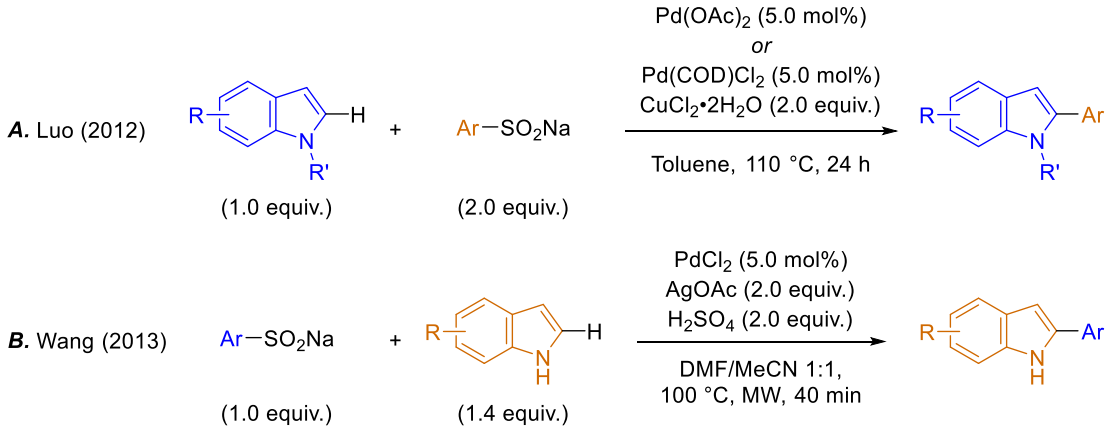
Sulfinate salts have also been used as arylating agents for C-H activation reactions. [40-41, 67] In these reactions, the sulfinate will once again act as the electrophilic or nucleophilic coupling partner, as described in **Section 1.2.2.** However, the mechanism of these C-H arylations with sulfinate salts is not well understood, and is most often based on limited or non-existent experimental data, or by analogy with previous reports also based on speculative material. For this reason, this section is organised according to the nature of the substrates or the reaction conditions, rather than the role of the sulfinate salt. Nevertheless, electrophilic or nucleophilic denominations will be used as described in these literature reports, and to avoid confusion, the electrophilic coupling partner will always appear first in blue, and the nucleophile second, in orange.

In 2011, the group of You reported the C-H arylation of caffeine derivatives as well as of a range of azole derivatives (***Scheme 1.9.A***).[68] Noticing that other oxidants than $Cu(OAc)_2$ were incapable of providing reactivity, they proposed that the heterocyclic substrate would be activated by copper(I) salts generated *in situ*. The latter would undergo transmetalation with an Ar-Pd-X complex generated by desulfination of the sulfinate salt. For this reason, they assigned the sulfinate salt as the electrophilic coupling partner. However, in the same year, Deng and co-workers independently reported the coupling of (benz)oxazoles and (benzo)thiazoles as well as caffein derivatives with aryl sulfinate salts using very similar conditions (***Scheme 1.9.B***).[69] The authors proposed a different mechanism in which the sulfinate salt acts as the nucleophilic coupling partner. This shows that the notions of electrophile/nucleophile in the field of C-H

activation should be examined carefully. Wang and co-workers reported a similar reaction in 2012, this time using TFA as a stoichiometric additive (***Scheme 1.9.C***).[70]



Scheme 1.9. C-H arylation of azoles and caffeine derivatives using sulfinate salts.

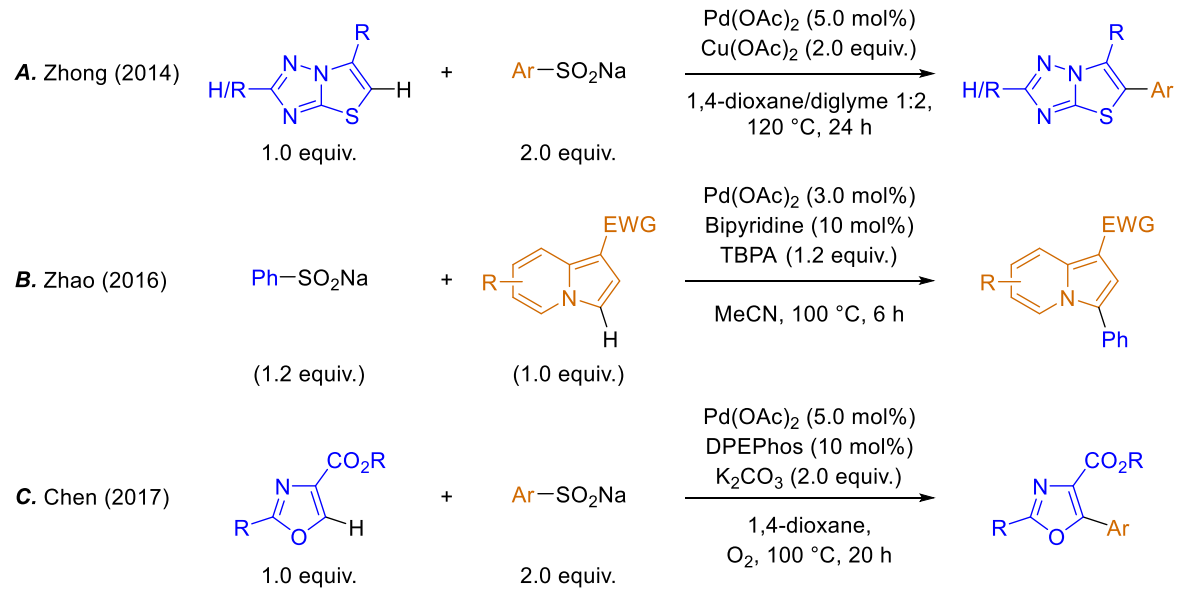


Scheme 1.10. C-H arylation of indoles using sulfinate salts.

Similar reaction conditions using $Pd(OAc)_2$ or $Pd(COD)Cl_2$ in combination with copper(II) chloride hydrate were subsequently reported for the C-H activation of indole substrates (***Scheme 1.10.A***).[71] The next year, this was extended to free N-H indoles by Wang and co-workers, this time using silver(I) acetate as an oxidant, and sulfuric acid as an additive (***Scheme***

1.10.B).[72] Once again, the mechanism of these reactions is unclear, as both reports assigned the role of the sulfinate differently.

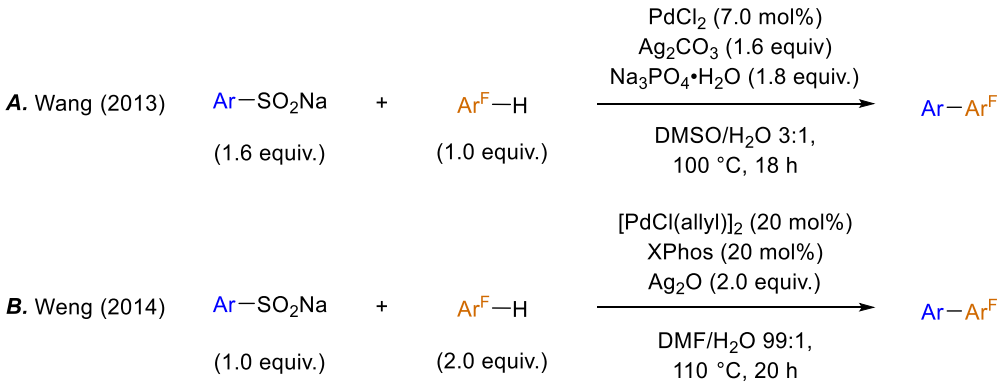
In more recent years, similar reactions were reported for a wider variety of heterocyclic substrates. The $Pd(OAc)_2/Cu(OAc)_2$ conditions reported in 2011 by the groups of You and Deng (***Scheme 1.9***) were applied by Zhong and co-workers to thiazolo[3,2-*b*]-1,2,4-triazole substrates (***Scheme 1.11.A***).[73] Interestingly, despite the presence of two potentially reactive C-H bonds, these conditions were selective for the C-H bond of the thiazole ring rather than the triazole. Zhao and co-workers showed that indolizines could be arylated using $Pd(OAc)_2$/bipyridine as a catalytic system and *tert*-butyl peroxyacetate as the stoichiometric oxidant (***Scheme 1.11.B***).[74] The arylation of oxazole-4-carboxylates by aryl sulfinate salts was mediated by a $Pd(OAc)_2$/DPEPhos catalytic system using O_2 as the oxidant (***Scheme 1.11.C***).[75] This demonstrated that ancillary phosphine ligands can also support the palladium catalyst in these direct C-H coupling processes.



Scheme 1.11. C-H arylation of various heterocylces using sulfinate salts.

Sulfinate salts were also used for the C-H arylation of polyfluorobenzene substrates. This was first reported by the Wang lab, using 7.0 mol% of $PdCl_2$ in combination with a phosphate base

and a stoichiometric silver oxidant (***Scheme 1.12.A***).[76] The Weng group subsequently reported the same arylation reaction using a phosphine supported palladium catalyst (***Scheme 1.12.B***).[77] However, these conditions are arguably not an improvement since 20 mol% of palladium allyl chloride dimer (representing 40 mol% of palladium) was required, together with 2.0 equivalents of silver oxide as the oxidant. In both of these couplings, the sulfinate was proposed to be the electrophilic coupling partner.

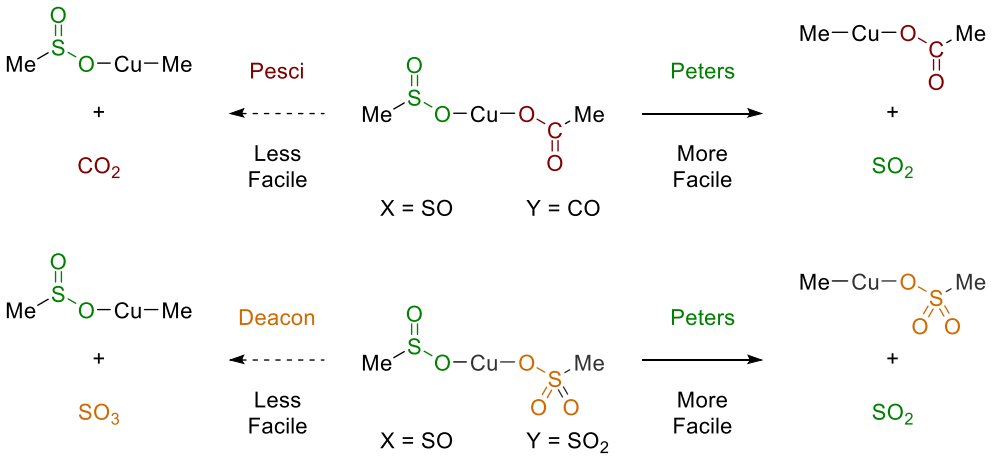


Scheme 1.12. C-H arylation polyfluorobenzenes using sulfinate salts.

1.3. Mechanistic Insights in Metal-Catalysed Desulfination Reactions

1.3.1. Desulfination *vs* Decarboxylation *vs* Desulfonation

The Peters desulfination reaction was described in 1905,[78] four years after the Pesci decarboxylation reaction,[79-80] while the Deacon desulfonation reaction was reported in 1971.[81] These three stoichiometric reactions proceeded *via* the thermal extrusion of SO_2, CO_2 and SO_3 under vacuum from the corresponding carboxylic, sulfinic, and sulfonic acid mercury salts. More recently, a DFT/MS study of desulfination at copper was conducted by the O'Hair group.[82] Ligand competition experiments in the copper complexes $[MeXOCuOYMe]^-$ where X = CO or SO and Y = SO or SO_2 (***Scheme 1.13***), showed that desulfination occurs more easily than decarboxylation and desulfonation, demonstrating the high potential of sulfinate derivatives as organometallic precursors.



Scheme 1.13. C-H arylation polyfluorobenzenes using sulfinate salts.

The O'Hair group also examined the reactivity of phenanthroline-ligated palladium complexes with aryl sulfinate and aryl carboxylate salts.[83] After a similar DFT/MS study, they concluded that similar to the copper complexes showed in ***Scheme 1.13***, the extrusion of SO_2 has a lower energy barrier that the extrusion of CO_2 with their phenanthroline-ligated cationic palladium complexes.

1.3.2. Palladium Sulfinate Complexes

Palladium sulfinate complexes can be obtained *via* three fundamental processes:[84]

- Insertion of SO_2 into the palladium-carbon bond of an organometallic complex *via* an electrophilic cleavage of the palladium-carbon bond (***Equation I.***)

$$\textit{I.} \quad RPd^{II}L_nX + SO_2 \longrightarrow RSO_2Pd^{II}L_nX$$

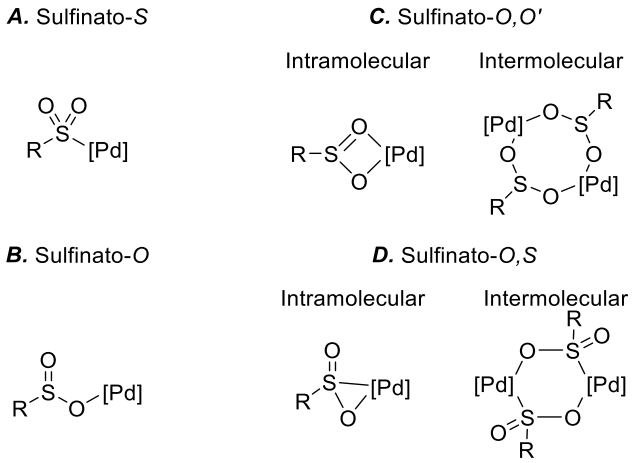
- Oxidative addition of sulfonyl derivatives into Pd(0) species (***Equation II.***)

$$\textit{II.} \quad RSO_2X + Pd^{0}L_n \longrightarrow RSO_2Pd^{II}L_nX$$

- Reaction of Pd(II) salts with alkali metal sulfinate salts (***Equation III.***)

$$\textit{III.} \quad m\ RSO_2[M^{alk}] + Pd^{II}L_nX_2 \longrightarrow (RSO_2)_mPd^{II}L_nX_{2-m} + m\ [M^{alk}]X$$

The sulfinate can then bind the central palladium atom in four different modes. In sulfinato-*S* complexes (***Scheme 1.14.A***), the palladium is linked directly to the sulfur, whereas in the sulfinato-*O* coordination mode, it is the oxygen that is binding the metal (***Scheme 1.14.B***). The sulfinate can also bind the palladium in a multidentate fashion, or bind two palladium atoms at the same time, forming dimers or higher aggregates. In these cases, the complexes are called sulfinato-*O,O'* (***Scheme 1.14.C***) or sulfinato-*O,S* (***Scheme 1.14.D***) depending on the nature of the binding atoms of the sulfinate salt.

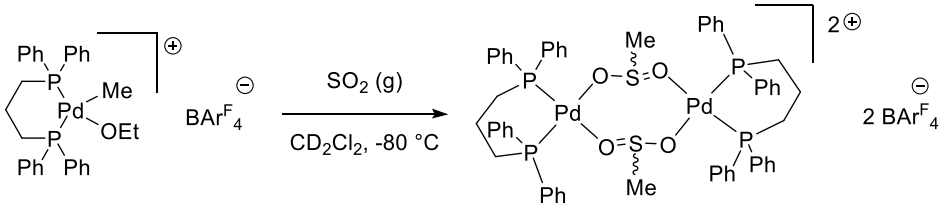


Scheme 1.14. Coordination modes available to sulfinate salts.

Coordination of sulfinate to metal complexes has been extensively studied by IR spectroscopy. It has been shown that the sulfinate preferentially adopts a sulfinato-*S* coordination mode when the metal is soft, whereas harder metal centres, *i.e.* those with higher oxidation number, higher effective charge, small ionic radius, low polarizability and low oxidisability, will generally lead to a sulfinato-*O* coordination mode.[84-86] Therefore, sulfinato-*S* coordination modes should be preferred with the soft palladium centre (see ***Section 1.1.2***). It is however possible to change the soft/hard character of metals by a suitable choice of ligands. For example, due to the σ-donating and π-accepting character of CN^- ligands, a sulfinato-*S* complex was observed with the intrinsically hard Co^{III} complex $[Co(SO_2R)CN)_5]^{3-}$.[87]

The nature of the binding of sulfinate salts to metal centres affects the SO_2 stretching vibration frequencies which can be observed by IR spectroscopy. General trends have emerged from extensive studies of metal complexes, but the predicted binding from IR data does not always agree with solid state structures.[84]

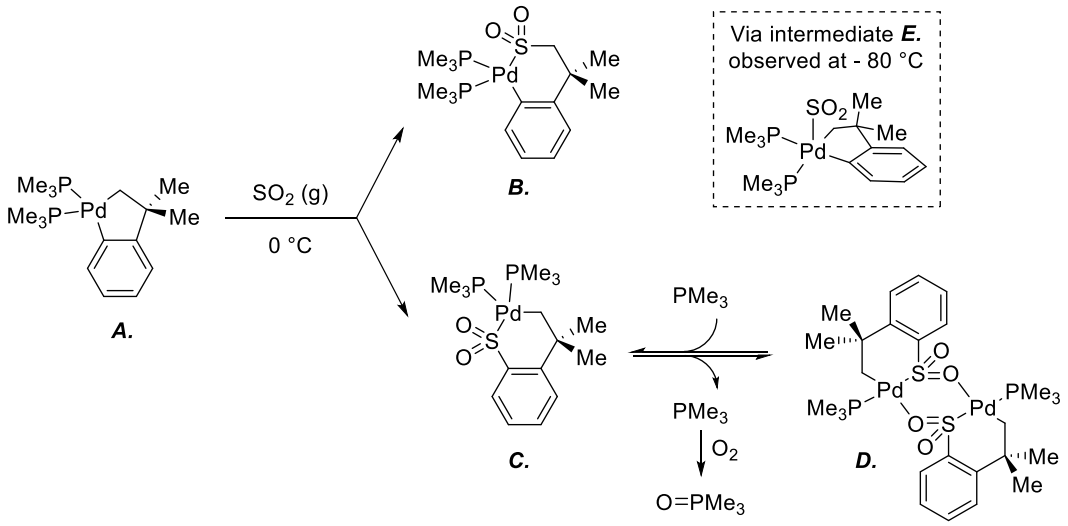
Despite the wide array of palladium sulfinate complexes reported in the literature, only a few have been characterised by X-ray crystallography. In 2000, the dimeric sulfinato-*O*-*O'* $[(dppp)Pd(SO_2Me)]_2[BAr^F{}_4]_2$ complex (***Scheme 1.15***) was prepared *via* the insertion of SO_2 into the Pd-Me bond of the corresponding cationic $[(dppp)Pd(Me)(OEt_2)]BAr^F{}_4$ complex.[88] Variable temperature NMR spectroscopy showed that the unprecedented dimeric eight-membered palladacycle was in equilibrium with different conformers. This was due to the ring inversion of the chair conformation of the dppp ligand in solution, rather than a conformation change at the stable sulfur centre.



Scheme 1.15. Synthesis of the dimeric sulfinato-*O,O'* complex $[(dppp)Pd(SO_2Me)]_2[BAr^F{}_4]_2$.

In 2001, two structural isomers of the sulfinato-*S* palladacycle $[(PMe_3)_2Pd(CH_2CMe_2C_6H_4SO_2)]$ (***Scheme 1.16***) were prepared *via* the insertion of SO_2 into the Pd-C_{alkyl} (*Compound* ***B***) or Pd-C_{aryl} (*Compound* ***C***) of the palladacycle ***A.***[89] A transient orange coloration during the insertion of SO_2, led the authors to monitor the reaction by NMR spectroscopy, and the pre-insertion SO_2-ligated palladium intermediate ***E*** was observed at - 80 °C. Single crystals suitable for an X-ray diffraction study could be grown from complex ***B***, which unambiguously confirmed its structure. However, the dimeric sulfinato-*S,O* complex ***D*** was obtained from the structural isomer ***C*** upon crystallisation. This was due to the presence

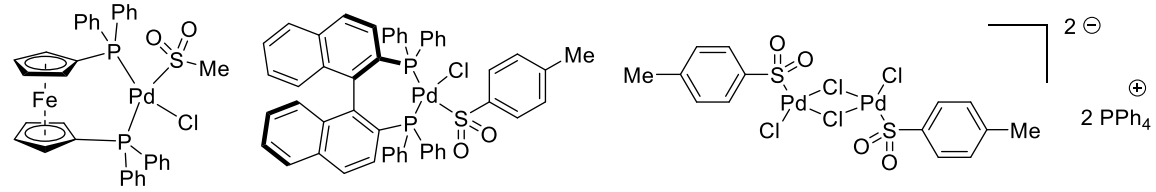
of traces of air under the crystallisation conditions that oxidised the PMe_3 after ligand dissociation. Compound ***C*** could be regenerated quantitatively upon reaction of ***D*** with PMe_3 under strict anaerobic conditions.



Scheme 1.16. Formation of sulfinato-*S* complexes via a pentacoordinated intermediate.

The sulfinato-*S* complex (dppf)Pd(SO_2Me)Cl (***Scheme 1.17.A***) was also prepared *via* the insertion of gaseous SO_2 in the corresponding chloro(methyl)palladium complex.[90] The corresponding COD complex was found to be unstable due to SO_2 de-insertion, showing the reversibility of the SO_2 insertion process and the low energy barrier associated with the extrusion of SO_2 in such complexes. The Weix lab reported a structurally similar tolyl sulfinate complex ***B.***[91] This time, it was not obtained by insertion of SO_2 into the corresponding oxidative addition complex, but was prepared by ligand exchange with sodium 4-methylbenzene sulfinate, as described in *Equation **3.*** Both complexes ***A*** and ***B*** have a sulfinato-*S* coordination mode with aryl or methyl groups positioned *trans* to the chloride atom. Shavnya and co-workers recently reported the crystal structure of the sulfinato-*S* complex [(4-Me-$C_6H_4SO_2$)$PdCl_2$]$_2$[PPh_4]$_2$ (***Scheme 1.17.C***).[92] In this dimeric complex, it is not the sulfinate that is responsible for the dimeric aggregation, which exists due to two bridging chloride anions.

Its catalytic activity was demonstrated in the sulfonylation of boronic acids using $K_2S_2O_5$, an inorganic SO_2 surrogate.



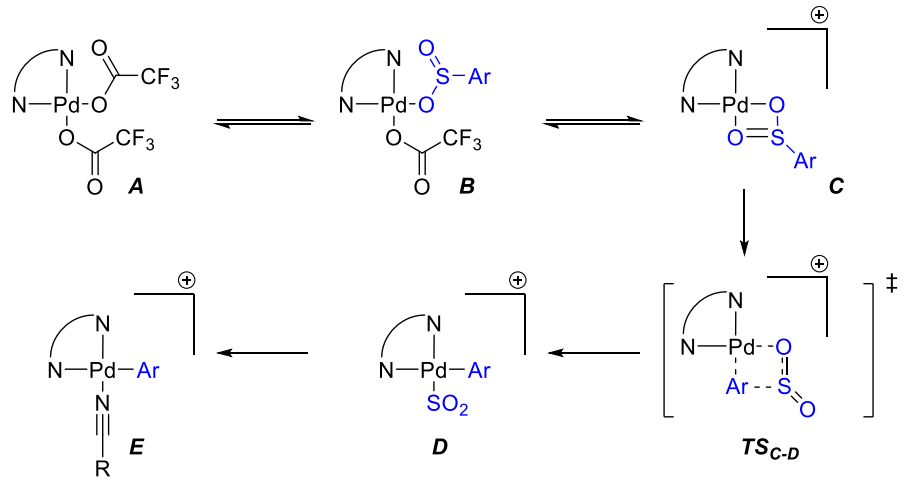
A. (dppf)Pd(SO_2Me)Cl ***B.*** (BINAP)Pd(4-Me-$C_6H_4SO_2$)Cl ***C.*** [(4-Me-$C_6H_4SO_2$)$PdCl_2$]$_2$(PPh_4)$_2$

Scheme 1.17. Other palladium sulfinate complexes.

Overall, there is only limited data on palladium sulfinate complexes. Their synthesis and characterisation by X-ray crystallography has brought some understanding to the mechanism of SO_2 insertion to aryl palladium halide oxidative addition complexes. However, the desulfination process from such palladium sulfinate complexes remains underexplored.

1.3.3. Desulfination at Palladium: Electrophilic Sulfinate

Aryl ketones can be synthesised form aryl sulfinate salts and nitriles in conjunction with palladium catalysis.[93-94] Although these reactions are not strictly cross-coupling arylation reactions, the sulfinate is involved as the electrophilic partner as defined in the **Section 1.2.2.** This process was studied by the Larhed group, who shed light on the sequence that leads to a cationic aryl Pd(II) complex from the combination of bipyridine, $Pd(TFA)_2$ and aryl sulfinate salts (***Scheme 1.18***). Exchange of two trifluoroacetate ligands for a sulfinate ligand (***A*** → ***C***), followed by extrusion of SO_2 (***C*** → ***D***), was proposed to generate a cationic Ar-$Pd(SO_2)(bipy)^+$ *Complex* ***D*** that is subsequently ligated by the nitrile to form *Complex* ***E***. An electrospray ionization mass spectrometry study revealed the presence of the key intermediates ***A***-***E***, therein supporting their theoretical DFT calculations.

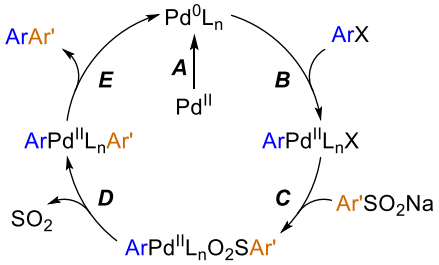


Scheme 1.18. C-H arylation polyfluorobenzenes using sulfinate salts.

In their 2014 report on the desulfinative cross-coupling of arylsulfinates with arylboronic acids catalysed by $PdCl_2$ and $Cu(TFA)_2$ (see ***Scheme 1.6.B***),[46] the Qi group calculated the bond dissociation enthalpies[95] in $PhSO_2[M]Cl$ complexes ([M] = Cu or Pd). They concluded that the desulfination step, which is more enthalpically favourable at palladium than at copper, happens in a concerted 4-membered transition state, similar to Larhed's transition state (***Scheme 1.18, $TS_{C\text{-}D}$***).

1.3.4. Desulfination at Palladium: Nucleophilic Sulfinate

The cross-coupling reaction of aryl sulfinate salts and aryl halides is believed to proceed *via* five key steps (***A***-***E***) as shown in ***Scheme 1.19.*** The active Pd(0) PdL_n species must first be generated (*step* ***A***), either by reduction of a Pd(II) precatalyst, or ligand exchange with a Pd(0) source such as $Pd_2(dba)_3$. The active catalyst subsequently inserts into the carbon-halide bond of the electrophile (*step* ***B***), forming an oxidative addition complex $(Ar)PdL_n(X)$. A putative palladium sulfinate complex, $(Ar)PdL_n(SO_2Ar')$, is formed in a transmetalation process (*step* ***C***). The latter involves an anion exchange between the alkali metal sulfinate salt and the halide of the oxidative addition complex. Extrusion of SO_2 (*step* ***D***) giving $(Ar)PdL_n(Ar')$, followed by reductive elimination (*step* ***E***), leads to the product and regenerates the active Pd(0) catalyst PdL_n.



Scheme 1.19. Accepted mechanism for palladium-catalysed cross-coupling reactions between aryl halides and aryl sulfinate salts.

The oxidative addition[96-98] and reductive elimination[99-101] steps of the mechanism depicted in ***Scheme 1.19*** are common to a wide range of palladium-catalysed cross-coupling reactions, and have been extensively studied with a myriad of ligands and aryl halides. However, the elementary steps involving the nucleophilic sulfinate salts, *i.e.* generation of the active Pd(0) species, transmetalation and extrusion of SO_2 have never been investigated.

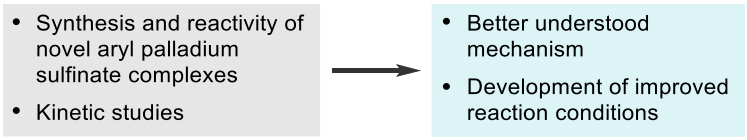
If the active Pd(0) species is generated from a Pd(0) precatalyst, this neutral ligand exchange step should be independent of the nature of the nucleophile. However, a common pathway for the reduction of Pd(II) salts to the active Pd(0) species, is a double transmetalation followed by reductive elimination.[102] This reduction pathway has been illustrated and studied with boronic acids as the nucleophilic coupling partner.[103-104] Given the ability of sulfinate salts to undergo homocoupling in presence of a Pd(II) catalyst (see ***Section 1.2.5***), the involvement of sulfinate salts in the reduction of the precatalyst is a scenario which should not be excluded, and which has not been studied.

Prior to our studies, post transmetalation aryl palladium sulfinate complexes, such as $(Ar)PdL_n(SO_2Ar')$, had never been reported. Similar complexes have been obtained with a variety of other nucleophiles, and the study of their reactivity has greatly improved the understanding of their corresponding coupling reactions.[105-107]

1.4. Research Aims

Palladium-catalysed carbon-carbon bond formation has revolutionised the field of organic synthesis in both academia and industry, as described in **Section 1.1**. In this context, aryl sulfinate salts have recently emerged as alternative coupling partners to conventional organometallic reagents. **Section 1.2** shows the significant growth in this field over the past decade. The use of sulfinate salts in palladium catalysed arylation reactions has proved particularly useful in the context of the 2-pyridyl organometallic cross-coupling problem. Their use as nucleophilic coupling partners, opens the door to arylation reactions with vast libraries of commercially available halogen-substituted arenes. However, this synthetically useful transformation remains poorly understood. This was detailed in **Section 1.3** which showed that there is limited data on the binding of aryl sulfinate salts to palladium and the process of SO_2 extrusion. In particular, little is known about the nucleophilic attack of sulfinate salts onto aryl palladium halide complexes, which leads to aryl palladium sulfinate complexes.

The objective of this research was to investigate the mechanism of the palladium-catalysed desulfinative cross-coupling of aryl bromides and (hetero)aryl sulfinate salts. The aim was to isolate and characterise palladium complexes relevant to the catalytic cycle, with a strong focus on the aryl palladium sulfinate intermediates. By investigating the kinetics of the reaction, I aimed to identify the resting state intermediates and turnover limiting steps of the catalytic cycle, so as to deliver improved and lower temperature versions of these synthetically important transformations (***Scheme 1.20***).



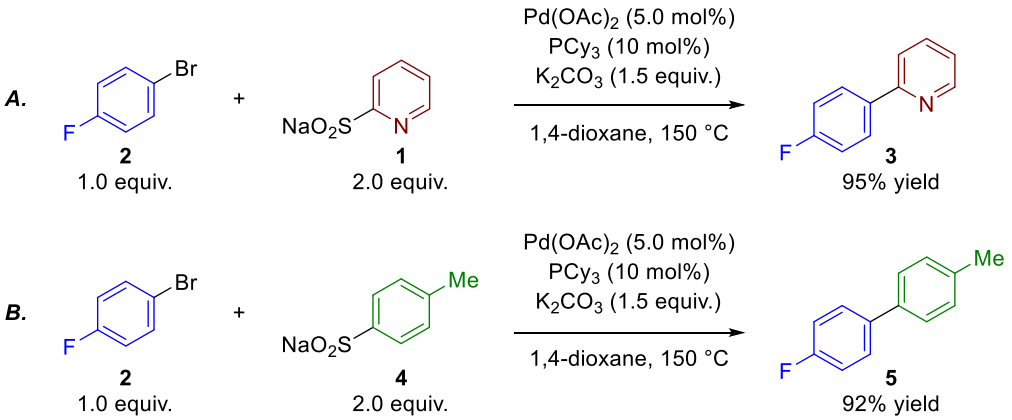
Scheme 1.20. Research aims.

Chapter 2 – Mechanistic Studies of the Palladium-Catalysed Desulfinative Cross-Coupling of Aryl Bromides and (Hetero)Aryl Sulfinate Salts

The results of these studies were published in the *Journal of the American Chemical Society*[108] and were highlighted in the journal *Trends in Chemistry*.[109] Dr Alasdair I. McKay solved all the X-ray structures that are featured in this chapter. DOSY NMR spectroscopy and high temperature NMR spectroscopy experiments were conducted with the help of Dr Nader Amin. All other experiments were conducted by myself.

2.1. Model Reactions and Substrates

The coupling of unsubstituted sodium pyridine-2-sulfinate salt **1** with 1-bromo-4-fluorobenzene **2** proceeds in 95% yield in presence of $Pd(OAc)_2$, PCy_3 and K_2CO_3 in 1,4-dioxane at 150 °C (***Scheme 2.1.A***). These cross-coupling conditions were initially developed for pyridine sulfinate salts,[58] before being extended to a larger class of heteroaromatic substrates.[61] In this study, the reactivity of 2-pyridyl substrate **1** was compared to sodium 4-methylbenzenesulfinate **4**. This carbocyclic sulfinate undergoes cross-coupling with 1-bromo-4-fluorobenzene under the same reaction conditions to deliver biaryl **5** in 92% yield (***Scheme 2.1.B***).



Scheme 2.1. Model reactions and substrates.

2.2. Formation of the Active Pd(0) Species

Palladium(II) acetate is employed as the palladium source for the two model reactions and in the preparative reactions, and therefore the active Pd(0) species must be generated *via* a reductive process. This step is often overlooked in the literature, although several pathways are known for the formation of Pd(0) species, the understanding of which is crucial for the study of reaction kinetics.[103, 110-112] The use of excess phosphine as a reducing agent is a common method to reduce Pd(II) precatalysts,[113] but the nucleophilic coupling partner involved in the cross-coupling such as organolithium reagents,[114] organostannanes,[115] alcohols,[116] and amines[117] can also mediate this transformation. Buchwald and co-workers judiciously used sub-stoichiometric amounts of an aryl boronic acid in order to ensure complete reduction of their Pd(II) precatalysts without loss of precious starting materials.[118] Furthermore, stoichiometric Pd(II)-mediated dimerisation of sulfinate salts was reported in the early seventies (see **Section 1.2.5**), showing the ability of sulfinate salts to take part in the formation of Pd(0) species from Pd(II) complexes. Therefore, examined the generation of the active catalyst was examined in the presence of 4-methylbenzenesulfinate **4**. The two coupling partners 1-bromo-4-fluorobenzene **2** and 4-methylbenzenesulfinate **4** were introduced to a Young's NMR tube together with K_2CO_3 and stoichiometric amounts of $Pd(OAc)_2$ and PCy_3 in a 2:1 ratio. A 2.5:1 mixture of 1,4-dioxane/benzene-d_6 was chosen as the solvent in order to mimic the reaction conditions whilst permitting NMR spectroscopic analysis. The NMR tube was then gradually heated at different temperatures and the reaction was monitored by $^{31}P\{^1H\}$ and $^{19}F\{^1H\}$ NMR spectroscopy (***Figure 2.1***).

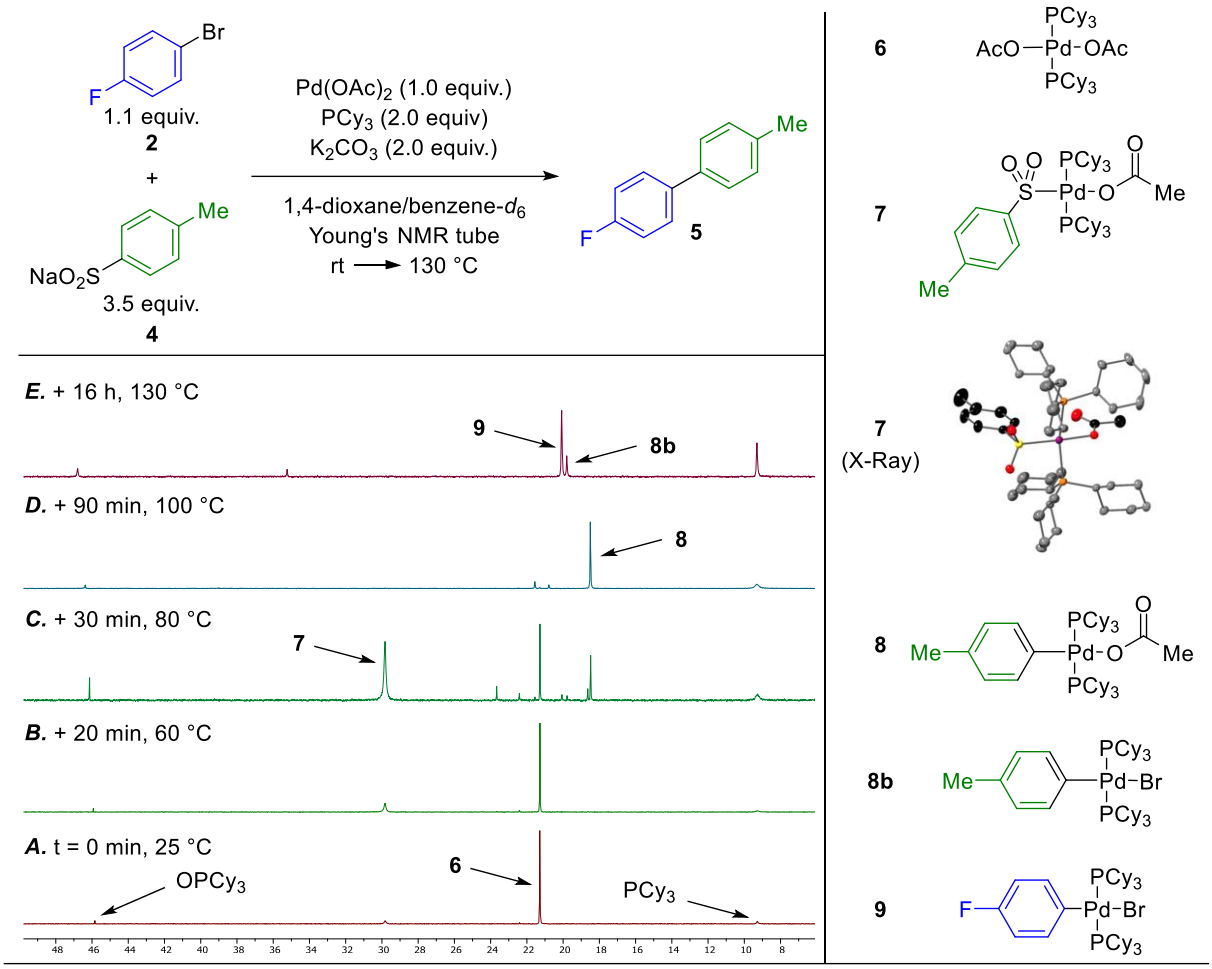


Figure 2.1. $^{31}P\{^{1}H\}$ monitoring of the formation of the active $Pd^{II}(OAc)_2$.

The known $Pd(PCy_3)_2(OAc)_2$ complex[119] **6** was rapidly formed at room temperature (***A***). Upon heating to 60-80 °C, the $^{31}P\{^{1}H\}$ resonance of **6** started to decay to a new complex **7**, characterised by a broad signal at 29.83 ppm (***B*** and ***C***). Complex **7** was synthesised independently, and single crystals suitable for an X-ray diffraction study were grown from CH_2Cl_2/hexane. The structure displays a square planar geometry around the palladium centre, with a *trans* arrangement of the phosphines. The palladium-sulfur bond length in **7** of 2.2755(4) Å, is shorter than those in (dppf)Pd(SO_2Me)Cl[90] and (BINAP)Pd($SO_2C_6H_4$Me)Cl[91] (2.3262(9) and 2.3331(7) Å, respectively). Whilst the palladium-oxygen bond length of 2.0975(13) Å, is notably longer than that in $(PCy_3)_2Pd(OAc)_2$ (2.0288(17) Å), reflecting the strong *trans* influence of the sulfinate ligand. Upon heating between 80 °C and 100 °C, complex **7** then undergoes extrusion of SO_2 to give complex **8** (δ_P = 18.50 ppm) (***C*** and ***D***). Similar aryl

palladium acetate complexes were reported and characterized by X-ray crystallography by Eastgate and coworkers,[103] and the identity of complex **8** was confirmed by its independent synthesis and characterisation according to these literature protocols. Above 100 °C, complex **8** is then likely to undergo a second acetate/aryl sulfinate exchange to form an aryl palladium sulfinate complex (Ar')Pd(PCy_3)$_2$(O_2SAr') followed by extrusion of SO_2 and reductive elimination to generate a Pd(0) intermediate and 4,4'-dimethylbiphenyl **5b**, the homocoupling product. None of these two intermediates were observed by NMR spectroscopy as the rate of extrusion of SO_2 from such palladium sulfinate complexes and of oxidative addition are fast at such temperatures (see **Sections 2.4** and **2.7**). Instead, the oxidative addition complex (4-F-C_6H_4)Pd(PCy_3)$_2$(Br) **9** (δ_P = 20.08 ppm) was observed (***E***). Complex **8** can also undergo an acetate/bromide exchange giving complex **8b** (δ_P = 19.79 ppm), which can then undergo the same transformations to form Pd(0) species and homocoupling product. Phosphine oxidation products were detected in trace amounts only, which is consistent with the observation made by Eastgate and co-workers that Pd(PCy_3)$_2$(OAc)$_2$ **6** is not easily reduced to Pd(0) via phosphine oxidation in absence of hydroxide bases.[103]

When the cross-coupling was performed with increasing amounts of Pd(OAc)$_2$ (5 – 18 mol%) with a ligand/palladium ratio fixed at two, a linear correlation was observed between the amount of homocoupling product **5b** formed and the amount of Pd(OAc)$_2$ introduced (***Figure 2.2***), which supports the proposed reduction pathway of the precatalyst. The gradient was found to be 0.76, which can be explained by the existence of minor reduction pathways or by catalyst deactivation/decomposition.

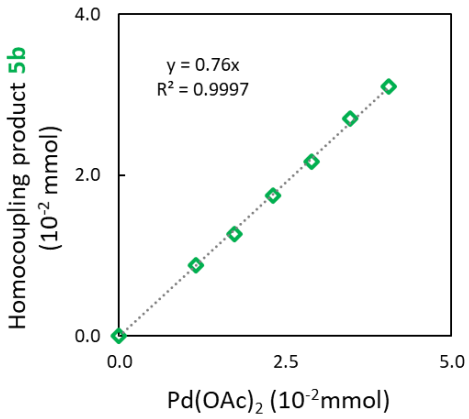
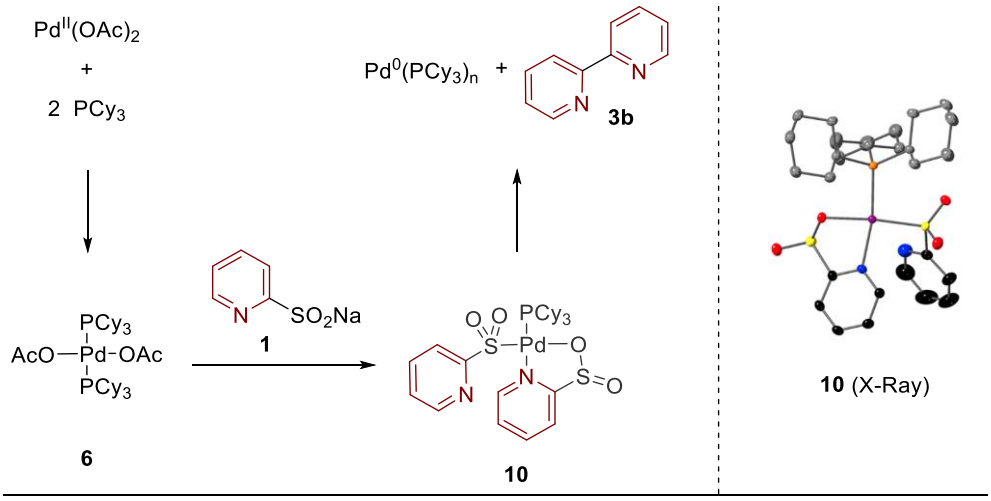


Figure 2.2. Correlation between the amount of homocoupling product formed and the amount of $Pd(OAc)_2$ introduced in the reaction mixture.

When attempting to synthesise the complex corresponding to **7** with pyridine-2-sulfinate **1**, a different palladium complex **10** was isolated (***Scheme 2.2***). This complex also displays a square planar geometry around the palladium centre, with a pyridine residue lying *trans* to the phosphine instead of a second phosphine ligand as in **7**. Two 2-pyridyl sulfinate groups are present in **10**. One chelates the palladium in a $\kappa^2_{N,O}$-mode affording a 5-membered metallocycle. This mode of ligand binding has precedence in copper 2-pyridyl sulfinate complexes.[120] The second 2-pyridyl sulfinate coordinates the palladium by the sulfur, *trans* to the oxygen binding. The palladium-sulfur bond length in **10** (2.2307(5) Å) is notably shorter than that in **7**, possibly reflecting the decreased steric congestion in the former due to the replacement of a bulky PCy_3 ligand by the less bulky pyridyl group.

When complex **10** was heated in presence of aryl bromide **2**, homocoupling product **3b** and the oxidative addition complex **9** were observed, suggesting that Pd(0) species are generated after double extrusion of SO_2 and reductive elimination.



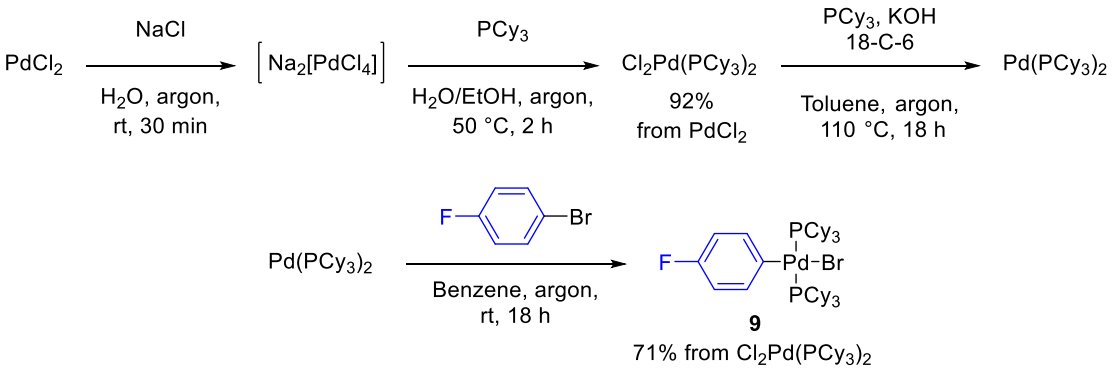
Scheme 2.2. Formation of the active Pd(0) species with 2-pyridyl sulfinate **1**.

2.3. Synthesis and Characterisation of Relevant Palladium Complexes

2.3.1. Oxidative Addition Complex

The insertion of $Pd(PCy_3)_2$ into the carbon-halide bond of aryl bromides leads to complexes of general formula $(Ar)Pd(PCy_3)_2(Br)$ which adopt a square planar geometry with the two phosphine ligands *trans* to each other.[121] This is in agreement with the Crystal Field Theory which predicts that for d^8 transition-metal complexes, the occupation of the orbitals d_{xz}, d_{yz}, d_{z^2} and d_{xy} in a square planar geometry is energetically advantageous compared to tetrahedral or octahedral geometries.[11, 122] Oxidative addition of bromobenzene to $Pd(PCy_3)_2$ has been investigated by Baird[123] and Hartwig.[96] These studies showed that the insertion of the two-coordinate Pd(0) complex $Pd(PCy_3)_2$ in the C-Br bond of bromobenzene is an irreversible process in nonpolar solvents at room temperature.

Oxidative addition complex **9** was synthesized according to literature procedures (***Scheme 2.3***), and its NMR spectroscopy resonances were in agreement with previous reports.[121, 124] As discussed previously, without the presence of a nucleophilic coupling partner that is able to dimerise, it is the combination of the hydroxide base KOH with excess PCy_3 acting as the reducing agent which promotes the reduction of $Cl_2Pd(PCy_3)_2$ to $Pd(PCy_3)_2$.



Scheme 2.3. Synthesis of the oxidative addition complex **9**.

Oxidative addition complex **9** proved to be a competent catalyst for the coupling of lithium 4-methoxybenzene sulfinate **4-OMe** and 1-bromo-4-fluorobenzene **2,** giving similar reaction rate and yield compared to the mixture of $Pd(OAc)_2$ and PCy_3 (***Figure 2.3***). The kinetics of the oxidative addition step will be examined in **Section 2.7.3.**

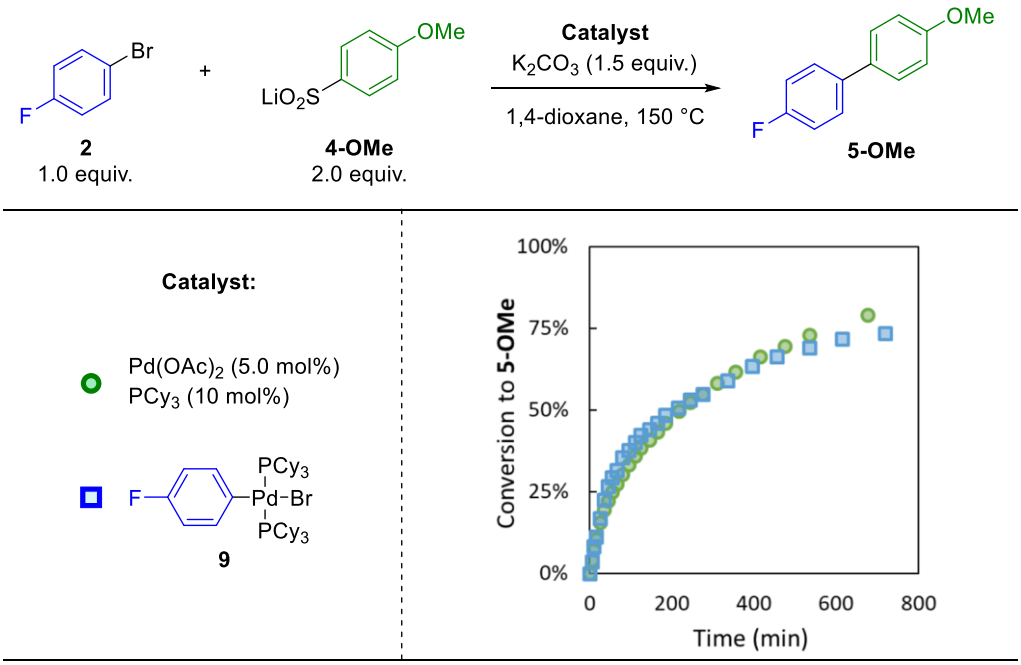


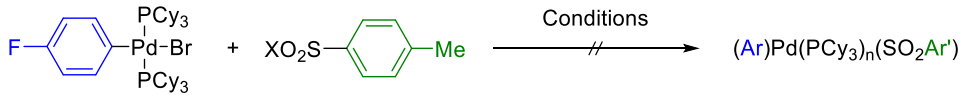
Figure 2.3. Oxidative addition complex **9** as a competent catalyst.

2.3.2. Aryl Palladium Sulfinate Complexes

As discussed in **Sections 1.3.2** and **1.3.4**, post-transmetalation aryl palladium sulfinate complexes of molecular formula $(Ar)PdL_n(SO_2Ar')$ had never been reported prior to these

studies. Given that post-transmetalation complexes of formula $(Ar)PdL_n(XR_m)$ involved in the cross-coupling of alcohols (X = O),[125-128] amines (X = N)[129-130] or thiols (X = S)[131] are known, the synthesis of these unprecedented aryl palladium sulfinate complexes was attempted starting from oxidative addition complex **9**.

Our first approach was to heat oxidative addition complex **9** at moderate to elevated temperatures (50-120 °C) in the presence of carbocyclic sulfinate salt **4** or its lithium **4-Li** and potassium **4-K** analogues (***Table 2.1***). However, formation of biaryl **5** and/or decomposition were observed depending on the temperature (*Entries 1-3*). This was also the case when the phase transfer additive TBAB was employed, or when different solvents were used (*Entry 4*).

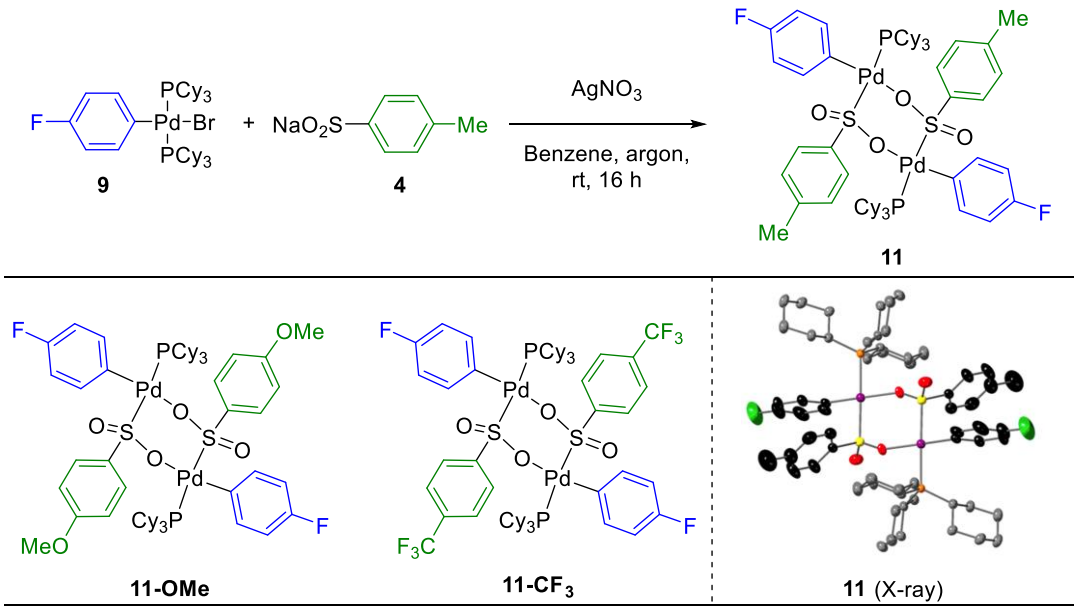


9 **4**, **4-Li**, **4-K** : X = Na, Li, K

Entry	*Sulfinate*	*Conditions*	*Outcome*
1	**4, 4-Li** or **4-K**	benzene-d_6, T = rt, 50 °C, 70 °C	**9** recovered
2	**4, 4-Li** or **4-K**	benzene-d_6, T = 90 °C	**9** recovered + Decomposition + Ar-Ar' **5** (traces)
3	**4, 4-Li** or **4-K**	benzene-d_6, T = 120 °C	**9** recovered + Decomposition + Ar-Ar' **5** (significant amounts)
4	**4**	TBAB, benzene or THF or dioxane T = 25 °C, 50 °C, 70 °C	**9** recovered

Table 2.1. Unsuccessful synthesis attempts of aryl palladium sulfinate complexes.

The use of silver nitrate was key to the formation of such aryl palladium sulfinate complexes under mild reaction conditions, thus allowing their isolation. In the presence of $AgNO_3$, the oxidative addition complex **9** was entirely consumed at room temperature, and the dimeric palladium sulfinate complex **11** was isolated (***Scheme 2.4***). This could be reproduced with the electron-rich sulfinate **4-OMe** and its electron-poor **4-CF$_3$** analogue, leading to complexes **11-OMe** and **11-CF$_3$**. These three Pd(II) complexes, which were all characterised by XRD, adopt a square planar geometry around the palladium centre, and the sulfinato-*O*,*S* dimeric structure resembles the one reported by Tiripicchio and co-workers[89] (**Experimental Section 7.2.15.4**).

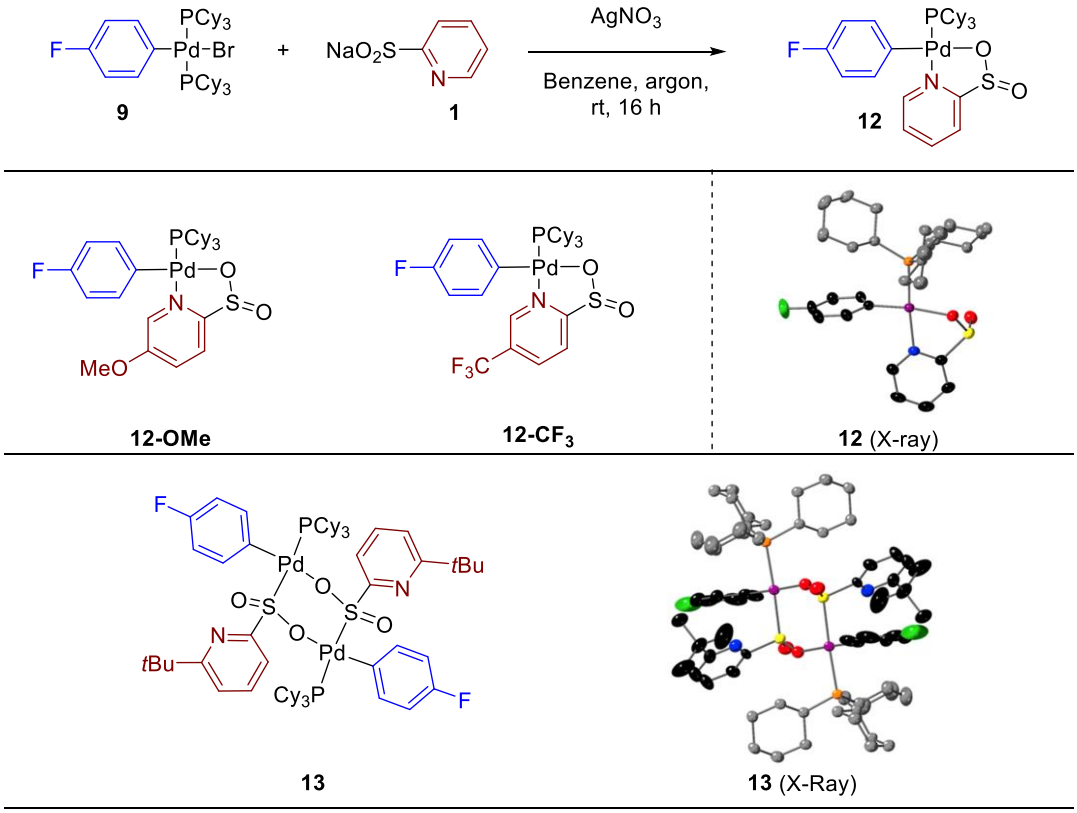


Scheme 2.4. Silver-mediated synthesis of aryl palladium sulfinate complexes with carbocyclic sulfinates.

When the pyridine-2-sulfinate substrate **1** was subjected to the same reaction conditions, the monomeric palladium sulfinate complex **12** was obtained (***Scheme 2.5***). The geometry about the palladium centre in **12** closely resembles that present in **10** (see ***Scheme 2.2***). The palladium oxygen bond length in complex **12** (2.132(2) Å) is elongated relative to that in complex **10** (2.0975(13) Å), reflecting the greater *trans* influence of the aryl ligand.

The degree of aggregation in these complexes is also maintained when either an electron-donating or -withdrawing substituent is introduced at the 5-position of the pyridine ring as in **12-OMe** and **12-CF$_3$** (**Experimental Section 7.2.15.4**). A notable exception is when steric bulk, in the form of a *tert*-butyl group, is placed at the 6-position of the pyridine. This prevents the $\kappa^2_{N,O}$-binding mode of the pyridine sulfinate, thereby affording a dimeric solid state structure **13** which resembles that of the 4-methylbenzenesulfinate substituted complex, **11**. X-ray suitable crystals could be obtained from CH_2Cl_2/hexane recrystallization of crude reaction mixtures, however, attempts to obtain analytically pure samples were unsuccessful for compound **13**.

The diffusion coefficients obtained by DOSY NMR spectroscopy in 1,4-dioxane/benzene-d_6 predicted masses for complex **11** and complex **12** in a 2:1 ratio, indicating the former maintains its dimeric structure in solution (**Experimental Section 7.2.6**).



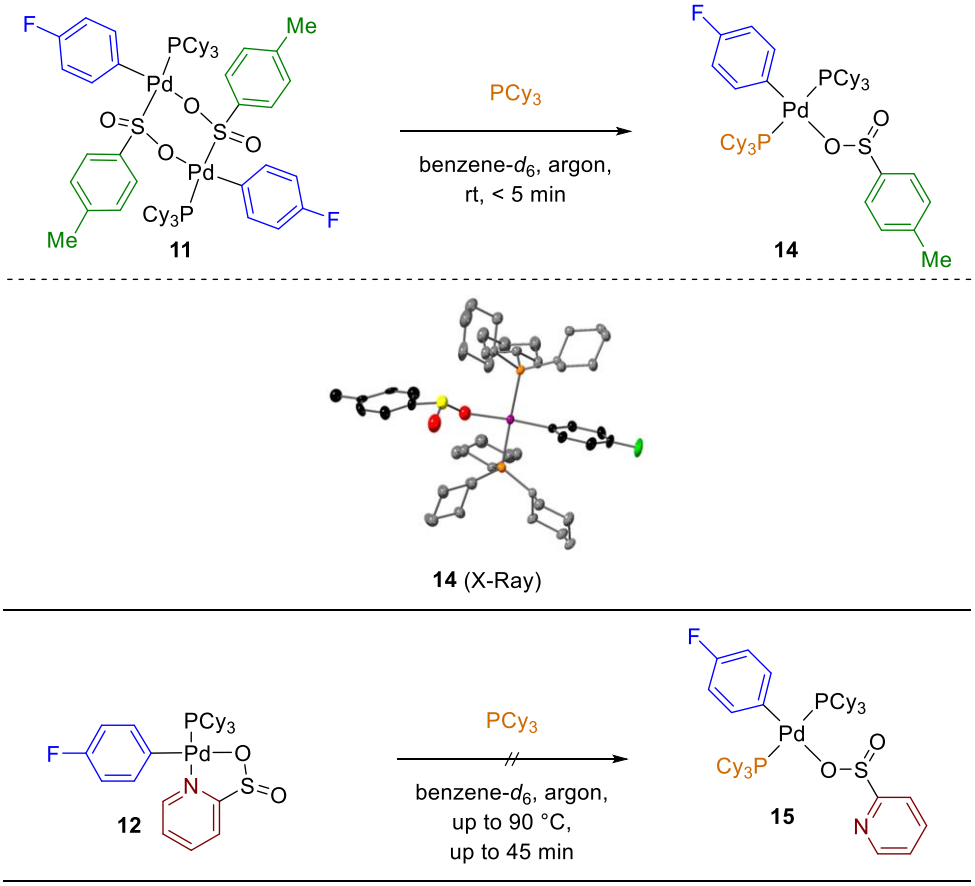
Scheme 2.5. Silver-mediated synthesis of aryl palladium sulfinate complexes with 2-pyridyl sulfinates.

2.4. Reactivity of Aryl Palladium Sulfinate Complexes

2.4.1. At Room Temperature in Presence of Tricyclohexylphosphine

Similarly to what was observed by Tiripicchio and co-workers,[89] dimeric complex **11** reacted quantitatively with tricyclohexylphosphine to give monomeric complex **14** (***Scheme 2.6***). Although conversion was quantitative according to $^{19}F\{^1H\}$ NMR spectroscopy, the new complex **14** was only isolated in 57% yield. Similarly to oxidative addition complex **9** (δ_P = 20.20 ppm, $J_{P\text{-}F}$ = 3.0 Hz), a doublet at δ_P = 21.95 ppm, $J_{P\text{-}F}$ = 3.0 Hz is characteristic of this novel aryl palladium sulfinate complex. Crystals suitable for XRD were obtained from CH_2Cl_2/hexane, which allowed us to confirm the solid-state structure of compound **14**, as a

square planar palladium complex bearing the two bulky PCy_3 ligands *trans* to each other. The sulfinate coordinates the palladium *via* a single O-Pd bond, which is consistent with a nucleophilic displacement of the sulfur atom from dimeric complex **11** with PCy_3. In contrast, palladacycle **12** was found to be unreactive under the same conditions, and compound **15** was not observed, suggesting that the Pd-N bond in **12** is much stronger than the Pd-S bond in the dimeric complex **11**.



Scheme 2.6. Reactivity of complexes **11** and **12** in presence of PCy_3.

We demonstrated in **Section 2.2** that the formation of the active Pd(0) species from the Pd(II) precatalyst is mediated by the homocoupling of two sulfinate substrates. As a consequence, the phosphine to palladium ratio is preserved during the reduction step and two phosphine ligands remain available per palladium atom during catalysis. This is why dimeric complexes **11**, **11-OMe**, **11-CF_3** and **13** are not believed to be involved in the reaction mechanism. Their

formation is most likely caused by the presence of $AgNO_3$ which can act as an oxidant.[89] In the following sections, only the aryl palladium sulfinates **12** and **14** will be considered as potential intermediates in the reaction mechanism.

2.4.2. Extrusion of SO_2 from Complexes 12 and 14

Complexes **12** and **14** were heated at 150 °C in 1,4-dioxane and the formation of products **3** and **5** was monitored by HPLC analysis of aliquots syringed out from the reaction. For this set of experiments, complex **14** was generated *in situ* from dimeric complex **11** and PCy_3. (**Experimental Section 7.2.7**). The results are shown in ***Figure 2.4.***

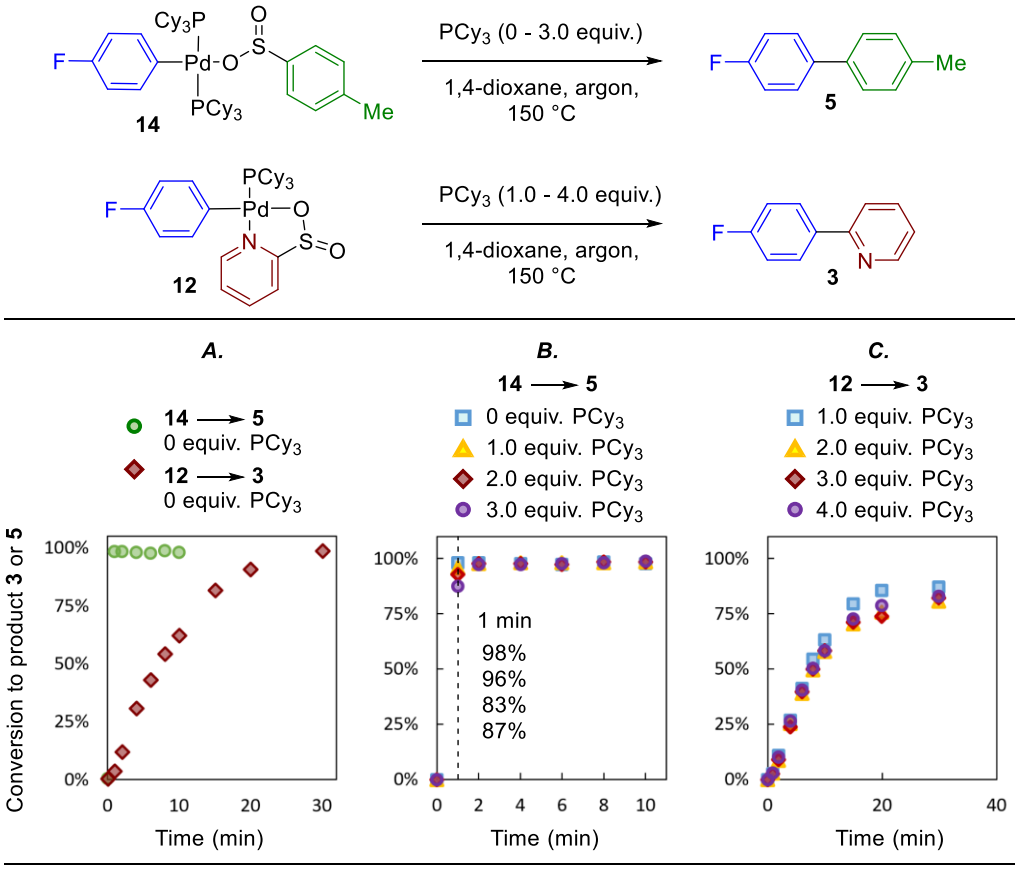


Figure 2.4. Extrusion of SO_2 from complexes **14** and **12**.

The rates of extrusion of SO_2 from complexes **12** and **14** are drastically different. At 150 °C in 1,4-dioxane, full conversion to biaryl **5** is obtained within one minute from complex **14**. In contrast, the extrusion of SO_2 from complex **12** is much slower and requires 30 min to reach

full conversion to compound **3** under the same reaction conditions (***Figure 2.4.A***). This suggests that the coordination of the sulfinate in complex **14** is weak, permitting an easy extrusion of SO_2, whereas the sulfinate strongly chelates the palladium centre in complex **12**, making the extrusion of SO_2 a more energy demanding process. The rates of extrusion of SO_2 from complexes **12** and **14** were then examined under various concentrations of PCy_3 at 150 °C in 1,4-dioxane. A small but significative decrease from 98% to 96%; 93% and 87% conversion after 1 minute of reaction time was observed for the extrusion of SO_2 from complex **14** in presence of 0; 1.0; 2.0 and 3.0 equivalents of tricyclohexylphosphine respectively (***Figure 2.4.B***). Desulfination from complex **12** however was unaffected by the presence of excess ligand (***Figure 2.4.C***).

The extrusion of SO_2 from complex **14** was also monitored at 90 °C in toluene-d_8 by quantitative ^{19}F NMR spectroscopy (***Figure 2.5***). Under these conditions, it is clear that the concentration of PCy_3 has a major impact on the rate of extrusion of SO_2 from complex **14**. We propose that the loss of a phosphine ligand is required prior to extrusion of SO_2 to allow a 4-coordinate transition (**TS^4**) state rather than an energetically less favourable 5-coordinate transition state (**TS^5**) if both ligands remain present.

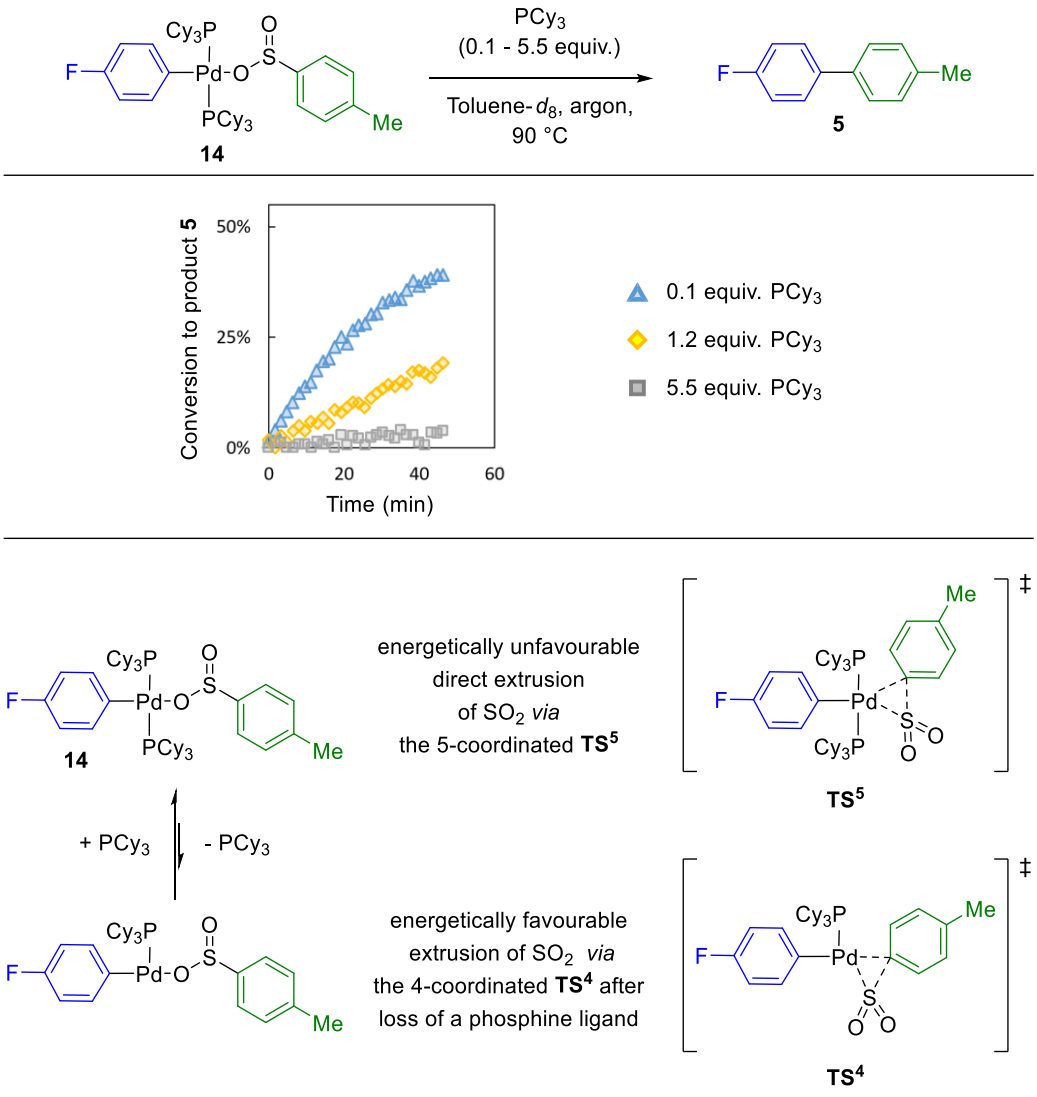


Figure 2.5. Extrusion of SO_2 from complex **14** at 90 °C in toluene-d_8.

Similarly, the extrusion of SO_2 from pyridyl complex **12** was monitored at 110 °C in toluene-d_8 by quantitative ^{19}F NMR spectroscopy (***Figure 2.6.A***). Under these conditions, the presence of added ligand did not affect the rate of extrusion of SO_2, in agreement with the results showed in ***Figure 2.5.C.*** Weakening of the Pd-N bond by adding an electron-withdrawing group on the pyridyl ring as in complex **12-CF3** increased the rate of extrusion of SO_2 in toluene-d_8, as 47% conversion to product **3-CF3** was obtained after 45 minutes of reaction time (***Figure 2.6.B***) compared to 11% conversion of complex **12** to complex **5**. This data suggests that extrusion of SO_2 from aryl palladium sulfinate chelates formed with 2-pyridyl sulfinate substrates is limited by breaking of the strong Pd-N bond, which does not depend on the concentration of PCy_3.

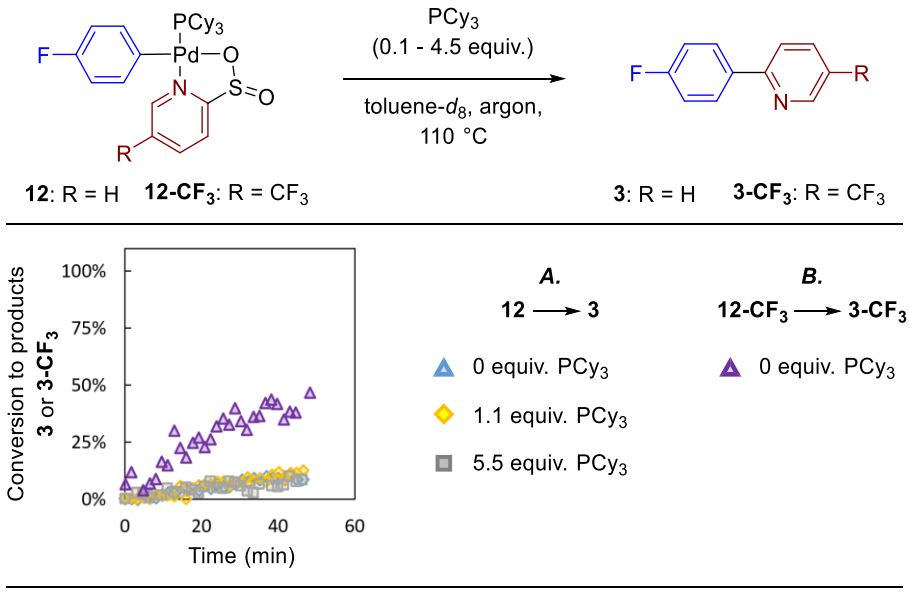


Figure 2.6. Extrusion of SO_2 from complexes **12** and **12-CF$_3$** at 110 °C in toluene-d_8.

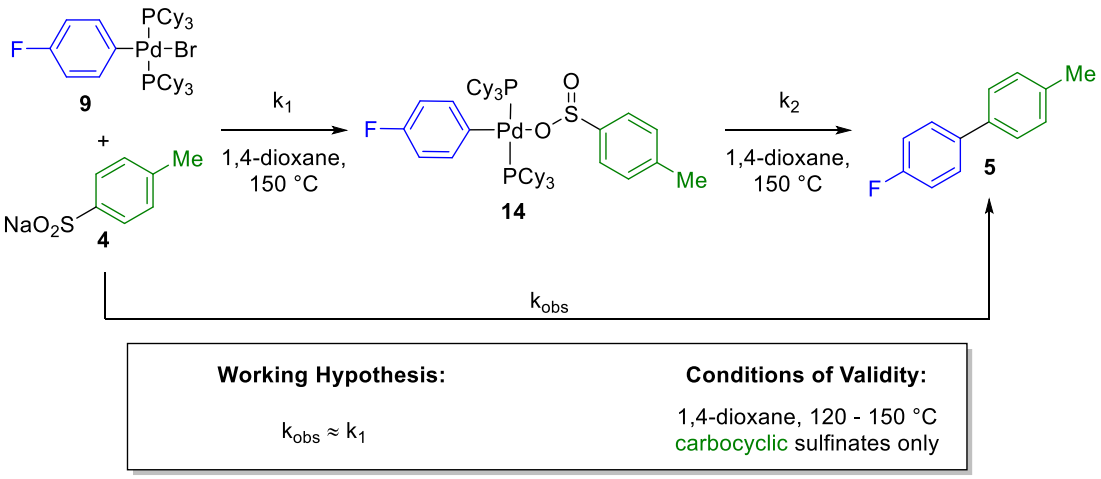
2.5. Study of the Transmetalation Step

2.5.1. Working Hypothesis

In this section, the stoichiometric reactions between oxidative addition complex **9** and aryl sulfinate salts was studied. Given the poor solubility of both **9** and sulfinate salts in common organic solvents and the requirement of high temperatures for the transmetalation step, accurate kinetic measurements by NMR spectroscopy were not possible. The stoichiometric reactions between complex **9** and aryl sulfinate salt **4** were therefore monitored by taking aliquots from the reaction mixtures and analysing them by HPLC (**Experimental Section 7.2.7**). With this experimental protocol, it was not possible to monitor the consumption of complex **9**, and formation of biaryl product **5** was measured instead. As a consequence, the observed rates are not the rates of transmetalation (k_1), but the rates of the sequence transmetalation/extrusion of SO_2/reductive elimination (k_{obs}) (***Scheme 2.7)***.

We showed in the previous **Section 2.4.2** that the rate of extrusion of SO_2 from the aryl palladium sulfinate complex **14** followed by reductive elimination to give biaryl **5** (k_2) is, under the reaction conditions (1,4-dioxane, 150 °C), extremely fast and happens within < 1.0 min

reaction time independently of the concentration of PCy_3 (***Figure 2.4.B***). These high rates of extrusion of SO_2 from complex **14** were rationalised by the weak coordination of 4-methylbenzene sulfinate to the palladium centre *via* one oxygen atom.



Scheme 2.7. Working hypothesis for the study of the transmetalation step with carbocyclic sulfinate salts.

In this section, we propose that the rate of formation of product **5** from a combination of the oxidative addition complex **9** and 4-methylbenzene sulfinate salt **4** can be approximated to the rate of the transmetalation step ($k_{obs} \approx k_1$).

In contrast, the extrusion of SO_2 from complex **12** in which the 2-pyridyl sulfinate strongly chelates the palladium centre in a $\kappa^2_{N,O}$ fashion requires significant reaction times (~30 min) in 1,4-dioxane at 150 °C (see ***Figure 2.4.A***). Therefore, such an approximation can not be justified for 2-pyridyl sulfinate substrates, and this section will focus on carbocyclic sulfinate salts.

2.5.2. Importance of the Sulfinate Counter Cation

Lithium, sodium, potassium and caesium sulfinate salts have been shown to be compatible with the reaction conditions used in this study.[58] In order to probe whether the nature of the sulfinate counter cation has an impact on the rate of the transmetalation step, the reaction between oxidative addition complex **9** and 4-methylbenzene sulfinate salts bearing a range of alkali and

organic counter cations **4**, **4-Li**, **4-K**, **4-Cs**, **4-NMe$_4$**, **4-N(TBA)$_4$** were monitored in 1,4-dioxane at 120 °C and 150 °C (***Figure 2.7.A***).

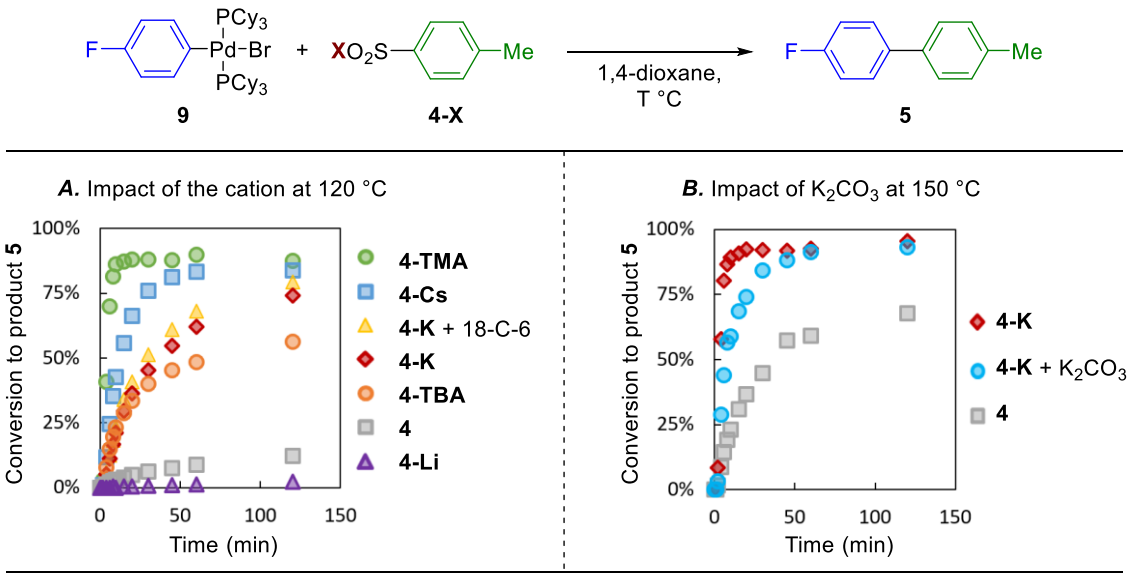


Figure 2.7. Importance of the sulfinate counter cation.

Lithium and sodium sulfinate salts **4-Li** and **4** were found to be very poor nucleophilic coupling partners under these conditions, with 2% and 12% product formation respectively in 2 hours. In contrast, 74% and 84% conversion to product **5** were obtained in 2 hours moving further down in the alkaline metals group, with potassium and caesium sulfinate salts **4-K** and **4-Cs**, respectively. Tetrabutylammonium sulfinate **4-TBA** had a similar initial rate compared to the potassium sulfinate substrate **4-K**, however, conversion stalled at 60%, even after five hours reaction time. Decomposition of the tetrabutylammonium cation *via* Hoffman-type elimination is likely to be responsible for this loss of reactivity. A slight but non-significant increase in reaction rate was observed when the 18-crown-6 was used in conjunction with potassium sulfinate **4-K**. However, the use of tetramethylammonium sulfinate salt as the nucleophilic coupling partner dramatically boosted the reaction rate, as 86% yield was obtained within the first 10 minutes. Tetramethylammonium salts have been used as organic silver surrogates for the abstraction of halide atoms from palladium complexes,[132] which might explain the excellent reactivity of sulfinate **4-TMA** in the transmetallation step. The low performance of

the tetrabutylammonium sulfinate salt compared to the potassium, or caesium sulfinates suggests that solubility of the sulfinate salt is not correlated to the rate of the transmetallation step. Indeed, the tetrabutylammonium sulfinate is entirely soluble in 1,4-dioxane at 120 °C, while the alkali sulfinates are not.

This set of stoichiometric experiments showed that the nature of the sulfinate counter cation is crucial for efficient transmetalation between oxidative addition complex **9** and 4-methylbenzene sulfinate salts. However, it also showed that the sodium sulfinate salt **4** does not seem to be a good partner in this process, with mediocre reactivity at 120 °C. In order to understand how the model reaction produces synthetically useful yields of product **5** while involving the sluggish sodium sulfinate salt **4**, the rates of transmetalation between **9** and sodium or potassium sulfinate salts **4** and **4-K** were compared to the rate of transmetalation between sodium sulfinate **4** and complex **9** in presence of K_2CO_3 (1:1 ratio) at 150 °C (***Figure 2.7.B***). At this higher temperature, sodium sulfinate salt **4** does mediate the transmetalation, reaching 68% conversion within two hours (grey squares). However, the rate of product formation was largely improved by the presence of K_2CO_3 as shown by the blue circles, while sulfinate **4-K** gave the highest rate of product formation (red diamonds). This observation suggests that a cation metathesis between the sodium sulfinate salt **4** and potassium carbonate is likely to take place under the reaction conditions (***Equation 4***), therein permitting the transmetalation step to happen at reasonable rates.

IV. $ArSO_2Na \xrightarrow{K_2CO_3} ArSO_2K$

2.5.3. Impact of the Concentration of PCy_3 on the Rate of Transmetalation

The stoichiometric reaction between oxidative addition complex **9** and 4-methylbenzene sulfinate salt **4-K** was carried out in 1,4-dioxane at 150 °C while varying the concentration of PCy_3 (***Figure 2.8***). The potassium sulfinate **4-K** was used rather than the sodium sulfinate **4** as

it was proposed that it is formed *in situ* prior to transmetalation, as discussed in the previous section.

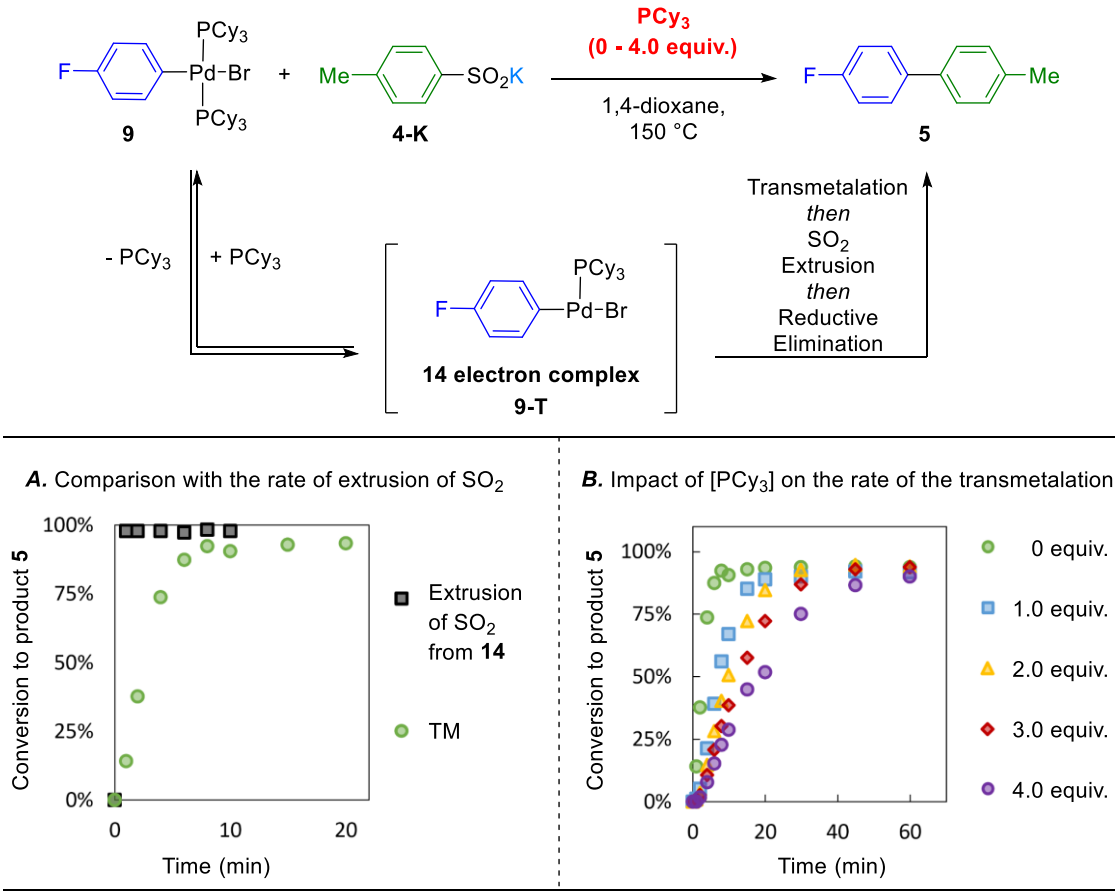


Figure 2.8. Transmetalation step with **4-K**: comparison with the extrusion of SO_2, and influence of [PCy_3].

In ***Figure 2.8.A***, the rate of transmetalation between **9** and **4-K** is compared with the rate of extrusion of SO_2 from complex **14**. It is evident from this first plot that the rate of the sequence transmetalation/extrusion of SO_2/reductive elimination (k_{obs} as defined in **Section 2.5.1**, ***Scheme 2.7***) is much slower than the rate of the extrusion of SO_2/reductive elimination k_2: $k_{obs} << k_2$.

A significant decrease in the rate of transmetalation was observed upon increasing the concentration of PCy_3 (***Scheme 2.8.B***). This suggests that dissociation of a phosphine ligand from the 16-electron complex **9** is necessary to release a coordination site and form a more

reactive 14-electron T-shaped oxidative addition complex **9-T** prior to transmetalation (phosphine dissociation from complex **9** is explored in more details in **Section 2.5.4**).

The rates of the sequence transmetalation/desulfination/reductive elimination between oxidative addition complex **9** and potassium pyridine-2-sulfinate **1-K** were also compared to the rate of desulfination/reductive elimination from palladium sulfinate **12** (***Figure 2.9.A***). For the extrusion of SO_2 from complex **12**, one equivalent of PCy_3 was added to the reaction mixture to ensure a 2:1 PCy_3/Pd ratio. In contrast to what was observed with carbocyclic sulfinate **4-K** and the corresponding palladium sulfinate complex **14**, the rates of both reactions are almost equal with the 2-pyridyl substrates. This further confirms that the hypothesis made in **Section 2.5.1** is not applicable to the transmetalation with potassium 2-pyridyl sulfinate **1-K**: $k_{obs} \neq k_1$. Instead, observing $k_{obs} \approx k_2$ suggests that the extrusion of SO_2 is the limiting step of the sequence transmetalation/extrusion of SO_2/reductive elimination for 2-pyridyl substrates due to the strong Pd-N bond in palladium sulfinate chelate **12**.

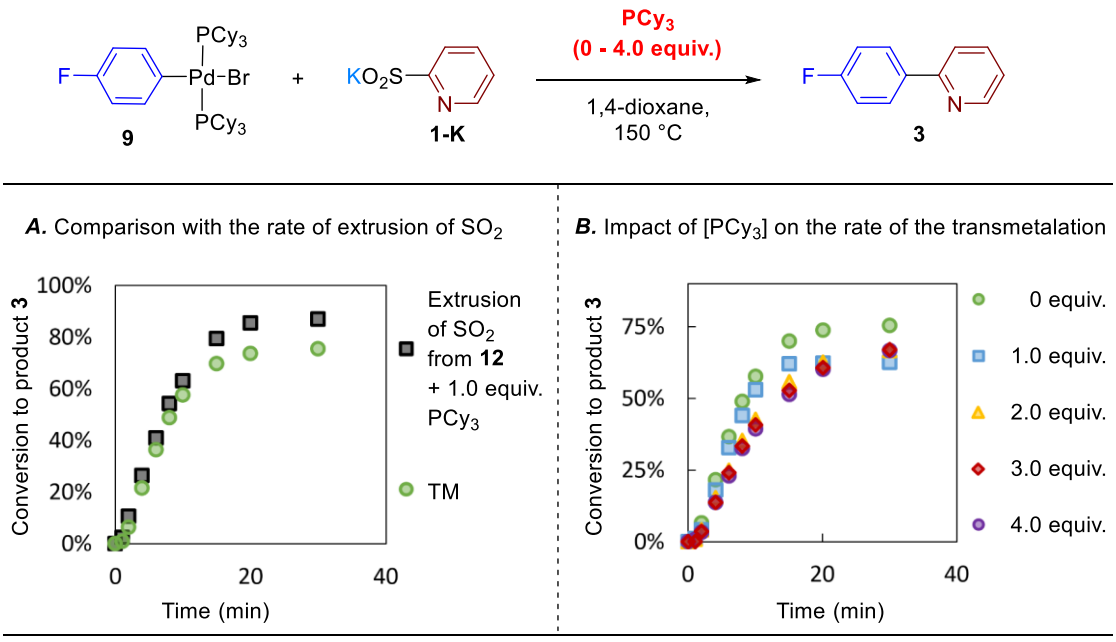


Figure 2.9. Transmetalation step with **1-K**: comparison with the extrusion of SO_2, and influence of [PCy_3].

The rates of the sequence transmetalation/extrusion of SO_2/reductive elimination were slightly affected by increasing amounts of PCy_3 (***Figure 2.9.B***). The dependence observed is once again consistent with ligand dissociation from oxidative addition complex **9** giving complex **9-T** prior to transmetalation. It is however important to highlight that the impact of the increasing concentration of PCy_3 on the reaction rates is less important than for the carbocyclic system. This is most likely due to the slow and limiting extrusion of SO_2 from complex **12** which does not depend on the concentration of PCy_3 as shown in **Section 2.4.2.** (***Figure 2.4.C***).

2.5.4. Lability of PCy_3 in the Oxidative Addition Complex 9

In order to support the ligand dissociation sequence deduced in the previous section and the involvement of a putative T-shaped oxidative addition complex **9-T** in the transmetalation step, the lability of PCy_3 in complex **9** was examined. Oxidative addition complex **9-*i*-Pr** was synthesised with tri-isopropylphosphine ligand P(*i*-Pr)$_3$, which is electronically and sterically similar to PCy_3. Similarly to complex **9**, a doublet at δ_P = 30.51 ppm, $J_{P\text{-}F}$ = 3.0 Hz could be observed, characteristic of a *trans* configuration of the two phosphine ligands.

The two oxidative addition complexes **9** and **9-*i*-Pr** were dissolved in a 5:1 mixture of 1,4-dioxane/benzene-d_6, and gradually heated from room temperature to 100 °C (***Figure 2.10***). After an hour at 50 °C, the two complexes had remained untouched. However, raising the temperature to 75 °C for 60 minutes led to scrambling of the phosphine ligands, and a novel complex that was assigned as **9-Cy-*i*-Pr** was observed, with each phosphine ligand giving a doublet of doublets ($\delta_{P(i\text{-}Pr)3}$ = 30.54 ppm, δ_{PCy3} = 19.37 ppm, $J_{PCy3\text{-}P(i\text{-}Pr)3}$ = 381.5 Hz, $J_{P\text{-}F}$ = 3.0 Hz). The equilibrium obtained at 75 °C remained unchanged after raising the temperature to 100 °C for another hour. This experiment confirms that PCy_3 is labile under the reaction conditions, which supports the phosphine dissociation/transmetallation sequence discussed in the previous ***Section 2.5.3.*** The ability of PCy_3 to dissociate from complex **9** is not surprising given previous studied by Tolman and co-workers on Ni(II) complexes.[20]

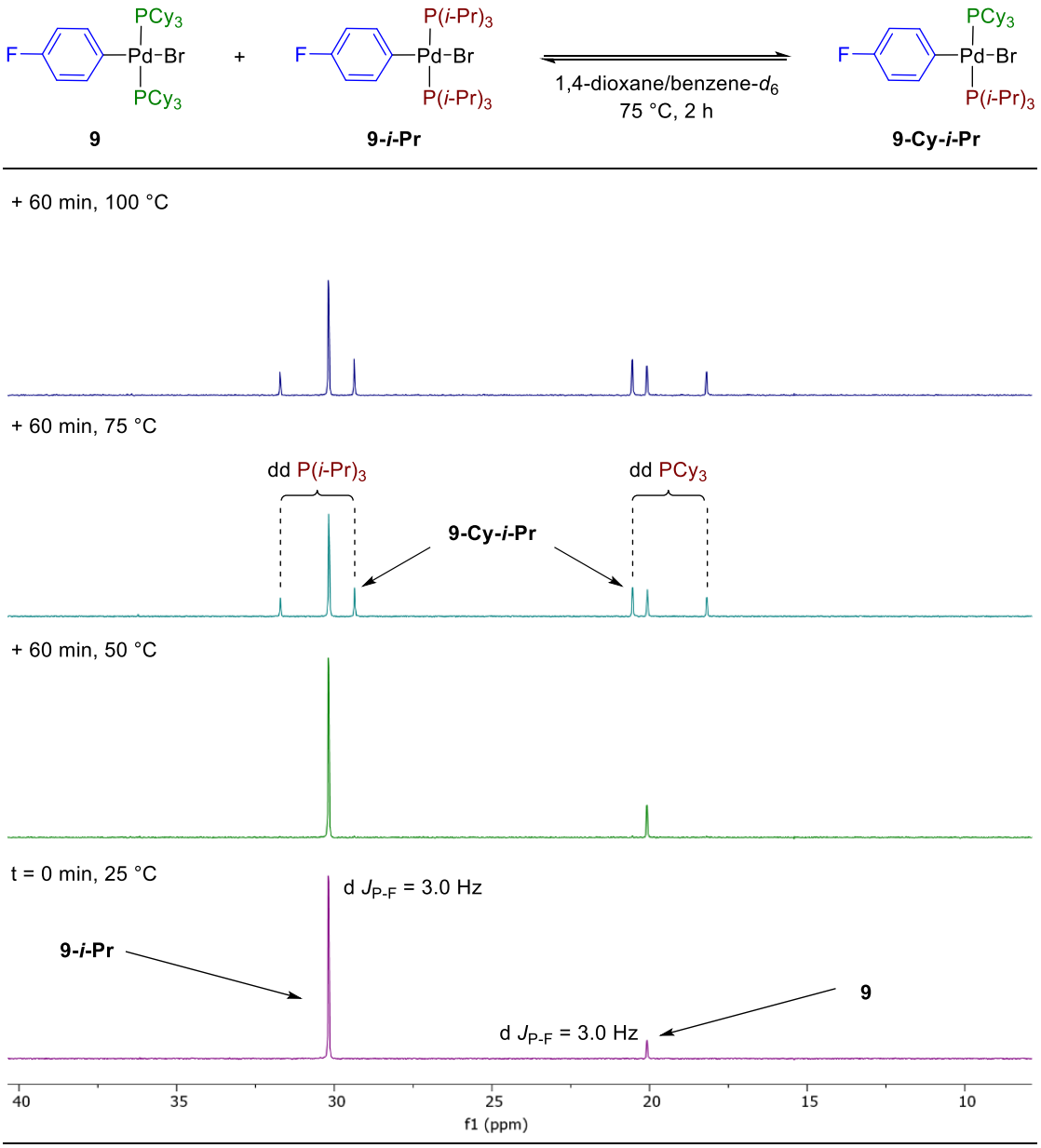


Figure 2.10. Ligand scrambling between oxidative addition complexes **9** and **9-*i*-Pr**.

2.6. Identification of the Resting State Intermediates

To identify the resting state intermediates (RSI) of the catalytic reactions, the desulfinative cross-couplings were monitored by $^{31}P\{^{1}H\}$ NMR and $^{19}F\{^{1}H\}$ NMR spectroscopy using sub-stoichiometric amounts of catalyst. The reactions were performed in a Young's NMR tube with 15 mol% of $Pd(OAc)_2$ and 30 mol% of PCy_3. The observed resonance peaks were compared to the signals of reference samples obtained from a similar 5:1 mixture of 1,4-dioxane/benzene-d_6. Due to poor stirring of the heterogeneous mixture in an NMR tube, the reaction kinetics

were found to be very slow. After 14 hours at 150 °C, at which point biaryl **5** was formed in 40% yield (≈ 2.7 turnovers), the resonance peak of oxidative addition complex **9** (δ_F = -124.26 ppm) was the only other signal observed on the $^{19}F\{^1H\}$ spectrum along with starting material, internal standard, and product (***Figure 2.11.A***). The corresponding characteristic doublet at δ_P = 20.08 ppm was also observed in the $^{31}P\{^1H\}$ spectrum, along with free PCy_3 (δ_P = 9.24 ppm), phosphine oxide (δ_P = 45.65 ppm) and oxidative addition complex **8b** (δ_P = 19.80 ppm) (***Figure 2.11.B***).

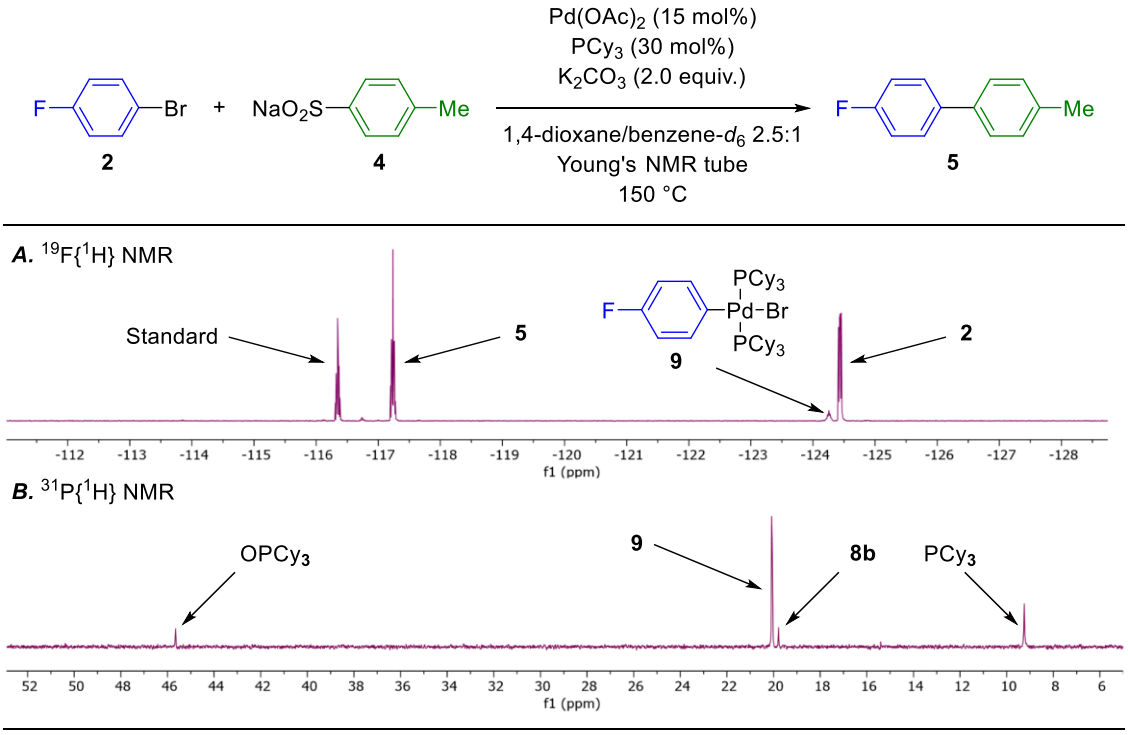


Figure 2.11. Identification of the RSI with 4-methylbenzene sulfinate **4**.

The same experiment was performed with the pyridine-2-sulfinate substrate **1**. After 14 hours reaction at 150 °C, the conversion to product **3** was lower than for the carbocyclic substrate (20%, ≈ 1.3 turnover). The oxidative addition product **9** was observed in a 1:1 ratio with the palladium sulfinate complex **12** (***Figure 2.12.A***). Presence of these species was confirmed by the $^{31}P\{^1H\}$ spectrum, where their corresponding phosphorus resonance peaks (δ_P = 38.03 and

δ_P = 20.08) were observed along with free PCy_3, its oxide, and minor unidentified resonances (***Figure 2.12.B***).

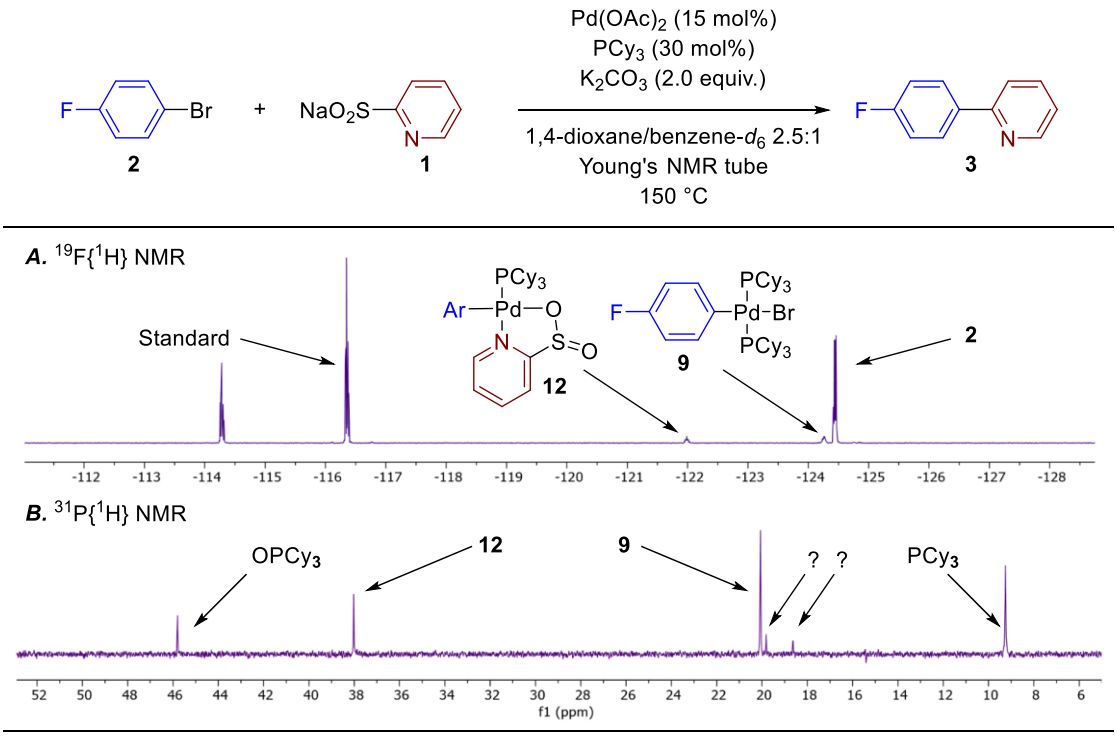


Figure 2.12. Identification of the RSI with pyridine-2-sulfinate **1**.

These experiments were also performed with sodium 5-(trifluoromethyl)pyridine-2-sulfinate **1-CF3**, sodium pyridine-4-sulfinate **16**, and lithium 6-(*tert*-butyl)pyridine-2-sulfinate **1-*t*-Bu**. For these three pyridyl sulfinate substrates, the oxidative addition complex **9** was the only complex observed by $^{19}F\{^1H\}$ NMR spectroscopy, and its corresponding resonance peak was found in the $^{31}P\{^1H\}$ NMR together with some minor unidentified signals. NMR spectra corresponding to these results are available in the **Experimental Section 7.2.11.**

Overall, the monitoring of the cross-coupling reactions between 1-bromo-4-fluorobenzene **2** and sulfinate salts **1**, **1-CF3**, **1-*t*-Bu**, **4** and **16** by $^{19}F\{^1H\}$ or $^{31}P\{^1H\}$ NMR spectroscopy suggests that the nature of the RSI depends on the ability of the sulfinate salt to form a strong aryl palladium sulfinate chelate such as complex **12**, from which the extrusion of SO_2 is a difficult process. The observation of complex **9** as the RSI for the reaction involving carbocyclic

sulfinate **4** is consistent with its inability to form such a chelate and with the high rates of extrusion of SO_2 observed in **Section 2.4.2.** Complex **9** was also observed to be the RSI in the reaction involving pyridine-4-sulfinate **16** which can not form a 5-membered ring chelate for evident geometrical reasons. Similarly, it was shown in **Section 2.3.2** that the palladium sulfinate complex **13** formed with 6-(*tert*-butyl)pyridine-2-sulfinate **1-*t*-Bu** is a dimer because the bulky *tert*-butyl group prevents formation of a Pd-N bond. Accordingly, complex **9** was observed to be the RSI of the reaction with sulfinate **1-*t*-Bu**. The electron-poor 5-(trifluoromethyl)pyridine-2-sulfinate **1-CF$_3$** is able to chelate the palladium in a $\kappa^2_{N,O}$-mode. However, it was demonstrated in **Section 2.4.2** that weakening of the N-Pd bond due to inductive effects of the trifluoromethyl group facilitates the extrusion of SO_2 from the corresponding complex (see **Section 2.4.2** ***Figure 2.6,*** **12** *vs* **12-CF$_3$**). As a consequence, oxidative addition complex **9** was once again observed to be the RSI of the reaction with sulfinate **1-CF$_3$**. It is only with the unsubstituted pyridine-2-sulfinate **1** that the corresponding palladium sulfinate chelate **12** was observed by NMR spectroscopy over the course of the reaction. This suggests that the strong chelation observed with this substrate provokes a change of RSI due to the difficulties associated with the extrusion of SO_2 from complex **12**.

2.7. Kinetics of the Catalytic Reaction

2.7.1. Experimental Procedure: Initial Rates of the Reaction

Productive catalytic reactions are performed at 150 °C in 1,4-dioxane (bp = 101 °C) and under these conditions, sulfinate salts and potassium carbonate are sparingly soluble. The heterogeneous nature of the reaction mixture and the high temperatures required prevented us from monitoring these cross-couplings by NMR spectroscopy. Instead, reaction progress was monitored by HPLC analysis of aliquots taken from the reaction mixture with a syringe. Under these conditions, the microwave caps employed to seal the reaction vials were quickly damaged and reactions could not be monitored for extended reaction times. It was however possible to

obtain reproducible results over shorter reaction times. Therefore, the partial orders in reagents and catalyst were obtained using the initial rate method.[133]

A precise addition order of the reagents was crucial in obtaining interpretable kinetic data. The amount of homocoupling product **5b** was monitored, as it is indicative of the formation of active Pd(0) species as discussed in **Section 2.2.** The data in ***Figure 2.13*** was obtained by injecting a solution of $Pd(OAc)_2$ and PCy_3 to a preheated solution of aryl bromide **2**, sulfinate **4** and K_2CO_3. With this addition order, catalyst activation (green circles) and product formation (blue diamonds) take place concurrently and the initial rates can not be easily interpreted, and the red dotted lines represent the uncertainty range for the initial rate.

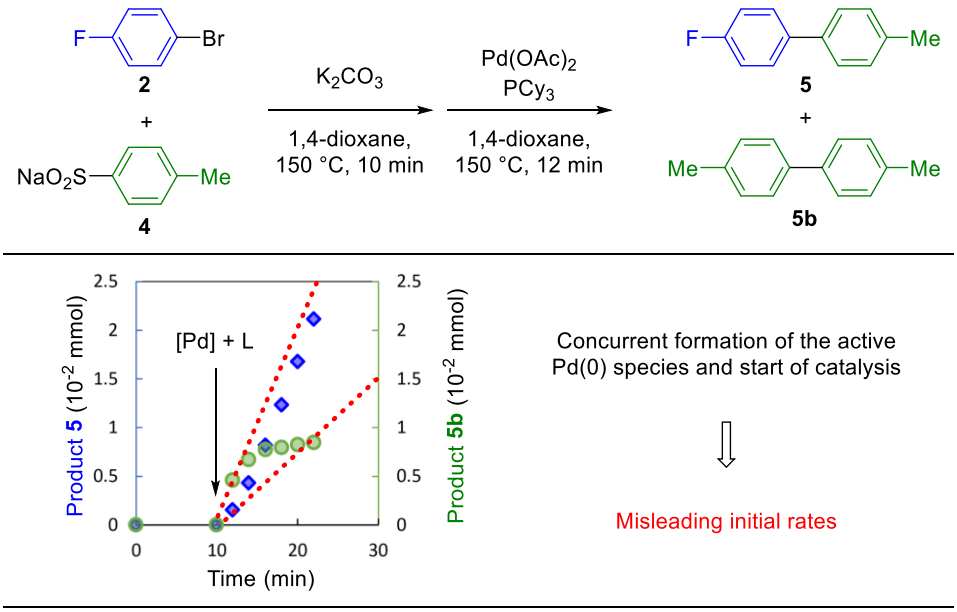


Figure 2.13. Measurement of the initial rate without catalyst pre-activation.

In order to suppress the induction period caused by the activation of $Pd(OAc)_2$, the precatalyst was first heated at 150 °C in presence of ligand, base and sulfinate **4** before addition of the aryl bromide **2** (***Figure 2.14***). This addition order, which permitted the precise measurement of the initial rate of the reaction (green dotted line), was employed for the entirety of the experiments figuring in **Section 2.7.**

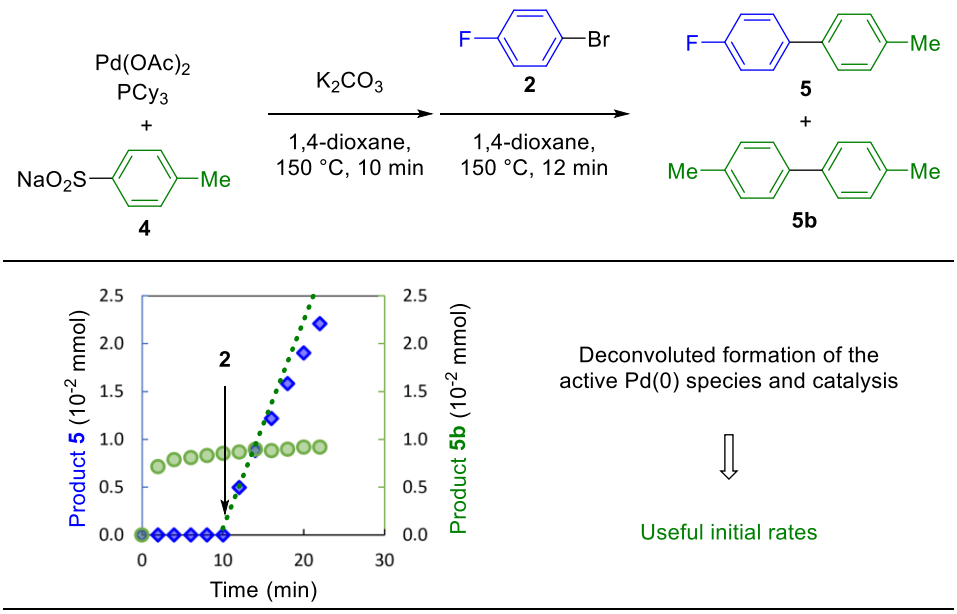


Figure 2.14. Measurement of the initial rate with catalyst pre-activation.

2.7.2. Heterogeneous *vs* Homogeneous Catalysis

The nature of the active catalyst in palladium-catalysed cross-couplings can be ambiguous.[5, 134-135] In order to verify that the reaction kinetics are not affected by a possible heterogeneous component, a mercury test was performed (***Figure 2.15***). To our surprise, the introduction of Hg(0) in the reaction mixture entirely stopped the catalysis, suggesting that the reaction could follow a heterogeneous pathway. However, the mercury poisoning test can sometimes lead to false positives, as Hg(0) can decompose Pd(0)/L and Pd(II)/L systems.[136-137] A filtration test was performed to gather more information on the nature of the true catalyst species (***Figure 2.16***). A reaction using typical stoichiometry and concentration[138] was halted after 20 minutes, at which point the conversion was 20% based on an internal standard, corresponding to a rate of 0.0023 mmol.min^{-1}. The solution was cooled, filtered through a 0.22 µm PTFE syringe filter under an inert atmosphere, and the filtrate was introduced in a new reaction vial containing K_2CO_3 and the sulfinate coupling partner **4**. Upon heating, the reaction started again with a similar rate of 0.0020 mmol.min^{-1}, as 41% conversion were reached after 20 minutes and 88% after 120 minutes. Although it is not possible to fully exclude a heterogeneous pathway, we

propose, based on the isolation of discrete homogeneous intermediates and this filtration test, that the major catalytic pathway is homogeneous in the studied reactions.

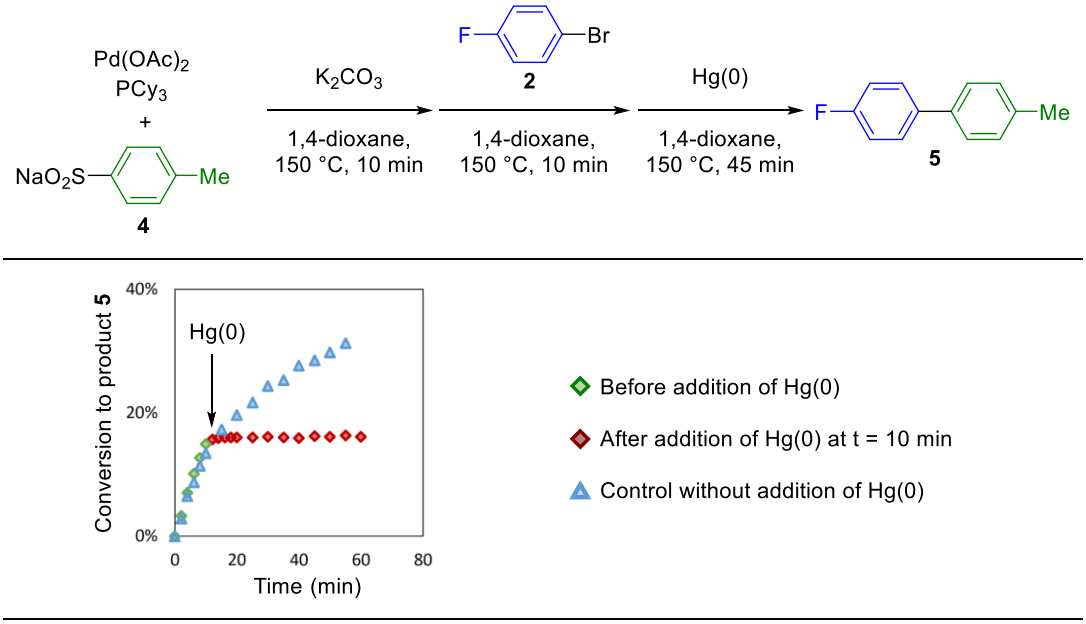


Figure 2.15. Mercury test.

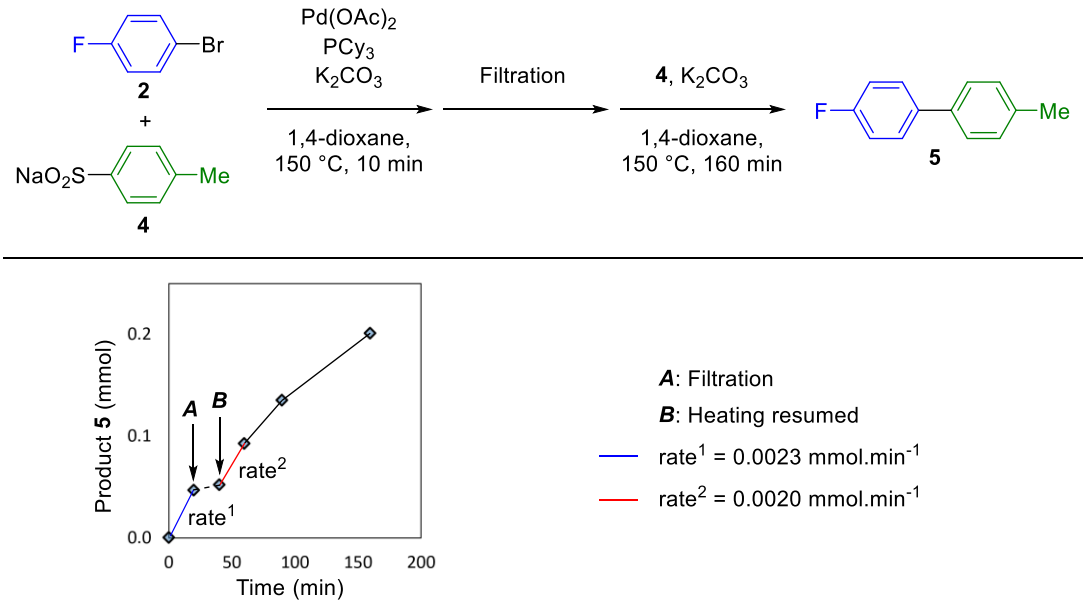


Figure 2.16. Filtration test.

2.7.3. Order in Aryl Bromide 2

The reactions of 4-methylbenzenesulfinate **4** and pyridine-2-sulfinate **1** were performed with different concentrations of aryl bromide **2** (0.025-0.15 mM). A zero order in aryl bromide was

observed with both sulfinate substrates as the initial rates were found to be independent of the concentration of aryl bromide **2** (***Figure 2.17***). This observation implies that the oxidative addition step is not the turnover limiting step (TLS) of the catalytic cycle. This is in good agreement with previous studies by the groups of Baird[123] and Hartwig[96] who showed that oxidative addition of $Pd^0(PCy_3)_2$ in bromobenzene happens at room temperature and with the observation of complexes **9** or **12** as the resting state intermediates.

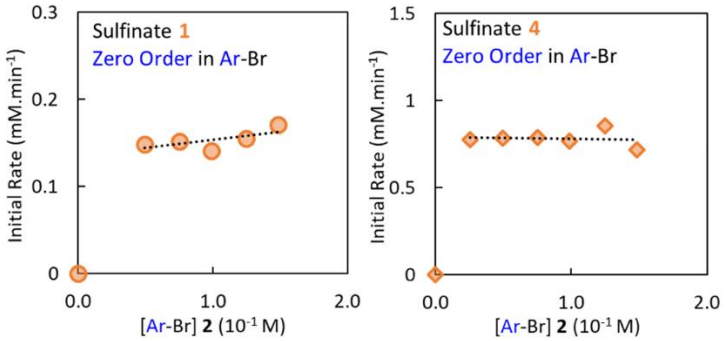


Figure 2.17. Plot of the initial rate of the reaction against the concentration of aryl bromide **2** with both 2-pyridyl sulfinate **1** (●) and carbocyclic sulfinate **4** (◆).

Despite the existence of $Pd^0(PCy_3)_2$ as a 12-electron complex in bromobenzene,[96, 123] it is not possible to rule out the potential formation of palladium(0) aggregates under the cross-coupling reaction conditions, which would be consistent with the results of the mercury poisoning test (***Section 2.7.2***). However, together with the aforementioned literature precedents, the observed zero-order in aryl bromide suggests that oxidative addition is fast and non-turnover determining in the studied reactions, and that formation of such aggregates does not appear to be catalytically relevant to the reaction kinetics.

2.7.4. Order in Sulfinate Salts and K_2CO_3

Given that sodium 4-methylbenzenesulfinate **4**, sodium pyridine-2-sulfinate **1** and potassium carbonate are not fully soluble in 1,4-dioxane at 150 °C at concentrations between 0.010 M and 0.10 M, their partial orders were not measured.

2.7.5. Order in Catalyst

The initial rates of the reaction between aryl bromide **2** and 4-methylbenzenesulfinate **4** were measured with different concentrations of $Pd(OAc)_2$ and PCy_3, keeping the ligand to palladium ratio fixed at two. A linear correlation was observed between the square root of the concentration of $Pd(OAc)_2$ and the measured initial rates: rate $\propto [Pd(OAc)_2]^{0.5}$ (***Figure 2.18.A***). Such half orders in catalyst have been observed when dimerisation of the active catalyst[139-141] or ligand coordination to the metal centre[142-143] lead to an inactive off cycle species in equilibrium with an active intermediate. Having observed both dimerisation to form dimer **11** as well as the important lability of PCy_3, the order in $Pd(OAc)_2$ was measured in presence of excess phosphine ligand ($[Pd(OAc)_2]/[PCy_3] < 0.10$) to clarify the origin of the observed half order. Under these conditions, a first order was measured in $Pd(OAc)_2$ (rate $\propto [Pd(OAc)_2]$) (***Figure 2.18.B***), confirming that the observed half order dependence in catalyst is due to a fast equilibrium between the resting state oxidative addition complex **9** and the catalytically active 14-electron complex **9-T**, as discussed in **Section 2.5.3.** Under these conditions where the inactive tris-ligated $Pd^0(PCy_3)_3$ is likely to be formed,[123] a zero order in aryl bromide **2** was still observed (***Figure 2.18.C***), confirming that a turnover limiting oxidative addition was not responsible for the different kinetic regimes observed.

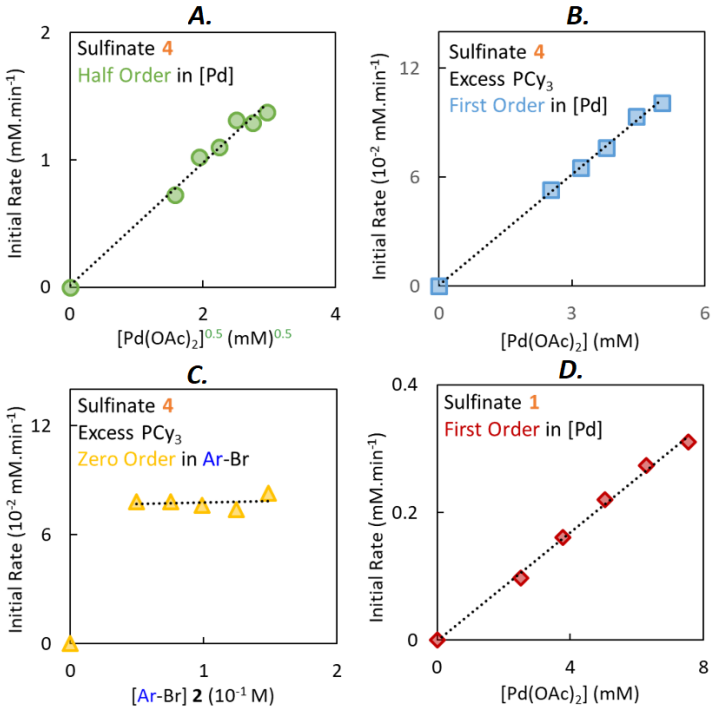


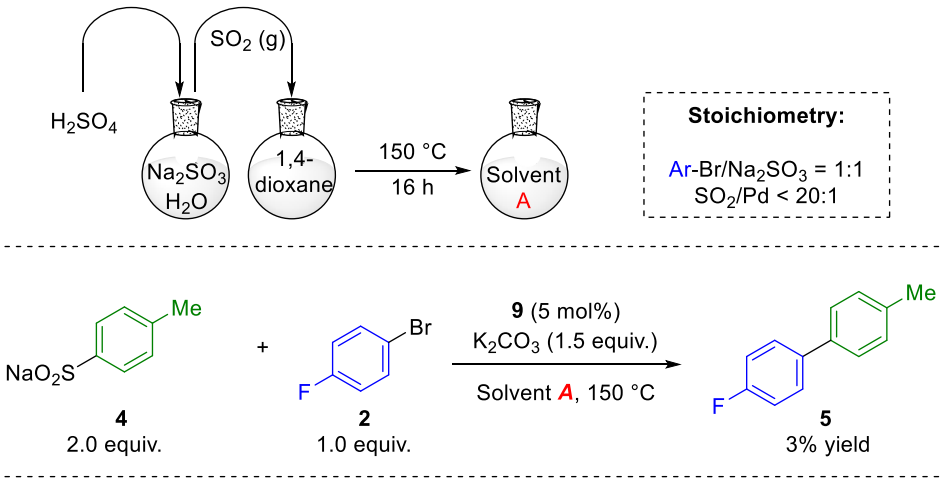
Figure 2.18. Determination of the order in catalyst. Plots of the initial rate between aryl bromide **2** and ***A.*** 4-methylbenzenesulfinate **4** (●), ***B.*** 4-methylbenzenesulfinate **4** using an excess of PCy_3 (■) ***C.*** 4-methylbenzenesulfinate **4** using an excess of PCy_3 (▲) ***D.*** pyridine-2-sulfinate **1** (◆).

In contrast, a first order in catalyst was observed for the reaction between aryl bromide **2** and 2-pyridine sulfinate **1**: rate ∝ $[Pd(OAc)_2]$ (***Figure 2.18.D***). This observation is in good agreement with the stoichiometric reactions of **Sections 2.4** and **2.5.** Because sulfinate **1** strongly chelates the palladium centre in complex **12**, extrusion of SO_2 becomes the TLS instead of the transmetalation, palladium sulfinate **12** becomes the RSI instead of complex **9**. Therefore, even if an equilibrium between **9** and **9-T** is likely to precede the transmetalation step, it does not have an apparent impact on the kinetics of the reaction which are limited by the extrusion of SO_2 from complex **12**.

2.8. SO_2 By-product

Sulfur dioxide is the main by-product of these desulfinative cross-coupling reactions, with one molecule of SO_2 extruded per molecule of product formed. As a consequence, SO_2 is present as a 20-fold excess compared to the catalyst towards the end of catalysis as $Pd(OAc)_2$ is

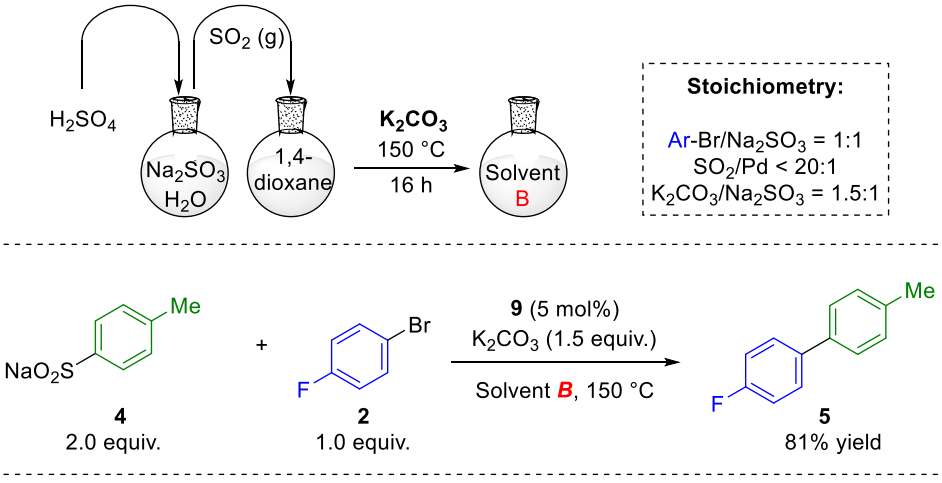
employed in a 5.0 mol% stoichiometry. Insertion of SO_2 in palladium complexes is well known (***Section 1.3.2***), and has been utilised in many palladium-catalysed C-S bond forming reactions.[144-149] Given the known reactivity of SO_2 with palladium complexes, it was puzzling to observe productive reactions under these conditions in which SO_2 co-exists with the palladium intermediates. In order to verify whether these reaction conditions are simply compatible with the presence of SO_2 gas or if SO_2 acts as a poison to the catalyst and must be therefore neutralised during the process, the cross-coupling reaction was first performed in presence of SO_2. SO_2 was generated by a slow addition of sulfuric acid to a solution of sodium sulfite in water, and the generated gas was bubbled in 1,4-dioxane *via* a canula. The generated solution ***A*** was heated overnight at 150 °C (***Scheme 2.19***).



Scheme 2.19. Cross-coupling reaction in presence of SO_2 (g).

Weighing the amount of Na_2SO_3 allowed us to control the concentration of SO_2 in solution which corresponded to a maximum of 1.0 equiv. compared to the aryl bromide **2** (20 equiv. compared to the catalyst). The oxidative addition complex **9** was chosen as the catalyst in order to deconvolute the generation of the active Pd(0) species and the productive catalytic cycle for this experiment. Under these reaction conditions, biaryl **5** was obtained in 3% yield, showing that presence of SO_2 is not compatible with catalysis.

Our attention was drawn to the role of K_2CO_3 in the reaction mechanism. It was demonstrated in **Section 2.5.2** that K_2CO_3 is involved in a cation metathesis with the sodium sulfinate salt to increase the rate of the transmetalation step. However, during the optimisation of this cross-coupling process, it had been observed that other potassium bases failed to provide synthetically useful yields, suggesting that the carbonate base is of crucial importance too.[58] Examination of the literature showed that carbonate bases have been employed to trap SO_2 from the waste stream of industrial combustion processes.[150-151] In order to verify the hypothesis that the presence of carbonate in the reaction mixture sequesters the SO_2 by-product and allows catalyst turnover, a 0.05 M solution of SO_2 in 1,4-dioxane was heated overnight in presence of K_2CO_3 in a 1:1.5 ratio, giving solvent B after filtration (***Scheme 2.20***).



Scheme 2.20. Trapping of SO_2 (g) by K_2CO_3.

When solvent ***B*** was used for the cross-coupling reaction between substrates **2** and **4**, biaryl **5** was obtained in 81% yield. These two experiments were repeated with 2-pyridyl sulfinate **1** and similar results were obtained (**Experimental Section 7.12.14**).

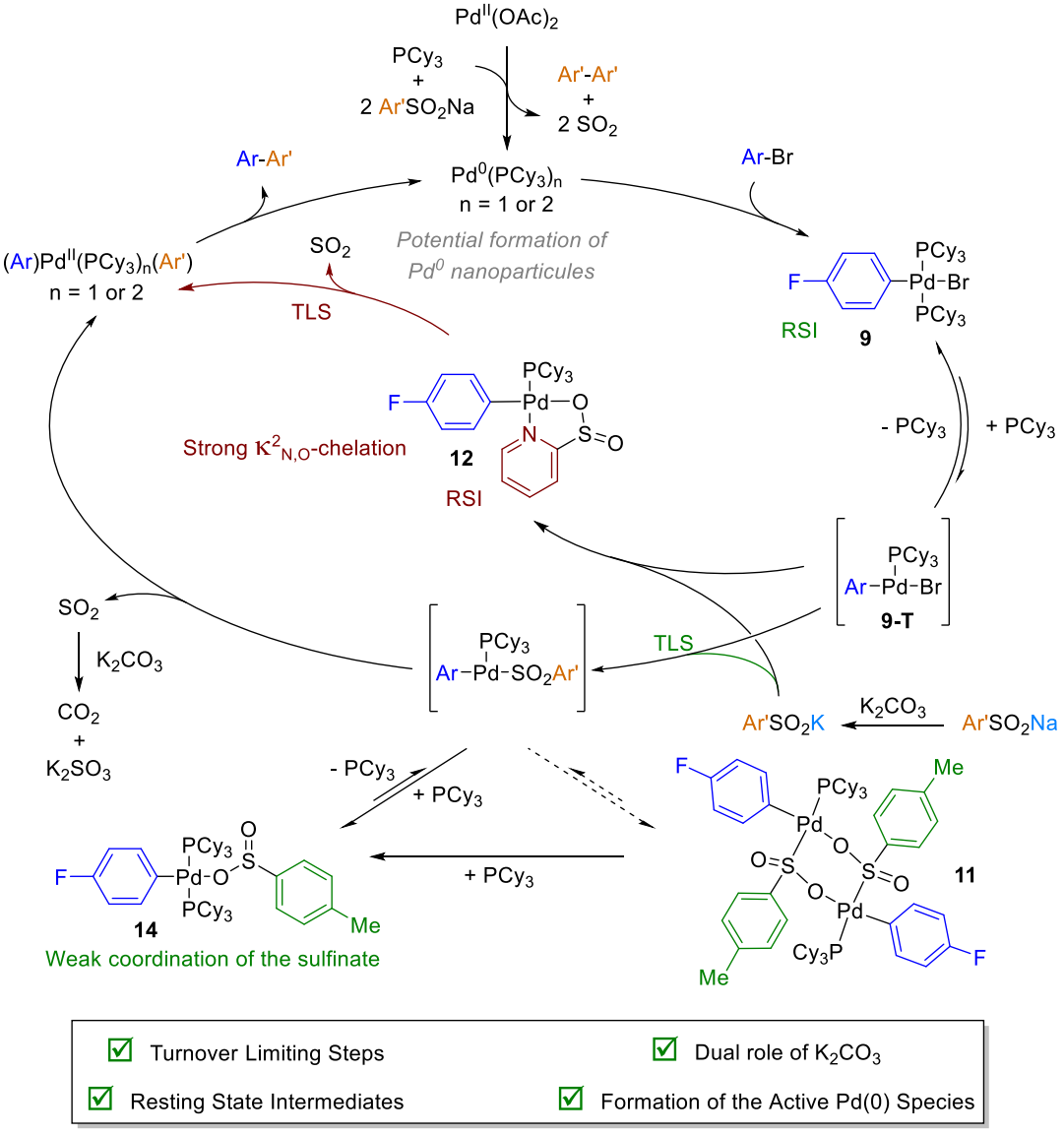
This demonstrates that the carbonate base is required in order to trap the gaseous SO_2 by-product, which was shown to be otherwise a poison for the catalytic system. Given literature

precedents,[152] we propose that sulfite anions and CO_2 are generated in this process, according to ***Equation 5.***

V. $SO_2 + K_2CO_3 \longrightarrow CO_2 + K_2SO_3$

2.9. Project Summary

We have investigated the mechanism of the palladium-catalysed desulfinative cross-coupling of 1-bromo-4-fluorobenzene **2** with pyridine-2-suflinate **1** and 4-methylbenzenesulfinate sulfinate **4**, and ***Scheme 2.8*** summarises our findings.



Scheme 2.8. Overall catalytic cycle, summary of our findings.

Formation of the active Pd(0) species is mediated by the homocoupling of two sulfinate salts, *via* double transmetalation, extrusion of SO_2 and reductive elimination to form homocoupling side-products **3b** and **5b**, preserving the phosphine/palladium ratio at 2:1.

After oxidative addition of active palladium(0) species into the C-Br bond of aryl bromide **2**, we proposed that oxidative addition complex **9** does not directly undergoes transmetalation with the nucleophilic coupling partner, but first dissociates a PCy_3 ligand to free a coordination site. The equilibrium between complexes **9** and **9-T** is supported by the observation of a half-order in catalyst in the catalytic reaction involving 4-methylbenzene sulfinate **4**, and by the strong dependence of the rate of transmetalation on the concentration of PCy_3 in stoichiometric experiments between oxidative addition complex **9** and potassium sulfinate **4-K**. Together with the observation of oxidative addition complex **9** by NMR spectroscopy over the course of the reaction, these results suggest that oxidative addition complex **9** is the resting state catalyst and the transmetalation is turnover limiting for the reaction of 4-methylbenzene sulfinate **4** with aryl bromide **2**.

In contrast, the nature of the RSI and TLS are shifted to palladium sulfinate **12** and extrusion of SO_2 respectively for the reaction of pyridine-2-sulfinate **1** with aryl bromide **2**, due to the ability of the 2-pyridyl sulfinate substrate to strongly chelate the palladium centre as in complex **12**, therefore making the extrusion of SO_2 a more energy demanding process. This was supported by the observation of a first order in catalyst in the catalytic reaction, and by the non-dependence of stoichiometric reactions involving oxidative addition complex **9** and potassium pyridine sulfinate **1-K** on the concentration of PCy_3. Accordingly, palladium sulfinate **12** could be observed by NMR spectroscopy over the course of the reaction.

Given the facility of extrusion of SO_2 from sulfinato-*O* complex **14**, we were able to formulate approximations that allowed us to study the transmetalation step between oxidative addition complex **9** and carbocyclic sulfinate **4**. Stoichiometric experiments revealed the importance of

the sulfinate cation for efficient transmetalation, and it was proposed that potassium carbonate is involved in a cation metathesis with sodium sulfinate salt **4** prior to transmetalation.

Formation of dimeric complex **11** was attributed to the oxidative properties of $AgNO_3$, which was required for the formation of palladium sulfinate complexes at lower temperatures. Such dimeric aggregates are however not believed to participate in the reaction mechanism.

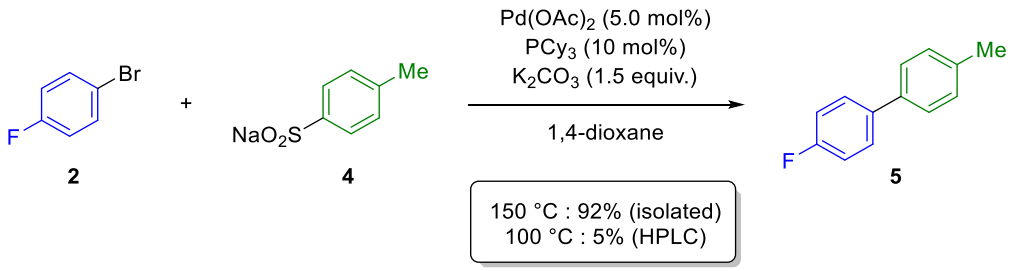
Finally, control experiments showed that the carbonate base is essential to sequester the SO_2 by-product and allow catalyst turnover.

Having identified the nature of the catalyst RSI and the TLS, as well as the role of the different substrates and additives in this reaction mechanism, I aimed at delivering a more efficient cross-coupling reaction compatible with lower reaction temperatures. This is the focus of **Chapter 3.**

Chapter 3 –Towards a Lower Temperature Cross-Coupling Reaction

3.1. Choice of the Model Substrates

In this chapter, the objective was to exploit our knowledge of the mechanism discussed in **Chapter 2** to promote desulfinative cross-coupling reactions between aryl halides and aryl sulfinate salts at reduced temperatures compared to the original conditions, which require a temperature of 150 °C.[58] 1-Bromo-4-fluorobenzene **2** and sodium 4-methylbenzenesulfinate salt **4** were chosen as model substrates to carry out this optimisation work. While the reaction between these two substrates is nearly quantitative when the reaction is performed at 150 °C allowing isolation of biaryl **5** in 92% yield, only 5% of product **5** are formed according to HPLC analysis of the crude reaction mixture when the temperature is reduced to 100 °C (***Scheme 3.1***). This illustrates the magnitude of the challenge associated with promoting desulfinative cross-coupling reactions at a lower temperature.



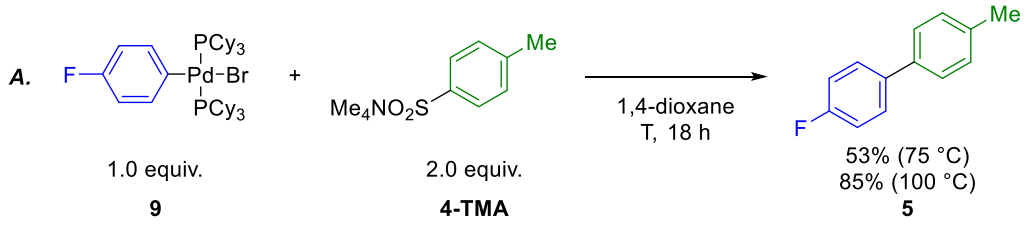
Scheme 3.1. Lowering the working temperature of desulfinative cross-coupling reactions: the challenge.

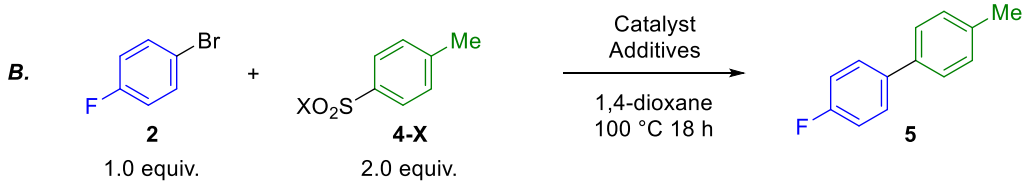
According to the mechanistic investigation discussed in **Chapter 2**, the transmetalation step between oxidative addition complex (4-F-C_6H_4)Pd(PCy_3)$_2$(Br) **9** and the poorly nucleophilic potassium sulfinate salt **4-K**, formed *in situ via* cation metathesis between sodium sulfinate **4** and K_2CO_3, is responsible for the high temperature requirements of this reaction. In order to facilitate this transmetalation step at 100 °C, the screening of the three main parameters was undertaken: additives, solvents, and ligands.

These efforts towards lower temperature palladium-catalysed desulfinative cross-coupling reactions are summarised in this chapter. Unless otherwise stated, reaction yields were measured by HPLC against 1,3,5-trimethoxybenzene as an internal standard. The general procedure employed for these optimisation reactions can be found in the **Experimental Section 7.3.1.**

3.2. Tetramethylammonium Cation

We showed in **Section 2.5.2** that the nature of the sulfinate counter cation had a tremendous effect on the rate of the transmetalation step. Among the organic and inorganic cations assessed, the tetramethylammonium cation was the most promising, proving superior when compared to caesium or potassium sulfinates salts, as high rates and conversions were observed at 120 °C (***Figure 2.7.A***).





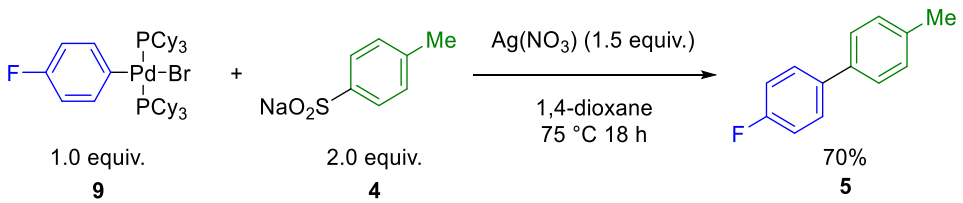
Entry	*Substrate*	*Catalyst*	*Additives*	*Yield*
1	X = NMe_4 : **4-TMA**	$Pd(OAc)_2$ (5.0 mol%) PCy_3 (10 mol%)	K_2CO_3 (1.5 equiv.)	7%
2	X = NMe_4 : **4-TMA**	**9** (5.0 mol%)	K_2CO_3 (1.5 equiv.)	19%
3	X = Na **4**	**9** (5.0 mol%)	K_2CO_3 (1.5 equiv.) NMe4Cl (1.5 equiv.) KOAc (1.5 equiv.)	2% (80 °C)
4	X = Na **4**	$Pd(OAc)_2$ (5.0 mol%) PCy_3 (10 mol%)	K_2CO_3 (1.5 equiv.) NMe_4Cl (1.5 equiv.)	7% (100 °C, 4 days)

Table 3.1. Tetramethyl ammonium substrate and additives.

When tetramethylammonium sulfinate salt **4-TMA** was employed in a stoichiometric reaction with complex **9** at 75 °C, biaryl product **5** was obtained in 53% yield (***Table 3.1.A***). This yield was increased to 85% upon raising the temperature to 100 °C. The use of **4-TMA** as a substrate in the catalytic reaction, however, proved to be disappointing (***Table 3.1.B***), with only 7-19% yield of biaryl **5** obtained after 18 hours at 100 °C depending on the catalyst used (*Entries 1-2*). Larossa and co-workers reported the use of NMe_4Cl in combination with KOAc as an alternative to silver additives to promote the palladium catalysed arylation of aromatic C-H bonds with iodoarenes,[132] but the use of these additives did not improve the efficiency of the coupling (*Entries 3-4*).

3.3. Silver Salts

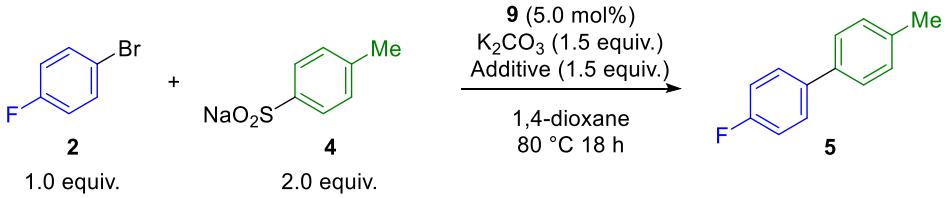
Silver nitrate was key to the formation of aryl palladium sulfinate complexes from oxidative addition complex **9** and various (hetero)aryl sodium sulfinate salts without the need for heating (**Section 2.3.2**). In other words, silver nitrate mediates the transmetalation step at room temperature. To illustrate the potential of silver salts as additives for lower temperature cross-coupling reactions, the stoichiometric reaction between complex **9** and sulfinate **4** was first performed at 75 °C in presence of silver nitrate, and provided 70% yield of biaryl **5** (***Scheme 3.2.*** This result was a significant improvement compared to the 53% yield obtained at the same temperature using tetramethylammonium substrate **4-TMA**.



Scheme 3.2. Formation of biaryl **5** using a stoichiometric amount of complex **9** and of $AgNO_3$.

Encouraged by this result, a range of salts were employed as stoichiometric additives in the Pd/PCy_3 catalysed coupling of aryl bromide **2** and sodium sulfinate **4** at 80 °C in 1,4-dioxane

(**Table 3.2**). Oxidative addition complex **9** was employed as the catalyst to deconvolute the formation of the active Pd(0) species with the productive catalytic cycle.



Additive	*Yield*	*Additive*	*Yield*	*Additive*	*Yield*	*Additive*	*Yield*
-	1%	$AgBF_4$	2%	Ag_2CO_3	6%	AgOTs	3%
$AgNO_3$	2%	$AgPF_6$	2%	AgF	5%	AgSCN	1%
AgOTf	2%	AgOAc	2%	AgOCN	2%	AgTFA	1%

Table 3.2. Silver salts as sub-stoichiometric additives.

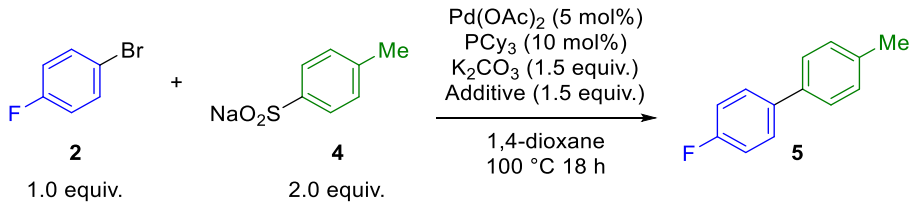
Disappointingly, all the silver salts investigated proved to not be compatible with these conditions, as none of these reactions gave biaryl **5** in yields above 6%, representing one turnover or less of the catalyst. This incompatibility is most likely due to the redox properties of silver salts and the involvement of a Pd(0) intermediate in the catalytic process.[153] Indeed, it was shown in **Chapter 2** that, similar to the report by Tiripicchio,[89] the use of silver in stoichiometric reactions with oxidative addition complex **9** resulted in the oxidation of a PCy_3 ligand, affording dimeric complex **11** $[(Ar)Pd(PCy_3)(SO_2Ar')]_2$ rather than sulfinato-*O* palladium complex **14** $[(Ar)Pd(PCy_3)_2(SO_2Ar')]$, therefore causing catalyst deactivation.

3.4. Copper Additives

Copper salts also have redox properties and have commonly been used as terminal oxidants[154] or as catalytic oxidant/electron transfer mediators in Pd(II)/Pd(0) catalytic cycles. The latter case was exemplified in **Section 1.2.3** with the Pd(II)-catalysed cross-coupling of aryl sulfinate salts with boronic acids as nucleophilic coupling partners,[46] and in **Section 1.2.5** with the Pd(II)-catalysed homocoupling reaction of aryl sulfinate salts.[65] However, conversely to silver salts, copper salts have also been frequently employed in the context of bimetallic catalysis for carbon-carbon bond forming reactions.[155] The Sonogashira reaction is probably the most

emblematic example of Pd/Cu dual catalysis, with Cu(I) halides being the most frequent copper sources employed to mediate the transmetalation between oxidative addition complexes and alkyne coupling partners.[35] Cu-sulfinate binding is also well precedented,[156] as copper salts have been used for the synthesis of unsymmetrical diaryl sulfones from sulfinate salts and iodoarenes as coupling partners, of which the mechanism was recently investigated.[157]

A range of Cu(I) and Cu(II) salts were therefore selected to promote the lower temperature cross-coupling of aryl bromide **2** and sodium sulfinate salt **4** at 100 °C (***Table 3.3***). A combination of $Pd(OAc)_2$ and PCy_3 was employed as the catalyst system, as the Sonogashira reaction provides a vast range of examples in which Pd(0) intermediates are successfully generated from Pd(II) precatalysts in the presence of copper additives.[35] This was supported by the detection of the homocoupling product **5b** in all reactions in 2-5% yield as discussed in **Section 2.2.** Unfortunately, the presence of these copper salts did not improve the yield of the desired product **5** at 100 °C, but was instead found to be detrimental to the reaction, with yields ranging in most cases from 1% to 5%, whereas the control copper-free reaction provided product **5** in 5% yield.



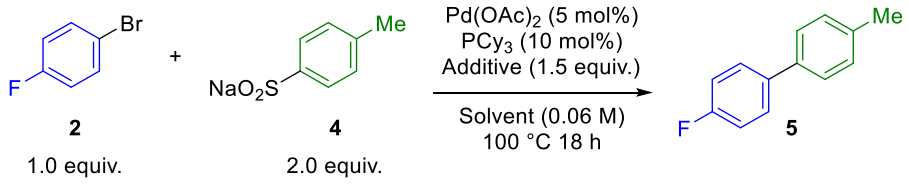
Additive	*Yield*	*Additive*	*Yield*	*Additive*	*Yield*	*Additive*	*Yield*
-	5%	$Cu(MeCN)_4(OTf)$	2%	CuOAc	3%	$Cu_2(CO_3)_2(OH)_2$	2%
CuBr	6%	$Cu(MeCN)_4(PF_6)$	1%	$Cu(OAc)_2$	2%	$CuOTf_2$	1%
CuI	6%	Cu(3-methylsalicylate)	4%	$Cu(BF_4)_2$	1%		

Table 3.3. Copper salts as stoichiometric additives.

3.5. Solubility of the Sulfinate Coupling Partner

The results discussed in **Section 2.5.2**, where the role of the sulfinate counter cation was investigated, indicated that the poor solubility of the sulfinate coupling partner was not

responsible for the difficulty of the transmetalation step. Indeed, both the rates of the stoichiometric reaction between either the non soluble potassium sulfinate salt **4-K** or the fully soluble tetrabutylammonium sulfinate **4-TBA** with oxidative addition complex **9** were found to be similar. To confirm this finding, a range of solvents and additives were explored (***Table 3.4***). While the use of DMSO (*Entry 2*), in which both sulfinate **4** and K_2CO_3 are soluble at the concentrations employed (0.06 M), slightly increased product yield to 10% compared to the standard reaction (*Entry 1*, 5%), switching to toluene, a less polar solvent, did not suppress reactivity (*Entry 3*, 6%). Solvent mixtures featuring DMSO were found beneficial (*Entries 4 and 5*, 8% and 10%) whereas the presence of isopropanol did not cause any major reactivity change (*Entry 6*, 4%). Using potassium bicarbonate as an additive instead of potassium carbonate or using the aryl sulfinic acid **4-H** were found to be detrimental to the reaction (*Entries 7 and 8*, 3% and 2%). Adding acetic acid, sodium acetate, or the commonly employed phase transfer reagent TBAB did not provoke any significant change in yield (*Entries 9-11*, 5-6% yield).



Entry	*Additive*	*Sovlent*	*Yield*
1	K_2CO_3	1,4-dioxane	5%
2	K_2CO_3	DMSO	10%
3	K_2CO_3	toluene	6%
4	K_2CO_3	toluene/DMSO 1:1	8%
5	K_2CO_3	toluene/DMSO/1,4-dioxane 1:1:1	10%
6	K_2CO_3	toluene/IPA 1:1	4%
7	$KHCO_3$	1,4-dioxane	3%
8	K_2CO_3*	1,4-dioxane	2%
9	K_2CO_3 + AcOH	1,4-dioxane	5%
10	K_2CO_3 + AcONa	1,4-dioxane	6%
11	K_2CO_3 + TBAB	1,4-dioxane	6%

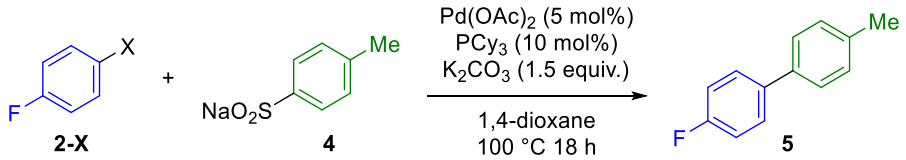
*The aryl sulfinic acid 4-Me-C_6H_4-SO_2H **4-H** was employed instead of sodium sulfinate **4**

Table 3.4. Solvent and additive screening to investigate the impact of the solubility of the sulfinate coupling partner.

Overall, these findings suggest that the solubility of the sulfinate salts and the nature of the solvent are indeed not crucial parameters at this point of optimisation.

3.6. Nature of the Aryl Halide

The nature of the electrophilic coupling partner was next explored (***Table 3.5***). 1-Iodo-4-fluorobenzene **2-I** showed similar sluggish reactivity at 100 °C (*Entry 2*, 6%) compared to the model reaction employing aryl bromide **2** (*Entry 1*, 5%). However, a significant increase to 19% yield of biaryl **5** was observed when aryl triflate **2-OTf** was used as the electrophile (*Entry 3*). Triflate anions coordinate the palladium comparably less than the corresponding bromide and iodide anions, therefore increasing the electrophilicity of the key oxidative addition complex. This is likely to favour the weak binding of the sulfinate to the palladium centre and facilitate the following displacement of the pseudo-halide.[158] Encouraged by this result, diazonium salt **2-N_2BF_4** was synthesised and subjected to the cross-coupling conditions. It was hypothesised that after oxidative addition and loss of N_2, the less coordinating BF_4 anion would further enhance the electrophilicity of the palladium intermediate and favour the coordination of the sulfinate salt. Unfortunately, biaryl **5** was not formed using the diazonium substrate, and solely decomposition products were observed (*Entry 4*).



Entry	*X*	*Yield*	*Entry*	*X*	*Yield*
1	Br	5%	3	OTf	19%
2	I	6%	4	N_2BF_4	0%

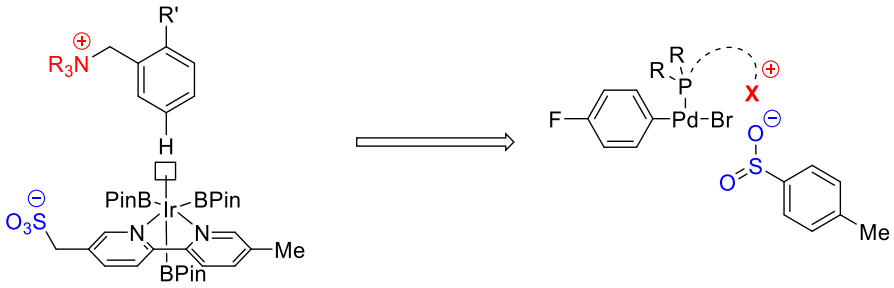
Table 3.5. Nature of the electrophilic coupling partner.

Despite the significant improvement observed when aryl triflates were employed as the electrophilic coupling partner, this lead was not further pursued. Indeed, while this finding was

interesting and provided us with an insight on the importance of the electrophilicity of the key oxidative addition complex, we judged that limiting the optimisation to aryl triflates was not desirable at this stage, as this does not constitute a general solution for lower temperature cross-coupling of aryl sulfinate salts in palladium-catalysed transformations.

3.7. Cationic Phosphine Ligands

Recently, the use of noncovalent interactions has emerged as a powerful strategy to control the selectivity of a range of transition-metal catalysed processes.[159] Inspired by the work of the Phipps group, which elegantly exploited the ion pairing between an anionic ligand and a positively charged substrate to control the selectivity of the iridium-catalysed C-H borylation of 1,2-substituted arenes (***Scheme 3.3.A***),[160] we sought to facilitate the transmetalation step by using positively charged phosphine ligands. It was hypothesised that the sulfinate salt could be brought into close proximity to the palladium centre *via* electrostatic interactions, therefore encouraging its binding and lowering the overall entropic cost of the transmetalation step without changing the nature of the electrophilic coupling partner (***Scheme 3.3.B***).

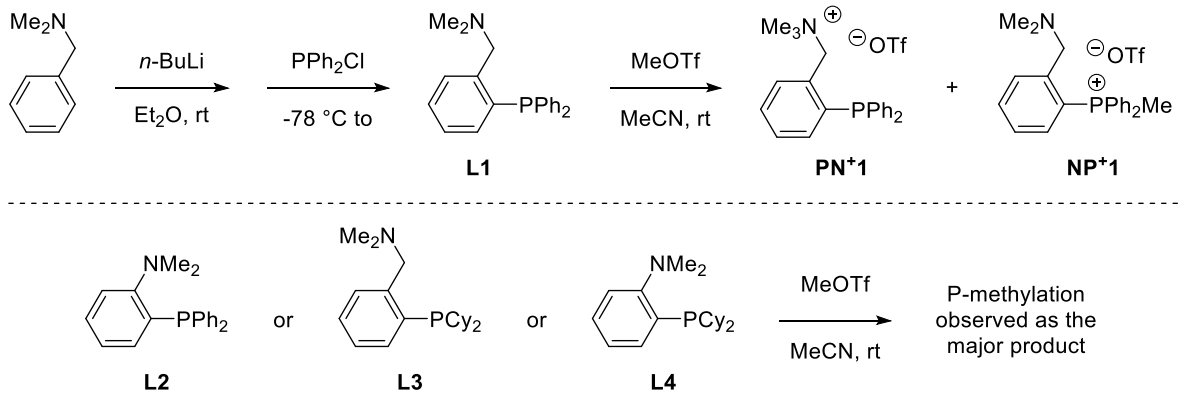


A. Phipps and co-workers ***B.*** Our ligand design

Scheme 3.3. Design of novel cationic ligands.

The two-step synthesis of *ortho*-diphenylphosphinobenzyl-ammonium cation **PN$^+$1** (***Scheme 3.4***) was reported in 2012 by Ooi and co-workers for the enantioselective allylation of α-nitrocarboxylate substrates using enantioenriched binol derivatives as counter anions.[161] However, in our hands the final methylation step was found to be a capricious reaction, and

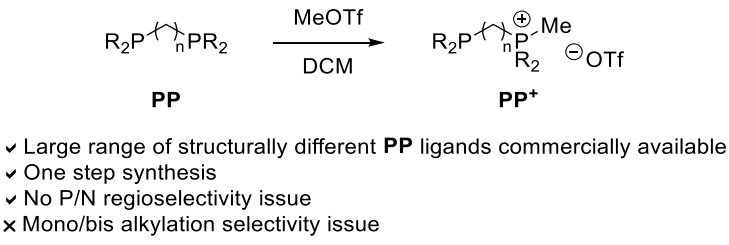
formation of the *P*-methylated side-product **NP⁺1** prevented us from obtaining analytically pure samples of **PN⁺1**.



Scheme 3.4. Capricious synthesis of ligand **L⁺1** and derivatives

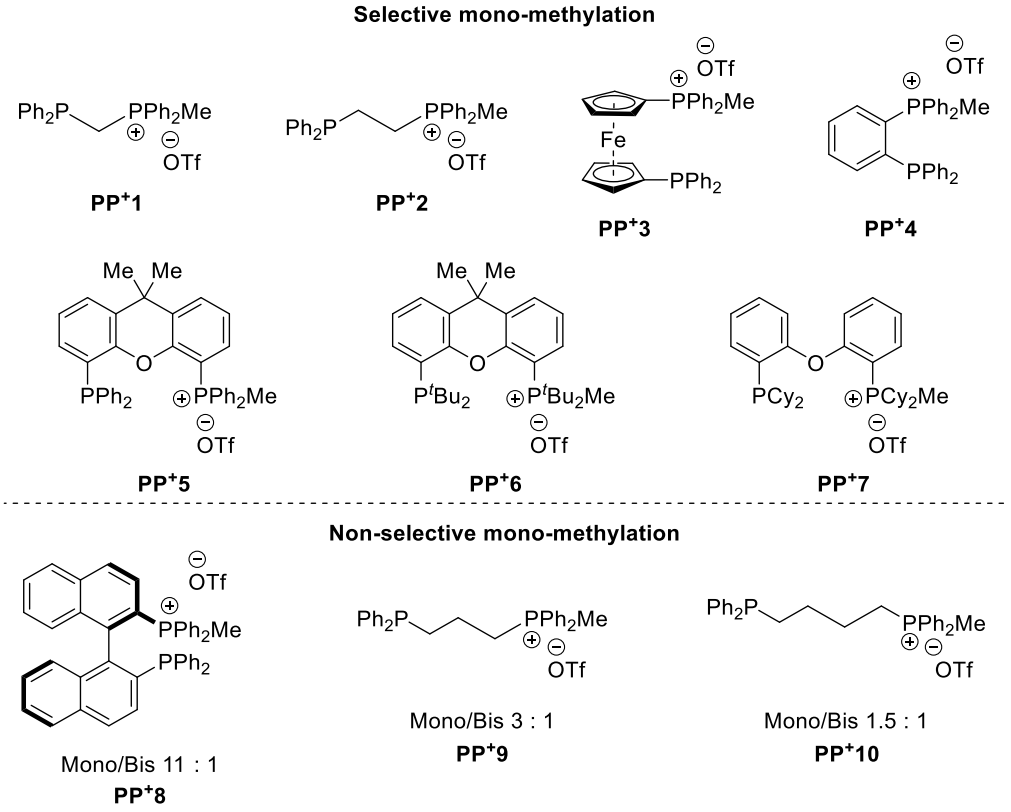
Ligands **L2**-**L4** were also prepared according to literature procedures, but due to the lower nucleophilicity of the nitrogen in **L2** and **L4**, compared to **L1**, or the higher nucleophilicity of the phosphorus in **L3** compared to **L1**, the corresponding *N*-methylated ammonium ligands could not be prepared.

Given the difficulties associated with the synthesis of such ammonium based cationic ligands, the ligand design was revisited. It was envisioned that mono-methylation of symmetrical bis-phosphines **PP** could give us access to a variety of structurally different mono-phosphine ligands **PP⁺** bearing a cationic group, in a single synthetic step from commercial compounds (***Scheme 3.5***). With this new route, the P/N regioselectivity issue was bypassed, however, bis-alkylated side-products could not be separated when formed.



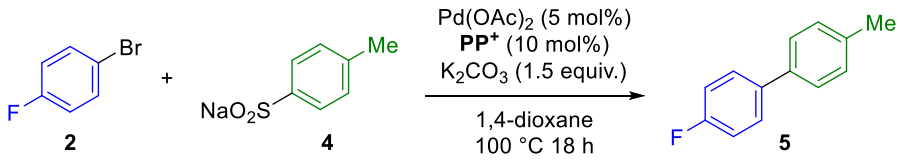
Scheme 3.5. Novel ligand design based on bis-phosphine ligands

Ten bis-phosphine ligands were selected to evaluate the potential of these cationic ligands **PP$^+$** in desulfinative cross-coupling reactions (***Scheme 3.6***). Methylation of these bis-phosphine ligands was performed using a slight excess of the bis-phosphine compared to the methylating agent to avoid bis-methylation (**Experimental Section 7.3.3.3**). These conditions allowed the selective mono-methylation of seven bis-phosphines **PP$^+$1** – **PP$^+$7**, but inseparable mixtures of mono- and bis-methylated products were obtained with ligands **PP$^+$8** – **PP$^+$10**.



Scheme 3.6. Alternative ligand design based on bis-phosphine ligands.

Ligands **PP$^+$1** – **PP$^+$8** and ammonium ligand **PN$^+$1** (5 : 1 mixture of P/N methylated products) were then used under the typical cross-coupling conditions (***Table 3.6***). A 2:1 ratio of ligand to palladium was employed as these mono-methylated bis-phosphines should not be acting as bidentate ligands.



Entry	*Ligand*	*Yield*	*Entry*	*Ligand*	*Yield*
1	**PP$^+$1**	3%	6	**PP$^+$6**	1%
2	**PP$^+$2**	6%	7	**PP$^+$7**	3%
3	**PP$^+$3**	8%	8	**PP$^+$8**	4%
4	**PP$^+$4**	8%	9	**PN$^+$1**	3%
5	**PP$^+$5**	12%	10	**PCy$_3$**	5%

Table 3.6. Cationic phosphine ligands under cross-coupling reaction conditions.

Unfortunately, none of these selected cationic ligands produced the desired cross-coupling product **5** in more than 12% yield. Ligand decomposition under prolonged heating might be responsible for the poor performance of these phosphonium ligands. Control experiments with non-methylated bis-phosphine ligands produced the biaryl coupling product in equal or better yields compared to their methylated analogues. Therefore, this strategy was not further investigated.

3.8. Other Phosphine Ligands

The number of phosphines that have been developed over the last three decades for palladium-catalysed cross-coupling reactions is immense, and only a limited number of ligands can be screened by hand in a reasonable amount of time. In this context, High Throughput Experimentation (HTE) is an invaluable tool for the optimisation of catalytic organic reactions, as it allows the rapid and accurate screening of large ligand libraries as well as other reaction parameters under reliable, controlled, and reproducible conditions, while using minimum amounts of materials.[162-163] Thanks to our collaboration with Vertex Pharmaceuticals, we were given the opportunity to screen a wide range of ligands using state of the art high throughput facilities located in Boston. The High Throughput Screening (HTS) experiments discussed in

this section were designed by myself with the help of Dr Liana Allen and Dr Chris Davis, and performed by Dr Liana Allen at Vertex in Boston.

The coupling reaction between 4-bromoanisole **2-OMe** and 4-methylbenzene sulfinate salt **4** was performed at 100 °C in 1,4-dioxane over 20 hours (***Figure 3.1***). 4-Bromoanisole **2-OMe** was chosen instead of 1-bromo-4-fluorobenzene **2** as the electrophilic coupling partner in order to get better product detection by mass spectrometry. In hindsight, this substrate was not ideal as the corresponding product **5-OMe** was not detected by ESI either. Product **5-OMe** was synthesised independently, and was identified in the reaction mixture from its HPLC retention time. Three equivalents of Cs_2CO_3 were employed as it was previously demonstrated that a carbonate base was required to allow catalyst turnover and the caesium cation was highly efficient for promoting transmetalation (see **Sections 2.5.2** and **2.8**). Reaction yields were not calculated against an internal standard. Given the high reproducibility of HTE, and the possibility to systematically inject an accurate volume for analysis of the crude reaction mixtures, quantitative data could be obtained directly from the peak area detected by HPLC (**Experimental Section 7.3.4.3**).

In an initial set of experiments (***Figure 3.1.***), 48 catalytic systems were screened, featuring a wide range of structurally diverse phosphine ligands, ranging from simple alkyl phosphines (CatacXium A, (t-Bu_3)P), bis-phosphine with different bite angles (DPPF, BINAP, Xantphos), Buchwald biphenyl mono-phosphines (BrettPhos, AlPhos, XPhos) and other miscellaneous ligands (MorDalphos, QPhos). NHC ligands were also included in this initial screen. The full list of ligands and their corresponding structures can be found at pages X-XII.

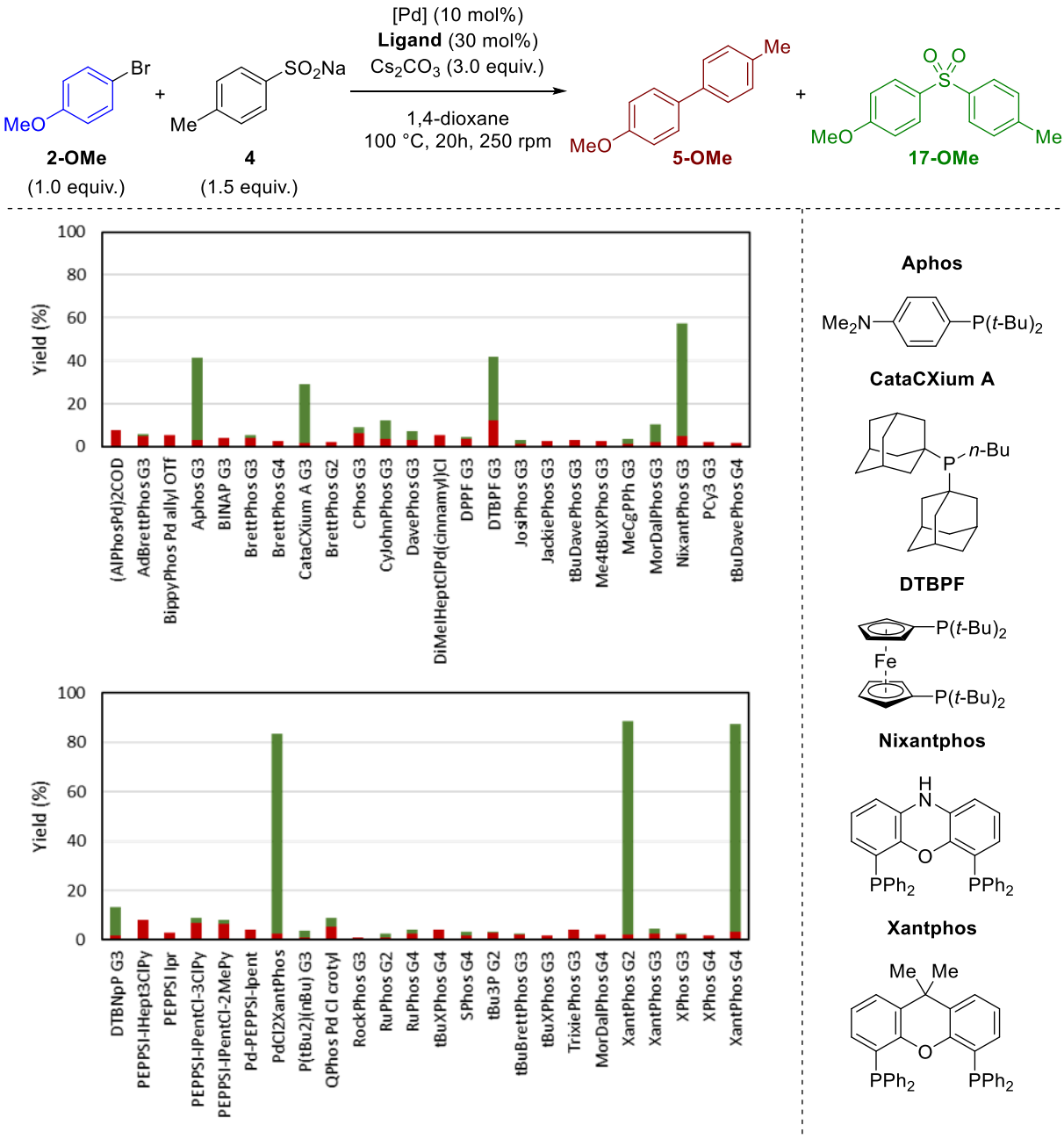


Figure 3.1. HTS#1: Screening of a large range of catalysts with the same reaction conditions. Red bars: biaryl product **5-OMe**. Green bars: sulfone product **17-OMe**.

Remarkably, none of these ligands provided the cross-coupling product **5-OMe** in significant quantities (red bars), with a maximum amount of 12% obtained with DTBPF. This once again shows the challenge associated with performing such desulfinative cross-coupling reactions at 100 °C. Instead, sulfone **17-OMe** was found to be the major product with APhos, CataCXium A, DTBPF, Nixantphos, DTBNpP and Xantphos ligands (green bars). Sulfone **17-**

OMe was formed in yields above 80% with Xantphos and Nixantphos ligands, independent of the nature of the palladium precatalyst ($PdCl_2$Xantphos, Pd-Xantphos G2, Pd-Xantphos G4).

A smaller set of 16 ligands was then selected to investigate the importance of the solvent for the formation of biaryl **5-OMe** (***Figure 3.2***). 1,4-Dioxane, toluene, and DMF were selected as the solvents of choice, as these three solvents are common for desulfinative cross-coupling reactions (see **Sections 1.2.3-1.2.5**). The use of (n-Bu)$_4$NCl as an additive has been shown to be either beneficial or detrimental to the Pd/Xantphos catalysed formation of diaryl sulfones depending on the nature of the coupling partners (see **Section 4.1**).[164] Therefore, all reactions of this second screening were also performed with or without (n-Bu)$_4$NCl as an additive to investigate its importance for the formation of the desired biaryl product.

Similarly to the previous screen, the yields of biaryl product **5-OMe** remained low: among the 96 reactions, 81 resulted in a yield lower than 15%. The average yield of this screening was 5.8%, and a maximum yield of 21% was obtained in toluene, with (n-Bu)$_4$NCl and ligand **L3** (see ***Scheme 3.7*** for the structure of the ligands **L1** – **L16**). In contrast, sulfone product **17-OMe** was again formed selectively and in high yields with Xantphos-Pd G4 (**L5**), Nixantphos-Pd G3 (**L6**) and Xantphos in combination with $Pd(OAc)_2$ (**L10**). The presence of (n-Bu)$_4$NCl did not provoke any significant change in product distribution in 1,4-dioxane. However its presence slightly increased the yields of biaryl product **5-OMe** in toluene and DMF. For the sulfone formation reaction with Xantphos-based ligands, higher yields were observed in 1,4-dioxane and toluene compared to DMF, but high conversions were observed in all cases, with the exception of Nixantphos-Pd G3 (**L6**) in DMF which did not lead to any sulfone formation.

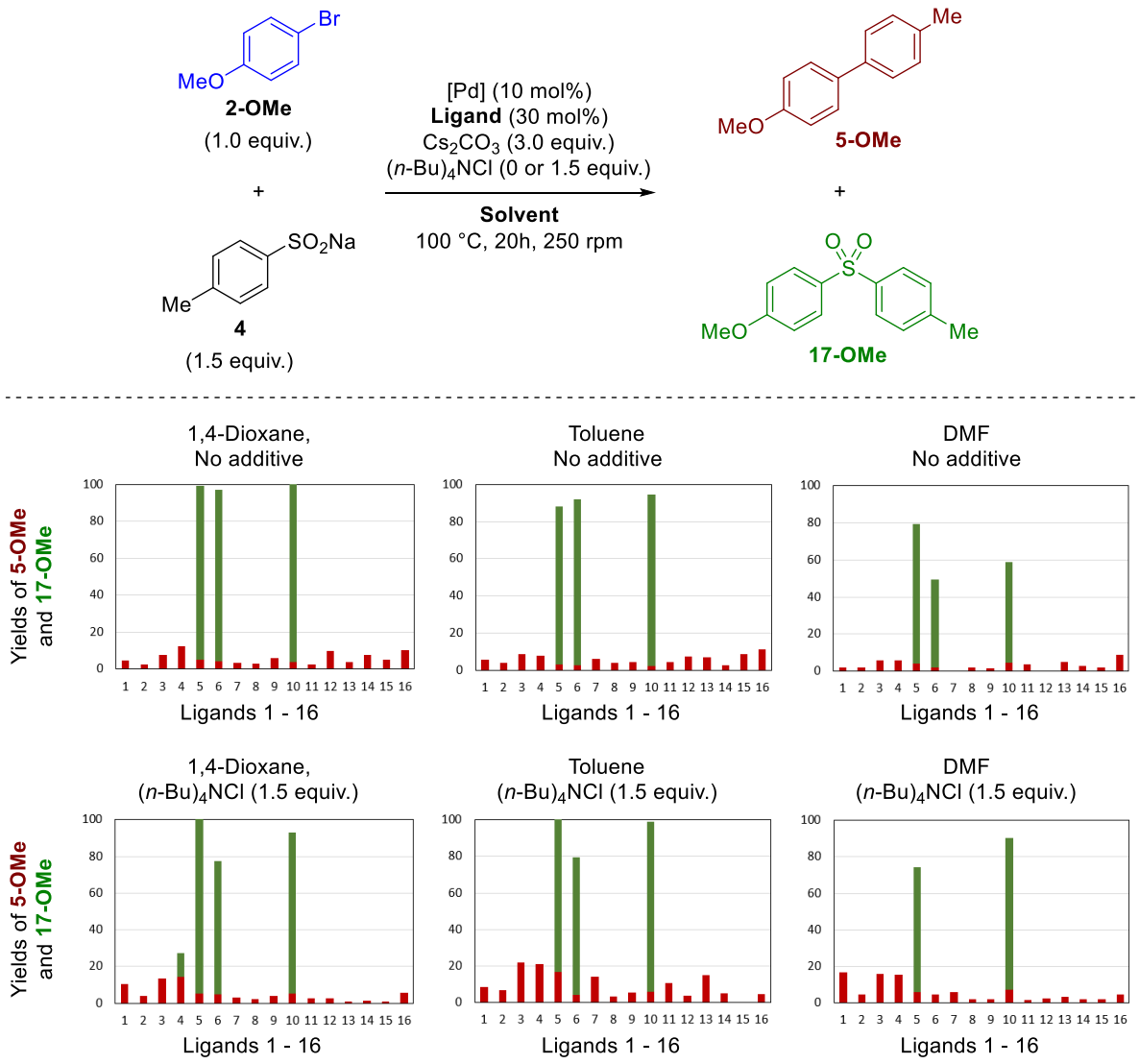
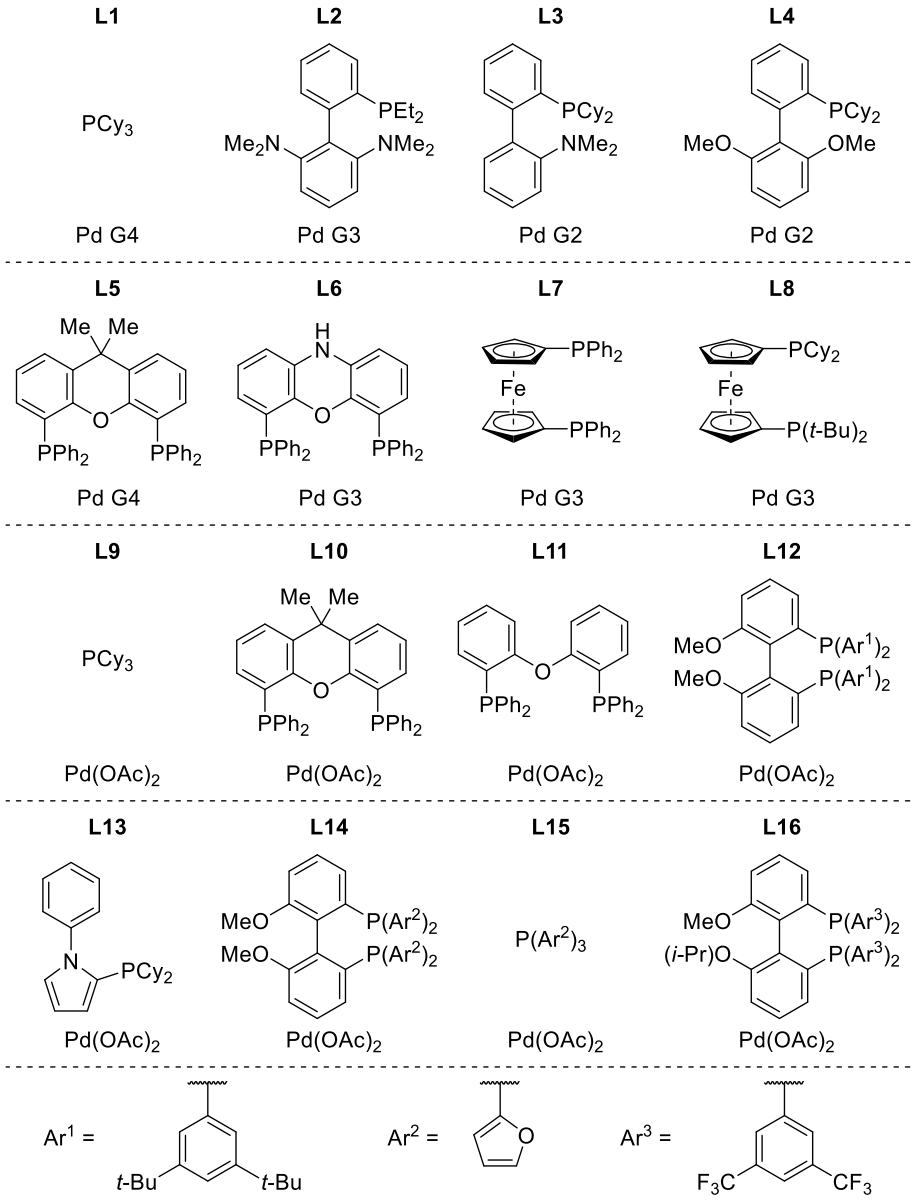


Figure 3.2. HTS#2: Screening of solvents and ligands with or without (n-Bu)$_4$NCl as an additive. See **Scheme 3.7** for the structures of the ligands **L1** – **L16** (next page).



Scheme 3.7. HTS#2: Ligands corresponding to ***Figure 3.2***.
Pd GX refers to the structure of the Pd precatalyst (10 mol%) as defined in page X,
$Pd(OAc)_2$ refers to the combination of the ligand (30 mol%) with $Pd(OAc)_2$ (10 mol%).

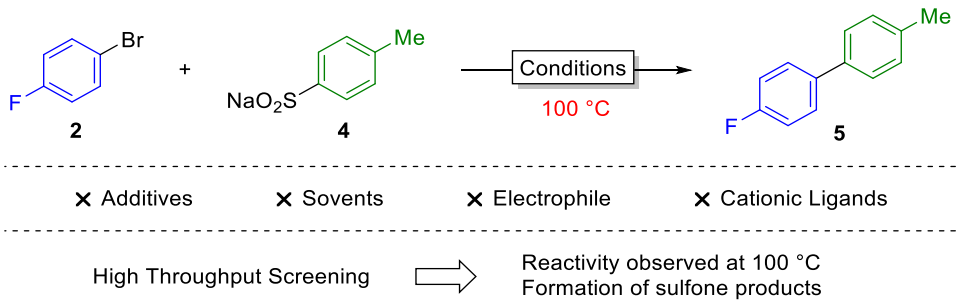
Similar trends were observed when these HTS were repeated with 2-pyridyl sulfinate **1** instead of carbocyclic sulfinate **4**. Results of these additional HTS can be found in the **Experimental Section 7.3.4.**

The outcome of these HTS illustrate once again the challenge associated with lower temperature cross-coupling reactions. Indeed, among the 144 conditions assessed, biaryl product **5-OMe**

was never detected in yields above 21%. The formation of sulfone **17-OMe** is, however, of particular interest, and will be discussed in depth in **Chapter 4**.

3.9. Summary of the Screening Strategy

A number of attempts to promote the cross-coupling reaction between aryl bromide **2** and aryl sulfinate salt **4** at 100 °C were described through this chapter and are summarised in ***Scheme 3.8.***



Scheme 3.8. Summary of our attempts to perform desulfinative cross-coupling reactions at 100 °C.

Based on the mechanistic studies of **Chapter 2**, the use of metal and ammonium additives was first explored to facilitate the turnover limiting transmetalation step. However, this additive based strategy was unsuccessful, as yields mostly remained under 10%, comparable to the additive-free control reaction. The nature of the solvent was not found to be crucial at this stage of optimisation. Aryl triflates were found to be better electrophilic coupling partners compared to aryl bromides and iodides at 100 °C. However, further optimisation was pursued with the more challenging aryl bromide substrates.

A new class of phosphine ligands, bearing a remote phosphonium group was designed to assist the transmetalation step. These phosphines were readily synthesised from commercially available bis-phosphine ligands *via* a simple methylation reaction. The mechanistic rational for this ligand design was to profit from the anionic nature of the sulfinate coupling partner and exploit ligand/substrate electrostatic interactions to reduce the entropic cost of the

transmetalation step. However, this strategy was unsuccessful as the desired biaryl cross-coupling product was not formed in yields above 12%.

Finally, we used High Throughput Experimentation to probe the reactivity of a large range of structurally different ancillary ligands. These screening experiments confirmed that reducing the temperature and maintaining the high efficiency of desulfinative cross-coupling reactions is a difficult challenge as biaryl product **5-OMe** was never formed in synthetically useful yields.

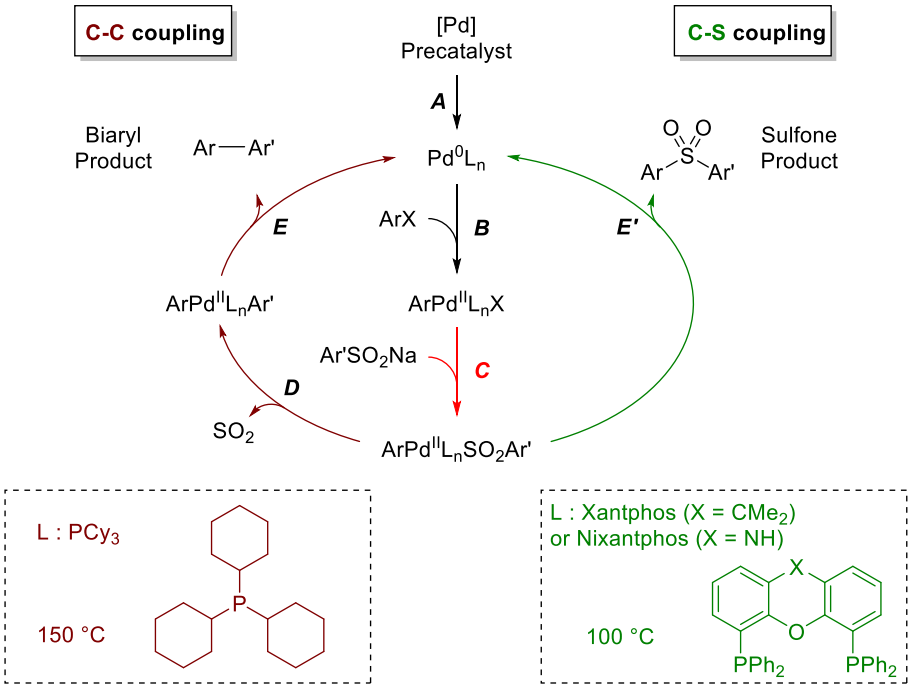
Interestingly, while starting material was recovered in most reactions, full conversion to the sulfone analogue of biaryl **5-OMe** was observed when Xantphos and Nixantphos ligands were used. This unique reactivity and the use of Xantphos-type ligands for desulfinative cross-coupling reactions are discussed in depth in **Chapter 4**.

Chapter 4 – Xantphos-Like Ligands

4.1. Introduction

4.1.1. Comparison of the Mechanisms for Sulfone or Biaryl Formation

Our HTE study (**Section 3.8**) revealed that sulfone products are formed in high yields when Xantphos or Nixantphos are employed as ligands. This finding is of significant importance because both C-S and C-C bond formation reactions follow very similar mechanisms (***Scheme 4.1***).

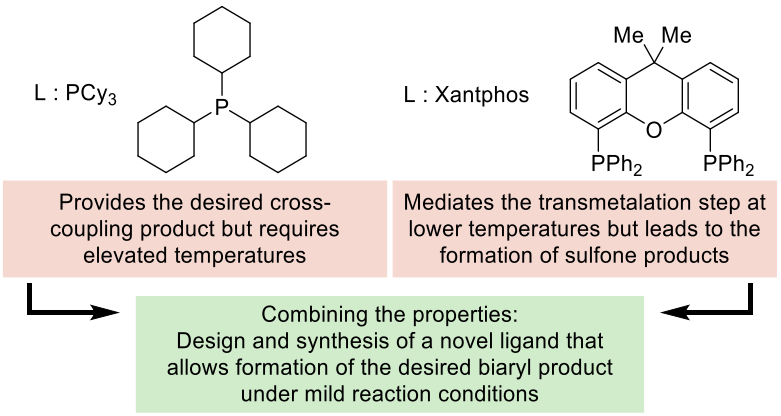


Scheme 4.1. Palladium-catalysed C-C and C-S coupling reactions: comparison of the mechanisms.

After generation of the active catalyst Pd^0L_n by either reduction of $Pd(OAc)_2$ or dba/phosphine exchange, if $Pd_2(dba)_3$ is the palladium source employed (***Step A***), oxidative addition into the carbon-(pseudo)halide bond of the electrophile leads to an oxidative addition complex $ArPd^{II}L_nX$ (***Step B***). Such oxidative addition complexes are known with both PCy_3 (**Chapter 2**) as well as Xantphos ligands (**Section 4.1.2**). Nucleophilic attack of the aryl sulfinate coupling partner subsequently displaces the (pseudo)halide from $ArPd^{II}L_nX$ to form an aryl palladium

sulfinate complex $ArPd^{II}L_nSO_2Ar'$ (***Step C***). Such complexes were studied in **Chapter 2** with PCy_3 as a ligand, but have never been reported with Xantphos as the ligand. It is only after such aryl palladium sulfinate complexes are formed that the mechanisms of both sulfone and biaryl formation diverge. With PCy_3 as a ligand, it was shown in **Chapter 2** that extrusion of SO_2 (***Step D***) is facile with carbocyclic sulfinates, and subsequent reductive elimination (***Step E***) affords the biaryl product and regenerates the zero valent palladium species. In contrast, sulfone products must be formed *via* direct reductive elimination (***Step E'***) from the putative aryl palladium sulfinate complex (Xantphos)Pd(Ar)(SO_2Ar').

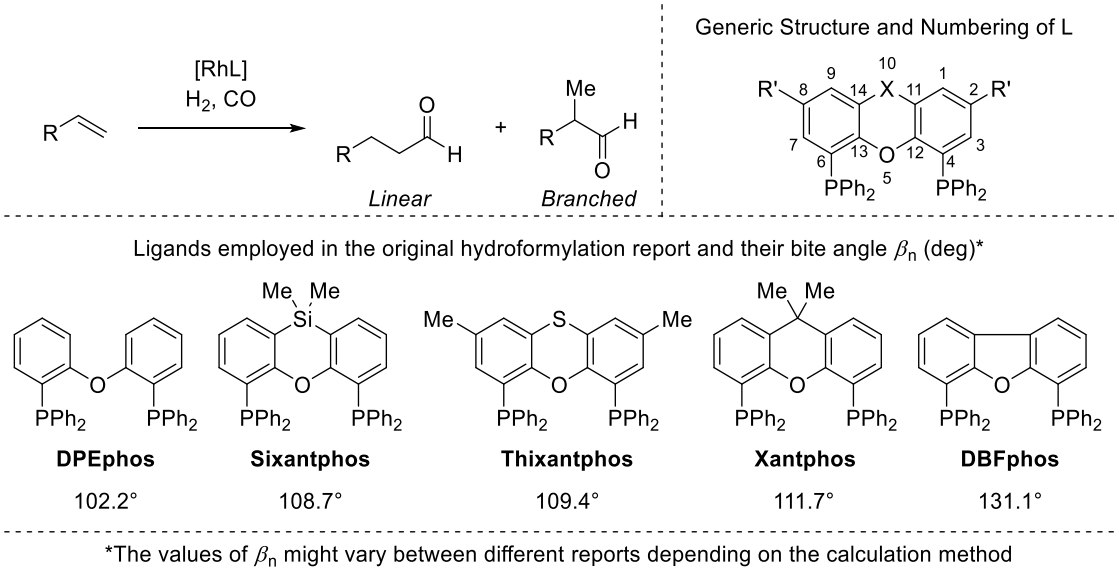
The transmetalation step (***Step C***) is therefore common to both reaction pathways. As the formation of sulfone **5-OMe** was observed to be quantitative at 100 °C in the reaction between 4-bromoanisole **2-OMe** and 4-methylbenzenesulfinate salt **4** (see **Section 3.8**), this suggests that the Xantphos ligand has the unique ability to promote the transmetalation between oxidative addition complex (Xantphos)Pd(Ar)(Br) and aryl sulfinate **4** at much reduced temperatures compared to PCy_3. In this **Chapter**, a study is presented that aimed to understand what structural features of the Xantphos ligand are that allow for such reactivity, and thus use Xantphos-like ligands to promote transmetalation followed by extrusion of SO_2 at 100 °C or below. In other words, our objective was to combine the properties of Xantphos and PCy_3 to allow lower temperature desulfinative cross-coupling reactions (**Scheme 4.2**).



Scheme 4.2. Combining the properties of PCy_3 and Xantphos for lower temperature desulfinative cross-coupling reactions.

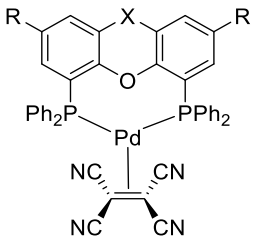
4.1.2. Xantphos Palladium Complexes

The van Leeuwen group pioneered the used of Xantphos as an ancillary ligand for transition-metal catalysis in 1995.[165] In their original report, they studied the effect of the bite angle on the regioselectivity of rhodium-catalysed hydroformylation reactions in a series of xanthene-like aromatic ligands (***Scheme 4.3***). Since these seminal studies, the rigidity and large natural bite angle of Xantphos and related ligands have proved to be beneficial for an immense range of cross-coupling reactions.[166-167]



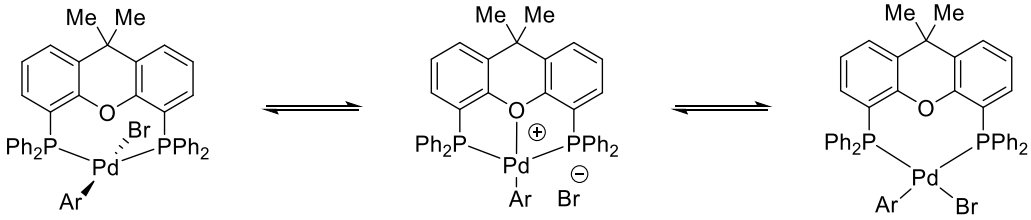
Scheme 4.3. Original report of xanthene-like phosphine ligands.

Pd(0) tetracyanoethylene complexes were obtained and characterised by X-ray crystallography with the same ligand series (***Scheme 4.4***).[168] In these complexes, the measured bite angles were found to be smaller than the calculated natural bite angle (104.6° against 111.7° for Xantphos), and such a difference was rationalised by the elongation of the Pd-P bond lengths due to electronic reasons. Generally, ligands with a large bite angle do not necessarily accelerate the rates of oxidative addition.[166]



Scheme 4.4. Pd(0) tetracyanotehtylene complexes

In 2002, both the Buchwald and van Leeuwen groups independently reported that Xantphos forms *trans*-chelating aryl Pd(II) bromide complexes in the solid state, with the oxygen atom located at the apical position of the square pyramidal complex (***Scheme 4.5.A***).[169-170] The *cis*-isomer remains however available in solution: the broad signal observed by ^{31}P NMR spectroscopy at room temperature at which *cis*-*trans* equilibrium takes place on the NMR time-scale resolves upon cooling down the sample to –40 °C to give a sharp singlet (*trans*-complex ***A***) and an AB system (*cis*-complex ***C***).[170] In contrast, the DPEphos oxidative addition complex is *cis* in both solid state and solution due to its smaller bite angle.



A.

trans-compound, major in solution, sharp singlet observed by ^{31}P NMR spectroscopy at -40 °C

B.

cationic $\kappa^3_{P,O,P}$ pincer-type complex, presence in solution suggested by high molar conductivities

C.

cis-compound, minor in solution, AB system observed by ^{31}P NMR spectroscopy at -40 °C

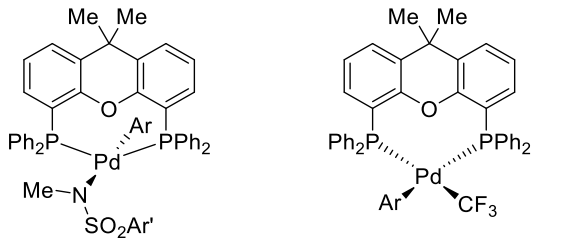
Scheme 4.5. *Cis*/*trans* equilibrium of aryl palladium(Xantphos) bromide complexes.

This *cis*-*trans* isomerisation mechanism of (Xantphos)Pd(Ar)(Br) was proposed to involve a cationic $\kappa^3_{P,O,P}$ pincer intermediate (complex ***B***), in which the oxygen atom coordinates the palladium centre. These pincer complexes were characterised by X-ray crystallography for Xantphos and other xanthene-like ligands, and their presence in solution was deduced from the

high values of conductivity measured.[158, 170] These cationic complexes were also proven to be competent catalysts in amination chemistry.[171]

The transmetalation step is specific to each nucleophile, meaning there are no general trends associated with the effect of the ligand bite angle. Literature data suggests that larger bite angle ligands are more likely to promote the formation of 5-coordinate complexes during the transmetalation process.[166]

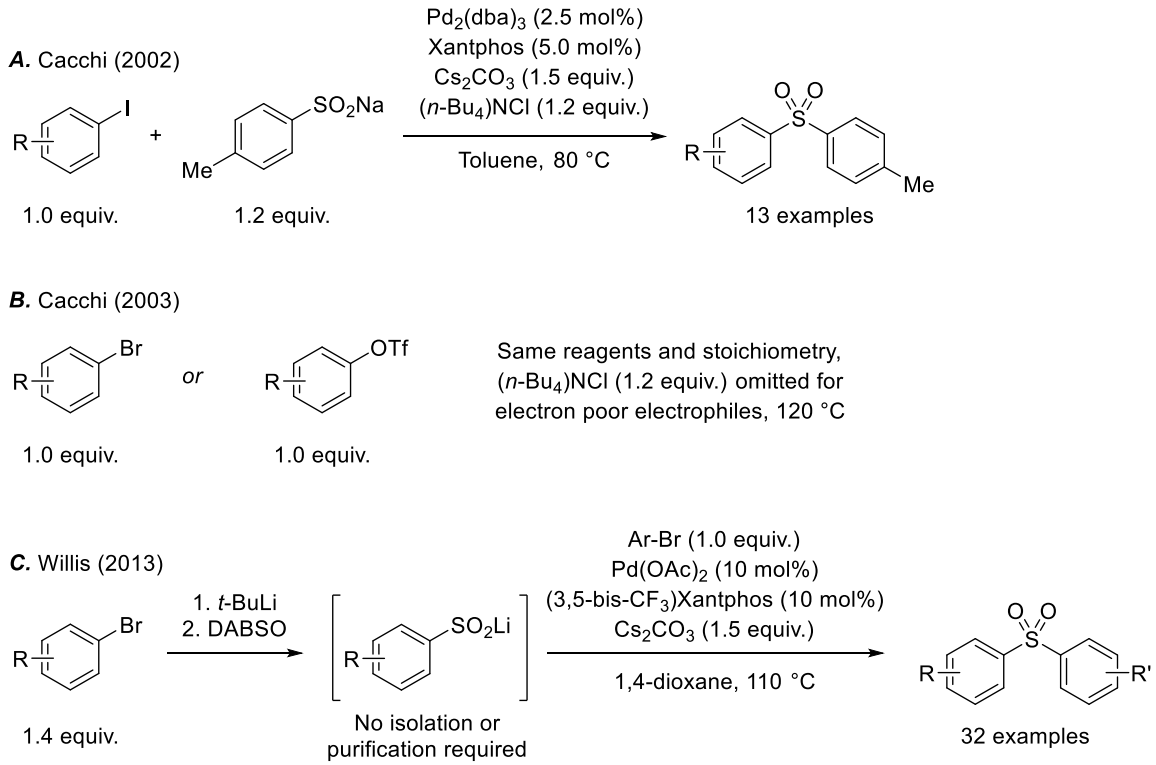
Post transmetalation complexes have been described in the context of amidation chemistry,[172] in which Xantphos has been observed to be *trans*-chelating (***Scheme 4.6.A***). Complex ***A***, as well as other amidate complexes, were found to be in equilibrium with their *cis*-isomers in solution, from which reductive elimination is believed to happen. In contrast, (Xantphos)Pd(Ar)(CF_3) ***B*** is *cis* in the solid state.[173] Although the free energy of its *trans*-isomer was calculated to be only higher by 0.9 kcal.mol^{-1}, the high energy barrier of the *cis*-*trans* transition state precludes isomerisation in solution,[174] and reductive elimination proceeds smoothly from complex ***B*** to give trifluorotoluene. As a general trend, reductive elimination in square planar Pd(II) complexes is strongly favoured by *cis* wide bite angle bidentate phosphines.[166]



Scheme 4.6. Post transmetalation Xantphos Pd(II) complexes.

4.1.3. Palladium-Catalysed Coupling of Aryl (Pseudo)Halides and Aryl Sulfinate Salts

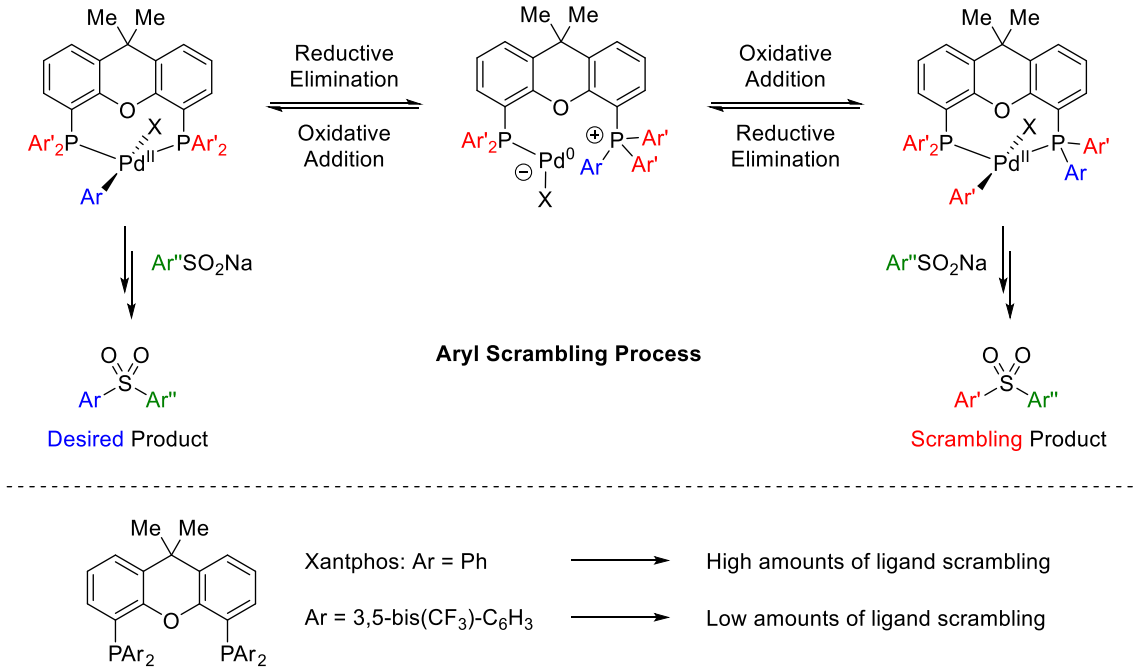
Cacchi and co-workers described the first palladium-catalysed cross-coupling of aryl iodides and aryl sulfinate salts in 2004 (***Scheme 4.7.A***).[175] A large range of mono and bis-phosphine ligands were explored, but sulfone formation was observed exclusively with Xantphos. The strong σ-donor NHC ligand class also failed to promote the reaction, although they were more recently used in a similar nickel-catalysed cross-coupling.[176] Combination of Cs_2CO_3 and (n-Bu)$_4$NCl proved to be optimal, and although up to 80% yield was obtained at 40 °C the scope of the reaction was obtained at 80 °C. Sodium 4-methylbenzene sulfinate was the only sulfinate salt employed, and the scope focused on the aryl halide coupling partner. Electron-rich (4-OMe-C_6H_4) or electron-poor (4-CF_3-C_6H_4 and 4-NO_2-C_6H_4) substituents were tolerated on the electrophile, and excellent chemoselectivity was observed when an aryl bromide was also present on the aromatic ring, however, *ortho*-substituents were not tolerated.



Scheme 4.7. Palladium-catalysed sulfone formation from aryl (pseudo)halides and aryl sulfinate salts.

By increasing the temperature of the reaction to 120 °C, the Cacchi group further extended the scope of their Pd/Xantphos-catalysed sulfone formation to aryl bromides and triflates.[164, 177] Under these conditions, the (n-Bu)$_4$NCl additive was only needed for electron-rich or neutral electrophiles, whereas its omission gave higher yields with electron-deficient ones. Once again, the sulfinate scope remained unexplored and sodium 4-methylbenzene sulfinate was the only sulfinate employed.

The Willis group revisited this coupling reaction in 2013 in order to expand the scope of the aryl sulfinate coupling partner.[178] Sulfinate salts were prepared by the addition of organolithium reagents to DABSO and were coupled without the need for isolation or purification, allowing the synthesis of a large range of unsymmetrical diaryl sulfones in an efficient two-step one-pot procedure. Good conversions were obtained at 85 °C with aryl iodides as the electrophilic coupling partners. Given the nature of the one-pot process and the presence of sulfinate-formation related bi-products, high catalyst loadings (10 mol% Pd(OAc)$_2$) were required to ensure high reaction yields. As a consequence, large amounts of side-products were observed due to aryl scrambling (***Scheme 4.8***).[179-181] To circumvent this problem, a range of Xantphos analogues bearing different aryl or alkyl groups on the phosphorus atoms were synthesised, and using the more electron-withdrawing 3,5-bis(CF_3)Xantphos derivative suppressed the formation of such aryl scrambling products. A detailed analysis of these substituent effects will be made in **Section 4.3**. The scope was performed with this electron-poor Xantphos variant which required a higher reaction temperature of 110 °C for efficient couplings. With these reaction conditions, (n-Bu)$_4$NCl was not required as an additive.



Scheme 4.8. Mechanism of ligand scrambling side product formation.

Overall, it appears that Xantphos and its electron-deficient analogue have so far been the only ligands able to promote the coupling between aryl (pseudo)halides and arylsulfinates salts to form diaryl sulfone compounds. This is consistent with our extensive HTE study in which sulfone formation was observed in synthetically useful yields exclusively with Xantphos and Nixantphos ligands (**Section 3.8**). Examination of these previous reports showed that depending on the reaction conditions, product formation can be observed at temperatures as low as 40 °C, demonstrating the high potential of this backbone to promote transmetalation between oxidative addition complexes and poorly nucleophilic sulfinate salts.

4.2. Mechanistic Insights

4.2.1. Importance of the Sulfinate Counter Cation

The importance of the counter cation for the Pd/Xantphos-catalysed sulfone formation reaction was assessed using the same method that was used for the Pd/PCy_3 catalysed desulfinative cross-coupling reaction (**Section 2.5.2**). Oxidative addition complex **19** was prepared from allyl palladium cyclopentadiene **18**, Xantphos and aryl bromide **2** (**Experimental Section 7.4.1**).

Stoichiometric reactions between complex **19** and 4-methylbenzene sulfinate salts: **4**, **4-Li**, **4-K**, **4-Cs**, **4-TMA**, **4-TBA**, were monitored by HPLC at 95 °C in 1,4-dioxane. The reactivity of these sulfinate salts followed the same trends that were observed in the desulfinative cross-coupling reaction (**Figure 4.1**). No product formation was observed with lithium and sodium sulfinate salts **4-Li** and **4**, whereas potassium and tetrabutylammonium sulfinate salts **4-K** and **4-TBA** were converted to sulfone **17** with similar reaction rates. These rates were outperformed by caesium sulfinate salt **4-Cs**, but as was previously observed, tetramethylammonium sulfinate salt **4-TMA** showed the best reactivity. Product yields were found to be generally low due to decomposition of oxidative addition complex **19** and the formation of by-product **17-H** *via* aryl scrambling between the diphenylphosphino groups and the 4-F-C_6H_4 group of oxidative addition complex **19** according to ***Scheme 4.8***.

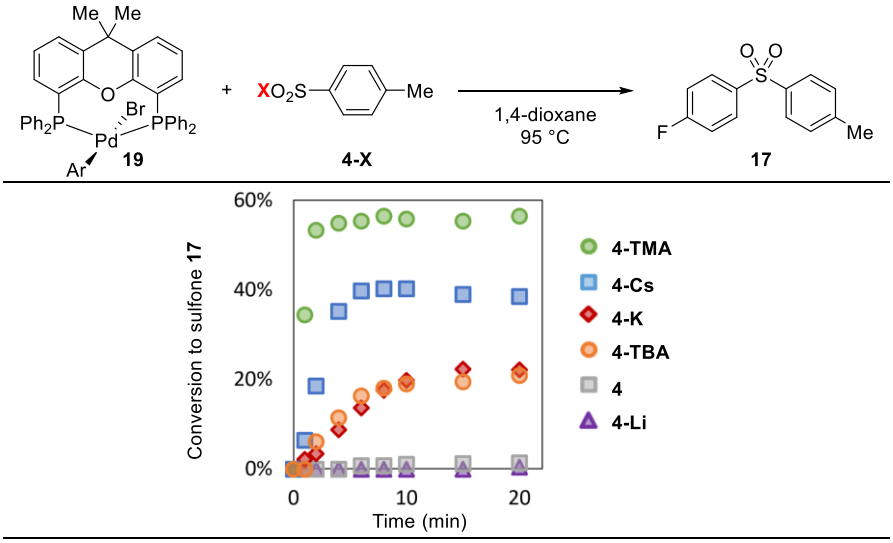


Figure 4.1. Impact of the sulfinate counter cation on the rate of sulfone formation.

4.2.2. Reversibility of the Transmetalation Step

We propose that the final reductive elimination step from the putative palladium sulfinato complex (Xantphos)Pd(Ar)(SO_2Ar') is not affected by the nature of the sulfinate counter cation. To the best of our knowledge, such a dependence of reductive elimination on the presence of inorganic salts has not been observed in palladium-catalysed cross-coupling reactions.[129-130,

[182-184] Furthermore, the alkali metal bromide salts generated upon transmetalation have poor solubilities in 1,4-dioxane and are therefore not likely to influence the rate or mechanism of the final reductive elimination step, as shown at the end of this section.

In order to assess the reversibility of the transmetalation step, the rate of sulfone formation was measured in the stoichiometric reaction between oxidative addition complex **19** and tetrabutylammonium sulfinate **4-TBA** in the presence of excess TBAB (***Figure 4.2.A***). Sulfinate **4-TBA** was chosen over its caesium or potassium analogues **4-Cs** and **4-K** to suppress the potential influence of cation metathesis between the sulfinate salt and the tetrabutylammonium additive on the rate of the reaction.

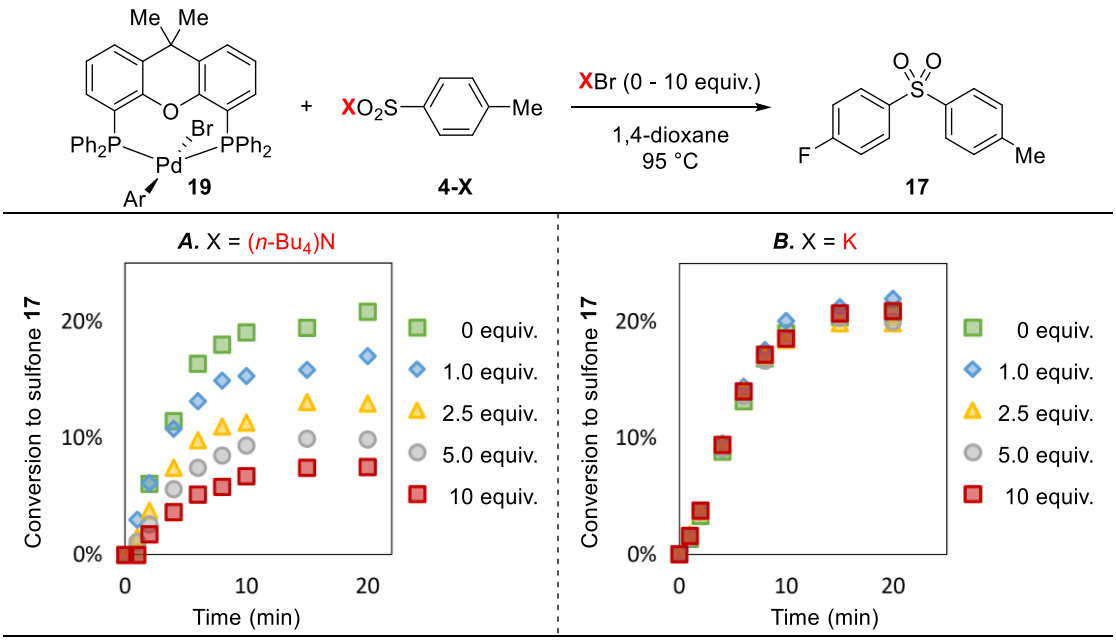


Figure 4.2. Effect of the addition of bromide salts on the rate of sulfone formation.

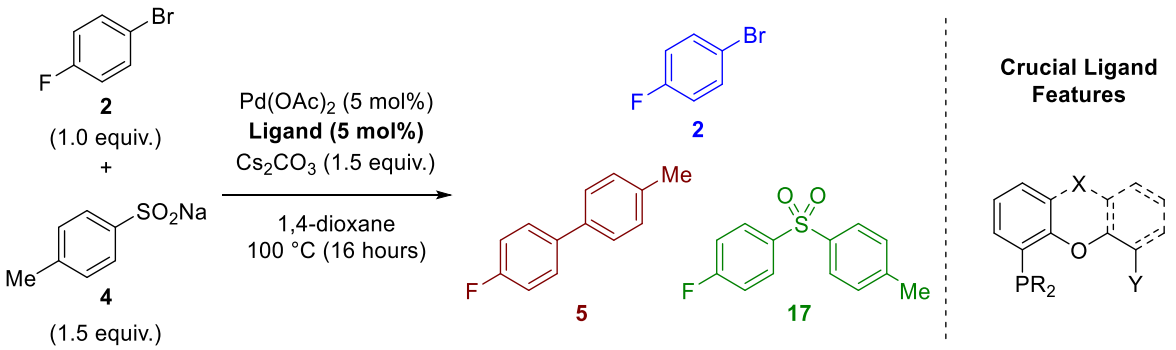
From this experiment, it is clear that the rate of sulfone formation decreases upon increasing the concentration of the tetrabutylammonium bromide salt, suggesting that transmetalation is a reversible process. However, when the same experiment was reproduced using the potassium sulfinate **4-K** together with potassium bromide (***Figure 4.2.B***), the rate of sulfone formation remained unaffected by the amount of KBr present in solution. These experiments suggest that

even if transmetalation is intrinsically a reversible process, it remains irreversible under the reaction conditions due to the poor solubility of KBr in 1,4-dioxane.

4.3. Key Structural Features of the Xantphos Ligand

4.3.1. Model System

In order to assess what the crucial features of the Xantphos ligand are, the reactivity of a range of xanthene-like ligands was compared in the cross-coupling reaction of 1-bromo-4-fluorobenzene **2** with carbocyclic 4-methylbenzene sodium sulfinate salt **4** at 100 °C (***Scheme 4.9***).

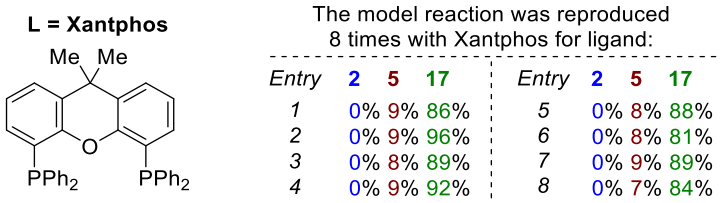


Scheme 4.9. Model reaction and substrates for the systematic study of the Xantphos ligand.

Tetramethylammonium carbonate is not a commercially available chemical, and requires special equipment for synthesis.[185] Therefore, Cs_2CO_3 was chosen as a stoichiometric additive according to the discussion of **Section 4.2.2.** 1,4-Dioxane was chosen as the reaction solvent as it was observed in the HTE study that sulfone formation happens in generally higher yields in 1,4-dioxane compared to toluene and DMF, and under these conditions, $(n\text{-Bu})_4NCl$ was omitted as it did not impact the outcome of the reaction (**Experimental Section 7.3.4**).

Reaction yields were determined by HPLC using 1,3,5-trimethoxybenzene as an internal standard. To assess the reproducibility of this method, a control experiment with Xantphos ligand was reproduced with each new set of ligands, ensuring that the stock solutions were correctly prepared (***Scheme 4.10***). Overall, this standard reaction with Xantphos ligand was

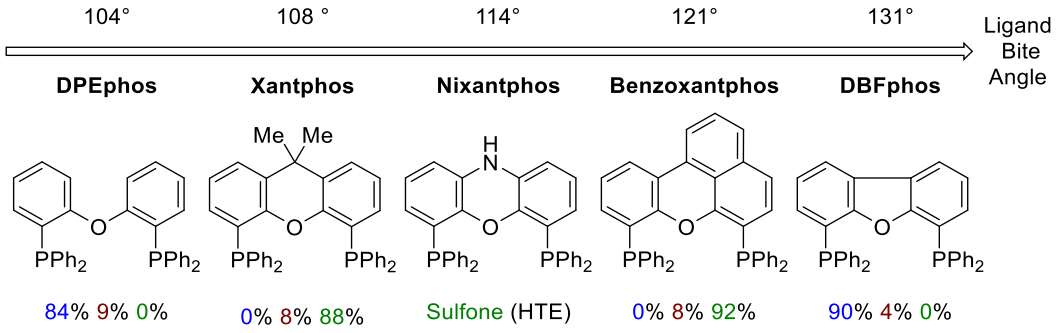
repeated 8 times, giving sulfone cross-coupling product **8** in 8 ± 1% yield and **17** in 88 ± 5%. However, because each of the reactions with other ligands were performed once without being reproduced, the maximum deviation needs to be considered instead of the standard deviation, which corresponds to an error of ± 8% on all the yields reported in this section. Yields were reported in the same order: aryl bromide **2** / biaryl **5** / sulfone **17**, in all the schemes in this section.



Scheme 4.10. Reproducibility of the reaction.

4.3.2. Variations of the Xanthene Backbone

The effect of the ligand bite angle was first examined. The HTE results showed that neither the sulfone nor the cross-coupling product were formed in significant amounts when **DPEphos** was used. In the model reaction conditions, sulfone **17** was not detected, cross-coupling product **5** was formed in 9% yield, and 84% of the starting aryl bromide **2** was recovered with **DPEphos** (***Figure 4.11***), in good agreement with the HTE study. This result suggests that rigidity of the backbone ligand is necessary to promote the cross-coupling reaction.



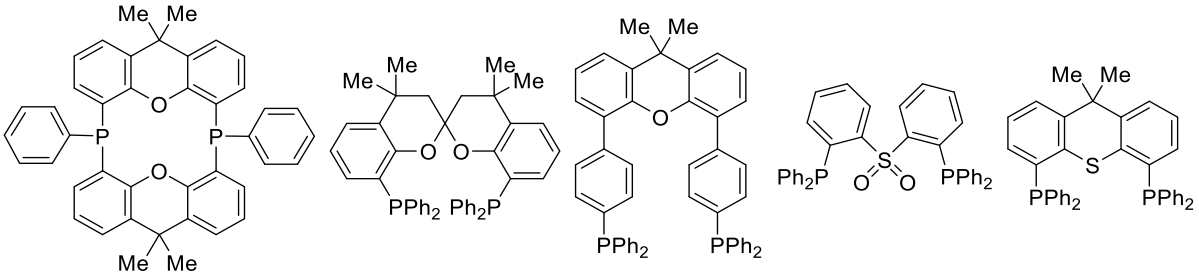
Scheme 4.11. Variations of the ligand bite angle. The values of the bite angle were taken from the review by van Leeuwen.[166] Yields are reported in the order **2**/**5**/**17**.

Nixantphos, in which the CMe_2 bridge of Xantphos is replaced by a free NH, has a slightly larger bite angle (114°) compared to Xantphos (108°) due to shorter Csp^2-NH bonds compared to Csp^2-CMe_2 bonds in Xantphos. The HTE screen showed that **Nixantphos** had similar catalytic activity to Xantphos in 1,4-dioxane, but this result was not reproduced with the model system. Nevertheless, it indicates that increasing the bite angle of the ligand while keeping its rigidity is not detrimental to sulfone formation. This was confirmed by the **Benzoxantphos** ligand, that has a larger bite angle of 121°, which produced sulfone product **17** in 92% yield and cross-coupling product **5** in 8%. However, using **DBFphos** entirely inhibited sulfone formation (0%), and did not promote desulfinative cross-coupling either, with 4% conversion to product **5**. Due to the geometry imposed by the central five-membered ring, DBFphos has a large bite angle of 131° and has been shown to be unable to form chelates with metal centres.[165] This suggests that chelation of the palladium centre is necessary to enable both transmetalation and selective reductive elimination to form sulfone **17**.

In summary, the bite angle and nature of the bridge of the Xantphos ligand does not seem to be crucial for reactivity or selectivity of sulfone formation, as long as the rigidity of the ligand is preserved, as shown by **DPEphos**, and the chelation ability of the ligand is not lost, as shown by **DBFphos**.

A variety of ligands with similar structures compared to the xanthene backbone were next compared (***Figure 4.12***). The cyclic bis-phosphine ligand **Bisxantphos**, which was reported by Kamer, van Leeuwen and co-workers, was synthesized by the reaction between dilithio-xanthene and dichlorophenylphosphine. According to X-ray crystallography analysis, **Bisxantphos** was obtained as a single stereoisomer in which the two phosphorus bridging groups are arranged in a *syn*-disposition, therefore orienting the phosphorus lone pairs *cis* to each other, making the formation of metal chelates possible.[186] Using **Bisxantphos** lowered the selectivity of the cross-coupling compared to the Xantphos ligand, as sulfone **17** and biaryl

5 were obtained approximately in a 1:1 ratio. However, given the low overall conversion (32% combined, 68% starting material recovered) and the difficulties associated with the preparation of this cyclic structure, Bisxantphos-type ligands were not further investigated.



Scheme 4.12. Variations of the ligand backbone.
Yields are reported in the order **2**/**5**/**17**.

The commercially available C_2-symmetric **Spanphos** ligand, which was also reported by the van Leeuwen group, was next used. The crystal structure of the free ligand revealed that the intramolecular P-P distance is 4.991 Å, resulting in an exclusive *trans*-configuration in solution in the related complexes [(**Spanphos**)PdXCl] where X = Me or Cl.[187] Despite the rigidity of this *trans*-chelating ligand, and its ability to form metal chelates, no sulfone formation was observed, and cross-coupling product **5** was formed in 9% yield while 90% of aryl bromide **2** was recovered. The oxygen atoms of complex [(**Spanphos**)$PtCl_2$] lie out of the plane defined by the aromatic rings of the chroman fragment, 3.110 Å and 3.097 Å respectively, away from the platinum atom, precluding oxygen coordination to the metal centre.[187] In comparison, the Pd-O atom distance in oxidative addition complex [(**Xantphos**)Pd(4-CN-C_6H_4)(Br)] is 2.698 Å, and 2.154 Å in the corresponding $\kappa^3_{P,O,P}$ cationic complex [(**Xantphos**)Pd(4-CN-C_6H_4)$^+$(OTf)$^-$].[170] To probe the importance of the availability of an oxygen atom at the apical position of oxidative addition complexes for the formation of sulfone products, the extended Xantphos ligand **XL-Xantphos** was synthesised. **XL-Xantphos** was designed by Whiteker and co-workers to mimic the bite angle and electronic properties of the Xantphos ligand without the

possibility of the oxygen atom to take part with metal coordination.[188] When **XL-Xantphos** was used in the model system, formation of the sulfone product **17** was completely inhibited, and aryl bromide **2** was largely recovered (84%), with small amounts of biaryl **5** formed as the major product (10%). Similarly, Whiteker and co-workers compared the reactivity of Xantphos and **XL-Xantphos** in the Pd-catalysed arylation of benzamides.[169] While product was formed in 92% yield with Xantphos, only <4% HPLC yield was observed with **XL-Xantphos** under the same reaction conditions.[188] The transmetalation step is often turnover-limiting in Pd-catalysed amination reactions,[158] and the bridging oxygen of the Xantphos ligand has been suggested to be involved in the transmetalation step.[189] The reactivity of **XL-Xantphos** in the model reaction therefore suggests a similar mechanism for the sulfone formation process.

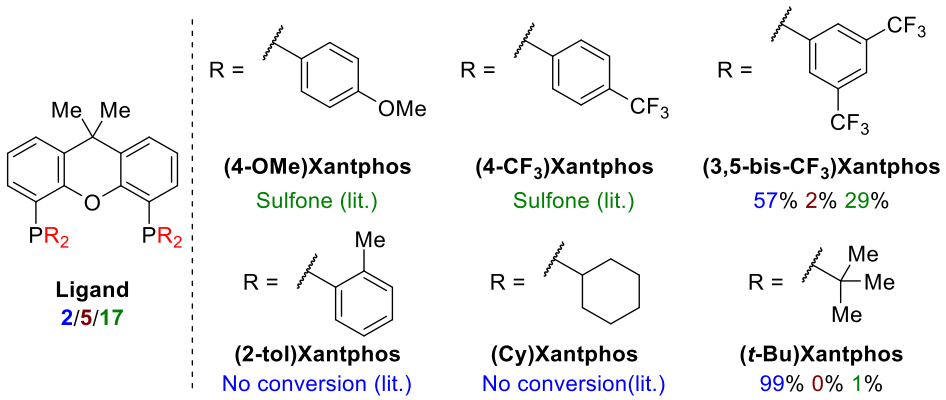
Sulfphos, which was readily synthesised from diphenylsulfone is structurally similar to **DPEphos**, but has a sulfone functional group replacing the oxygen of the ether linker. Almost no reactivity was observed when Sulfphos was employed in the model system (99% **2**, 2% 5, 0% **17**), which consistent with our discussion on the importance of the rigidity of the ligand backbone and of the presence of an oxygen group at the bridging position.

Finally, **Thioxantphos** ligand, which is the sulfur analogue of Xantphos, was shown to have no catalytic activity in amination chemistry due to the high affinity between the sulfur and the palladium atom, forming an inactive $\kappa^3_{P,S,P}$ cationic complex from which transmetalation does not occur.[171] Considering the poor nucleophilicity of sulfinate salts compared to anilines in palladium catalysed arylation reactions, the **Thioxantphos** ligand was not synthesised and studied with the model reaction.

Overall, it appears that the availability of an oxygen at bridging position 5 of the Xantphos ligand is a crucial ligand feature, without which, good conversion of the aryl bromide coupling partner **2** and formation of the sulfone product **17** are not observed. This is most likely due to the involvement of $\kappa^3_{P,O,P}$ pincer type complexes in the transmetalation step.

4.3.3. Symmetrical Variation of the Diphenylphosphino Groups

Having observed that the xanthene backbone is required in order to ensure high conversion of aryl bromide **2**, the phosphorus substituents were next varied. This strategy had been employed by the Willis group in 2013 to lower the amounts of bi-products formed by aryl scrambling (***Scheme 4.13***).[178-181].

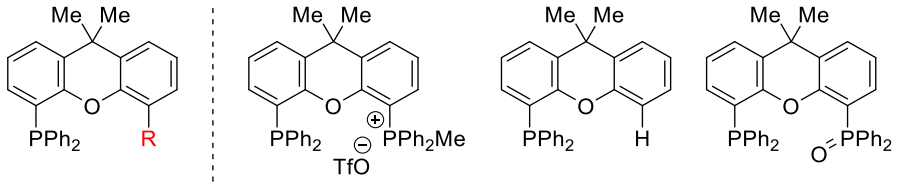


Scheme 4.13. Variations of the phosphine substituents.
Yields are reported in the order **2**/**5**/**17**.

In the reaction between 1-iodo-4-methylbenzene and lithium phenyl sulfinate salt generated *in situ* from phenyl lithium and DABCO, it was shown that **4-OMe-**, **4-CF3-** and **3,5-bis(CF3)Xantphos** ligands gave good to excellent conversions to the sulfone product, whereas starting material was recovered for with the bulky **(2-tol)-**, **Cy-** and **(*t*-Bu)Xantphos** ligands.[178] When the electron poor **3,5-bis(CF3)Xantphos** ligand was used in the model system, excellent selectivity towards the sulfone product **17** was observed, with 29% yield of sulfone compared to 2% yield of biaryl **5**. The lower conversion was in good agreement with literature results which indicated the need for higher temperatures (110 °C) with this electron-poor Xantphos analogue, most likely due to reduced rates in the oxidative addition step. Reactivity of the commercially available bulky **(*t*-Bu)Xantphos** was also assessed in the model system, and the starting aryl bromide **2** was fully recovered, in good agreement with the results reported by Willis and co-workers.

4.3.4. Chelating Ability of the Ligand

The poor reactivity observed with the large bite angle **DPFphos** ligand (**Section 4.3.2**) suggests that the chelating ability of Xantphos is a crucial feature for efficient conversion of aryl bromide **2** to sulfone **17**. The complete inhibition of sulfone formation and high recovery of the starting aryl bromide **2** (87%) when mono-methylated Xantphos ligand **Xantphos.MeOTf** was employed is in good agreement with this hypothesis (***Scheme 4.14***). To further illustrate the importance of the capability of the ligand to form chelates, the ligand **PPh_2-Xanthene**, in which one of the two diphenylphosphino groups was replaced by a proton, was synthesised. As expected, this mono-phosphine behaved very similarly to **Xantphos.MeOTf**, as aryl bromide **2** was recovered in 92% yield, biaryl **5** was obtained in 8%, and sulfone formation was not observed.



Scheme 4.14. Importance of the chelation. *Using K_2CO_3 instead of Cs_2CO_3. Yields are reported in the order **2**/**5**/**17**.

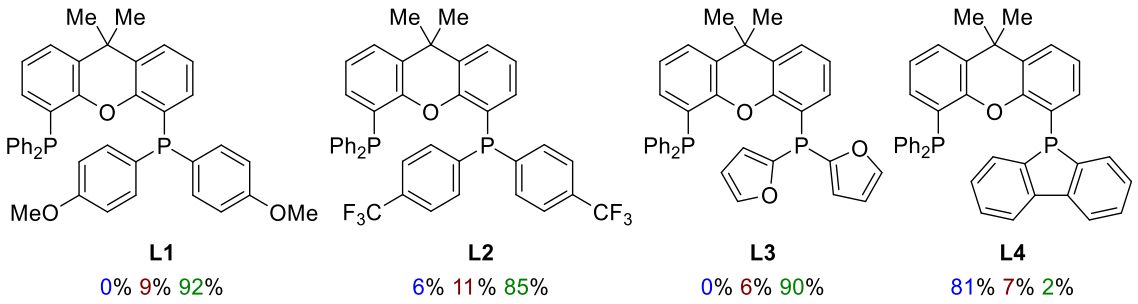
Similarly to Buchwald's dialkylbiphenyl phosphine ligands, the Xantphos ligand is resistant to aerobic oxidation.[166, 190] Nevertheless, the hemi-labile **Ox-Xantphos** has been shown to be formed *in situ* and become the catalytically active species in the palladium-mediated C-H arylation of imidazoles.[191] **Ox-Xantphos** has been shown to be *cis*-chelating in the oxidative addition complex [(**Ox-Xantphos**)Pd(3-pyrrole)(Br)], and dissociation of the phosphine oxide moiety was proposed to be preceding the turnover limiting concerted metalation-deprotonation step. To assess the potential involvement of such a hemi-labile ligand, **Ox-Xantphos** was synthesised and used in the model reaction. Once again, sulfone formation was completely

inhibited, and biaryl **5** was formed in 7% yield while aryl bromide **2** was recovered in 91% yield. This demonstrates that **Ox-Xantphos** does not take part in this catalysis, and further supports that the presence of two strongly binding phosphine ligands is required to promote reactivity and selectively to form sulfone product **17**.

4.3.5. Variation of One Diphenylphosphino Group

In order to fine tune the reactivity of Xantphos-derived ligands, the substituents of one of the two phosphorus atoms were modified while keeping phenyl groups on the other constant. This strategy allowed us to deconvolute the steric and electronic properties of the two phosphines and modify the overall reactivity of the bidentate ligand without altering its backbone, which was shown to be crucial in the previous sections of this chapter. Such non symmetrical bis-phosphine ligands were prepared with a ferrocenyl core by Hartwig and co-workers to determine the trans effect on the rates of reductive elimination from arylpalladium(II) amido complexes.[183] These non-symmetrical bis-phosphine ligands were, however, limited to 4-CF_3 or 4-OMe substituted phenyl rings. To the best of our knowledge, such non-symmetrical bis-phosphine ligands have never been reported with the xanthene backbone.

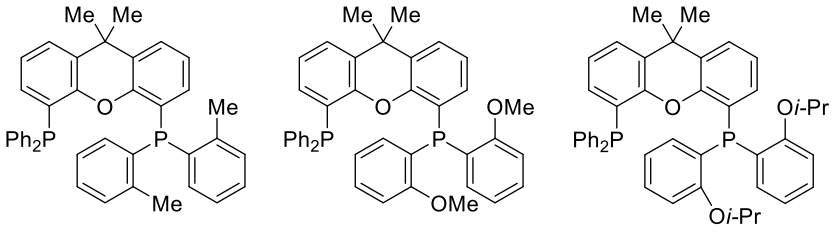
The presence of electron-donating groups on the phenyl rings of one of the two phosphorus atoms, as in ligand **L1** (***Scheme 4.15***), did not affect either conversion or selectivity of the cross-coupling process. Full conversion of aryl bromide **2** was observed, with sulfone **17** being the major product (92%), against 9% of the desired biaryl product **5**. In contrast, full conversion was not obtained with the electron-deficient 4-CF_3-C_6H_4 groups, as 6% of the aryl bromide **2** was recovered. Product distribution between sulfone **17** and biaryl **5** did not change significantly (85% sulfone, 11% biaryl). Both these results are consistent with the work reported by Willis and co-workers on the symmetrical Xantphos-type ligands and discussed in **Section 4.3.3**. The 2-furyl analogue **L3** gave a similar reactivity profile, with an excellent conversion to sulfone **17** in 90% yield, against 6% of biaryl product **5**.



Scheme 4.15. Non-symmetrical ligands #1: Electronic and conformation changes. Yields are reported in the order **2**/**5**/**17**.

In contrast, replacing a diphenylphosphino group of Xantphos by the fused benzophosphindole motif as in ligand **L4** drastically inhibited both C-S and C-C product formation reactions, allowing the recovery of the starting aryl bromide **2** in 81% yield. This behaviour suggests that changes in ligand conformation have a much stronger influence on the reaction compared to simple variations of the ligand electronics.

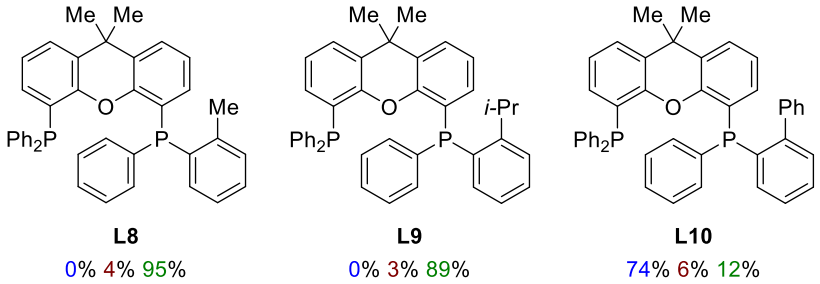
Steric effects were next investigated by functionalising the phenyl rings of one of the two diphenylphosphino groups at their 2-position (***Scheme 4.16***). Reactivity was strongly reduced by ligand **L5**, which features 2-tolyl substituents, as 83% of the starting aryl bromide **2** was recovered. Sulfone **17** remained the major product with 11% yield against 5% yield of biaryl product **5**. In contrast, 2-OMe groups were well tolerated, as the use of ligand **L6** only caused a slight drop in reactivity with sulfone **17** and biaryl **5** being formed in 71% and 8% yield respectively. A moderate conversion was still observed with ligand **L7**, in which bulkier isopropyl ether groups are present at the 2-position of both phenyl rings (45% aryl bromide **2** recovered, 39% sulfone **17** and 8% biaryl **5** formed).



Scheme 4.16. Non-symmetrical ligands #2: 2-substituted phenyl groups. Yields are reported in the order **2**/**5**/**17**.

Overall, increasing the steric bulk around the phosphorus atom with 2-substituted phenyl groups is detrimental to conversion of aryl bromide **2**, but does not affect the selectivity of the coupling. Indeed, sulfone product **17** was formed as the major product with the three ligands **L5**, **L6** and **L7**.

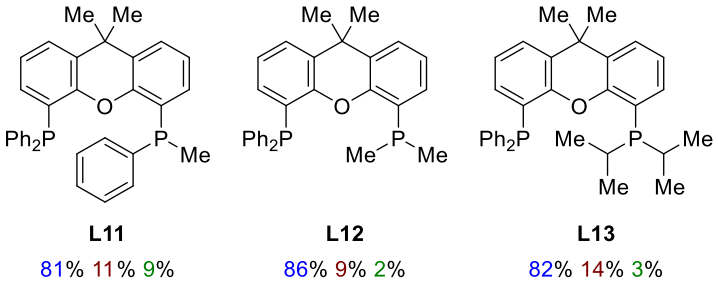
To further probe the importance of substituents on the 2-position of phenyl rings, only one of the four phenyl groups of the Xantphos ligand was changed to a 2-tolyl aromatic ring in **L8** (***Scheme 4.17***). In contrast to ligand **L5** which features two tolyl substituents, with **L8**, full conversion was obtained with an excellent selectivity towards sulfone product **17** (95%). Increasing the steric bulk of the substituent with ligand **L9**, in which the 2-methyl group was replaced by a 2-isopropyl group did not alter the reactivity; full conversion of aryl bromide **2** was also obtained with a similar selectivity for sulfone formation (89%). These two ligands, **L8** and **L9**, therefore behaved similarly to Xantphos; the presence of one alkyl substituent on the 2-position of one phenyl ring did not have any effect on the outcome of the reaction. Moving away from aliphatic substituents, the 2-phenyl substituted ligand **L10** did, however, shut down reactivity. The starting aryl bromide **2** was recovered in 74% yield while biaryl **5** and sulfone **17** were only formed in 6% and 12% yield respectively.



Scheme 4.17. Non-symmetrical ligands #3: single substitution at the 2-position. Yields are reported in the order **2**/**5**/**17**.

The presence of a single substituent at the 2-position of one out of the four phenyl groups of Xantphos can therefore either inhibit both C-C and C-S cross-couplings reactions as with **L10**, or leave reactivity entirely unaffected as with **L8** and **L9**. It is at this stage unclear why this is the case.

Aliphatic substituents were next explored as an alternative to aromatic groups on the phosphorus atom (***Scheme 4.18***). In ligand **L11**, one out of the four phenyl groups of Xantphos was replaced by a methyl substituent. When this ligand was employed, reactivity was strongly retarded, with 81% starting material **2** being recovered. In contrast to ligands **L1**-**L10**, however, biaryl **5** and sulfone **17** were formed approximately in a 1:1 ratio (11% and 9% respectively) when using **L11**. Selectivity towards biaryl product **5** was further increased with ligand **L12**, in which both the phenyl groups were replaced by methyl substituents on the same phosphorus atom. This increase in selectivity was not due to the formation of biaryl **5** in higher yields (9% with **L12** compared to 11% with **L11**), but resulted from the inhibition of sulfone formation (2% with **L12** compared to 9% with **L11**). Replacing both methyl by isopropyl substituents in **L13** slightly increased the amounts of biaryl product **5** formed to 14% without increasing sulfone formation (3%).



Scheme 4.18. Non-symmetrical ligands #4: aliphatic substituents. Yields are reported in the order **2**/**5**/**17**.

Overall, replacing one or two aromatic groups by aliphatic substituents in ligands **L11**-**L13** resulted in a change of selectivity between biaryl **5** and sulfone **17**. Indeed, independently of their steric bulk, ligands **L1**-**L10** all favoured formation of product **17**, whereas it is the biaryl **5** which was formed as the major product with ligands **L11**-**L13**. Ligand **L4**, in which the two aromatic rings are fused in a benzophosphindole moiety, stands out as an exception, most likely due to conformational restrictions.

4.4. Conclusion

The xanthene scaffold has been identified as a promising ligand backbone to promote the desulfinative cross-coupling reaction of aryl bromide **2** and aryl sulfinate **4** at 100 °C. Indeed, Xantphos has been shown to have the unique ability to promote the palladium-catalysed formation of diaryl sulfones from aryl halides and aryl sulfinate salts. By surveying previous literature reports, one can observe that sulfone products can be formed at temperatures as low as 40 °C, which is in sharp contrast with the temperatures required for desulfinative cross-coupling reactions (120-150 °C). This finding is of significant importance because the transmetalation step which was found to be turnover limiting for desulfinative cross-couplings is common to both C-C and C-S bond formating reactions.

Performing the stoichiometric reaction between oxidative addition complex [(Xantphos)Pd(4-F-C_6H_4)(Br)] **19** and aryl sulfinate salts bearing a variety of organic and inorganic counter

cations showed that the rate of product formation was significantly affected by the identity of such counter cations. Similar trends were observed for both sulfone and biaryl product formating reactions, suggesting that a cation metathesis between the sulfinate salt and the carbonate base is also preceding the transmetalation step in the Pd/Xantphos cross-coupling reaction. Running such stoichiometric reactions with increasing amounts of potassium and tetrabutylammonium salts showed that even if transmetalation is intrinsically a reversible process, it is not likely to be reversible when the inorganic K_2CO_3 base is employed due to the poor solubility of KBr in 1,4-dioxane. These experimental results are, however, not sufficient to fully exclude the reductive elimination as the turnover limiting step of the catalytic cycle.

By synthesising a range of xanthene-derived phosphines, a detailed structure/reactivity portrait of the Xantphos ligand was built. Three parameters were found to be crucial to ensure good conversion of the aryl bromide coupling partner **2** to sulfone product **17**: 1) rigidity of the backbone; 2) presence of an oxygen on the bottom bridge (position 5); and, 3) ability of the bis-phosphine to form chelates with the palladium centre. The identity of the substituents at the top bridge (position 10) was not found to be important.

Finally, a range of non symmetrical ligands were designed to further understand the reactivity of Xantphos and fine tune it to form selectively the desired biaryl product **5**. While the presence of aryl groups on both phosphorus atoms strongly favours the formation of sulfone **17**, switching from diaryl- to dialkylphosphino groups allowed biaryl **5** to be formed as the major product. However, this change also caused a major drop in conversion, with most of the aryl bromide **2** remaining unreacted.

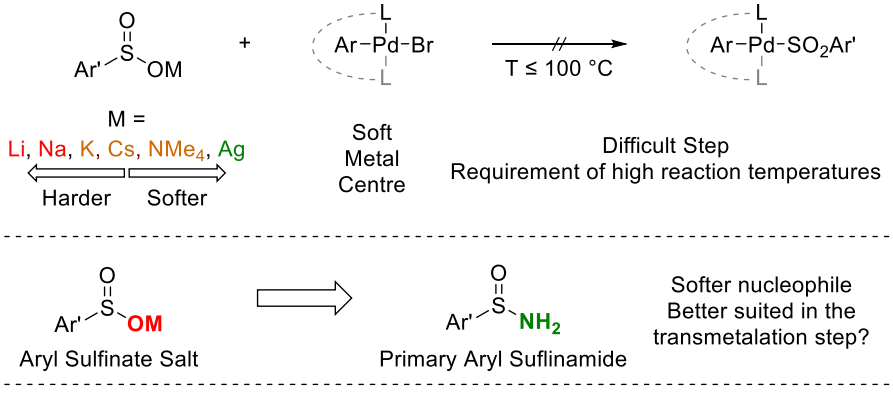
Synthesis of putative palladium sulfinate complexes [(Xantphos)Pd(Ar)(SO_2Ar')] *via* the reported $\kappa^3_{P,O,P}$ cationic pincer type complexes[(Xantphos)Pd(Ar)]$^+$, and their characterisation to identify the bonding between the sulfinate salt and the palladium centre would be pivotal to further our understanding of the mechanism of this C-S cross-coupling reaction. The synthesis

of such complexes would complete the current data set and allow the identification of the RSI and TLS of this synthetically important transformation. Indeed, in order to improve both conversion and selectivity towards biaryl product **5**, it is key to understand what becomes the limiting step (transmetalation *vs* reductive elimination or extrusion of SO_2) upon varying the phosphine substituents. To that end, the synthesis of a larger range of ligands and theoretical analysis of the corresponding transition states would be desirable. Computational work towards this is currently ongoing.

Chapter 5 – Aryl Sulfinamides as Novel Nucleophiles for Palladium-Catalysed Carbon-Carbon Bond-Forming Reactions

5.1. Introduction

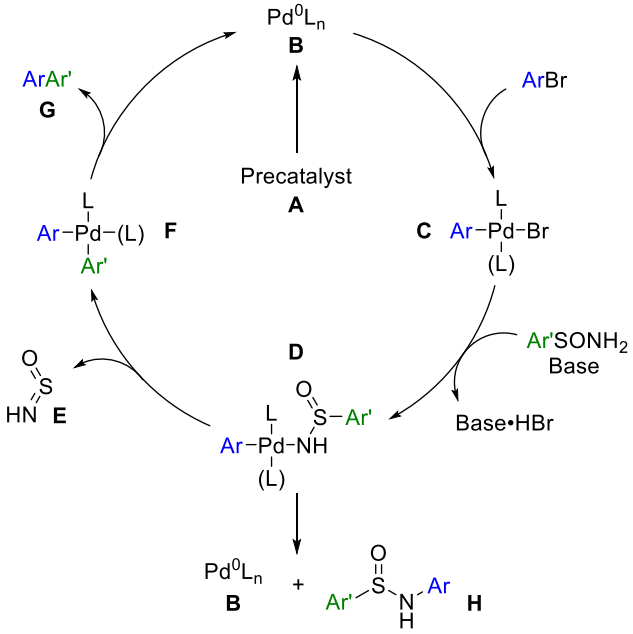
Alkali metal sulfinate salts require high temperatures to react with aryl palladium halide oxidative addition complexes. It was shown in **Section 2.5.2** that moving down the alkaline metal group of the periodic table, therefore increasing the softness of the alkaline metal, led to faster rates of transmetalation with oxidative addition complex **9**. Accordingly, sulfinate salts bearing softer counter cations, such as tetramethylammonium or silver, gave the highest rates of transmetalation. We envisioned that replacing the hard anionic oxygen atom of the sulfinate salt for the softer and neutral amine group as in the sulfinamide functional group, might improve the transmetalation process by increasing the affinity with the soft palladium metal centre and allow lower temperatures for the reaction (***Scheme 5.1***).[9-10] Furthermore, sulfinamides are more functional group tolerant compared to sulfinate salts, are easier to purify and can be readily accessed *via* a wide range of synthetic routes.[192-193]



Scheme 5.1. Primary aryl sulfinamides as alternative, softer nucleophiles.

A putative mechanism for the palladium-catalysed cross-coupling reaction between aryl bromides and primary aryl sulfinamides is depicted in ***Scheme 5.2.*** By analogy with desulfinative cross-coupling reactions, formation of on-cycle palladium(0) species **B** from a

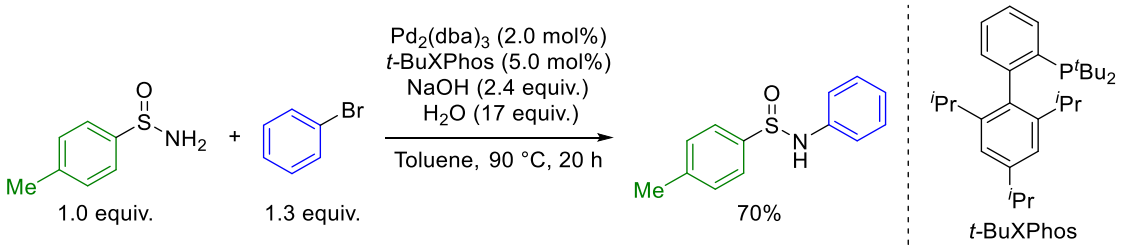
precatalyst **A**, followed by reaction with the aryl bromide coupling partner, leading to an aryl palladium(II) oxidative addition complex is to be expected. However, in contrast to reactions involving aryl sulfinate salts, which formally do not necessitate a base as the sulfinate salt is already anionic, a base is required to sequester the stoichiometric HBr by-product that is formed during the transmetalation step (**C → D**). The attack of nitrogen-based nucleophiles onto such aryl palladium oxidative addition complexes is a common transformation that is very well precedented in the context of palladium catalysed C-N bond-forming reactions.[194]



Scheme 5.2. Proposed mechanism for the palladium-catalysed cross-coupling of aryl bromides and primary aryl sulfinamides.

Once the key intermediate **D** is formed, extrusion of the sulfinyl amine HNSO **E** is required to give complex **F** that delivers the desired biaryl product **G** and regenerates the palladium(0) catalyst upon reductive elimination. Extrusion of HNSO has been proposed to be responsible for the base-mediated decomposition of *N*-benzoxyaryl sulfinamides,[195] but to the best of our knowledge, generation of this gas has never been reported in the context of transition-metal catalysis. An alternative, commonly observed reaction pathway in C-N coupling reactions is direct reductive elimination from **D** which would lead to *N*-arylated sulfinamide product

Ar'SONHAr **H** and regenerate the palladium(0) species **B**. *N*-arylation of *tert*-butyl sulfinamides was reported by Zeng and co-workers using the palladium(0) source $Pd_2(dba)_3$ in conjunction with the Buchwald biaryl ligand *t*-BuXPhos in toluene at 90 °C.[196] They also showed that 4-tolylsulfinamide could be arylated with bromobenzene in moderate yield under the same reaction conditions (***Scheme 5.3***). Although this pathway is unproductive in the desired transformation, these reactions indicate that the transmetalation step does not require particularly harsh reaction conditions in comparison to sulfinate salts.



Scheme 5.3. Palladium-catalysed *N*-arylation of primary sulfinamides with aryl bromides as reported by Zeng and co-workers.[196]

In this chapter, efforts towards the optimisation of a novel palladium-catalysed cross-coupling of aryl sulfinamides with aryl bromides to form biaryl products are described.

5.2. Initial Evaluation at 150 °C

The potential of sulfinamide derivatives as nucleophilic coupling partners was first evaluated using standard conditions[58] developed for desulfinative cross-coupling reactions (***Figure 5.1***). To our delight, the desired cross-coupling product **5** was obtained in 80% yield according to HPLC analysis of the crude reaction mixture when primary 4-methylbenzenesulfinamide **20** was used, accounting for most of the consumption of aryl bromide **2**. In contrast, lower yields ranging from 25% to 32% were obtained with *N*-alkyl (*t*-Bu and *n*-Bu), -allyl and -benzyl sulfinamides, despite measuring high conversions of starting material. The HPLC chromatograms of these crude reaction mixtures were complex, and did not reveal the presence of a major reaction by-product. Aryl bromide **2** remained unreacted when the sulfinamide was

substituted with a carbonyl containing functional group (*N*-benzoyl, -pivaloyl, -boc) or an aromatic group *N*-Ar. At this stage, it is difficult to explain this reactivity pattern, which could be due to the incompatibility of these substituents with either the transmetalation step, the deprotonation step, or the loss of the RNSO fragment. The latter is expected to be more difficult with *N*-substituted sulfinamides, as HNSO is a gas whereas RNSO derivatives are not expected to be, therefore resulting in the loss of the entropic driving force of the reaction. The primary sulfinamide **20** was therefore selected for further optimisation at lower temperatures.

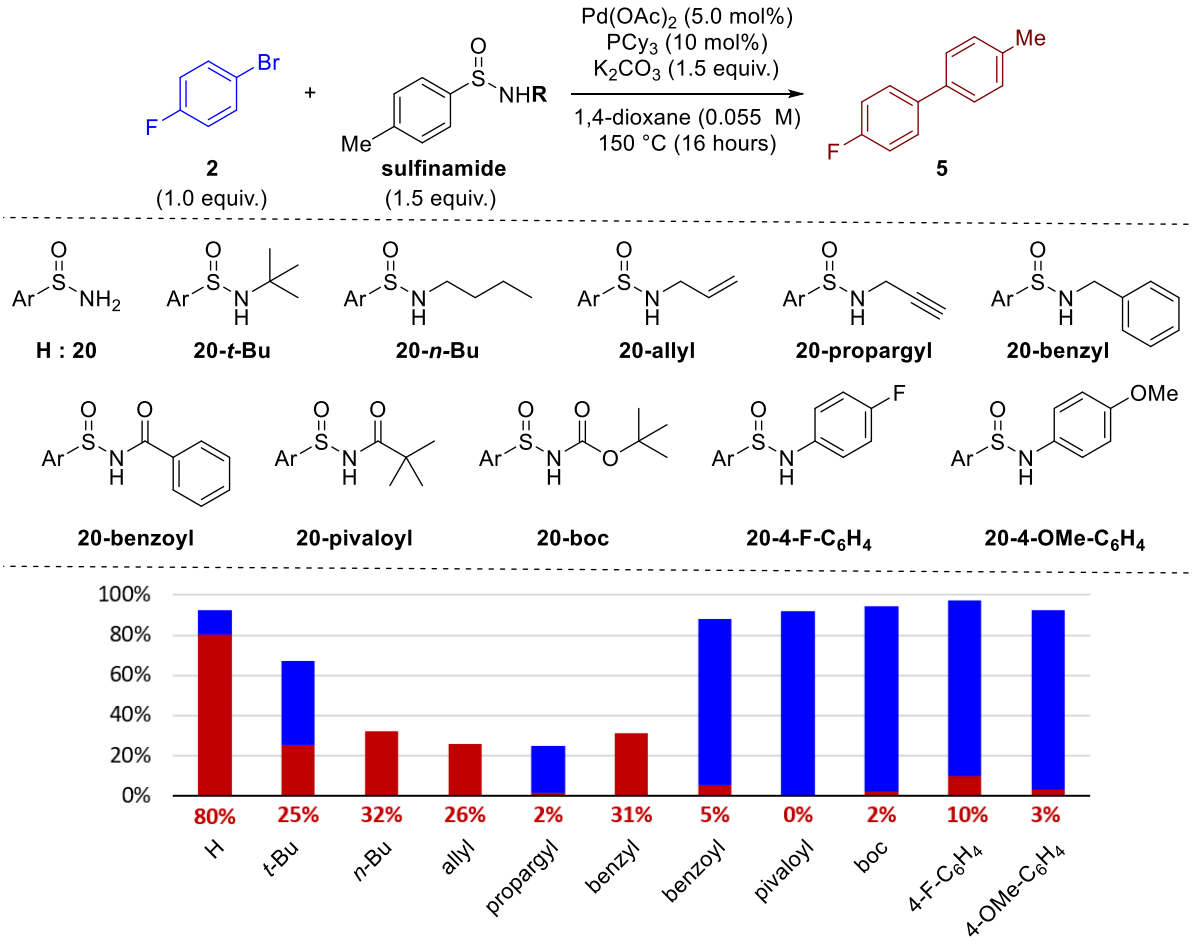


Figure 5.1. Sulfinamides as nucleophilic coupling partners: Importance of the *N*-substituent. Red bars and reaction yields (%): biaryl product **5**. Blue bars: starting material **2**.

5.3. Lowering the Reaction Temperature to 100 °C, Base and Solvent Screening

Lowering the temperature to 100 °C resulted in the complete loss of reactivity, with 3% yield of cross-coupling product **5** and full recovery of the electrophilic coupling partner **2** (***Figure 5.2***). Replacing the potassium carbonate base by its caesium analogue Cs_2CO_3 (pK_a conjugate acid = 10.3 in H_2O)[197] proved to be beneficial, giving a promising 22% yield of biaryl **5**. In comparison, the highest yields of biaryl **5** obtained from desulfinative cross-coupling at 100 °C were 19% in **Chapter 3** using aryl triflate **2-OTf** instead of aryl bromide **2**, and 15% in **Chapter 4** using the non-selective **Bisxantphos** ligand. This result therefore demonstrates the superiority of primary sulfinamide **20** as a nucleophilic coupling partner at lower temperatures compared to 4-methylbenzene sulfinate salt **4** when used with the same electrophilic coupling partner.

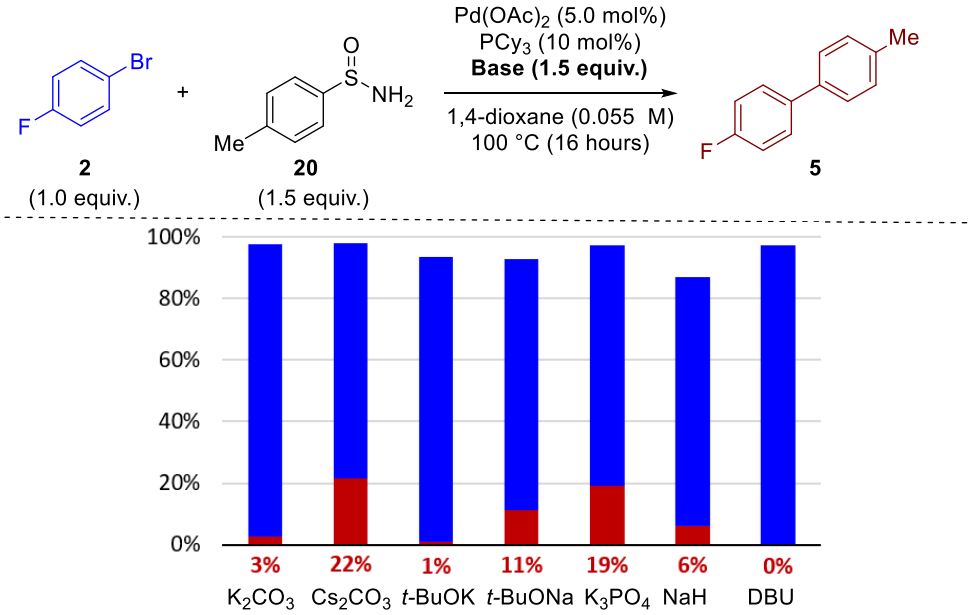


Figure 5.2. Screening of common bases at 100 °C.
Red bars and reaction yields (%): biaryl product **5**. Blue bars: starting material **2**.

Tert-butoxide bases (pK_a *t*-BuOH = 32.4 in DMSO)[198] are the most commonly employed bases in palladium-catalysed amination chemistry. They have been shown to lead to the formation of *tert*-butoxide palladium intermediates by displacing the halide of the oxidative addition complex, or deprotonating the amine after its coordination to the oxidative addition

complex, therefore lowering its pK_a.[199-200] Disappointingly, in the model reaction, 1% and 11% yield of biaryl **5** were obtained when using *t*-BuOK and *t*-BuONa, respectively. Potassium phosphate tribasic K_3PO_4 (pK_a conjugate acid = 12.3 in H_2O)[201], which is also used frequently in amination chemistry, provided cross-coupling product **5** in 19% yield, performing similarly to Cs_2CO_3. Using the stronger hydride base, NaH, only provided product in 6% yield, and no product was formed using the organic base DBU (1,8-Diazabicyclo(5.4.0)undec-7-ene, pK_a conjugate acid = 11.5 in H_2O).[202] The yields of cross-coupling product are therefore not directly correlated with the pK_a of the basic additive. The higher yields obtained with Cs_2CO_3 and K_3PO_4 compared to K_2CO_3 may be due to the lower solubility of the latter in 1,4-dioxane.[13]

A small number of organic solvents commonly used in palladium-catalysed arylation reactions were selected and evaluated with the model reaction using Cs_2CO_3 as a base (***Figure 5.3***). Similarly to what was observed for the cross-coupling reaction between aryl bromide **2** and sodium 4-methylbenzene sulfinate salt **4** (**Section 3.8**), 1,4-dioxane, DMF and toluene gave similar yields of cross-coupling product **5**, 24%, 27% and 21%, respectively. Reactivity was similar with THF (27%), whereas a slight erosion in yield was observed with DMSO. Methanol was however incompatible with this system, as no product formation was observed despite the entire consumption of aryl bromide **2**. Despite the lower yield of product **5** observed with 1,4-dioxane, this solvent was preferred over DMF and THF for the following optimisation reactions due to the toxicity and environmental cost of DMF, and the low boiling point of THF.

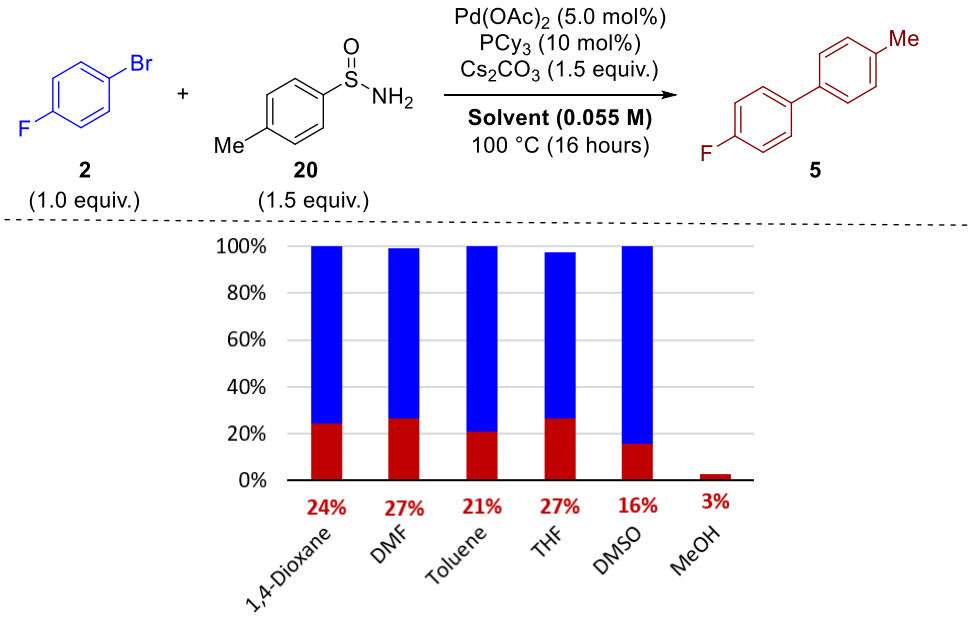


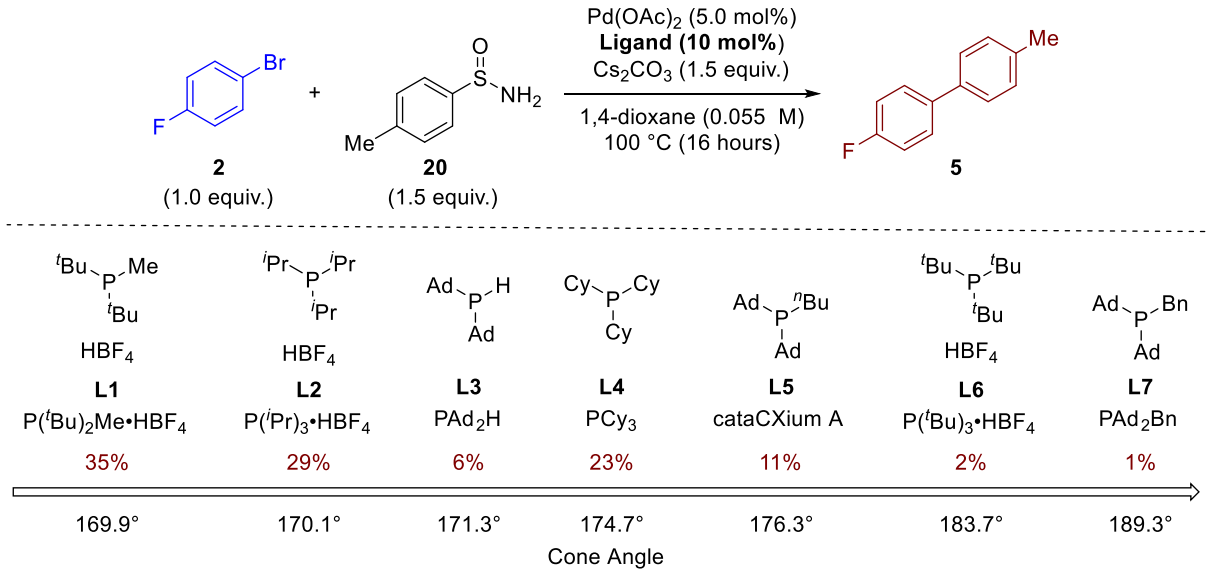
Figure 5.3. Solvent screening. Red bars and reaction yields (%): biaryl product **5**. Blue bars: starting material **2**.

5.4. Ligand Screening

A total of 56 ligands were evaluated for this cross-coupling reaction, and the full data is available in the **Experimental Section 7.4.** $Pd(OAc)_2$ and the ligand were employed in a 2:1 stoichiometry for mono-phosphine ligands, whereas a 1:1 stoichiometry was used for bis-phosphine ligands, therefore ensuring the same ratio of phosphine to palladium.

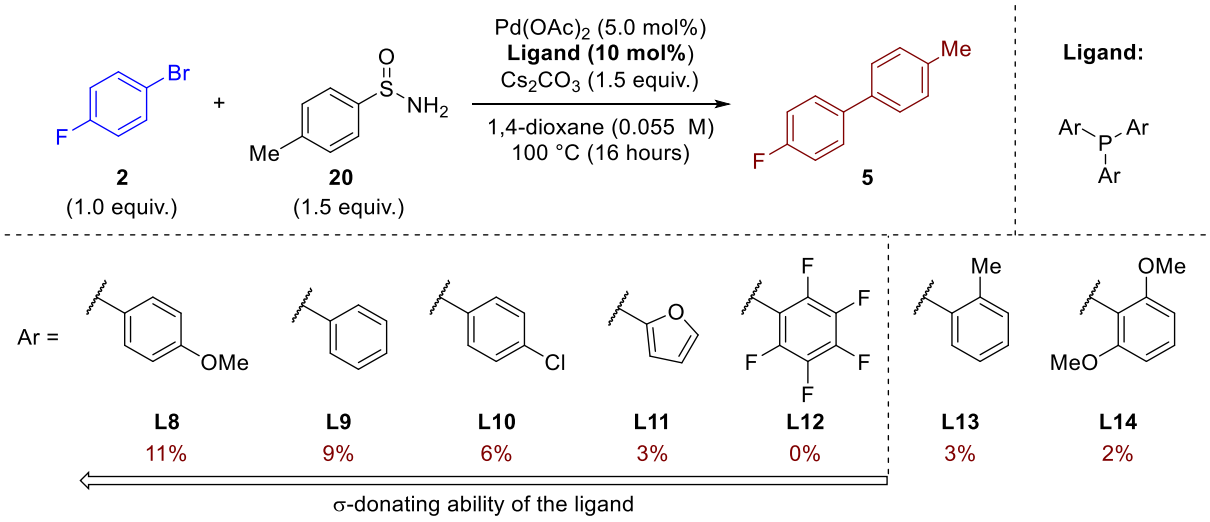
Sterically demanding and strongly σ-donating trialkylphosphines[12, 203] have proved to be successful ligands for desulfinative cross-coupling reactions.[58, 61] Within this ligand series, reaction yields ranged from 1% with PAd_2Bn **L7**, up to 35% with $P(t\text{-Bu})_2Me{\bullet}HBF_4$ **L1** (***Scheme 5.4***). Reactions were found to give clean HPLC chromatograms for all the phosphine ligands investigated, with unreacted starting material accounting for the mass balance (**Experimental Section 7.5** for the corresponding bar charts). The activity of these mono-phosphine ligands showed good correlation with their computed ligand cone angles,[204] with higher yields observed for ligands with smaller cone angle, with the exception of diadamantyl phosphine **L3**, most likely due to electronic factors. Following this trend, it would be interesting

to assess the reactivity of trialkylphosphines with smaller cone angles such as PPr_3 and PEt_3, as time pressure precluded the study of these ligands.



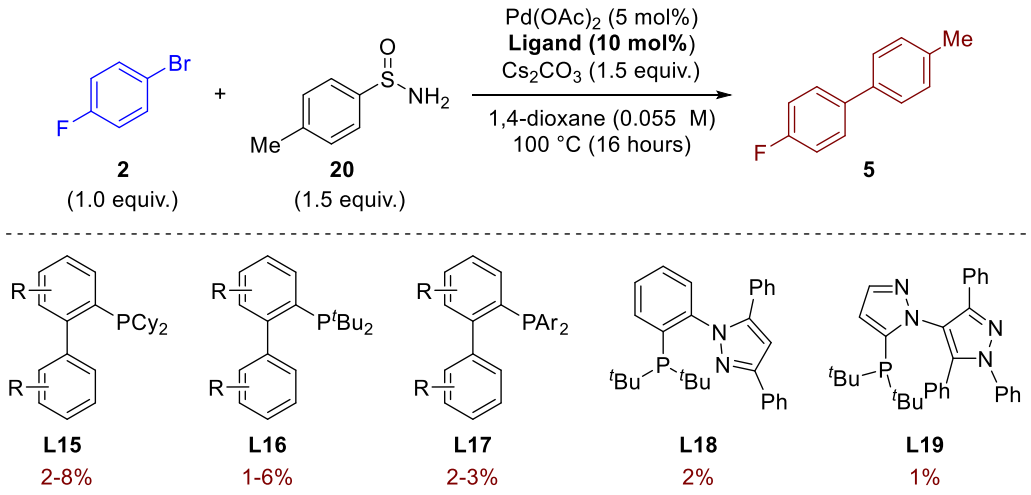
Scheme 5.4. Trialkylphosphine ligands showing good correlation between cone angle and reactivity.

A number of triarylphosphines, which were until the end of the 1990s the most largely used ligand class in palladium-catalysed cross-coupling reactions,[205] were tested in the model reaction. Despite a significantly smaller cone angle compared to trialkylphosphine ligands for the non-*ortho*-substituted triarylphopshines (165.8° for PPh_3 **L9** and 166.0° for P(4-Cl-C_6H_4)$_3$ **L10**),[204] their use resulted in lower yields; product **5** was obtained in 9%, 11% and 6% yields, respectively with PPh_3 **L9**, P(4-OMe-C_6H_4)$_3$ **L8** and P(4-Cl-C_6H_4)$_3$ **L10**. This suggests the strong σ-donation of trialkylphosphines ligands is required in this cross-coupling process (ν_{CO} = 2056 cm^{-1} (PPh_3) vs 2069 cm^{-1} (PCy_3)).[13] Within the triarylphosphine series, this trend is confirmed with decreasing yields upon decreasing the donating ability of the ligand (***Scheme 5.5***). Indeed, IR investigations have confirmed that the 2-furyl substituent acts as an electron withdrawing group on phosphorus nuclei with respect to standard phenyl rings.[206] Sterically hindered triarylphosphines, which have the combination of large cone angle with no increased σ-donation, performed very poorly, as shown with P(2-Me-C_6H_4)$_3$ **L13** (183.4°)[204] and P(2,6-*bis*-OMe-C_6H_3)$_3$ **L14**.



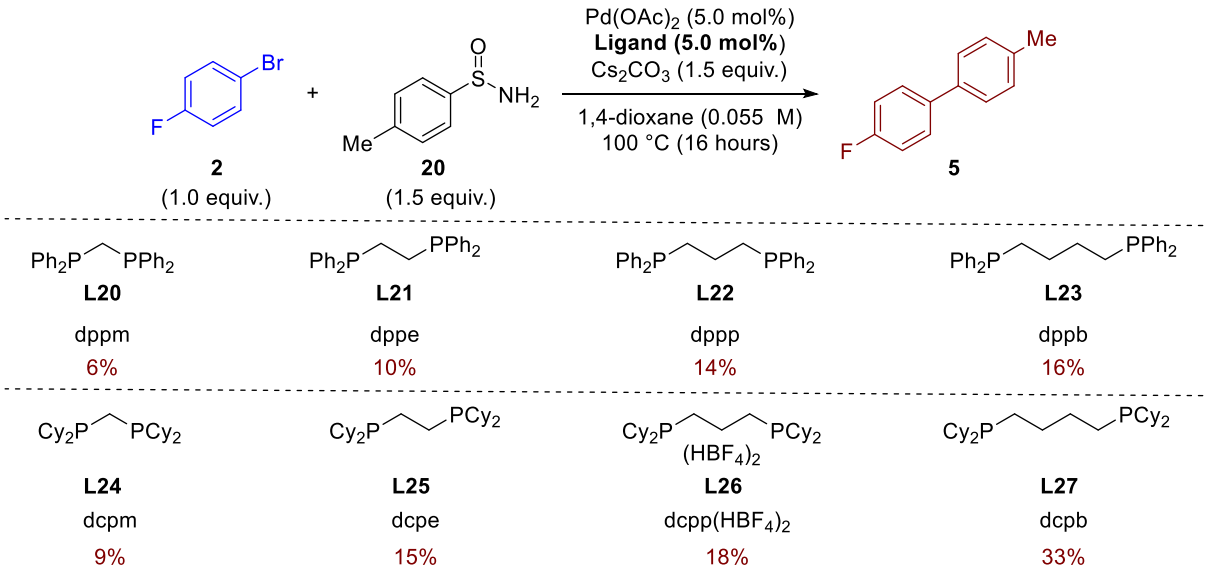
Scheme 5.5. Screening of triarylphoshine ligands.
Correlation between reactivity and σ-donation properties of the ligand.

Buchwald-type biaryl phosphines are prevalent in cross-coupling chemistry, especially in palladium-catalysed amination reactions.[207-208] However, this class of ligands performed poorly with the model reaction conditions, with yields of biaryl **5** averaging at 5% independent of the nature of the phosphine substituents (Cy, *t*-Bu, or Ar) as in **L15-L17** (***Scheme 5.6***). Importantly, the sulfinamide *N*-arylation product was not detected and the aryl bromide was recovered in yields above 90%. This is consistent with the observation of Zeng and co-workers, that hydroxide and water were crucial additives for the formation of the *N*-arylation product using *t*-BuXPhos (***Scheme 5.3***).[7] Similarly, heteroaromatic variants **L18** and BippyPhos **L19** were found to be inactive in this reaction. In contrast, BippyPhos **L19** was shown to have high catalytic activity in Buchwald-Hartwig amination and amidation reactions with (hetero)aryl chlorides under similar cross-coupling reaction conditions (1,4-dioxane or toluene, 90 °C to 110 °C).[209]



Scheme 5.6. Buchwald biphenyl phosphine ligands: poor reactivity.

Bis-phosphine ligands play an important role in homogeneous catalysis. Since the first report of dppe (**L21** in ***Scheme 5.7***) being used in 1959,[210] the number of ligand backbones and phosphine substituents that have been reported have grown dramatically. For bis-phosphine ligands, the bite angle is more commonly used as a method of comparison, in preference to the Tolman cone angle.[166-167] Interestingly, both diphenylphosphino and dicyclohexylphosphino alkane ligand series exhibited a similar correlation between the number of carbons in the alkyl chain linker and the reaction yields, which increased with the length of the linker (***Scheme 5.7***). More flexible phosphines with a larger bite angle, such as dppb **L23** and dcpb **L27**, are more likely to result in a *trans*-coordination mode, and as a general rule, smaller bite-angle ligands tend to give more sluggish reactions compared to their wider bite-angle analogues.[166] Here, these trends can also be rationalised if de-coordination of a phosphine ligand is required in the mechanism to free a coordination site on the palladium, whether it is for the transmetalation step or the extrusion of HNSO. This is further supported by the similar results obtained with both dcpb **L27** (5 mol%) and P(*t*-Bu)$_2$Me•HBF$_4$ **L1** (10 mol%), which gave 33% and 35% yields, respectively. Indeed, given its long linker length, dcpb can be seen as two almost independent equivalents of PCy$_2$(alkyl), therefore acting as a trialkylphosphine with a low Tolman cone angle.



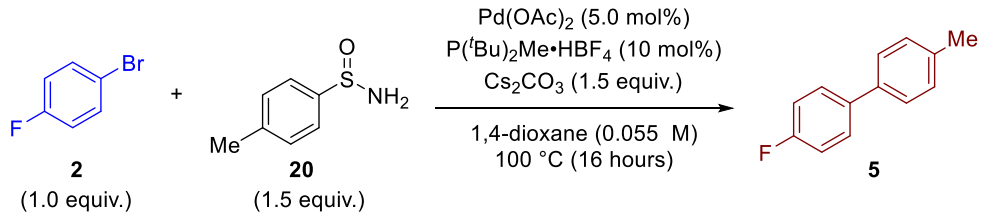
Scheme 5.7. Diphenylphosphino and dicyclohexylphosphino alkane ligand series. Correlation between the length of the ligand backbone and the yield of product **5**.

Other common bidentate ligands such as Xantphos, dppbenz, dppf, as well as tri- and tetradentate phosphines such as triphos or tetraphos were also evaluated, but yields remained poor (0-10%) without showing any clear trends. Complete data and experimental procedures for these screening experiments can be found in the **Experimental Section 7.4**.

5.5. Palladium Precatalyst

$Pd(OAc)_2$ was compared to four other palladium sources using P(*t*-Bu)$_2$Me•HBF_4 as a ligand (***Table 5.1***). The control reaction which employed $Pd(OAc)_2$ gave biaryl product **5** in 38% yield (*Entry 1*), illustrating the reproducibility of the reaction (35% under the same reaction conditions in ***Scheme 5.4***). The reaction yield dropped significantly with $Pd(TFA)_2$ and $PdCl_2$ to 26% and 16%, respectively (*Entries 2 and 3*), showing that the nature of the acetate ligand is of importance in this process. Allylpalladium cyclopentadiene is known to be a reliable precursor of low-valent palladium phosphine complexes after coordination of a phosphine ligand and reductive elimination to form C_3H_5-C_5H_5 as a mixture of isomers.[111, 211] However, its use only resulted in the formation of biaryl **5** in 20% yield (*Entry 4*). Similarly, biaryl **5** was obtained in 20% yield with the palladium(0) precatalyst $Pd_2(dba)_3$ (*Entry 5*). Once again,

reactions were found to give clean HPLC chromatograms with all five palladium precatalysts investigated, with unreacted starting material accounting for the mass balance. This excludes the possibility that presence of dba or C_3H_5-C_5H_5 might lead to the formation of side-products, therefore resulting in the observed erosion of the reaction yields. These results further support that acetate ligands might be required to maintain reactivity. Indeed, acetate ligands have been shown to favour the formation of anionic zero-valent intermediates in Heck reactions[110, 113, 212] as well as in the palladium-catalysed cross-coupling of carboxylic acid anhydrides with arylboronic acids.[213]



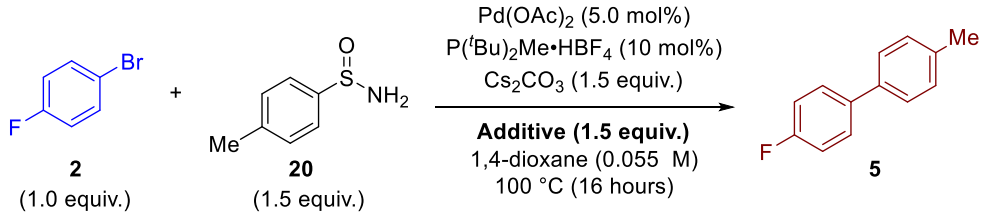
Entry	*Palladium Precatalyst*	*Yield*
1	$Pd(OAc)_2$	38%
2	$Pd(TFA)_2$	26%
3	$PdCl_2$	16%
4	(Allyl)Pd(Cp)	20%
5	$Pd_2(dba)_3$	20%

Table 5.1. Importance of the palladium source.

5.6. Additives

A range of additives were used to further increase the yield of the reaction (***Table 5.2***). Tetrabutylammonium halides inhibited the reaction, as yields dropped from 35-38% (control reaction without additive, *Entry 1*) to 8-13% (*Entries 2-4*). Employing tetramethylammonium chloride was detrimental as well, but to a lesser extent (*Entry 5*, 24%). Similarly, other (pseudo)halide sources NaI and NaOTf lowered the reaction yields (*Entries 6* and *7*). Given the discussion in the previous section about the role of acetate ligands, the presence of additional acetate additives was investigated. The reaction yield dropped to 18% in presence of NaOAc (*Entry 8*) but remained at 38% with CsOAc (*Entry 9*). The conjugate acid HOAc, however,

almost entirely stopped the catalytic process, with 8% yield in biaryl **5** being achieved (*Entry 10*).

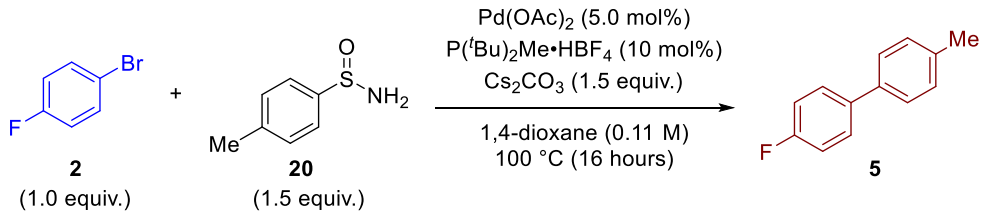


Entry	*Additive*	*Yield*	*Entry*	*Additive*	*Yield*
1	-	35-38%	8	NaOAc	18%
2	$(n\text{-Bu})_4NCl$	10%	9	CsOAc	36%
3	$(n\text{-Bu})_4NBr$	8%	10	HOAc	8%
4	$(n\text{-Bu})_4NI$	13%	11	NEt_3	35%
5	Me_4NCl	24%	12	NaH	38%
6	NaI	12%	13	KOH	3%
7	NaOTf	17%	14	H_2O (15 equiv.)	15%

Table 5.2. Additive screening.

Basic additives were also employed under the same reaction conditions, and although the presence of NEt_3 and NaH was well tolerated, they did not improve the yield (*Entries 12* and *13*, 35% and 38%). Whereas the addition of potassium hydroxide completely inhibited product formation (*Entry 13*, 3%). Importantly, water (15 equiv., 30 µL) was detrimental to the reaction. This is in clear contrast with the report by Zeng and co-workers, who showed that these two additives were crucial for the Pd/*t*-BuXPhos mediated *N*-arylation of sulfinamide **20**.[7]

The effect of the stoichiometry and of additional bases was further probed with higher reaction concentrations of 0.11 M compared to 0.055 M employed so far (***Table 5.3***). A control experiment with no additive gave biaryl product **5** in 40% yield (*Entry* 1), representing a slight yield increase due to the more concentrated reaction mixture. Increasing the stoichiometry of the base to 3.0 equiv. instead of 1.5 equiv. resulted in a yield increase to 49% (*Entry 2*). However, a simultaneous increase of both the base and sulfinamide was not beneficial to product formation (*Entry 3*, 42%), showing that maintaining a high base/sulfinamide ratio is important in this coupling process.



Entry	*Changes from the reaction scheme*	*Yield*
1	-	40%
2	Cs_2CO_3 (3.0 equiv)	49%
3	Cs_2CO_3 (3.0 equiv) and **20** (3.0 equiv)	42%
4	*t*-BuOK (1.5 equiv.)	2%
5	*t*-BuONa (1.5 equiv.)	27%
6	*t*-BuOLi (1.5 equiv.)	2%
7	KHMDS (1.5 equiv.)	1%
8	Caesium pivalate (1.5 equiv.)	48%
9	**20** deprotonated with *n*-BuLi	4%
10	Sodium sulfinate **4** instead of **20**	9%

Table 5.3. Screening of basic additives.

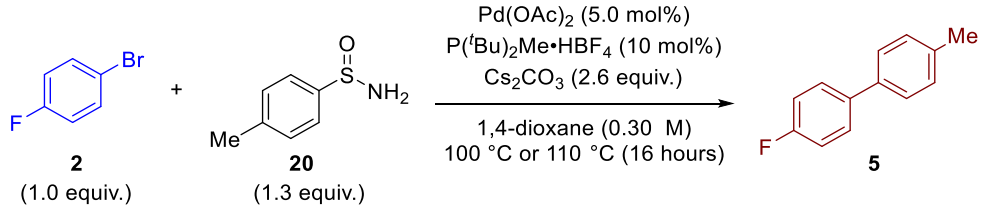
The presence of *tert*-butoxide bases was again assessed, but this time they were employed as an additive, together with Cs_2CO_3, rather than as the only base in the system as in **Section 5.3.** Their inclusion resulted in partial or complete inhibition of the coupling, in good agreement with previous observations (*Entries 4-6*). Similarly, the strong amide base KHMDS entirely suppressed reactivity (*Entry 7*, 1% yield). Using caesium pivalate as an additive increased the reaction yield to 48% (*Entry 8*). Given the previous observations with acetate additives and the stoichiometry of the carbonate base, we propose that this beneficial effect is due to increased quantities of caesium in the reaction mixture, rather than the presence of pivalate anions. When sulfinamide **20** was treated with *n*-BuLi prior to injection to a reaction tube containing the other components for the coupling reaction, the yield plummeted to 4% (*Entry 9*). This suggests that deprotonation of the sulfinamide coupling partner by the carbonate base is more likely to occur after its coordination to the oxidative addition complex.

Finally, the conditions of *Entry 1* were reproduced with sodium 4-methylbenzene sulfinate salt **4** (*Entry 10*) instead of sulfinamide **20**. Under those conditions, biaryl **5** was only obtained in 9% yield. This once again illustrates the superiority of sulfinamides as nucleophilic coupling

partners compared to sulfinate salts in palladium-catalysed carbon-carbon bond formation reactions.

5.7. Preparative Scale and Isolation

With these elements in hand, a preparative scale (0.30 mmol) reaction was performed to verify the screening results. Having observed that increasing the ratio of base to sulfinamide coupling partner was beneficial to the reaction yields, a 1:1.3:2.6 stoichiometry of aryl bromide/sulfinamide/base was chosen, and the reaction concentration was further increased to 0.30 M. Under these conditions, the product was obtained in 49% HPLC yield (***Table 5.4***, *Entry 1*), similarly to the previous best result (***Table 5.3***, *Entry 2*). Lowering the stoichiometry was therefore not detrimental and was encouraging from an atom economy perspective. After workup and purification of the product by flash column chromatography, biaryl **5** was isolated in 41% yield. This reaction was then repeated at 110 °C, and the HPLC yield increased to 63% yield, giving **5** in 61% yield upon isolation. Similarly to desulfinative cross-couplings, the drastic improvement caused by a small temperature difference highlights the crucial importance of the reaction temperature for these types of cross-coupling processes.



Entry	*Temperature*	*HPLC Yield*	*Isolated Yield*
1	100 °C	49%	41%
2	110 °C	63%	61%

Table 5.4. Isolation of biaryl product **5**, comparison of HPLC and isolated yields.

5.8. Conclusion and Future Work

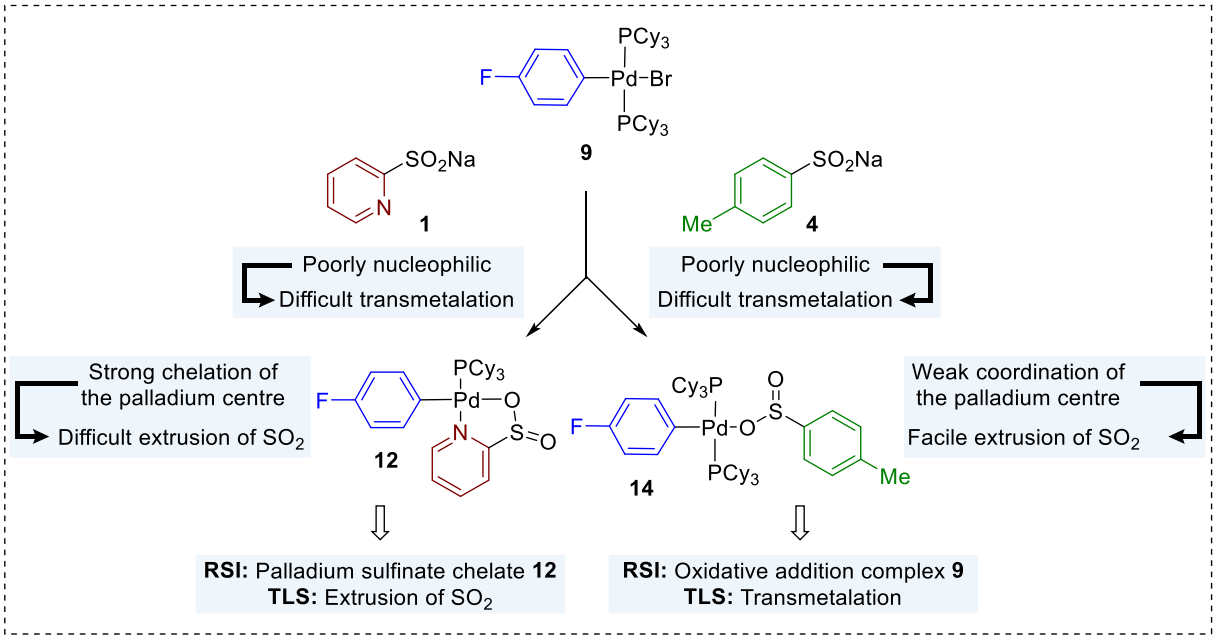
In summary, this **Chapter 5** shows that primary sulfinamides can be employed as novel nucleophilic coupling partner for palladium-catalysed carbon-carbon bond forming cross-coupling reactions. Synthetically useful yields can be achieved at high temperatures (80% HPLC yield at 150 °C), but more interestingly, the sulfinamide functional group has showed a high potential for their use at lower temperatures. Indeed, after screenings of the base, solvent, phosphine ligand, palladium source, additives and the stoichiometry of the reactants, biaryl **5** could be isolated in 41% yield, on a preparative scale, compared to 9% HPLC yield when the corresponding sulfinate salt was employed.

In order to fully demonstrate the value of this transformation, improvements on the current conditions are still required. DMF and THF were found to give slightly higher product yields compared to 1,4-dioxane under non-optimised reaction conditions and should therefore be reassessed with the best catalytic system, along with other polar solvents. The current system employs high loadings of Cs_2CO_3, but this base is expensive, and hygroscopic. As it was shown that these reaction conditions are sensitive to water, it would perhaps be beneficial to use the less expensive and less hygroscopic K_3PO_4, which was found to be a promising alternative base in initial screenings.

Finally, if required, raising the temperature to 110 °C or 120 °C would still make this cross-coupling reaction a valuable transformation, as primary aryl sulfinamides offer advantages over sulfinate salts in terms of functional group tolerance and ease of preparation. Furthermore, the possibility of sp^3-sp^2 cross-coupling reactions is also improved as alkyl sulfinamides are relatively common compared to alkyl sulfinates. Substrate functionalisation, orthogonality with other cross-coupling methods and application to 2-pyridyl substrates are also to be investigated.

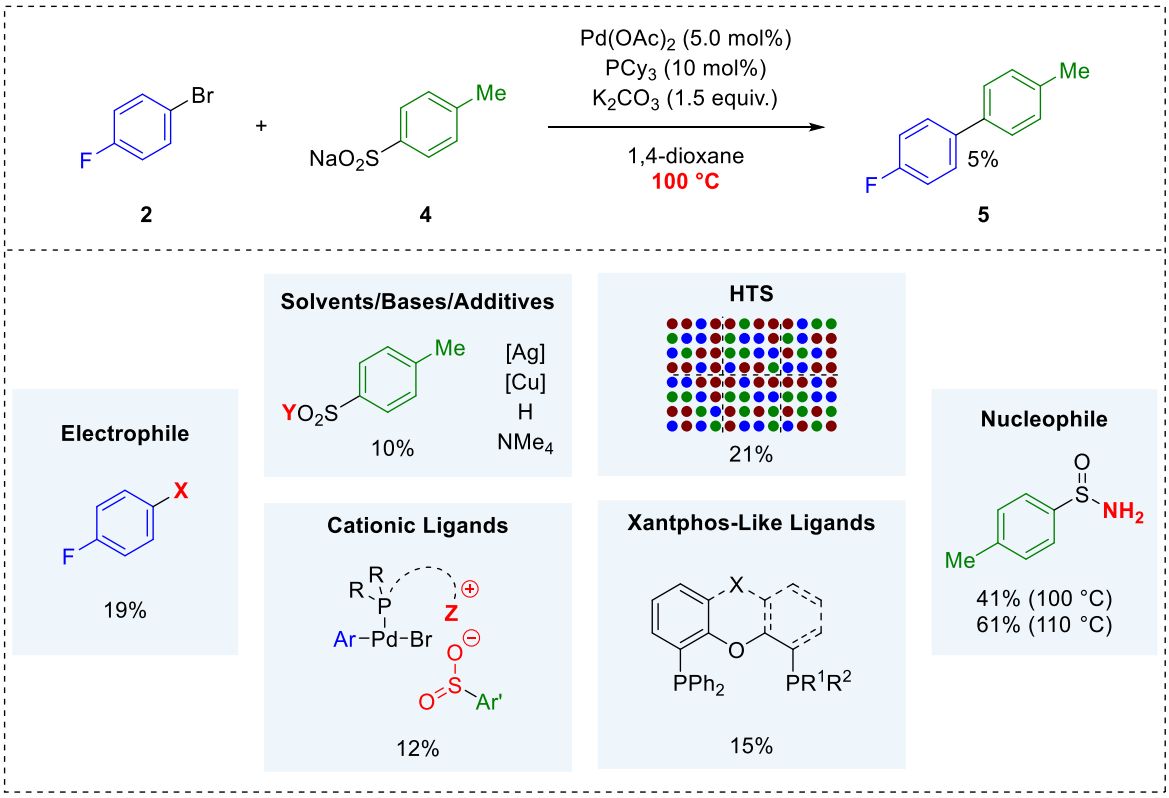
Chapter 6 – Conclusion

Mechanistic studies of the palladium-catalysed desulfinative cross-coupling of aryl bromides and (hetero)aryl sulfinate salts were described in **Chapter 2**. The isolation of novel palladium sulfinate complexes and study of their reactivity allowed us to deconvolute the elementary steps of the reaction. Both the heterocyclic 2-pyridyl sulfinate salt **1** and the carbocyclic 4-methylbenzene sulfinate salt **4** were found to be poorly nucleophilic, resulting in a difficult transmetalation step that required high temperatures. However, a key finding was the difference between the strong $\kappa^2_{N,O}$ chelation of 2-pyridyl sulfinate **1** in complex **12**, and the weak coordination of carbocyclic sulfinate **4** in complex **14**, leading to different rates of extrusion of SO_2. Consequently, the nature of the turnover limiting steps and resting state intermediates is different for these two substrates, as shown by a set of stoichiometric experiments and study of the kinetics of the catalytic process (***Scheme 6.1***). Additionally, the dual role of the carbonate base and the generation of the active palladium(0) species from the precatalyst $Pd(OAc)_2$ were investigated.



Scheme 6.1. Key findings on the nature of the RSI and TLS of the palladium-catalysed desulfinative cross-coupling of aryl bromides and (hetero)aryl sulfinate salts.

Following on from these mechanistic studies, a variety of approaches were undertaken to overcome the challenge of the transmetalation step, and promote the desulfinative cross-coupling of aryl bromide **2** and sodium 4-methylbenzene sulfinate **4** at 100 °C. The significance of this challenge was illustrated by the formation of biaryl product **5** in 5% yield upon decreasing the temperature from 150 °C to 100 °C (***Scheme 6.2***). In **Chapter 3**, the importance of solvents, bases, additives and electrophilic coupling partners was investigated, but reactivity remained poor with all the reaction conditions trialled. In an attempt to profit from the anionic nature of sulfinate salts, cationic phosphine ligands were synthesised *via* the methylation of bis-phosphine ligands, and were employed in the cross-coupling reaction. However, none of these ligands performed better than their non-methylated analogues. A high throughput screen, conducted in collaboration with Vertex, showed that with a broad scope of phosphine ligands, the reactions conditions that were optimal at 150 °C gave no more than 21% yield of cross-coupling product at 100 °C.

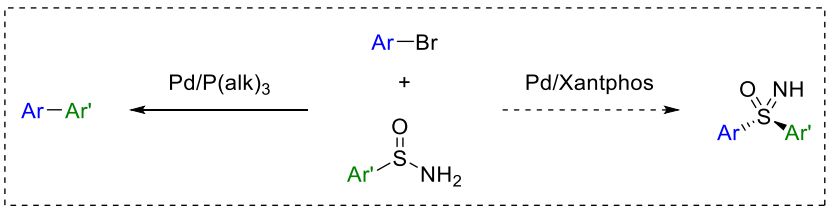


Scheme 6.2. Summary of our strategies to lower the temperature of palladium-catalysed desulfinative cross-coupling reactions.

In **Chapter 4**, efforts were directed to the synthesis of novel Xantphos-like bis-phosphine ligands. Indeed, Xantphos has the unique ability to promote the palladium-catalysed formation of diaryl sulfones from aryl halides and aryl sulfinate salts. Therefore promoting the transmetalation step at the target temperature of 100 °C. A range of ligands were designed and synthesised in order to fine-tune the reactivity of the system and favour the formation of biaryl over sulfone products. Unfortunately, reaction yields have so far remained poor, but computational work is ongoing to guide future ligand design.

Finally, **Chapter 5** reports initial results on the first palladium-catalysed desulfinamidative cross-coupling between aryl bromide **2** and 4-methylbenzene sulfinamide **20**. Comparison of sulfinamide **20** and sulfinate **4** under the same reaction conditions, showed that although sulfinate salt **4** performed better at 150 °C, sulfinamide **20** was superior at lower temperatures, with up to 61% isolated yield at 110 °C.

In summary, sulfinate salts are versatile substrates in palladium-catalysed cross-coupling chemistry as they can be employed for the formation of either biaryl or sulfone products, depending on the nature of the ligand involved. By combining our knowledge and efforts on Xantphos-like ligands and sulfinamides derivatives, it is possible to foresee the use of sulfinamides for the synthesis of diaryl sulfoximines as well as biaryl synthesis at lower temperatures.



Scheme 6.2. Primary aryl sulfinamides as promising reagents for palladium-catalysed synthesis of biaryls and sulfoximines.

Chapter 7 – Experimental Data and Procedures

Table of Contents

7.1. General Considerations 124

7.2. Experimental Data and Procedures for Chapter 2 126

7.2.1. Synthetic Procedures and Characterisation Data 126

7.2.1.1. List of Compounds Prepared According to Literature Procedures 126

7.2.1.2. Synthesis and Characterisation of Cross-Coupling Products 126

7.2.1.3. Synthesis and Characterisation of Palladium Complexes 129

7.2.1.4. Synthesis and Characterisation of Sulfinate Salts 141

7.2.2. Calibration Curves for HPLC Analysis 151

7.2.3. Formation of the Active Pd(0) Species 154

7.2.3.1. NMR Spectroscopy Monitoring 154

7.2.3.2. Correlation Between the Amount of Homocoupling Product (**5b**) Formed and the Amount of $Pd(OAc)_2$ Introduced in the Reaction Mixture 157

7.2.4. Oxidative Addition Complex **9** as a Competent Catalyst 158

7.2.5. Catalytic Activity of Palladium Complexes **9**, **11**, **12** and **14** 159

7.2.6. DOSY NMR Data 160

7.2.7. Reactivity of Complexes **9**, **11**, **14**, **12** and **12-CF$_3$** in 1,4-dioxane 163

7.2.8. Extrusion of SO2 from Complexes **11**, **14**, **12** and **12-CF$_3$** in toluene-d_8 and Monitored by $^{19}F\{1H\}$ NMR spectroscopy 166

7.2.9. Importance of the Sulfinate Counter Cation 171

7.2.10. Lability of PCy_3 in the Oxidative Addition Complex **9** 173

7.2.11. Identification of the Resting State Intermediates 173

7.2.12. Homogeneous vs Heterogeneous Catalysis 177

7.2.12.1. Mercury Test 177

7.2.12.2. Filtration Test 178

7.2.13. Initial Rate Studies 180

7.2.13.1. Influence of the Addition Order of the Reagents on the Initial Rate 180

7.2.13.2. Determination of the Reaction Order in [$Pd(OAc)_2$ + 2 PCy_3] With Sodium 4-methylbenzenesulfinate **4** 182

7.2.13.3. Determination of the Reaction Order in [$Pd(OAc)_2$ + 2 PCy_3] With Sodium Pyridine-2-sulfinate **1** 185
7.2.13.4. Determination of the Reaction Order in Ar-Br **2** With Sodium 4-methylbenzene Sulfinate **4** 187
7.2.13.5. Determination of the Reaction Order in Ar-Br **2** With Sodium Pyridine-2-sulfinate **1** 190
7.2.13.6. Determination of the Reaction Order in [$Pd(OAc)_2$ + 2 PCy_3] With Sodium 4-methylbenzenesulfinate **4** and Pd/PCy_3 ratio < 0.10 193
7.2.13.7. Determination of the Reaction Order in Ar-Br **2** With Sodium 4-methylbenzenesulfinate **4** and Pd/PCy_3 ratio < 0.10 195
7.2.14. Role of the Carbonate Base 198
7.2.14.1. Preparation of the solutions of SO_2 in 1,4-dioxane 198
7.2.14.2. Cross-Coupling Reactions Using Solvents A and B 199
7.2.15. Crystallographic and Refinement Data 200
7.2.15.1. Crystal Structure Determinations 200
7.2.15.2. Further Comments on Individual Crystal Structures 201
7.2.15.3. Selected bond length (Å) and angles (°) 202
7.2.15.4. Further Crystal Structures 203
7.2.15.5. Selected Crystallographic and Refinement Data 205

7.3. Experimental Data and Procedures for Chapter 3 206
7.3.1. General Procedure for the Screening Reactions 206
7.3.2. Stoichiometric Reactions With Oxidative Addition Complex **9** 206
7.3.2.1. Using Sulfinate **4-TMA** 206
7.3.2.2. Using Sulfinate **4** and $AgNO_3$ as an Additive 207
7.3.3. Synthetic Procedures and Characterisation Data 207
7.3.3.1. Sulfone Products 207
7.3.3.2. Ammonium-based ligand **PN^+1** 210
7.3.3.3. Methylation of Bis-Phosphine Ligands 211
7.3.4. High Throughput Screening Data 218
7.3.4.1. General Procedure 218
7.3.4.2. Work-up 219
7.3.4.3. Calculation of the Reaction Yields 219
7.3.4.4. Calibration Curves 220

7.3.4.5. Screening Data: HTS#1 224
7.3.4.6. Screening Data: HTS#2 226
7.3.4.7. Screening Data: HTS#3 230
7.3.4.8. Screening Data: HTS#4 232

7.4. Experimental Data and Procedures for Chapter 4 236
7.4.1. Oxidative Addition Complex **19** 236
7.4.2. Literature Procedures for the Synthesis of Phosphinic Acids 237
7.4.3. Novel Phosphinic Acids 237
7.4.4. (5-Iodo-9,9-dimethyl-9*H*-xanthen-4-yl)diphenylphosphane 242
7.4.5. General Procedures for the Synthesis of Ligands **L1-L13** 244
7.4.6. Characterisation Data for Ligands **L1-L13** 246
7.4.7. Other Novel Phosphine Ligands 256

7.5. Experimental Data and Procedures for Chapter 5 262
7.5.1. General Procedure for the Screening Reactions 262
7.5.2. Additional Ligand Screening Data 263
7.5.3. Additional Bar Charts 267
7.5.4. Preparative Scale and Isolation of the Product **5** 268

7.1. General Considerations

Reactions were performed in oven dried glassware under an atmosphere of dried argon with anhydrous solvents unless otherwise stated. Anhydrous CH_2Cl_2, Et_2O, C_6H_6, 1,4-dioxane and toluene were obtained by passing through alumina columns using an Innovative Technology Inc. PS-400-7 solvent purification system, these solvents were then degassed with argon prior to use. All other solvents were purchased as anhydrous from a commercial source. Reagents, ligands and catalysts were purchased from Sigma-Alrdrich Chemical Co. Ltd., Alfa Aesar, Arcos Organic Ltd., Fluorochem Ltd., Strem Chemicals Inc. or Insight Biotechnology Ltd. and were used as supplied unless otherwise stated. Tricyclohexylphosphine was purchased from Sigma-Alrdrich Chemical Co. Ltd. and palladium acetate was purchased from Strem Chemicals Inc.

Reactions were monitored by HPLC analysis and/or thin layer chromatography (TLC) using pre-coated aluminum-backed silica plates (Merck Kieselgel 60 F254). Plates were visualised under ultraviolet light (254 nm) followed by staining with KMnO4. Flash column chromatography was carried out using Geduran® Si 60, 40-63 micron silica gel; the compound to be purified was either loaded as oil or pre-absorbed onto silica. Petrol refers to the fraction of light Petroleum ether boiling in the range 40-60 °C. HPLC samples were analyzed using an Ascentis® Express C18 10 cm x 4.6 mm, 2.7 µm column (cat# 53827-U). Data was processed using Chem Station for LC systems Rev.B.04.01.SP1.

^{1}H NMR spectra were obtained on a Brüker AVIII HD 400 (400 MHz), AVII 500 (500 MHz) or AVIII HD 500 (500 MHz) spectrometer using the residual solvent as an internal standard. $^{13}C\{^{1}H\}$ NMR spectra were obtained on a Brüker AVIII HD 400 (101 MHz), AVII 500 (126 MHz) or AVIII HD 500 (126 MHz) spectrometer using the ^{1}H decoupling method and the residual solvent as an internal standard. ^{19}F NMR spectra were obtained on a Brüker AVIII HD

400 (377 MHz) spectrometer using the ^{1}H decoupling method. Acquisitions were carried out at room temperature unless otherwise stated. Chemical shifts (δ) are reported in parts per million (ppm) from the residual solvent peak and coupling constants (J) were given in Hertz (Hz) and rounded to the nearest 0.5 Hz. Proton multiplicity is assigned using the following abbreviations: singlet (s), doublet (d), triplet (t), quartet (q), quintet (p), multiplet (m), broad (br), apparent (app.).

High resolution mass spectra were recorded either on a Brüker MicroTOF spectrometer under electrospray ionization conditions (ESI) or on a Waters LCT Premier spectrometer under the conditions of chemical ionization (CI) by the internal service at Chemistry Research Laboratory, University of Oxford. Samples for mass spectra were prepared as 1 mg/mL solution in MeOH (HRMS-ESI). Values quoted are a ratio of mass to charge in Daltons. High resolution values are calculated to four decimal places from the molecular formula, all found within a tolerance of five ppm.

Infrared spectra were recorded on a Brüker Tensor 27 FT-IR spectrometer. Melting points were determined using a Stuart Scientific Melting Point Apparatus SMP1.

Cross-coupling reactions were performed using Kinesis KX Microwave Vials w/ Crimp Cap, 5 mL, Silicone/PTFE, 20 mm. This allowed the safe use of high reaction temperatures without the need for a blast shield.

7.2. Experimental Data and Procedures for Chapter 2

7.2.1. Synthetic Procedures and Characterisation Data

7.2.1.1. List of Compounds Prepared According to Literature Procedures

Dichlorobis(tricyclohexylphosphine)palladium(II)[124]

(η^3-Allyl)(η^5-cyclopentadienyl)palladium(II)[214]

2-Bromo-5-*tert*-butylpyridine[215]

3-Methoxy-3-oxopropane-1-sulfinate (*SMOPS*)[216]

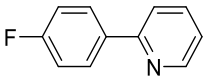
Pyridine-2-sulfinate (**1**)[61]

N-methylpyrrolidine SO_2 adduct (*TIMSO*)[58]

$[Pd(OAc)_2(PCy_3)_2]$ (**6**)[217]

7.2.1.2. Synthesis and Characterisation of Cross-Coupling Products

2-(4-Fluorophenyl)pyridine (3)



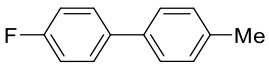
Modified procedure from Markovic *et al*.[58] Sodium pyridine-2-sulfinate (132 mg, 0.80 mmol, 2.0 equiv.), potassium carbonate (83 mg, 0.60 mmol, 1.5 equiv.), palladium acetate (4.5 mg, 0.020 mmol, 0.05 equiv.), tricyclohexylphosphine (11.2 mg, 0.040 mmol, 0.10 equiv.) were added to a microwave vial equipped with a stirrer bar. The vial was sealed with a microwave vial cap, evacuated (< 0.1 mbar) and back-filled with argon twice, then 1,4-dioxane (4.0 mL) and 1-bromo-4-fluorobenzene (44 µL, 0.40 mmol, 1.0 equiv.) were added. The reaction was heated at 150 °C for 16 hours. The mixture was allowed to cool to room temperature, then filtered through a pad of silica using EtOAc. The solvent was removed under reduced pressure,

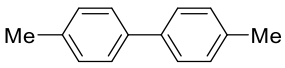
and the crude material was purified by column chromatography (gradient of EtOAc 0% to 5% in petrol) to yield the title compound in 95% yield (66 mg, 0.38 mmol) as a light yellow oil.

^{1}H NMR (400 MHz, $CDCl_3$) δ 8.67 (ddd, J = 5.0, 2.0, 1.0 Hz, 1H), 8.02 – 7.90 (m, 2H), 7.74 (ddd, J = 8.0, 7.5, 2.0 Hz, 1H), 7.67 (dt, J = 8.0, 1.0 Hz, 1H), 7.22 (ddd, J = 7.5, 5.0, 1.5 Hz, 1H), 7.19 – 7.11 (m, 2H); **^{13}C{^{1}H} NMR** (101 MHz, $CDCl_3$) δ 163.7 (d, J = 248.0 Hz), 156.6, 149.8, 136.9, 135.7 (d, J = 3.0 Hz), 128.8 (d, J = 8.5 Hz), 122.1, 120.3, 115.8 (d, J = 22.0 Hz); HRMS: m/z (EI) calculated for ($C_{11}H_8FN$) $[M+H]^+$: 174.0714, found: 174.0714.

Data consistent with the literature.[218]

4-Fluoro-4'-methyl-1,1'-biphenyl (5) and 4,4'-dimethyl-1,1'-biphenyl (5b)





Modified procedure from Markovic *et al.*[58] Sodium 4-methylbenzenesulfinate (143 mg, 0.80 mmol, 2.0 equiv.), potassium carbonate (83 mg, 0.60 mmol, 1.5 equiv.), palladium acetate (4.5 mg, 0.020 mmol, 0.05 equiv.) and tricyclohexylphosphine (11.2 mg, 0.040 mmol, 0.10 equiv.) were added to a microwave vial equipped with a stirrer bar. The vial was sealed with a microwave vial cap, evacuated (< 0.1 mbar) and back-filled with argon twice, then 1,4-dioxane (4.0 mL) and 1-bromo-4-fluorobenzene (44 µL, 0.40 mmol, 1.0 equiv.) were added. The reaction was heated at 150 °C for 16 hours. The mixture was allowed to cool to room temperature, filtered through a pad of silica and washed with EtOAc. The solvent was removed under reduced pressure, and purification of the crude material by flash chromatography (Gradient of EtOAc 0% to 2% in petrol) led to 75.5 mg of a 10.0:1.0 mixture of **5**/**5b** according to HPLC analysis corresponding to a yield of 92% (0.37 mmol) for compound **5**. This mixture was loaded on a preparative thin layer chromatography in order to obtain pure analytical samples. **5** was obtained as a white solid.

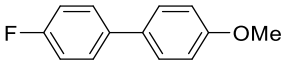
IR (thin film, cm^{-1}) 2945, 1603, 1498, 1264, 1225, 1157, 1096, 1007, 845, 809, 736, 704, 656; **^{1}H NMR** (400 MHz, $CDCl_3$) δ 7.56 – 7.50 (m, 2H), 7.47 – 7.41 (m, 2H), 7.28 – 7.21 (m, 2H), 7.15 – 7.05 (m, 2H), 2.40 (s, 3H); **^{13}C{^{1}H} NMR** (101 MHz, $CDCl_3$) δ 162.4 (d, J = 246.0 Hz), 137.5, 137.4 (d, J = 3.5 Hz), 137.2, 129.7, 128.6 (d, J = 8.0 Hz), 127.0, 115.7 (d, J = 21.5 Hz), 21.2; **^{19}F NMR** (377 MHz, $CDCl_3$) δ -116.30 (tt, J = 9.0, 5.5 Hz).

Data consistent with the literature.[219]

9 was obtained as a white solid (6.7 mg, 0.04 mmol). **^{1}H NMR** (400 MHz, $CDCl_3$) δ 7.63 – 7.47 (m, 2H), 7.29 – 7.23 (m, 2H), 2.42 (s, 3H); **^{13}C{^{1}H} NMR** (101 MHz, $CDCl_3$) δ 138.4, 136.8, 129.6, 126.9, 21.2.

Data consistent with the literature.[220]

4-Fluoro-4'-methoxy-1,1'-biphenyl (5-OMe)



Modified procedure from Markovic *et al*.[58] Lithium 4-methoxybenzene sulfinate (75 mg, 0.42 mmol, 2.0 equiv.), potassium carbonate (44 mg, 0.31 mmol, 1.5 equiv.), palladium acetate (2.4 mg, 0.01 mmol, 0.05 equiv.), tricyclohexylphosphine (5.9 mg, 0.02 mmol, 0.10 equiv.) were added to a microwave vial equipped with a stirrer bar. The vial was sealed with a microwave vial cap, evacuated (< 0.1 mbar) and back-filled with argon twice, then 1,4-dioxane (4.6 mL) and 1-bromo-4-fluorobenzene (23 µL, 0.21 mmol, 1.0 equiv.) were added. The reaction was heated at 150 °C for 16 hours. The mixture was allowed to cool to room temperature, then filtered through a pad of silica using EtOAc. The solvents were removed under reduced pressure, and the crude material was purified by column chromatography (gradient of EtOAc 0% to 2% in petrol) to yield the title compound in 87% yield (37 mg, 0.18 mmol) as a white solid.

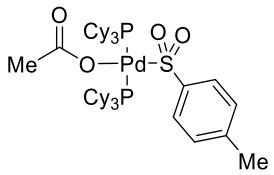
IR (thin film, cm^{-1}) 3016, 2967, 2843, 2360, 1893, 1599, 1573, 1494, 1466, 1442, 1399, 1326, 1307, 1290, 1268, 1255, 1234, 1182, 1160, 1131, 1037, 1012, 952, 826, 811, 791, 706, 627; **^{1}H NMR** (400 MHz, $CDCl_3$) δ 7.54 – 7.44 (m, 4H), 7.16 – 7.07 (m, 2H), 7.03 – 6.92 (m, 2H), 3.86 (s, 3H); **^{13}C{^{1}H} NMR** (101 MHz, $CDCl_3$) δ 162.1 (d, J = 245.5 Hz), 159.1, 137.0 (d, J = 3.0 Hz), 132.8, 128.2 (d, J = 8.0 Hz), 128.1, 115.5 (d, J = 21.5 Hz), 114.3, 55.4; **^{19}F{^{1}H} NMR** (377 MHz, $CDCl_3$) δ -116.70.

Data consistent with the literature.[221]

7.2.1.3. Synthesis and Characterisation of Palladium Complexes

Mass Spectroscopy analysis was conducted on the palladium complexes, but this method of characterisation was found unsuitable sur such compounds.

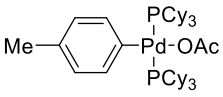
[Pd(OAc)(PCy$_3$)$_2$)(κ$_S$-4-CH$_3$-C$_6$H$_4$-SO$_2$)] (7)



Palladium acetate (30 mg, 0.13 mmol, 1.0 equiv.), tricyclohexylphosphine (75 mg, 0.27 mmol, 2.0 equiv.), sodium 4-methylbenzene sulfinate (84 mg, 0.47 mmol, 3.5 equiv.) and potassium carbonate (37 mg, 0.27 mmol, 2.0 equiv.) were introduced in a Schlenk flask. The flask was sealed with a septum, evacuated (< 0.1 mbar) and back-filled with argon twice, then 1,4-dioxane (2.7 mL) was added. The reaction was heated at 50 °C for 16 hours. After cooling to room temperature, the reaction was filtered under an inert atmosphere of argon and the solvent removed under vacuum. Pentane (7 mL) was added, and the solid that formed was washed with pentane (2 x 7 mL) then dried under high vacuum giving the title compound as a yellow solid. X-ray suitable crystals were obtained by recrystallization from CH_2Cl_2/hexane.

mp (decomp.) 123–128 °C (from CH_2Cl_2/hexane); **IR** (thin film, cm^{-1}) 3407, 2922, 2846, 2161, 1620, 1603, 1480, 1443, 1380, 1317, 1297, 1265, 1229, 1196, 1174, 1128, 1110, 1074, 1052, 1006, 914, 888, 849, 819, 794, 736, 710, 652, 617; **^{1}H NMR** (400 MHz, C_6D_6) δ 8.96 (d, broad, *J* = 7.5 Hz, 2H), 7.05 (d, *J* = 8.0 Hz, 2H), 2.77 – 2.54 (m, 6H), 2.28 – 2.07 (m, 15H), 2.01 (s, 3H), 1.86 – 1.45 (m, 30H), 1.41 – 1.06 (m, 18H); **^{13}C{^{1}H} NMR** (101 MHz, C_6D_6) δ 175.2, 155.3, 140.5, 129.3, 125.0, 34.1, 30.5, 28.3, 26.9, 25.6, 21.2; **^{31}P{^{1}H} NMR** (162 MHz, C_6D_6) δ 29.92.

[(4-Me-C_6H_4)Pd(PCy_3)$_2$(OAc)] (8)

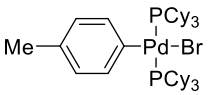


[(4-Me-C_6H_4)Pd(PCy_3)$_2$(Br)] (69 mg, 0.082 mmol, 1.0 equiv.) and silver acetate (15 mg, 0.090 mmol, 1.1 equiv.) were introduced in a 25 mL round bottom flask. The flask was sealed with a septum, evacuated (< 0.1 mbar) and back-filled with argon twice, then toluene (3.5 mL) was added. The reaction was stirred at room temperature for 16 hours. The dark brown reaction mixture was filtered through a pad of Celite® which was flushed with toluene, and concentrated under reduced pressure. Pentane (20 mL) was added, and the solid that formed was washed with pentane (2 x 20 mL) before drying under high vacuum to give the title compound as an off white solid in 19% yield (13 mg, 0.016 mmol).

mp (decomp.) 176–181 °C (from pentane); **IR** (thin film, cm^{-1}) 1619, 1481, 1447, 1366, 1318, 1298, 1267, 1228, 1200, 1175, 1129, 1111, 1074, 1053, 1005, 915, 888, 849, 799, 735, 709, 660, 615; **^{1}H NMR** (400 MHz, C_6D_6) δ 7.58 (d, *J* = 7.5 Hz, 1H), 6.91 (d, *J* = 7.5 Hz, 2H), 2.28 (s, 3H), 2.23 (s, 3H), 2.15 – 1.93 (m, 18H), 1.81 – 1.55 (m, 30H), 1.34 – 1.07 (m, 18H); **^{13}C{^{1}H} NMR** (126 MHz, C_6D_6) δ 174.6, 143.7, 138.9 (t, *J* = 3.5 Hz), 131.0, 34.2 (t, *J* = 8.5 Hz), 30.2,

28.27 (t, *J* = 5.0 Hz), 27.0, 25.8, 20.9 (one carbon under the residual benzene peak according to HSQC); **$^{31}P\{^{1}H\}$ NMR** (162 MHz, C_6D_6) δ 18.78.

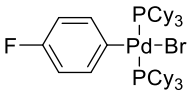
[(4-Me-C_6H_4)Pd(PCy_3)$_2$(Br)] (8b)



Cyclopentadienyl allyl palladium (100 mg, 0.47 mmol, 1.0 equiv.), tricyclohexylphosphine (283 mg, 1.00 mmol, 1.1 equiv.) and 1-bromo-4-methylbenzene (164 mg, 0.96 mmol, 2.0 equiv.) were introduced in a 25 mL round bottom flask. The flask was sealed with a septum, evacuated (< 0.1 mbar) and back-filled with argon twice, then benzene (3.5 mL) was added. The reaction was stirred at room temperature for 16 hours. Pentane (20 mL) was added resulting in the precipitation of a yellow solid. The reaction mixture was filtered, the filtrate was concentrated, and the resulting yellow slurry was triturated in pentane (20 mL) resulting in the precipitation of a solid an off white micro crystalline solid. The mixture was filtered and the solid dried under high vacuum to yield the title compound in 28% yield (110 mg, 0.13 mmol).

mp (decomp.) 150–155 °C (from pentane); **IR** (thin film, cm^{-1}) 1479, 1446, 1328, 1298, 1267, 1206, 1174, 1111, 1074, 1051, 1005, 915, 889, 849, 799, 734; **^{1}H NMR** (400 MHz, C_6D_6) δ 7.52 (d, *J* = 7.5 Hz, 2H), 6.92 (d, *J* = 7.5 Hz, 2H), 2.42 – 2.27 (m, 6H), 2.25 (s, 3H), 2.15 – 2.05 (m, 12H), 1.86 – 1.67 (m, 24H), 1.67 – 1.56 (m, 6H), 1.29 – 1.02 (m, 18H); **$^{13}C\{^{1}H\}$ NMR** (101 MHz, $CDCl_3$) δ 137.8 (t, *J* = 3.0 Hz), 130.9, 128.5, 127.8, 34.3 (t, *J* = 9.5 Hz), 30.2, 27.8 (t, *J* = 5.0 Hz), 26.7, 20.8; **$^{31}P\{^{1}H\}$ NMR** (162 MHz, C_6D_6) δ 19.92.

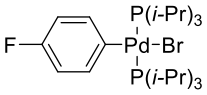
[(PCy_3)$_2$Pd(4-F-C_6H_4)(Br)] (9)



1-Bromo-4-fluorobenzene (315 µL, 2.87 mmol, 1.1 equiv.) was added to a schlenk flask containing [Pd(PCy_3)$_2$], which was generated *in situ* from [(PCy_3)$_2$Pd(Cl)$_2$] (1.92 g, 2.60 mmol, 1.0 equiv.) according to the procedure of Grushin *et al*.[124] After stirring at room temperature for 16 hours, the white precipitate was collected by filtration under air and washed with cold Et_2O to yield 71% (1.55 g, 1.84 mmol) of the title compound as a white solid.

mp (decomp.) 175–177 °C (from Et_2O); **IR** (thin film, cm^{-1}) 2927, 2851, 1475, 1447, 1211, 1007, 910, 849, 818, 733; **^{1}H NMR** (500 MHz, $CDCl_3$) δ 7.33 – 7.27 (m, 2H), 6.79 – 6.67 (m, 2H), 2.11 – 1.96 (m, 6H), 1.95 – 1.80 (m, 12H), 1.78 – 1.68 (m, 12H), 1.68 – 1.61 (m, 6H), 1.61 – 1.48 (m, 12H), 1.24 – 1.12 (m, 6H), 1.12 – 0.99 (m, 12H); **^{13}C{^{1}H} NMR** (126 MHz, $CDCl_3$) δ 160.0 (d, J = 240.0 Hz), 146.4 (q, J = 4.0 Hz), 138.1 (q, J = 4.0 Hz), 113.7 (d, J = 18.0 Hz), 34.2 (t, J = 9.5 Hz), 30.2, 27.8 (t, J = 5.0 Hz), 26.7; **^{31}P{^{1}H} NMR** (162 MHz, $CDCl_3$) δ 19.65 (d, J = 3.0 Hz); **^{19}F{^{1}H} NMR** (377 MHz, $CDCl_3$) δ -123.92 (t, J = 3.0 Hz).

[(PiPr$_3$)$_2$Pd(4-F-C_6H_4)(Br)] (9-*i*-Pr)

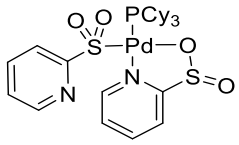


Tri-isopropylphosphine (420 µL, 2.34 mmol, 4.7 equiv.) was added to a solution of cyclopentadienyl allyl palladium (100 mg, 0.47 mmol, 1.0 equiv.) in benzene (4.0 mL) under an inert atmosphere of argon. The reaction was stirred at room temperature for 16 hours. The solvent was then removed under vacuum, and a white precipitate formed upon addition of hexane (5.0 mL). The obtained solid was washed with hexane (2 x 5 mL) and dried under high vacuum to yield the title compound in 55% yield (140 mg, 0.26 mmol) as a white solid.

mp (decomp.) 139–142 °C (from hexane); **IR** (thin film, cm^{-1}) 2962, 2869, 2160, 2033, 1569, 1475, 1387, 1368, 1290, 1247, 1210, 1151, 1091, 1057, 1038, 1008, 965, 927, 879, 813, 705, 654; **^{1}H NMR** (400 MHz, C_6D_6) δ 7.32 – 7.22 (m, 2H), 6.80 – 6.72 (m, 2H), 2.32 (ddh, *J* =

11.0, 7.0, 3.5 Hz, 6H), 1.14 (app. q, *J* = 7.0 Hz, 36H); **$^{13}C\{^{1}H\}$ NMR** (101 MHz, $CDCl_3$) δ 160.3 (d, *J* = 240.0 Hz), 141.4 (q, *J* = 4.0, Hz), 139.0 (q, *J* = 4.0 Hz), 113.8 (d, *J* = 18.5 Hz), 25.1 (t, *J* = 10.0 Hz), 20.2; **$^{31}P\{^{1}H\}$ NMR** (162 MHz, C_6D_6) δ 30.51 (d, *J* = 3.0 Hz); **^{19}F NMR** (377 MHz, C_6D_6) δ -122.22 (ttt, *J* = 10.0, 6.5, 3.0 Hz).

[(κS-2-pyridyl-SO_2)Pd(PCy_3))(κ^{2}N,O-pyridine-2-SO_2)] (10)

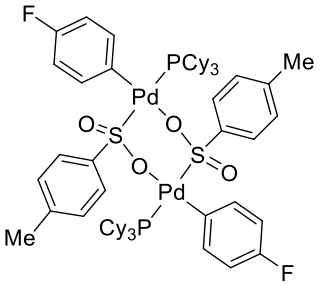


Palladium acetate (30 mg, 0.13 mmol, 1.0 equiv.), tricyclohexylphosphine (75 mg, 0.27 mmol, 2.0 equiv.), sodium pyridine-2-sulfinate (77 mg, 0.47 mmol, 3.5 equiv.) and potassium carbonate (37 mg, 0.27 mmol, 2.0 equiv.) were introduced in a Schlenk flask. The flask was sealed with a septum, evacuated (< 0.1 mbar) and back-filled with argon twice, then 1,4-dioxane (2.7 mL) was added. The reaction was heated at 50 °C for 16 hours. After cooling down, the reaction was filtered under an inert atmosphere of argon and the solvent removed under vacuum. Pentane (7 mL) was added, and the solid that formed was washed with pentane (2 x 7 mL) before drying under high vacuum to give the title compound as a yellow solid in 19% yield (17 mg, 0.025 mmol). X-ray suitable crystals were obtained by recrystallization from CH_2Cl_2/hexane.

mp (decomp.) 95–100 °C (from pentane); **IR** (thin film, cm^{-1}) 2926, 2850, 2360, 2161, 2023, 1592, 1574, 1560, 1446, 1298, 1269, 1213, 1176, 1130, 1086, 1060, 1004, 897, 848, 821, 773, 740, 723, 642, 619; **^{1}H NMR** (400 MHz, Toluene-d_8) δ 9.33 – 9.21 (m, 1H), 8.21 – 8.08 (m, 1H), 7.84 – 7.69 (m, 1H), 7.03 – 6.98 (m, 1H), 6.89 (td, *J* = 7.5, 2.0 Hz, 1H), 6.60 (td, *J* = 7.5, 1.5 Hz, 1H), 6.37 (ddd, *J* = 7.5, 5.0, 1.0 Hz, 1H), 6.29 – 6.18 (m, 1H), 3.03 – 2.75 (m, 3H), 2.28 – 2.15 (m, 6H), 1.92 – 1.78 (m, 6H), 1.78 – 1.68 (m, 6H), 1.67 – 1.54 (m, 3H), 1.39 – 1.07 (m, 9H); **$^{13}C\{^{1}H\}$ NMR** (126 MHz, Toluene-d_8) δ 178.0 (d, *J* = 2.0 Hz), 168.4 (d, *J* = 3.0 Hz),

150.9, 149.2, 139.3, 137.3, 125.4, 124.6 (d, *J* = 2.5 Hz), 121.4, 117.7, 34.1 (d, *J* = 23.0 Hz), 30.7, 28.3 (d, *J* = 12.0 Hz), 27.2; **$^{31}P\{^{1}H\}$ NMR** (162 MHz, Toluene-d_8) δ 52.69.

[(PCy_3)Pd(4-F-C_6H_4)(κ$_S$-κ$_O$'-4-Me-C_6H_4-SO_2)]$_2$ (11)

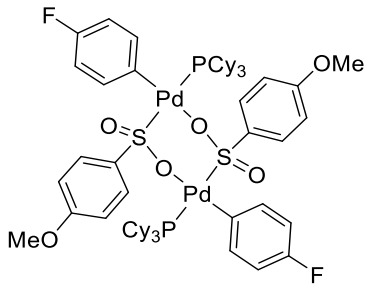


[(PCy_3)$_2$Pd(4-F-C_6H_4)(Br)] (750 mg, 0.89 mmol, 1.0 equiv.), silver nitrate (303 mg, 1.78 mmol, 2.0 equiv.), and sodium 4-methylbenzene sulfinate (317 mg, 1.78 mmol, 2.0 equiv.) were stirred in methanol under an argon atmosphere for 16 hours. The workup was performed under air. The solvent was removed under reduced pressure at room temperature. The resulting mixture was dissolved in benzene, then filtered through a pad of Celite® which was flushed with benzene, and concentrated under reduced pressure. Pentane (30 mL) was added, and the solid that formed was washed with pentane (2 x 30 mL) before drying under high vacuum to give the title compound as a white solid in 67% yield (381 mg, 0.60 mmol). X-ray suitable crystals were obtained by recrystallization from CH_2Cl_2/hexane.

mp (decomp.) 158–162 °C (from CH_2Cl_2/hexane); **IR** (thin film, cm^{-1}) 2925, 2851, 2161, 2033, 1567, 1474, 1442, 1295, 1204, 1161, 1147, 1086, 1053, 1026, 1012, 1001, 918, 886, 850, 820, 743, 708, 640; **^{1}H NMR** (500 MHz, C_6D_6) δ 7.90 (d, *J* = 8.0 Hz, 2H), 7.30 (m, 2H), 6.96 (d, *J* = 8.0 Hz, 2H), 6.69 (m , 2H), 2.02 (s, 3H), 1.94 – 1.79 (m, 9H), 1.63 – 1.54 (m, 6H), 1.53 – 1.39 (m, 9H), 1.14 – 0.87 (m, 9H); **$^{13}C\{^{1}H\}$ NMR** (126 MHz, C_6D_6) δ 161.3 (d, *J* = 240.0 Hz), 149.3 (d, *J* = 11.0 Hz), 139.9, 138.9 (d, *J* = 6.0 Hz), 138.0 – 137.3 (m), 128.8 – 127.9 (m), 126.8, 113.5 (d, *J* = 19.0 Hz), 33.7 (d, *J* = 19.0 Hz), 29.97, 27.8 (d, *J* = 11.0 Hz), 26.6, 21.2;

$^{31}P\{^{1}H\}$ NMR (162 MHz, C_6D_6) δ 27.79; **^{19}F NMR** (377 MHz, C_6D_6) δ -122.42 (app. dqd, *J* = 9.5, 6.5, 3.0 Hz).

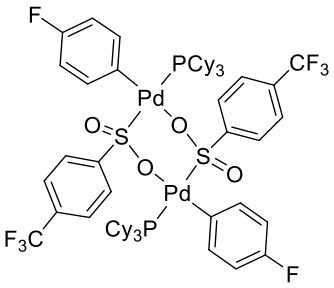
[(PCy$_3$)Pd(4-F-C$_6$H$_4$)(κ$_S$-κ$_O$'-4-MeO-C$_6$H$_4$-SO$_2$)]$_2$ (11-OMe)



[(PCy$_3$)$_2$Pd(4-F-C$_6$H$_4$)(Br)] (100 mg, 0.12 mmol, 1.0 equiv.), silver nitrate (22 mg, 0.13 mmol, 1.1 equiv.), and sodium 4-methoxybenzenesulfinate (25 mg, 0.13 mmol, 1.1 equiv.) were stirred in methanol under an argon atmosphere for 16 hours. The solvent was removed under reduced pressure at room temperature. The workup was performed under air. The resulting mixture was dissolved in CH_2Cl_2then filtered through a pad of Celite® which was flushed with CH_2Cl_2, and concentrated under reduced pressure. Et_2O (5 mL) was added, and the solid that formed was washed with Et_2O (2 x 5 mL) and recrystallized at –20 °C in CH_2Cl_2/hexane to yield the title compound in 49% yield (38 mg, 0.029 mmol) as a white solid.

mp (decomp.) 125–130 °C (from CH_2Cl_2/hexane); **IR** (thin film, cm^{-1}) 2925, 2850, 2161, 1593, 1493, 1476, 1445, 1300, 1249, 1210, 1149, 1088, 984, 913, 848, 812, 729, 644, 626; **^{1}H NMR** (400 MHz, $CDCl_3$) δ 7.48 (m, 2H), 6.91 (m, 2H), 6.75 (m, 2H), 6.45 (m, 2H), 3.81 (s, 3H), 1.81 – 1.50 (m, 18H), 1.47 – 1.28 (m, 6H), 1.22 – 1.01 (m, 3H), 0.99 – 0.80 (m, 6H); **$^{13}C\{^{1}H\}$ NMR** (101 MHz, $CDCl_3$) δ 160.7, 160.6 (d, J = 239.0 Hz), 143.3, 136.7, 127.8, 113.1 (d, J = 19.0 Hz), 112.8 33.2 (d, J = 19.5 Hz), 29.6, 27.6 (d, J = 11.0 Hz), 26.4; **^{31}P NMR** (162 MHz, $CDCl_3$) δ 27.79; **$^{19}F\{^{1}H\}$ NMR** (377 MHz, $CDCl_3$) δ -123.41.

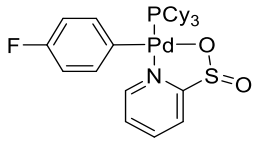
[(PCy$_3$)Pd(4-F-C$_6$H$_4$)(κ$_S$-κ$_O$'-4-CF$_3$-C$_6$H$_4$-SO$_2$)]$_2$ (11-CF$_3$)



[$(PCy_3)_2Pd(4\text{-}F\text{-}C_6H_4)(Br)$] (100 mg, 0.12 mmol, 1.0 equiv.), silver nitrate (22 mg, 0.13 mmol, 1.1 equiv.), and sodium 4-(trifluoromethyl)benzenesulfinate (30 mg, 0.13 mmol, 1.1 equiv.) were stirred in methanol under an argon atmosphere for 16 hours. The workup was performed under air. The solvent was removed under reduced pressure at room temperature. The resulting mixture was dissolved in CH_2Cl_2then filtered through a pad of Celite® which was flushed with CH_2Cl_2, and concentrated under reduced pressure. Et_2O (5 mL) was added, and the solid that formed was washed with Et_2O (2 x 5 mL) then recrystallized at –20 °C in CH_2Cl_2/hexane to yield the title compound in 37% yield (30 mg, 0.022 mmol) as a white solid.

mp (decomp.) 130–135 °C (from CH_2Cl_2/hexane); **IR** (thin film, cm^{-1}) 2361, 2341, 2161, 2029, 1572, 1476, 1447, 1400, 1323, 1209, 1164, 1127, 1101, 1060, 1025, 997, 911, 817, 735, 701, 613; **^{1}H NMR** (400 MHz, $CDCl_3$) δ 7.61 (d, J = 8.0 Hz, 2H), 7.49 (d, J = 8.0 Hz, 2H), 6.94 – 6.80 (m, 2H), 6.47 – 6.33 (m, 2H), 1.75 – 1.66 (m, 6H), 1.66 – 1.50 (m, 12H), 1.48 – 1.29 (m, 6H), 1.23 – 1.02 (m, 3H), 0.85 (m, 6H); **^{13}C{^{1}H} NMR** (101 MHz, $CDCl_3$) δ 160.7 (d, J = 241.5 Hz), 153.9 (d, J = 12.0 Hz), 136.7, 131.6 (d, J = 32.5 Hz), 126.5, 125.4, 124.7 (d, J = 4.0 Hz), 122.7, 113.6 (d, J = 19.0 Hz), 33.4 (d, J = 20.0 Hz), 29.7, 27.6 (d, J = 11.0 Hz), 26.3; **^{31}P{^{1}H} NMR** (162 MHz, $CDCl_3$) δ 28.97; **^{19}F NMR** (377 MHz, $CDCl_3$) δ -62.66, -122.51 – -122.62 (m).

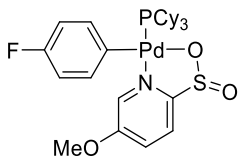
[$(PCy_3)Pd(4\text{-}F\text{-}C_6H_4)(\kappa^2_{N,O}$-pyridine-2-$SO_2$)] (12)



[$(PCy_3)_2Pd(4\text{-}F\text{-}C_6H_4)(Br)$] (750 mg, 0.89 mmol, 1.0 equiv.), silver nitrate (303 mg, 1.78 mmol, 2.0 equiv.), and sodium pyridine-4-sulfinate (294 mg, 1.78 mmol, 2.0 equiv.) were stirred in methanol under an argon atmosphere for 16 hours. The workup was performed under air. The solvent was removed under reduced pressure at room temperature. The resulting mixture was dissolved in benzene then filtered through a pad of Celite® which was flushed with CH_2Cl_2, and concentrated under reduced pressure. Pentane (30 mL) was added and the compound was allowed to crystallize over five hours at room temperature. The off-white crystals were washed with pentane and dried to give the title compound in 60% yield (0.53 mmol, 329 mg). X-ray suitable crystals were obtained by recrystallization from CH_2Cl_2/hexane.

mp (decomp.) 165–170 °C (from CH_2Cl_2/hexane); **IR** (thin film, cm^{-1}) 2917, 2849, 2159, 2029, 1589, 1570, 1475, 1447, 1286, 1211, 1151, 1126, 1073, 1006, 943, 914, 886, 850, 822, 777, 738, 709, 644; **^{1}H NMR** (400 MHz, $CDCl_3$) δ 7.89 – 7.67 (m, 2H), 7.51 – 7.34 (m, 2H), 7.21 – 7.17 (m, 1H), 7.16 – 7.06 (m, 1H), 6.90 – 6.79 (m, 2H), 2.06 – 1.87 (m, 9H), 1.84 – 1.73 (m, 6H), 1.73 – 1.54 (m, 9H), 1.34 – 1.19 (m, 3H), 1.12 (m, 6H); **^{13}C{^{1}H} NMR** (101 MHz, $CDCl_3$) δ 177.2, 160.9 (d, *J* = 241.5 Hz), 148.3, 144.5 (dd, *J* = 5.5, 2.5 Hz), 139.0, 136.1 (dd, *J* = 5.5, 3.5 Hz), 125.2 (d, *J* = 2.0 Hz), 122.6, 114.7 (d, *J* = 19.0 Hz), 34.4 (d, *J* = 24.0 Hz), 29.8, 27.6 (d, *J* = 11.0 Hz), 26.4; **^{31}P{^{1}H}** NMR (162 MHz, $CDCl_3$) δ 37.88; **^{19}F NMR** (377 MHz, $CDCl_3$) δ -121.02 – -121.15 (m).

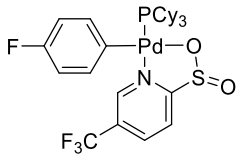
[$(PCy_3)Pd(4\text{-}F\text{-}C_6H_4)(\kappa^2_{N,O}\text{-}5\text{-}MeO\text{-}pyridine\text{-}2\text{-}SO_2)$] (12-OMe)



[(PCy_3)$_2$Pd(4-F-C_6H_4)(Br)] (100 mg, 0.12 mmol, 1.0 equiv.), silver nitrate (22 mg, 0.13 mmol, 1.1 equiv.), and sodium 5-methoxypyridine-2-sulfinate (26 mg, 0.13 mmol, 1.1 equiv.) were stirred in methanol under an argon atmosphere for 16 hours. The workup was performed under air. The solvent was removed under reduced pressure at room temperature. The resulting mixture was dissolved in CH_2Cl_2then filtered through a pad of Celite® which was flushed with CH_2Cl_2, and concentrated under reduced pressure. Et_2O (5 mL) was added, and the solid that formed was washed with Et_2O (2 x 5 mL) and recrystallized at –20 °C in CH_2Cl_2/hexane to yield the title compound in 49% yield (38 mg, 0.058 mmol) as a white solid.

mp (decomp.) 155–160 °C (from CH_2Cl_2/hexane); **IR** (thin film, cm^{-1}) 2921, 2847, 2161, 2029, 1568, 1475, 1443, 1326, 1291, 1276, 1241, 1206, 1174, 1155, 1106, 1081, 1052, 1033, 941, 918, 888, 851, 827, 753, 736, 704, 659, 620; **^{1}H NMR** (400 MHz, $CDCl_3$) δ 7.69 (dd, J = 8.5, 1.0 Hz, 1H), 7.41 (ddd, J = 8.5, 6.0, 2.0 Hz, 2H), 7.30 (dd, J = 8.5, 2.5 Hz, 1H), 6.85 (t, J = 9.0 Hz, 2H), 6.80 (t, J = 2.5 Hz, 1H), 3.57 (s, 3H), 2.07 – 1.91 (m, 9H), 1.84 – 1.73 (m, 6H), 1.72 – 1.52 (m, 9H), 1.36 – 1.18 (m, 3H), 1.18 – 1.04 (m, 6H); **^{13}C{^{1}H} NMR** (126 MHz, $CDCl_3$) δ 169.4 (d, J = 1.5 Hz), 160.9 (d, J = 241.5 Hz), 156.9 (d, J = 2.5 Hz), 145.0 (dd, J = 6.0, 3.0 Hz), 136.1 (dd, J = 5.5, 3.0 Hz), 135.6, 123.7, 123.2 (d, J = 2.0 Hz), 114.7 (dd, J = 19.0, 1.5 Hz), 55.8, 34.4 (d, J = 24.0 Hz), 29.8, 27.6 (d, J = 11.5 Hz), 26.4; **^{31}P{^{1}H} NMR** (162 MHz, $CDCl_3$) δ 38.11; **^{19}F NMR** (377 MHz, $CDCl_3$) δ -120.98 – -121.10 (m).

[(PCy_3)Pd(4-F-C_6H_4)($\kappa^2_{N,O}$-5-CF_3-pyridine-2-SO_2)] (12-CF_3)

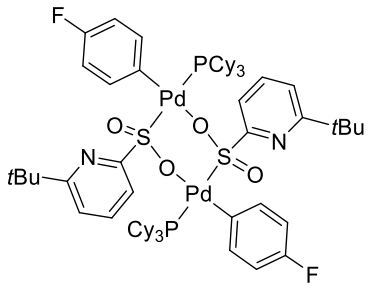


[(PCy_3)$_2$Pd(4-F-C_6H_4)(Br)] (100 mg, 0.12 mmol, 1.0 equiv.), silver nitrate (22 mg, 0.13 mmol, 1.1 equiv.), and sodium 5-methoxypyridine-2-sulfinate (30 mg, 0.13 mmol, 1.1 equiv.) were stirred in methanol under an argon atmosphere for 16 hours. The workup was performed under

air. The solvent was removed under reduced pressure at room temperature. The resulting mixture was dissolved in CH_2Cl_2then filtered through a pad of Celite® which was flushed with CH_2Cl_2, and concentrated under reduced pressure. Et_2O (5 mL) was added, and the solid that formed was washed with Et_2O (2 x 5 mL) and recrystallized at –20 °C in CH_2Cl_2/hexane to yield the title compound in 27% yield (22 mg, 0.032 mmol) as a white solid.

mp (decomp.) 150–155 °C (from CH_2Cl_2/hexane); **IR** (thin film, cm^{-1}) 2925, 2850, 2161, 1593, 1493, 1476, 1445, 1300, 1249, 1210, 1149, 1088, 984, 914, 849, 812, 729, 644, 626; **^{1}H NMR** (500 MHz, $CDCl_3$) δ 8.05 (dd, *J* = 8.0, 2.0 Hz, 1H), 7.91 (d, *J* = 8.0 Hz, 1H), 7.42 – 7.37 (m, 3H), 6.87 (t, *J* = 9.0 Hz, 2H), 2.06 – 1.93 (m, 6H), 1.84 – 1.75 (m, 6H), 1.73 – 1.55 (m, 9H), 1.31 – 1.20 (m, 6H), 1.18 – 1.07 (m, 6H); **^{13}C{^{1}H} NMR** (126 MHz, $CDCl_3$) δ 180.8, 161.1 (d, *J* = 242.5 Hz), 145.4 (q, *J* = 4.5 Hz), 143.4 (dd, *J* = 5.5, 3.0 Hz), 136.1 (q, *J* = 3.5 Hz), 135.8 (dd, *J* = 5.5, 3.0 Hz), 128.9 – 127.9 (m), 122.7 (d, *J* = 1.5 Hz), 122.3 (q, *J* = 272.9 Hz), 115.1 (dd, *J* = 19.0, 2.0 Hz), 34.5 (d, *J* = 24.0 Hz), 29.8, 27.6 (d, *J* = 11.5 Hz), 26.3; **^{31}P{^{1}H} NMR** (162 MHz, $CDCl_3$) δ 39.20; **^{19}F NMR** (377 MHz, $CDCl_3$) δ -62.91, -120.21 – -120.36 (m).

[(PCy_3)Pd(4-F-C_6H_4)(κ$_S$-κ$_O$-6-*t*Bu-pyridine-2-SO_2)]$_2$ (13)

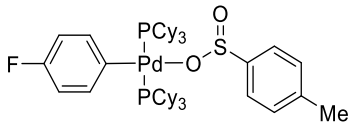


[(PCy_3)$_2$Pd(4-F-C_6H_4)(Br)] (100 mg, 0.12 mmol, 1.0 equiv.), silver nitrate (22 mg, 0.13 mmol, 1.1 equiv.), and lithium 6-(*tert*-butyl)pyridine-2-sulfinate (53 mg, 0.26 mmol, 2.2 equiv.) were stirred in methanol under an argon atmosphere for 16 hours. The solvent was removed under reduced pressure at room temperature. The resulting mixture was dissolved in benzene, then filtered through a pad of Celite® which was flushed with benzene and concentrated under

reduced pressure. Attempts to purify the crude mixture by precipitation and washing with Et_2O or pentane were unsuccessful. X-ray suitable crystals were obtained from the crude material by recrystallization from CH_2Cl_2/hexane at -20 °C. The following characterization data was obtained from the impure crude sample.

^{1}H NMR (400 MHz, $CDCl_3$) δ 7.79 (m, 1H), 7.71 – 7.51 (m, 1H), 7.36 (m, 1H), 7.33 – 7.28 (m, 2H), 6.75 (m, 2H), 2.31 – 2.11 (m, 7H), 1.76 (m, 30H), 1.55 – 1.40 (m, 9H), 1.36 – 0.97 (m, 27H); **^{31}P{^{1}H} NMR** (162 MHz, $CDCl_3$) δ 18.61 (d, J = 3.0 Hz); **^{19}F{^{1}H} NMR** (377 MHz, $CDCl_3$) δ -123.13 (t, J = 3.0 Hz).

[Pd(4-F-C_6H_4) (PCy_3)$_2$(κO-4-Me-C_6H_4-SO_2)] (14)



[Pd(4-F-C_6H_4)(PCy_3)(κS-κO'-4-Me-C_6H_4-SO_2)]$_2$ (122 mg, 0.096 mmol, 1.0 equiv.) and tricyclohexylphosphine (161 mg, 0.57 mmol, 6.0 equiv.) were introduced in a flask with a stirrer bar. The flask was sealed with a septum, evacuated (< 0.1 mbar) and back-filled with argon twice, then benzene (3.8 mL) was added. The reaction was stirred for 5 minutes, then the workup was carried out under air. The solvent was removed under vacuum, and pentane (10 mL) was added. The solid that formed was washed with pentane (2 x 10 mL) before drying under high vacuum to give the title compound title compound as a white solid in 57% yield (97 mg, 0.11 mmol). Washing the solid with Et_2O did not improve its purity. X-ray suitable crystals were obtained by recrystallization from dichloromethane/hexane.

mp (decomp.) 151–154 °C (from Et_2O); **IR** (thin film, cm^{-1}) 2922, 2850, 2160, 1475, 1447, 1204, 1086, 1070, 1051, 1005, 925, 889, 849, 817, 736, 617; **^{1}H NMR** (500 MHz, C_6D_6) δ 8.00 (d, *J* = 8.0 Hz, 2H), 7.43 – 7.33 (m, 2H), 7.11 (d, *J* = 8.0 Hz, 2H), 6.88 – 6.70 (m, 2H), 2.21 – 2.13 (m, 6H), 2.11 (s, 3H), 2.07 – 2.01 (m, 12H), 1.78 – 1.69 (m, 12H), 1.69 – 1.54 (m, 18H),

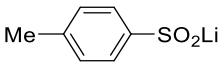
1.30 – 1.08 (m, 18H); **$^{13}C\{^{1}H\}$ NMR** (126 MHz, C_6D_6) δ 160.7 (d, *J* = 240.0 Hz), 155.54 139.0 (q, *J* = 4.0 Hz), 138.4, 128.9, 125.3, 113.9 (d, *J* = 18.5 Hz), 34.5 (t, *J* = 9.0 Hz), 30.5, 27.9 (t, *J* = 5.5 Hz), 26.9, 21.3; **$^{31}P\{^{1}H\}$ NMR** (162 MHz, C_6D_6) δ 22.04 (d, *J* = 3.0 Hz); **$^{19}F\{^{1}H\}$ NMR** (377 MHz, C_6D_6) δ -123.18 (t, *J* = 3.0 Hz).

7.2.1.4. Synthesis and Characterisation of Sulfinate Salts

General Procedure A: Synthesis of 4-methylphenylsulfinate salts with different counter cations

The reaction was performed under air. Sodium 4-methylbenzene sulfinate (1.0 equiv.) was dissolved in a 1:1 mixture of H_2O and CH_2Cl_2 (0.06 M). The reaction mixture was cooled to 0 °C before addition of HCl (2.0 equiv.). The reaction mixture was stirred for 5 minutes at 0 °C, then transferred to a separating funnel. The organic layer was quickly collected and cooled to 0 °C. The aqueous layer was discarded. H_2O (25 mL per gram of sodium sulfinate introduced) was added and the base XOH was added (0.5 equiv.) and stirred for 5 minutes at 0 °C. The reaction was transferred to a separating funnel, and layers were quickly separated. The organic layer was discarded, and the aqueous layer was concentrated under vacuum by forming an azeotrope with acetonitrile to yield the title compound without further purification.

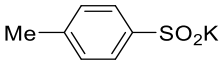
Lithium 4-methylbenzenesulfinate (4-Li)



General Procedure A was followed using sodium 4-methylbenzene sulfinate (2.00 g, 11.2mmol, 1.0 equiv.), 37% w/w aq. HCl (1.8 mL , 21.9 mmol, 2.0 equiv.) and lithium hydroxide monohydrate (235 mg, 5.6 mmol, 0.50 equiv.). The title compound was obtained as in 93% yield (846 mg, 5.2 mmol) as a white solid.

mp > 325 °C (from H_2O/MeCN); **IR** (thin film, cm^{-1}) 2916, 2160, 2032, 1598, 1491, 1370, 1086, 1031, 1013, 989, 813, 710, 639, 624; **^{1}H NMR** (400 MHz, CD_3OD) δ 7.59 – 7.50 (m, 2H), 7.27 – 7.20 (m, 2H), 2.36 (s, 3H); **^{13}C{^{1}H} NMR** (101 MHz, CD_3OD) δ 154.3, 140.6, 130.0, 125.3, 21.3; **HRMS**: m/z (EI) calculated for ($C_7H_7LiO_2S$) $[M–Li]^-$: 155.0172, found: 155.0170.

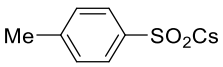
Potassium 4-methylbenzenesulfinate (4-K)



General Procedure A was followed using sodium 4-methylbenzene sulfinate (1.0 g, 5.6 mmol, 1.0 equiv.), 37% w/w aq. HCl (920 µL, 11.2 mmol, 2.0 equiv.) and potassium hydroxide (150 mg, 2.7 mmol, 0.48 equiv.). The title compound was obtained in 76% yield (520 mg, 2.1 mmol) as a white solid.

mp > 325 °C (from H_2O/MeCN); **IR** (thin film, cm^{-1}) 3382, 2919, 2162, 1674, 1596, 1487, 1389, 1078, 1019, 975, 811, 713, 686, 616; **^{1}H NMR** (400 MHz, CD_3OD) δ 7.61 – 7.41 (m, 2H), 7.30 – 7.15 (m, 2H), 2.36 (s, 3H); **^{13}C{^{1}H} NMR** (101 MHz, CD_3OD) δ 154.1, 140.8, 130.1, 125.3, 21.4; **HRMS**: m/z (EI) calculated for ($C_7H_7KO_2S$) $[M–K]^-$: 155.0172, found: 155.0170.

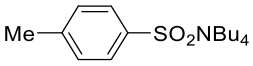
Caesium 4-methylbenzenesulfinate (4-Cs)



General Procedure A was followed using sodium 4-methylbenzene sulfinate (2.00 g, 11.2mmol, 1.0 equiv.), 37% w/w aq. HCl (1.8 mL , 21.9 mmol, 2.0 equiv.) and caesium hydroxide monohydrate (853 mg, 5.7 mmol, 0.51 equiv.). The title compound was obtained in 88% yield (1.42 g, 4.9 mmol) as a white solid.

mp 255–260 °C (from H_2O/MeCN); **IR** (thin film, cm^{-1}) 3245, 2360, 1486, 1076, 1053, 1015, 975, 815, 716, 618; **^{1}H NMR** (400 MHz, CD_3OD) δ 7.58 – 7.50 (m, 2H), 7.30 – 7.21 (m, 2H), 2.36 (s, 3H); **^{13}C{^{1}H} NMR** (101 MHz, CD_3OD) δ 154.2, 140.8, 130.0, 125.2, 21.3; **HRMS**: m/z (EI) calculated for ($C_7H_7CsO_2S$) $[M–Cs]^–$: 155.0172, found: 155.0170.

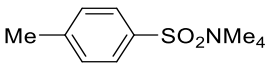
Tetrabutylammonium 4-methylbenzenesulfinate (4-TBA)



General Procedure A was followed using sodium 4-methylbenzene sulfinate (2.00 g, 11.2mmol, 1.0 equiv.), 37% w/w aq. HCl (1.8 mL , 21.9 mmol, 2.0 equiv.) and tetra-*n*-butylammonium hydroxide solution 1 M in MeOH (5.6 mL, 5.6 mmol, 0.50 equiv.). The title compound was obtained in 27% yield (592 mg, 1.49 mmol) as a white gel.

IR (thin film, cm^{-1}) 2959, 2874, 1487, 1381, 1199, 1119, 1033, 1012, 974, 883, 813, 739, 712, 678, 613; **^{1}H NMR** (400 MHz, CD_3OD) δ 7.57 – 7.51 (m, 2H), 7.26 – 7.20 (m, 2H), 3.27 – 3.16 (m, 8H), 2.35 (s, 3H), 1.72 – 1.58 (m, 8H), 1.41 (h, *J* = 7.5 Hz, 8H), 1.02 (t, *J* = 7.5 Hz, 12H); **^{13}C{^{1}H} NMR** (101 MHz, CD_3OD) δ 154.5, 140.5, 130.0, 125.3, 60.0 – 58.9 (m), 24.8, 21.3, 20.7 (m), 13.9; **HRMS**: m/z (EI) calculated for ($C_{23}H_{43}NO_2S$) $[M–NBu_4]^–$: 155.0172, found: 155.0170.

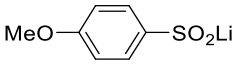
Tetramethylammonium 4-methylbenzenesulfinate (4-TMA)



General Procedure A was followed using sodium 4-methylbenzene sulfinate (2.00 g, 11.2mmol, 1.0 equiv.), 37% w/w HCl (1.8 mL , 21.9 mmol, 2.0 equiv.) and tetramethylammonium hydroxide 25% w/w in H_2O (2.0 mL, 5.6 mmol, 0.50 equiv.). The title compound was obtained as an extremely hygroscopic white solid in 87% yield (1.12 g, 4.9 mmol).

mp 180–185 °C (from H_2O /MeCN); **IR** (thin film, cm^{-1}) 3346, 3018, 2160, 1662, 1595, 1489, 1424, 1194, 1121, 1076, 1033, 969, 953, 815, 913, 681, 616; **^{1}H NMR** (400 MHz, CD_3OD) δ 7.66 – 7.48 (m, 2H), 7.34 – 7.20 (m, 2H), 3.14 (s, 12H), 2.37 (s, 3H); **^{13}C{^{1}H} NMR** (101 MHz, CD_3OD) δ 154.1, 140.8, 130.1, 125.3, 57.6 – 54.1 (m), 21.4; **HRMS**: m/z (EI) calculated for ($C_{11}H_{19}NO_2S$) $[M–NMe_4]^–$: 155.0172, found: 155.0170.

Lithium 4-methoxybenzenesulfinate 4-OMe

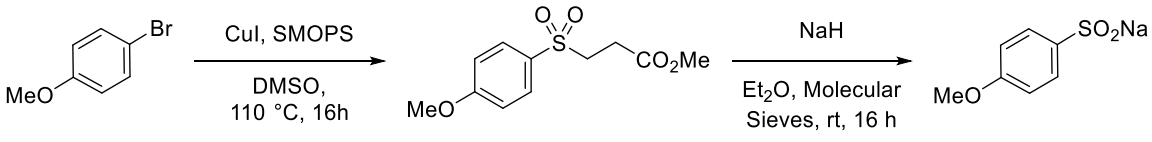


A solution of *n*-BuLi (2.50 M in Hexane) (3.4 mL, 8.5 mmol, 0.9 equiv.) was added to a solution of 1-bromo-4-methoxybenzene (1.2 mL, 9.6 mmol, 1.0 equiv.) in THF at -78 °C. The reaction was stirred at -78 °C for 40 minutes before slow addition of *TIMSO* (1.43 g, 9.6 mmol, 1.0 equiv.) at -78 °C. The mixture was allowed to warm to room temperature and stirred for 10 minutes. The reaction mixture was quenched with MeOH, and the solvents were removed under reduced pressure. The residue was suspended in a 1:1 mixture of acetone/ Et_2O and stirred for 2 hours. The suspension was filtered and washed extensively with acetone and Et_2O, then dried under high vacuum to yield the title compound as a white solid in 74% yield (1.12 g, 6.3 mmol).

^{1}H NMR (400 MHz, CD_3OD) δ 7.57 (d, J = 8.5 Hz, 2H), 6.96 (d, J = 8.5 Hz, 2H), 3.81 (s, 3H); **^{13}C{^{1}H} NMR** (101 MHz, CD_3OD) δ 162.2, 149.1, 126.8, 114.67, 55.8; **HRMS**: m/z (EI) calculated for ($C_7H_7LiO_3S$) $[M–Li]^–$: 171.0121, found: 171.0120.

Data consistent with the literature[58]

Sodium 4-methoxybenzenesulfinate (4-OMe-Na)



4-Bromoanisole (1.50 g, 8.02 mmol, 1.0 equiv.) was added to a solution of CuI (4.58 g, 24.1 mmol, 3.0 equiv.) and *SMOPS* (4.19 g, 24.1 mmol, 3.0 equiv.) in DMSO (24 mL). The reaction was stirred under a nitrogen atmosphere at 110 °C for 16 hours. The mixture was then cooled to room temperature, diluted with EtOAc (50 mL) and filtered through a pad of silica. The filtrate was washed with H_2O (3 x 50 mL), brine (3 x 50 mL), dried over magnesium sulfate, and concentrated under reduced pressure. The product was purified by column chromatography (Gradient of ETOAC30% to 40% in PETROL) to yield 45% (939 mg, 3.64 mmol) of methyl 3-((4-methoxyphenyl)sulfonyl)propanoate as a white solid.

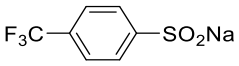
mp 34–35 °C (from EA/PETROL); **IR** (thin film, cm^{-1}) 3934, 5161, 2034, 1732 ,1598, 1578, 1500, 1457, 1434, 1412, 1369, 1311, 1285, 1261, 1207, 1159, 1137, 1090, 1062, 1023, 973, 942, 834, 820, 804, 745, 711; **^{1}H NMR** (400 MHz, $CDCl_3$) δ 7.83 (d, J = 9.0 Hz, 2H), 7.03 (d, J = 9.0 Hz, 2H), 3.89 (s, 3H), 3.65 (s, 3H), 3.49 – 3.24 (m, 2H), 2.77 – 2.71 (m, 2H); **^{13}C{^{1}H} NMR** (101 MHz, $CDCl_3$) δ 170.7, 164.1, 130.5, 130.1, 114.7, 55.9, 52.4, 51.9, 27.9; **HRMS**: m/z (EI) calculated for ($C_{11}H_{14}O_5S$) $[M+H]^+$: 259.0635, found: 259.0634.

A solution of methyl 3-((4-methoxyphenyl)sulfonyl)propanoate (500 mg, 1.94 mmol, 1.0 equiv.) in Et_2O (39 mL) was slowly added to a flask containing sodium hydride (60% in mineral oil, 77.4 mg, 1.94 mmol, 1.0 equiv.) and 3 Å activated molecular sieves (5.00 g) under nitrogen atmosphere at 0 °C. The resulting mixture was stirred for 16 hours at room temperature, then quenched with MeOH at 0 °C, filtered through a pad of Celite® which was flushed with methanol, and concentrated under reduced pressure. The resulting solid was dissolved in H_2O (5 mL), washed with CH_2Cl_2 (3 x 5 mL), and the solvents were removed under reduced pressure by forming an azeotrope with acetonitrile to yield the title compound in 96% (360 mg, 1.85 mmol) as a white solid.

mp (decomp.) 275–280 °C (from H_2O/MeCN); **IR** (thin film, cm^{-1}) 1635, 1591, 1574, 1489, 1467, 1439, 1370, 1299, 1244, 1171, 1084, 1045, 976, 837, 823, 792, 722, 623; **^{1}H NMR** (400

MHz, CD_3OD) δ 7.57 (d, J = 9.0 Hz, 2H), 6.95 (d, J = 9.0 Hz, 2H), 3.81 (s, 3H); **$^{13}C\{^1H\}$ NMR** (101 MHz, CD_3OD) δ 162.2, 149.3, 126.7, 114.7, 55.8; **HRMS**: m/z (EI) calculated for ($C_7H_7NaO_3S$) $[M–Na]^–$: 171.0121, found: 171.0119.

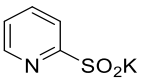
Sodium 4-(trifluoromethyl)benzenesulfinate (4-CF_3)



The reaction was performed under air. Hydrogen peroxide solution (30% w/w in H_2O, 271 µL, 2.80 mmol, 1.0 equiv.) was slowly added to a solution of 4-(trifluoromethyl)benzenethiol and sodium hydroxide (101 mg, 2.53 mmol, 0.9 equiv.) in methanol (12 mL) and H_2O (12 mL) at 0 °C. The resulting mixture was allowed to warm to room temperature over 16 hours. The solvent was removed under reduced pressure, and the solid was washed with EtOAc (Et_2O should be used instead to avoid formation of NaOAc). The obtained off-white solid was dissolved in a minimum amount of H_2O and precipitated by addition of acetonitrile leading to 49% (275 mg, 1.18 mmol) of the title compound.

mp (decomp.) 275–280 °C (from H_2O/MeCN); **IR** (thin film, cm^{-1}) 1667, 1601, 1398, 1328, 1132, 1104, 1059, 1034, 1016, 989, 976, 925, 854, 842, 741, 720, 696, 652, 611; **^1H NMR** (500 MHz, CD_3OD) δ 7.83 (d, J = 8.0 Hz, 2H), 7.73 (d, J = 8.0 Hz, 2H); **$^{13}C\{^1H\}$ NMR** (126 MHz, CD_3OD) δ 180.5 (s, CH_3CO_2Na impurity), 161.5 (d, J = 1.5 Hz), 132.3 (q, J = 32.0 Hz), 126.5 (q, J = 4.0 Hz), 126.1, 125.60 (q, J = 271.5 Hz), 24.2 (s, CH_3CO_2Na impurity); **^{19}F NMR** (377 MHz, CD_3OD) δ -63.98; **HRMS**: m/z (EI) calculated for ($C_7H_4F_3NaO_2S$) $[M–Na]^–$: 208.9890, found: 208.9888.

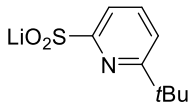
Potassium pyridine-2-sulfinate (1-K)



Pyridine-2-thiol (1.00 g, 9.0 mmol, 1.0 equiv.) and potassium hydroxide (454 mg, 8.1 mmol, 0.9 equiv.) were dissolved in methanol (40 mL) and H_2O (5.0 mL). The reaction mixture was cooled to 0 °C, and hydrogen peroxide 30% w/w in H_2O (1.7 mL, 17.5 mmol, 2.0 equiv.) was added dropwise. The reaction was allowed to warm to room temperature over 16 hours, after which 30 mL of H_2O and 100 mL of dichloromethane were added. The aqueous layer was concentrated under vacuum by forming an azeotrope with acetonitrile to yield the title compound without further purification as an extremely hygroscopic off white solid in 69% yield (1.13 g, 6.2 mmol).

mp 185–190 °C (from H_2O/MeCN); **IR** (thin film, cm^{-1}) 1574, 1560, 1453, 1418, 1276, 1209, 1145, 1062, 1041, 1008, 979, 778, 767, 750, 741, 715, 632, 618; **^{1}H NMR** (200 MHz, CD_3OD) δ 8.52 (ddd, *J* = 5.0, 1.5, 1.0 Hz, 1H), 8.10 – 7.74 (m, 2H), 7.41 (ddd, *J* = 7.0, 5.0, 2.0 Hz, 1H); **^{13}C{^{1}H} NMR** (101 MHz, CD_3OD) δ 174.6, 149.5, 139.4, 125.7, 118.8; **HRMS**: m/z (EI) calculated for ($C_5H_4KNO_2S$) $[M–K]^–$: 141.9957, found: 141.9960.

Lithium 6-(tert-butyl)pyridine-2-sulfinate (1-*t*-Bu)

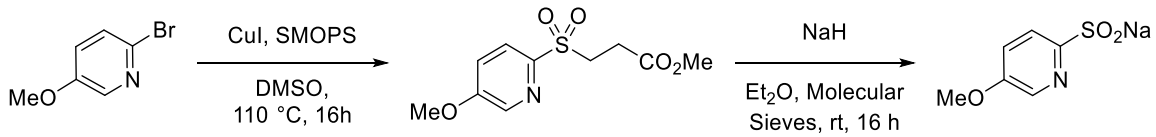


A solution of *n*-BuLi (2.15 M in Hexane) (1.3 mL, 2.80 mmol, 0.93 equiv.) was added to a solution of 2-bromo-6-(*tert*-butyl)pyridine (650 mg, 3.04 mmol, 1.0 equiv.) in THF at -78 °C. The reaction was stirred at -78 °C for 40 minutes before slow addition of *TIMSO* (450 mg, 3.02 mmol, 1.0 equiv.) at -78 °C. The mixture was allowed to warm to room temperature over 10 minutes. The reaction mixture was quenched with MeOH, and the solvents were removed under reduced pressure. The residue was suspended in Et_2O, loaded on a silica plug, and washed thoroughly with Et_2O. The Et_2O fractions were all discarded, then MeOH was added and the

product was collected. Removing the solvent under vacuum yielded the title compound as a white solid in 93% yield (536 mg, 2.61 mmol).

mp 150–155 °C (from methanol); **IR** (thin film, cm^{-1}) 2958, 2160, 2025, 1581, 1558, 1479, 1437, 1396, 1362, 1204, 1169, 1140, 1035, 977, 859, 810, 769, 747, 673; **^{1}H NMR** (400 MHz, CD_3OD) δ 7.80 (app. t, *J* = 8.0 Hz, 1H), 7.68 (dd, *J* = 8.0, 1.0 Hz, 1H), 7.41 (dd, *J* = 8.0, 1.0 Hz, 1H), 1.38 (s, 9H); **^{13}C{^{1}H} NMR** (101 MHz, CD_3OD) δ 173.6, 169.7, 138.8, 120.7, 114.7, 38.5, 30.6; **HRMS**: m/z (EI) calculated for ($C_9H_{12}KNO_2S$) $[M–Li]^-$: 198.0594, found: 198.0590.

Sodium 5-methoxypyridine-2-sulfinate



2-Bromo-5-methoxypyridine (1.00 g, 5.32 mmol, 1.0 equiv.) was added to a solution of CuI (3.04 g, 16.0 mmol, 3.0 equiv.) and *SMOPS* (2.78 g, 16.0 mmol, 3.0 equiv.) in DMSO (16 mL). The reaction was stirred under a nitrogen atmosphere at 110 °C for 16 hours. The mixture was cooled to room temperature, diluted with EtOAc (40 mL) and filtered through a pad of silica. The filtrate was washed with H_2O (3 x 40 mL), brine (3 x 40 mL), dried over magnesium sulfate, and concentrated under reduced pressure. The product was purified by column chromatography (Toluene/dichloromethane/EtOAc 45:40:15) to yield 11% (154 mg, 0.60 mmol) of methyl 3-((5-methoxypyridin-2-yl)sulfonyl)propanoate as a light yellow oil.

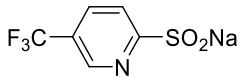
IR (thin film, cm^{-1}) 2950, 1735, 1573, 1463, 1437, 1394, 1365, 1307, 1278, 1248, 1200, 1159, 1129, 1097, 1059, 1017, 980, 835, 753, 722; **^{1}H NMR** (400 MHz, $CDCl_3$) δ 8.37 (dd, J = 3.0, 0.5 Hz, 1H), 8.01 (dd, J = 9.0, 0.5 Hz, 1H), 7.34 (dd, J = 9.0, 3.0 Hz, 1H), 3.94 (s, 3H), 3.68 – 3.61 (m, 5H), 2.84 – 2.73 (m, 2H); **^{13}C{^{1}H} NMR** (101 MHz, $CDCl_3$) δ 170.4, 158.7, 148.1,

139.4 – 139.0 (m), 124.2, 120.4, 56.2 (d, J = 13.2 Hz), 52.4 (d, J = 10.7 Hz), 48.2, 27.6; **HRMS**: m/z (EI) calculated for ($C_{10}H1_3NO_5S$) $[M+ H]^+$: 260.0587, found: 260.0588.

A solution of methyl 3-((5-methoxypyridin-2-yl)sulfonyl)propanoate (140 mg, 0.54 mmol, 1.0 equiv.) in Et_2O (11 mL) was slowly added to a flask containing sodium hydride (60% in mineral oil, 22 mg, 0.54 mmol, 1.0 equiv.) and 3Å activated molecular sieves (1.4 g) under nitrogen atmosphere at 0 °C. The resulting mixture was stirred for 16 hours at room temperature, then quenched with MeOH at 0 °C, filtered through a pad of Celite® which was flushed with methanol and concentrated under reduced pressure. The resulting solid was dissolved in H_2O (5 mL), washed with dichloromethane (3 x 5 mL), and the solvents were removed under reduced pressure using by forming an azeotrope with acetonitrile to yield the title compound in 82% yield (86 mg, 0.44 mmol) as a white solid.

mp (decomp.) 245–250 °C (from H_2O/MeCN); **IR** (thin film, cm^{-1}) 3404, 1632, 1578, 1566, 1464, 1385, 1290, 1269, 1238, 1109, 1057, 1015, 980, 838, 750, 642, 612; **^{1}H NMR** (400 MHz, CD_3OD) δ 8.19 (dd, J = 3.0, 0.5 Hz, 1H), 7.81 (dd, J = 9.0, 0.5 Hz, 1H), 7.49 (dd, J = 9.0, 3.0 Hz, 1H), 3.90 (s, 3H); **^{13}C{^{1}H} NMR** (101 MHz, CD_3OD) δ 166.4, 158.1, 137.1, 123.0, 120.1, 56.4; **HRMS**: m/z (EI) calculated for ($C_6H_6NNaO_3S$) $[M–Na]^–$: 172.0074, found: 172.0072.

Sodium 5-(trifluoromethyl)pyridine-2-sulfinate

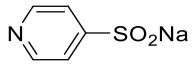


Procedure performed under air. Hydrogen peroxide solution (30% w/w in H_2O, 590 µL, 6.11 mmol, 2.0 equiv.) was slowly added to a solution of 5-(trifluoromethyl)pyridine-2-thiol (547 mg, 3.05 mmol, 1.0 equiv.) and sodium hydroxide (147 mg, 3.68 mmol, 1.2 equiv.) in methanol (15 mL) and H_2O (15 mL) at 0 °C. The resulting mixture was allowed to warm to room temperature over 16 hours. The solvents were removed under reduced pressure by

forming an azeotrope with acetonitrile. The crude solid was recrystallized in acetone (100 mL) and H_2O (6 mL) yielding 24% (174 mg, 0.75 mmol) of the title compound as white needles.

mp (decomp.) 240–245 °C (from H_2O/MeCN); **IR** (thin film, cm^{-1}) 3247, 2161, 1594, 1569, 1378, 1327, 1251, 1169, 1130, 1103, 1062, 1021, 988, 948, 850, 766, 706, 620; **^{1}H NMR** (400 MHz, CD_3OD) δ 8.86 – 8.84 (m, 1H), 8.26 (ddd, J = 8.0, 2.0, 0.5 Hz, 1H), 8.04 (dt, J = 8.0, 0.5 Hz, 1H); **^{13}C{^{1}H} NMR** (126 MHz, CD_3OD) δ 178.6 (d, J = 1.5 Hz), 146.7 (q, J = 4.0 Hz), 136.4 (q, J = 3.5 Hz), 128.1 (q, J = 33.0 Hz), 123.9 (q, J = 272.2 Hz), 119.2; **^{19}F NMR** (377 MHz, CD_3OD) δ -63.82; **HRMS**: m/z (EI) calculated for ($C_6H_3F_3NNaO_2S$) $[M–Na]^-$: 209.9842, found: 209.9837.

Sodium pyridine-4-sulfinate (16)



The reaction was performed under air. Pyridine-4-thiol (1.03 g, 9.3 mmol, 1.0 equiv.) and sodium hydroxide (445 mg, 11.1 mmol, 1.2 equiv.) were dissolved in methanol (45 mL) and H_2O (45 mL). The reaction mixture was cooled to 0 °C, and hydrogen peroxide 30% w/w in H_2O (1.6 mL, 18.2 mmol, 2.0 equiv.) was added dropwise. The reaction was allowed to warm to room temperature over 16 hours. The solvents were removed under vacuum by forming an azeotrope with acetonitrile. The crude off-white solid was recrystallized in a mixture of acetone/ H_2O 15:1 which gave the title compound in 11% yield as a white solid (161 mg, 0.97 mmol).

mp (decomp.) 298–303 °C (from acetone/H_2O); **IR** (thin film, cm^{-1}) 2161, 2034, 1579, 1554, 1481, 1407, 1312, 1222, 1085, 1036, 1003, 987, 970, 885, 819, 741, 695; **^{1}H NMR** (500 MHz, CD_3OD) δ 8.61 (d, *J* = 6.0 Hz, 1H), 7.66 (d, *J* = 6.0 Hz, 1H); **^{13}C{^{1}H} NMR** (126 MHz, CD_3OD) δ 166.6, 150.5, 120.6; **HRMS**: m/z (EI) calculated for ($C_5H_4NNaO_2S$) $[M–Na]^-$: 141.9968, found: 141.9966.

7.2.2. Calibration Curves for HPLC Analysis

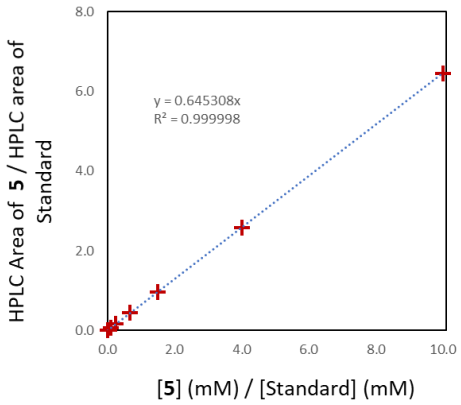
A 0.04 M solution of substrate in 1,4-dioxane and a 0.04 M solution of 1,3,5-trimethoxybenzene in 1,4-dioxane were prepared. Using a 100 µL glass syringe, six different ratios of these solutions were mixed in six different vials which were topped up with an ~ 10:1 MeCN/H_2O mixture.

Volume Substrate Solution (µL)	Volume Standard Solution (µL)	Amount Substrate (µmol)	Amount Standard (µmol)	Substrate / Standard Ratio
10	100	0.4	4	0.10
20	80	0.8	3.2	0.25
40	60	1.6	2.4	0.67
60	40	2.4	1.6	1.5
80	20	3.2	0.8	4.0
100	10	4.0	0.4	10

A linear relation between the ratios of the peak areas obtained and the substrate/standard ratio was obtained using Microsoft® Excel.

4-fluoro-4'-methyl-1,1'-biphenyl (5) against 1,3,5-trimethoxybenzene

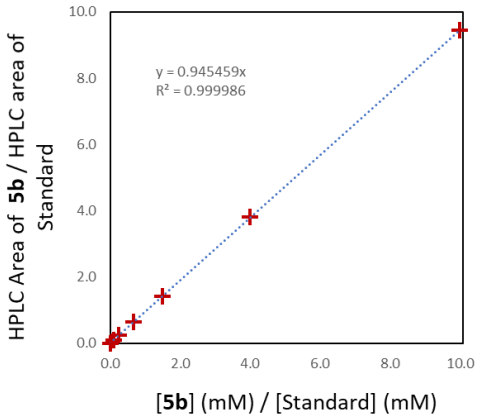
Substrate/Standard Ratio	Ratio HPLC area substrate / HPLC area Standard
0	0.00
0.10	0.07
0.25	0.17
0.67	0.44
1.5	0.97
4.0	2.58
10	6.45



$$[\mathbf{5}\ (mM)] = \frac{1}{0.65} * \frac{HPLC\ area\ \mathbf{5}}{HPLC\ Area\ Standard} * [Standard\ (mM)]$$

4,4'-dimethyl-1,1'-biphenyl (5b) against 1,3,5-trimethoxybenzene

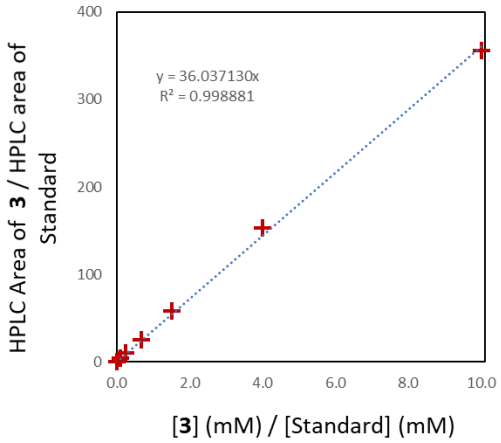
Substrate/Standard Ratio	Ratio HPLC area substrate / HPLC area Standard
0	0.00
0.10	0.10
0.25	0.24
0.67	0.63
1.5	1.40
4.0	3.81
10	9.45



$$[\mathbf{5b}\ (mM)] = \frac{1}{0.95} * \frac{HPLC\ area\ \mathbf{5b}}{HPLC\ Area\ Standard} * [Standard\ (mM)]$$

2-(4-fluorophenyl)pyridine (3) against 1,3,5-trimethoxybenzene

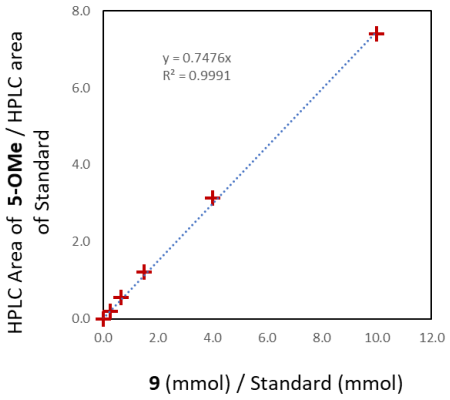
Substrate/Standard Ratio	Ratio HPLC area substrate / HPLC area Standard
0	0.0
0.10	4.0
0.25	9.9
0.67	26
1.5	58
4.0	153
10	356



$$[\mathbf{3}\ (mM)] = \frac{1}{36} * \frac{HPLC\ area\ \mathbf{3}}{HPLC\ Area\ Standard} * [Standard\ (mM)]$$

4-fluoro-4'-methoxy-1,1'-biphenyl (5-OMe) against 4,4'-dimethyl-1,1'-biphenyl

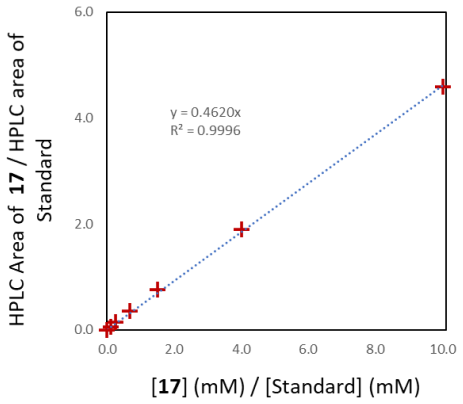
Substrate/Standard Ratio	Ratio HPLC area /HPLC area Standard
0	0.00
0.25	0.190
0.67	0.546
1.5	1.21
4.0	3.13
10	7.40



$$[\mathbf{5-OMe}\ (mmol)] = \frac{1}{0.75} * \frac{HPLC\ area\ \mathbf{5-OMe}}{HPLC\ Area\ Standard} * [Standard\ (mmol)]$$

1-fluoro-4-tosylbenzene (17) against 1,3,5-trimethoxybenzene

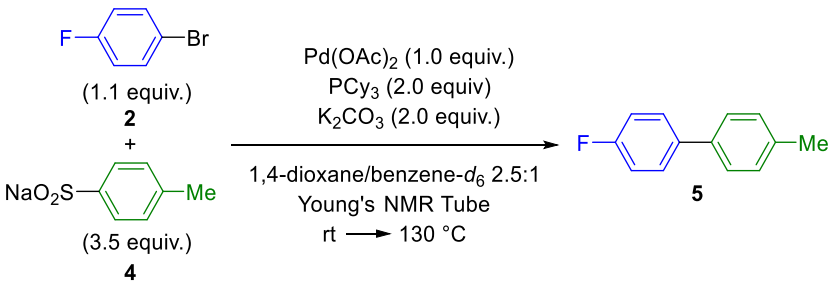
Substrate/Standard Ratio	Ratio HPLC area substrate / HPLC area Standard
0	0.00
0.10	0.06
0.25	0.14
0.67	0.36
1.5	0.75
4.0	1.90
10	4.59



$$[\mathbf{17}\ (mmol)] = \frac{1}{0.46} * \frac{HPLC\ area\ \mathbf{17}}{HPLC\ Area\ Standard} * [Standard\ (mmol)]$$

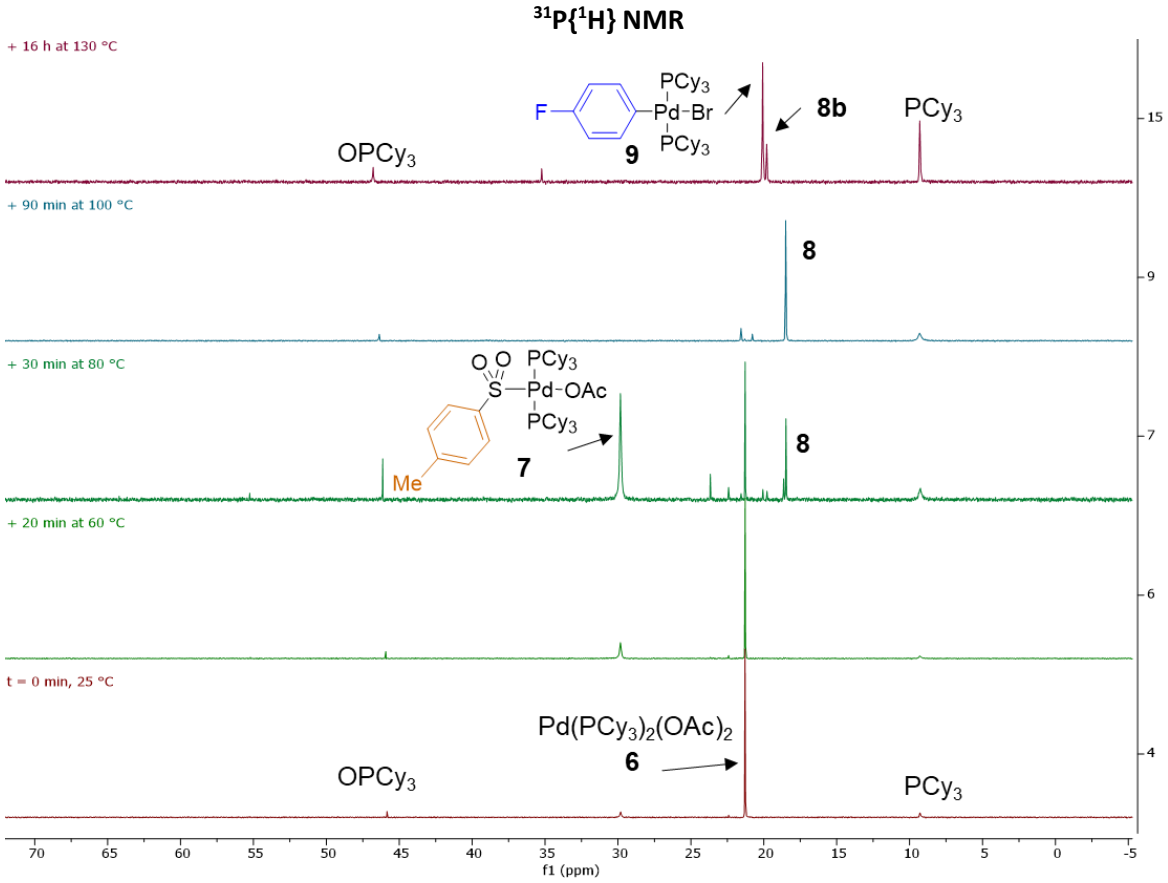
7.2.3. Formation of the Active Pd(0) Species

7.2.3.1. NMR Spectroscopy Monitoring

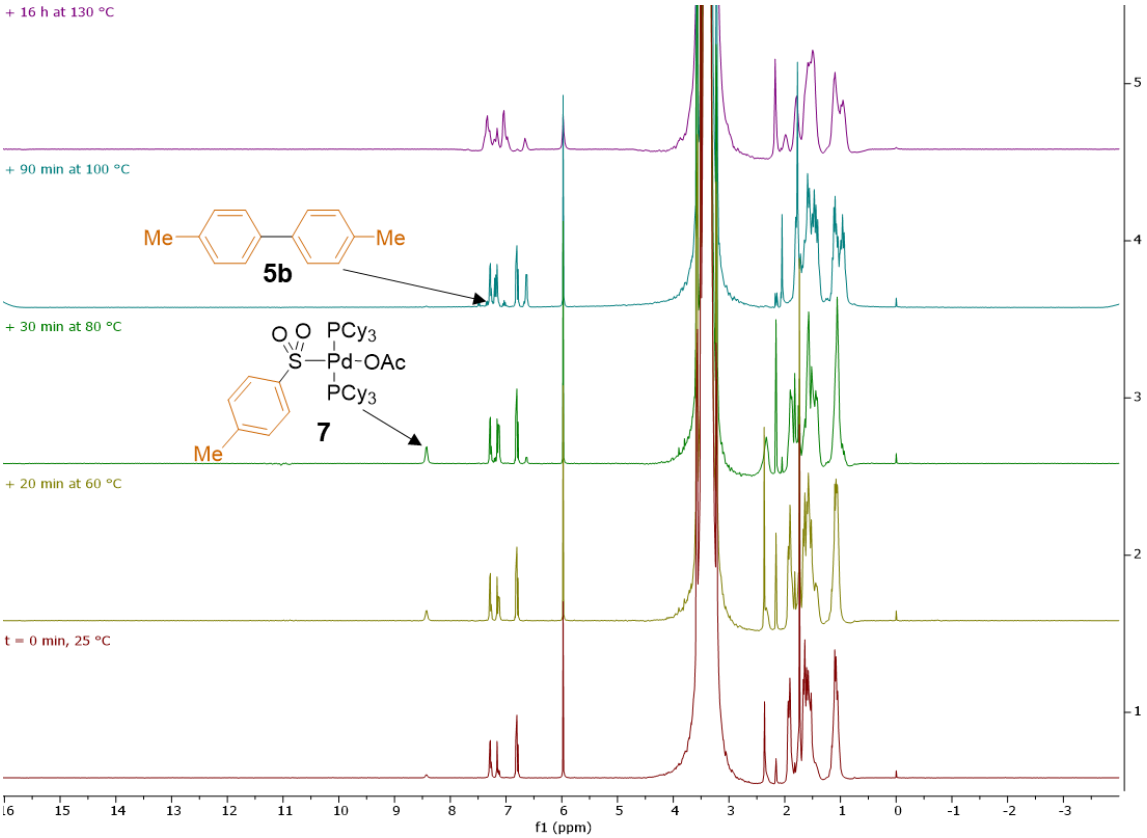


Palladium acetate (5.6 mg, 0.025 mmol, 1.0 equiv.), tricyclohexylphosphine (14 mg, 0.050 mmol, 2.0 equiv.), potassium carbonate (6.9 mg, 0.050 mmol, 2.0 equiv.), sodium 4-methylbenzenesulfinate (16 mg, 0.090 mmol, 3.6 equiv.) and trimethoxybenzene (2.1 mg, 0.012 mmol, 0.5 equiv.) were introduced into a Young's NMR tube. The NMR tube was evacuated (< 0.1 mbar) and back-filled with argon twice. 1,4-Dioxane (500 µL), benzene-d_6

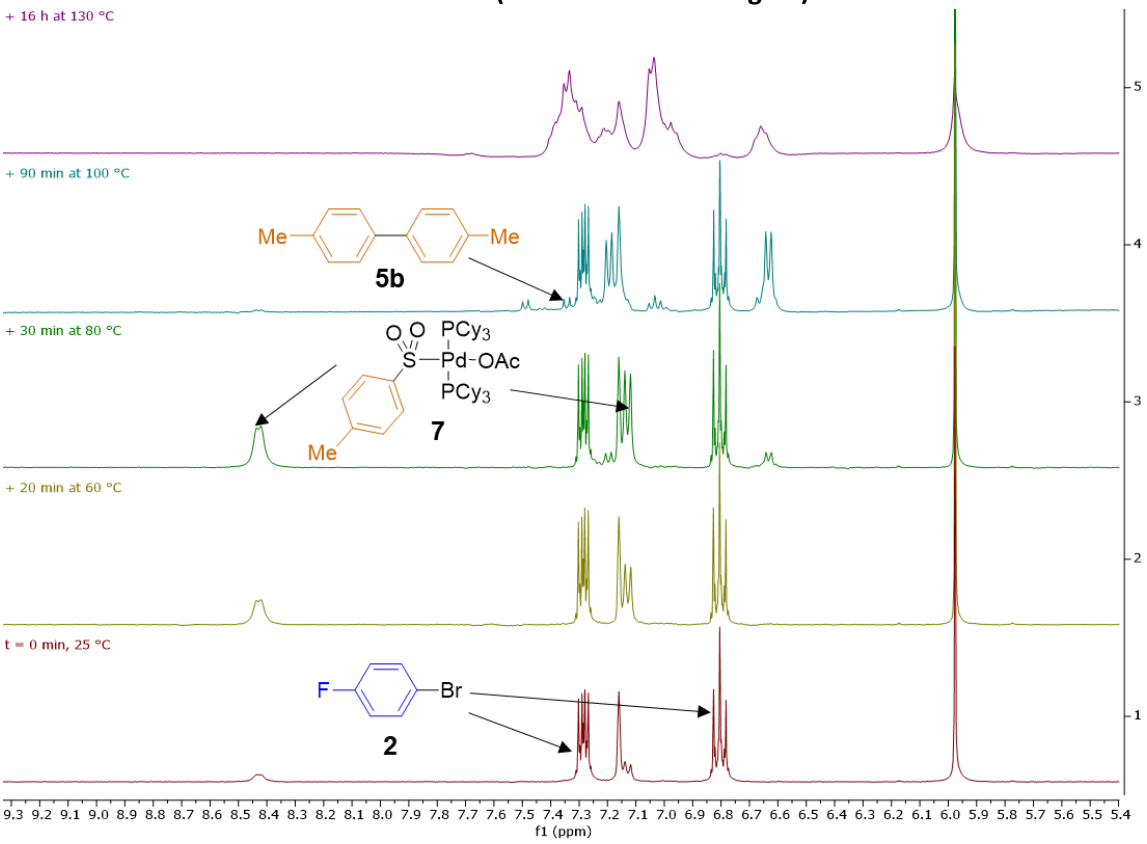
(200 µL) and 1-bromo-4-fluorobenzene (3.0 µL, 0.027 mmol, 1.1 equiv.) were then added to the Young's NMR tube. The NMR tube was sealed, vigorously shaken, and a first set of NMR spectra (^{1}H, ^{19}F, $^{31}P\{^{1}H\}$) was taken (t = 0 min, 25 °C). The same Young's NMR tube was then heated in a heating block filled with sand for 20 minutes at 60 °C and a second set of NMR spectra was taken (+ 20 min at 60 °C). The following times and temperatures were then employed: (+ 30 min at 80 °C); (+ 90 min at 100 °C); (+ 16 h at 130 °C).

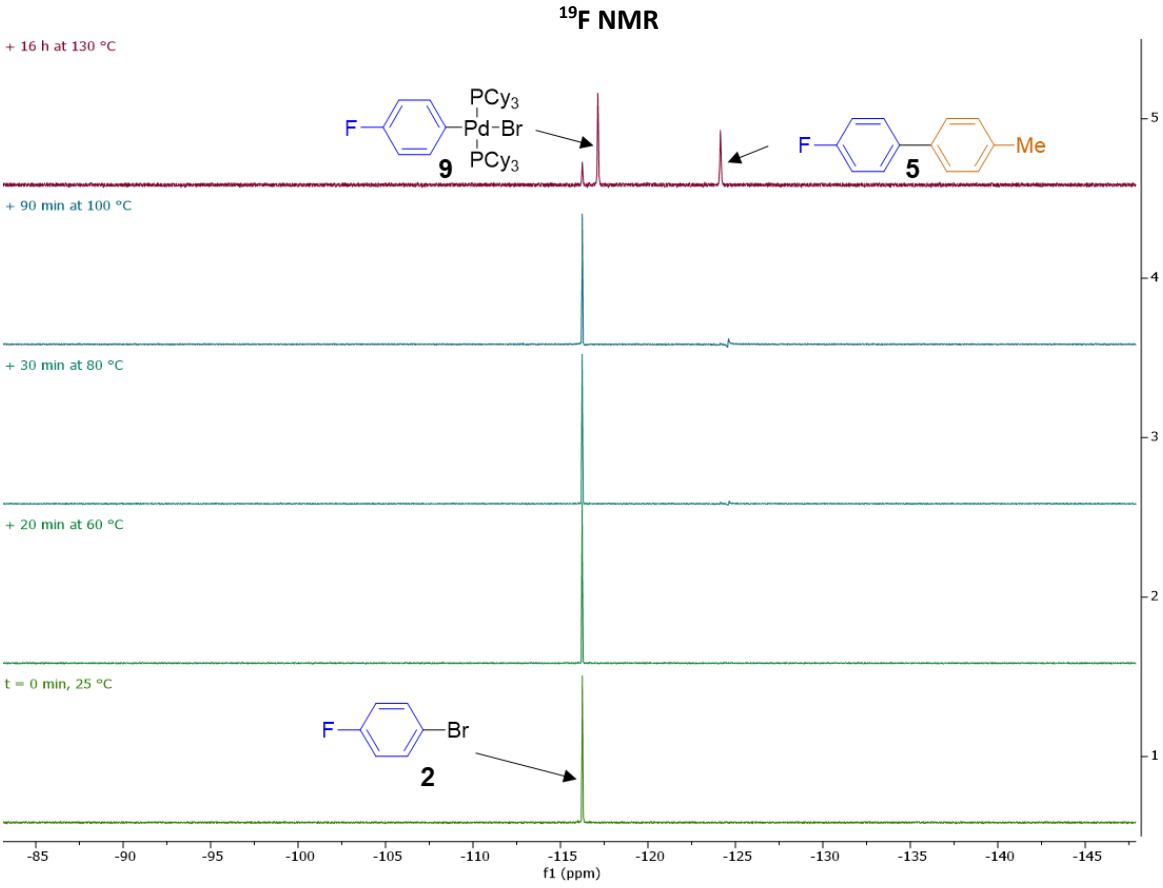


^{1}H NMR

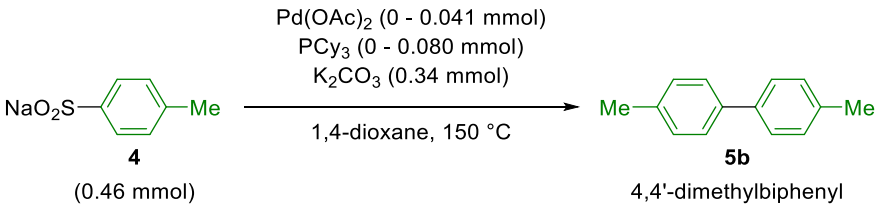


^{1}H NMR (zoom in aromatic region)





7.2.3.2. Correlation Between the Amount of Homocoupling Product (5b) Formed and the Amount of $Pd(OAc)_2$ Introduced in the Reaction Mixture

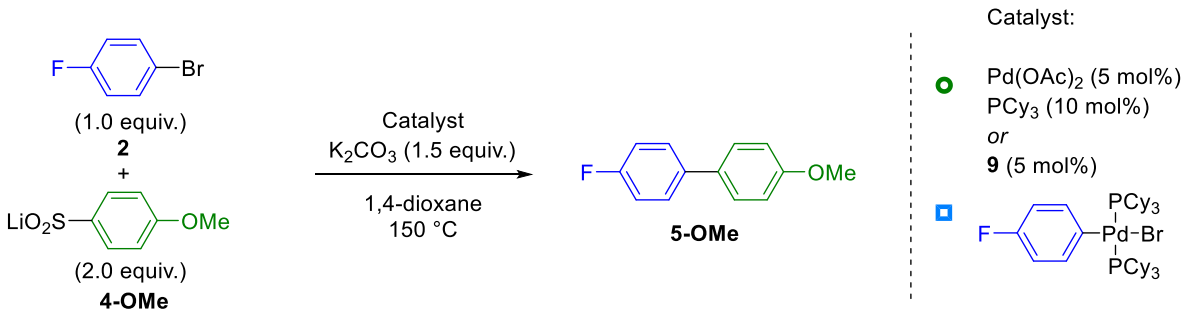


Sodium 4-methylbenzenesulfinate (81 mg, 0.46 mmol, 2.0 equiv.), 1,3,5-trimethoxybenzene (19 mg, 0.11 mmol, 0.50 equiv.), K_2CO_3 (47 mg, 0.34 mmol, 1.5 equiv.), palladium acetate (X mmol) and PCy_3 (2*X mmol) were added to a microwave vial equipped with a stirrer bar. The vial was sealed with a microwave vial cap, evacuated (< 0.1 mbar) and back-filled with argon twice, then 1,4-dioxane (4.6 mL) was added. The vial was then placed in a preheated heating block at 150 °C and stirred for 15 minutes, after which an aliquot was taken. This aliquot was

analyzed by HPLC, and the amount of 4,4'-dimethylbiphenyl was determined using 1,3,5-trimethoxybenzene as the internal standard.

n($PdOAc_2$) (10^{-2} mmol)	0	1.2	2.3	3.5	1.7	2.9	4.1
5b (10^{-2} mmol) Run 1	0	0.8	1.8	2.7	1.3	2.2	3.1
5b (10^{-2} mmol) Run 2	0	0.9	1.8	2.6	1.2	2.2	3.1
5b (10^{-2} mmol) Run 3	0	0.8	1.7	2.8	1.3	2.1	3.1
5b (10^{-2} mmol) Average	0	0.9	1.8	2.7	1.3	2.2	3.1

7.2.4. Oxidative Addition Complex 9 as a Competent Catalyst



Lithium 4-methoxybenzene sulfinate (75 mg, 0.42 mmol, 2.0 equiv.), potassium carbonate (44 mg, 0.31 mmol, 1.5 equiv.), 4,4'-dimethyl-1,1'-biphenyl (15 mg, 0.080 mmol, 0.38 equiv.), palladium acetate (2.4 mg, 0.011 mmol, 0.05 equiv.) and tricyclohexylphosphine (5.9 mg, 0.02 mmol, 0.10 equiv.) or [(Ar)Pd(PCy_3)$_2$(Br)] (8.8 mg, 0.011 mmol, 0.05 equiv.) were added to a microwave vial equipped with a stirrer bar. The vial was sealed with a microwave vial cap, evacuated (< 0.1 mbar) and back-filled with argon twice, then 1,4-dioxane (4.6 mL) and 1-bromo-4-fluorobenzene (23 µL, 0.21 mmol, 1.0 equiv.) were added. The vial was then placed in a preheated heating block at 150 °C and the yield of product **5-OMe** was determined by HPLC using 4,4'-dimethyl-1,1'-biphenyl as the internal standard.

Catalyst:	$Pd(OAc)_2$ + 2 PCy_3	Catalyst:	$(Ar)Pd(PCy_3)_2(Br)$
Time (min)	Conversion to **5-OMe**	Time (min)	Conversion to **5-OMe**
0	0%	0	0%
5	4%	5	4%
10	7%	10	8%
15	10%	15	11%
25	16%	25	17%
35	20%	35	23%
45	22%	45	27%
55	25%	55	29%
65	27%	65	32%
80	30%	80	35%
95	33%	95	38%
110	36%	110	40%
125	38%	125	42%
145	41%	145	44%
165	43%	165	46%
185	46%	185	49%
217	50%	215	51%
245	52%	245	53%
275	55%	275	55%
311	58%	335	59%
355	62%	395	63%
415	66%	455	66%
475	70%	535	69%
535	73%	615	72%
677	79%	720	73%

7.2.5. Catalytic Activity of Palladium Complexes 9, 11, 12 and 14

Sodium 4-methylbenzenesulfinate (81 mg, 0.46 mmol, 2.0 equiv.) or sodium pyridine-2-sulfinate (75 mg, 0.46 mmol, 2.0 equiv.), 1,3,5-trimethoxybenzene (19 mg, 0.11 mmol, 0.50 equiv.), K_2CO_3 (47 mg, 0.34 mmol, 1.5 equiv.), and the following catalysts were added to a microwave vial equipped with a stirrer bar:

a) **11** (7.2 mg, 0.006 mmol, 0.025 equiv.)

b) **11** (7.2 mg, 0.006 mmol, 0.025 equiv.) and PCy_3 (3.2 mg, 0.011 mmol, 0.05 equiv.)

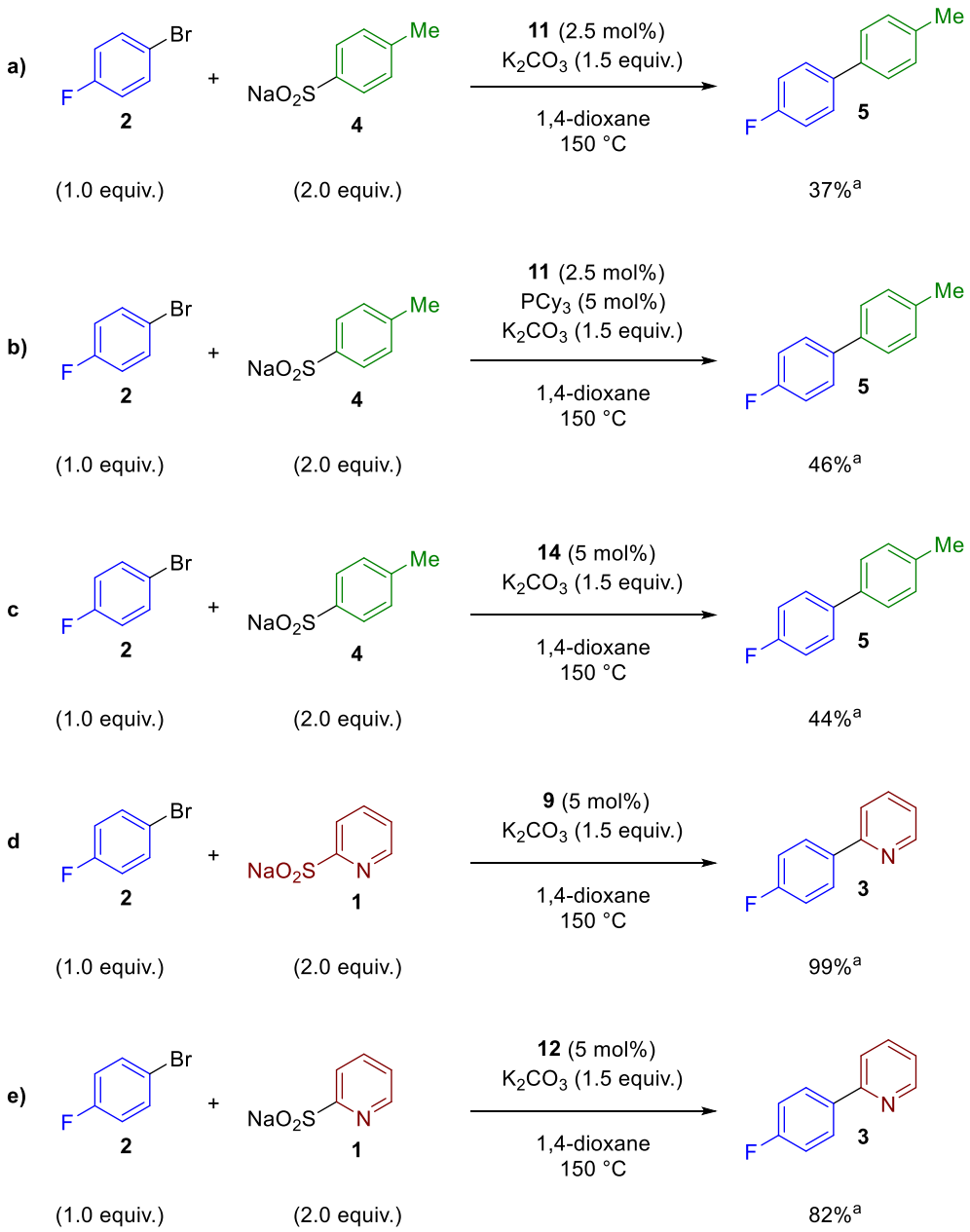
c) **14** (10.4 mg, 0.011 mmol, 0.05 equiv.)

d) **9** (9.6 mg, 0.011 mmol, 0.05 equiv.)

e) **12** (7.1 mg, 0.011 mmol, 0.05 equiv.)

The vial was sealed with a microwave vial cap, evacuated (< 0.1 mbar) and back-filled with argon twice, then 1,4-dioxane (4.6 mL) and 1-bromo-4-fluorobenzene (25 µL, 0.23 mmol, 1.0 equiv.) were added. The vial was then placed in a preheated heating block at 150 °C and

stirred for 16 hours. The yield of products **3** or **5** were determined by HPLC using 1,3,5-trimethoxybenzene as the internal standard.



7.2.6. DOSY NMR Data

DOSY experiments used the Bruker Double Stimulated Echo (DSTE) pulse sequence with solvent suppression by presaturation during the relaxation delay. 16 spectra with 32K data points were collected for each experiment. The duration of the pulsed field gradient (P30) was 1 ms, and the diffusion time (D_2O) was varied between 100-120 ms to allow 5% residual signal

with the maximum gradient strength. The gradient strength was incremented in 16 steps from 5% to 95% of the maximum value in a squared ramp. The diffusion data was analysed using the Dynamics module in Topspin 3.

For **11**

Peak 1 at 7.337 ppm
Diff Con. = 3.191e-010 m2/s
Peak 2 at 6.912 ppm
Diff Con. = 3.145e-010 m2/s
Peak 3 at 6.835 ppm
Diff Con. = 3.114e-010 m2/s
Peak 4 at 6.358 ppm
Diff Con. = 3.138e-010 m2/s

Peak 5 at 1.588 ppm
Diff Con. = 3.181e-010 m2/s
Peak 6 at 1.423 ppm
Diff Con. = 3.166e-010 m2/s
Peak 7 at 1.282 ppm
Diff Con. = 3.133e-010 m2/s
Peak 8 at 0.951 ppm
Diff Con. = 3.190e-010 m2/s

Average diffusion constant = 3.16E-10 m^2 s^{-1}

Predicted molecular weight from diffusion constant = 853 $g.mol^{-1}$

Actual molecular weight = 1274 $g.mol^{-1}$

For **12**

Peak 1 at 7.523 ppm
Diff Con. = 4.291e-010 m2/s
Peak 2 at 7.317 ppm
Diff Con. = 4.238e-010 m2/s
Peak 3 at 7.032 ppm
Diff Con. = 4.279e-010 m2/s
Peak 4 at 6.855 ppm
Diff Con. = 4.294e-010 m2/s

Peak 5 at 6.726 ppm
Diff Con. = 4.167e-010 m2/s
Peak 6 at 1.853 ppm
Diff Con. = 4.221e-010 m2/s
Peak 7 at 1.603 ppm
Diff Con. = 4.280e-010 m2/s
Peak 8 at 1.498 ppm
Diff Con. = 4.194e-010 m2/s

Average diffusion constant = 4.27 E-10 m^2 s^{-1}

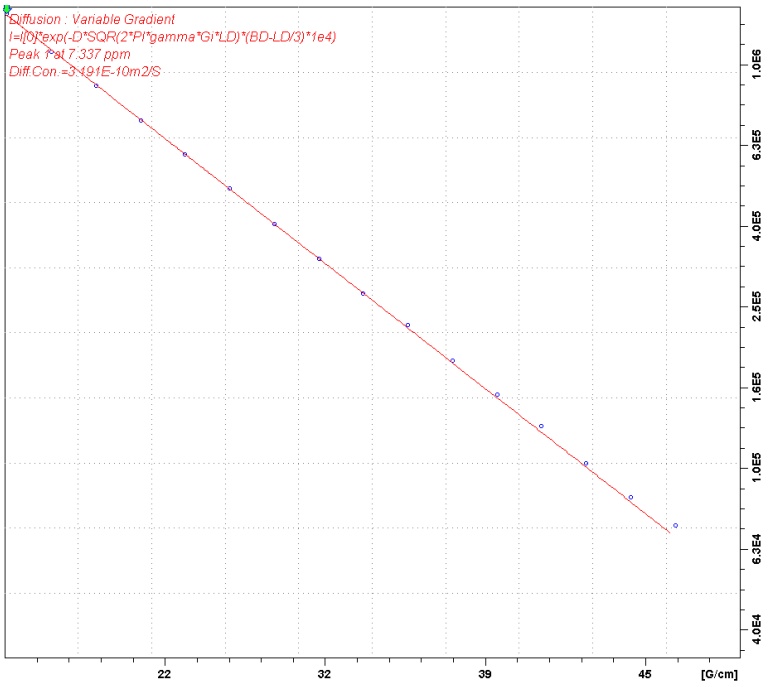
Predicted molecular weight from diffusion constant = 445 $g.mol^{-1}$

Actual molecular weight = 624 $g.mol^{-1}$

Although the predicted molecular weight values are significantly different compared to the actual molecular weight values, they show that compound **11** is approximately two times heavier than compound **12**, suggesting that compound **11** is dimeric in solution.

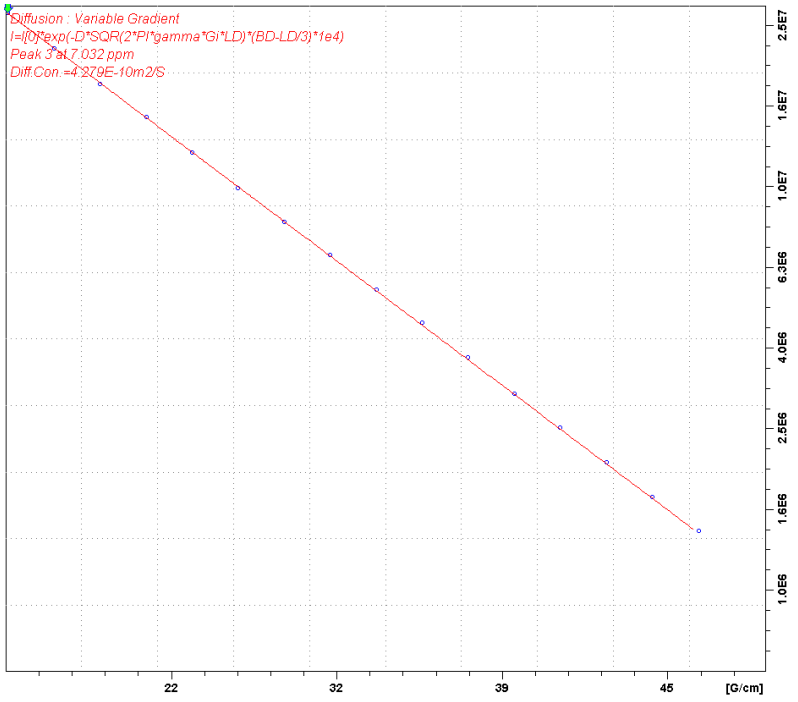
Example of line fitting quality for **11**

Aromatic peak δ = 7.337 ppm: Diffusion constant = 3.191 E-10 $m^2.s^{-1}$

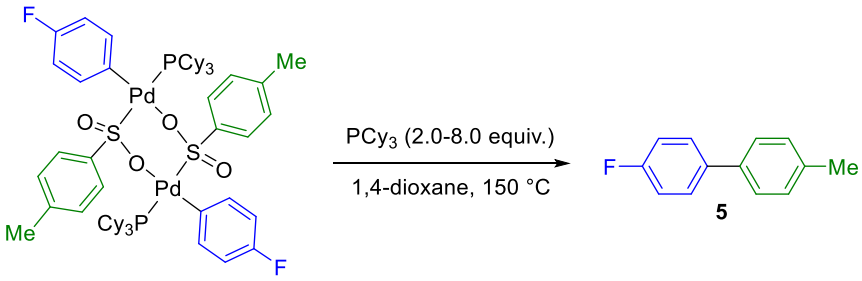


Example of line fitting quality for **12**

Aromatic peak δ = 7.032 ppm: Diffusion constant = 4.279 E-10 $m^2.s^{-1}$



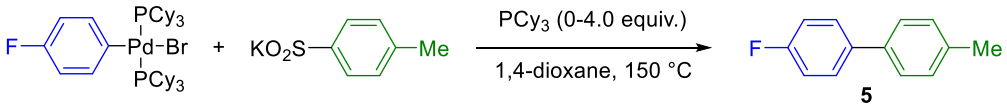
7.2.7. Reactivity of Complexes 9, 11, 14, 12 and 12-CF_3 in 1,4-dioxane



11 (1.0 equiv.)

Tricyclohexylphosphine (8.3-33 mg, 0.030-0.12 mmol, 2.0-8.0 equiv.) was added to a microwave vial equipped with a stirrer bar. The vial was sealed with a microwave vial cap, evacuated (< 0.1 mbar) and back-filled with argon twice, then 1,4-dioxane (3.0 mL) was added. The vial was placed in a preheated heating block at 150 °C and stirred for 5 minutes. A stock solution of $[Pd(4\text{-}F\text{-}C_6H_4)(PCy_3)(\kappa_S\text{-}\kappa_O\text{-}4\text{-}Me\text{-}C_6H_4\text{-}SO_2)]_2$ (7.5 µM, 0.015 mmol, 1.0 equiv.) and 1,3,5-trimethoxybenzene (30 µM, 0.060 mmol, 4.0 equiv.) in 1,4-dioxane (2.0 mL) was then injected. Aliquots were taken at the indicated times. The yield of product **5** was determined by HPLC against 1,3,5-trimethoxybenzene as the internal standard.

Amount of PCy_3	0.030 mmol (2.0 equiv.)	0.060 mmol (4.0 equiv.)	0.090 mmol (6.0 equiv.)	0.12 mmol (8.0 equiv.)
Time (min)	Conversion to **5**	Conversion to **5**	Conversion to **5**	Conversion to **5**
0	0%	0%	0%	0%
1	98%	96%	93%	87%
2	98%	98%	98%	97%
4	98%	98%	98%	97%
6	97%	98%	97%	98%
8	98%	98%	98%	98%
10	98%	98%	98%	99%

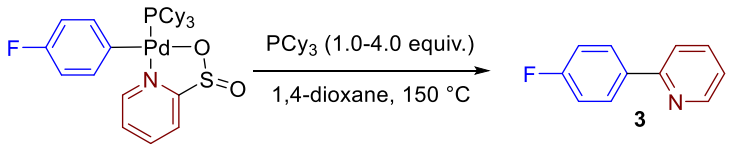


9 (1.0 equiv.) **25** (2.0 equiv.)

Tricyclohexylphosphine (0-33 mg, 0-0.12 mmol, 0-4.0 equiv.) and potassium 4-methylbenzenesulfinate (11.5 mg, 0.060 mmol, 2.0 equiv.) were added to a microwave vial equipped with a stirrer bar. The vial was sealed with a microwave vial cap, evacuated (< 0.1

mbar) and back-filled with argon twice, then 1,4-dioxane (3.0 mL) was added. The vial was placed in a preheated heating block at 150 °C and stirred for 5 minutes. A stock solution of [$(PCy_3)_2Pd(4\text{-}F\text{-}C_6H_4)(Br)$] (0.015 mM, 30 µmol, 1.0 equiv.) and 1,3,5-trimethoxybenzene (30 µM, 0.060 mmol, 2.0 equiv.) in 1,4-dioxane (2.0 mL) was then injected. Aliquots were taken at the indicated times. The yield of product **5** was determined by HPLC against 1,3,5-trimethoxybenzene as the internal standard.

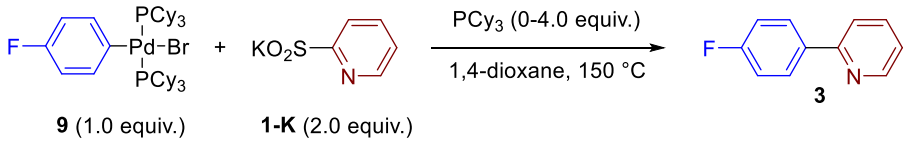
Amount of PCy_3	0 mmol (0 equiv.)	0.030 mmol (1.0 equiv.)	0.060 mmol (2.0 equiv.)	0.090 mmol (3.0 equiv.)	0.12 mmol (4.0 equiv.)
Time (min)	Conversion to **5**	Conversion to **5**	Conversion to **5**	Conversion to **5**	Conversion to **5**
0	0%	0%	0%	0%	0%
1	14%	1%	1%	1%	0%
2	38%	5%	3%	3%	2%
4	74%	21%	15%	11%	8%
6	87%	39%	28%	21%	15%
8	92%	56%	40%	30%	23%
10	91%	67%	51%	39%	29%
15	93%	85%	72%	57%	45%
20	94%	89%	85%	72%	52%
30	94%	90%	93%	87%	75%
45	94%	92%	95%	93%	87%
60	94%	92%	94%	94%	90%



12 (1.0 equiv.) **3**

Tricyclohexylphosphine (8.3-33 mg, 0.030-0.12 mmol, 1.0-4.0 equiv.) was added to a microwave vial equipped with a stirrer bar. The vial was sealed with a microwave vial cap, evacuated (< 0.1 mbar) and back-filled with argon twice, then 1,4-dioxane (3.0 mL) was added. The vial was placed in a preheated heating block at 150 °C and stirred for 5 minutes. A stock solution of [$(PCy_3)Pd(4\text{-}F\text{-}C_6H_4)(\kappa^2_{N,O}\text{-pyridine-2-}SO_2)$] (15 µM, 0.0030 mmol, 1.0 equiv.) and 1,3,5-trimethoxybenzene (30 µM, 0.060 mmol, 2.0 equiv.) in 1,4-dioxane (2.0 mL) was then injected. Aliquots were taken at the indicated times. The yield of product **3** was determined by HPLC against 1,3,5-trimethoxybenzene as the internal standard.

Amount of PCy_3	0.030 mmol (1.0 equiv.)	0.060 mmol (2.0 equiv.)	0.090 mmol (3.0 equiv.)	0.12 mmol (4.0 equiv.)
Time (min)	Conversion to **3**	Conversion to **3**	Conversion to **3**	Conversion to **3**
0	0%	0%	0%	0%
1	2%	3%	3%	3%
2	11%	9%	9%	10%
4	27%	25%	24%	26%
6	41%	39%	40%	40%
8	54%	49%	50%	50%
10	63%	58%	58%	58%
15	80%	70%	71%	73%
20	86%	76%	74%	79%
30	87%	81%	82%	83%

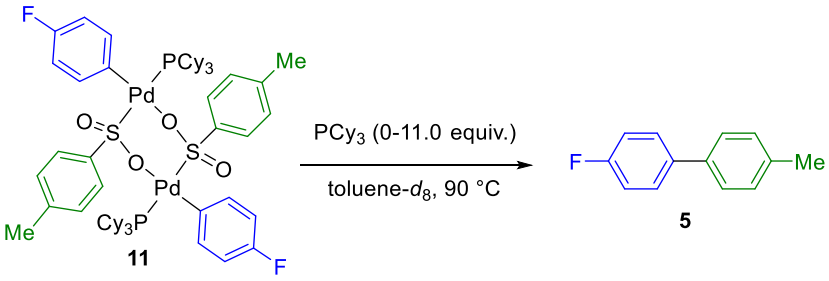


9 (1.0 equiv.) **1-K** (2.0 equiv.)

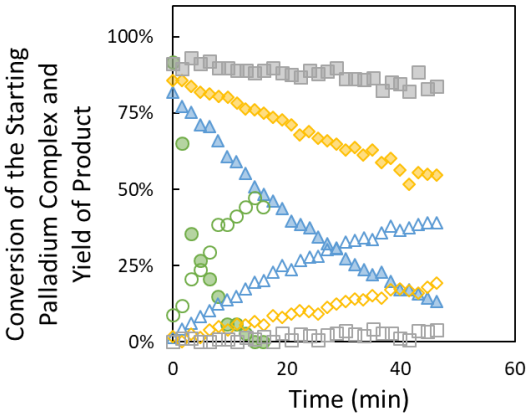
Tricyclohexylphosphine (0-33 mg, 0-0.12 mmol, 0-4.0 equiv.) and potassium pyridine-2-sulfinate (10.8 mg, 0.060 mmol, 2.0 equiv.) were added to a microwave vial equipped with a stirrer bar. The vial was sealed with a microwave vial cap, evacuated (< 0.1 mbar) and back-filled with argon twice, then 1,4-dioxane (3.0 mL) was added. The vial was placed in a preheated heating block at 150 °C and stirred for 5 minutes. A stock solution of [$(PCy_3)_2Pd(4\text{-}F\text{-}C_6H_4)(Br)$] (0.015 mM, 30 µmol, 1.0 equiv.) and 1,3,5-trimethoxybenzene (30 µM, 0.060 mmol, 2.0 equiv.) in 1,4-dioxane (2.0 mL) was then injected. Aliquots were taken at the indicated times. The yield of product **3** was determined by HPLC against 1,3,5-trimethoxybenzene as the internal standard.

Amount of PCy_3	0 mmol (0 equiv.)	0.030 mmol (1.0 equiv.)	0.060 mmol (2.0 equiv.)	0.090 mmol (3.0 equiv.)	0.12 mmol (4.0 equiv.)
Time (min)	Conversion to **3**	Conversion to **3**	Conversion to **3**	Conversion to **3**	Conversion to **3**
0	0%	0%	0%	0%	0%
1	1%	1%	1%	1%	0%
2	7%	4%	4%	3%	4%
4	22%	18%	15%	14%	14%
6	37%	33%	25%	23%	24%
8	49%	44%	35%	33%	33%
10	58%	53%	43%	39%	41%
15	70%	62%	56%	51%	53%
20	74%	62%	63%	60%	61%
30	76%	63%	67%	67%	67%

7.2.8. Extrusion of SO_2 from Complexes 11, 14, 12 and 12-CF_3 in toluene-d_8 and Monitored by $^{19}F\{^1H\}$ NMR spectroscopy



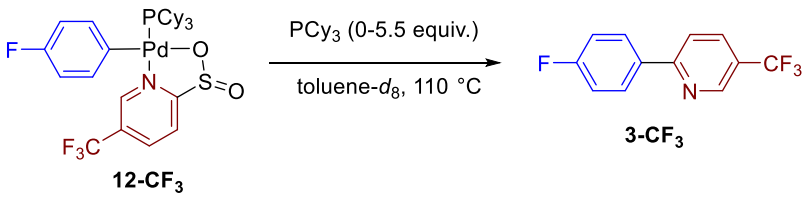
$[(PCy_3)Pd(4\text{-}F\text{-}C_6H_4)(\kappa_S\text{-}\kappa_{O'}\text{-}4\text{-}Me\text{-}C_6H_4\text{-}SO_2)]_2$ (5.0 mg, 0.0039 mmol, 1.0 equiv.) and tricyclohexylphosphine (0-12 mg, 0-0.043 mmol, 0-11 equiv.) were introduced into a Young's NMR tube. The NMR tube was evacuated (< 0.1 mbar) and back-filled with argon twice. A 0.013 M solution of 1,3,5-trifluorobenzene in toluene-d_8 (600 µL, 0.0077 mmol, 2.0 equiv.) was added to the Young's NMR tube. The NMR tube was sealed, vigorously shaken, and placed in a 500 MHz NMR spectrometer that had been pre-equilibrated at 90 °C. NMR experiments were then collected at 90 °C. Conversion of the starting material and yield of product were measured against 1,3,5-trifluorobenzene as the internal standard.



(●) 0 equiv. PCy_3, (▲) 2.2 equiv. PCy_3, (◆) 4.4 equiv. PCy_3, (■) 11.0 equiv. PCy_3.

0 mmol PCy_3	(0 equiv.)	$0.86*10^{-2}$ mmol PCy_3	(2.2 equiv.)	$1.7*10^{-2}$ mmol PCy_3	(4.4 equiv.)	$4.3*10^{-2}$ mmol PCy_3	(11.0 equiv.)
Time (min)	% Starting Material	Time (min)	% Starting Material	Time (min)	% Starting Material	Time (min)	% Starting Material
0.0	92%	0.0	82%	0.0	86%	0.0	91%
1.6	65%	1.6	77%	1.6	86%	1.6	90%
3.2	35%	3.2	75%	3.2	84%	3.2	93%
4.8	27%	4.8	71%	4.8	82%	4.8	91%
6.4	21%	6.4	71%	6.4	81%	6.4	92%
7.9	15%	8.0	66%	8.0	80%	8.0	90%
9.5	6%	9.5	61%	9.6	80%	9.6	90%
11.1	6%	11.1	59%	11.2	78%	11.2	89%
12.7	3%	12.7	55%	12.8	76%	12.8	89%
14.3	0%	14.4	51%	14.4	76%	14.4	88%
15.9	0%	16.0	48%	16.0	75%	16.0	89%
		17.5	46%	17.6	74%	17.6	90%
		19.2	44%	19.1	73%	19.2	88%
		20.8	40%	20.7	71%	20.8	88%
		22.4	38%	22.3	68%	22.4	87%
		23.9	38%	23.9	69%	23.9	89%
		25.5	34%	25.5	67%	25.5	88%
		27.1	32%	27.1	66%	27.1	89%
		28.7	31%	28.7	65%	28.7	90%
		30.3	27%	30.3	63%	30.3	86%
		31.9	25%	31.9	64%	31.9	86%
		33.5	24%	33.5	61%	33.5	86%
		35.1	22%	35.0	63%	35.1	87%
		36.7	23%	36.6	59%	36.7	82%
		38.3	20%	38.2	60%	38.3	85%
		39.9	17%	39.8	56%	39.9	85%
		41.4	17%	41.5	52%	41.5	82%
		43.1	16%	43.1	56%	43.1	88%
		44.7	14%	44.7	55%	44.7	83%
		46.3	13%	46.3	55%	46.3	84%

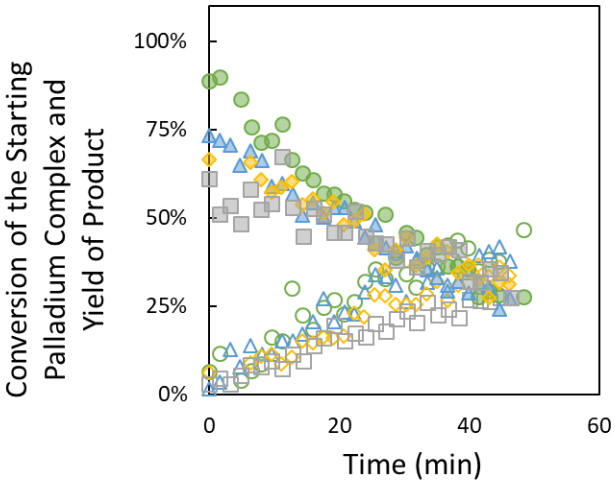
0 mmol PCy_3	(0 equiv.)	$0.86*10^{-2}$ mmol PCy_3	(2.2 equiv.)	$1.7*10^{-2}$ mmol PCy_3	(4.4 equiv.)	$4.3*10^{-2}$ mmol PCy_3	(11.0 equiv.)
Time (min)	% Product **5**	Time (min)	% Product **5**	Time (min)	% Product **5**	Time (min)	% Product **5**
0.0	9%	0.0	1%	0.0	2%	0.0	0%
1.6	12%	1.6	4%	1.6	0%	1.6	1%
3.2	21%	3.2	6%	3.2	3%	3.2	1%
4.8	24%	4.8	8%	4.8	1%	4.8	0%
6.4	30%	6.4	10%	6.4	4%	6.4	0%
7.9	38%	8.0	12%	8.0	5%	8.0	1%
9.5	38%	9.5	14%	9.6	4%	9.6	1%
11.1	41%	11.1	15%	11.2	6%	11.2	0%
12.7	44%	12.7	17%	12.8	6%	12.8	1%
14.3	47%	14.4	20%	14.4	7%	14.4	1%
15.9	44%	16.0	20%	16.0	6%	16.0	2%
		17.5	23%	17.6	9%	17.6	0%
		19.2	25%	19.1	8%	19.2	3%
		20.8	24%	20.7	9%	20.8	1%
		22.4	27%	22.3	10%	22.4	3%
		23.9	28%	23.9	10%	23.9	2%
		25.5	28%	25.5	9%	25.5	1%
		27.1	30%	27.1	11%	27.1	2%
		28.7	30%	28.7	12%	28.7	3%
		30.3	33%	30.3	13%	30.3	4%
		31.9	33%	31.9	14%	31.9	3%
		33.5	34%	33.5	14%	33.5	2%
		35.1	34%	35.0	15%	35.1	4%
		36.7	36%	36.6	14%	36.7	3%
		38.3	38%	38.2	17%	38.3	3%
		39.9	37%	39.8	17%	39.9	1%
		41.4	38%	41.5	17%	41.5	1%
		43.1	38%	43.1	16%	43.1	4%
		44.7	39%	44.7	18%	44.7	3%
		46.3	39%	46.3	19%	46.3	4%



12-CF_3 **3-CF_3**

[(PCy_3)Pd(4-F-C_6H_4)($\kappa^2_{N,O}$-pyridine-5-CF_3-2-SO_2)] (5.4 mg, 0.0078 mmol, 1.0 equiv.) and tricyclohexylphosphine (0-12 mg, 0-0.043 mmol, 0-5.5 equiv.) were introduced into a Young's

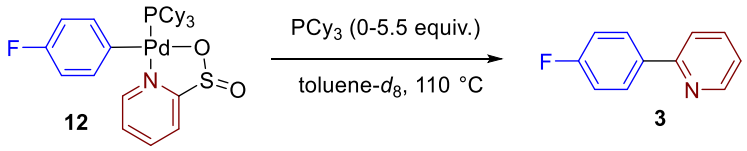
NMR tube. The NMR tube was evacuated (< 0.1 mbar) and back-filled with argon twice. A 0.013 M solution of 1,3,5-trifluorobenzene in toluene-d_8 (600 µL, 0.0077 mmol, 1.0 equiv.) was added to the Young's NMR tube. The NMR tube was sealed, vigorously shaken, and placed in a 500 MHz NMR spectrometer that had been pre-equilibrated at 110 °C. NMR experiments were then collected at 110 °C. Conversion of the starting material and yield of product were measured against 1,3,5-trifluorobenzene as the internal standard.



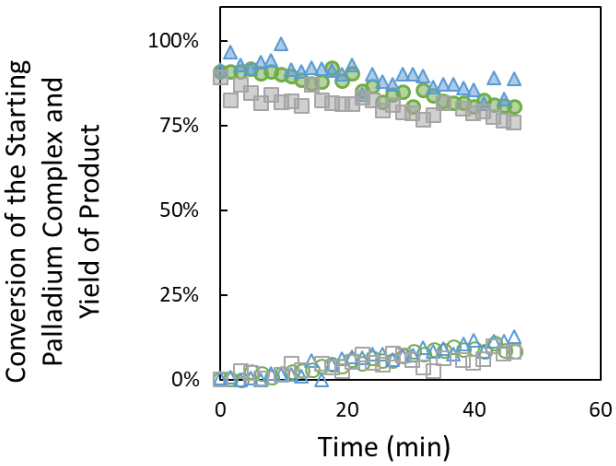
(●) 0 equiv. PCy_3, (▲) 1.1 equiv. PCy_3, (◆) 2.2 equiv. PCy_3, (■) 5.5 equiv. PCy_3.

0 mmol PCy_3	(0 equiv.)	$0.86*10^{-2}$ mmol PCy_3	(1.1 equiv.)	$1.7*10^{-2}$ mmol PCy_3	(2.2 equiv.)	$4.3*10^{-2}$ mmol PCy_3	(5.5 equiv.)
Time (min)	% Starting Material	Time (min)	% Starting Material	Time (min)	% Starting Material	Time (min)	% Starting Material
0.0	89%	0.0	73%	0.0	67%	0.0	61%
1.6	90%	1.6	72%		0%	1.6	51%
	86%	3.2	70%		0%	3.2	53%
4.8	83%	4.8	65%		0%	4.8	48%
6.4	76%	6.4	69%	6.4	66%	6.4	58%
8.0	71%	8.0	66%	8.0	61%	8.0	52%
9.6	72%	9.6	59%	9.5	57%	9.6	54%
11.2	76%	11.2	60%	11.1	59%	11.2	67%
12.7	67%	12.8	57%	12.7	60%	12.9	53%
14.3	63%	14.4	51%	14.3	54%	14.4	45%
15.9	61%	16.0	54%	15.9	55%	16.0	53%
17.5	57%	17.6	50%	17.5	51%	17.6	51%
19.1	57%	19.2	53%	19.1	54%	19.3	46%
20.7	55%	20.8	53%	20.7	48%	20.9	46%
22.3	52%	22.4	49%	22.3	49%	22.4	52%
23.9	52%	24.0	44%	23.8	51%	24.0	45%
25.5	43%	25.5	48%	25.4	41%	25.6	43%
27.1	51%	27.1	42%	27.0	35%	27.2	42%
28.7	39%	28.7	41%	28.6	41%	28.8	38%
30.2	46%	30.3	42%	30.2	44%	30.4	44%
31.8	44%	31.9	38%	31.8	37%	32.0	36%
33.4	40%	33.5	35%	33.4	39%	33.6	41%
35.0	42%	35.1	33%	35.0	42%	35.2	39%
36.6	36%	36.7	29%	36.6	40%	36.8	42%
38.2	36%	38.2	32%	38.2	34%	38.4	41%
39.8	35%	39.8	29%	39.8	37%	40.0	32%
41.4	28%	41.5	32%	41.4	32%	41.6	32%
42.9	29%	43.1	30%	43.0	27%	43.2	36%
44.5	28%	44.6	24%	44.6	32%	44.8	34%
48.3	28%	46.2	27%	46.2	31%	46.4	27%

0 mmol PCy_3	(0 equiv.)	$0.86*10^{-2}$ mmol PCy_3	(1.1 equiv.)	$1.7*10^{-2}$ mmol PCy_3	(2.2 equiv.)	$4.3*10^{-2}$ mmol PCy_3	(5.5 equiv.)
Time (min)	% Product **5**-CF_3	Time (min)	% Product **5**-CF_3	Time (min)	% Product **5**-CF_3	Time (min)	% Product **5**-CF_3
0.0	7%	0.0	2%	0.0	6%	0.0	3%
1.6	12%	1.6	3%		0%	1.6	5%
	0%	3.2	13%		0%	3.2	3%
4.8	4%	4.8	8%		0%	4.8	6%
6.4	7%	6.4	14%	6.4	9%	6.4	8%
8.0	9%	8.0	11%	8.0	11%	8.0	8%
9.6	16%	9.6	11%	9.5	11%	9.6	9%
11.2	15%	11.2	15%	11.1	9%	11.2	7%
12.7	30%	12.8	15%	12.7	10%	12.9	11%
14.3	23%	14.4	17%	14.3	15%	14.4	9%
15.9	18%	16.0	21%	15.9	15%	16.0	14%
17.5	25%	17.6	27%	17.5	16%	17.6	16%
19.1	27%	19.2	21%	19.1	16%	19.3	19%
20.7	23%	20.8	23%	20.7	17%	20.9	15%
22.3	26%	22.4	23%	22.3	23%	22.4	17%
23.9	32%	24.0	29%	23.8	22%	24.0	16%
25.5	35%	25.5	34%	25.4	28%	25.6	20%
27.1	33%	27.1	33%	27.0	28%	27.2	18%
28.7	40%	28.7	31%	28.6	25%	28.8	21%
30.2	34%	30.3	26%	30.2	25%	30.4	24%
31.8	30%	31.9	38%	31.8	26%	32.0	20%
33.4	36%	33.5	32%	33.4	29%	33.6	26%
35.0	36%	35.1	36%	35.0	32%	35.2	23%
36.6	42%	36.7	31%	36.6	27%	36.8	24%
38.2	44%	38.2	38%	38.2	31%	38.4	22%
39.8	42%	39.8	35%	39.8	35%	40.0	27%
41.4	35%	41.5	39%	41.4	37%	41.6	27%
42.9	38%	43.1	40%	43.0	33%	43.2	26%
44.5	38%	44.6	42%	44.6	36%	44.8	27%
48.3	47%	46.2	38%	46.2	34%	46.4	



[(PCy_3)Pd(4-F-C_6H_4)($\kappa^2_{N,O}$-pyridine-2-SO_2)] (4.9 mg, 0.0079 mmol, 1.0 equiv.) and tricyclohexylphosphine (0-12 mg, 0-0.043 mmol, 0-5.5 equiv.) were introduced into a Young's NMR tube. The NMR tube was evacuated (< 0.1 mbar) and back-filled with argon twice. A 0.013 M solution of 1,3,5-trifluorobenzene in toluene-d_8 (600 µL, 0.0077 mmol, 1.0 equiv.) was added to the Young's NMR tube. The NMR tube was sealed, vigorously shaken, and placed in a 500 MHz NMR spectrometer that had been pre-equilibrated at 110 °C. NMR experiments were then collected at 110 °C. Conversion of the starting material and yield of product were measured against 1,3,5-trifluorobenzene as the internal standard.

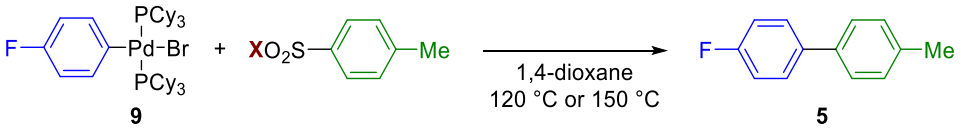


(●) 0 equiv. PCy_3, (▲) 1.1 equiv. PCy_3, (■) 5.5 equiv. PCy_3.

0 mmol PCy_3	(0 equiv.)	$0.86*10^{-2}$ mmol PCy_3	(1.1 equiv.)	$4.3*10^{-2}$ mmol PCy_3	(5.5 equiv.)
Time (min)	% Starting Material	Time (min)	% Starting Material	Time (min)	% Starting Material
0.0	91%	0.0	91%	0.0	89%
1.6	91%	1.6	97%	1.6	83%
3.3	91%	3.2	93%	3.2	87%
4.9	92%	4.8	92%	4.8	85%
6.5	90%	6.4	94%	6.4	82%
8.1	91%	8.0	94%	8.0	84%
9.7	90%	9.6	99%	9.6	82%
11.3	89%	11.1	92%	11.1	82%
12.8	88%	12.7	91%	12.7	81%
14.4	87%	14.4	92%	14.3	87%
16.0	88%	16.0	92%	15.9	83%
17.6	92%	17.5	91%	17.5	82%
19.2	88%	19.1	90%	19.1	81%
20.8	90%	20.7	93%	20.7	81%
22.4	85%	22.3	84%	22.3	83%
24.0	86%	24.0	90%	23.9	82%
25.6	82%	25.6	88%	25.5	80%
27.2	84%	27.2	87%	27.1	81%
28.8	85%	28.8	90%	28.7	79%
30.5	80%	30.4	90%	30.3	79%
32.1	85%	31.9	90%	31.9	77%
33.6	84%	33.6	86%	33.5	78%
35.2	82%	35.2	87%	35.1	82%
36.8	82%	36.8	87%		
38.4	82%	38.4	86%	38.3	80%
40.0	80%	40.0	85%	39.9	79%
41.7	82%	41.6	82%	41.5	79%
43.3	81%	43.2	89%	43.0	78%
44.9	81%	44.8	83%	44.7	76%
46.4	81%	46.4	89%	46.3	76%

0 mmol PCy_3	(0 equiv.)	$0.86*10^{-2}$ mmol PCy_3	(1.1 equiv.)	$4.3*10^{-2}$ mmol PCy_3	(5.5 equiv.)
Time (min)	% Product **3**	Time (min)	% Product **3**	Time (min)	% Product **3**
0.0	0%	0.0	0%	0.0	0%
1.6	0%	1.6	1%		
3.3	0%	3.2	0%	3.2	3%
4.9	2%	4.8	0%	4.8	2%
6.5	2%	6.4	0%	6.4	1%
8.1	1%	8.0	2%		
9.7	2%	9.6	2%	9.6	2%
11.3	2%	11.1	2%	11.1	5%
12.8	3%	12.7	1%	12.7	3%
14.4	3%	14.4	6%		
16.0	4%	16.0	0%	15.9	5%
17.6	5%	17.5	5%	17.5	4%
19.2	4%	19.1	6%	19.1	3%
20.8	6%	20.7	7%	20.7	5%
22.4	5%	22.3	6%	22.3	8%
24.0	7%	24.0	8%	23.9	5%
25.6	6%	25.6	8%	25.5	5%
27.2	6%	27.2	6%	27.1	8%
28.8	7%	28.8	7%	28.7	7%
30.5	8%	30.4	7%	30.3	6%
32.1	8%	31.9	10%	31.9	4%
33.6	9%	33.6	8%	33.5	3%
35.2	9%	35.2	9%	35.1	6%
36.8	10%	36.8	8%		4%
38.4	9%	38.4	11%	38.3	6%
40.0	9%	40.0	12%	39.9	5%
41.7	8%	41.6	8%	41.5	6%
43.3	11%	43.2	11%	43.0	10%
44.9	9%	44.8	11%	44.7	8%
46.4	8%	46.4	13%	46.3	8%

7.2.9. Importance of the Sulfinate Counter Cation



9 **5**

Sodium 4-methylbenzenesulfinate (10.6 mg, 0.060 mmol, 2.0 equiv.), 1,3,5-trimethoxybenzene (10 mg, 0.060 mmol, 2.0 equiv.), and $[(PCy_3)_2Pd(4\text{-}F\text{-}C_6H_4)(Br)]$ (25 mg, 30 µmol, 1.0 equiv.) were added to a microwave vial equipped with a stirrer bar. The vial was sealed with a microwave vial cap, evacuated (< 0.1 mbar) and back-filled with argon twice, then 1,4-dioxane (3.0 mL) was added. The vial was then placed in a preheated heating block at 120 °C and the reaction was monitored by taking aliquots over 5 hours. The yield of product **5** was determined by HPLC against 1,3,5-trimethoxybenzene as the internal standard.

The above procedure was repeated by replacing sodium 4-methylbenzenesulfinate with:

- Lithium 4-methylbenzenesulfinate (9.6 mg, 0.060 mmol, 2.0 equiv.)

- Tetra-*n*-butylammonium 4-methylbenzenesulfinate (23.6 mg, 0.060 mmol, 2.0 equiv.)
- Potassium 4-methylbenzenesulfinate (11.5 mg, 0.060 mmol, 2.0 equiv.)
- Potassium 4-methylbenzenesulfinate (11.5 mg, 0.060 mmol, 2.0 equiv.) with 18-crown-6 (19.6 mg, 0.075 mmol, 2.5 equiv.)
- Cesium 4-methylbenzenesulfinate (17.1 mg, 0.060 mmol, 2.0 equiv.)
- Tetramethylammonium 4-methylbenzenesulfinate (13.6 mg, 0.060 mmol, 2.0 equiv.)

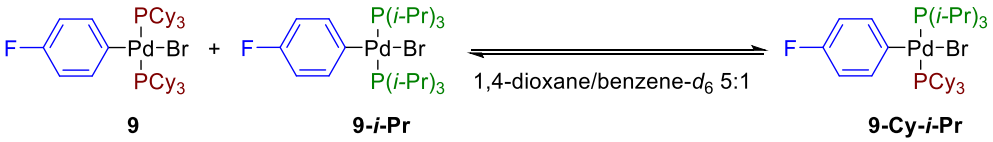
Sulfinate	X = Li (**27**)	X = Na (**4**)	X = K (**27**)	X = K (**27**) + 18-C-6	X = NBu4 (**29**)	X = Cs (**28**)	X = NMe4 (**30**)
Time (min)	Conversion to **5**	Conversion to **5**	Conversion to **5**	Conversion to **5**	Conversion to **5**	Conversion to **5**	Conversion to **5**
0	0%	0%	0%	0%	0%	0%	0%
1	0%	0%	0%	0%	0%	0%	0%
2	0%	0%	1%	1%	1%	1%	3%
4	0%	1%	5%	6%	8%	12%	41%
6	0%	2%	11%	12%	15%	25%	70%
8	0%	3%	17%	18%	20%	35%	81%
10	0%	3%	21%	23%	23%	43%	86%
15	0%	4%	30%	34%	29%	56%	87%
20	0%	5%	36%	41%	33%	66%	88%
30	1%	6%	45%	51%	40%	76%	88%
45	1%	7%	55%	61%	45%	81%	88%
60	1%	9%	62%	68%	48%	83%	90%
120	2%	12%	74%	79%	56%	84%	88%
180	3%	15%	80%	82%	59%	84%	89%
240	4%	18%	81%	84%	59%	85%	89%
300	6%	20%	83%	86%	59%	85%	91%

The above procedure was then repeated at 150 °C and monitored for 3 hours with:

- Sodium 4-methylbenzenesulfinate (10.6 mg, 0.060 mmol, 2.0 equiv.)
- Potassium 4-methylbenzenesulfinate (11.5 mg, 0.060 mmol, 2.0 equiv.)
- Sodium 4-methylbenzenesulfinate (10.6 mg, 0.060 mmol, 2.0 equiv.) with K_2CO_3 (8.2 mg, 0.060 mmol, 2.0 equiv.)

Sulfinate	X = Na (**4**)	X = K (**27**)	X = Na (**4**) + K2CO3
Time (min)	Conversion to **5**	Conversion to **5**	Conversion to **5**
0	0%	0%	0%
1	0%	0%	0%
2	2%	8%	3%
4	9%	58%	29%
6	14%	80%	44%
8	19%	87%	57%
10	23%	89%	59%
15	31%	91%	68%
20	37%	92%	74%
30	45%	92%	84%
45	57%	92%	88%
60	59%	93%	91%
120	68%	95%	93%
180	67%	95%	94%

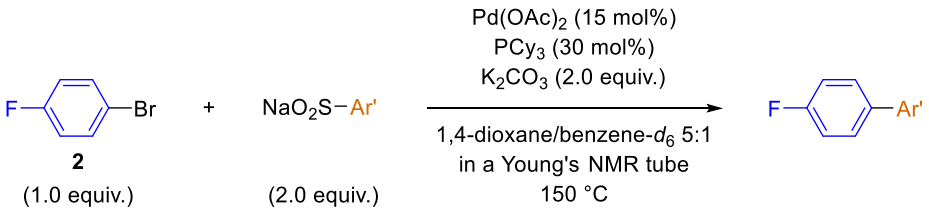
7.2.10. Lability of PCy_3 in the Oxidative Addition Complex 9



9 **9-*i*-Pr** **9-Cy-*i*-Pr**

$[(PCy_3)_2Pd(4\text{-}F\text{-}C_6H_4)(Br)]$ (7.0 mg, 0.0083 mmol, 1.0 equiv.) and $[(P\textit{i}\text{-}Pr_3)_2Pd(4\text{-}F\text{-}C_6H_4)(Br)]$ (5.0 mg, 0.0083 mmol, 1.0 equiv.) were introduced into a Young's NMR tube. The NMR tube was evacuated (< 0.1 mbar) and back-filled with argon twice. 1,4-Dioxane (500 µL) and benzene-d_6 (100 µL) were added to the Young's NMR tube. The NMR tube was sealed, vigorously shaken, and a first $^{31}P\{^1H\}$ NMR spectrum was taken (t = 0 min, 25 °C). The same Young's NMR tube was then heated in a heating block filled with sand for 60 minutes at 50 °C, and a second NMR spectrum was taken (+ 60 min at 50 °C). The following times and temperatures were then employed: (+ 60 min at 75 °C); (+ 60 min at 100 °C).

7.2.11. Identification of the Resting State Intermediates



a) Sodium 4-methylbenzenesulfinate (10.7 mg, 0.060 mmol, 2.0 equiv.) and potassium carbonate (6.2 mg, 0.045 mmol, 1.5 equiv.) were introduced into a Young's NMR tube. The

NMR tube was evacuated (< 0.1 mbar) and back-filled with argon twice. A stock solution containing 1-bromo-4-fluorobenzene (0.060 M, 0.030 mmol, 1.0 equiv.), palladium acetate (0.0090 M, 0.0045 mmol, 0.15 equiv.), tricyclohexylphosphine (0.018 M, 0.009 mmol 0.30 equiv.) and 1-fluoronaphtalene (0.030 M, 0.015, 0.5 equiv.) in 1,4-dioxane (500 µL) was added, followed by 100 µL of benzene-d_6. The NMR tube was sealed, vigorously shaken, and heated at 150 °C for 14 hours. The NMR tube was allowed to cool to room temperature, and a set of NMR spectra (^{19}F, $^{31}P\{^1H\}$) was recorded.

The above procedure was by replacing sodium 4-methylbenzenesulfinate with:

b) sodium pyridine-2-sulfinate (9.9 mg, 0.060 mmol, 2.0 equiv.)

c) lithium 6-(*tert*-butyl)pyridine-2-sulfinate (12.2 mg, 0.059 mmol, 2.0 equiv.)

d) Sodium 5-(trifluoromethyl)pyridine-2-sulfinate (4.7 mg, 0.020 mmol, 1.0 equiv.) and potassium carbonate (2.1 mg, 0.015 mmol, 1.5 equiv.) were introduced into a Young's NMR tube. The NMR tube was evacuated (< 0.1 mbar) and back-filled with argon twice. A stock solution containing 1-bromo-4-fluorobenzene (0.020 M, 0.010 mmol, 1.0 equiv.), palladium acetate (0.0030 M, 0.0015 mmol, 0.15 equiv.), tricyclohexylphosphine (0.0060 M, 0.0030 mmol, 0.30 equiv.) and 1,3,5-trifluorobenzene (0.005 M, 0.0025 mmol, 0.25 equiv.) in 1,4-dioxane (500 µL) was added, followed by 100 µL of benzene-d_6. The NMR tube was sealed, vigorously shaken, and heated at 150 °C for 14 hours. The NMR tube was allowed to cool to room temperature, and a set of NMR spectra (^{19}F, $^{31}P\{^1H\}$) was recorded.

The above procedure was repeated by replacing sodium 5-(trifluoromethyl)pyridine-2-sulfinate with:

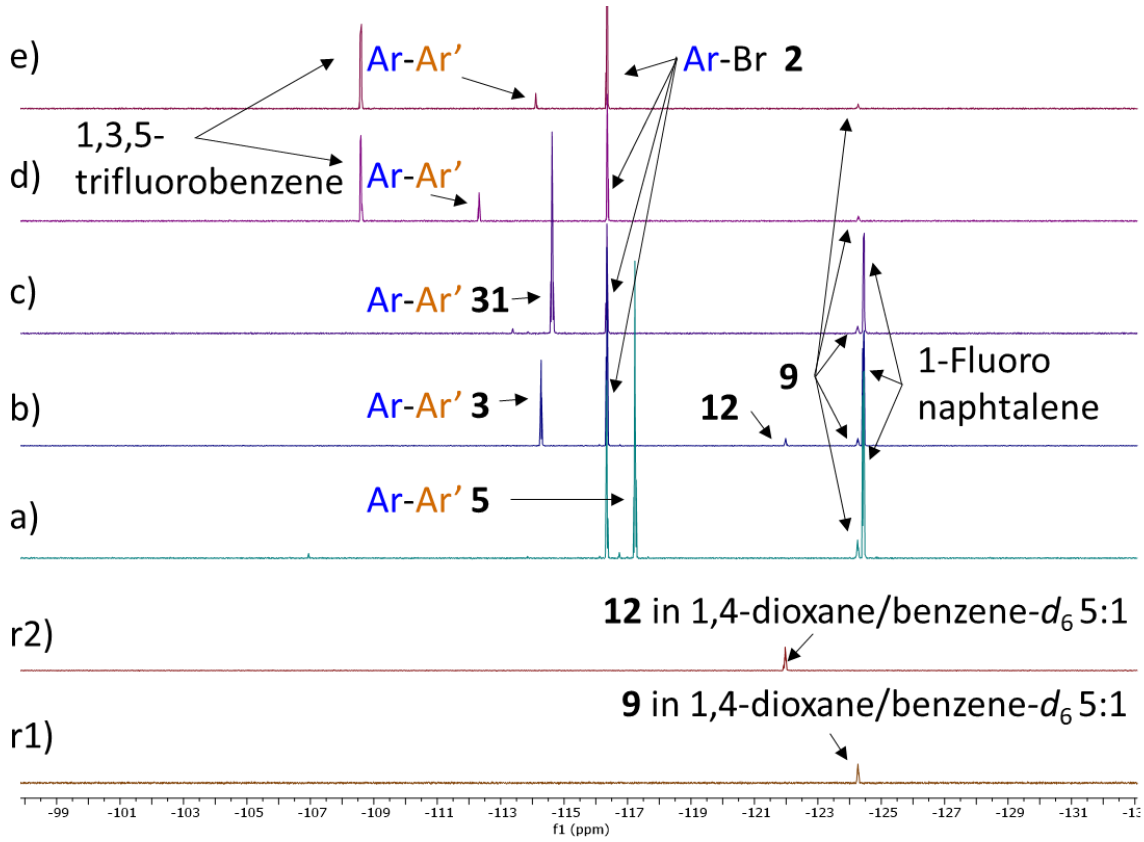
e) sodium pyridine-4-sulfinate **16** (3.3 mg, 0.020 mmol, 2.0 equiv.)

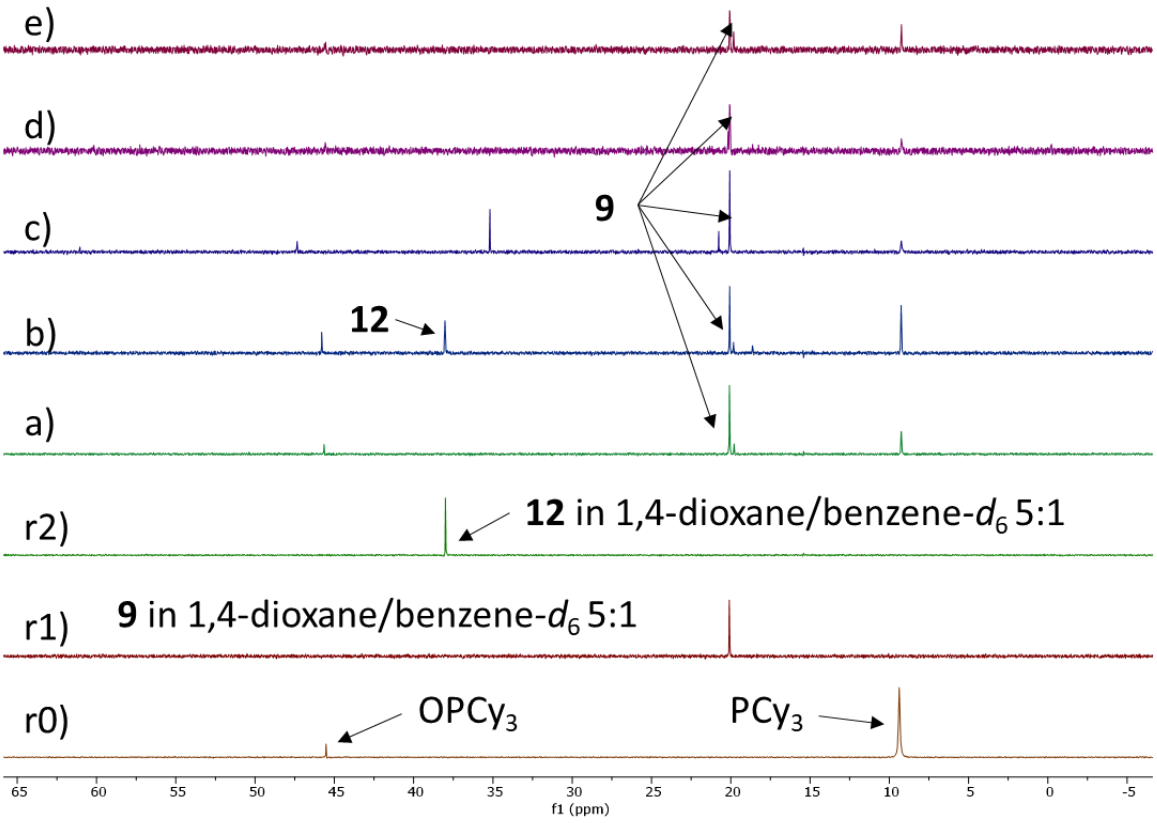
Reference spectra in 1,4-dioxane/benzene-d_6 5:1:

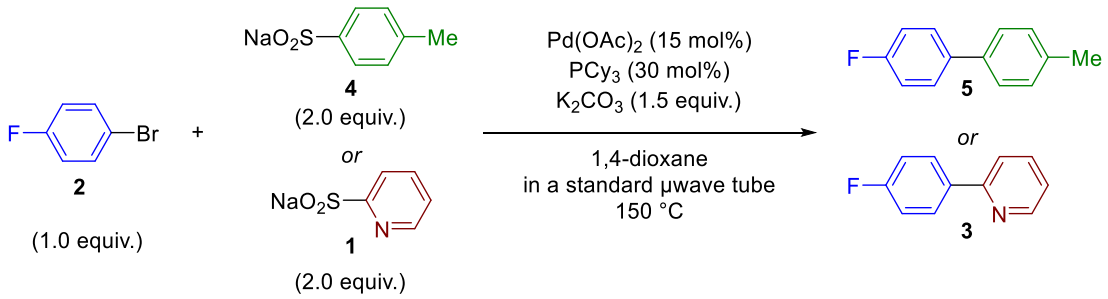
r0) PCy_3

r1) Compound **12**

r2) Compound **9**



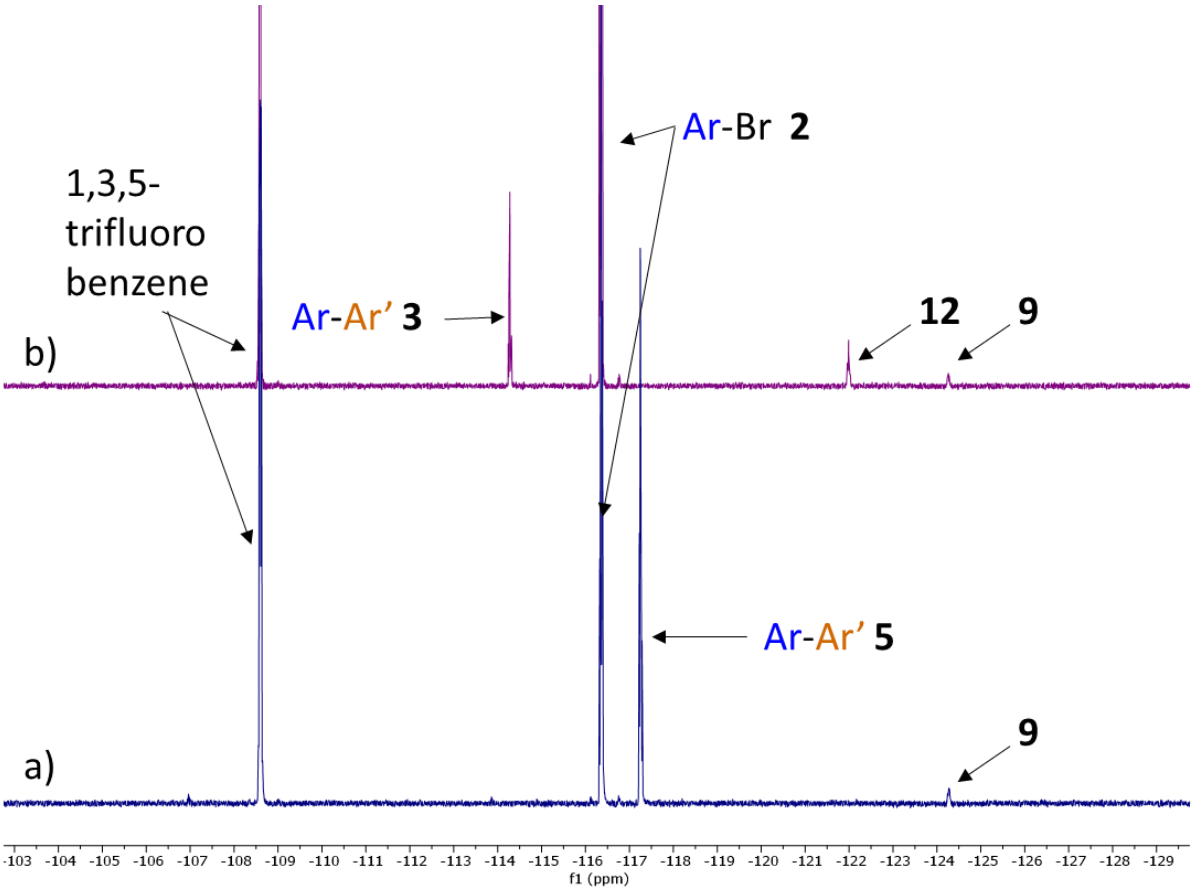




a) Sodium 4-methylbenzenesulfinate (81 mg, 0.46 mmol, 2.0 equiv.), 1,3,5-trimethoxybenzene (19.1 mg, 0.11 mmol, 0.50 equiv.), K_2CO_3 (47.2 mg, 0.34 mmol, 1.5 equiv.), palladium acetate (2.6 mg, 0.012 mmol, 0.05 equiv.) and PCy_3 (6.4 mg, 0.023 mmol, 0.10 equiv.) were added to a microwave vial equipped with a stirrer bar. The vial was sealed with a microwave vial cap, evacuated (< 0.1 mbar) and back-filled with argon twice, then 1,4-dioxane (4.6 mL) and 1-bromo-4-fluorobenzene (25 µL, 0.23 mmol, 1.0 equiv.) were added. The microwave tube was placed in a preheated heating block at 150 °C, and stirred for 120 minutes. It was then cooled

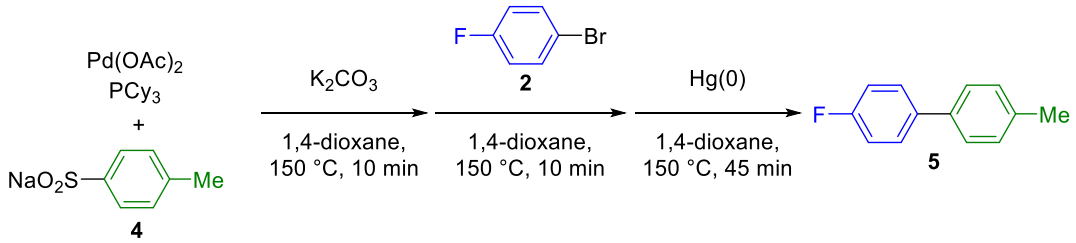
to room temperature with a water bath, a 500 µL aliquot was taken and mixed with 100 µL of benzene-d_6 in a Young's NMR tube, and a ^{19}F NMR spectrum was recorded

b) The above procedure was repeated by replacing sodium 4-methylbenzenesulfinate with sodium pyridine-2-sulfinate (75 mg, 0.46 mmol, 2.0 equiv.).



7.2.12. Homogeneous *vs* Heterogeneous Catalysis

7.2.12.1. Mercury Test



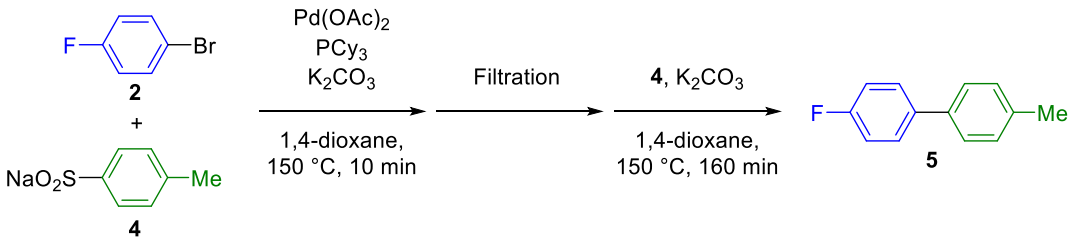
Sodium 4-methylbenzenesulfinate (81 mg, 0.45 mmol, 2.0 equiv.), potassium carbonate (47 mg, 0.34 mmol, 1.5 equiv.), palladium acetate (2.6 mg, 0.012 mmol, 0.05 equiv.),

tricyclohexylphosphine (6.4 mg, 0.023 mmol, 0.10 equiv.) and 1,3,5-trimethoxybenzene (19 mg, 0.11 mmol, 0.50 equiv.) were added to a microwave vial equipped with a stirrer bar. The vial was sealed with a microwave vial cap, evacuated (< 0.1 mbar) and back-filled with argon twice, then 1,4-dioxane (4.3 mL) was added. The vial was then placed in a preheated heating block at 150 °C and stirred for 20 minutes. A stock solution of 1-bromo-4-fluorobenzene (0.76 M, 0.23 mmol, 1.0 equiv.) in 1,4-dioxane (300 µL) was then injected and aliquots were taken every two minutes for 10 minutes (◆). Then, mercury(0) (4.6 g, 22.9 mmol, 100 equiv.) was added and the reaction was monitored for another 45 minutes (◆). The yield of product **5** was determined by HPLC using 1,3,5-trimethoxybenzene as the internal standard.

The above procedure was also performed without the addition of mercury as a control experiment (▲).

Addition of Hg(0) after t = 10 min		No Addition of Hg(0)	
Time (min)	Conversion to **5**	Time (min)	Conversion to **5**
0	0%	0	0%
2	3%	2	3%
4	7%	4	7%
6	10%	6	9%
8	13%	8	11%
10	15%	10	13%
12	16%	15	17%
14	16%	20	20%
16	16%	25	22%
18	16%	30	24%
20	16%	35	25%
25	16%	40	28%
30	16%	45	29%
35	16%	50	30%
40	16%	55	31%
45	16%		
50	16%		
55	16%		

7.2.12.2. Filtration Test

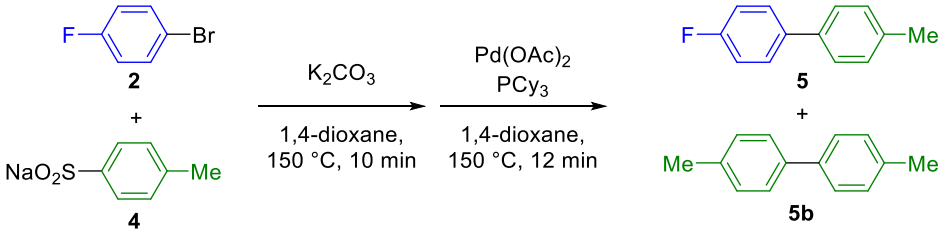


Sodium 4-methylbenzenesulfinate (81 mg, 0.45 mmol, 2.0 equiv.), potassium carbonate (47 mg, 0.34 mmol, 1.5 equiv.), palladium acetate (2.6 mg, 0.012 mmol, 0.05 equiv.), tricyclohexylphosphine (6.4 mg, 0.023 mmol, 0.10 equiv.) and 1,3,5-trimethoxybenzene (19 mg, 0.11 mmol, 0.50 equiv.) were added to a microwave vial equipped with a stirrer bar. The vial was sealed with a microwave vial cap, evacuated (< 0.1 mbar) and back-filled with argon twice, then 1,4-dioxane (4.6 mL) and 1-bromo-4-fluorobenzene (25 µL, 0.23 mmol, 1.0 equiv.) were added. The vial was then placed in a preheated heating block at 150 °C and stirred for 20 minutes. The vial was rapidly cooled to room temperature using a water bath, and a first sample was taken (t_1 = 20 min). 4-methylbenzenesulfinate (81 mg, 0.45 mmol, 2.0 equiv.) and potassium carbonate (47 mg, 0.34 mmol, 1.5 equiv.) were introduced in a second microwave vial equipped with a stirrer bar. The vial was sealed with a microwave vial cap, evacuated (< 0.1 mbar) and back-filled with argon twice. The first reaction mixture was then filtered under an inert atmosphere of argon through a 0.22 µm PTFE syringe filter (Gilson Scientific Ldt, CAT #ANP2522) and the filtrate was immediately injected into the second microwave vial after which a second HPLC sample was then taken (t_2 = 40 min). The vial was then placed in a preheated heating block at 150 °C, and aliquots were taken at t_3 = 60 min, t_4 = 90 min, and t_5 = 160 min. The yield of product **5** was determined by HPLC using 1,3,5-trimethoxybenzene as the internal standard.

Time (min)	Amount of **5** (mmol)
0	0.000
20	0.047
40	0.052
60	0.093
90	0.135
160	0.201

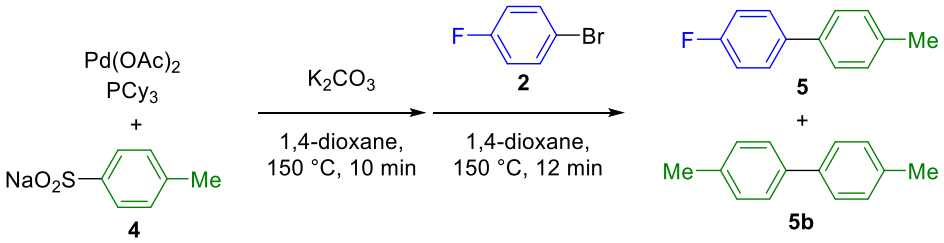
7.2.13. Initial Rate Studies

7.2.13.1. Influence of the Addition Order of the Reagents on the Initial Rate



Sodium 4-methylbenzenesulfinate (81 mg, 0.46 mmol, 2.0 equiv.), 1,3,5-trimethoxybenzene (19 mg, 0.11 mmol, 0.50 equiv.), K_2CO_3 (47 mg, 0.34 mmol, 1.5 equiv.) were added to a microwave vial equipped with a stirrer bar. The vial was sealed with a microwave vial cap, evacuated (< 0.1 mbar) and back-filled with argon twice, then 1,4-dioxane (4.2 mL) and 1-bromo-4-fluorobenzene (25 µL, 0.23 mmol, 1.0 equiv.) were added. A first aliquot was taken and the vial was placed in a preheated heating block at 150 °C and stirred for 10 minutes. A second aliquot was taken, then 400 µL of a solution of palladium acetate (0.029 mM, 0.011 mmol, 0.05 equiv.) and PCy_3 (0.057 mM, 0.023 mmol, 0.10 equiv.) was injected. Aliquots were taken every two minutes for 12 minutes and the amounts of product **5** and 4,4'-dimethylbiphenyl **5b** were measured by HPLC against 1,3,5-trimethoxybenzene as the internal standard.

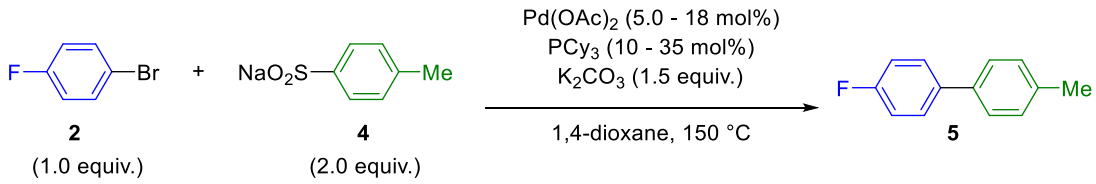
Time (min)	Amount of **5** (10^{-2} mmol)	Amount of **5b** (10^{-2} mmol)
0	0.00	0.00
10	0.00	0.00
12	0.15	0.46
14	0.43	0.67
16	0.81	0.77
18	1.23	0.79
20	1.67	0.82
22	2.12	0.85



Sodium 4-methylbenzenesulfinate (81 mg, 0.46 mmol, 2.0 equiv.), 1,3,5-trimethoxybenzene (19 mg, 0.11 mmol, 0.50 equiv.), K_2CO_3 (47.2 mg, 0.34 mmol, 1.5 equiv.), palladium acetate (2.6 mg, 0.012 mmol, 0.05 equiv.) and PCy_3 (6.4 mg, 0.023 mmol, 0.10 equiv.) were added to a microwave vial equipped with a stirrer bar. The vial was sealed with a microwave vial cap, evacuated (< 0.1 mbar) and back-filled with argon twice, then 1,4-dioxane (4.6 mL) was added and a first aliquot was taken. The vial was then placed in a preheated heating block at 150 °C and stirred for 10 minutes, aliquots were taken every two minute during this period. Then, 1-bromo-4-fluorobenzene (25 µL, 0.23 mmol, 1.0 equiv.) was injected and aliquots were taken every two minutes for 12 more minutes. The amounts of product **5** and 4,4'-dimethylbiphenyl **5b** were measured by HPLC against 1,3,5-trimethoxybenzene as the internal standard.

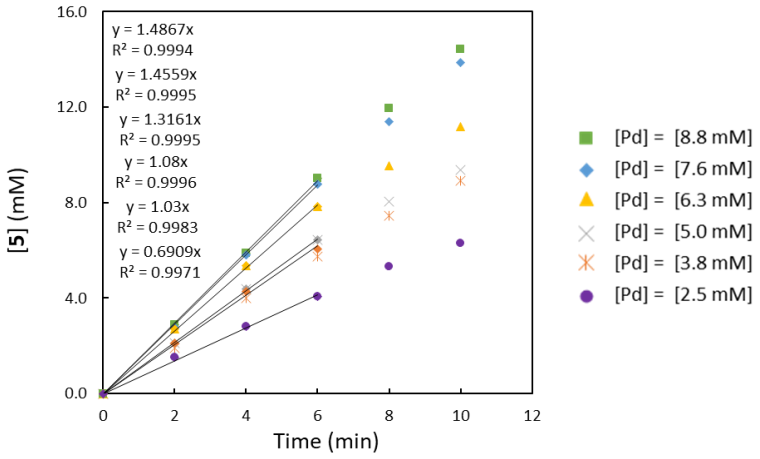
Time (min)	Amount of **5** (10^{-2} mmol)	Amount of **5b** (10^{-2} mmol)
0	0.00	0.00
2	0.00	0.71
4	0.00	0.79
6	0.00	0.81
8	0.00	0.84
10	0.00	0.85
12	0.49	0.87
14	0.88	0.89
16	1.22	0.88
18	1.58	0.89
20	1.90	0.92
22	2.21	0.92

7.2.13.2. Determination of the Reaction Order in [$Pd(OAc)_2$ + 2 PCy_3] With Sodium 4-methylbenzenesulfinate 4



Sodium 4-methylbenzenesulfinate (81 mg, 0.46 mmol, 2.0 equiv.), 1,3,5-trimethoxybenzene (19 mg, 0.11 mmol, 0.50 equiv.), K_2CO_3 (47 mg, 0.34 mmol, 1.5 equiv.), palladium acetate (X mmol) and PCy_3 (2*X mmol) were added to a microwave vial equipped with a stirrer bar. The vial was sealed with a microwave vial cap, evacuated (< 0.1 mbar) and back-filled with argon twice, then 1,4-dioxane (4.6 mL) was added. The vial was then placed in a preheated heating block at 150 °C and stirred for 10 minutes. 1-Bromo-4-fluorobenzene (25 µL, 0.23 mmol, 1.0 equiv.) was injected at t = 0 min. Aliquots were taken every two minutes for 10 minutes. The yield of product **5** was determined by HPLC using 1,3,5-trimethoxybenzene as the internal standard.

Initial rates were obtained from the first four points of the plot of product formation against time with Microsoft® Excel as described in the following figure.



Representative plot for six concentrations of [$Pd(OAc)_2$ + 2 PCy_3].

The 1 : 2 ratio palladium/ligand ratio was kept constant, and each concentration was repeated three times (runs 1, 2 and 3).

		Run 1	Run 2	Run 3		
	Reaction time (min)	Product (mM)	Product (mM)	Product (mM)		
	0	0.0	0.0	0.0		
$m(Pd(OAc)_2)$ (mg)	2	1.5	1.5	1.6		
2.6	4	2.8	2.9	3.2	Average Initial Rate	0.72
$m(PCy_3)$ (mg)	6	4.1	4.1	4.7	Standard Deviation	0.05
6.4	8	5.3	5.3	5.4	Relative Error	7%
Concentration $[Pd(OAc)_2]$ (M)	10	6.3	6.5	6.1		
0.0025						
	Initial Rate (mM/min)	0.70	0.70	0.78		

		Run 1	Run 2	Run 3		
	Reaction time (min)	Product (mM)	Product (mM)	Product (mM)		
	0	0.0	0.0	0.0		
m(Pd(OAc)2) (mg)	2	2.1	1.9	2.1		
3.9	4	4.3	4.0	4.3	Average Initial Rate	1.02
$m(PCy_3)$ (mg)	6	6.1	5.7	6.3	Standard Deviation	0.04
9.6	8	7.8	7.4	8.1	Relative Error	4%
Concentration $[Pd(OAc)_2]$ (M)	10	9.2	8.9	9.7		
0.0038						
	Initial Rate (mM/min)	1.02	0.98	1.07		

		Run 1	Run 2	Run 3		
	Reaction time (min)	Product (mM)	Product (mM)	Product (mM)		
	0	0.0	0.0	0.0		
m(Pd(OAc)2) (mg)	2	2.3	2.1	2.1		
5.2	4	4.6	4.3	4.4	Average Initial Rate	1.10
$m(PCy_3)$ (mg)	6	7.1	6.2	6.4	Standard Deviation	0.07
12.8	8	8.9	8.0	8.1	Relative Error	6%
Concentration $[Pd(OAc)_2]$ (M)	10	10.9	9.6	9.4		
0.0050						
	Initial Rate (mM/min)	1.17	1.04	1.09		

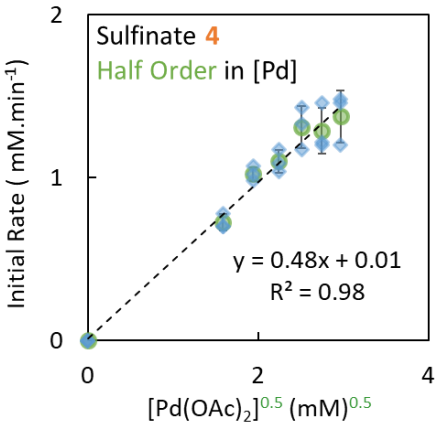
		Run 1	Run 2	Run 3		
	Reaction time (min)	Product (mM)	Product (mM)	Product (mM)		
	0	0.0	0.0	0.0		
m(Pd(OAc)2) (mg)	2	2.7	2.7	2.3		
6.5	4	5.3	5.8	4.7	Average Initial Rate	1.31
$m(PCy_3)$ (mg)	6	7.8	8.7	7.1	Standard Deviation	0.13
16	8	9.6	11.5	9.3	Relative Error	10%
Concentration $[Pd(OAc)_2]$ (M)	10	11.2	13.8	11.6		
0.0063						
	Initial Rate (mM/min)	1.33	1.43	1.17		

		Run 1	Run 2	Run 3		
	Reaction time (min)	Product (mM)	Product (mM)	Product (mM)		
	0	0.0	0.0	0.0		
m(Pd(OAc)2) (mg)	2	2.8	2.4	2.4		
7.8	4	5.8	4.8	4.9	Average Initial Rate	1.29
m(PCy_3) (mg)	6	8.8	7.1	7.2	Standard Deviation	0.14
19.2	8	11.4	8.8	8.2	Relative Error	11%
Concentration [$Pd(OAc)_2$] (M)	10	13.9	10.5	9.2		
0.0076						
	Initial Rate (mM/min)	1.46	1.20	1.22		

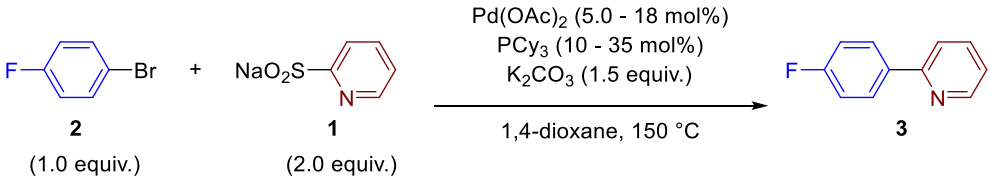
		Run 1	Run 2	Run 3		
	Reaction time (min)	Product (mM)	Product (mM)	Product (mM)		
	0	0.0	0.0	0.0		
m(Pd(OAc)2) (mg)	2	2.9	3.1	2.4		
9.1	4	5.9	5.8	4.7	Average Initial Rate	1.38
m(PCy_3) (mg)	6	9.0	8.7	7.2	Standard Deviation	0.16
22.4	8	11.9	11.4	9.7	Relative Error	11%
Concentration [$Pd(OAc)_2$] (M)	10	14.4	14.1	12.1		
0.0088						
	Initial Rate (mM/min)	1.48	1.46	1.20		

$[Pd(OAc)_2]^{0.5}$ $(mM)^{0.5}$	Average Initial Rate (mM/min)
0.0	0.00
1.6	0.72
1.9	1.02
2.2	1.10
2.5	1.31
2.7	1.29
3.0	1.38

The following plot shows all data points (◆), average values (●) and error bars.

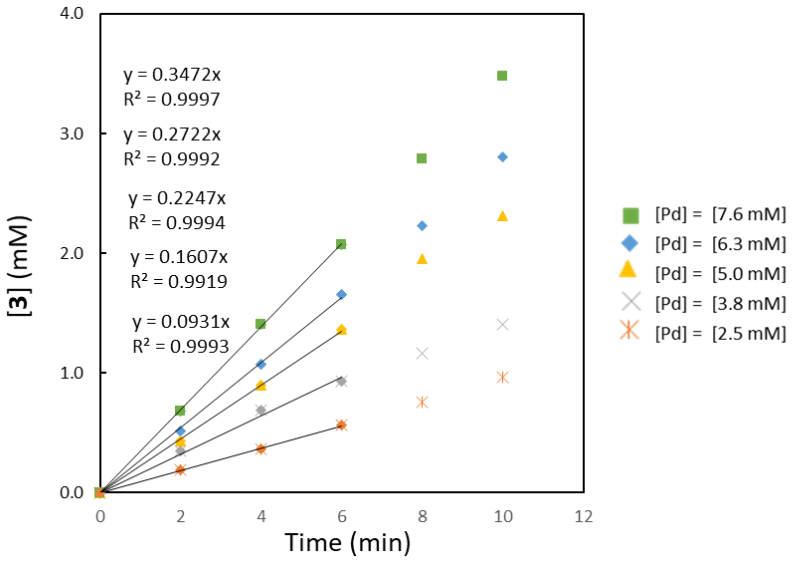


7.2.13.3. Determination of the Reaction Order in [$Pd(OAc)_2$ + 2 PCy_3] With Sodium Pyridine-2-sulfinate 1



Sodium pyridine-2-sulfinate (75 mg, 0.46 mmol, 2.0 equiv.), 1,3,5-trimethoxybenzene (19 mg, 0.11 mmol, 0.50 equiv.), K_2CO_3 (47.2 mg, 0.34 mmol, 1.5 equiv.), palladium acetate (X mmol) and PCy_3 (2*X mmol) were added to a microwave vial equipped with a stirrer bar. The vial was sealed with a microwave vial cap, evacuated (< 0.1 mbar) and back-filled with argon twice, then 1,4-dioxane (4.6 mL) was added. The vial was then placed in a preheated heating block at 150 °C and stirred for 10 minutes. 1-Bromo-4-fluorobenzene (25 µL, 0.23 mmol, 1.0 equiv.) was injected at t = 0 min. Aliquots were taken every two minutes for 10 minutes. The yield of product **3** was determined by HPLC using 1,3,5-trimethoxybenzene as the internal standard.

Initial rates were obtained from the first four points of the plot of product formation against time with Microsoft® Excel as described in the following figure.



Representative plot for five concentrations of [$Pd(OAc)_2$ + 2 PCy_3].

The 1 : 2 ratio palladium/ligand ratio was kept constant, and each concentration was repeated three times (runs 1, 2 and 3).

		Run 1	Run 2	Run 3		
	Reaction time (min)	Product (mM)	Product (mM)	Product (mM)		
	0	0.00	0.00	0.00		
$m(Pd(OAc)_2)$ (mg)	2	0.19	0.21	0.19		
2.6	4	0.36	0.39	0.39	Average Initial Rate	0.10
$m(PCy_3)$ (mg)	6	0.56	0.60	0.60	Standard Deviation	0.003
6.4	8	0.75	0.82	0.80	Relative Error	3%
Concentration $[Pd(OAc)_2]$ (M)	10	0.96	1.04	1.01		
0.0025						
	Initial Rate (mM/min)	0.09	0.10	0.10		

		Run 1	Run 2	Run 3		
	Reaction time (min)	Product (mM)	Product (mM)	Product (mM)		
	0	0.00	0.00	0.00		
$m(Pd(OAc)_2)$ (mg)	2	0.36	0.31	0.35		
3.9	4	0.67	0.60	0.68	Average Initial Rate	0.16
$m(PCy_3)$ (mg)	6	1.05	0.89	0.93	Standard Deviation	0.013
9.6	8	1.41	1.01	1.16	Relative Error	8%
Concentration $[Pd(OAc)_2]$ (M)	10	1.79	1.52	1.41		
0.0038						
	Initial Rate (mM/min)	0.17	0.15	0.16		

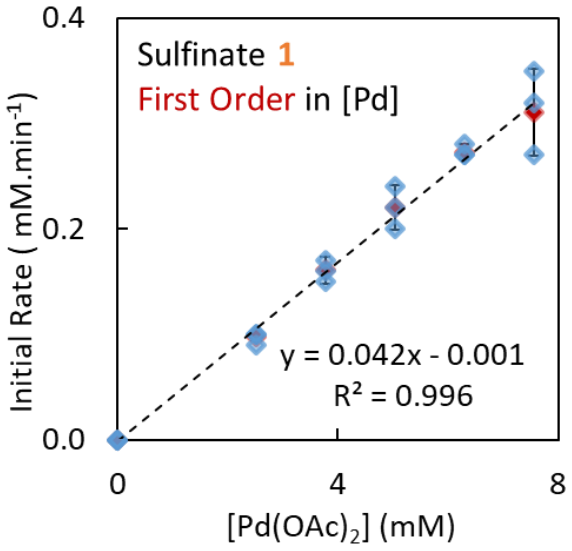
		Run 1	Run 2	Run 3		
	Reaction time (min)	Product (mM)	Product (mM)	Product (mM)		
	0	0.00	0.00	0.00		
$m(Pd(OAc)_2)$ (mg)	2	0.50	0.25	0.43		
5.2	4	0.84	0.55	0.89	Average Initial Rate	0.22
$m(PCy_3)$ (mg)	6	1.13	0.78	1.36	Standard Deviation	0.021
12.8	8	1.44	1.05	1.96	Relative Error	9%
Concentration $[Pd(OAc)_2]$ (M)	10	1.76	1.33	2.32		
0.0050						
	Initial Rate (mM/min)	0.20	0.24	0.22		

		Run 1	Run 2	Run 3		
	Reaction time (min)	Product (mM)	Product (mM)	Product (mM)		
	0	0.00	0.00	0.00		
$m(Pd(OAc)_2)$ (mg)	2	0.52	0.51	0.48		
6.5	4	1.08	1.13	1.05	Average Initial Rate	0.27
$m(PCy_3)$ (mg)	6	1.65	1.68	1.63	Standard Deviation	0.007
16	8	2.23	2.21	2.19	Relative Error	2%
Concentration $[Pd(OAc)_2]$ (M)	10	2.80	2.68	2.82		
0.0063						
	Initial Rate (mM/min)	0.27	0.28	0.27		

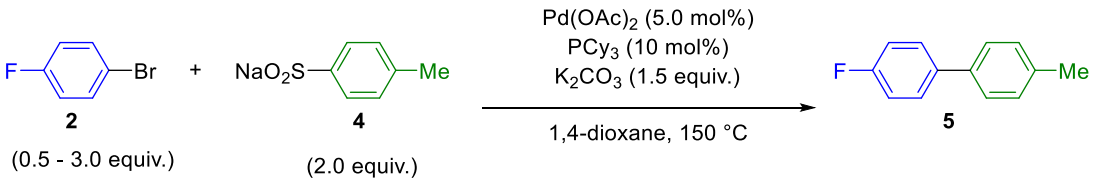
		Run 1	Run 2	Run 3		
	Reaction time (min)	Product (mM)	Product (mM)	Product (mM)		
	0	0.00	0.00	0.00		
$m(Pd(OAc)_2)$ (mg)	2	0.45	0.68	0.60		
7.8	4	1.03	1.41	1.21	Average Initial Rate	0.31
$m(PCy_3)$ (mg)	6	1.66	2.07	1.95	Standard Deviation	0.041
19.2	8	2.25	2.79	2.33	Relative Error	13%
Concentration $[Pd(OAc)_2]$ (M)	10	2.80	3.48	2.73		
0.0076						
	Initial Rate (mM/min)	0.27	0.35	0.32		

Concentration [$Pd(OAc)_2$] (mM)	Average Initial Rate (mM/min)
0.0	0.00
2.5	0.10
3.8	0.16
5.0	0.22
6.3	0.27
7.6	0.31

The following plot shows all data points (◆), average values (◆) and error bars.



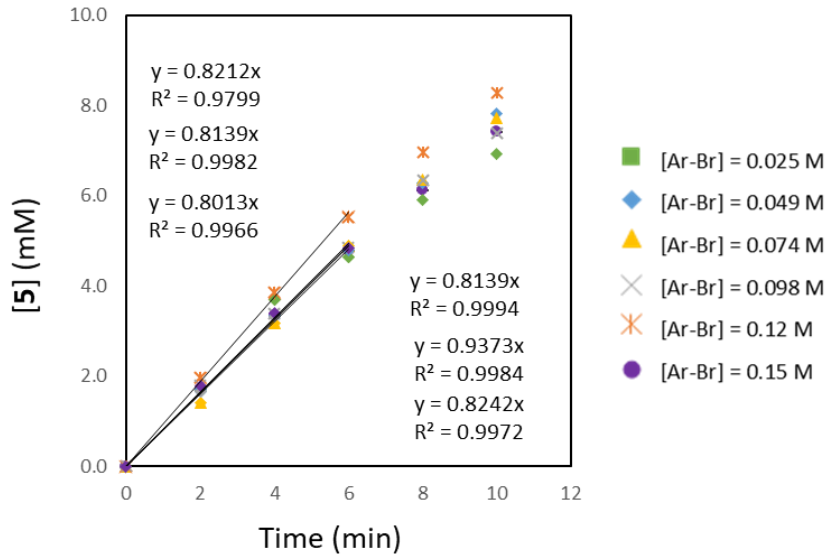
7.2.13.4. Determination of the Reaction Order in Ar-Br 2 With Sodium 4-methylbenzene Sulfinate 4



Sodium 4-methylbenzenesulfinate (81 mg, 0.46 mmol, 2.0 equiv.), 1,3,5-trimethoxybenzene (19 mg, 0.11 mmol, 0.50 equiv.), K_2CO_3 (47 mg, 0.34 mmol, 1.5 equiv.), palladium acetate (2.6 mg, 0.012 mmol, 0.05 equiv.) and PCy_3 (6.4 mg, 0.023 mmol, 0.10 equiv.) were added to a microwave vial equipped with a stirrer bar. The vial was sealed with a microwave vial cap, evacuated (< 0.1 mbar) and back-filled with argon twice, then 1,4-dioxane (4.6 mL) was added. The vial was then placed in a preheated heating block at 150 °C and stirred for 10 minutes. 1-

Bromo-4-fluorobenzene (X mmol) was injected at t = 0 min. Aliquots were taken every two minutes for 10 minutes. The yield of product **5** was determined by HPLC using 1,3,5-trimethoxybenzene as the internal standard.

Initial rates were obtained from the first four points of the plot of product formation against time with Microsoft® Excel as described in the following figure.



Representative plot for six concentrations of 1-bromo-4-fluorobenzene.

Each concentration was repeated three times (runs 1, 2 and 3).

		Run 1	Run 2	Run 3		
	Reaction time (min)	Product (mM)	Product (mM)	Product (mM)		
	0	0.0	0.0	0.0		
V(Ar-Br) (µL)	2	1.7	1.3	2.0		
13	4	3.7	2.6	3.5	Average Initial Rate	0.78
	6	4.6	3.9	4.9	Standard Deviation	0.11
Concentration [Ar-Br] (M)	8	5.9	4.5	5.8	Relative Error	14%
0.026	10	6.9	5.2	6.9		
	Initial Rate (mM/min)	0.83	0.65	0.85		

		Run 1	Run 2	Run 3		
	Reaction time (min)	Product (mM)	Product (mM)	Product (mM)		
	0	0.0	0.0	0.0		
V(Ar-Br) (µL)	2	1.7	1.5	1.8		
25	4	3.4	3.0	3.4	Average Initial Rate	0.78
	6	4.8	4.4	4.7	Standard Deviation	0.04
Concentration [Ar-Br] (M)	8	6.1	5.5	5.8	Relative Error	5%
0.049	10	7.4	7.0	6.6		
	Initial Rate (mM/min)	0.80	0.74	0.80		

		Run 1	Run 2	Run 3		
	Reaction time (min)	Product (mM)	Product (mM)	Product (mM)		
	0	0.0	0.0	0.0		
V(Ar-Br) (µL)	2	2.0	1.4	1.2		
38	4	3.7	3.2	2.6	Average Initial Rate	0.79
	6	5.3	4.9	4.0	Standard Deviation	0.13
Concentration [Ar-Br] (M)	8	6.9	6.4	5.2	Relative Error	17%
0.075	10	8.1	7.7	6.1		
	Initial Rate (mM/min)	0.91	0.80	0.65		

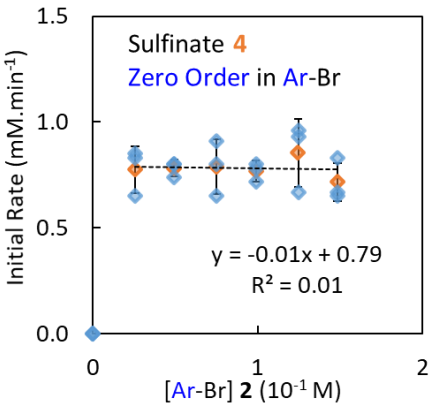
		Run 1	Run 2	Run 3		
	Reaction time (min)	Product (mM)	Product (mM)	Product (mM)		
	0	0.0	0.0	0.0		
V(Ar-Br) (µL)	2	2.0	1.7	1.9		
50	4	3.0	3.3	3.2	Average Initial Rate	0.77
	6	4.0	4.8	4.5	Standard Deviation	0.05
Concentration [Ar-Br] (M)	8	4.9	6.3	5.6	Relative Error	6%
0.099	10	5.8	7.8	6.7		
	Initial Rate (mM/min)	0.72	0.80	0.78		

		Run 1	Run 2	Run 3		
	Reaction time (min)	Product (mM)	Product (mM)	Product (mM)		
	0	0.0	0.0	0.0		
V(Ar-Br) (µL)	2	2.0	2.0	1.2		
63	4	3.8	3.8	2.7	Average Initial Rate	0.86
	6	5.5	5.7	4.1	Standard Deviation	0.16
Concentration [Ar-Br] (M)	8	7.0	7.0	5.5	Relative Error	18%
0.12	10	8.3	8.3	6.7		
	Initial Rate (mM/min)	0.93	0.96	0.67		

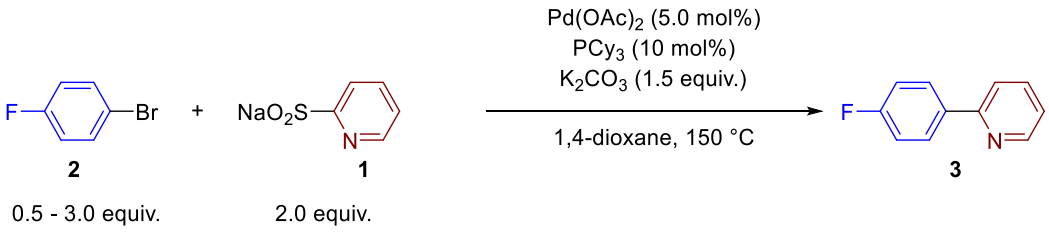
		Run 1	Run 2	Run 3		
	Reaction time (min)	Product (mM)	Product (mM)	Product (mM)		
	0	0.0	0.0	0.0		
V(Ar-Br) (µL)	2	1.8	1.3	1.2		
75	4	3.4	2.7	2.7	Average Initial Rate	0.72
	6	4.8	4.1	3.8	Standard Deviation	0.09
Concentration [Ar-Br] (M)	8	6.3	5.5	4.3	Relative Error	13%
0.15	10	7.4	6.8	4.9		
	Initial Rate (mM/min)	0.83	0.67	0.65		

[Ar-Br] (10^{-1} M)	Average Initial Rate (mM/min)
0.00	0.00
0.26	0.78
0.49	0.78
0.75	0.79
0.99	0.77
1.2	0.86
1.5	0.72

The following plot shows all data points (◆), average values (◆) and error bars.

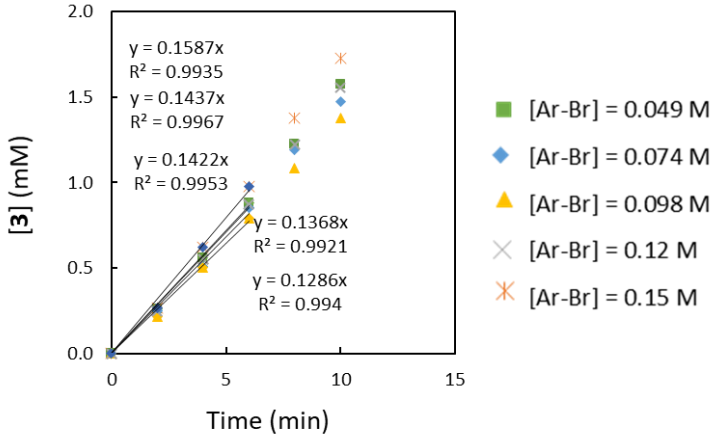


7.2.13.5. Determination of the Reaction Order in Ar-Br 2 With Sodium Pyridine-2-sulfinate 1



Sodium pyridine-2-sulfinate (75 mg, 0.46 mmol, 2.0 equiv.), 1,3,5-trimethoxybenzene (19 mg, 0.11 mmol, 0.50 equiv.), K_2CO_3 (47 mg, 0.34 mmol, 1.5 equiv.), palladium acetate (2.6 mg, 0.012 mmol, 0.05 equiv.) and PCy_3 (6.4 mg, 0.023 mmol, 0.10 equiv.) were added to a microwave vial equipped with a stirrer bar. The vial was sealed with a microwave vial cap, evacuated (< 0.1 mbar) and back-filled with argon twice, then 1,4-dioxane (4.6 mL) was added. The vial was then placed in a preheated heating block at 150 °C and stirred for 10 minutes. 1-Bromo-4-fluorobenzene (X mmol) was injected at t = 0 min. Aliquots were taken every two minutes for 10 minutes. The yield of product **3** was determined by HPLC using 1,3,5-trimethoxybenzene as the internal standard.

Initial rates were obtained from the first four points of the plot of product formation against time with Microsoft® Excel as described in the following figure.



Representative plot for five concentrations of 1-bromo-4-fluorobenzene.

Each concentration was repeated two times (runs 1 and 2).

		Run 1	Run 2		
	Reaction time (min)	Product (mM)	Product (mM)		
	0	0.00	0.00		
V(Ar-Br) (µL)	2	0.26	0.29		
25	4	0.56	0.61	Average Initial Rate	0.15
	6	0.88	0.95	Standard Deviation	0.005
Concentration [Ar-Br] (M)	8	1.2	1.3	Relative Error	3%
0.049	10	1.6	1.6		
	Initial Rate (mM/min)	0.15	0.15		

		Run 1	Run 2		
	Reaction time (min)	Product (mM)	Product (mM)		
	0	0.00	0.00		
V(Ar-Br) (µL)	2	0.25	0.29		
38	4	0.51	0.57	Average Initial Rate	0.15
	6	0.85	0.93	Standard Deviation	0.009
Concentration [Ar-Br] (M)	8	1.2	1.3	Relative Error	6%
0.075	10	1.5	1.6		
	Initial Rate (mM/min)	0.15	0.16		

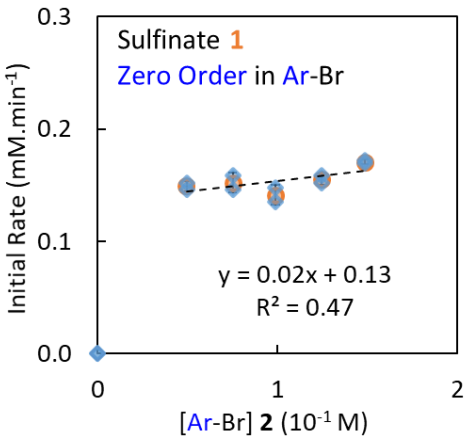
		Run 1	Run 2		
	Reaction time (min)	Product (mM)	Product (mM)		
	0	0.00	0.00		
V(Ar-Br) (µL)	2	0.22	0.26		
50	4	0.51	0.55	Average Initial Rate	0.14
	6	0.79	0.87	Standard Deviation	0.009
Concentration [Ar-Br] (M)	8	1.1	1.2	Relative Error	7%
0.099	10	1.4	1.5		
	Initial Rate (mM/min)	0.13	0.15		

		Run 1	Run 2		
	Reaction time (min)	Product (mM)	Product (mM)		
	0	0.00	0.00		
V(Ar-Br) (µL)	2	0.25	0.27		
63	4	0.55	0.57	Average Initial Rate	0.16
	6	0.88	0.93	Standard Deviation	0.005
Concentration [Ar-Br] (M)	8	1.2	1.3	Relative Error	3%
0.12	10	1.6	1.6		
	Initial Rate (mM/min)	0.15	0.16		

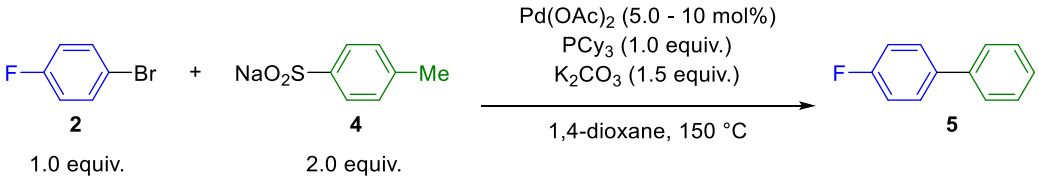
		Run 1	Run 2		
	Reaction time (min)	Product (mM)	Product (mM)		
	0	0.00	0.00		
V(Ar-Br) (µL)	2	0.27	0.26		
75	4	0.62	0.61	Average Initial Rate	0.17
	6	1.0	1.1	Standard Deviation	0.002
Concentration [Ar-Br] (M)	8	1.4	1.4	Relative Error	1%
0.15	10	1.7	1.8		
	Initial Rate (mM/min)	0.17	0.17		

[Ar-Br] (10^{-1} M)	Average Initial Rate (mM/min)
0.00	0.00
0.49	0.15
0.75	0.15
0.99	0.14
1.2	0.16
1.5	0.17

The following plot shows all data points (◆), average values (●) and error bars.

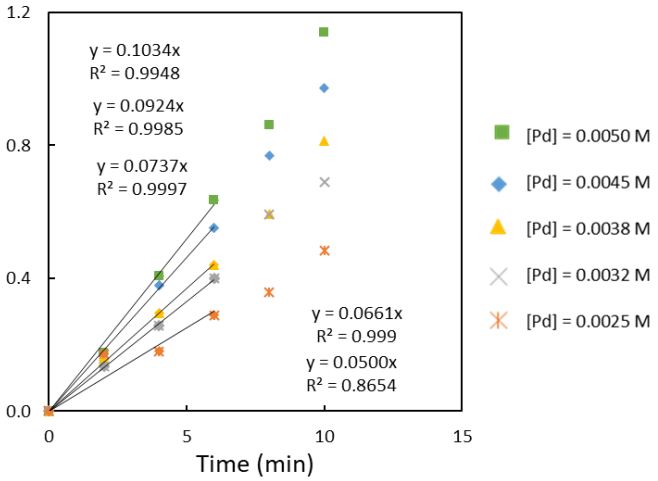


7.2.13.6. Determination of the Reaction Order in [$Pd(OAc)_2$ + 2 PCy_3] With Sodium 4-methylbenzenesulfinate 4 and Pd/PCy_3 ratio < 0.10



Sodium 4-methylbenzenesulfinate (81 mg, 0.46 mmol, 2.0 equiv.), 1,3,5-trimethoxybenzene (19 mg, 0.11 mmol, 0.50 equiv.), K_2CO_3 (47 mg, 0.34 mmol, 1.5 equiv.), palladium acetate (X mmol) and PCy_3 (64 mg, 0.23 mmol, 1.0 equiv.) were added to a microwave vial equipped with a stirrer bar. The vial was sealed with a microwave vial cap, evacuated (< 0.1 mbar) and back-filled with argon twice, then 1,4-dioxane (4.6 mL) was added. The vial was then placed in a preheated heating block at 150 °C and stirred for 15 minutes. 1-Bromo-4-fluorobenzene (25 µL, 0.23 mmol, 1.0 equiv.) was injected at t = 0 min. Aliquots were taken every two minutes for 20 minutes. The yield of product **5** was determined by HPLC using 1,3,5-trimethoxybenzene as the internal standard.

Initial rates were obtained from the first four points of the plot of product formation against time with Microsoft® Excel as described in the following figure.



Representative plot for five concentrations of $Pd(OAc)_2$.

The palladium/ligand ratio was kept ≤ 0.1, and each concentration was repeated two times (runs 1 and 2).

		Run 1	Run 2		
	Reaction time (min)	Product (mM)	Product (mM)		
	0	0.00	0.00		
$m(Pd(OAc)_2)$ (mg)	2	0.17	0.25		
2.6	4	0.18	0.22	Average Initial Rate	0.053
$m(PCy_3)$ (mg)	6	0.29	0.32	Standard Deviation	0.005
63.8	8	0.36	0.43	Relative Error	9%
Concentration $[Pd(OAc)_2]$ (M)	10	0.48	0.56		
0.0025					
	Initial Rate (mM/min)	0.050	0.057		

		Run 1	Run 2		
	Reaction time (min)	Product (mM)	Product (mM)		
	0	0.00	0.00		
$m(Pd(OAc)_2)$ (mg)	2	0.13	0.13		
3.3	4	0.26	0.26	Average Initial Rate	0.065
$m(PCy_3)$ (mg)	6	0.40	0.39	Standard Deviation	0.000
63.8	8	0.59	0.51	Relative Error	0%
Concentration $[Pd(OAc)_2]$ (M)	10	0.69	0.66		
0.0032					
	Initial Rate (mM/min)	0.065	0.065		

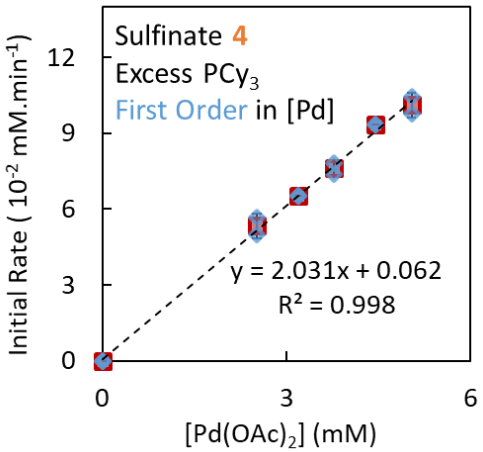
		Run 1	Run 2		
	Reaction time (min)	Product (mM)	Product (mM)		
	0	0.00	0.00		
$m(Pd(OAc)_2)$ (mg)	2	0.15	0.15		
3.9	4	0.29	0.29	Average Initial Rate	0.076
$m(PCy_3)$ (mg)	6	0.44	0.49	Standard Deviation	0.003
63.8	8	0.59	0.65	Relative Error	4%
Concentration $[Pd(OAc)_2]$ (M)	10	0.81	0.82		
0.0038					
	Initial Rate (mM/min)	0.074	0.078		

		Run 1	Run 2		
	Reaction time (min)	Product (mM)	Product (mM)		
	0	0.00	0.00		
$m(Pd(OAc)_2)$ (mg)	2	0.17	0.19		
4.6	4	0.38	0.39	Average Initial Rate	0.093
$m(PCy_3)$ (mg)	6	0.55	0.54	Standard Deviation	0.000
63.8	8	0.77	0.73	Relative Error	0%
Concentration $[Pd(OAc)_2]$ (M)	10	0.97	0.97		
0.0045					
	Initial Rate (mM/min)	0.093	0.093		

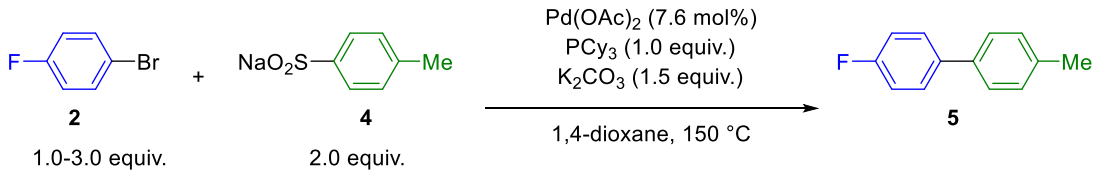
		Run 1	Run 2		
	Reaction time (min)	Product (mM)	Product (mM)		
	0	0.00	0.00		
$m(Pd(OAc)_2)$ (mg)	2	0.18	0.18		
5.2	4	0.41	0.37	Average Initial Rate	0.101
$m(PCy_3)$ (mg)	6	0.63	0.60	Standard Deviation	0.005
63.8	8	0.86	0.84	Relative Error	5%
Concentration $[Pd(OAc)_2]$ (M)	10	1.14	1.04		
0.0050					
	Initial Rate (mM/min)	0.104	0.098		

[Pd(OAc)$_2$] (mM)	Average Initial Rate (10^{-2} mM/min)
0.0	0.0
2.5	5.3
3.2	6.5
3.8	7.6
4.5	9.3
5.0	10.1

The following plot shows all data points (◆), average values (■) and error bars.



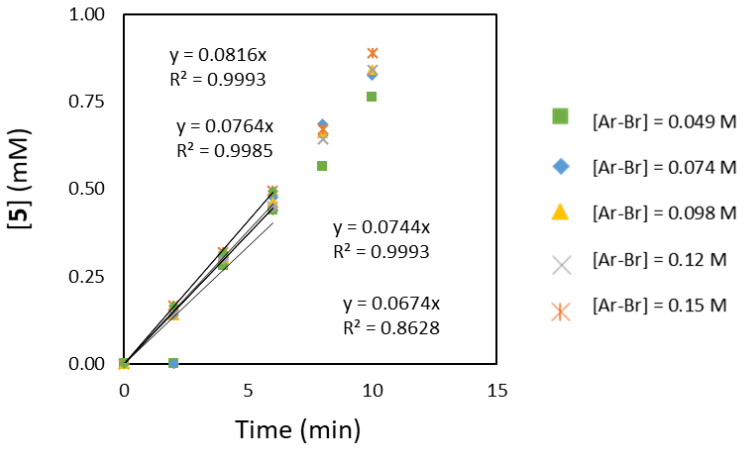
7.2.13.7. Determination of the Reaction Order in Ar-Br 2 With Sodium 4-methylbenzenesulfinate 4 and Pd/PCy$_3$ ratio < 0.10



Sodium 4-methylbenzenesulfinate (81 mg, 0.46 mmol, 2.0 equiv.), 1,3,5-trimethoxybenzene (19 mg, 0.11 mmol, 0.50 equiv.), K_2CO_3 (47 mg, 0.34 mmol, 1.5 equiv.), palladium acetate (3.9 mg, 0.017 mmol, 0.076 equiv.) and PCy_3 (64 mg, 0.23 mmol, 1.0 equiv.) were added to a microwave vial equipped with a stirrer bar. The vial was sealed with a microwave vial cap, evacuated (< 0.1 mbar) and back-filled with argon twice, then 1,4-dioxane (4.6 mL) was added. The vial was then placed in a preheated heating block at 150 °C and stirred for 15 minutes. 1-Bromo-4-fluorobenzene (X mmol) was injected at t = 0 min. Aliquots were taken every two

minutes for 10 minutes. The yield of product **5** was determined by HPLC using 1,3,5-trimethoxybenzene as the internal standard.

Initial rates were obtained from the first four points of the plot of product formation against time with Microsoft® Excel as described in the following figure.



Plot for five concentrations of Ar-Br.

		Run 1
	Reaction time (min)	Product (mM)
	0	0.00
V(Ar-Br) (µL)	2	0.00
25	4	0.28
	6	0.44
Concentration [Ar-Br] (M)	8	0.57
0.049	10	0.76
	Initial Rate (mM/min)	0.078

		Run 1
	Reaction time (min)	Product (mM)
	0	0.00
V(Ar-Br) (µL)	2	0.00
38	4	0.30
	6	0.48
Concentration [Ar-Br] (M)	8	0.69
0.075	10	0.83
	Initial Rate (mM/min)	0.078

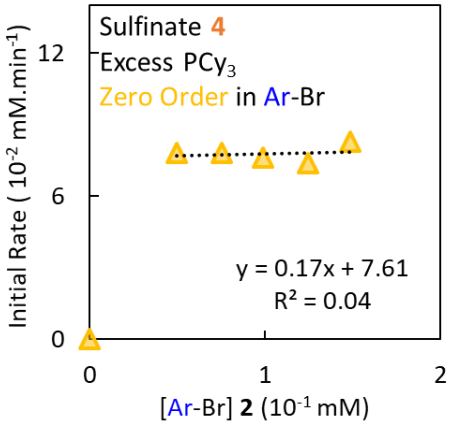
		Run 1
	Reaction time (min)	Product (mM)
	0	0.00
V(Ar-Br) (µL)	2	0.14
50	4	0.30
	6	0.46
Concentration [Ar-Br] (M)	8	0.66
0.099	10	0.84
	Initial Rate (mM/min)	0.076

		Run 1
	Reaction time (min)	Product (mM)
	0	0.00
V(Ar-Br) (µL)	2	0.14
63	4	0.30
	6	0.45
Concentration [Ar-Br] (M)	8	0.64
0.12	10	0.84
	Initial Rate (mM/min)	0.074

		Run 1
	Reaction time (min)	Product (mM)
	0	0.00
V(Ar-Br) (µL)	2	0.16
75	4	0.32
	6	0.49
Concentration [Ar-Br] (M)	8	0.67
0.15	10	0.89
	Initial Rate (mM/min)	0.083

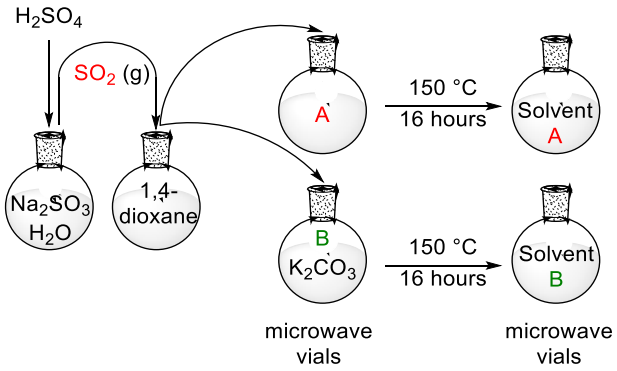
[Ar-Br] (10^{-1} M)	Average Initial Rate (10^{-2} mM/min)
0.0	0.0
0.5	7.8
0.8	7.8
1.0	7.6
1.2	7.4
1.5	8.3

The following plot shows all data points (▲).



7.2.14. Role of the Carbonate Base

7.2.14.1. Preparation of the solutions of SO_2 in 1,4-dioxane



Sodium sulfite (441 mg, 3.50 mmol) was introduced in a round bottomed flask equipped with a stirrer bar. The flask was sealed with a septum, evacuated (< 0.1 mbar) and back-filled with argon twice, then H_2O (1.5 mL) was added. A canula was used to connect this first flask to a second sealed round bottomed flask containing 70 mL of 1,4-dioxane under argon. Sulfuric acid was added dropwise to the first flask, and the SO_2 gas generated was bubbled through the 1,4-dioxane *via* the canula. When no more gas bubbles were observed, the canula was removed, and the flask containing SO_2 and 1,4-dioxane was stirred for 30 minutes.

Preparation of Solvent A

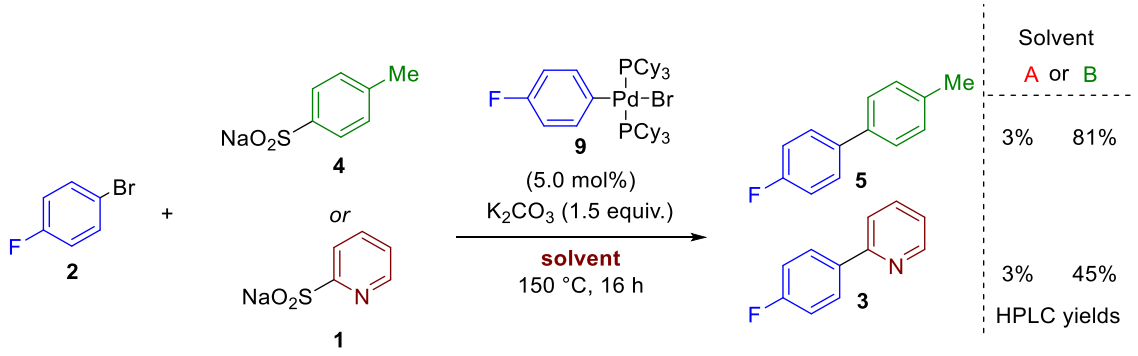
A microwave vial equipped with a stirrer bar was sealed with a microwave vial cap, evacuated (< 0.1 mbar) and back-filled with argon twice. 6 mL of the ca. 0.05M solution of SO_2 in 1,4-dioxane (0.3 mmol, 1.0 equiv.) was added to the microwave vial. The solution was stirred at 150 °C for 16 hours in the sealed microwave vial.

Preparation of Solvent B

K_2CO_3 (62 mg, 0.45 mmol, 1.5 equiv.) was added to a microwave vial equipped with a stirrer bar. The vial was sealed with a microwave vial cap, evacuated (< 0.1 mbar) and back-filled with argon twice. 6 mL of the ca. 0.05M solution of SO_2 in 1,4-dioxane (0.3 mmol, 1.0 equiv.)

was added to the microwave vial. The solution was stirred at 150 °C for 16 hours in the sealed microwave vial.

7.2.14.2. Cross-Coupling Reactions Using Solvents A and B



Sodium 4-methylbenzenesulfinate (81 mg, 0.46 mmol, 2.0 equiv.) or sodium pyridine-2-sulfinate (75.2 mg, 0.46 mmol, 2.0 equiv.), 1,3,5-trimethoxybenzene (19 mg, 0.11 mmol, 0.50 equiv.), K_2CO_3 (47 mg, 0.34 mmol, 1.5 equiv.) and $[(PCy_3)_2Pd(4\text{-}F\text{-}C_6H_4)(Br)]$ (9.6 mg, 0.011 mmol, 0.05 equiv.) were added to a microwave vial equipped with a stirrer bar. The vial was sealed with a microwave vial cap, evacuated (< 0.1 mbar) and back-filled with argon twice, then the solvent was added:

Solvent A: 4.6 mL (0.23 mmol of SO_2, 1.0 equiv. with respect to **2**, 20 equiv. with respect to **9**)

Solvent B: 4.6 mL were taken carefully after the carbonate base had settled at the bottomed of the vial (unknown amount of SO_2 as solvent B was stirred with K_2CO_3 for 16 hours).

1-Bromo-4-fluorobenzene **2** (25 µL, 0.23 mmol, 1.0 equiv.) was added last. Then, the sealed vials were placed in a preheated heating block at 150 °C and stirred for 4 hours after which an aliquot was taken from each of the four reactions and The yield of product **5** was determined by HPLC against 1,3,5-trimethoxybenzene as the internal standard giving the following yields:

Solvent A, sulfinate **4**: 3%

Solvent B, sulfinate **4**: 81%

Solvent A, sulfinate **1**: 3%

Solvent B, sulfinate **1**: 45%

7.2.15. Crystallographic and Refinement Data

Preparation of the X-ray samples was done by myself.

The data was acquired either by Dr Alasdair I. McKay or by myself.

Analysis of the data and refinement of the structures was done by Dr Alasdair I. McKay.

This section was kindly written by Dr Alasdair I. McKay.

7.2.15.1. Crystal Structure Determinations

Single crystal X-ray diffraction data for all samples were collected as follows: a typical crystal was mounted on a MiTeGen micromounts using perfluoropolyether oil and cooled rapidly in a stream of nitrogen gas using an Oxford Cryosystems unit.[222] Data were collected with an Agilent SuperNova diffractometer (Cu K_α radiation, $\lambda = 1.54180$ Å), a Rigaku XtaLAB Mini II diffractometer (Mo K_α radiation, $\lambda = 0.71073$ Å) or a Rigaku XtaLAB Synergy diffractometer (Mo K_α radiation, $\lambda = 0.71073$ Å). Raw frame data were reduced using CrysAlisPro.[223] The structures were solved using SHELXT[224] and refined using full-matrix least squares refinement on all F^2 data using the SHELXL-18[225-226] using the interface OLEX2.[227] All hydrogen atoms were placed in calculated positions (riding model). Further comments regarding individual crystal structures can be found below. Crystallographic data have been deposited with the Cambridge Crystallographic Data Centre under CCDC 1964568-1964578. These data can be obtained free of charge from The Cambridge Crystallographic Data Centre via www.ccdc.cam.ac.uk/data_request/cif. Full bond length and bond angle data may be found in the CIFs.

7.2.15.2. Further Comments on Individual Crystal Structures

Compound 6: The asymmetric unit contains two independent half molecules. One acetate was modelled as disordered over two sites. Restraints were applied with the aid of the FragmentDB module.[228-229] The second acetate is likewise incompletely occupied, however, attempts to introduce a disorder model were not successful, giving rise to the two Level B Checkcif alerts.

Compound 10: A disordered molecule of CH_2Cl_2 in the lattice was modelled over two sites. Restraints were applied with the aid of the FragmentDB module.[228-229]

Compound 11-CF_3: Minor peaks of electron density were observed adjacent to F1 and C31 atom of the aryl. This was modelled as a substitutional disorder of the CF_3 and F units. The occupancies in the final model are 0.77/0.23.

Compound 12: A disordered molecule of hexane lying on a special position in the lattice modelled over two sites. Restraints were applied with the aid of the FragmentDB module.[228-229]

Compound 12-OMe: A molecule of dichloromethane lying on a special position in the lattice was modelled with the aid of the FragmentDB module.[228-229]

Compound 13: The sulfinate was modelled as disordered over two sites. A molecule of chloroform in the lattice was modelled as disordered over three sites with the aid of the FragmentDB module.[228-229]

Compound 14: The sulfinate was found to be incompletely occupied (0.85). This was modelled as substitutional disorder with the starting bromide (0.15). The bromide was modelled with isotropic displacement parameters as the refinement became unstable when anisotropic displacement parameters were employed in the refinement. The data was also modelled as an inversion twin.

Compound 11-OMe: The collected crystal was found to be twinned. The twin matrix [-1.000, 0.000, 0.000, 0.000, -1.000, 0.000, -0.351, -0.922, 1.000] was applied with the twin scale factor refining to 0.16. The sulfinate and aryl groups displayed prolate displacement ellipsoids. These were modelled over two sites employing restraints to geometries and displacement parameters.

Compound 12-CF_3: The asymmetric unit contains two independent molecules.

7.2.15.3. Selected bond length (Å) and angles (°)

7: Pd1-P1 2.4084(4), Pd1-P2 2.3982(4), Pd1-O3 2.0838(12), Pd1-S1 2.2755(4), P1-Pd1-Pd2 164.468(15), P1-Pd1-O3 87.76(3), P1-Pd1-S1 93.829(15), P2-Pd1-O3 86.29(3), P2-Pd1-S1 93.899(15), O3-Pd1-S1 172.64(4).

10: Pd1-P1 2.2812(5), Pd1-N1 2.1513(15), Pd1-O1 2.0975(13), Pd1-S2 2.2307(5), P1-Pd1-N1 168.27(4), P1-Pd1-O1 89.34(4), P1-Pd1-S2 97.193(17), N1-Pd1-O1 80.45(6), N1-Pd1-S2 93.53(4), O1-Pd1-S2 171.69(4).

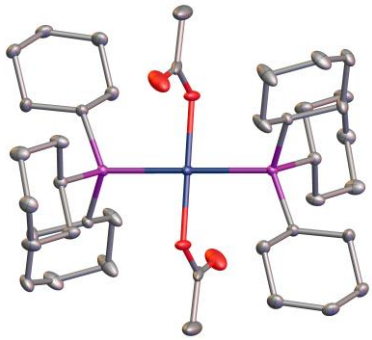
11: Pd1-P1 2.3255(7), Pd1-S1 2.3097(8), Pd1-O1' 2.155(2), Pd1-C19 2.001(3), P1-Pd1-S1 178.85(3), P1-Pd1-O1' 87.50(6), P1-Pd1-C19 91.81(8), C19-Pd1-S1 87.06(8), C19-Pd1-O1' 175.24(12), S1-Pd1-O1' 93.65(6).

12: Pd1-P1 2.2608(8), Pd1-N1 2.147(2), Pd1-O1 2.132(2), Pd1-C19 1.979(3), P1-Pd1-N1 174.65(7), P1-Pd1-O1 95.41(6), P1-Pd1-C19 91.20(8), N1-Pd1-O1 80.33(9), N1-Pd1-C19 93.17(10), O1-Pd1-C19 173.16(10).

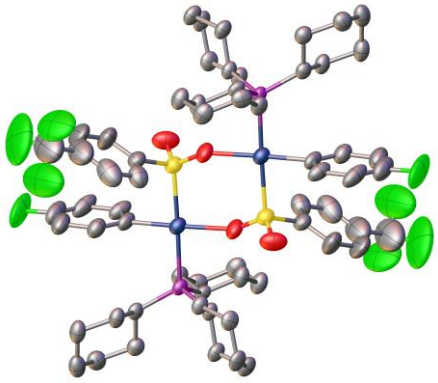
13: Pd1-P1 2.3219(11), Pd1-S1 2.392(7), Pd1-O1' 2.281(11), Pd1-C19 1.987(5), P1-Pd1-S1 172.1(3), P1-Pd1-O1' 87.1(2), P1-Pd1-C19 91.16(13), C19-Pd1-S1 81.5(3), C19-Pd1-O1' 177.1(4), S1-Pd1-O1' 100.4(3).

14: Pd1-P1 2.3633(14), Pd1-P2 2.3708(14), Pd1-O1 2.156(5), Pd1-C37 2.004(5), P1-Pd1-P2 170.48(5), P1-Pd1-O1 94.49(17), P1-Pd1-C37 89.67(16), P2-Pd1-C37 89.75(16), P2-Pd1-O1 85.78(17), C37-Pd1-O1 175.3(2).

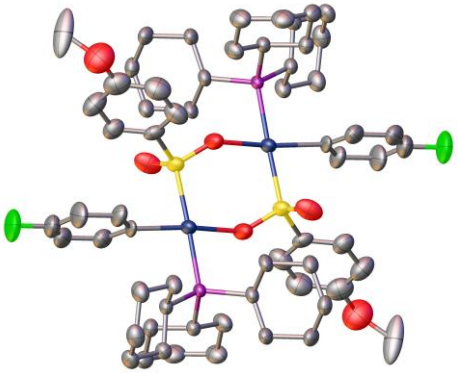
7.2.15.4. Further Crystal Structures



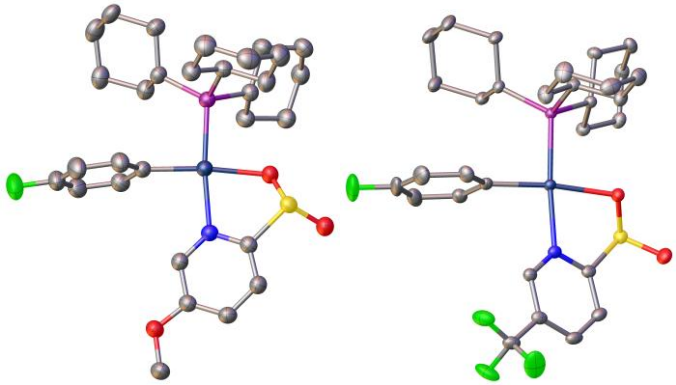
Molecular structure of **6** with displacement ellipsoids at 50% probability. Complete molecule generated through symmetry operation: 1-X,1-Y,-Z. Hydrogen atoms, lower occupancy disordered components and the second molecule in the asymmetric unit have been omitted for clarity. Selected bond lengths (Å): Pd1-P1 2.3543(4), Pd1-O1 2.0237(15).



Molecular structure of **11-CF$_3$** with displacement ellipsoids at 50% probability. Complete dimer generated through symmetry operation: 1-X,1-Y,1-Z. All lower occupancy disorder components and hydrogen atoms have been omitted for clarity. Selected bond lengths (Å): Pd1-P1 2.3160(13), Pd1-S1 2.3052(14), Pd1-O1' 2.137(4), Pd1-C19 1.994(5).



Molecular structure of **11-OMe** with displacement ellipsoids at 50% probability. Complete dimer generated through symmetry operation: 1-X,-Y,1-Z. All lower occupancy disorder components and hydrogen atoms have been omitted for clarity. Selected bond lengths (Å): Pd1-P1 2.3197(15), Pd1-S1 2.3119(16), Pd1-O1' 2.164(8), Pd1-C19 2.044(15).



Molecular structures of **12-OMe** (left) and **12-CF$_3$** (right). Displacement ellipsoids shown at 50% probability. Hydrogen atoms, solvent molecules and the second molecule in the asymmetric unit of **20** have been omitted for clarity. Selected bond lengths (Å) for **12-OMe** and **20** {in parentheses}: Pd1-P1 2.2611(6) {2.2620(4)}, Pd1-O1 2.1199(19) {2.1544(14)}, Pd1-N1 2.136(2) {2.1246(15)}, Pd1-C19 1.994(3) {1.991(2)}.

7.2.15.5. Selected Crystallographic and Refinement Data

	6	**7**	**10**	**11**	**11-CF_3**	**12**
Chemical formula	$C_{40}H_{72}O_4P_2Pd$	$C_{45}H_{76}O_4P_2PdS$	$C_{29}H_{43}Cl_2N_2O_4PPdS_2$	$C_{62}H_{88}F_2O_4P_2Pd_2S_2$	$C_{62}H_{82}F_8O_4P_2Pd_2S_2$	$C_{32}H_{48}FNO_2PPdS$
Formula weight	785.31	881.45	756.04	1274.18	1382.13	667.14
Temperature (K)	100(1)	170(1)	170(1)	170(1)	150(1)	170(1)
Radiation (λ)	0.71073	0.71073	0.71073	0.71073	1.54184	0.71073
Crystal system	triclinic	triclinic	monoclinic	monoclinic	monoclinic	monoclinic
Space group	*P*-1	*P*-1	$P2_1/c$	$P2_1/c$	$P2_1/c$	$C2/c$
a (Å)	9.5870(2)	10.2937(3)	10.0029(2)	13.3684(4)	13.5764(10)	33.707(2)
b (Å)	13.1727(3)	13.7632(3)	29.0336(8)	24.2919(6)	24.600(2)	9.0995(3)
c (Å)	16.0211(3)	17.3117(4)	11.5546(3)	9.5064(2)	9.5037(6)	27.7743(18)
α (deg)	91.788(2)	87.089(2)	90	90	90	90
β (deg)	91.2280(10)	73.891(2)	97.295(2)	99.501(2)	100.444(7)	130.842(11)
γ (deg)	91.613(2)	76.606(2)	90	90	90	90
V (Å^3)	2020.96(7)	2291.99(10)	3328.53(14)	3044.80(14)	3121.5(4)	6444.7(10)
Z	2	2	4	2	2	8
ρ(calcd) (g cm^{-3})	1.291	1.277	1.509	1.390	1.471	1.375
μ (mm^{-1})	0.575	0.559	0.928	0.762	6.338	0.724
F(000)	840	940	1560	1328	1424	2792
Reflections collected	32404	77121	57892	59366	17104	92978
Unique reflections	8912	10025	7301	6673	6435	7123
Parameters / Restraints	466 / 100	480 / 0	398 / 44	335 / 0	406 / 323	372 / 34
R_{int}	0.0340	0.0419	0.0392	0.0586	0.0537	0.1018
R_1 [$I > 2\sigma(I)$]	0.0260	0.0259	0.0252	0.0408	0.0611	0.0386
wR_2 [all data]	0.0659	0.0642	0.0559	0.0803	0.1502	0.0885
GooF	1.053	1.053	1.019	1.163	1.071	1.058
Residual electron density (e Å^{-3})	1.46 / -0.33	0.80 / -0.55	0.37 / -0.42	0.82 / -0.58	1.28 / -1.12	0.80 / -0.56
CCDC no.	1964568	1964569	1964570	1964572	1964571	1964576

	12-OMe	**13**	**14**	**11-OMe**	**12-CF_3**
Chemical formula	$C_{30.5}H_{44}ClFNO_3PPdS$	$C_{68}H_{100}Cl_6F_2N_2O_4P_2Pd_2S_2$	$C_{47.95}H_{75.95Br}Br_{0.15}FNO_{1.7}P_2PdS_{0.85}$	$C_{62}H_{88}F_2O_6P_2Pd_2S_2$	$C_{30}H_{40}F_4NO_2PPdS$
Formula weight	696.54	1599.05	906.21	1306.18	692.06
Temperature (K)	150(1)	150(1)	170(1)	150(1)	150(1)
Radiation (λ)	1.54184	1.54184	0.71073	1.54184	1.54184
Crystal system	triclinic	triclinic	orthorhombic	triclinic	monoclinic
Space group	*P*-1	*P*-1	$P2_12_12_1$	*P*-1	$P2_1/c$
a (Å)	8.8944(3)	12.1932(7)	9.7818(3)	9.5185(6)	10.58590(10)
b (Å)	10.3439(3)	13.1620(7)	13.9735(4)	13.3787(6)	20.2148(2)
c (Å)	17.8359(7)	13.4651(8)	33.9579(9)	14.2586(8)	28.1308(3)
α (deg)	79.425(3)	64.568(5)	90	62.876(5)	90
β (deg)	82.298(3)	86.354(5)	90	78.221(5)	95.5300(10)
γ (deg)	78.361(2)	77.968(5)	90	78.401(4)	90
V (Å^3)	1571.88(10)	1907.9(2)	4641.6(2)	1569.84(17)	5991.75(10)
Z	2	1	4	1	8
ρ(calcd) (g cm^{-3})	1.472	1.392	1.297	1.382	1.534
μ (mm^{-1})	6.953	7.038	0.675	6.150	6.615
F(000)	722	828	1924	680	2848
Reflections collected	14930	15361	29170	15016	37849
Unique reflections	6464	7882	10201	15016	12423
Parameters / Restraints	371 / 22	596 / 504	511 / 0	499 / 598	721 / 0
R_{int}	0.0321	0.0264	0.0382	0.0393	0.0332
R_1 [$I > 2\sigma(I)$]	0.0393	0.0463	0.0468	0.0685	0.0275
wR_2 [all data]	0.0971	0.1324	0.1023	0.2219	0.0688
GooF	1.043	1.034	1.108	1.055	1.051
Residual electron density (e Å^{-3})	1.22 / -0.32	1.16 / -1.82	1.20 / -0.56	1.96 / -1.20	0.73 / -0.97
CCDC no.	1964574	1964575	1964577	1964573	1964578

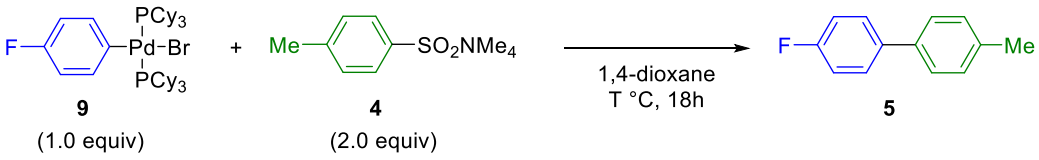
7.3. Experimental Data and Procedures for Chapter 3

7.3.1. General Procedure for the Screening Reactions

Solid reagents were added in a microwave vial with the indicated stoichiometry. The vial was sealed with a microwave vial cap, evacuated (< 0.1 mbar) and back-filled with argon twice, then the solvent was added, followed by any liquid reagent or additive. The reaction was then heated at the indicated temperature and time. The yields of products were measured by HPLC against 1,3,5-trimethoxybenzene as the internal standard using the calibration curves described in **Section 7.2.2**.

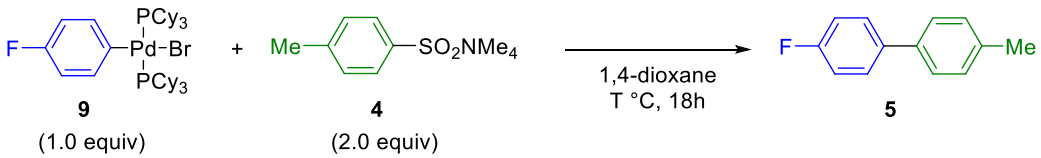
Unless otherwise stated, the reactions were performed with 0.11 mmol of aryl bromide **2** (1.0 equiv.), with 2 mL of solvent, corresponding to a reaction concentration of 0.056 M.

The internal standard was introduced at the beginning of the reaction with the solid reagents (0.5 equiv. compared to Ar-Br **2**).



7.3.2. Stoichiometric Reactions With Oxidative Addition Complex 9

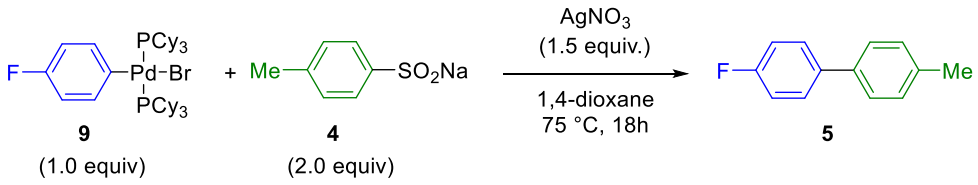
7.3.2.1. Using Sulfinate 4-TMA



Tetramethylammonium 4-methylbenzenesulfinate (13.6 mg, 0.060 mmol, 2.0 equiv.), 1,3,5-trimethoxybenzene (10 mg, 0.060 mmol, 2.0 equiv.) and [$(PCy_3)_2Pd(4\text{-}F\text{-}C_6H_4)(Br)$] (25 mg, 0.030 mmol, 1.0 equiv.) were added to a microwave vial equipped with a stirrer bar. The vial was sealed with a microwave vial cap, evacuated (< 0.1 mbar) and back-filled with argon twice,

then 1,4-dioxane (5.0 mL) was added. The vial was placed in a preheated heating block at 75 °C or 100 °C and stirred for 18 hours, after which an aliquot was taken. The yield of product **5** was determined by HPLC analysis using 1,3,5-trimethoxybenzene as the internal standard. 75 °C : 53%; 100 °C : 85%.

7.3.2.2. Using Sulfinate 4 and $AgNO_3$ as an Additive

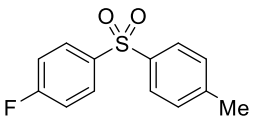


Sodium 4-methylbenzenesulfinate (10.6 mg, 0.060 mmol, 2.0 equiv.), 1,3,5-trimethoxybenzene (10 mg, 0.060 mmol, 2.0 equiv.), [$(PCy_3)_2Pd(4\text{-}F\text{-}C_6H_4)(Br)$] (25 mg, 30 µmol, 1.0 equiv.) and silver nitrate (7.6 mg, 0.045 mmol, 1.5 equiv.) were added to a microwave vial equipped with a stirrer bar. The vial was sealed with a microwave vial cap, evacuated (< 0.1 mbar) and back-filled with argon twice, then 1,4-dioxane (5.0 mL) was added. The vial was placed in a preheated heating block at 75 °C and stirred for 16 hours, after which an aliquot was taken. The yield of product **5** was determined to be 70% by HPLC analysis using 1,3,5-trimethoxybenzene as the internal standard.

7.3.3. Synthetic Procedures and Characterisation Data

7.3.3.1. Sulfone Products

1-fluoro-4-tosylbenzene (17)



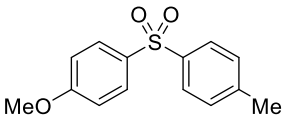
Sodium 4-methylbenzenesulfinate (61 mg, 0.34 mmol, 1.5 eqfuiv.), caesium carbonate (111 mg, 0.34 mmol, 1.5 equiv.), palladium acetate (5.1 mg, 0.023 mmol, 0.10 equiv.) and

Xantphos (14 mg, 0.023 mmol, 0.10 equiv.) were added to a microwave vial equipped with a stirrer bar. The vial was sealed with a microwave vial cap, evacuated (< 0.1 mbar) and back-filled with argon twice, then 1,4-dioxane (4.0 mL) and 1-bromo-4-methoxybenzene (25 µL, 0.23 mmol, 1.0 equiv.) were added. The reaction was heated at 100 °C for 18 hours. The mixture was allowed to cool to room temperature, filtered through a pad of silica and washed with EtOAc. The solvent was removed under reduced pressure, and purification of the crude material by flash chromatography (EtOAc 10% in petrol) gave the title compound in 54% yield (31 mg, 0.12 mmol) as a white solid. The yield was observed to be 90% according to HPLC and 1H NMR analysis, but only 54% were isolated as pure fractions due to overlap with the ligand scrambling by-product $PhSO_2(4\text{-}Me\text{-}C_6H_4)$.

^{1}H NMR (400 MHz, $CDCl_3$) δ 8.01 – 7.89 (m, 2H), 7.84 – 7.78 (m, 2H), 7.30 (d, *J* = 8.0 Hz, 2H), 7.20 – 7.10 (m, 2H), 2.39 (s, 3H); **^{13}C{^{1}H} NMR** (101 MHz, $CDCl_3$) δ 165.5 (d, *J* = 255.5 Hz), 144.5, 138.7, 138.3 (d, *J* = 3.0 Hz), 130.4 (d, *J* = 9.5 Hz), 130.1, 127.8, 116.6 (d, *J* = 22.5 Hz), 21.7; **^{19}F NMR{^{1}H}** (376 MHz, $CDCl_3$) δ -104.64 (tt, *J* = 8.3, 5.1 Hz); **HRMS**: m/z (EI) calculated for ($C_{13}H_{11}FO_2S$) $[M+H]^+$: 251.0537, found: 251.0538.

Data consistent with the literature.[230]

1-methoxy-4-tosylbenzene (17-OMe)



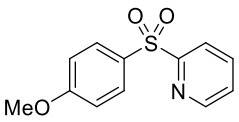
Sodium 4-methylbenzenesulfinate (128 mg, 0.72 mmol, 1.5 equiv.), caesium carbonate (234 mg, 0.75 mmol, 1.5 equiv.), palladium acetate (5.4 mg, 0.024 mmol, 0.05 equiv.) and Xantphos (14 mg, 0.024 mmol, 0.10 equiv.) were added to a microwave vial equipped with a stirrer bar. The vial was sealed with a microwave vial cap, evacuated (< 0.1 mbar) and back-filled with argon twice, then 1,4-dioxane (4.0 mL) and 1-bromo-4-methoxybenzene (60 µL,

0.48 mmol, 1.0 equiv.) were added. The reaction was heated at 100 °C for 18 hours. The mixture was allowed to cool to room temperature, filtered through a pad of silica and washed with EtOAc. The solvent was removed under reduced pressure, and purification of the crude material by flash chromatography (Gradient of EtOAc 10% to 15 % in petrol) gave the title compound in 82% yield (103 mg, 0.39 mmol) as a white solid.

^{1}H NMR (400 MHz, $CDCl_3$) δ 7.87 (d, *J* = 9.0 Hz, 2H), 7.80 (d, *J* = 8.0 Hz, 2H), 7.28 (d, *J* = 8.0 Hz, 2H), 6.96 (d, *J* = 9.0 Hz, 2H), 3.83 (s, 3H), 2.39 (s, 3H); **^{13}C{^{1}H} NMR** (101 MHz, $CDCl_3$) δ 163.3, 143.8, 139.5, 133.6, 129.9, 129.8, 127.4, 114.5, 55.7, 21.6; **HRMS**: m/z (EI) calculated for ($C_{14}H_{14}O_3S$) $[M+H]^+$: 263.0736, found: 263.0735.

Data consistent with the literature.[231]

2-((4-methoxyphenyl)sulfonyl)pyridine (17-OMe-2-pyr)

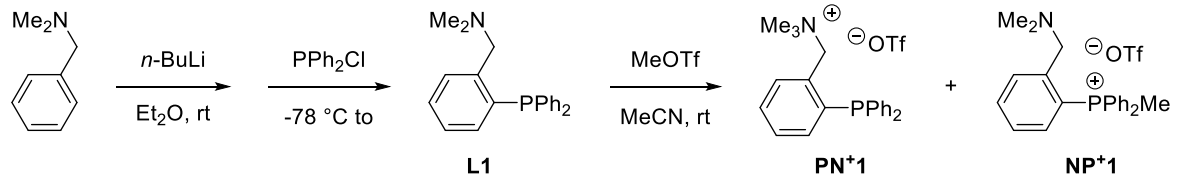


Sodium pyridine-2-sulfinate (119 mg, 0.72 mmol, 1.5 equiv.), caesium carbonate (234 mg, 0.75 mmol, 1.5 equiv.), palladium acetate (5.4 mg, 0.024 mmol, 0.05 equiv.) and Xantphos (14 mg, 0.024 mmol, 0.10 equiv.) were added to a microwave vial equipped with a stirrer bar. The vial was sealed with a microwave vial cap, evacuated (< 0.1 mbar) and back-filled with argon twice, then 1,4-dioxane (4.0 mL) and 1-bromo-4-methoxybenzene (60 µL, 0.48 mmol, 1.0 equiv.) were added. The reaction was heated at 100 °C for 18 hours. The mixture was allowed to cool to room temperature, filtered through a pad of silica and washed with EtOAc. The solvent was removed under reduced pressure, and purification of the crude material by flash chromatography (EtOAc 30% in petrol) gave the title compound in 16 % yield (103 mg, 0.0.79 mmol) as a white solid.

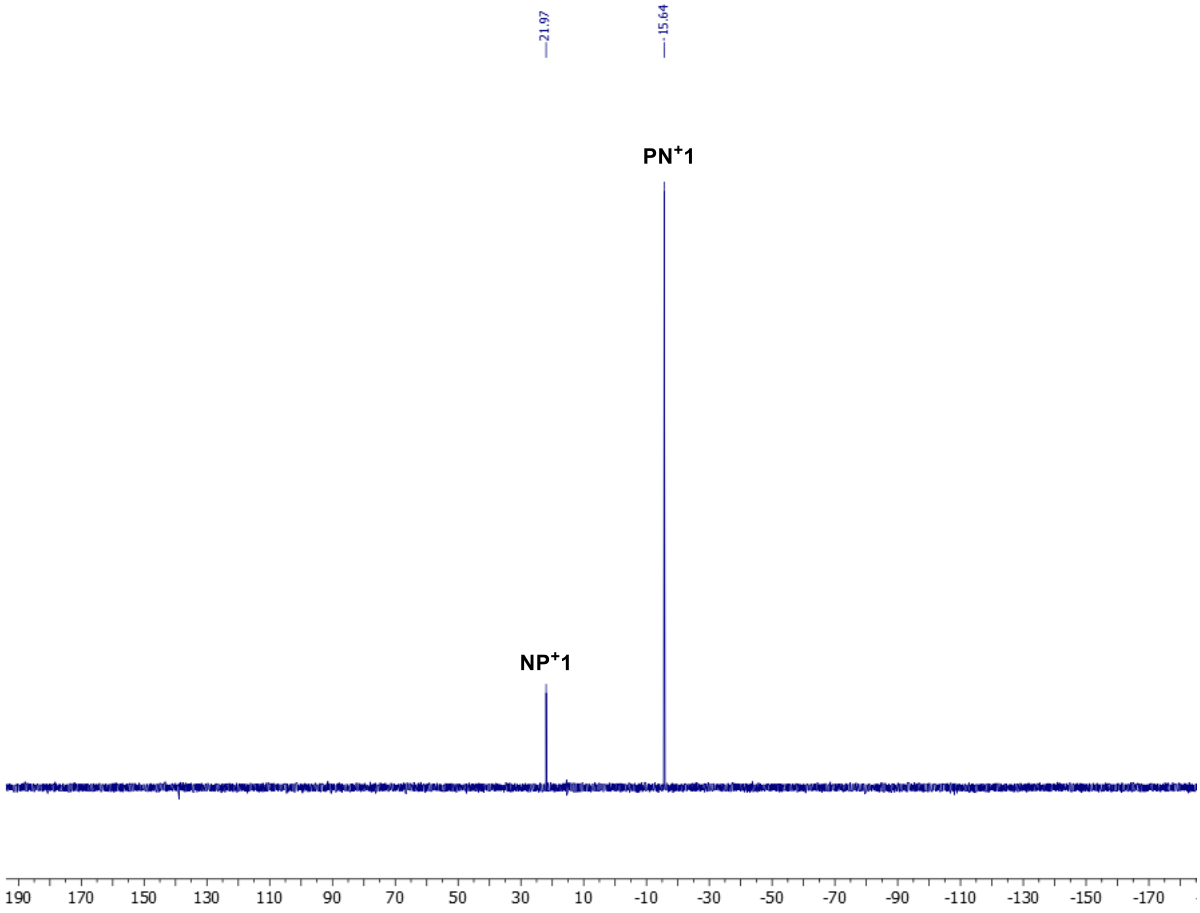
^{1}H NMR (400 MHz, $CDCl_3$) δ 8.65 (ddd, *J* = 4.5, 2.0, 1.0 Hz, 1H), 8.16 (dt, *J* = 8.0, 1.0 Hz, 1H), 7.98 (d, *J* = 9.0 Hz, 2H), 7.90 (td, *J* = 8.0, 2.0 Hz, 1H), 7.42 (ddd, *J* = 8.0, 4.5, 1.0 Hz, 1H), 6.98 (d, *J* = 9.0 Hz, 2H), 3.84 (s, 3H); **^{13}C{^{1}H} NMR** (101 MHz, $CDCl_3$) δ 164.0, 159.5, 150.5, 138.2, 131.3, 130.4, 126.8, 121.9, 114.5, 55.8; **HRMS**: m/z (EI) calculated for ($C_{12}H_{11}NO_3S$) $[M+H]^+$: 250.0532, found: 250.0532.

Data consistent with the literature.[232]

7.3.3.2. Ammonium-based ligand PN$^+$1

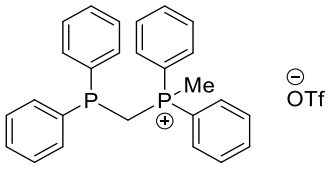


Synthesis and characterisation of Ligand **PN$^+$1** can be found in a paper from Ooi and co-workers.[161] In our hands formation of product **NP+1** occurred, showing a resonance peak at 21.97 ppm in $^{31}P\{^{1}H\}$ spectrum:



7.3.3.3. Methylation of Bis-Phosphine Ligands

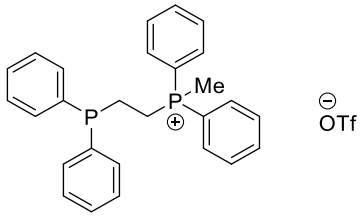
((Diphenylphosphaneyl)methyl)(methyl)diphenylphosphonium trifluoromethanesulfonate $PP^{+}1$



A solution of 1,2-bis(diphenylphosphino)methane (54 mg, 0.14 mmol, 1.0 equiv.) and methyl triflate (15 µL, 0.13 mmol, 0.95 equiv.) in CH_2Cl_2 (1.0 mL) was stirred at room temperature under a nitrogen atmosphere for 1 hour. After removal of all volatiles under reduced pressure, the resulting residue was triturated and rinsed with Et_2O, giving the title compound as a white solid.

mp 150–152 °C (from CH_2Cl_2); **IR** (thin film, cm^{-1}) 2917, 1588, 1484, 1438, 1257, 1224, 1152, 1119, 1030, 999, 901, 815, 743, 690, 637; **^{1}H NMR** (400 MHz, CD_3OD) δ 7.82 – 7.69 (m, 6H), 7.61 – 7.52 (m, 4H), 7.50 – 7.41 (m, 4H), 7.36 – 7.24 (m, 6H), 3.91 (dd, *J* = 15.5, 1.0 Hz, 2H), 2.54 (dd, *J* = 14.0, 1.0 Hz, 3H); **^{13}C{^{1}H} NMR** (101 MHz, CD_3OD) δ 136.7 (dd, *J* = 12.0, 8.5 Hz), 135.8 (d, *J* = 3.0 Hz), 134.1 (d, *J* = 22.0 Hz), 133.5 (dd, *J* = 10.5, 1.5 Hz), 131.0, 131.0 (d, *J* = 13.0 Hz), 130.0 (d, *J* = 8.0 Hz), 121.6 (dd, *J* = 87.0, 2.0 Hz), 22.2 (dd, *J* = 52.5, 35.0 Hz), 8.0 (dd, *J* = 58.5, 7.5 Hz); **^{31}P{^{1}H} NMR** (162 MHz, CD_3OD) δ 25.33 (d, *J* = 46.5 Hz), -12.66 (d, *J* = 46.5 Hz); **^{19}F{^{1}H} NMR** (377 MHz, CD_3OD) δ -79.96; **HRMS**: m/z (EI) calculated for ($C_{27}H_{25}F_3O_3P_2S$) $[M–OTf]^+$: 399.1426, found: 399.1424.

(2-(Diphenylphosphaneyl)ethyl)(methyl)diphenylphosphonium trifluoromethanesulfonate PP$^+$2

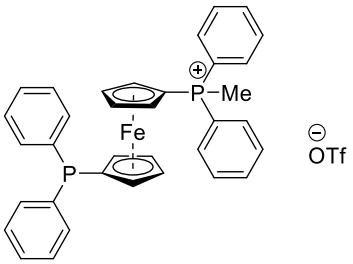


A solution of 1,2-bis(diphenylphosphino)ethane (50 mg, 0.13 mmol, 1.0 equiv.) and methyl triflate (14 µL, 0.12 mmol, 0.95 equiv.) in THF (1.0 mL) was stirred at room temperature under a nitrogen atmosphere for 1 hour. After removal of all volatiles under reduced pressure, the resulting residue was triturated and rinsed with Et_2O, giving the title compound as a white solid.

mp 55–60 °C (from CH_2Cl_2); **IR** (thin film, cm^{-1}) 2915, 1588, 1483, 1438, 1258, 1224, 1153, 1119, 1030, 999, 903, 744, 722, 691, 637; **^{1}H NMR** (400 MHz, CD_3OD) δ 7.82 (tt, *J* = 7.0, 2.0 Hz, 2H), 7.78 – 7.59 (m, 8H), 7.42 – 7.31 (m, 10H), 3.02 – 2.87 (m, 2H), 2.61 (d, *J* = 14.0 Hz, 3H), 2.33 – 2.14 (m, 2H); **^{13}C{^{1}H} NMR** (101 MHz, CD_3OD) δ 137.9 (d, *J* = 13.5 Hz), 136.0 (d, *J* = 3.0 Hz), 133.8 (d, *J* = 19.5 Hz), 133.5 (d, *J* = 10.0 Hz), 131.3 (d, *J* = 12.5 Hz), 130.5, 130.0 (d, *J* = 7.0 Hz), 120.8 (d, *J* = 85.5 Hz), 21.0 – 20.1 (m), 6.15 (d, *J* = 56.0 Hz); **^{31}P{^{1}H}**

NMR (162 MHz, CD_3OD) δ 22.74 (d, *J* = 63.0 Hz), -28.29 (d, *J* = 63.0 Hz). **$^{19}F\{^1H\}$** NMR (377 MHz, CD_3OD) δ -80.00; **HRMS**: m/z (EI) calculated for ($C_{28}H_{27}F_3O_3P_2S$) $[M–OTf]^+$: 413.1583, found: 413.1583.

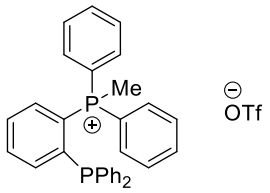
(1'-(Diphenylphosphaneyl)ferrocenyl)(methyl)diphenylphosphonium trifluoromethanesulfonate PP$^+$3



A solution of 1,1′-ferrocenediyl-bis(diphenylphosphine) (50 mg, 0.090 mmol, 1.0 equiv.) and methyl triflate (10.0 µL, 0.088 mmol, 0.95 equiv.) in THF (1.0 mL) was stirred at room temperature under a nitrogen atmosphere for 1 hour. After removal of all volatiles under reduced pressure, the resulting residue was triturated and rinsed with Et_2O, giving the title compound as an orange solid.

mp 75–80 °C (from CH_2Cl_2); **IR** (thin film, cm^{-1}) 3060, 2361, 1482, 1438, 1259, 1224, 1196, 1153, 1117, 1071, 1030, 998, 896, 842, 747, 823, 694, 637; **^{1}H NMR** (400 MHz, CD_3OD) δ 7.87 – 7.79 (m, 2H), 7.76 – 7.64 (m, 8H), 7.40 – 7.23 (m, 10H), 4.72 (q, *J* = 2.0 Hz, 2H), 4.60 (q, *J* = 2.0 Hz, 2H), 4.46 (t, *J* = 2.0 Hz, 2H), 4.18 (q, *J* = 2.0 Hz, 2H), 2.83 (d, *J* = 14.0 Hz, 3H); **$^{13}C\{^1H\}$ NMR** (101 MHz, CD_3OD) δ 139.2 (d, *J* = 9.5 Hz), 135.9 (d, *J* = 3.0 Hz), 134.5 (d, *J* = 20.0 Hz), 133.6 (d, *J* = 11.0 Hz), 131.1 (d, *J* = 13.0 Hz), 130.2, 129.5 (d, *J* = 7.0 Hz), 123.2 (d, *J* = 91.0 Hz), 81.6 (d, *J* = 11.5 Hz), 77.0 (d, *J* = 11.0 Hz), 76.2 (d, *J* = 14.0 Hz), 74.9 (d, *J* = 13.0 Hz), 74.3 (d, *J* = 3.5 Hz), 8.6 (dd, *J* = 61.0, 2.0 Hz); **$^{31}P\{^1H\}$ NMR** (162 MHz, CD_3OD) δ 23.29, -19.20; **$^{19}F\{^1H\}$ NMR** (377 MHz, CD_3OD) δ -80.00; **HRMS**: m/z (EI) calculated for ($C_{36}H_{31}F_3FeO_3P_2S$) $[M–OTf]^+$: 569.1245, found: 569.1248.

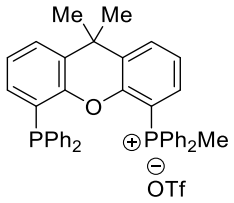
(2-(Diphenylphosphaneyl)phenyl)(methyl)diphenylphosphonium trifluoromethanesulfonate PP^{+}4



A solution of 1,2-bis(diphenylphosphino)benzene (100 mg, 0.22 mmol, 1.0 equiv.) and methyl triflate (24 µL, 0.21 mmol, 0.95 equiv.) in THF (1.0 mL) was stirred at room temperature under a nitrogen atmosphere for 1 hour. After removal of all volatiles under reduced pressure, the resulting residue was triturated and rinsed with Et_2O, giving the title compound as a white solid.

mp 160–162 °C (from CH_2Cl_2); **IR** (thin film, cm^{-1}) 2917, 1587, 1481, 1438, 1259, 1224, 1151, 1114, 1029, 998, 901, 745, 692, 637; **^{1}H NMR** (400 MHz, CD_3OD) δ 7.84 (tdd, *J* = 7.5, 2.0, 1.5 Hz, 1H), 7. 76 – 7.68 (m, 7H), 7.64 – 7.55 (m, 5H), 7.49 (dddd, *J* = 15.0, 8.0, 3.5, 1.5 Hz, 1H), 7.40 – 7.34 (m, 2H), 7.29 (ddd, *J* = 8.5, 6.5, 1.5 Hz, 4H), 7.04 – 6.95 (m, 4H), 3.27 (dd, *J* = 14.0, 1.5 Hz, 3H); **^{13}C{^{1}H} NMR** (101 MHz, CD_3OD) δ 144.2 (dd, *J* = 18.5, 12.0 Hz), 140.3 (d, *J* = 11.5 Hz), 137.6 (dd, *J* = 13.0, 9.5 Hz), 136.1 (d, *J* = 3.0 Hz), 135.8 (d, *J* = 3.0 Hz), 135.2 (d, *J* = 6.5 Hz), 134.3 (d, *J* = 19.0 Hz), 134.2 (d, *J* = 2.0 Hz), 132.1 (d, *J* = 13.0 Hz), 131.2 (d, *J* = 13.0 Hz), 130.6, 130.0 (d, *J* = 7.0 Hz), 128.1 (dd, *J* = 89.5, 35.5 Hz), 122.0 (dd, *J* = 89.5, 2.5 Hz), 12.4 (dd, *J* = 59.0, 20.0 Hz); **^{31}P{^{1}H} NMR** (162 MHz, CD_3OD) δ 22.48 (d, *J* = 26.0 Hz), -15.49 (d, *J* = 26.0 Hz); **^{19}F{^{1}H} NMR** (377 MHz, CD_3OD) δ -79.98; **HRMS**: m/z (EI) calculated for ($C_{32}H_{27}F_3O_3P_2S$) $[M–OTf]^+$: 461.1583, found: 461.1584.

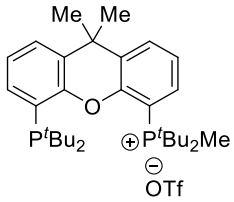
(5-(Diphenylphosphaneyl)-9,9-dimethyl-9H-xanthen-4-yl)(methyl)diphenylphosphonium trifluoromethanesulfonate PP^{+}5



A solution of Xantphos (81 mg, 0.14 mmol, 1.0 equiv.) and methyl triflate (15 µL, 0.13 mmol, 0.95 equiv.) in CH_2Cl_2 (1.0 mL) was stirred at room temperature under a nitrogen atmosphere for 1 hour. After removal of all volatiles under reduced pressure, the resulting residue was triturated and rinsed with Et_2O, giving the title compound as a white solid.

mp 70–75 °C (from CH_2Cl_2); **IR** (thin film, cm^{-1}) 3059, 1586, 1478, 1438, 1405, 1263, 1236, 1152, 1114, 1031, 905, 788, 745, 794, 637; **^{1}H NMR** (400 MHz, CD_3OD) δ 8.12 (dt, *J* = 8.0, 1.5 Hz, 1H), 7.80 (tq, *J* = 6.5, 1.5 Hz, 2H), 7.74 – 7.60 (m, 9H), 7.43 – 7.25 (m, 7H), 7.08 (t, *J* = 7.5 Hz, 1H), 6.99 – 6.93 (m, 4H), 6.82 (ddd, *J* = 15.5, 7.5, 1.5 Hz, 1H), 6.57 (ddd, *J* = 7.5, 4.0, 1.5 Hz, 1H), 2.95 (dd, *J* = 14.5, 1.5 Hz, 3H), 1.75 (s, 6H); **^{13}C{^{1}H} NMR** (101 MHz, CD_3OD) δ 154.4 (t, *J* = 2.0 Hz), 152.6 (d, *J* = 19.5 Hz), 137.3 (d, *J* = 11.5 Hz), 136.1 – 136.0 (m), 135.6 (d, *J* = 8.5 Hz), 134.7 – 134.3 (m), 134.2 (d, *J* = 6.0 Hz), 131.3 (d, *J* = 13.0 Hz), 131.1 (d, *J* = 2.5 Hz), 130.1, 129.8 (d, *J* = 6.5 Hz), 129.2, 126.3, 126.1 (d, *J* = 13.5 Hz), 125.4 (d, *J* = 18.0 Hz), 120.9 (dd, *J* = 91.0, 1.5 Hz), 107.5 (d, *J* = 89.5 Hz), 35.7 (t, *J* = 1.5 Hz), 32.6, 8.8 (dd, *J* = 57.5, 13.0 Hz); **^{31}P{^{1}H} NMR** (162 MHz, CD_3OD) δ 23.09, -21.02; **^{19}F{^{1}H} NMR** (377 MHz, CD_3OD) δ -79.88; **HRMS**: m/z (EI) calculated for ($C_{41}H_{35}F_3O_4P_2S$) $[M–OTf]^+$: 593.2158, found: 593.2158.

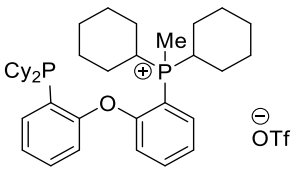
Di-tert-butyl(5-(di-tert-butylphosphaneyl)-9,9-dimethyl-9H-xanthen-4-yl)(methyl)phosphonium trifluoromethanesulfonate PP$^+$6



A solution of *t*-BuXantphos (70 mg, 0.14 mmol, 1.0 equiv.) and methyl triflate (15 µL, 0.13 mmol, 0.95 equiv.) in CH_2Cl_2 (1.0 mL) was stirred at room temperature under a nitrogen atmosphere for 1 hour. After removal of all volatiles under reduced pressure, the resulting residue was triturated and rinsed with Et_2O, giving the title compound as a white solid.

mp 105–110 °C (from CH_2Cl_2); **IR** (thin film, cm^{-1}) 2977, 1599, 1473, 1396, 1365, 1264, 1223, 1149, 1031, 905, 868, 796, 752, 737; **^{1}H NMR** (400 MHz, CD_3OD) δ 8.02 (d, *J* = 8.0 Hz, 1H), 7.94 (dd, *J* = 12.0, 8.0 Hz, 1H), 7.78 (d, *J* = 7.5 Hz, 1H), 7.67 (d, *J* = 7.5 Hz, 1H), 7.47 (td, *J* = 8.0, 2.0 Hz, 1H), 7.29 (t, *J* = 7.5 Hz, 1H), 3.25 (dd, *J* = 13.0, 6.5 Hz, 3H), 1.64 (s, 6H), 1.58 (d, *J* = 16.0 Hz, 18H), 1.24 (d, *J* = 12.0 Hz, 18H); **^{13}C{^{1}H} NMR** (101 MHz, CD_3OD) δ 156.7, 155.9 (d, *J* = 21.0 Hz), 136.7 – 135.9 (m), 135.3 (d, *J* = 5.5 Hz), 134.6 (d, *J* = 6.0 Hz), 133.9 (d, *J* = 2.5 Hz), 132.2 (d, *J* = 3.5 Hz), 128.5, 124.9, 124.7, 124.6 (d, *J* = 11.5 Hz), 105.8 (d, *J* = 71.0 Hz), 37.4 (d, *J* = 38.5 Hz), 36.1, 33.7 (d, *J* = 21.5 Hz), 31.3, 31.0 (d, *J* = 14.5 Hz), 28.2, 5.3 (dd, *J* = 45.5, 41.0 Hz); **^{31}P{^{1}H} NMR** (162 MHz, CD_3OD) δ 44.31 (d, *J* = 4.5 Hz), 8.76 (d, *J* = 4.5 Hz); **^{19}F{^{1}H} NMR** (377 MHz, CD_3OD) δ -79.96; **HRMS**: m/z (EI) calculated for ($C_{33}H_{51}F_3O_4P_2S$) $[M–OTf]^+$: 513.3410, found: 513.3414.

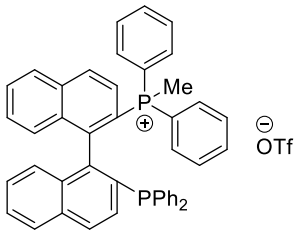
Dicyclohexyl(2-(2-(dicyclohexylphosphaneyl)phenoxy)phenyl)(methyl)phosphonium trifluoromethanesulfonate PP$^+$7



A solution of DCEphos (79 mg, 0.14 mmol, 1.0 equiv.) and methyl triflate (15 µL, 0.13 mmol, 0.95 equiv.) in CH_2Cl_2 (1.0 mL) was stirred at room temperature under a nitrogen atmosphere for 1 hour. After removal of all volatiles under reduced pressure, the resulting residue was triturated and rinsed with Et_2O, giving the title compound as a white solid.

mp 85–90 °C (from CH_2Cl_2); **IR** (thin film, cm^{-1}) 2925, 2852, 1593, 1567, 1464, 1446, 1432, 1255, 1224, 1152, 1086, 1064, 1030, 1005, 923, 874, 851, 757, 637; **^{1}H NMR** (400 MHz, CD_3OD) δ 7.80 – 7.61 (m, 3H), 7.49 (ddd, *J* = 8.5, 7.5, 1.5 Hz, 1H), 7.46 – 7.33 (m, 2H), 7.09 (ddd, *J* = 8.0, 4.0, 1.0 Hz, 1H), 7.00 (ddd, *J* = 9.0, 5.0, 1.0 Hz, 1H), 2.22 (d, *J* = 12.5 Hz, 3H), 2.15 – 0.98 (m, br. 44H); **^{13}C{^{1}H} NMR** (101 MHz, CD_3OD) δ 161.0 (d, *J* = 2.0 Hz), 159.8 (d, *J* = 19.5 Hz), 137.6 (d, *J* = 2.0 Hz), 136.3 (d, *J* = 2.5 Hz), 136.0 (d, *J* = 5.5 Hz), 132.3, 128.6 (d, *J* = 23.0 Hz), 126.7, 125.4 (d, *J* = 11.0 Hz), 119.8 (d, *J* = 2.5 Hz), 118.7 (d, *J* = 6.5 Hz), 108.3 (d, *J* = 79.5 Hz), 28.1 – 27.7 (m), 27.5, 27.2 (d, *J* = 14.0 Hz), 26.4 (d, *J* = 2.0 Hz), -1.1 (d, *J* = 53.5 Hz); **^{31}P{^{1}H} NMR** (162 MHz, CD_3OD) δ 34.90, -20.44; **^{19}F{^{1}H} NMR** (377 MHz, CD_3OD) δ -79.98; **HRMS**: m/z (EI) calculated for ($C_{38}H_{55}F_3O_4P_2S$) $[M–OTf]^+$: 577.3723, found: 577.3729.

(2'-(Diphenylphosphaneyl)-[1,1'-binaphthalen]-2-yl)(methyl)diphenylphosphonium trifluoromethanesulfonate PP$^+$8



A solution of *rac*-BINAP (87 mg, 0.14 mmol, 1.0 equiv.) and methyl triflate (15 µL, 0.13 mmol, 0.95 equiv.) in CH_2Cl_2 (1.0 mL) was stirred at room temperature under a nitrogen atmosphere for 1 hour. After removal of all volatiles under reduced pressure, the resulting residue was triturated and rinsed with Et_2O, giving the title compound as a white solid.

Mixture of mono- and bis-methylated products in 11:1 ratio as judged by ^{1}H NMR spectroscopy and integration of the C*H*$_3$-P protons. The reported data corresponds to the major mono-methylated compound. **mp** 122–127 °C (from CH_2Cl_2); **IR** (thin film, cm^{-1}) 3058, 1586, 1480, 1438, 1261, 1223, 1152, 1111, 1030, 998, 905, 821, 776, 745, 719, 698, 636; **^{1}H NMR** (400

MHz, CD_3OD) δ 8.29 (dd, *J* = 8.5, 2.5 Hz, 1H), 8.00 (d, *J* = 8.0 Hz, 1H), 7.95 (d, *J* = 8.5 Hz, 1H), 7.90 (d, *J* = 8.5 Hz, 1H), 7.82 (dd, *J* = 12.5, 9.0 Hz, 1H), 7.73 – 7.67 (m, 1H), 7.66 – 7.60 (m, 1H), 7.58 – 7.54 (m, 1H), 7.53 – 7.41 (m, 9H), 7.38 (dd, *J* = 8.5, 3.0 Hz, 1H), 7.35 – 7.24 (m, 3H), 7.23 – 7.14 (m, 2H), 7.04 (ddt, *J* = 7.5, 5.5, 1.5 Hz, 2H), 6.96 – 6.76 (m, 6H), 6.52 (d, *J* = 8.5 Hz, 1H), 2.05 (d, *J* = 13.5 Hz, 3H); **^{13}C NMR** (101 MHz, CD_3OD) δ 148.1 (t, *J* = 8.5 Hz), 141.3, 140.9 (d, *J* = 5.0 Hz), 138.5 (d, *J* = 15.0 Hz), 137.1 (d, *J* = 10.5 Hz), 136.6 (d, *J* = 2.5 Hz), 135.9 (d, *J* = 9.5 Hz), 135.9 – 135.3 (m), 134.8 (d, *J* = 3.0 Hz), 134.7, 134.5 (d, *J* = 6.5 Hz), 134.2 (d, *J* = 2.0 Hz), 134.4 – 134.0 (m), 134.1 (d, *J* = 2.0 Hz), 134.0 (d, *J* = 2.0 Hz), 131.4, 131.2 – 130.5 (m), 130.1 – 129.8 (m), 129.8 – 129.4 (m), 129.2, 128.9, 128.8 (d, *J* = 4.0 Hz), 127.0 (d, *J* = 2.5 Hz), 122.1 (d, *J* = 88.5 Hz), 121.0 (d, *J* = 88.5 Hz), 116.5 (d, *J* = 2.0 Hz), 115.6 (d, *J* = 2.5 Hz), 11.4 (dd, *J* = 57.5, 2.5 Hz); **^{19}F NMR** (377 MHz, CD_3OD) δ -79.97; **HRMS**: m/z (EI) calculated for ($C_{46}H_{35}F_3O_3P_2S$) $[M–OTf]^+$: 637.2209, found: 637.2207.

7.3.4. High Throughput Screening Data

7.3.4.1. General Procedure

Reactions were prepared by Dr Liana Allen at Vertex Boston.

The reactions were set under a nitrogen atmosphere in a glovebox.

Reactants and reagents were dispensed into 48-well plates containing 2.0 mL HPLC-sized vials in a 6x8 array, or 96-well plates containing 1.0 mL vials in a 8x12 array. https://www.analytical-sales.com/product-category/photoredox-parallel-synthesis/aluminum-reaction-blocks/

The palladium catalyst (1.0 µmol, 0.10 equiv.) and ligand (if required: 3.0 µmol, 30 mol%), were first added using a Mettler Toledo-Trajan Chronect Solid Handler (https://www.trajanscimed.com/collections/automation-systems/products/leap-powder-liquid-automation). The dispensing takes approximately 1 minute per dose. The catalyst/ligand mixture was then stirred in the reaction solvent for 30 minutes before addition of the other

reagents. This pre-stirring step was not performed when pre-ligated palladium catalysts were used. Then, caesium carbonate (9.8 mg, 30 µmol, 3.0 equiv.) and tetrabutylammonium chloride (if required: 4.2 mg, 15 µmol, 1.5 equiv.) were solid dosed in this specific order using the Chronect Solid Handler. Then, 4-bromoanisole (1.3 µL, 10 µmol, 1.0 equiv.) and sodium 4-methylbenzenesulfinate (2.7 mg, 15 µmol, 1.5 equiv.) or sodium pyridine-2-suflinate (2.5 mg, 15 µmol, 1.5 equiv.) were added manually *via* a single channel pipette using a wide-bore pipette tip made by Eppendorf in the reaction solvent at the reaction concentration (0.10 M). This step was performed manually due to the stock solutions being slurries. The vials were then sealed manually using a plate lid, and were stirred in a V&P Tumble Stirrer at 100 °C. These tumble stirrers ensure uniform heating and stirring across a rectangular plate http://vp-sci.com/products/stirrers-mixers/stirring-microplates/vertical-tumble-stirrers/vp-710p5x.html.

The experiments were not replicated.

7.3.4.2. Work-up

After 20 hours reaction time, 500µL of the reaction solvent were added to each reaction well. 40µL of these diluted solutions were taken and further diluted in 600 µL of solvent. 1 µL of each solution was injected into a UPLC-MS for analysis.

7.3.4.3. Calculation of the Reaction Yields

In the following calculations, the amount n_{inj} (µmol) of product injected in the UPLC is calculated.

After reaction, x µmol of product were formed and are in 100 µL of solvent:

$$(0 \leq x \leq 10) \text{ µmol}$$

Concentration of product is therefore equal to C_0::

$$C_0 = \frac{x\ \mu mol}{100\ \mu L}$$

After the first dilution with 500 µL of solvent, the concentration C_1 of product is equal to:

$$C_1 = \frac{x\ \mu mol}{(100 + 500)\ \mu L} = \frac{x}{600}\ \mu mol.\ \mu L^{-1}$$

40 µL of this diluted solutions were taken, therefore containing n_1 µmol of product:

$$n_1 = C_1 * V = \frac{x}{600}\ \mu mol.\ \mu L^{-1} * 40\ \mu L = 0.6667 * x\ \mu mol$$

This amount of product n_1 in 40 µL of solvent was further diluted with 600 µL of solvent, resulting in a solution of concentration C_2:

$$C_2 = \frac{n_1}{V_{total}} = \frac{0.6667 * x\ \mu mol}{(600 + 40)\ \mu L} = 0.000104 * x\ \mu mol.\ \mu L^{-1}$$

Then, V_{inj} = 1 µL of this solution of concentration C_2 was injected into the UPLC-MS, corresponding to an amount injected n_{inj}:

$$n_{inj} = C_2 * V_{inj} = 0.000104 * x\ \mu mol.\ \mu L^{-1} * 1\ \mu L = 0.000104 * x\ \mu mol$$

If the reaction had reached full conversion to product, a maximum of 10 µmol of product would have been generated: $x_{max} = 10\ \mu mol$

This corresponds to a maximum injection: $n_{inj-max} = 0.000104 * 10 = 0.00104\ \mu mol$

This value $n_{inj-max}$ was used to determine the yields of products **5-OMe** and **17-OMe** using to the calibration curves shown in the next section.

7.3.4.4. Calibration Curves

Stock solutions of known concentrations of each of the products were prepared, and 1µL; 2µL and 3µL of each of these stock solutions were injected in the UPLC-MS. Each injection was

done in triplicates. The peak area of the UV-detection at 254 nm was then plotted against the amount of product injected n_{inj} in µmol.

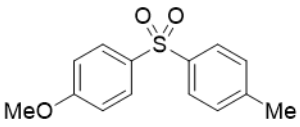
This gives the linear expression:

$$Peak\ Area\ (UV254) = \alpha * n_{inj} + \beta$$

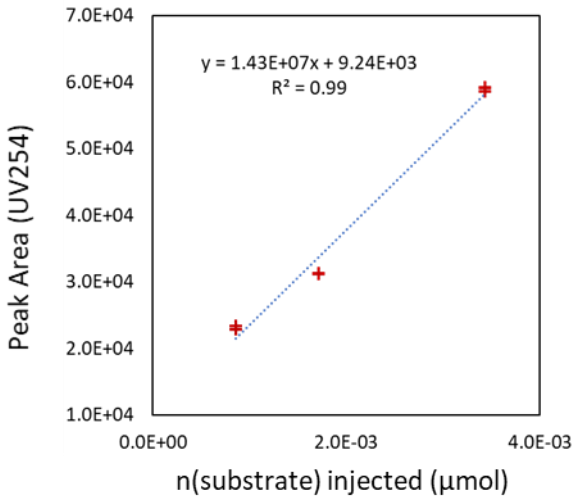
Using the value $n_{inj-max}$ gives the maximum value of $Peak\ Area\ (UV254)_{max}$ corresponding to 100% yield for each of the products. This value $Peak\ Area\ (UV254)_{max}$was employed to obtain the yield product in each screening reaction.

$$Product\ Yield = \frac{Peak\ Area\ (UV254)_{measured}}{Peak\ Area\ (UV254)_{max}}$$

1-methoxy-4-tosylbenzene 17-OMe

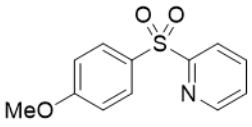


n substrate injected (µmol)	Peak Area (UV254)
8.6E-04	2.3E+04
8.6E-04	2.3E+04
8.6E-04	2.3E+04
1.7E-03	3.1E+04
1.7E-03	3.1E+04
1.7E-03	3.1E+04
3.4E-03	5.9E+04
3.4E-03	5.9E+04
3.4E-03	5.9E+04

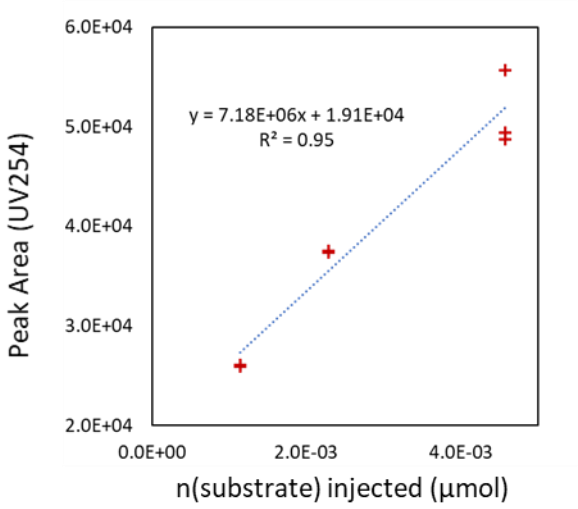


$Peak\ Area\ (UV254)_{max}$= 24112

2-((4-methoxyphenyl)sulfonyl)pyridine 17-OMe-2-pyr

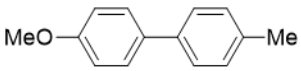


n substrate injected (µmol)	Peak Area (UV254)
1.1E-03	2.6E+04
1.1E-03	2.6E+04
1.1E-03	2.6E+04
2.3E-03	3.8E+04
2.3E-03	3.8E+04
2.3E-03	3.7E+04
4.6E-03	4.9E+04
4.6E-03	4.9E+04
4.6E-03	5.6E+04

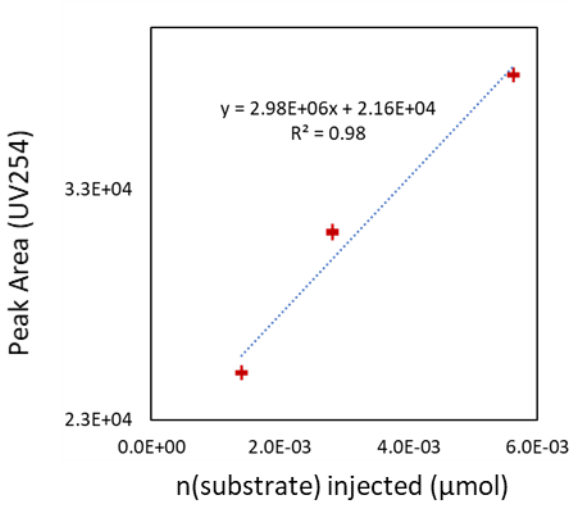


$Peak\ Area\ (UV254)_{max}$ = 26567

4-methoxy-4'-methyl-1,1'-biphenyl 5-OMe

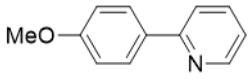


n substrate injected (µmol)	Peak Area (UV254)
1.4E-03	2.5E+04
1.4E-03	2.5E+04
1.4E-03	2.5E+04
2.8E-03	3.1E+04
2.8E-03	3.1E+04
2.8E-03	3.1E+04
5.6E-03	3.8E+04
5.6E-03	3.8E+04
5.6E-03	3.8E+04

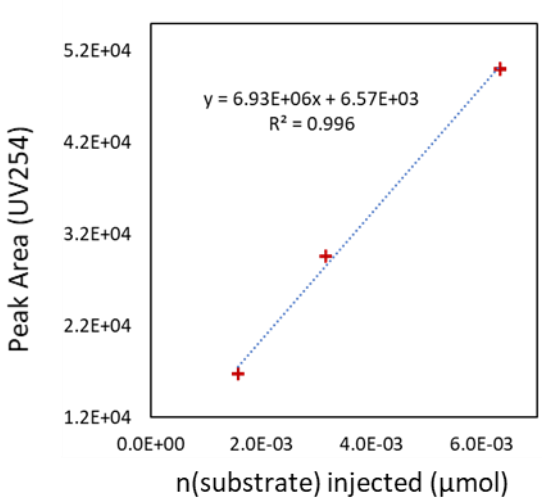


$Peak\ Area\ (UV254)_{max}$ = 24699

2-(4-methoxyphenyl)pyridine 5-OMe-2-pyr

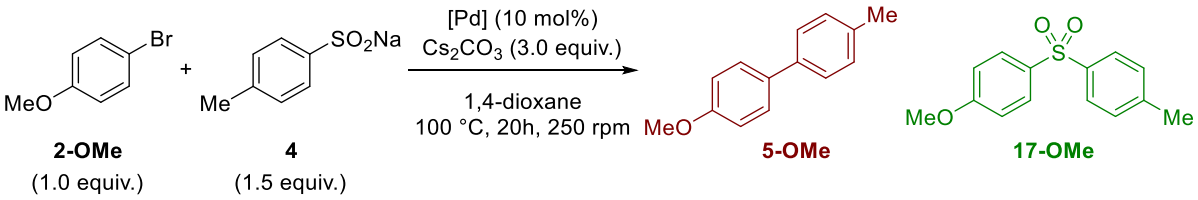


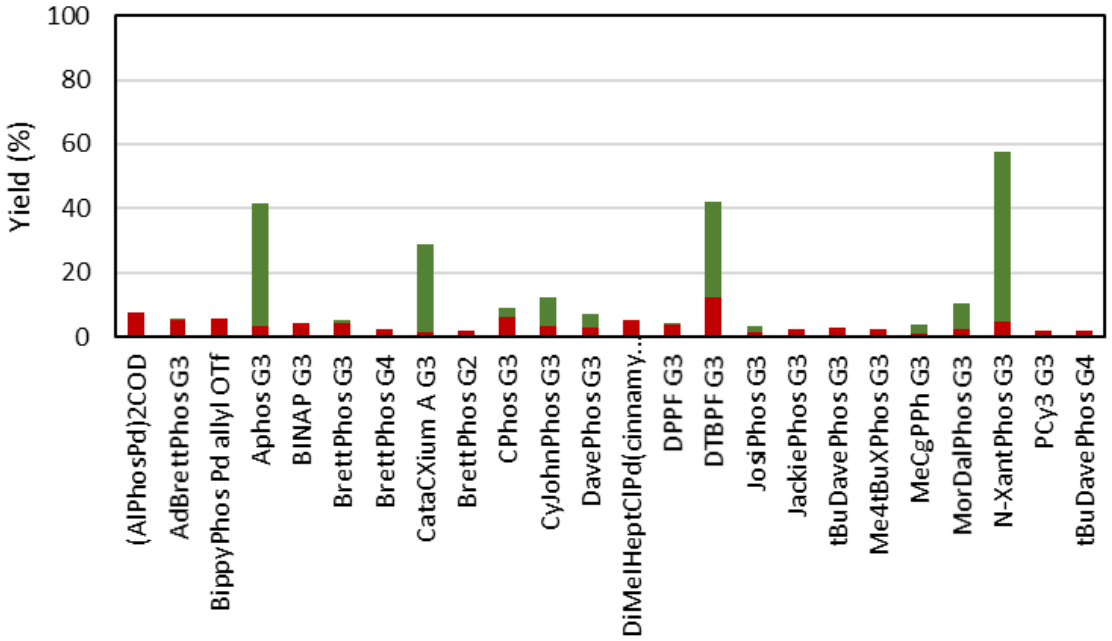
n substrate injected (µmol)	Peak Area (UV254)
1.6E-03	1.7E+04
1.6E-03	1.7E+04
1.6E-03	1.7E+04
3.2E-03	3.0E+04
3.2E-03	3.0E+04
3.2E-03	3.0E+04
6.3E-03	5.0E+04
6.3E-03	5.0E+04
6.3E-03	5.0E+04

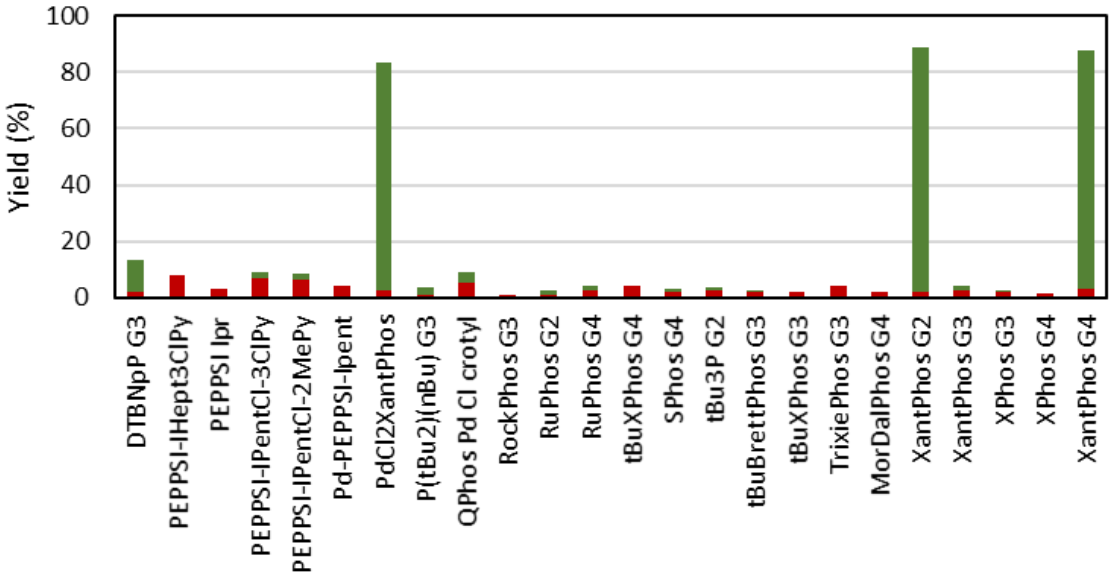


$Peak\ Area\ (UV254)_{max}$= 13777

7.3.4.5. Screening Data: HTS#1

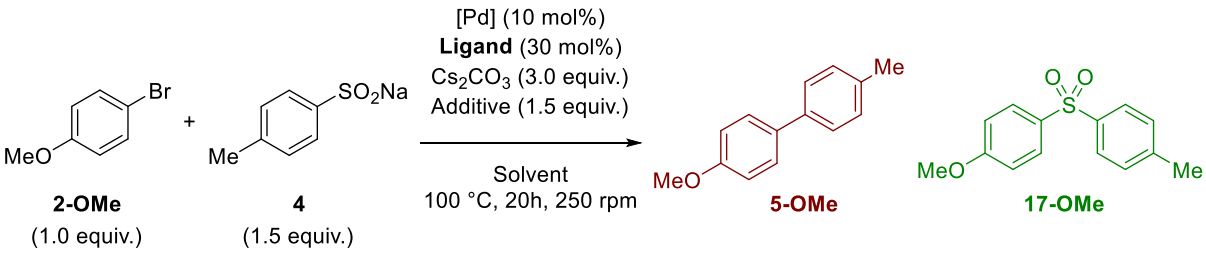






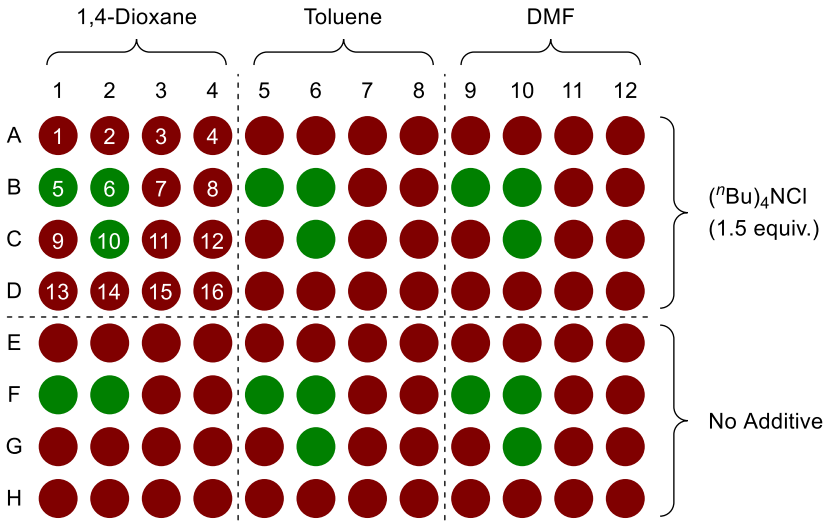
	5-OMe (%)	17-OMe (%)
(AlPhosPd)2COD	7.7	0.0
AdBrettPhos G3	5.1	0.9
BippyPhos Pd allyl OTf	5.6	0.0
Aphos G3	3.3	38.2
BINAP G3	4.2	0.0
BrettPhos G3	4.2	1.2
BrettPhos G4	2.6	0.0
CataCXium A G3	1.6	27.4
BrettPhos G2	2.1	0.0
CPhos G3	6.4	2.8
CyJohnPhos G3	3.5	8.8
DavePhos G3	3.1	4.1
DiMeIHeptClPd(cinnamyl)Cl	5.4	0.0
DPPF G3	3.6	0.8
DTBPF G3	12.2	29.7
JosiPhos G3	1.5	1.7
JackiePhos G3	2.6	0.0
tBuDavePhos G3	3.0	0.0
Me4tBuXPhos G3	2.6	0.0
MeCgPPh G3	1.1	2.5
MorDalPhos G3	2.2	8.4
N-XantPhos G3	4.8	52.6
PCy3 G3	2.1	0.0
tBuDavePhos G4	1.7	0.0
DTBNpP G3	1.8	11.4
PEPPSI-IHept3ClPy	8.0	0.0
PEPPSI Ipr	2.9	0.0
PEPPSI-IPentCl-3ClPy	6.9	2.1
PEPPSI-IPentCl-2MePy	6.6	1.7
Pd-PEPPSI-Ipent	4.3	0.0
PdCl2XantPhos	2.7	80.8
P(tBu2)(nBu) G3	1.0	2.7
QPhos Pd Cl crotyl	5.3	3.8
RockPhos G3	1.0	0.0
RuPhos G2	1.1	1.6
RuPhos G4	2.7	1.4
tBuXPhos G4	4.0	0.0
SPhos G4	1.9	1.4
tBu3P G2	2.8	0.7
tBuBrettPhos G3	2.1	0.5
tBuXPhos G3	1.8	0.0
TrixiePhos G3	4.3	0.0
MorDalPhos G4	2.0	0.0
XantPhos G2	2.3	86.6
XantPhos G3	2.4	1.9
XPhos G3	2.3	0.2
XPhos G4	1.8	0.0
XantPhos G4	3.2	84.4

7.3.4.6. Screening Data: HTS#2

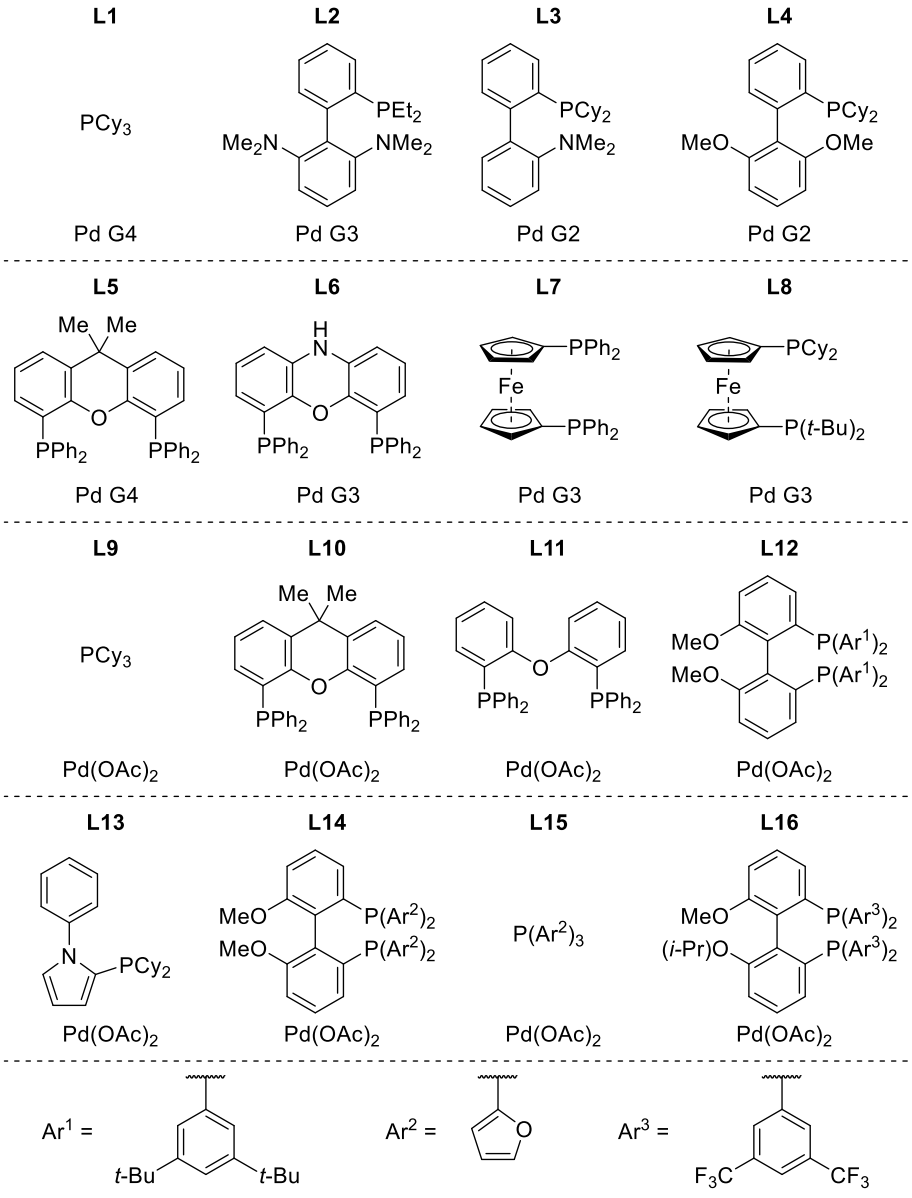


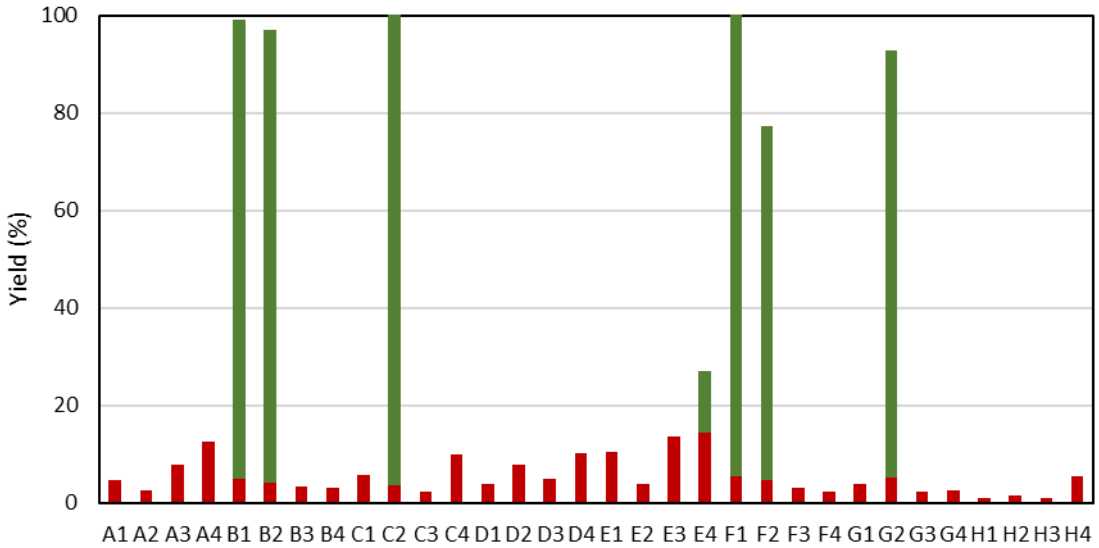
2-OMe (1.0 equiv.) + **4** (1.5 equiv.) → **5-OMe** + **17-OMe**

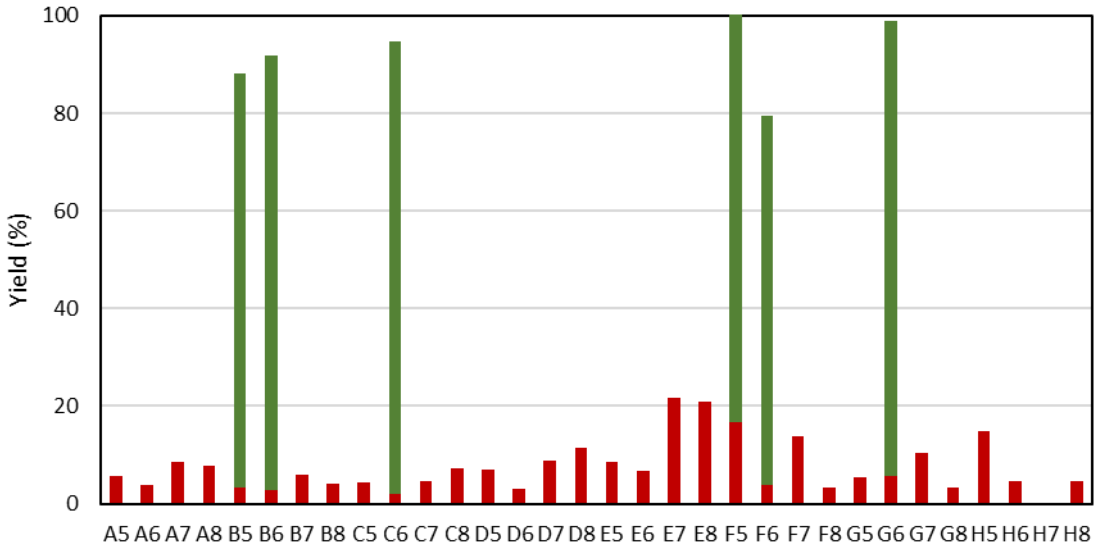
Well highlighted with the colour of the major product:

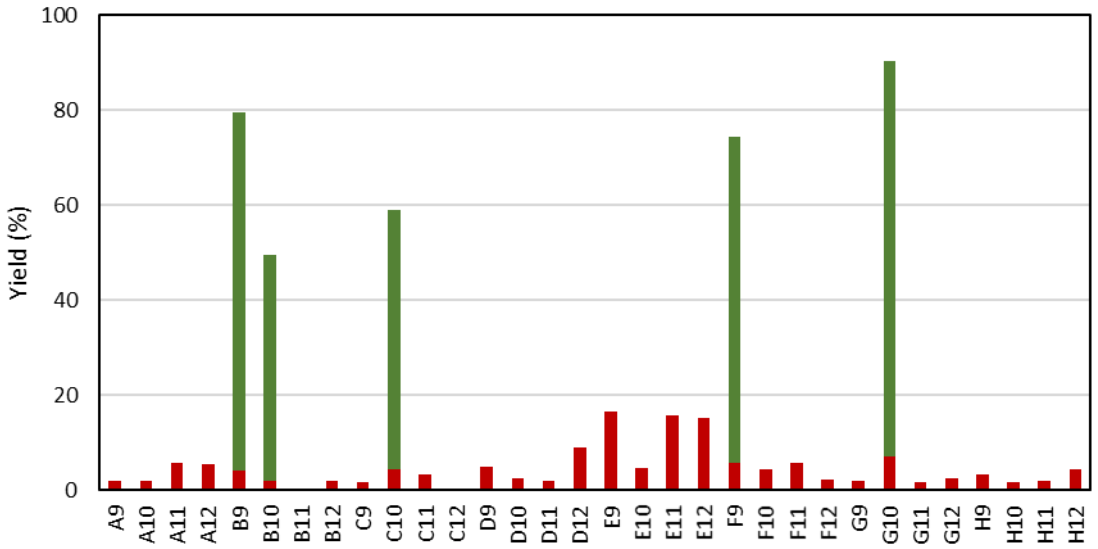


Structure of catalysts 1-16 are shown in the next figure


L1
PCy3
Pd G4
L2
PEt2
Me2N
NMe2
Pd G3
L3
PCy2
NMe2
Pd G2
L4
PCy2
MeO
OMe
Pd G2
L5
Me Me
O
PPh2
PPh2
Pd G4
L6
H
N
O
PPh2
PPh2
Pd G3
L7
PPh2
Fe
PPh2
Pd G3
L8
PCy2
Fe
P(t-Bu)2
Pd G3
L9
PCy3
Pd(OAc)2
L10
Me Me
O
PPh2
PPh2
Pd(OAc)2
L11
O
PPh2
PPh2
Pd(OAc)2
L12
MeO
MeO
P(Ar1)2
P(Ar1)2
Pd(OAc)2
L13
N
PCy2
Pd(OAc)2
L14
MeO
MeO
P(Ar2)2
P(Ar2)2
Pd(OAc)2
L15
P(Ar2)3
Pd(OAc)2
L16
MeO
(i-Pr)O
P(Ar3)2
P(Ar3)2
Pd(OAc)2
Ar1 =
t-Bu
t-Bu
Ar2 =
O
Ar3 =
F3C
CF3

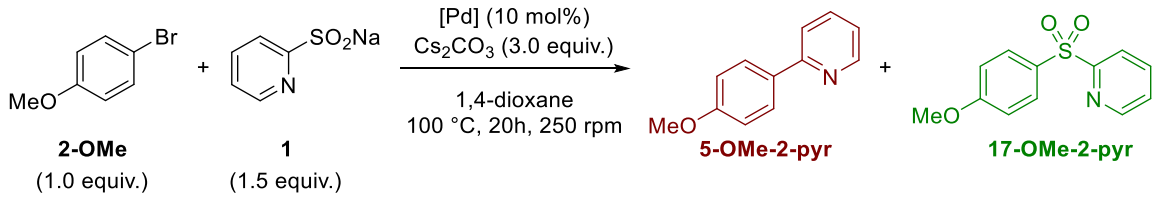

Yield (%)
100
80
60
40
20
0
A1 A2 A3 A4 B1 B2 B3 B4 C1 C2 C3 C4 D1 D2 D3 D4 E1 E2 E3 E4 F1 F2 F3 F4 G1 G2 G3 G4 H1 H2 H3 H4

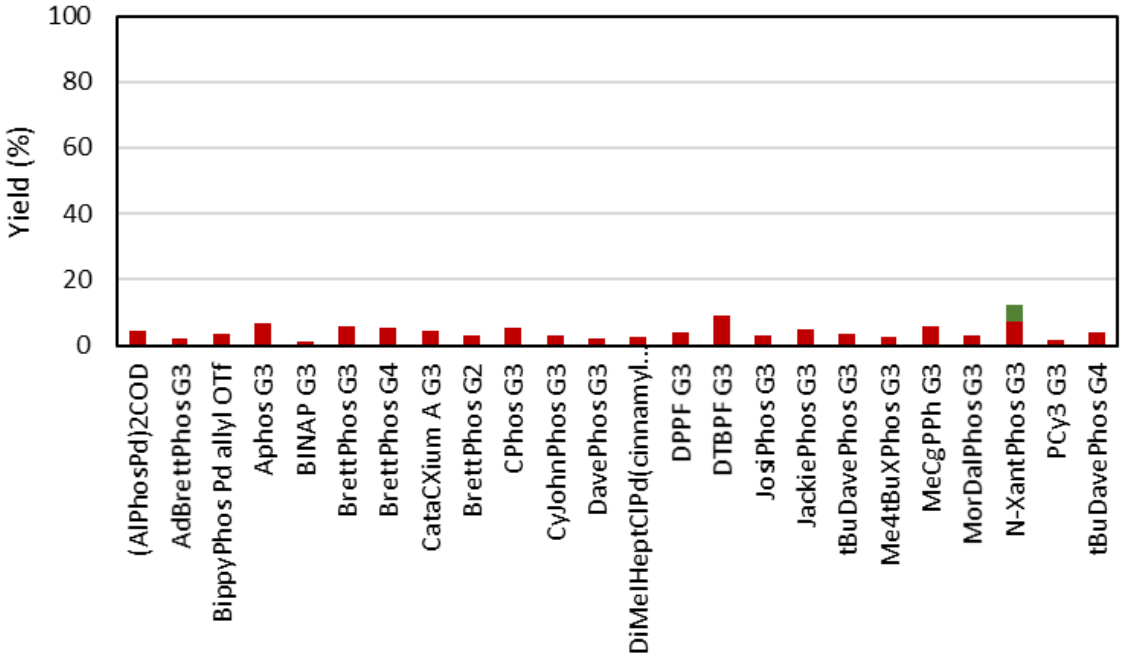

Yield (%)
100
80
60
40
20
0
A5 A6 A7 A8 B5 B6 B7 B8 C5 C6 C7 C8 D5 D6 D7 D8 E5 E6 E7 E8 F5 F6 F7 F8 G5 G6 G7 G8 H5 H6 H7 H8

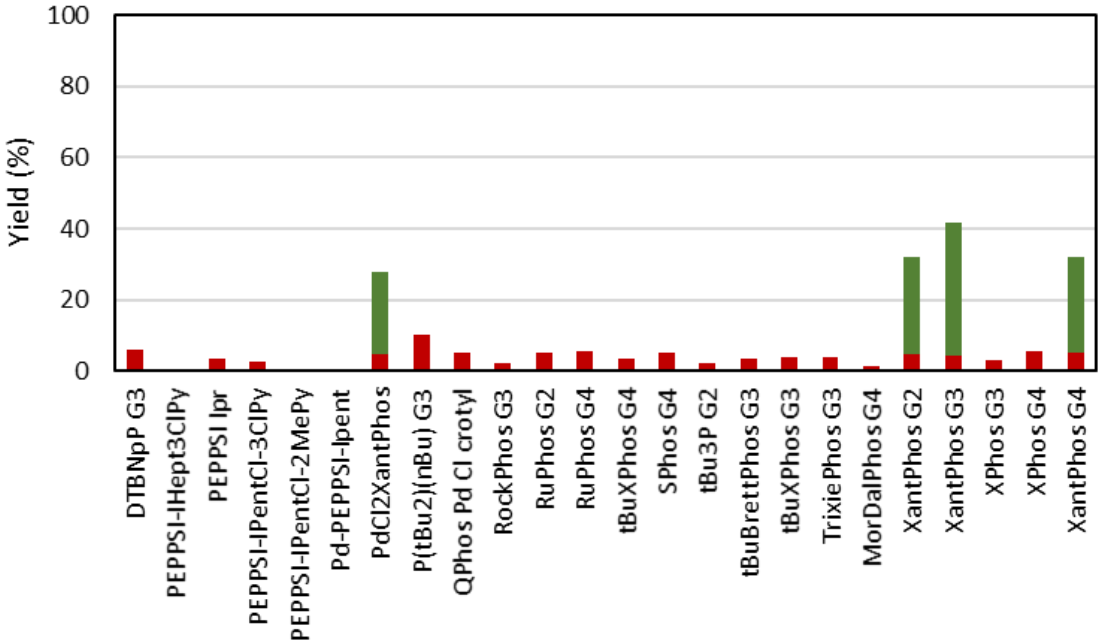

Yield (%)
100
80
60
40
20
0
A9 A10 A11 A12 B9 B10 B11 B12 C9 C10 C11 C12 D9 D10 D11 D12 E9 E10 E11 E12 F9 F10 F11 F12 G9 G10 G11 G12 H9 H10 H11 H12

	1,4-dioxane	1,4-dioxane		toluene	toluene		DMF	DMF
Well	**5-OMe** (%)	**17-OMe** (%)	Well	**5-OMe** (%)	**17-OMe** (%)	Well	**5-OMe** (%)	**17-OMe** (%)
A1	4.7	0.0	A5	5.8	0.0	A9	2.1	0.0
A2	2.7	0.0	A6	3.9	0.0	A10	2.0	0.0
A3	7.8	0.0	A7	8.6	0.0	A11	5.8	0.0
A4	12.5	0.0	A8	7.8	0.0	A12	5.5	0.0
B1	5.1	94.1	B5	3.2	84.9	B9	4.2	75.4
B2	4.0	92.9	B6	2.9	89.0	B10	1.9	47.6
B3	3.4	0.0	B7	6.0	0.0	B11	0.0	0.0
B4	3.1	0.0	B8	4.0	0.0	B12	1.8	0.0
C1	5.8	0.0	C5	4.3	0.0	C9	1.5	0.0
C2	3.6	97.9	C6	2.1	92.6	C10	4.5	54.6
C3	2.3	0.0	C7	4.6	0.0	C11	3.4	0.0
C4	9.9	0.0	C8	7.3	0.0	C12	0.0	0.0
D1	4.0	0.0	D5	6.9	0.0	D9	5.0	0.0
D2	7.8	0.0	D6	2.9	0.0	D10	2.5	0.0
D3	4.9	0.0	D7	8.9	0.0	D11	1.9	0.0
D4	10.1	0.0	D8	11.4	0.0	D12	8.9	0.0
E1	10.6	0.0	E5	8.5	0.0	E9	16.5	0.0
E2	3.8	0.0	E6	6.7	0.0	E10	4.6	0.0
E3	13.5	0.0	E7	21.7	0.0	E11	15.7	0.0
E4	14.5	12.7	E8	21.0	0.0	E12	15.2	0.0
F1	5.4	102.0	F5	16.6	93.0	F9	5.7	68.7
F2	4.6	72.7	F6	3.8	75.7	F10	4.4	0.0
F3	3.2	0.0	F7	13.7	0.0	F11	5.7	0.0
F4	2.3	0.0	F8	3.3	0.0	F12	2.1	0.0
G1	4.0	0.0	G5	5.4	0.0	G9	1.9	0.0
G2	5.1	87.7	G6	5.6	93.5	G10	7.0	83.5
G3	2.4	0.0	G7	10.3	0.0	G11	1.6	0.0
G4	2.5	0.0	G8	3.4	0.0	G12	2.5	0.0
H1	0.9	0.0	H5	14.9	0.0	H9	3.2	0.0
H2	1.5	0.0	H6	4.7	0.0	H10	1.8	0.0
H3	1.1	0.0	H7	0.0	0.0	H11	2.1	0.0
H4	5.6	0.0	H8	4.6	0.0	H12	4.4	0.0

7.3.4.7. Screening Data: HTS#3

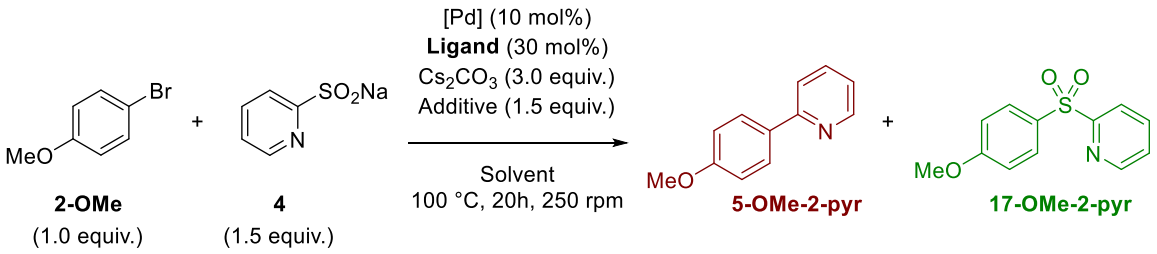




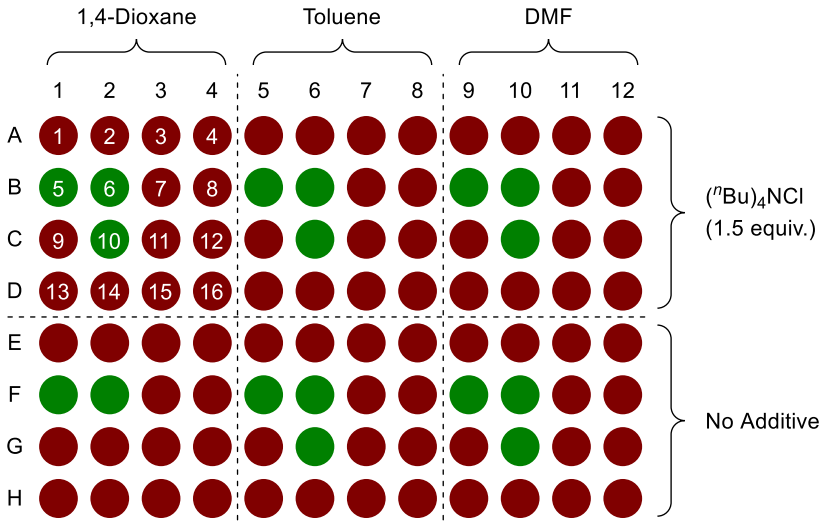


	5-OMe-2-pyr (%)	17-OMe-2-pyr (%)
(AlPhosPd)2COD	4.6	0.0
AdBrettPhos G3	2.2	0.0
BippyPhos Pd allyl OTf	3.4	0.0
Aphos G3	6.8	0.0
BINAP G3	1.2	0.0
BrettPhos G3	5.8	0.0
BrettPhos G4	5.1	0.0
CataCXium A G3	4.6	0.0
BrettPhos G2	3.2	0.0
CPhos G3	5.2	0.0
CyJohnPhos G3	3.0	0.0
DavePhos G3	2.0	0.0
DiMeIHeptClPd(cinnamyl)Cl	2.5	0.0
DPPF G3	4.0	0.0
DTBPF G3	9.3	0.0
JosiPhos G3	3.0	0.0
JackiePhos G3	4.7	0.0
tBuDavePhos G3	3.6	0.0
Me4tBuXPhos G3	2.5	0.0
MeCgPPh G3	5.9	0.0
MorDalPhos G3	3.3	0.0
N-XantPhos G3	7.3	4.8
PCy3 G3	1.7	0.0
tBuDavePhos G4	3.8	0.0
DTBNpP G3	5.8	0.0
PEPPSI-IHept3ClPy	0.0	0.0
PEPPSI Ipr	3.3	0.0
PEPPSI-IPentCl-3ClPy	2.5	0.0
PEPPSI-IPentCl-2MePy	0.0	0.0
Pd-PEPPSI-Ipent	0.0	0.0
PdCl2XantPhos	4.5	23.4
P(tBu2)(nBu) G3	10.3	0.0
QPhos Pd Cl crotyl	5.1	0.0
RockPhos G3	2.3	0.0
RuPhos G2	5.2	0.0
RuPhos G4	5.4	0.0
tBuXPhos G4	3.4	0.0
SPhos G4	5.1	0.0
tBu3P G2	2.2	0.0
tBuBrettPhos G3	3.3	0.0
tBuXPhos G3	3.9	0.0
TrixiePhos G3	3.8	0.0
MorDalPhos G4	1.3	0.0
XantPhos G2	4.5	27.4
XantPhos G3	4.4	37.4
XPhos G3	2.8	0.0
XPhos G4	5.6	0.0
XantPhos G4	5.2	26.6

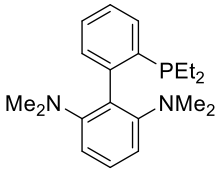
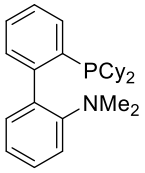
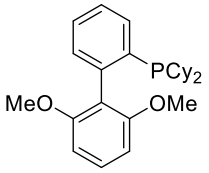
7.3.4.8. Screening Data: HTS#4

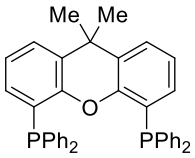
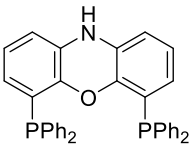
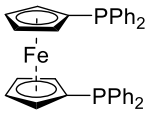
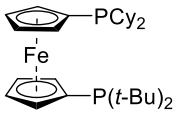


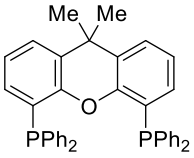
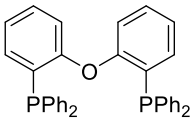
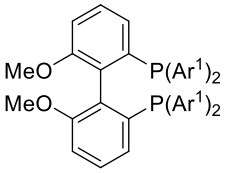
Well highlighted with the colour of the major product:

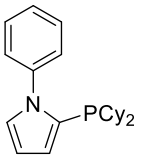
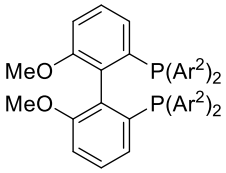
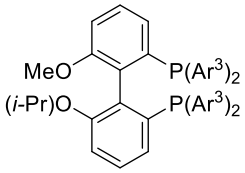


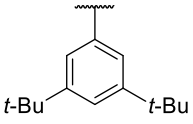
Structure of catalysts 1-16 are shown in the next figure

L1	L2	L3	L4
			
Pd G4	Pd G3	Pd G2	Pd G2

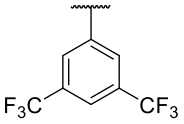
L5	L6	L7	L8
			
Pd G4	Pd G3	Pd G3	Pd G3

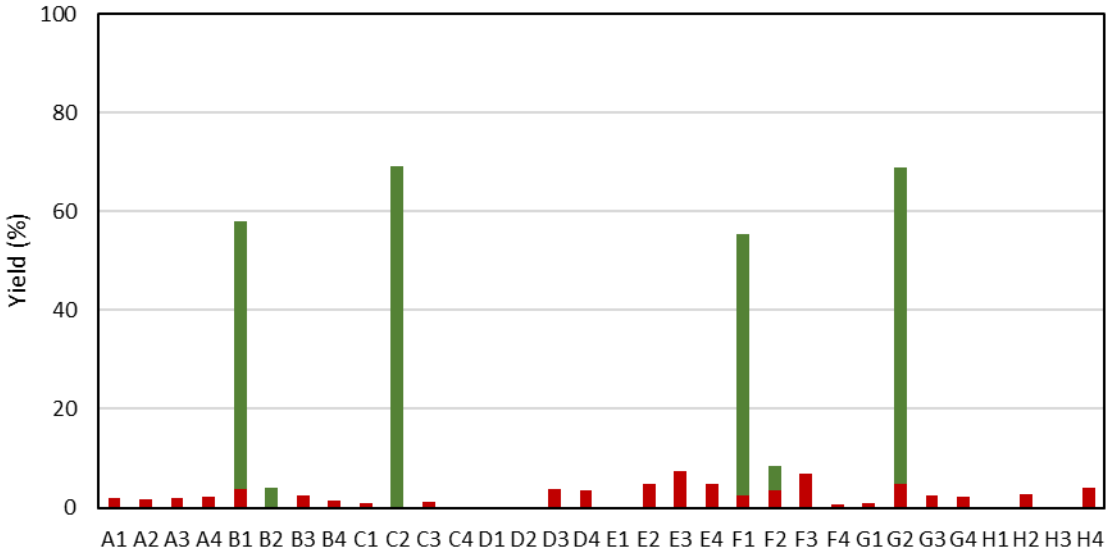
L9	L10	L11	L12
			
$Pd(OAc)_2$	$Pd(OAc)_2$	$Pd(OAc)_2$	$Pd(OAc)_2$

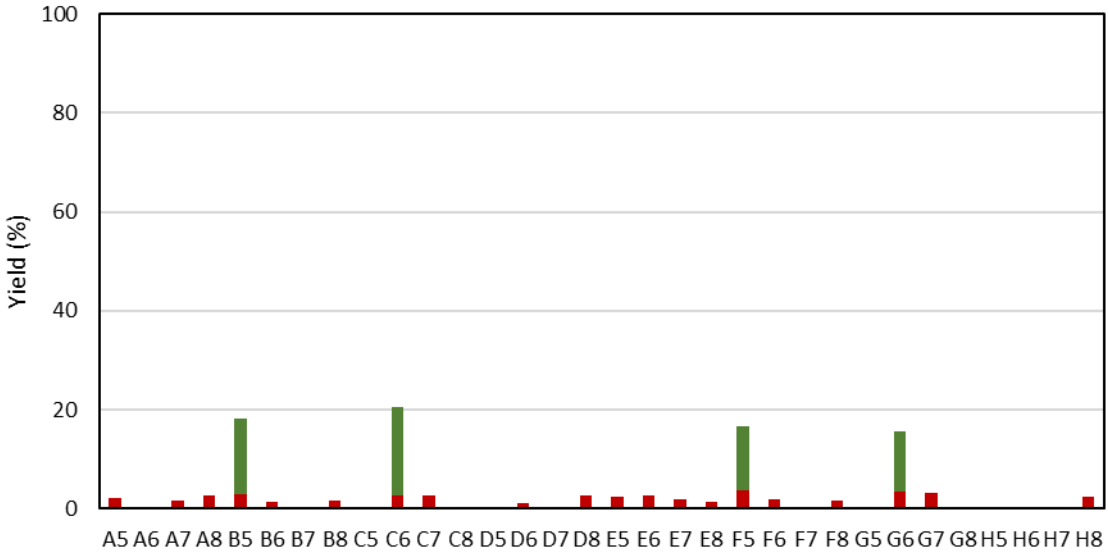
L13	L14	L15	L16
			
$Pd(OAc)_2$	$Pd(OAc)_2$	$Pd(OAc)_2$	$Pd(OAc)_2$

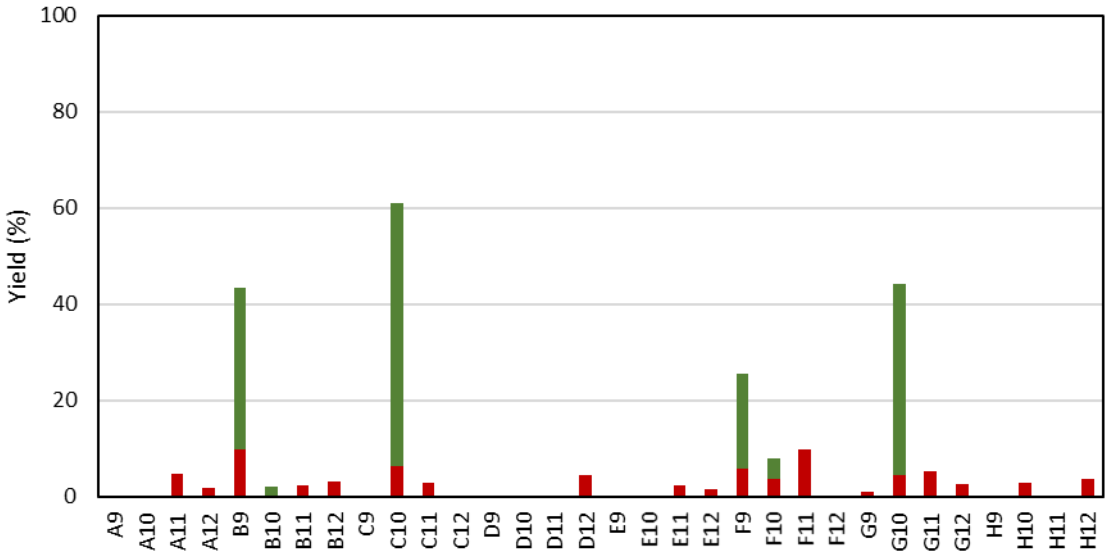
Ar^1 = 

Ar^2 = 

Ar^3 = 


100
80
60
40
20
0
Yield (%)
A1 A2 A3 A4 B1 B2 B3 B4 C1 C2 C3 C4 D1 D2 D3 D4 E1 E2 E3 E4 F1 F2 F3 F4 G1 G2 G3 G4 H1 H2 H3 H4

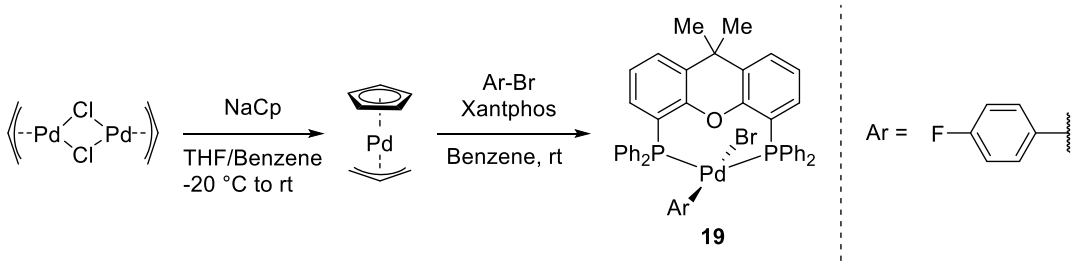

100
80
60
40
20
0
Yield (%)
A5 A6 A7 A8 B5 B6 B7 B8 C5 C6 C7 C8 D5 D6 D7 D8 E5 E6 E7 E8 F5 F6 F7 F8 G5 G6 G7 G8 H5 H6 H7 H8


100
80
60
40
20
0
Yield (%)
A9 A10 A11 A12 B9 B10 B11 B12 C9 C10 C11 C12 D9 D10 D11 D12 E9 E10 E11 E12 F9 F10 F11 F12 G9 G10 G11 G12 H9 H10 H11 H12

	1,4-dioxane	1,4-dioxane		toluene	toluene		DMF	DMF
Well	**5-OMe** (%)	**17-OMe** (%)	Well	**5-OMe** (%)	**17-OMe** (%)	Well	**5-OMe** (%)	**17-OMe** (%)
A1	1.9	0.0	A5	2.2	0.0	A9	0.0	0.0
A2	1.7	0.0	A6	0.0	0.0	A10	0.0	0.0
A3	2.1	0.0	A7	1.6	0.0	A11	4.8	0.0
A4	2.3	0.0	A8	2.7	0.0	A12	1.8	0.0
B1	3.9	54.1	B5	3.0	15.1	B9	9.9	33.5
B2	0.0	4.1	B6	1.4	0.0	B10	0.0	2.2
B3	2.5	0.0	B7	0.0	0.0	B11	2.5	0.0
B4	1.3	0.0	B8	1.6	0.0	B12	3.1	0.0
C1	0.8	0.0	C5	0.0	0.0	C9	0.0	0.0
C2	0.0	69.2	C6	2.8	17.8	C10	6.5	54.6
C3	1.2	0.0	C7	2.7	0.0	C11	3.0	0.0
C4	0.0	0.0	C8	0.0	0.0	C12	0.0	0.0
D1	0.0	0.0	D5	0.0	0.0	D9	0.0	0.0
D2	0.0	0.0	D6	1.2	0.0	D10	0.0	0.0
D3	3.7	0.0	D7	0.0	0.0	D11	0.0	0.0
D4	3.6	0.0	D8	2.6	0.0	D12	4.4	0.0
E1	0.0	0.0	E5	2.4	0.0	E9	0.0	0.0
E2	4.8	0.0	E6	2.6	0.0	E10	0.0	0.0
E3	7.5	0.0	E7	1.9	0.0	E11	2.4	0.0
E4	4.7	0.0	E8	1.2	0.0	E12	1.6	0.0
F1	2.6	52.7	F5	3.7	13.1	F9	5.8	19.8
F2	3.6	5.0	F6	1.9	0.0	F10	3.7	4.2
F3	6.9	0.0	F7	0.0	0.0	F11	9.9	0.0
F4	0.8	0.0	F8	1.7	0.0	F12	0.0	0.0
G1	0.9	0.0	G5	0.0	0.0	G9	1.1	0.0
G2	4.9	63.9	G6	3.3	12.2	G10	4.4	39.8
G3	2.5	0.0	G7	3.1	0.0	G11	5.4	0.0
G4	2.2	0.0	G8	0.0	0.0	G12	2.7	0.0
H1	0.0	0.0	H5	0.0	0.0	H9	0.0	0.0
H2	2.7	0.0	H6	0.0	0.0	H10	3.0	0.0
H3	0.0	0.0	H7	0.0	0.0	H11	0.0	0.0
H4	4.0	0.0	H8	2.3	0.0	H12	3.8	0.0

7.4. Experimental Data and Procedures for Chapter 4

7.4.1. Oxidative Addition Complex 19

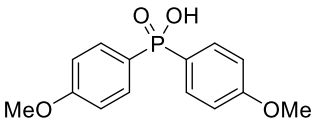


Allyl(cyclopentadienyl)palladium was synthesised from allyl palladium chloride dimer according to literature procedure.[233]

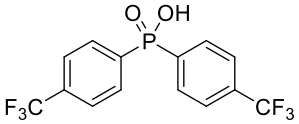
Allyl(cyclopentadienyl)palladium (500 mg, 2.35 mmol, 1.0 equiv.) and Xantphos (1.50 g, 2.64 mmol, 1.1 equiv.) were added to a round-bottom flask equipped with a stirrer bar. The flask was sealed with a septum, evacuated (< 0.1 mbar) and back-filled with argon twice, then benzene (20 mL) was added. The reaction was stirred at room temperature under argon atmosphere for 18 hours. The workup was carried out under air. The reaction mixture was filtered through a sintered funnel, and the obtained solid was triturated and rinsed with pentane (50 mL) then cold Et_2O (50 mL) before drying under high vacuum to give the title compound title compound as a yellow solid in 97% yield (1.96 g, 2.28 mmol).

mp (decomp.) 202-207 °C (from Et_2O); **IR** (thin film, cm^{-1}) 2161, 2020, 1474, 1433, 1398, 1212, 1151, 1094, 871, 820, 801, 790, 744, 696 ; **^{1}H NMR** (400 MHz, $CDCl_3$) δ 7.62 (dd, *J* = 7.0, 2.0 Hz, 2H), 7.41 – 7.30 (m, br. 7H), 7.29 – 7.22 (m, 5H), 7.19 – 7.08 (m, 12H), 6.44 (s, br. 2H), 5.91 (app. t, *J* = 9.0 Hz, 2H), 1.79 (s, 6H); **^{13}C{^{1}H} NMR** (101 MHz, CD_2Cl_2) δ 156.3, 150.1, 135.9 – 135.6 (m), 135.5 – 135.3 (m), 132.3, 132.1, 131.9, 131.7, 130.3, 128.4 (app. t, *J* = 5.0 Hz), 127.8, 124.8 (app. t, *J* = 3.5 Hz), 122.9 – 122.3 (m), 113.7, 113.5, 36.8, 28.6; **^{31}P{^{1}H} NMR** (162 MHz, $CDCl_3$) δ 8.54 (d, *J* = 4.0 Hz); **^{19}F NMR** (376 MHz, $CDCl_3$) δ -126.12 (tt, *J* = 12.0, 4.0 Hz).

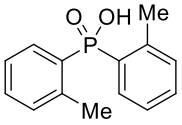
7.4.2. Literature Procedures for the Synthesis of Phosphinic Acids



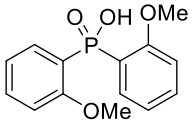
bis(4-methoxyphenyl)phosphinic acid



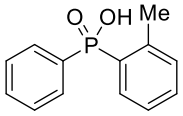
bis(4-(trifluoromethyl)phenyl)phosphinic acid



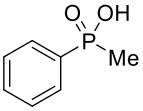
di-*o*-tolylphosphinic acid



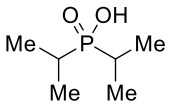
bis(2-methoxyphenyl)phosphinic acid



phenyl(*o*-tolyl)phosphinic acid



methyl(phenyl)phosphinic acid



diisopropylphosphinic acid

Bis(4-methoxyphenyl)phosphinic acid was purchased from Sigma Aldrich.

Bis(4-(trifluoromethyl)phenyl)phosphinic acid.[234]

Di-*o*-tolylphosphinic acid.[235]

Bis(2-methoxyphenyl)phosphinic acid.[236]

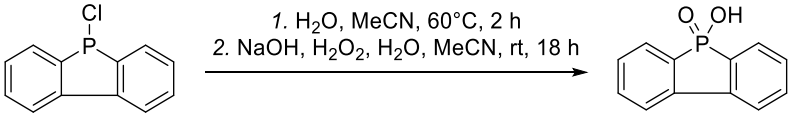
Phenyl(*o*-tolyl)phosphinic acid.[237]

Methyl(phenyl)phosphinic acid.[238]

Diisopropylphosphinic acid.[239]

7.4.3. Novel Phosphinic Acids

5-Hydroxybenzo[*b*]phosphindole 5-oxide

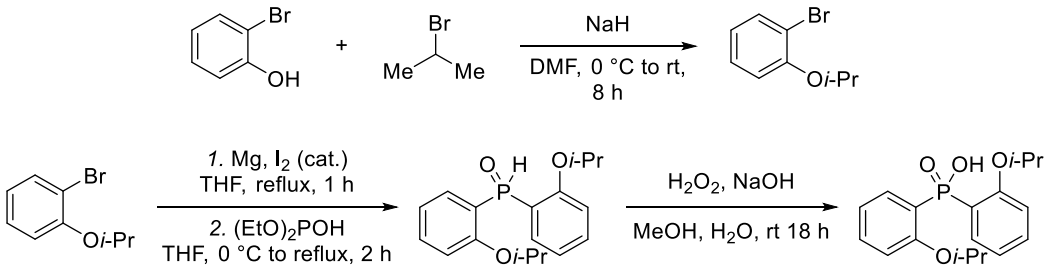


5-Chlorobenzo[*b*]phosphindole was purchased from Sigma Aldrich. The chlorophosphine (225 mg, 1.03 mmol, 1.0 equiv.) was dissolved in MeCN (5 mL) and H_2O (2 mL) and heated

to 60 °C for two hours. The reaction mixture was cooled to room temperature, then H_2O (10 mL), NaOH (1.03 g, 25.7 mmol, 25 equiv.) and H_2O_2 (30% w/w in H_2O, 530 µL, mmol, 5.0 equiv.) were added, and the mixture was stirred at room temperature for 18 hours. The reaction mixture was concentrated, the resulting solid was triturated and thoroughly washed with H_2O, then dried under high vacuum, giving title compound as a white solid in 57% yield over two steps (127 mg, 0.6 mmol).

mp 237-242 °C (from H_2O); **IR** (thin film, cm^{-1}) 3060, 2359, 1602, 1472, 1441, 1285, 1168, 1140, 1073, 964, 864, 748, 717, 695, 620; **^{1}H NMR** (400 MHz, $CDCl_3$) δ 7.92 (dd, *J* = 11.0, 7.5 Hz, 2H), 7.77 (dd, *J* = 8.0, 3.5 Hz, 2H), 7.59 (app. t, *J* = 7.5 Hz, 2H), 7.45 (td, *J* = 7.5, 3.5 Hz, 2H), 3.77 (s, 1H); **^{13}C{^{1}H} NMR** (101 MHz, CD_3OD) δ 141.3 (d, *J* = 28.5 Hz), 134.7 (d, *J* = 2.5 Hz), 131.3 (d, *J* = 138.0 Hz), 130.5 (d, *J* = 11.5 Hz), 128.8 (d, *J* = 9.0 Hz), 122.4 (d, *J* = 12.5 Hz); **^{31}P{^{1}H} NMR** (162 MHz, CD_3OD) δ 40.11; **HRMS**: m/z (EI) calculated for ($C_{12}H_9O_2P$) $[M–H]^–$: 215.0267, found: 215.0258.

Bis(2-isopropoxyphenyl)phosphinic acid



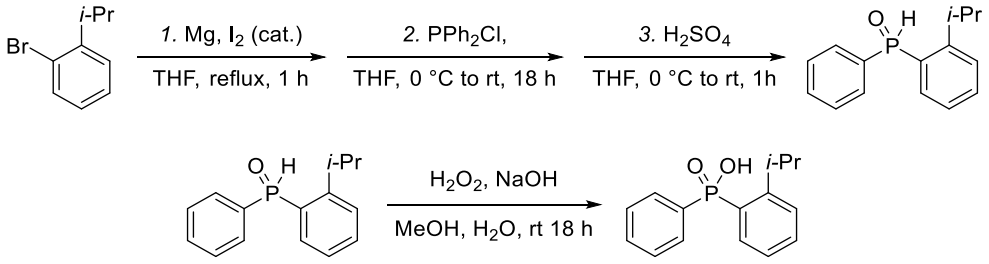
1-Bromo-2-isopropoxybenzene was synthesised according to literature procedure.[240]

Magnesium turnings (452 mg, 18.6 mmol, 3.3 equiv.) and I_2 (5 – 10 mg) were added to a two-neck round-bottom flask with a stirrer bar and a condenser. The flask was sealed with a septum, evacuated (< 0.1 mbar) and back-filled with argon twice, then a solution of 1-bromo-2-isopropoxybenzene (4.00 g, 18.6 mmol, 3.3 equiv.) in THF (20 mL) was slowly added. The resulted mixture was heated to reflux for 1 hour, then cooled to 0 °C. A solution of diethyl

phosphite (720 µL, 5.6 mmol, 1.0 equiv.) in THF (10 mL) was slowly added and the resulting mixture was heated to reflux for 2 hours. The reaction mixture was cooled to 0 °C, and brine was added followed by conc. HCl until pH = 1 was reached. The two phases were separated and the aqueous layer was extracted with EtOAc (3 ×100 mL). The combined organic extracts were dried with anhydrous $MgSO_4$, filtered and concentrated under reduced pressure. The crude product was dissolved in MeOH (75 mL) and H_2O (75 mL), then NaOH (5.60 g, 140 mmol, 25 equiv.) and H_2O_2 (30% w/w in H_2O, 2.9 mL, 28.1 mmol, 5.0 equiv.) were added. The resulting mixture was stirred for 18 hours at room temperature then concentrated under reduced pressure. The residue was dissolved in H_2O (100 mL), and conc. HCl was added at 0 °C until formation of a yellow precipitate. The solution was filtered through a sintered funnel, and the precipitate was thoroughly washed with H_2O, then dried under high vacuum for 18 hours giving the title compound as a yellow solid in 53% yield over two steps (988 mg, 3.0 mmol).

mp 173–178 °C (from H_2O); **IR** (thin film, cm^{-1})1590, 1473, 1443, 1374, 1278, 1243, 1173, 1140, 1113, 1082, 1043, 950, 869, 791, 756, 716, 609; **^{1}H NMR** (400 MHz, $CDCl_3$) δ 10.59 (s, 1H), 8.02 (ddd, *J* = 14.0, 7.5, 2.0 Hz, 2H), 7.34 (tdd, *J* = 8.0, 2.0, 1.0 Hz, 2H), 6.92 (tdd, *J* = 7.5, 2.5, 1.0 Hz, 2H), 6.71 (dd, *J* = 8.0, 6.0 Hz, 2H), 4.37 (hept, *J* = 6.0 Hz, 2H), 0.88 (d, *J* = 6.0 Hz, 12H); **^{13}C{^{1}H} NMR** (101 MHz, $CDCl_3$) δ 159.1 (d, *J* = 5.0 Hz), 134.9 (d, *J* = 6.5 Hz), 132.9 (d, *J* = 2.0 Hz), 123.1 (d, *J* = 145.0 Hz), 119.5 (d, *J* = 13.0 Hz), 112.1 (d, *J* = 8.0 Hz), 69.5, 21.3; **^{31}P{^{1}H} NMR** (162 MHz, $CDCl_3$) δ 30.57; **HRMS**: m/z (EI) calculated for ($C_{18}H_{23}O_4P$) $[M–H]^-$: 333.1261, found: 333.1258.

(2-Isopropylphenyl)(phenyl)phosphinic acid

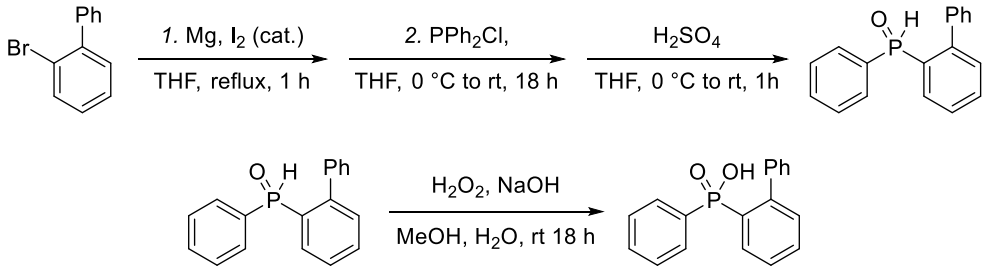


Magnesium turnings (269 mg, 11.1 mmol, 1.1 equiv.) and I_2 (5 – 10 mg) were added to a two-neck round-bottom flask equipped with a stirrer bar and a condenser. The flask was sealed with a septum, evacuated (< 0.1 mbar) and back-filled with argon twice, then a solution of 1-bromo-2-isopropylbenzene (2.00 g, 10.0 mmol, 1.0 equiv.) in THF (10 mL) was slowly added. The resulted mixture was heated to reflux for 1 hour, then cooled to 0 °C. A solution of dichlorophenylphosphine (1.4 mL, 10.3 mmol, 1.0 equiv.) in THF (10 mL) was slowly added and the resulting mixture was stirred at room temperature for 18 h. The reaction mixture was cooled to 0 °C and 100 mL of a 10% v/v solution of H_2SO_4 was added. After 10 min, the ice bath was removed and the reaction mixture was allowed to warm to room temperature. The two phases were separated and the aqueous layer was extracted with EtOAc (3 × 100 mL). The combined organic extracts were dried with anhydrous $MgSO_4$, filtered and concentrated under reduced pressure. The crude product was dissolved in MeOH (75 mL) and H_2O (75 mL), then NaOH (10.0 g, 250 mmol, 25 equiv.) and H_2O_2 (30% w/w in H_2O, 5.2 mL, 50 mmol, 5.0 equiv.) were added. The resulting mixture was stirred for 18 hours at room temperature then concentrated under reduced pressure. The residue was dissolved in H_2O (100 mL), and conc. HCl was added at 0 °C until formation of a yellow precipitate. The solution was filtered through a sintered funnel, and the precipitate was thoroughly washed with H_2O, then dried under high vacuum for 18 hours giving title compound as a yellow solid in 75% yield over two steps (1.96 g, 7.5 mmol).

mp 118–123 °C (from H_2O); **IR** (thin film, cm^{-1}) 2969, 1590, 1565, 1475, 1436, 1387, 1362, 1193, 1164, 1128, 1084, 1309, 1024, 980, 955, 770, 764, 752, 716, 695, 680; **^{1}H NMR** (400

MHz, $CDCl_3$) δ 12.27 (s, 1H), 7.94 (dd, *J* = 13.0, 7.5 Hz, 1H), 7.65 (dd, *J* = 13.0, 7.5 Hz, 2H), 7.51 – 7.40 (m, 2H), 7.38 – 7.29 (m, 3H), 7.24 – 7.17 (m, 1H), 3.47 (p, *J* = 6.5 Hz, 1H), 0.96 (d, *J* = 6.5 Hz, 6H); **$^{13}C\{^1H\}$ NMR** (101 MHz, $CDCl_3$) δ 153.1 (d, *J* = 12.0 Hz), 134.2 (d, *J* = 138.5 Hz), 133.1 (d, *J* = 9.5 Hz), 132.7, 131.7, 131.1 (d, *J* = 11.0 Hz), 129.4 (d, *J* = 139.0 Hz), 128.3 (d, *J* = 13.0 Hz), 126.7 (d, *J* = 12.5 Hz), 125.5 (d, *J* = 12.5 Hz), 31.3 (d, *J* = 4.0 Hz), 23.9; **$^{31}P\{^1H\}$ NMR** (162 MHz, $CDCl_3$) δ 34.61; **HRMS**: m/z (EI) calculated for ($C_{15}H_{17}O_2P$) $[M+H]^+$: 261.1039, found: 261.1039.

[1,1'-Biphenyl]-2-yl(phenyl)phosphinic acid

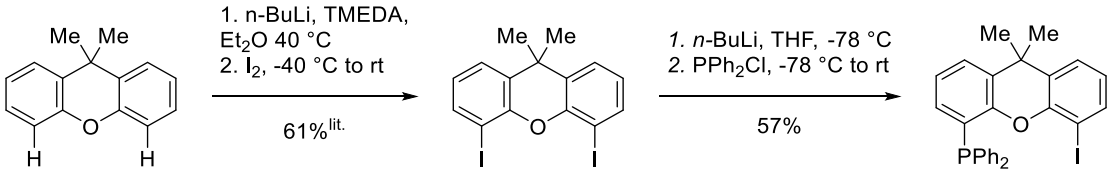


Magnesium turnings (310 mg, 12.8 mmol, 1.1 equiv.) and I_2 (5 – 10 mg) were added to a two-neck round-bottom flask equipped with a stirrer bar and a condenser. The flask was sealed with a septum, evacuated (< 0.1 mbar) and back-filled with argon twice, then a solution of 2-bromo-1,1'-biphenyl (2.0 mL, 11.6 mmol, 1.0 equiv.) in THF (10 mL) was slowly added. The resulted mixture was heated to reflux for 1 hour, then cooled to 0 °C. A solution of dichlorophenylphosphine (1.8 mL, 13.3 mmol, 1.1 equiv.) in THF (10 mL) was slowly added and the resulting mixture was stirred at room temperature for 18 h. The reaction mixture was cooled to 0 °C and 100 mL of a 10% v/v solution of H_2SO_4 was added. After 10 min, the ice bath was removed and the reaction mixture was allowed to warm to room temperature. The two phases were separated and the aqueous layer was extracted with EtOAc (3 × 100 mL). The combined organic extracts were dried with anhydrous $MgSO_4$, filtered and concentrated under reduced pressure. The crude product was dissolved in MeOH (75 mL) and H_2O (75 mL), then

NaOH (11.6 g, 290 mmol, 25 equiv.) and H_2O_2 (30% w/w in H_2O, 6.0 mL, 50 mmol, 5.0 equiv.) were added. The resulting mixture was stirred for 18 hours at room temperature then concentrated under reduced pressure. The residue was dissolved in H_2O (100 mL), and conc. HCl was added at 0 °C until formation of a white precipitate. The solution was filtered through a sintered funnel, and the precipitate was thoroughly washed with H_2O, then dried under high vacuum for 18 hours giving the title compound as a white solid in 30% yield over two steps (1.02 g, 3.5 mmol).

mp 167–172 °C (from H_2O); **IR** (thin film, cm^{-1}) 3053, 1586, 1563, 1468, 1434, 1401, 1361, 1285, 1237, 1189, 1136, 1095, 1068, 1027, 937, 909, 884, 780, 766, 744, 718, 695, 618; **^{1}H NMR** (400 MHz, $CDCl_3$) δ 12.18 (s, 1H), 8.19 (dd, *J* = 13.0, 7.5 Hz, 1H), 7.53 – 7.47 (m, 1H), 7.44 – 7.37 (m, 1H), 7.28 – 7.21 (m, 1H), 7.20 – 7.02 (m, 8H), 7.01 – 6.95 (m, 2H); **^{13}C{^{1}H} NMR** (101 MHz, $CDCl_3$) δ 146.4 (d, *J* = 12.0 Hz), 140.5 (d, *J* = 3.4 Hz), 133.1 (d, *J* = 141.5 Hz), 133.0 (d, *J* = 8.5 Hz), 131.7 – 131.0 (m), 131.2 (d, *J* = 135.1 Hz), 131.2 (d, *J* = 12.0 Hz), 130.0, 127.6 (d, *J* = 13.5 Hz), 127.2, 127.1, 126.8 (d, *J* = 12.0 Hz); **^{31}P{^{1}H} NMR** (162 MHz, $CDCl_3$) δ 32.63; **HRMS**: m/z (EI) calculated for ($C_{18}H_{15}O_2P$) $[M–H]^–$: 293.0737, found: 293.0731.

7.4.4. (5-Iodo-9,9-dimethyl-9*H*-xanthen-4-yl)diphenylphosphane



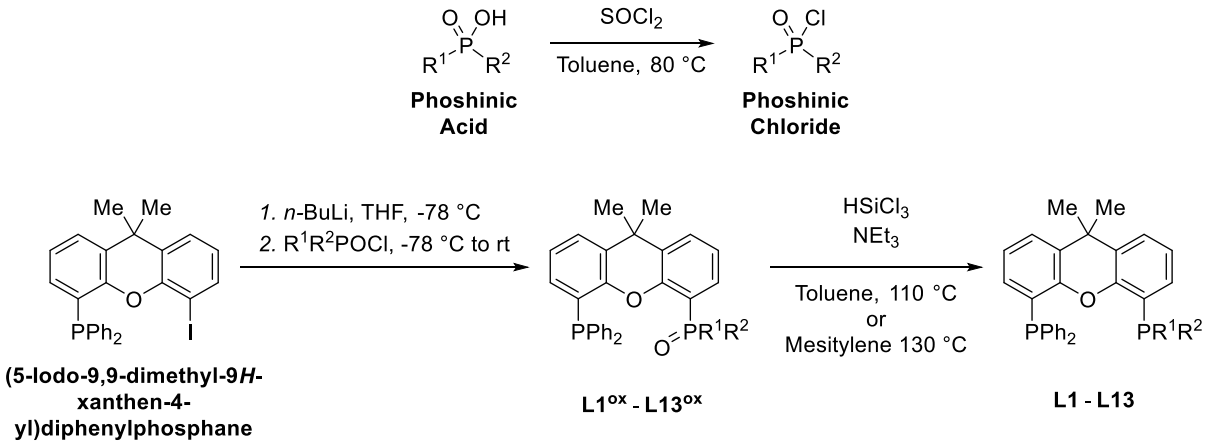
4,5-Diiodo-9,9-dimethyl-9*H*-xanthene was synthesised from 9,9-dimethyl-9*H*-xanthene according to literature procedure.[241]

4,5-Diiodo-9,9-dimethyl-9*H*-xanthene (6.40 g, 14.0 mmol, 1.0 equiv.) was added to a round-bottom flask with a stirrer bar. The flask was sealed with a septum, evacuated (< 0.1 mbar) and

back-filled with argon twice, then THF (100 mL) was added. After dissolution of the solid, the flask was cooled to -78 °C and *n*-BuLi (2.54 M in hexanes, 5.5 mL, 14.0 mmol, 1.0 equiv.) was added over 2 minutes. Lithium-iodide exchange was found to be complete within 1 minute according to HPLC analysis of the reaction mixture. Diphenylchlorophosphine (3.4 mL, 18.9 mmol, 1.4 equiv.) was then added over 2 minutes and the reaction was stirred at -78 °C for 10 minutes. The dry ice bath was then removed and the reaction was stirred for another 18 hours. The reaction flask was then opened to air, sat. aq. NH_4Cl (5 mL) was slowly added followed by brine (100 mL). The two phases were separated and the aqueous layer was extracted with EtOAc (3 × 50 mL). The combined organic extracts were dried with anhydrous $MgSO_4$, filtered and concentrated under reduced pressure. The crude product was purified by flash column chromatography (gradient of CH_2Cl_2 0% to 30% in petrol), giving the title compound as a white solid in 57% yield (4.12 g, 7.92 mmol).

mp 174-179 °C (from CH_2Cl_2/petrol); **IR** (thin film, cm^{-1}) 3068, 2970, 1585, 1557, 1477, 1434, 1408, 1284, 1247, 1206, 1194, 1140, 1097, 1067, 1027, 907, 884, 834, 814, 777, 730, 695, 665, 648 ; **^{1}H NMR** (400 MHz, $CDCl_3$) δ 7.60 (dd, *J* = 8.0, 1.5 Hz, 1H), 7.42 (ddd, *J* = 8.0, 1.5, 1.0 Hz, 1H), 7.39 – 7.32 (m, 11H), 7.01 (td, *J* = 7.5, 1.0 Hz, 1H), 6.79 (t, *J* = 8.0 Hz, 1H), 6.57 (ddd, *J* = 7.5, 4.0, 1.5 Hz, 1H), 1.64 (s, 6H); **^{13}C{^{1}H} NMR** (101 MHz, $CDCl_3$) δ 152.2 (d, *J* = 16.5 Hz), 149.7 (d, *J* = 2.0 Hz), 137.8, 136.6 (d, *J* = 10.5 Hz), 134.4 (d, *J* = 20.0 Hz), 131.9, 131.2, 129.7 (d, *J* = 1.5 Hz), 128.8, 128.7 – 128.3 (m), 126.7, 126.0, 125.5 (d, *J* = 17.0 Hz), 124.8, 123.9, 35.0 (d, *J* = 1.5 Hz), 32.4; **^{31}P{^{1}H} NMR** (162 MHz, $CDCl_3$) δ -14.25; **HRMS**: m/z (EI) calculated for ($C_{27}H_{22}IOP$) $[M+H]^+$: 521.0526, found: 521.0518.

7.4.5. General Procedures for the Synthesis of Ligands L1-L13



General Procedure B-1: Preparation of the Phosphinic Chloride Fragment

The phosphinic acid (1.0 equiv.) was added to a 50 mL round-bottom flask equipped with a stirrer bar. The flask was sealed with a septum, evacuated (< 0.1 mbar) and back-filled with argon twice, then toluene was added (obtained concentration of phosphinic acid in toluene: 0.25M), followed by $SOCl_2$ (10 equiv.). The reaction mixture was heated to 80 °C until complete conversion was observed by $^{31}P\{^1H\}$ NMR spectroscopy (ca. 30 min – 2 h), after which the reaction was cooled to room temperature and concentrated under reduced pressure on a rotavapor, minimising the time during which the flask was opened to air. The residue was further dried under high vacuum for 10 min at room temperature with stirring, after which THF was added, giving a ca. 0.1 M solution of phosphinic chloride in THF.

General Procedure B-2: Preparation of ***L1^{ox}-L13^{ox}***

(5-Iodo-9,9-dimethyl-9*H*-xanthen-4-yl)diphenylphosphane (1.0 equiv.) was added to a 50 mL round-bottom flask equipped with a stirrer bar. The flask was sealed with a septum, evacuated (< 0.1 mbar) and back-filled with argon twice, then THF was added (concentration of substrate: 0.06 M). After dissolution of the solid, the flask was cooled to -78 °C and *n*-BuLi (2.50 M in hexanes, 1.1 equiv.) was added over 30 seconds. Lithium-iodide exchange was found to be

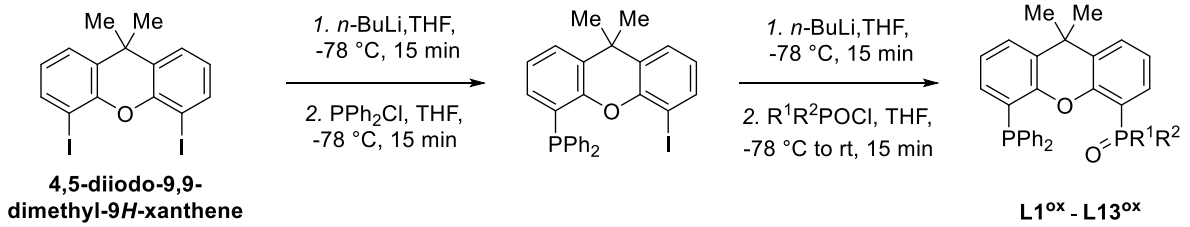
complete within 1 minute according to HPLC analysis of the reaction mixture. The phosphinic chloride (1.3 equiv.) prepared according to the procedure described above was then added over 30 seconds. The reaction mixture was stirred for 10 minutes after which the cooling bath was removed, allowing the flask to warm to room temperature and stir for 18 hours. Sat. aq.NH_4Cl (1-5 mL) and brine (20 mL) were sequentially added to the reaction mixture, then the two phases were separated and the aqueous layer was extracted with EtOAc (3 × 25 mL). The combined organic extracts were dried with anhydrous $MgSO_4$, filtered and concentrated under reduced pressure. The crude product was purified by flash column chromatography (gradient of EtOAc in petrol), giving ligands **L1^{ox}-L13^{ox}**. These ligands were not pure at this stage as phosphine oxide related compounds always co-eluted during the flash column chromatography.

*General Procedure B-3: Reduction of **L1^{ox}-L13^{ox}***

Ligands **L1^{ox}-L13^{ox}** were added to a high pressure reaction tube equipped with a stirrer bar. The flask was sealed with a septum, evacuated (< 0.1 mbar) and back-filled with argon twice, then toluene or mesitylene was added (concentration of substrate: 0.05 – 0.2 M), followed by NEt_3 (5.5 equiv.) and $HSiCl_3$ (5.0 equiv.). The septum was then removed and the pressure tube was sealed and heated to 110 °C (toluene) or 130 °C (mesitylene) for 18 hours. High pressure tubes were required due to the low boiling points of NEt_3 (bp = 89 °C) and $HSiCl_3$ (bp = 32 °C). The reaction flask was cooled to room temperature and the mixture was slowly added to a round-bottom flask containing a solution of aq. NaOH (1.0 M, 10 equiv. compared to $HSiCl_3$) at 0 °C. CH_2Cl_2 was added, then the two phases were separated and the aqueous layer was extracted with DCM (3 × 25 mL). The combined organic extracts were dried with anhydrous $MgSO_4$, filtered and concentrated under reduced pressure. The crude product was purified by flash column chromatography (gradient of CH_2Cl_2 in petrol), giving ligands **L1-L13**.

Yields were calculated against the amount of (5-Iodo-9,9-dimethyl-9*H*-xanthen-4-yl)diphenylphosphane used.

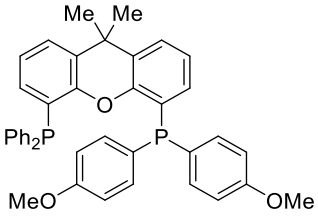
General Procedure C: Alternative Preparation of ***L1^{ox}-L13^{ox}***



4,5-Diiodo-9,9-dimethyl-9*H*-xanthene (1.0 equiv.) was added to a 50 mL round-bottom flask equipped with a stirrer bar. The flask was sealed with a septum, evacuated (< 0.1 mbar) and back-filled with argon twice, then THF was added (concentration of substrate: 0.09 M). After dissolution of the solid, the flask was cooled to -78 °C and *n*-BuLi (2.50 M in hexanes, 1.0 equiv.), PPh_2Cl (1.1 equiv.), *n*-BuLi (2.50 M in hexanes, 2.0 equiv.) and R^1R^2POCl (2.5 equiv.) were added sequentially every 15 minutes at – 78°C. The cooling bath was then removed, allowing the flask to warm to room temperature and stir for 15 minutes. Sat. aq.NH_4Cl (1 mL) and brine (20 mL) were sequentially added to the reaction mixture, then the two phases were separated and the aqueous layer was extracted with EtOAc (3 × 25 mL). The combined organic extracts were dried with anhydrous $MgSO_4$, filtered and concentrated under reduced pressure. The crude product was purified by flash column chromatography (gradient of EtOAc in petrol), giving ligands **L1^{ox}-L13^{ox}**. These ligands were not pure at this stage as phosphine oxide related compounds always co-eluted during the flash column chromatography.

7.4.6. Characterisation Data for Ligands L1-L13

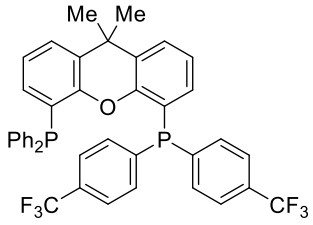
(5-(Bis(4-methoxyphenyl)phosphaneyl)-9,9-dimethyl-9*H*-xanthen-4-yl)diphenylphosphane L1



Isolated in 11% yield (62 mg, 0.097 mmol) from 4,5-diiodo-9,9-dimethyl-9*H*-xanthene (400 mg, 0.87 mmol, 1.0 equiv.) using General Procedures B-1 and C and B-2.

mp 132–137 °C (from $CDCl_3$); **IR** (thin film, cm^{-1}) 2961, 1593, 1567, 1497, 1461, 1434, 1401, 1284, 1239, 1177, 1094, 1029, 907, 882, 825, 789, 729, 696, 648; **^{1}H NMR** (400 MHz, $CDCl_3$) δ 7.46 – 7.37 (m, 2H), 7.31 – 7.09 (m, 14H), 7.04 – 6.94 (m, 2H), 6.81 – 6.74 (m, 4H), 6.64 – 6.53 (m, 2H), 3.80 (s, 6H), 1.67 (s, 6H); **^{13}C{^{1}H} NMR** (101 MHz, $CDCl_3$) δ 159.9, 153.1 – 152.7 (m), 152.6 – 152.2 (m), 137.7 (d, *J* = 14.0 Hz), 135.4 (d, *J* = 21.5 Hz), 134.0 (d, *J* = 20.0 Hz), 132.3, 131.9, 130.2 – 129.9 (m), 128.5 – 128.1 (m), 126.5, 126.2, 125.8 (d, *J* = 19.0 Hz), 123.4 (d, *J* = 3.5 Hz), 114.0 (d, *J* = 8.0 Hz), 55.2, 34.6 – 34.3 (m), 31.9; **^{31}P{^{1}H} NMR** (162 MHz, $CDCl_3$) δ -18.24 (d, *J* = 32.0 Hz), -20.17 (d, *J* = 32.0 Hz); **HRMS**: m/z (EI) calculated for ($C_{41}H_{36}O_3P_2$) $[M+H]^+$: 639.2212, found: 639.2210.

(5-(Bis(4-(trifluoromethyl)phenyl)phosphaneyl)-9,9-dimethyl-9*H*-xanthen-4-yl)diphenylphosphane L2

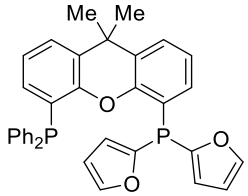


Isolated in 10% yield (64 mg, 0.097 mmol) from 4,5-diiodo-9,9-dimethyl-9*H*-xanthene (400 mg, 0.90 mmol, 1.0 equiv.) using General Procedures B-1 and C and B-2.

mp 141–146 °C (from $CDCl_3$); **IR** (thin film, cm^{-1}) 2361, 1604, 1433, 1404, 1322, 1239, 1168, 1125, 1106, 1059, 1016, 882, 839, 829, 789, 768, 743, 696; **^{1}H NMR** (400 MHz, $CDCl_3$) δ 7.53 – 7.47 (m, 5H), 7.45 (dd, *J* = 7.5, 1.5 Hz, 1H), 7.33 – 7.11 (m, 14H), 7.07 – 6.96 (m, 2H), 6.52 (ddq, *J* = 16.0, 7.5, 1.5 Hz, 2H), 1.70 (s, 6H); **^{13}C{^{1}H} NMR** (101 MHz, $CDCl_3$) δ 153.0 – 152.6 (m), 152.6 – 152.2 (m), 142.0 – 141.5 (m), 137.1 – 136.8 (m), 133.9 (ddd, *J* = 24.5, 12.0, 9.0

Hz), 132.2, 131.8, 130.6, 130.5 (q, *J* = 32.5 Hz), 129.9, 128.5, 128.2 (t, *J* = 3.5 Hz), 127.2, 126.4, 125.6 (d, *J* = 9.5 Hz), 124.1 (q, *J* = 272.0 Hz), 125.0 (q, *J* = 3.5 Hz), 123.8 (d, *J* = 4.5 Hz), 123.7 – 123.3 (m), 35.0 – 34.3 (m), 31.7; **^{31}P{^{1}H} NMR** (162 MHz, $CDCl_3$) δ -17.4 (app. s); **^{19}F{^{1}H} NMR** (377 MHz, $CDCl_3$) δ -62.66; **HRMS**: m/z (EI) calculated for ($C_{41}H_{30}F_6OP_2$) $[M+H]^+$: 715.1749, found: 715.1740.

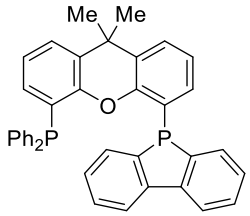
(5-(Di(furan-2-yl)phosphaneyl)-9,9-dimethyl-9*H*-xanthen-4-yl)diphenylphosphane L3



Isolated in 3.5% yield (6.5 mg, 0.012 mmol) from (5-iodo-9,9-dimethyl-9*H*-xanthen-4-yl)diphenylphosphane (175 mg, 0.34 mmol, 1.0 equiv.) using General Procedures B-1, B-2 and B-3.

mp 203–208 °C (from CH_2Cl_2/petrol); **IR** (thin film, cm^{-1}) 2924, 1459, 1434, 1403, 1364, 1284, 1262, 1239, 1211, 1151, 1111, 1067, 1026, 1006, 902, 883, 789, 740, 696, 654; **^{1}H NMR** (400 MHz, $CDCl_3$) δ 7.57 (dd, *J* = 2.0, 1.0 Hz, 2H), 7.42 – 7.38 (m, 2H), 7.33 – 7.29 (m, 10H), 7.05 – 6.92 (m, 3H), 6.56 (ddd, *J* = 7.5, 4.0, 1.5 Hz, 1H), 6.52 (dt, *J* = 3.5, 1.0 Hz, 2H), 6.29 (dt, *J* = 3.5, 1.5 Hz, 2H), 1.62 (s, 6H); **^{13}C{^{1}H} NMR** (126 MHz, $CDCl_3$) δ 207.1, 152.5 (dd, *J* = 17.5, 1.5 Hz), 152.4 – 152.1 (m), 150.7 (d, *J* = 13.0 Hz), 147.1 (d, *J* = 2.5 Hz), 137.3 (d, *J* = 12.5 Hz), 134.2 (d, *J* = 20.0 Hz), 132.2, 130.1 (dd, *J* = 14.5, 2.0 Hz), 128.6 – 128.3 (m), 127.0, 126.7, 125.7 (d, *J* = 18.0 Hz), 123.5 (d, *J* = 9.0 Hz), 123.0 (d, *J* = 8.5 Hz), 121.1 (dd, *J* = 23.5, 15 Hz), 110.7 (d, *J* = 5.5 Hz), 34.5 (t, *J* = 2.0 Hz), 32.0; **^{31}P{^{1}H} NMR** (162 MHz, $CDCl_3$) δ -17.17 (d, *J* = 32.0 Hz), -62.73 (d, *J* = 32.0 Hz); **HRMS**: m/z (EI) calculated for ($C_{35}H_{28}O_3P_2$) $[M+H]^+$: 559.1586, found: 559.1586.

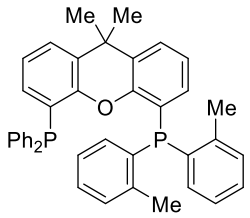
5-(5-(Diphenylphosphaneyl)-9,9-dimethyl-9*H*-xanthen-4-yl)-5*H*-benzo[*b*]phosphindole L4



Isolated in 35% yield (68 mg, 0.12 mmol) from (5-iodo-9,9-dimethyl-9*H*-xanthen-4-yl)diphenylphosphane (175 mg, 0.34 mmol, 1.0 equiv.) using General Procedures B-1, B-2 and B-3.

mp 227–232 °C (from CH_2Cl_2/petrol); **IR** (thin film, cm^{-1}) 2972, 1563, 1477, 1434, 1403, 1284, 1239, 1197, 1107, 1068, 1028, 907, 882, 787, 745, 725, 696, 648; **^{1}H NMR** (400 MHz, $CDCl_3$) δ 7.98 – 7.88 (m, 2H), 7.52 (ddd, *J* = 8.0, 1.5, 1.0 Hz, 1H), 7.48 – 7.30 (m, 15H), 7.17 (tdd, *J* = 7.5, 3.0, 1.0 Hz, 2H), 7.11 (t, *J* = 7.5 Hz, 1H), 6.81 – 6.71 (m, 2H), 6.49 (ddd, *J* = 7.5, 4.0, 1.5 Hz, 1H), 1.67 (s, 6H); **^{13}C{^{1}H} NMR** (101 MHz, $CDCl_3$) δ 153.6 (dd, *J* = 19.0, 1.5 Hz), 153.1 – 152.7 (m), 143.8 (d, *J* = 3.0 Hz), 142.8 (d, *J* = 6.5 Hz), 137.0 (d, *J* = 12.0 Hz), 134.4 (d, *J* = 20.0 Hz), 132.2, 131.3 (dd, *J* = 21.5, 2.0 Hz), 130.6 (dd, *J* = 14.0, 2.0 Hz), 129.0 (d, *J* = 3.0 Hz), 128.8, 128.7, 128.6, 128.3, 127.3 (d, *J* = 7.0 Hz), 126.6, 126.6, 125.8 (d, *J* = 17.0 Hz), 124.9 (d, *J* = 26.0 Hz), 123.8, 123.7, 121.2, 34.9 – 34.6 (m), 31.7; **^{31}P{^{1}H} NMR** (162 MHz, $CDCl_3$) δ -17.54 (d, *J* = 34.5 Hz), -24.33 (d, *J* = 34.5 Hz); **HRMS**: m/z (EI) calculated for ($C_{39}H_{30}OP_2$) $[M+H]^+$: 577.1845, found: 577.1844.

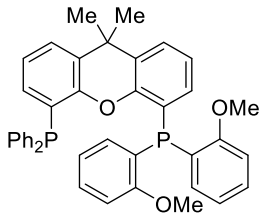
(5-(Di-*o*-tolylphosphaneyl)-9,9-dimethyl-9*H*-xanthen-4-yl)diphenylphosphane L5



Isolated in 7% yield (23 mg, 0.038 mmol) from (5-iodo-9,9-dimethyl-9*H*-xanthen-4-yl)diphenylphosphane (300 mg, 0.58 mmol, 1.0 equiv.) using General Procedures B-1, B-2 and B-3.

mp 142–147 °C (from CH_2Cl_2/petrol); **IR** (thin film, cm^{-1}) 3055, 2923, 2854, 1588, 1564, 1467, 1452, 1434, 1402, 1283, 1240, 1200, 1120, 1028, 882, 788, 745, 718, 695; **^{1}H NMR** (400 MHz, $CDCl_3$) δ 7.48 – 7.36 (m, 2H), 7.25 – 7.10 (m, 14H), 7.03 – 6.89 (m, 4H), 6.67 (ddd, *J* = 7.5, 4.0, 1.5 Hz, 2H), 6.57 – 6.45 (m, 2H), 2.31 (s, 6H), 1.66 (s, 6H); **^{13}C{^{1}H} NMR** (101 MHz, $CDCl_3$) δ 153.9 – 151.9 (m), 142.9 (d, *J* = 27.5 Hz), 137.8 (d, *J* = 14.5 Hz), 135.6 (d, *J* = 14.5 Hz), 134.0 (d, *J* = 20.0 Hz), 132.9, 132.4 – 131.5 (m), 130.1 – 129.6 (m), 128.6 – 128.0 (m), 126.4 (d, *J* = 5.5 Hz), 126.1 – 125.8 (m), 124.6 – 124.0 (m), 123.5 (d, *J* = 16.5 Hz), 34.6, 31.9, 21.6 – 21.2 (m); **^{31}P{^{1}H} NMR** (162 MHz, $CDCl_3$) δ -17.62 (d, *J* = 29.5 Hz), -32.99 (d, *J* = 29.5 Hz); **HRMS**: m/z (EI) calculated for ($C_{41}H_{36}OP_2$) $[M+H]^+$: 607.2314, found: 607.2310.

(5-(Bis(2-methoxyphenyl)phosphaneyl)-9,9-dimethyl-9*H*-xanthen-4-yl)diphenylphosphane L6

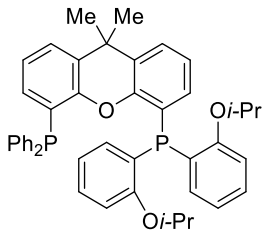


Isolated in 4% yield (7.2 mg, 0.011 mmol) from (5-iodo-9,9-dimethyl-9*H*-xanthen-4-yl)diphenylphosphane (140 mg, 0.27 mmol, 1.0 equiv.) using General Procedures B-1, B-2 and B-3.

mp 221–226 °C (from CH_2Cl_2/petrol); **IR** (thin film, cm^{-1}) 2959, 2919, 2851, 1586, 1572, 1474, 1460, 1431, 1403, 1275, 1241, 1180, 1162, 1124, 1095, 1080, 1025, 908, 880, 793, 748, 726, 694, 644; **^{1}H NMR** (400 MHz, $CDCl_3$) δ 7.42 (ddd, *J* = 15.5, 7.8, 1.5 Hz, 2H), 7.32 – 7.24 (m,

3H), 7.23 – 7.10 (m, 9H), 6.97 (dt, *J* = 12.5, 7.5 Hz, 2H), 6.83 (dd, *J* = 8.5, 5.0 Hz, 2H), 6.74 (t, *J* = 7.5 Hz, 2H), 6.65 – 6.56 (m, 3H), 6.54 (ddd, *J* = 7.5, 3.5, 1.5 Hz, 1H), 3.74 (s, 6H), 1.66 (s, 6H); **^{13}C{^{1}H} NMR** No ^{13}C data available for this compound; **^{31}P{^{1}H} NMR** (162 MHz, $CDCl_3$) δ -18.80, -19.03; **HRMS**: m/z (EI) calculated for ($C_{41}H_{36}O_3P_2$) $[M+H]^+$: 639.2212, found: 639.2211.

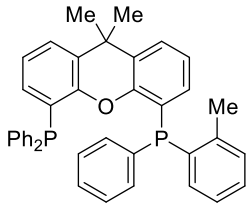
(5-(Bis(2-isopropoxyphenyl)phosphaneyl)-9,9-dimethyl-9*H*-xanthen-4-yl)diphenylphosphane L7



Isolated in 32% yield (130 mg, 0.19 mmol) from (5-iodo-9,9-dimethyl-9*H*-xanthen-4-yl)diphenylphosphane (300 mg, 0.58 mmol, 1.0 equiv.) using General Procedures B-1, B-2 and B-3.

mp 57–62 °C (from CH_2Cl_2/petrol); **IR** (thin film, cm^{-1}) 3057, 2975, 2828, 1582, 1468, 1436, 1402, 1384, 1372, 1275, 1236, 1179, 1133, 1109, 1067, 1041, 1027, 955, 908, 884, 797, 731, 696, 648; **^{1}H NMR** (400 MHz, $CDCl_3$) δ 7.40 (dd, *J* = 8.0, 1.5 Hz, 2H), 7.31 – 7.1 (m, br. 12H), 6.96 (app. t, *J* = 7.5 Hz, 2H), 6.90 – 6.68 (m, br. 7H), 6.57 (ddd, *J* = 7.5, 3.5, 1.5 Hz, 1H), 4.58 – 4.43 (m, 2H), 1.66 (s, 6H), 1.16 – 1.01 (m, 12H); **^{13}C{^{1}H} NMR** (126 MHz, $CDCl_3$) δ 159.9, 159.8, 153.2 – 152.9 (m), 137.7 – 137.2 (m), 134.4 (d, *J* = 5.5 Hz), 134.1 (d, *J* = 20.5 Hz), 133.4, 131.8, 129.9, 128.2 (d, *J* = 14.5 Hz), 126.4, 123.4 (t, *J* = 21.5 Hz), 120.9 – 120.4 (m), 71.1 – 70.2 (m), 34.6, 32.1, 22.0, 21.9; **^{31}P{^{1}H} NMR** (162 MHz, $CDCl_3$) δ -18.55, -18.75; **HRMS**: m/z (EI) calculated for ($C_{45}H_{44}O_3P_2$) $[M+H]^+$: 695.2838, found: 695.2831.

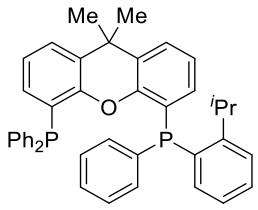
(9,9-Dimethyl-5-(phenyl(*o*-tolyl)phosphaneyl)-9*H*-xanthen-4-yl)diphenylphosphane L8



Isolated in 58% yield (198 mg, 0.33 mmol) from (5-iodo-9,9-dimethyl-9*H*-xanthen-4-yl)diphenylphosphane (300 mg, 0.58 mmol, 1.0 equiv.) using General Procedures B-1, B-2 and B-3.

mp 193–198 °C (from CH_2Cl_2/petrol); **IR** (thin film, cm^{-1}) 3052, 2972, 2359, 1586, 1563, 1476, 1433, 1402, 1284, 1240, 1199, 1109, 1067, 1027, 908, 882, 788, 744, 730, 696, 649; **^{1}H NMR** (400 MHz, $CDCl_3$) δ 7.42 (dd, *J* = 7.5, 1.5 Hz, 2H), 7.35 – 7.07 (m, 17H), 7.00 – 6.93 (m, 3H), 6.69 (ddd, *J* = 7.5, 4.0, 1.5 Hz, 1H), 6.56 (ddd, *J* = 7.5, 3.5, 1.5 Hz, 1H), 6.51 (ddd, *J* = 7.5, 3.5, 1.5 Hz, 1H), 2.33 (d, *J* = 1.5 Hz, 3H), 1.69 (s, 3H), 1.66 (s, 3H); **^{13}C{^{1}H} NMR** (101 MHz, $CDCl_3$) δ 153.0 – 152.5 (m), 142.5, 142.2, 138.0 – 137.0 (m), 136.7 – 136.0 (m), 134.9 – 133.4 (m), 132.6 – 131.8 (m), 130.0 (d, *J* = 4.5 Hz), 129.1 – 127.8 (m), 126.4 (d, *J* = 6.5 Hz), 126.0 (d, *J* = 19.5 Hz), 125.8, 125.3 (d, *J* = 18.5 Hz), 123.5 (d, *J* = 8.5 Hz), 34.6 (d, *J* = 1.5 Hz), 32.0, 31.8, 21.7 – 21.2 (m); **^{31}P{^{1}H} NMR** (162 MHz, $CDCl_3$) δ -17.81 (d, *J* = 30.0 Hz), -24.97 (d, *J* = 30.0 Hz); **HRMS**: m/z (EI) calculated for ($C_{40}H_{34}OP_2$) [$[M+H]^+$: 593.2158, found: 593.2152.

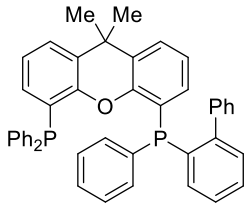
(5-(Diphenylphosphaneyl)-9,9-dimethyl-9*H*-xanthen-4-yl)(2-isopropylphenyl)(phenyl)phosphane L9



Isolated in 35% yield (126 mg, 0.20 mmol) from (5-iodo-9,9-dimethyl-9*H*-xanthen-4-yl)diphenylphosphane (300 mg, 0.58 mmol, 1.0 equiv.) using General Procedures B-1, B-2 and B-3.

mp 87–92 °C (from CH_2Cl_2/petrol); **IR** (thin film, cm^{-1}) 3052, 1586, 1563, 1471, 1433, 1402, 1361, 1285, 1238, 1146, 1109, 1067, 1027, 999, 882, 844, 787, 741, 695; **^{1}H NMR** (400 MHz, $CDCl_3$) δ 7.41 (dd, *J* = 7.5, 1.5 Hz, 2H), 7.37 – 7.14 (m, 17H), 7.01 – 6.93 (m, 3H), 6.77 (ddd, *J* = 7.5, 4.0, 1.5 Hz, 1H), 6.60 (ddd, *J* = 7.5, 3.5, 1.5 Hz, 1H), 6.51 (ddd, *J* = 7.5, 3.5, 1.5 Hz, 1H), 3.78 – 3.61 (m, 1H), 1.68 (s, 3H), 1.65 (s, 3H), 1.20 (d, *J* = 7.0 Hz, 3H), 1.02 (d, *J* = 7.0 Hz, 3H); **^{13}C{^{1}H} NMR** (101 MHz, $CDCl_3$) δ 153.6, 152.9 – 152.3 (m), 138.1 – 137.4 (m), 135.1 (d, *J* = 14.0 Hz), 134.5 (d, *J* = 21.0 Hz), 134.3, 134.1, 133.9 133.3, 132.7, 132.2, 130.0 (dd, *J* = 5.5, 1.5 Hz), 129.0, 128.4, 128.3 – 128.2 (m), 126.4 (d, *J* = 13.5 Hz), 126.1 (dd, *J* = 20.0, 4.0 Hz), 125.9, 125.4 (d, *J* = 4.5 Hz), 123.4, 34.6, 32.2, 31.7, 31.1 (d, *J* = 26.0 Hz), 24.3, 24.1 (d, *J* = 3.0 Hz); **^{31}P{^{1}H} NMR** (162 MHz, $CDCl_3$) δ -18.83 (d, *J* = 26.0 Hz), -26.87 (d, *J* = 26.0 Hz); **HRMS**: m/z (EI) calculated for ($C_{42}H_{38}OP_2$) $[M+H]^+$: 621.2471, found: 621.2463.

[1,1'-Biphenyl]-2-yl(5-(diphenylphosphaneyl)-9,9-dimethyl-9*H*-xanthen-4-yl)(phenyl)phosphane L10

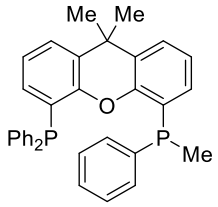


Isolated in 13% yield (50 mg, 0.076 mmol) from (5-iodo-9,9-dimethyl-9*H*-xanthen-4-yl)diphenylphosphane (300 mg, 0.58 mmol, 1.0 equiv.) using General Procedures B-1, B-2 and B-3.

mp 85–90 °C (CH_2Cl_2/petrol); **IR** (thin film, cm^{-1}) 3052, 1584, 1478, 1433, 1402, 1305, 1237, 1150, 1107, 1068, 1027, 998, 910, 878, 845, 787, 770, 740, 694, 667, 617; **^{1}H NMR** (400 MHz,

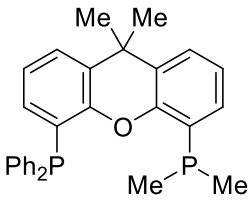
$CDCl_3$) δ 7.46 – 7.35 (m, 4H), 7.32 – 7.03 (m, 21H), 7.02 – 6.91 (m, 3H), 6.63 (ddd, *J* = 7.5, 3.5, 1.5 Hz, 1H), 6.55 (ddd, *J* = 7.5, 3.5, 1.5 Hz, 1H), 1.67 (s, 3H), 1.64 (s, 3H); **^{13}C{^{1}H} NMR** (101 MHz, $CDCl_3$) δ 153.0 – 152.3 (m), 147.1 (d, *J* = 25.0 Hz), 138.1 – 137.0 (m), 136.5, 136.3, 135.1 (d, *J* = 22.0 Hz), 134.1 (d, *J* = 20.0 Hz), 133.9 (d, *J* = 20.0 Hz), 132.9, 132.6, 132.3, 130.3 – 129.7 (m), 128.6 – 127.9 (m), 127.4, 127.0, 126.7, 126.5, 126.3, 126.1 (d, *J* = 4.0 Hz), 125.9 (d, *J* = 3.0 Hz), 123.4 (d, *J* = 4.5 Hz), 34.6 (t, *J* = 1.5 Hz), 32.5, 31.6 – 31.1 (m); **^{31}P{^{1}H} NMR** (162 MHz, $CDCl_3$) δ -19.83 (d, *J* = 26.0 Hz), -20.95 (d, *J* = 26.0 Hz); **HRMS**: m/z (EI) calculated for ($C_{45}H_{36}OP_2$) $[M+H]^+$: 655.2314, found: 655.2306.

(9,9-Dimethyl-5-(methyl(phenyl)phosphaneyl)-9*H*-xanthen-4-yl)diphenylphosphane L11



mp 114–119 °C (from CH_2Cl_2/petrol); **IR** (thin film, cm^{-1}) 2920, 2850, 1564, 1478, 1433, 1401, 1283, 1237, 1197, 1147, 1109, 1093, 1068, 1027, 999, 907, 881, 844, 786, 743, 728, 695, 647; **^{1}H NMR** (400 MHz, $CDCl_3$) δ 7.47 – 7.27 (m, 17H), 7.01 (t, *J* = 7.5 Hz, 1H), 6.92 (t, *J* = 7.5 Hz, 1H), 6.66 (ddd, *J* = 7.5, 4.0, 1.5 Hz, 1H), 6.59 (ddd, *J* = 7.5, 4.0, 1.5 Hz, 1H), 1.68 (s, 3H), 1.63 (s, 3H), 1.24 (d, *J* = 4.0 Hz, 3H); **^{13}C{^{1}H} NMR** (126 MHz, $CDCl_3$) δ 152.5 (d, *J* = 17.0 Hz), 152.0 (d, *J* = 17.0 Hz), 138.4 (d, *J* = 12.0 Hz), 137.3 (d, *J* = 12.0 Hz), 137.0 (d, *J* = 12.0 Hz), 134.5 (d, *J* = 20.5 Hz), 133.9 (d, *J* = 20.0 Hz), 132.9 (d, *J* = 19.0 Hz), 132.2, 130.2, 130.0, 129.7, 129.2 – 128.1 (m), 126.7, 126.1, 125.4, 125.3, 123.5, 123.4, 34.5, 33.0, 31.5, 11.2 – 10.6 (m); **^{31}P{^{1}H} NMR** (162 MHz, $CDCl_3$) δ -17.22 (d, *J* = 33.0 Hz), -37.45 (d, *J* = 33.0 Hz); **HRMS**: m/z (EI) calculated for ($C_{34}H_{30}OP_2$) $[M+H]^+$: 517.1845, found: 517.1843.

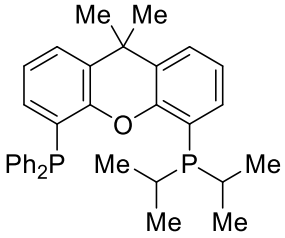
(5-(Dimethylphosphaneyl)-9,9-dimethyl-9*H*-xanthen-4-yl)diphenylphosphane L12



Isolated in 13% yield (19 mg, 0.042 mmol) from (5-iodo-9,9-dimethyl-9*H*-xanthen-4-yl)diphenylphosphane (165 mg, 0.32 mmol, 1.0 equiv.) using General Procedures B-1, B-2 and B-3.

mp 112–117 °C (from CH_2Cl_2/petrol); **IR** (thin film, cm^{-1}) 2965, 1563, 1477, 1433, 1401, 1284, 1235, 1197, 1111, 1068, 1027, 940, 907, 785, 730, 695, 646; **^{1}H NMR** (400 MHz, $CDCl_3$) δ 7.43 (dd, *J* = 8.0, 1.5 Hz, 1H), 7.40 – 7.29 (m, 11H), 7.20 – 7.05 (m, 2H), 6.99 (t, *J* = 7.5 Hz, 1H), 6.55 (ddd, *J* = 7.5, 4.0, 1.5 Hz, 1H), 1.64 (s, 6H), 1.04 (s, br. 6H); **^{13}C{^{1}H} NMR** (101 MHz, $CDCl_3$) δ 152.0 (d, *J* = 14.5 Hz), 137.5 – 137.0 (m), 134.3 (d, *J* = 20.0 Hz), 132.0, 130.0, 129.7, 128.7, 128.5 (d, *J* = 7.0 Hz), 127.4, 126.7, 125.5, 123.5 (d, *J* = 5.5 Hz), 34.5, 32.1, 13.3 (d, *J* = 14.0 Hz); **^{31}P{^{1}H} NMR** (162 MHz, $CDCl_3$) δ -16.88 (d, *J* = 37.0 Hz), -55.33 (d, *J* = 37.0 Hz); **HRMS**: m/z (EI) calculated for ($C_{29}H_{28}OP_2$) $[M+H]^+$: 455.1688, found: 455.1685.

(5-(Diisopropylphosphaneyl)-9,9-dimethyl-9*H*-xanthen-4-yl)diphenylphosphane L13



Isolated in 27% yield (53 mg, 0.12 mmol) from 4,5-diiodo-9,9-dimethyl-9*H*-xanthene (200 mg, 0.43 mmol, 1.0 equiv.) using General Procedures B-1 and C and B-2.

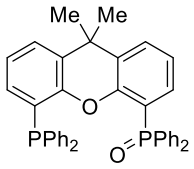
mp 102–107 °C (from CH_2Cl_2/petrol); **IR** (thin film, cm^{-1}) 3064, 1565, 1477, 1459, 1432, 1397, 1362, 1306, 1224, 1196, 1148, 1106, 1071, 1027, 874, 843, 786, 770, 741, 696, 657, 607; **^{1}H NMR** (400 MHz, $CDCl_3$) δ 7.49 – 7.40 (m, 2H), 7.38 – 7.27 (m, 11H), 7.04 (t, *J* = 7.5 Hz, 1H),

6.99 (t, *J* = 7.5 Hz, 1H), 6.62 (ddd, *J* = 7.5, 4.0, 1.5 Hz, 1H), 2.52 (s, br. 2H), 1.64 (s, 6H), 1.05 (dd, *J* = 15.0, 7.0 Hz, 6H), 0.69 (dd, *J* = 12.5, 7.0 Hz, 6H); **^{13}C{^{1}H} NMR** (101 MHz, $CDCl_3$) δ 153.5 – 152.8 (m), 137.5 (d, *J* = 13.0 Hz), 134.2 (d, *J* = 20.0 Hz), 132.6, 130.1 (d, *J* = 2.0 Hz), 129.9, 128.6 – 128.3 (m), 126.9 – 126.7 (m), 125.2 – 124.8 (m), 123.4, 122.6 (d, *J* = 7.5 Hz), 34.5, 32.2, 23.1 (dd, *J* = 12.5, 5.0 Hz), 20.9 (d, *J* = 21.0 Hz), 20.4 (d, *J* = 12.0 Hz); **^{31}P{^{1}H} NMR** (162 MHz, $CDCl_3$) δ -16.7, -16.8; **HRMS**: m/z (EI) calculated for ($C_{33}H_{36}OP_2$) $[M+H]^+$: 511.2314, found: 511.2309.

7.4.7. Other Novel Phosphine Ligands

(5-(Diphenylphosphaneyl)-9,9-dimethyl-9*H*-xanthen-4-yl)diphenylphosphine oxide

Ox-Xantphos

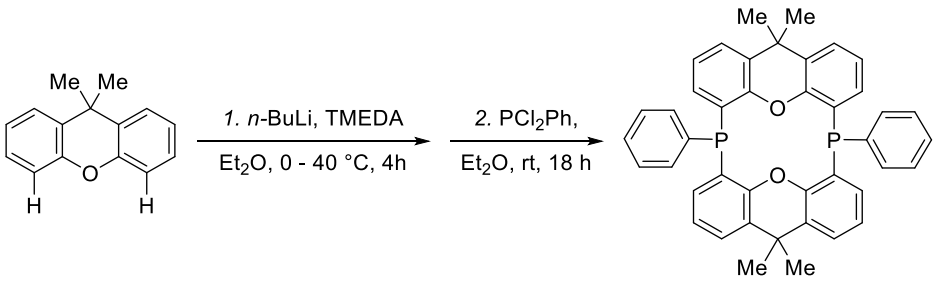


Isolated in 10% yield (49 mg, 0.082 mmol) from 4,5-diiodo-9,9-dimethyl-9*H*-xanthene (400 mg, 0.87 mmol, 1.0 equiv.) using General Procedures B-1 and B-2. After flash column chromatography, the product containing fractions were recrystallised from MeOH to give the title compound as a white solid.

mp 218–223 °C (from MeOH); **IR** (thin film, cm^{-1}) 3056, 2219, 1585, 1478, 1435, 1401, 1228, 1182, 1122, 1098, 1069, 1027, 908, 879, 851, 778, 727, 693, 643; **^{1}H NMR** (400 MHz, $CDCl_3$) δ 7.90 – 7.75 (m, 4H), 7.73 – 7.63 (m, 2H), 7.46 (dd, *J* = 7.5, 1.5 Hz, 1H), 7.42 – 7.37 (m, 2H), 7.35 – 7.19 (m, 11H), 7.06 – 6.95 (m, 5H), 6.64 (ddd, *J* = 7.5, 3.5, 1.5 Hz, 1H), 1.69 (s, 6H); **^{13}C{^{1}H} NMR** (101 MHz, $CDCl_3$) δ 152.9 – 152.1 (m), 138.3 (d, *J* = 17.0 Hz), 134.2 – 133.9 (m), 133.6 (d, *J* = 1.5 Hz), 133.6 (d, *J* = 20.0 Hz), 132.5, 132.3 (d, *J* = 3.0 Hz), 132.2 (d, *J* = 3.0 Hz), 131.6 (d, *J* = 3.0 Hz), 131.1 (d, *J* = 6.0 Hz), 130.8, 129.8, 128.5 – 128.0 (m), 127.0, 125.5

(d, *J* = 23.0 Hz), 123.9, 123.4 (d, *J* = 12.0 Hz), 119.4 (d, *J* = 99.5 Hz), 34.4, 32.5; **$^{31}P\{^{1}H\}$ NMR** (162 MHz, $CDCl_3$) δ 27.8, -21.7; **HRMS**: m/z (EI) calculated for ($C_{39}H_{32}O_2P_2$) $[M+H]^+$: 595.1950, found: 595.1948.

21,21,22,22-Tetramethyl-10,20-diphenyl-10*H*,20*H*-4,6:14,16-dimethanotetrabenzo[*b*,*e*,*h*,*k*][1,7]dioxa[4,10]diphosphacyclododecine BisXantphos

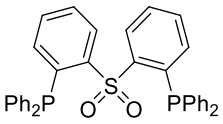


9,9-Dimethyl-9*H*-xanthene (2.0 g, 9.5 mmol, 1.0 equiv.) was added to a two-neck round-bottom flask with a stirrer bar and a condenser. The flask was sealed with a septum, evacuated (< 0.1 mbar) and back-filled with argon twice, then Et_2O (20 mL) and TMEDA (2.9 mL, 19.0 mmol, 2.0 equiv.) were added. After dissolution of the solid, the flask was cooled to 0 °C and *n*-BuLi (2.42 M in hexanes, 8.6 mL, 2.2 equiv.) was added over 5 minutes. The reaction mixture was stirred for 5 minutes, then the cooling bath was removed, allowing the flask to warm to room temperature. The flask was then heated to 40 °C for 4 hours, then was allowed to cool to room temperature. Both the reaction mixture and a solution of PCl_2Ph (1.3 mL, 9.5 mmol, 1.0 equiv.) in Et_2O were added at approximately the same rate over 20 minutes using cannulas to a round-bottom flask equipped with a stirrer bar and containing 100 mL of Et_2O under an argon atmosphere, and the obtained reaction mixture was stirred for 18 hours. Sat. aq. NH_4Cl (10 mL) and brine (100 mL) were sequentially added to the flask, then the two phases were separated and the aqueous layer was extracted with EtOAc (3 × 100 mL). The combined organic extracts were dried with anhydrous $MgSO_4$, filtered and concentrated under reduced pressure. The crude product was purified by flash column chromatography (gradient of CH_2Cl_2 5% to 30% in

PETROL), and the product containing fractions were concentrated then recrystallised from CH_2Cl_2/MeOH giving the title compound in 8% yield (75 mg, 0.12 mmol).

mp >300 °C (from CH_2Cl_2/petrol); **IR** (thin film, cm^{-1}) 2954, 1584, 1480, 1468, 1432, 1403, 1266, 1233, 1198, 1147, 1106, 1065, 1027, 908, 876, 839, 820, 797, 768, 747, 736, 704, 666, 617; **^{1}H NMR** (400 MHz, $CDCl_3$) δ 7.56 – 7.43 (m, 8H), 7.42 – 7.23 (m, 10H), 7.06 (t, *J* = 7.5 Hz, 4H), 1.67 (s, 6H), 1.56 (s, 6H); **^{13}C{^{1}H} NMR** (126 MHz, $CDCl_3$) δ 154.6 (t, *J* = 12.0 Hz), 138.1 (t, *J* = 5.0 Hz), 132.9 – 132.7 (m), 131.2 (t, *J* = 2.0 Hz), 128.0 – 127.8 (m), 127.0, 126.8, 126.8 – 126.6 (m), 123.9, 33.8, 28.4; **^{31}P{^{1}H} NMR** (162 MHz, $CDCl_3$) δ -39.6; **HRMS**: m/z (EI) calculated for ($C_{42}H_{34}O_2P_2$) $[M+H]^+$: 633.2107, found: 633.2106.

(Sulfonylbis(2,1-phenylene))bis(diphenylphosphane) SulfPhos

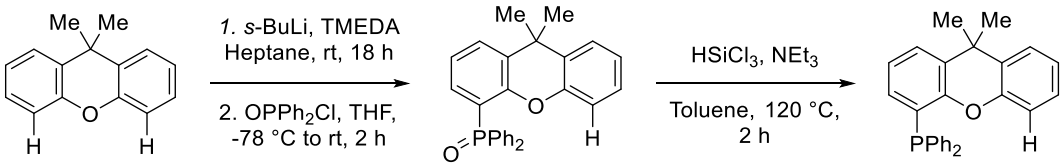


Diphenyl sulfone (500 mg, 2.3 mmol, 1.0 equiv.) was added to a two-neck round-bottom flask with a stirrer bar and a condenser. The flask was sealed with a septum, evacuated (< 0.1 mbar) and back-filled with argon twice, then THF (20 mL) was added. After dissolution of the solid, the flask was cooled to -78 °C and *s*-BuLi (1.24 M in hexanes, 5.5 mL, 3.0 equiv.) was added over 5 minutes. The reaction mixture was stirred for 30 minutes, at -78 °C, then a solution of PPh_2Cl (1.6 mL, 9.1 mmol, 4.0 equiv.) in THF (10 mL) was added over 5 minutes. The reaction mixture was stirred for 15 minutes, then the cooling bath was removed, allowing the flask to warm to room temperature, and the reaction mixture was stirred for 18 hours. Sat. aq. NH_4Cl (2 mL) was slowly added to the flask at 0 °C followed by brine (50 mL), then the two phases were separated and the aqueous layer was extracted with EtOAc (3 × 50 mL). The combined organic extracts were dried with anhydrous $MgSO_4$, filtered and concentrated under reduced pressure. The crude product was purified by flash column chromatography (gradient of EtOAc

0% to 10% in PETROL), and the product containing fractions were concentrated then triturated in CH_2Cl_2/PE, giving the title compound in 20% yield (271 mg, 0.46 mmol) as a light yellow solid.

mp 218–223 °C (from CH_2Cl_2/petrol); **IR** (thin film, cm^{-1}) 3052, 1586, 1478, 1433, 1402, 1306, 1238, 1150, 1106, 1068, 1027, 998, 909, 879, 846, 787, 740, 694, 667; **^{1}H NMR** (400 MHz, $CDCl_3$) δ 8.74 – 8.65 (m, 2H), 7.51 (td, *J* = 7.7, 1.4 Hz, 2H), 7.41 (td, *J* = 7.5, 1.5 Hz, 2H), 7.33 – 7.18 (m, 13H), 7.11 (ddd, *J* = 7.5, 3.0, 1.4 Hz, 2H), 7.06 – 6.99 (m, 7H); **^{13}C{^{1}H} NMR** (101 MHz, $CDCl_3$) δ 146.7 (d, *J* = 26.0 Hz), 137.3 (d, *J* = 29.0 Hz), 137.2 (d, *J* = 38.0 Hz), 136.8 (d, *J* = 13.5 Hz), 136.7, 134.0 (d, *J* = 3.0 Hz), 133.8 (d, *J* = 4.0 Hz), 133.6, 133.4, 133.1, 132.5 (d, *J* = 4.5 Hz), 132.3 (d, *J* = 4.5 Hz), 129.0, 128.7 – 128.2 (m); **^{31}P{^{1}H} NMR** (162 MHz, $CDCl_3$) δ -15.0; **HRMS**: m/z (EI) calculated for ($C_{36}H_{28}O_2P_2S$) $[M+H]^+$: 587.1358, found: 587.1359.

(9,9-Dimethyl-9*H*-xanthen-4-yl)diphenylphosphane PPh$_2$-Xanthene



9,9-Dimethyl-9*H*-xanthene (2.50 g, 11.9 mmol, 1.0 equiv.) was added to a two-neck round-bottom flask with a stirrer bar and a condenser. The flask was sealed with a septum, evacuated (< 0.1 mbar) and back-filled with argon twice, then heptane (75 mL) and TMEDA (1.8 mL, 11.9 mmol, 1.0 equiv) were added. After dissolution of the solid, the flask was cooled to 0 °C and *s*-BuLi (1.26 M in hexanes, 8.5 mL, 0.9 equiv.) was added over 5 minutes. The reaction mixture was stirred for 10 minutes, then the cooling bath was removed, allowing the flask to warm to room temperature, and the reaction mixture was stirred for 18 hours. The flask was then cooled to -78 °C and a solution of diphenylphosphinic chloride (3.0 mL, 15.5 mmol, 1.3 equiv.) in THF (25 mL) was added over 10 minutes. The reaction mixture was stirred for 10

minutes, then the cooling bath was removed, allowing the flask to warm to room temperature, and the reaction mixture was stirred for 2 hours. Sat. aq. NH_4Cl (5 mL) was slowly added to the flask at 0 °C followed by brine (50 mL), then the two phases were separated and the aqueous layer was extracted with EtOAc (3 × 100 mL). The combined organic extracts were dried with anhydrous $MgSO_4$, filtered and concentrated under reduced pressure. The crude product was purified by flash column chromatography (gradient of EtOAc 50% to 75% in PETROL), and the product containing fractions were concentrated then recrystallised from EtOAc/hexane to give (9,9-dimethyl-9*H*-xanthen-4-yl)diphenylphosphine oxide in 26% yield (1.13 g, 2.8 mmol) as a white solid.

IR (thin film, cm^{-1}) 3057, 2971, 1596, 1572, 1489, 1423, 1307, 1267, 1243, 1186, 1158, 1119, 1107, 1097, 885, 812, 795, 749, 738, 723, 695; **^{1}H NMR** (400 MHz, $CDCl_3$) δ 7.89 – 7.79 (m, 4H), 7.76 (ddd, *J* = 13.0, 7.5, 1.5 Hz, 1H), 7.68 – 7.62 (m, 1H), 7.56 – 7.49 (m, 2H), 7.47 – 7.41 (m, 4H), 7.35 (dd, *J* = 7.5, 2.0 Hz, 1H), 7.22 (td, *J* = 7.5, 2.0 Hz, 1H), 7.03 (td, *J* = 7.5, 1.5 Hz, 1H), 6.98 (td, *J* = 7.5, 2.0 Hz, 1H), 6.10 (dd, *J* = 8.0, 1.5 Hz, 1H), 1.60 (s, 6H); **^{13}C{^{1}H} NMR** (101 MHz, $CDCl_3$) δ 152.0 (d, *J* = 3.0 Hz), 149.7, 133.3 (d, *J* = 107.5 Hz), 133.0 (d, *J* = 7.0 Hz), 131.9 (d, *J* = 10.5 Hz), 131.8 (d, *J* = 3.0 Hz), 131.5 (d, *J* = 6.0 Hz), 130.7 (d, *J* = 2.0 Hz), 130.3, 128.5 (d, *J* = 12.5 Hz), 127.4, 125.5, 123.8, 123.4 (d, *J* = 12.0 Hz), 119.7 (d, *J* = 102 Hz), 116.1, 34.5 (d, *J* = 1.5 Hz), 31.6; **^{31}P{^{1}H} NMR** (162 MHz, $CDCl_3$) δ 26.36; **HRMS**: m/z (EI) calculated for ($C_{27}H_{23}OP$) $[M+H]^+$: 411.1508, found: 411.1502.

9,9-Dimethyl-9*H*-xanthen-4-yl)diphenylphosphine oxide was reduced according to General Procedure B-3 in toluene at 120 °C, giving the title compound as a white solid in 96% yield (1.03 g, 2.61 mmol).

mp 97–102 °C (from CH_2Cl_2/petrol); **IR** (thin film, cm^{-1}) 3053, 2971, 2586, 1568, 1489, 1458, 1434, 1416, 1386, 1362, 1307, 1243, 1204, 1155, 1125, 1096, 1069, 1027, 885, 809, 787, 744, 696, 631; **^{1}H NMR** (400 MHz, $CDCl_3$) δ 7.50 – 7.31 (m, 12H), 7.10 – 6.97 (m, 3H), 6.67 (ddd,

J = 7.5, 5.0, 1.5 Hz, 1H), 6.63 – 6.58 (m, 1H), 1.64 (s, 6H); **$^{13}C\{^{1}H\}$ NMR** (101 MHz, $CDCl_3$) δ 152.4 (d, *J* = 14.0 Hz), 150.6, 136.3 (d, *J* = 8.5 Hz), 134.2 (d, *J* = 20.5 Hz), 131.5 (d, *J* = 3.0 Hz), 130.5, 130.5, 129.0, 128.6 (d, *J* = 7.5 Hz), 127.3, 126.8, 125.4, 124.8 (d, *J* = 12.5 Hz), 123.4, 123.3 (d, *J* = 2.0 Hz), 116.6, 34.5, 31.6; **$^{31}P\{^{1}H\}$ NMR** (162 MHz, $CDCl_3$) δ -14.8; **HRMS**: m/z (EI) calculated for ($C_{27}H_{23}OP$) $[M+H]^+$: 395.1559, found: 395.1557.

7.5. Experimental Data and Procedures for Chapter 5

7.5.1. General Procedure for the Screening Reactions

All sulfinamide derivatives were kindly prepared and characterised by Charles Bell.

Unless otherwise stated, the reactions were performed with 0.11 mmol of aryl bromide **2** (1.0 equiv.), in 2.0 mL of solvent, corresponding to a reaction concentration of 0.056 M.

The internal standard was introduced at the beginning of the reaction with the solid reagents (0.5 equiv. compared to Ar-Br **2**).

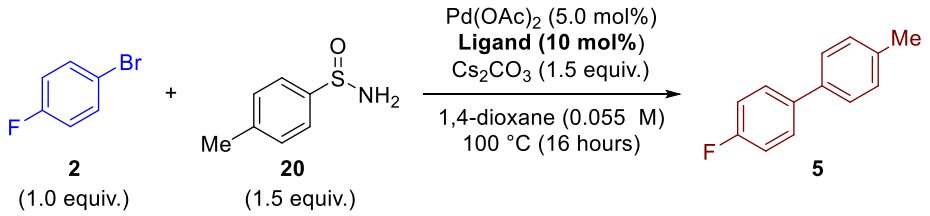
Stock solutions were employed to minimise weighing errors. For example, when the ligand was screened, a stock solution of Ar-Br **2** (0.056 M, 1.0 equiv.), sulfinamide **20** (1.5 equiv./Ar-Br), $Pd(OAc)_2$ (0.05 equiv./ArBr), and 1,3,5-trimethoxybenzene (0.5 equiv./Ar-Br) was prepared in 1,4-dioxane. Cs_2CO_3 (1.5 equiv./Ar-Br) and the ligand (0.05 or 0.10 equiv./Ar-Br) were added in a microwave, then the vial was sealed with a microwave vial cap, evacuated (< 0.1 mbar) and back-filled with argon twice. Then, the stock solution was added (2.0 mL). The reaction was then heated at the indicated temperature and time. The yields of products were measured by HPLC against 1,3,5-trimethoxybenzene as the internal standard using the calibration curves described in **Section 7.2.2**. As another example, when the palladium source was screened, the ligand of choice was added with the stock solution, and the precatalyst was weighed and added with the vial with Cs_2CO_3.

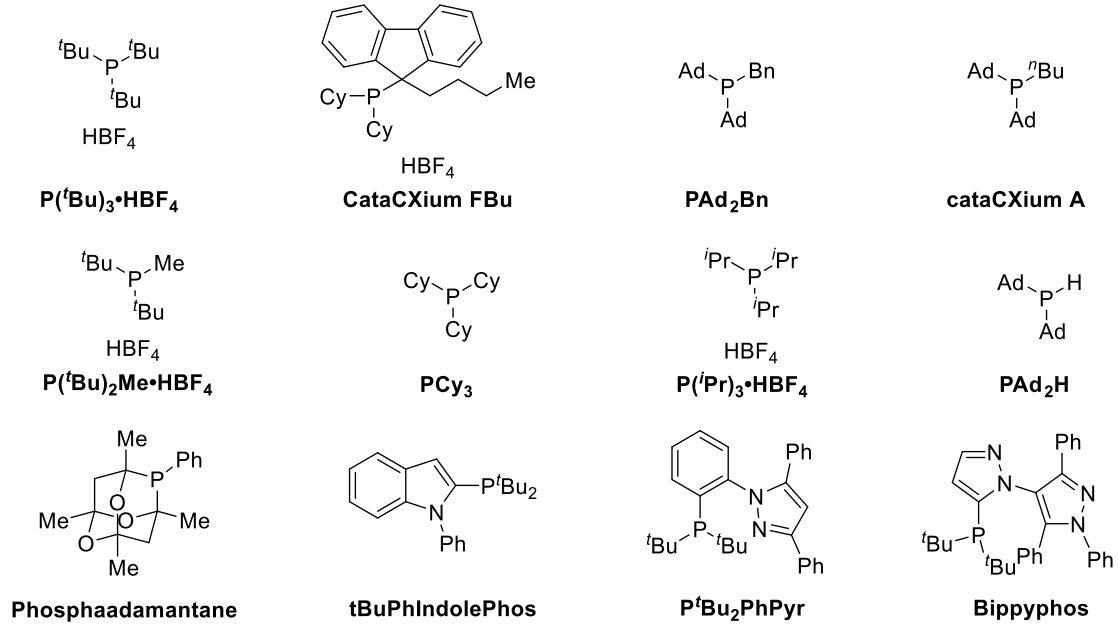
A control reaction was reproduced with each new screening to ensure the reproducibility of the experimental procedure and the quality of the stock solutions.

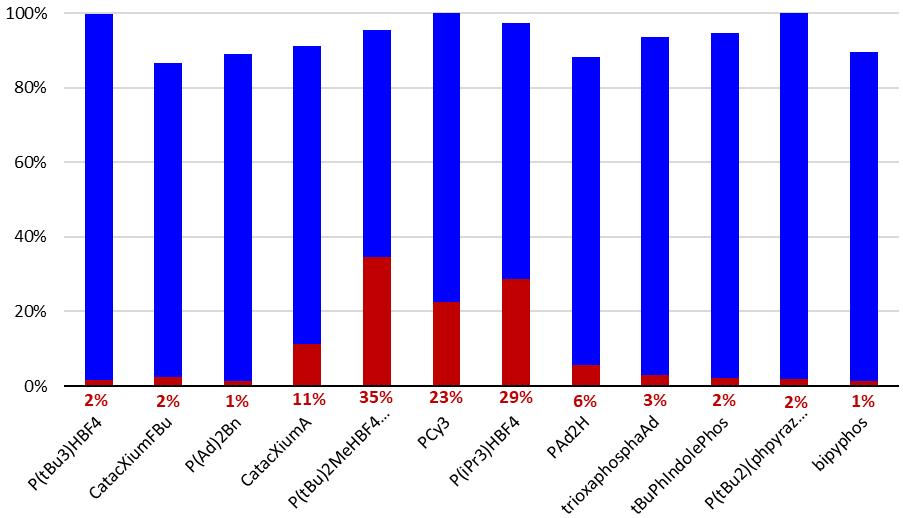
If liquids reagents were required, they were introduced last in the reaction vial, after addition of the solvent or stock solution.

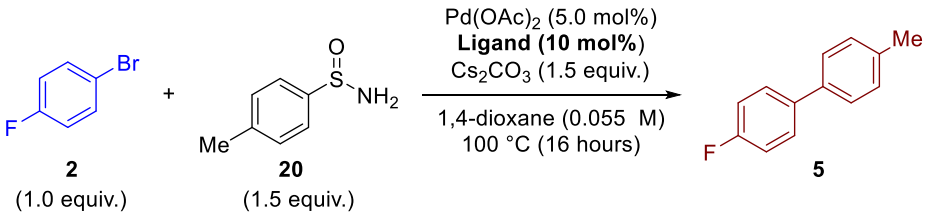
The screening of solvents was performed on a 0.23 mmol scale as stock solutions could not be prepared.

7.5.2. Additional Ligand Screening Data

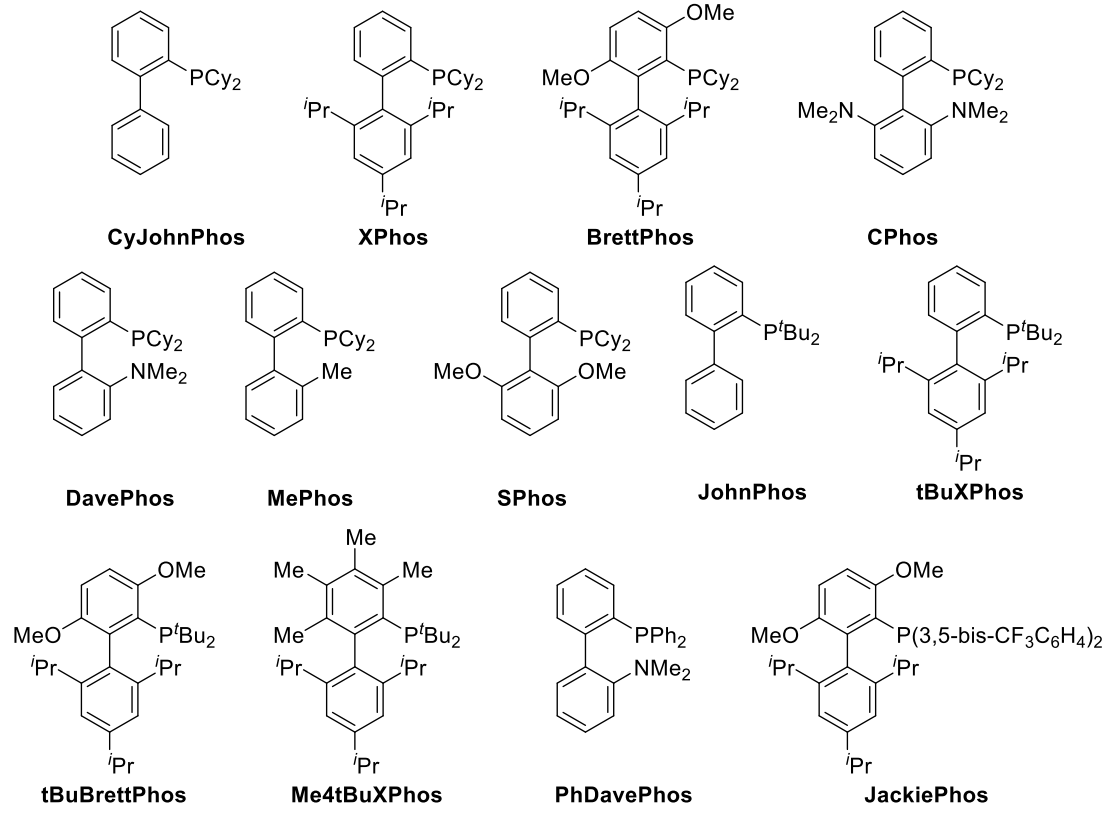


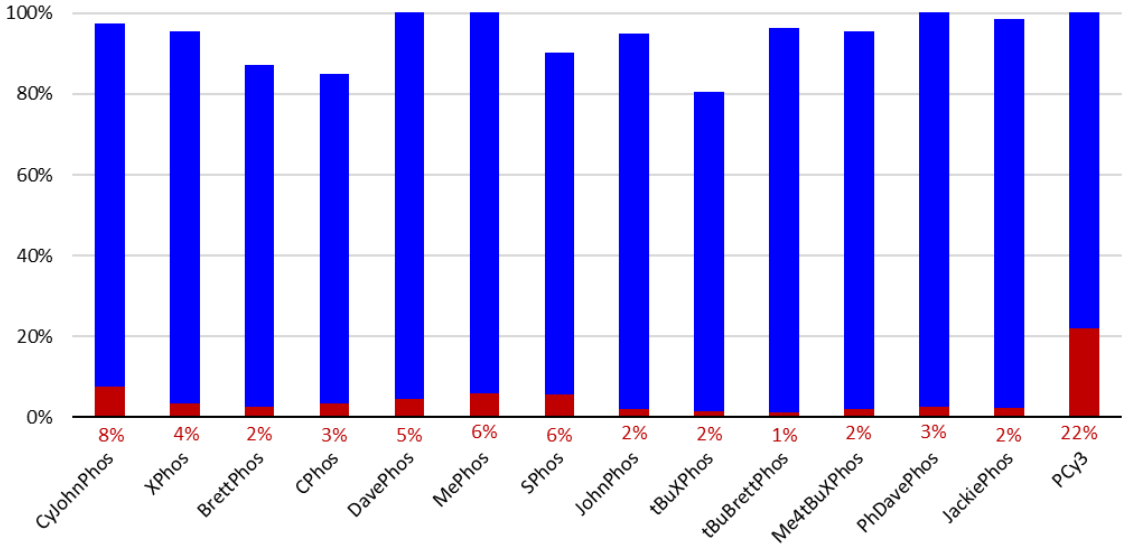


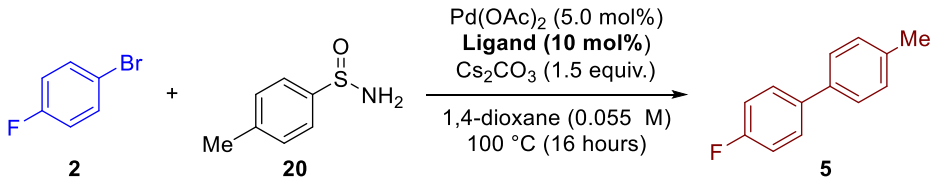




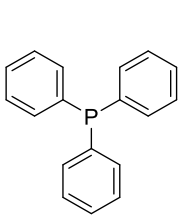
2 (1.0 equiv.) + **20** (1.5 equiv.) → **5**



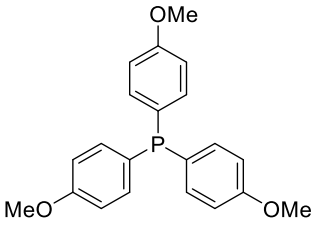




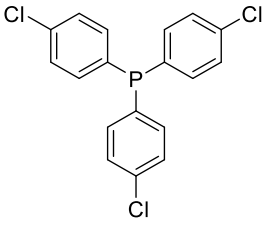
2 (1.0 equiv.) + **20** (1.5 equiv.) → **5**



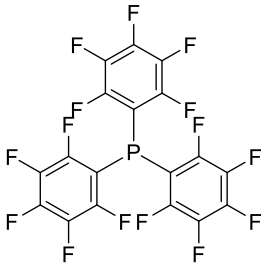
PPh_3



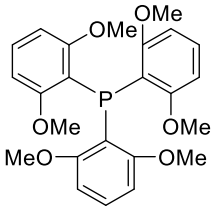
$P(4\text{-}OMe\text{-}C_6H_4)_3$



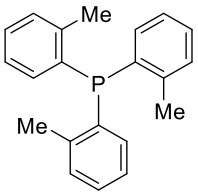
$P(4\text{-}Cl\text{-}C_6H_4)_3$



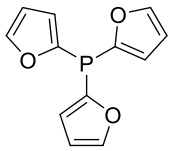
$P(C_6H_5)_3$



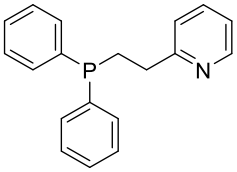
$P(2,6\text{-}bis\text{-}OMe\text{-}C_6H_4)_3$



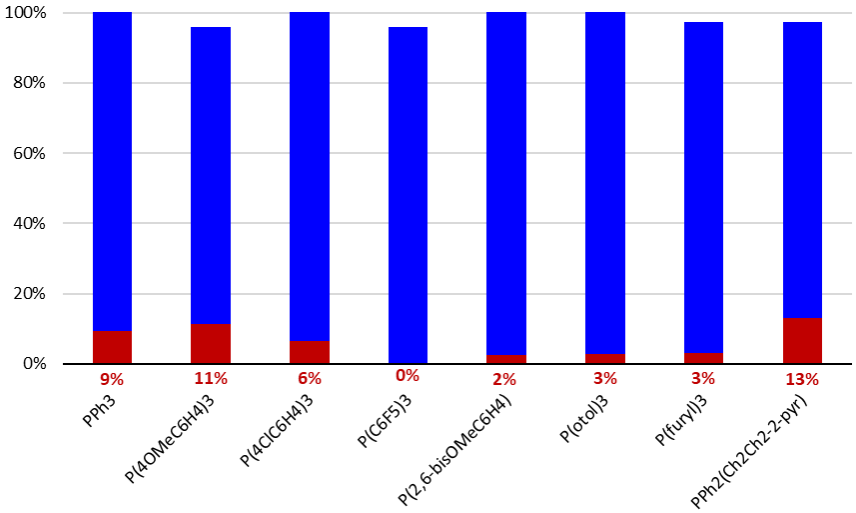
$P(o\text{-}tol)_3$

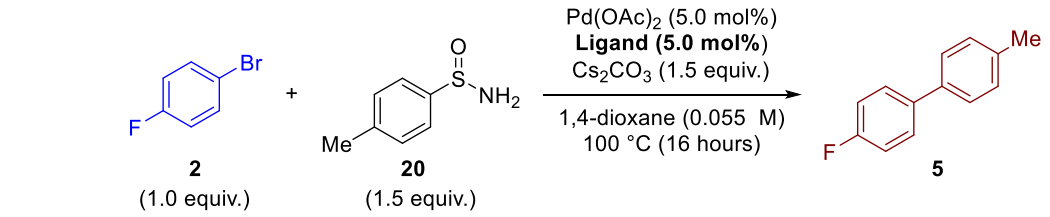


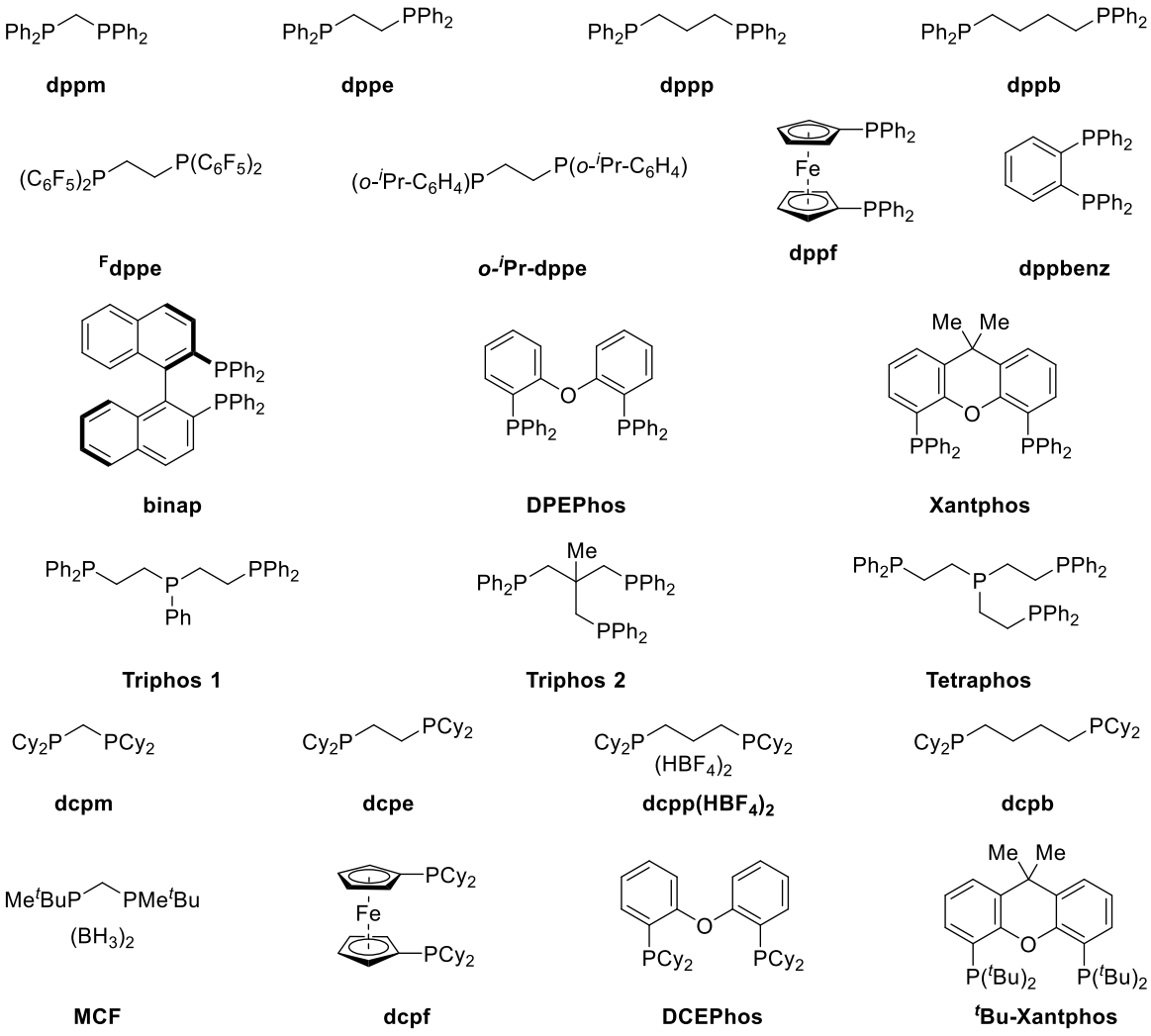
$P(furyl)_3$

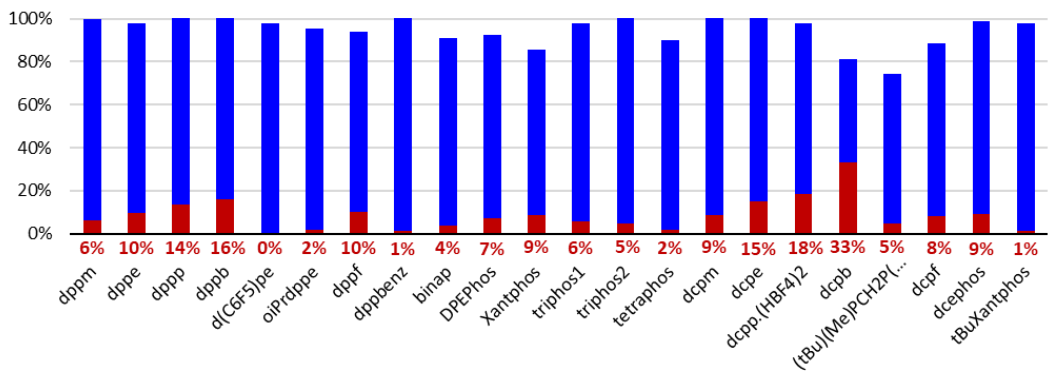


$PPh_2(Et\text{-}2\text{-}pyr)$

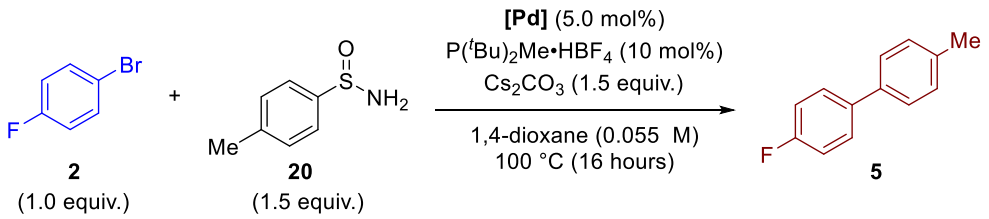


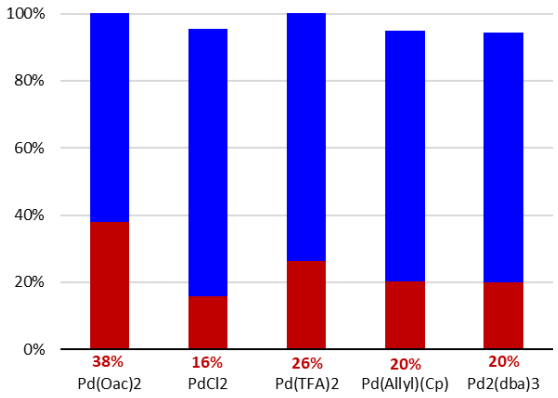

Pd(OAc)2 (5.0 mol%)
Ligand (5.0 mol%)
Cs2CO3 (1.5 equiv.)
1,4-dioxane (0.055 M)
100 °C (16 hours)
2
(1.0 equiv.)
20
(1.5 equiv.)
5

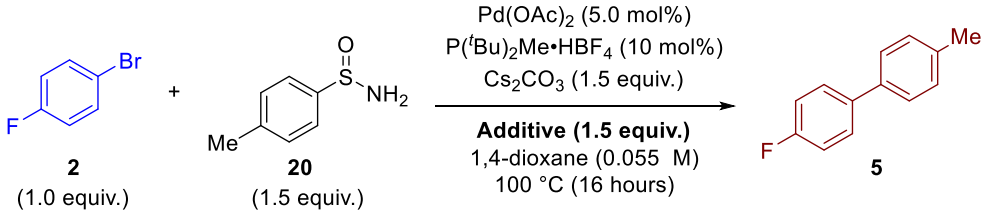

dppm
dppe
dppp
dppb
FdppeF
o-iPr-dppe
dppf
dppbenz
binap
DPEPhos
Xantphos
Triphos 1
Triphos 2
Tetraphos
dcpm
dcpe
dcpp(HBF4)2
dcpb
MCF
dcpf
DCEPhos
tBu-Xantphos

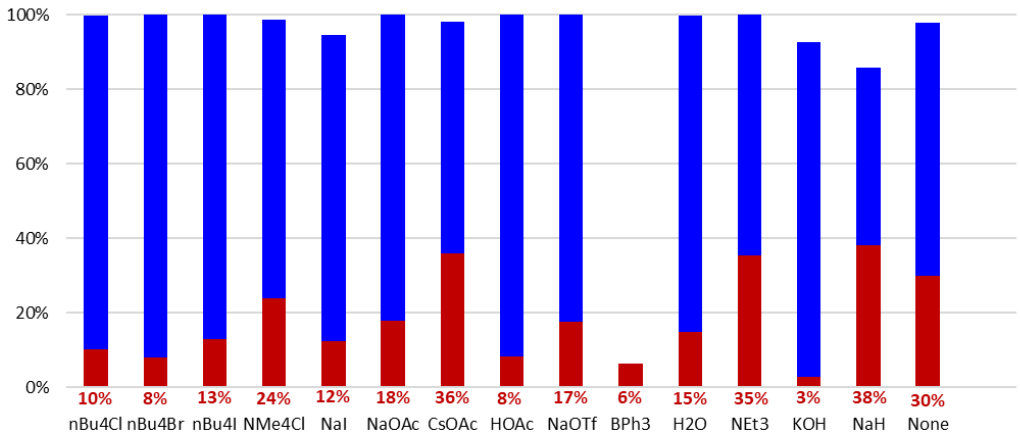

100%
80%
60%
40%
20%
0%
6% 10% 14% 16% 0% 2% 10% 1% 4% 7% 9% 6% 5% 2% 9% 15% 18% 33% 5% 8% 9% 1%
dppm
dppe
dppp
dppb
d(C6F5)pe
oiPrdppe
dppf
dppbenz
binap
DPEPhos
Xantphos
triphos1
triphos2
tetraphos
dcpm
dcpe
dcpp.(HBF4)2
dcpb
(tBu)(Me)PCH2P(...
dcpf
dcephos
tBuXantphos

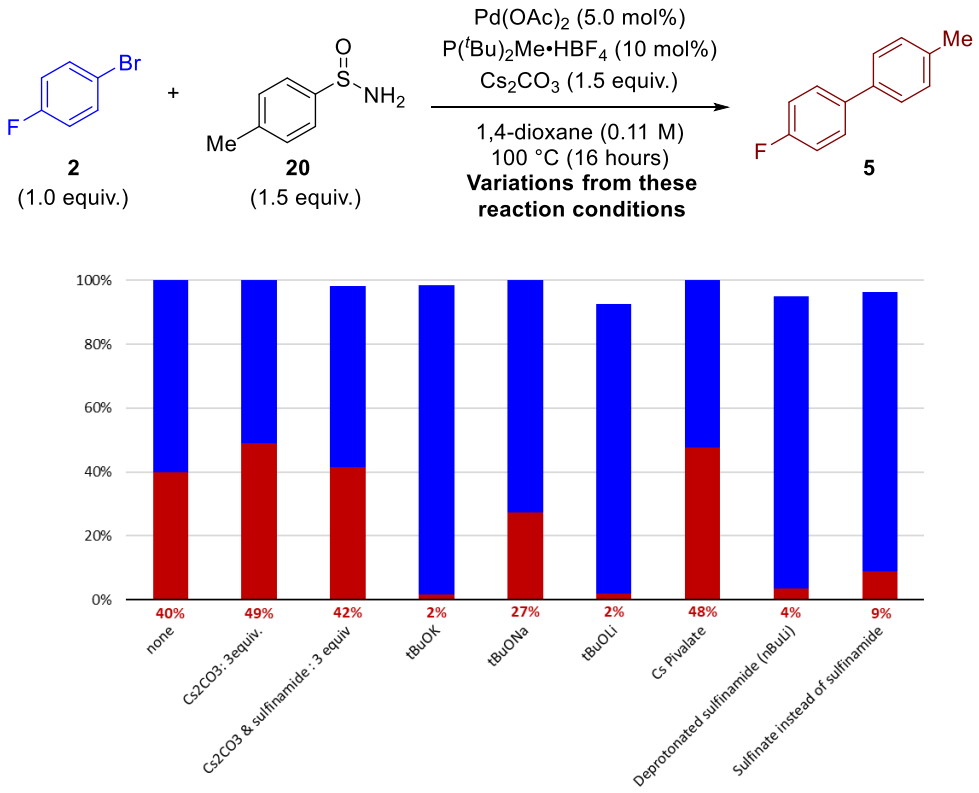
7.5.3. Additional Bar Charts











7.5.4. Preparative Scale and Isolation of the Product 5

4-Methylbenzenesulfinamide (61 mg, 0.39 mmol, 1.3 equiv.), caesium carbonate (255 mg, 0.78 mmol, 1.6 equiv.), palladium acetate (3.4 mg, 0.015 mmol, 0.05 equiv.), di-*tert*-butyl(methyl)phosphonium tetrafluoroborate (7.4 mg, 0.030 mmol, 0.10 equiv.) and 1,3,5-trimethoxybenzene (25 mg, 0.15 mmol, 0.5 equiv.) were added to a microwave vial equipped with a stirrer bar. The vial was sealed with a microwave vial cap, evacuated (< 0.1 mbar) and back-filled with argon twice, then 1,4-dioxane (1.0 mL) and 1-bromo-4-fluorobenzene (33 µL, 0.30 mmol, 1.0 equiv.) were added. The reaction was heated at the indicated temperature for 16 hours. The mixture was allowed to cool to room temperature, then filtered through a pad of silica using EtOAc. The solvents were removed under reduced pressure, and the crude material was purified by column chromatography (gradient of CH_2Cl_2 0% to 2% in petrol) to yield compound **5** white solid. Analytical data matched the one reported in **Section 7.2.1.2.**

100 °C : 41% yield (23 mg, 0.12 mmol); 110 °C : 61% yield (34 mg, 0.18 mmol)

8. References

[1] Beller, M. *Chem. Soc. Rev.* **2011**, *40*, 4891.
[2] Brown, D. G.; Boström, J. *J. Med. Chem.* **2016**, *59*, 4443-4458.
[3] Johansson Seechurn, C. C. C.; Kitching, M. O.; Colacot, T. J.; Snieckus, V. *Angew. Chem. Int. Ed.* **2012**, *51*, 5062-5085.
[4] Li, H.; Johansson Seechurn, C. C. C.; Colacot, T. J. *ACS Catal.* **2012**, *2*, 1147-1164.
[5] Biffis, A.; Centomo, P.; Del Zotto, A.; Zecca, M. *Chem. Rev.* **2018**, *118*, 2249-2295.
[6] Mironenko, R. M.; Belskaya, O. B.; Likholobov, V. A. *Catal. Today* **2020**, *357*, 152-165.
[7] Lindlar, H. *Helv. Chim. Acta* **1952**, *35*, 446-456.
[8] Pearson, R. G. *J. Am. Chem. Soc.* **1963**, *85*, 3533-3539.
[9] Pearson, R. G. *J. Chem. Educ.* **1968**, *45*, 581.
[10] Pearson, R. G. *J. Chem. Educ.* **1968**, *45*, 643.
[11] Hartwig, J. F. *University Science Books, Sausalito* **2010**, ISBN 978-1891389535.
[12] Tolman, C. A. *Chem. Rev.* **1977**, *77*, 313-348.
[13] Tolman, C. A. *J. Am. Chem. Soc.* **1970**, *92*, 2953-2956.
[14] Collman, J. P.; Hegedus, L. S.; Norton, J. R.; Finke, R. G. *Advanced Inorganic Chemistry, 5th ed.* **1988**, Wiley-Interscience: New York, pp 64-65.
[15] Dunne, B. J.; Morris, R. B.; Orpen, A. G. *J. Chem. Soc., Dalton Trans.* **1991**, 653.
[16] Orpen, A. G.; Connelly, N. G. *Organometallics* **1990**, *9*, 1206-1210.
[17] Leyssens, T.; Peeters, D.; Orpen, A. G.; Harvey, J. N. *Organometallics* **2007**, *26*, 2637-2645.
[18] Xiao, S.; Trogler, W. C.; Ellis, D. E.; Berkovitch-Yellin, Z. *J. Am. Chem. Soc.* **1983**, *105*, 7033-7037.
[19] Marynick, D. S. *J. Am. Chem. Soc.* **1984**, *106*, 4064-4065.
[20] Tolman, C. A. *J. Am. Chem. Soc.* **1970**, *92*, 2956-2965.
[21] Fey, N.; Koumi, A.; Malkov, A. V.; Moseley, J. D.; Nguyen, B. N.; Tyler, S. N. G.; Willans, C. E. *Dalton Trans.* **2020**, *49*, 8169-8178.
[22] Durand, D. J.; Fey, N. *Chem. Rev.* **2019**, *119*, 6561-6594.
[23] Fey, N. *Chem. Cent. J.* **2015**, *9*.
[24] Fey, N.; Orpen, A. G.; Harvey, J. N. *Coord. Chem. Rev.* **2009**, *253*, 704-722.
[25] Buchwald, S. L. *Acc. Chem. Res.* **2008**, *41*, 1439-1439.
[26] Dorel, R.; Grugel, C. P.; Haydl, A. M. *Angew. Chem. Int. Ed.* **2019**, *58*, 17118-17129.
[27] Hartwig, J. F. *Nature* **2008**, *455*, 314-322.
[28] Glaser, C. *Ber. Dtsch. Chem. Ges.* **1869**, 422-424.
[29] Hooshmand, S. E.; Heidari, B.; Sedghi, R.; Varma, R. S. *Green Chem.* **2019**, *21*, 381-405.
[30] Knappke, C. E. I.; Jacobi Von Wangelin, A. *Chem. Soc. Rev.* **2011**, *40*, 4948-4962.
[31] Haas, D.; Hammann, J. M.; Greiner, R.; Knochel, P. *ACS Catal.* **2016**, *6*, 1540-1552.
[32] Cordovilla, C.; Bartolomé, C.; Martínez-Ilarduya, J. M.; Espinet, P. *ACS Catal.* **2015**, *5*, 3040-3053.
[33] Komiyama, T.; Minami, Y.; Hiyama, T. *ACS Catal.* **2017**, *7*, 631-651.
[34] Mc Cartney, D.; Guiry, P. J. *Chem. Soc. Rev.* **2011**, *40*, 5122.
[35] Chinchilla, R.; Nájera, C. *Chem. Soc. Rev.* **2011**, *40*, 5084.
[36] Rodriguez, N.; Goossen, L. J. *Chem. Soc. Rev.* **2011**, *40*, 5030-5048.
[37] Goossen, L. J.; Deng, G.-J.; Levy, L. M. *Science* **2006**, *313*, 662-664.
[38] Ortgies, D. H.; Hassanpour, A.; Chen, F.; Woo, S.; Forgione, P. *Eur. J. Org. Chem.* **2016**, *2016*, 408-425.
[39] Kalle, W. *Justus Liebigs Ann. Chem.* **1861**, *119*, 153-164.
[40] Aziz, J.; Messaoudi, S.; Alami, M.; Hamze, A. *Org. Biomol. Chem.* **2014**, *12*, 9743-9759.
[41] Li, H.; Sasmal, A.; Shi, X.; Soulé, J.-F.; Doucet, H. *Org. Biomol. Chem.* **2018**, *16*, 4399-4423.
[42] Kaiser, D.; Klose, I.; Oost, R.; Neuhaus, J.; Maulide, N. *Chem. Rev.* **2019**, *119*, 8701-8780.

[43] Mei, H.; Pajkert, R.; Wang, L.; Li, Z.; Röschenthaler, G.-V.; Han, J. *Green Chem.* **2020**, *22*, 3028-3059.
[44] Liang, S.; Hofman, K.; Friedrich, M.; Manolikakes, G. *Eur. J. Org. Chem.* **2020**, *2020*, 4664-4676.
[45] Cheng, K.; Hu, S.; Zhao, B.; Zhang, X. M.; Qi, C. *J. Org. Chem.* **2013**, *78*, 5022-5025.
[46] Cheng, K.; Yu, H.-Z.; Zhao, B.; Hu, S.; Zhang, X.-M.; Qi, C. *RSC Adv.* **2014**, *4*, 57923-57928.
[47] Chang, S.; Sun, Y. B.; Zhang, X. R.; Dong, L. L.; Zhu, H. Y.; Lai, H. W.; Wang, D. *Appl. Organometal. Chem.* **2018**, *32*, e3970.
[48] Sato, K.; Okoshi, T. *US5159082A* **1992**.
[49] Zhou, C.; Liu, Q.; Li, Y.; Zhang, R.; Fu, X.; Duan, C. *J. Org. Chem.* **2012**, *77*, 10468-10472.
[50] Zhou, C.; Li, Y.; Lu, Y.; Zhang, R.; Jin, K.; Fu, X.; Duan, C. *Chinese J. Chem.* **2013**, *31*, 1269-1273.
[51] Forgione, P.; Ortgies, D.; Barthelme, A.; Aly, S.; Desharnais, B.; Rioux, S. *Synthesis* **2013**, *45*, 694-702.
[52] Forgione, P.; Ortgies, D. *Synlett* **2013**, *24*, 1715-1721.
[53] Colomb, J.; Billard, T. *Tetrahedron Lett.* **2013**, *54*, 1471-1474.
[54] Gund, S. H.; Balsane, K. E.; Nagarkar, J. M. *Tetrahedron* **2016**, *72*, 5051-5056.
[55] Sevigny, S.; Forgione, P. *Chem. Eur. J.* **2013**, *19*, 2256-2260.
[56] Sévigny, S.; Forgione, P. *New J. Chem.* **2013**, *37*, 589-592.
[57] Mangel, D.; Buonomano, C.; Sévigny, S.; Di Censo, G.; Thevendran, G.; Forgione, P. *Heterocycles* **2015**, *90*, 1228-1239.
[58] Markovic, T.; Rocke, B. N.; Blakemore, D. C.; Mascitti, V.; Willis, M. C. *Chem. Sci.* **2017**, *8*, 4437-4442.
[59] Mungalpara, M. N.; Plieger, P. G.; Rowlands, G. J. *Adv. Synth. Catal.* **2020**.
[60] Cook, X. A. F.; de Gombert, A.; McKnight, J.; Pantaine, L. R. E.; Willis, M. C. *Angew. Chem. Int. Ed.* **2020**, *59*, 2-26.
[61] Markovic, T.; Rocke, B. N.; Blakemore, D. C.; Mascitti, V.; Willis, M. C. *Org. Lett.* **2017**, *19*, 6033-6035.
[62] Markovic, T.; Murray, P. R. D.; Rocke, B. N.; Shavnya, A.; Blakemore, D. C.; Willis, M. C. *J. Am. Chem. Soc.* **2018**, *140*, 15916-15923.
[63] Campeau, L.-C.; Rousseaux, S.; Fagnou, K. *J. Am. Chem. Soc.* **2005**, *127*, 18020-18021.
[64] Garves, K. *J. Org. Chem.* **1970**, *35*, 3273-3275.
[65] Rao, B.; Zhang, W.; Hu, L.; Luo, M. *Green Chem.* **2012**, *14*, 3436-3440.
[66] Ortgies, D. H.; Chen, F.; Forgione, P. *Eur. J. Org. Chem.* **2014**, *2014*, 3917-3922.
[67] Yuan, K.; Soulé, J.-F.; Doucet, H. *ACS Catal.* **2015**, *5*, 978-991.
[68] Liu, B.; Guo, Q.; Cheng, Y.; Lan, J.; You, J. *Chem. Eur. J.* **2011**, *17*, 13415-13419.
[69] Chen, R.; Liu, S.; Liu, X.; Yang, L.; Deng, G.-J. *Org. Biomol. Chem.* **2011**, *9*, 7675.
[70] Wang, M.; Li, D.; Zhou, W.; Wang, L. *Tetrahedron* **2012**, *68*, 1926-1930.
[71] Wu, M.; Luo, J.; Xiao, F.; Zhang, S.; Deng, G.-J.; Luo, H.-A. *Adv. Synth. Catal.* **2012**, *354*, 335-340.
[72] Miao, T.; Li, P.; Wang, G.-W.; Wang, L. *Chem. Asian. J.* **2013**, *8*, 3185-3190.
[73] Wang, S.; Liu, W.; Lin, J.; Jiang, Y.; Zhang, Q.; Zhong, Y. *Synlett* **2014**, *25*, 586-590.
[74] Wang, C.; Jia, H.; Li, Z.; Zhang, H.; Zhao, B. *RSC Adv.* **2016**, *6*, 21814-21821.
[75] Tang, X.; Yang, K.; Zeng, L.; Liu, Q.; Chen, H. *Org. Biomol. Chem.* **2017**, *15*, 8504-8507.
[76] Miao, T.; Wang, L. *Adv. Synth. Catal.* **2014**, *356*, 429-436.
[77] Lin, X.; You, Y.; Weng, Z. *J. Fluor. Chem.* **2014**, *165*, 76-80.
[78] Peters, W. *Ber. Dtsch. Chem. Ges.* **1905**, *38*, 2565.
[79] Pesci, L. *Atti. Accad. Nazionale Lincei* **1901**, *10*, 362-363.
[80] Pesci, L. *J. Chem. Soc., Abstr.* **1901**, *80*, 576.
[81] Cookson, P. G.; Deacon, G. B. *J. Organomet. Chem.* **1971**, *27*, C9-C10.

[82] Sraj, L. O. C.; Khairallah, G. N.; da Silva, G.; O'Hair, R. A. J. *Organometallics* **2012**, *31*, 1801-1807.
[83] Wang, Z.; Yang, Y.; Donnelly, P. S.; Canty, A. J.; O'Hair, R. A. J. *J. Organomet. Chem.* **2019**, *882*, 42-49.
[84] Vitzthum, G.; Lindner, E. *Angew. Chem. Int. Ed.* **1971**, *10*, 315-326.
[85] Chiswell, B.; Venanzi, L. M. *J. Chem. Soc. A* **1966**, *0*, 1246-1248.
[86] Dudley, C. W.; Oldham, C. *Inorganica Chim. Acta* **1969**, *3*, 3-7.
[87] Yamamoto, K.; Shono, T.; Shinra, K. *J. Chem. Soc. Japan* **1967**, *88*.
[88] Gates, D. P.; White, P. S.; Brookhart, M. *Chem. Commun.* **2000**, 47-48.
[89] Cámpora, J.; López, J. A.; Palma, P.; Del Rio, D.; Carmona, E.; Valerga, P.; Graiff, C.; Tiripicchio, A. *Inorg. Chem.* **2001**, *40*, 4116-4126.
[90] Li, K.; Guzei, I. A.; Darkwa, J. *Polyhedron* **2003**, *22*, 805-810.
[91] Shrestha, R.; Brennessel, W. W.; Weix, D. J. *Acta Crystallogr Sect E Struct Rep Online* **2011**, *e67*, m1830.
[92] Shavnya, A.; Hesp, K. D.; Mascitti, V.; Smith, A. C. *Angew. Chem., Int. Ed.* **2015**, *54*, 13571-13575.
[93] Behrends, M.; Sävmarker, J.; Sjöberg, P. J. R.; Larhed, M. *ACS Catal.* **2011**, *1*, 1455-1459.
[94] Skillinghaug, B.; Skold, C.; Rydfjord, J.; Svensson, F.; Behrends, M.; Savmarker, J.; Sjoberg, P. J.; Larhed, M. *J. Org. Chem.* **2014**, *79*, 12018-12032.
[95] Yu, H.-Z.; Fu, F.; Zhang, L.; Fu, Y.; Dang, Z.-M.; Shi, J. *Phys. Chem. Chem. Phys.* **2014**, *16*, 20964-20970.
[96] Barrios-Landeros, F.; Carrow, B. P.; Hartwig, J. F. *J. Am. Chem. Soc.* **2009**, *131*, 8141-8154.
[97] Ariafard, A.; Lin, Z. *Organometallics* **2006**, *25*, 4030-4033.
[98] Galardon, E.; Ramdeehul, S.; Brown, J. M.; Cowley, A.; Hii, K. K.; Jutand, A. *Angew. Chem. Int. Ed.* **2002**, *41*, 1760-1763.
[99] Negishi, E.-i.; Takahashi, T.; Akiyoshi, K. *J. Organomet. Chem.* **1987**, *334*, 181-194.
[100] PéRez-RodríGuez, M. N.; Braga, A. A. C.; Garcia-Melchor, M.; PéRez-Temprano, M. N. H.; Casares, J. A.; Ujaque, G.; De Lera, A. R.; ÁLvarez, R.; Maseras, F.; Espinet, P. *J. Am. Chem. Soc.* **2009**, *131*, 3650-3657.
[101] Ananikov, V. P.; Musaev, D. G.; Morokuma, K. *Eur. J. Inorg. Chem.* **2007**, *2007*, 5390-5399.
[102] Xue, L.; Lin, Z. *Chem. Soc. Rev.* **2010**, *39*, 1692-1705.
[103] Wei, C. S.; Davies, G. H.; Soltani, O.; Albrecht, J.; Gao, Q.; Pathirana, C.; Hsiao, Y.; Tummala, S.; Eastgate, M. D. *Angew. Chem., Int. Ed.* **2013**, *52*, 5822-5826.
[104] Batsanov, A. S.; Collings, J. C.; Fairlamb, I. J. S.; Holland, J. P.; Howard, J. A. K.; Lin, Z.; Marder, T. B.; Parsons, A. C.; Ward, R. M.; Zhu, J. *J. Org. Chem.* **2005**, *70*, 703-706.
[105] Tymonko, S. A.; Smith, R. C.; Ambrosi, A.; Ober, M. H.; Wang, H.; Denmark, S. E. *J. Am. Chem. Soc.* **2015**, *137*, 6200-6218.
[106] Grushin, V. V.; Alper, H. *J. Am. Chem. Soc.* **1995**, *117*, 4305-4315.
[107] Thomas, A. A.; Denmark, S. E. *Science* **2016**, *352*, 329-332.
[108] de Gombert, A.; McKay, A. I.; Davis, C. J.; Wheelhouse, K. M.; Willis, M. C. *J. Am. Chem. Soc.* **2020**, *142*, 3564-3576.
[109] de Gombert, A.; Willis, M. C. *Trends Chem.* **2020**, *2*, 865-866.
[110] Amatore, C.; Jutand, A.; Amine M'Barki, M. *Organometallics* **1992**, *11*, 3009-3013.
[111] Norton, D. M.; Mitchell, E. A.; Botros, N. R.; Jessop, P. G.; Baird, M. C. *J. Org. Chem.* **2009**, *74*, 6674-6680.
[112] Li, H.; Grasa, G. A.; Colacot, J. *Org. Lett.* **2010**, *12*, 3332-3335.
[113] Amatore, C.; Jutand, A. *Acc. Chem. Res.* **2000**, *33*, 314-321.
[114] Negishi, E.; Takahashi, T.; Akiyoshi, K. *J. Chem. Soc., Chem. Comm.* **1986**, 1338-1339.
[115] Milstein, D.; Stille, J. K. *J. Am. Chem. Soc.* **1979**, *101*, 4992-4998.
[116] Steinhoff, B. A.; Stahl, S. S. *Org. Lett.* **2002**, *4*, 4179-4181.
[117] Louie, J.; Hartwig, J. F. *Angew. Chem., Int. Ed.* **1996**, *35*, 2359-2361.
[118] Huang, X.; Anderson, K. W.; Zim, D.; Jiang, L.; Klapars, A.; Buchwald, S. L. *J. Am. Chem. Soc.* **2003**, *125*, 6653-6655.

[119] Thirupathi, N.; Amoroso, D.; Bell, A.; Protasiewicz, J. D. *Organometallics* **2007**, *26*, 3157-3166.
[120] Higashi, L. S.; Lundeen, M.; Hilti, E.; Seff, K. *Inorg. Chem.* **1977**, *16*, 310-313.
[121] Stambuli, J. P.; Incarvito, C. D.; Bühl, M.; Hartwig, J. F. *J. Am. Chem. Soc.* **2004**, *126*, 1184-1194.
[122] Baker, S. J. *Thesis submitted in accordance with the requirements of the University of Cardiff for the degree of Doctor in Philosophy* **2007**, UMI Number: U584975.
[123] Mitchell, E. A.; Jessop, P. G.; Baird, M. C. *Organometallics* **2009**, *28*, 6732-6738.
[124] Grushin, V. V.; Bensimon, C.; Alper, H. *Inorg. Chem.* **1994**, *33*, 4804-4806.
[125] Lindsell, W. E.; Palmer, D. D.; Preston, P. N.; Rosair, G. M.; Jones, R. V. H.; Whitton, A. J. *Organometallics* **2005**, *24*, 1119-1133.
[126] Hartwig, J. F. *Angew. Chem., Int. Ed.* **1998**, *37*, 2046-2067.
[127] Widenhoefer, R. A.; Buchwald, S. L. *J. Am. Chem. Soc.* **1998**, *120*, 6504-6511.
[128] Widenhoefer, R. A.; Zhong, H. A.; Buchwald, S. L. *J. Am. Chem. Soc.* **1997**, *119*, 6787-6795.
[129] Klinkenberg, J. L.; Hartwig, J. F. *J. Am. Chem. Soc.* **2010**, *132*, 11830-11833.
[130] Arrechea, P. L.; Buchwald, S. L. *J. Am. Chem. Soc.* **2016**, *138*, 12486-12493.
[131] Alvaro, E.; Hartwig, J. F. *J. Am. Chem. Soc.* **2009**, *131*, 7858-7868.
[132] Arroniz, C.; Denis, J. G.; Ironmonger, A.; Rassias, G.; Larrosa, I. *Chem. Sci.* **2014**, *5*, 3509-3514.
[133] Casado, J.; Lopez-Quintela, M. A.; Lorenzo-Barral, F. M. *J. Chem. Educ.* **1986**, *63*, 450-452.
[134] Phan, N. T. S.; Van Der Sluys, M.; Jones, C. W. *Adv. Synth. Catal.* **2006**, *348*, 609-679.
[135] Mpungose, P.; Vundla, Z.; Maguire, G.; Friedrich, H. *Molecules* **2018**, *23*, 1676-1700.
[136] Gorunova, O. N.; Novitskiy, I. M.; Grishin, Y. K.; Gloriozov, I. P.; Roznyatovsky, V. A.; Khrustalev, V. N.; Kochetkov, K. A.; Dunina, V. V. *Organometallics* **2018**, *37*, 2842-2858.
[137] Chernyshev, V. M.; Astakhov, A. V.; Chikunov, I. E.; Tyurin, R. V.; Eremin, D. B.; Ranny, G. S.; Khrustalev, V. N.; Ananikov, V. P. *ACS Catal.* **2019**, *9*, 2984-2995.
[138] ArBr (1.0 equiv.), Ar'SO_2Na (2.0 equiv.), K_2CO_3 (1.5 equiv.), $Pd(OAc)_2$ (5 mol%), PCy_3 (10 mol%), 1,4-dioxane (0.05 M).
[139] F. van Strijdonck, G. P.; Boele, M. D. K.; Kamer, P. C. J.; de Vries, J. G.; van Leeuwen, P. W. N. M. *Eur. J. Inorg. Chem.* **1999**, *1999*, 1073-1076.
[140] Sewell, L. J.; Huertos, M. A.; Dickinson, M. E.; Weller, A. S.; Lloyd-Jones, G. C. *Inorg. Chem.* **2013**, *52*, 4509-4516.
[141] Rosner, T.; Le Bars, J.; Pfaltz, A.; Blackmond, D. G. *J. Am. Chem. Soc.* **2001**, *123*, 1848-1855.
[142] Dias, E. L.; Nguyen, S. T.; Grubbs, R. H. *J. Am. Chem. Soc.* **1997**, *119*, 3887-3897.
[143] Marshall, J. E.; Keister, J. B.; Diver, S. T. *Organometallics* **2011**, *30*, 1319-1321.
[144] Emmett, E. J.; Hayter, B. R.; Willis, M. C. *Angew. Chem., Int. Ed.* **2014**, *53*, 10204-10208.
[145] An, Y.; Xia, H.; Wu, J. *Org. Biomol. Chem.* **2016**, *14*, 1665-1669.
[146] Nguyen, B.; Emmett, E. J.; Willis, M. C. *J. Am. Chem. Soc.* **2010**, *132*, 16372-16373.
[147] Richards-Taylor, C. S.; Blakemore, D. C.; Willis, M. C. *Chem. Sci.* **2014**, *5*, 222-228.
[148] Shavnya, A.; Coffey, S. B.; Smith, A. C.; Mascitti, V. *Org. Lett.* **2013**, *15*, 6226-6229.
[149] Ye, S.; Wu, J. *Chem. Commun.* **2012**, *48*, 10037-10039.
[150] Anthony, E. J.; Granatstein, D. L. *Prog. Energy Combust. Sci.* **2001**, *27*, 215-236.
[151] Wappel, D.; Joswig, S.; Khan, A. A.; Smith, K. H.; Kentish, S. E.; Shallcross, D. C.; Stevens, G. W. *Int. J. Greenhouse Gas. Control.* **2011**, *5*, 1454-1459.
[152] Kimura, S.; Smith, J. M. *AIChE J.* **1987**, *33*, 1522-1532.
[153] Beccalli, E. M.; Broggini, G.; Martinelli, M.; Sottocornola, S. *Chem. Rev.* **2007**, *107*, 5318-5365.
[154] Zhu, C.; Liu, J.; Li, M.-B.; Bäckvall, J.-E. *Chem. Soc. Rev.* **2020**, *49*, 341-353.
[155] Pye, D. R.; Mankad, N. P. *Chem. Sci.* **2017**, *8*, 1705-1718.
[156] Suzuki, H.; Abe, H. *Tetrahedron Lett.* **1995**, *36*, 6239-6242.
[157] Ge, X.; Sun, F.; Liu, X.; Chen, X.; Qian, C.; Zhou, S. *Mol. Catal.* **2018**, *449*, 72-78.

[158] Becica, J.; Dobereiner, G. E. *ACS Catal.* **2017**, *7*, 5862-5870.
[159] Davis, H. J.; Phipps, R. J. *Chem. Sci.* **2017**, *8*, 864-877.
[160] Davis, H. J.; Mihai, M. T.; Phipps, R. J. *J. Am. Chem. Soc.* **2016**, *138*, 12759-12762.
[161] Ohmatsu, K.; Ito, M.; Kunieda, T.; Ooi, T. *Nat. Chem.* **2012**, *4*, 473-477.
[162] Allen, C. L.; Leitch, D. C.; Anson, M. S.; Zajac, M. A. *Nat. Catal.* **2019**, *2*, 2-4.
[163] Mennen, S. M.; Alhambra, C.; Allen, C. L.; Barberis, M.; Berritt, S.; Brandt, T. A.; Campbell, A. D.; Castañón, J.; Cherney, A. H.; Christensen, M.; Damon, D. B.; Eugenio De Diego, J.; García-Cerrada, S.; García-Losada, P.; Haro, R.; Janey, J.; Leitch, D. C.; Li, L.; Liu, F.; Lobben, P. C.; Macmillan, D. W. C.; Magano, J.; McInturff, E.; Monfette, S.; Post, R. J.; Schultz, D.; Sitter, B. J.; Stevens, J. M.; Strambeanu, I. I.; Twilton, J.; Wang, K.; Zajac, M. A. *Org. Process Res. Dev.* **2019**, *23*, 1213-1242.
[164] Cacchi, S.; Fabrizi, G.; Goggiamani, A.; Parisi, L. M. *Synlett* **2003**, 0361-0364.
[165] Kranenburg, M.; van der Burgt, Y. E. M.; Kamer, P. C. J.; van Leeuwen, P. W. N. M.; Goubitz, K.; Fraanje, J. *Organometallics* **1995**, *14*, 3081-3089.
[166] Birkholz, M.-N.; Freixa, Z.; van Leeuwen, P. W. N. M. *Chem. Soc. Rev.* **2009**, *38*, 1099-1118.
[167] van Leeuwen, P. W. N. M.; Kamer, P. C. J.; Reek, J. N. H.; Dierkes, P. *Chem. Rev.* **2000**, *100*, 2741-2770.
[168] Kranenburg, M.; G. P. Delis, J.; C. J. Kamer, P.; W. N. M. van Leeuwen, P.; Vrieze, K.; Veldman, N.; L. Spek, A.; Goubitz, K.; Fraanje, J. *J. Chem. Soc., Dalton Trans.* **1997**, 1839-1850.
[169] Yin, J.; Buchwald, S. L. *J. Am. Chem. Soc.* **2002**, *124*, 6043-6048.
[170] Zuideveld, M. A.; Swennenhuis, B. H. G.; Boele, M. D. K.; Guari, Y.; van Strijdonck, G. P. F.; Reek, J. N. H.; Kamer, P. C. J.; Goubitz, K.; Fraanje, J.; Lutz, M.; Spek, A. L.; van Leeuwen, P. W. N. M. *J. Chem. Soc., Dalton Trans.* **2002**, 2308-2317.
[171] Guari, Y.; van Strijdonck, G. P. F.; Boele, M. D. K.; Reek, J. N. H.; Kamer, P. C. J.; van Leeuwen, P. W. N. M. *Chem. Eur. J.* **2001**, *7*, 475-482.
[172] Fujita, K.-i.; Yamashita, M.; Puschmann, F.; Alvarez-Falcon, M. M.; Incarvito, C. D.; Hartwig, J. F. *J. Am. Chem. Soc.* **2006**, *128*, 9044-9045.
[173] Grushin, V. V.; Marshall, W. J. *J. Am. Chem. Soc.* **2006**, *128*, 12644-12645.
[174] Bakhmutov, V. I.; Bozoglian, F.; Gómez, K.; González, G.; Grushin, V. V.; Macgregor, S. A.; Martin, E.; Miloserdov, F. M.; Novikov, M. A.; Panetier, J. A.; Romashov, L. V. *Organometallics* **2012**, *31*, 1315-1328.
[175] Cacchi, S.; Fabrizi, G.; Goggiamani, A.; Parisi, L. M. *Org. Lett.* **2002**, *4*, 4719-4721.
[176] Liu, N.-W.; Liang, S.; Margraf, N.; Shaaban, S.; Luciano, V.; Drost, M.; Manolikakes, G. *Eur. J. Org. Chem.* **2018**, *2018*, 1208-1210.
[177] Cacchi, S.; Fabrizi, G.; Goggiamani, A.; Parisi, L. M.; Bernini, R. *J. Org. Chem.* **2004**, *69*, 5608-5614.
[178] Emmett, E. J.; Hayter, B. R.; Willis, M. C. *Angew. Chem., Int. Ed.* **2013**, *52*, 12679-12683.
[179] Kong, K. C.; Cheng, C. H. *J. Am. Chem. Soc.* **1991**, *113*, 6313-6315.
[180] Hamann, B. C.; Hartwig, J. F. *J. Am. Chem. Soc.* **1998**, *120*, 3694-3703.
[181] Goodson, F. E.; Wallow, T. I.; Novak, B. M. *J. Am. Chem. Soc.* **1997**, *119*, 12441-12453.
[182] Hartwig, J. F. *Acc. Chem. Res.* **1998**, *31*, 852-860.
[183] Yamashita, M.; Cuevas Vicario, J. V.; Hartwig, J. F. *J. Am. Chem. Soc.* **2003**, *125*, 16347-16360.
[184] Hartwig, J. F. *Inorg. Chem.* **2007**, *46*, 1936-1947.
[185] Zheng, Z.; Wu, T.; Zhou, X. *Chem. Commun.* **2006**, 1864.
[186] Den Heeten, R.; Zuidema, E.; Lutz, M.; Spek, A. L.; Van Leeuwen, P. W. N. M.; Kamer, P. C. J. *J. Organomet. Chem.* **2011**, *696*, 3113-3120.
[187] Freixa, Z.; Beentjes, M. S.; Batema, G. D.; Dieleman, C. B.; Van Strijdonck, G. P. F.; Reek, J. N. H.; Kamer, P. C. J.; Fraanje, J.; Goubitz, K.; Van Leeuwen, P. W. N. M. *Angew. Chem. Int. Ed.* **2003**, *42*, 1284-1287.
[188] Whiteker, G. T.; Li, F.; Froese, R. D. J.; Tulchinsky, M. L.; Hazari, A.; Klosin, J. *Organometallics* **2019**, *38*, 2233-2238.

[189] Hicks, J. D.; Hyde, A. M.; Cuezva, A. M.; Buchwald, S. L. *J. Am. Chem. Soc.* **2009**, *131*, 16720-16734.
[190] Barder, T. E.; Buchwald, S. L. *J. Am. Chem. Soc.* **2007**, *129*, 5096-5101.
[191] Ji, Y.; Plata, R. E.; Regens, C. S.; Hay, M.; Schmidt, M.; Razler, T.; Qiu, Y.; Geng, P.; Hsiao, Y.; Rosner, T.; Eastgate, M. D.; Blackmond, D. G. *J. Am. Chem. Soc.* **2015**, *137*, 13272-13281.
[192] Lo, P. K. T.; Oliver, G. A.; Willis, M. C. *J. Org. Chem.* **2020**, *85*, 5753-5760.
[193] Chatterjee, S.; Makai, S.; Morandi, B. *Angew. Chem. Int. Ed.* **2021**, *60*, 758-765.
[194] Ruiz-Castillo, P.; Buchwald, S. L. *Chem. Rev.* **2016**, *116*, 12564-12649.
[195] Bonifácio, V. D. B.; Kumar, R. P.; Prabhakar, S.; Lobo, A. M. *Arkivoc* **2011**, *(x)*, 266-276.
[196] Sun, X.; Tu, X.; Dai, C.; Zhang, X.; Zhang, B.; Zeng, Q. *J. Org. Chem.* **2012**, *77*, 4454-4459.
[197] Gimenez, D.; Dose, A.; Robson, N. L.; Sandford, G.; Cobb, S. L.; Coxon, C. R. *Org. Biomol. Chem.* **2017**, *15*, 4081-4085.
[198] Olmstead, W. N.; Margolin, Z.; Bordwell, F. G. *J. Org. Chem.* **1980**, *45*, 3295-3299.
[199] Wolfe, J. P.; Buchwald, S. L. *J. Org. Chem.* **2000**, *65*, 1144-1157.
[200] Shekhar, S.; Ryberg, P.; Hartwig, J. F.; Mathew, J. S.; Blackmond, D. G.; Strieter, E. R.; Buchwald, S. L. *J. Am. Chem. Soc.* **2006**, *128*, 3584-3591.
[201] Beitia, J. *Synlett* **2011**, *2011*, 139-140.
[202] Ravalico, F.; James, S. L.; Vyle, J. S. *Green Chem.* **2011**, *13*, 1778.
[203] Fleckenstein, C. A.; Plenio, H. *Chem. Soc. Rev.* **2010**, *39*, 694-711.
[204] Jover, J.; Cirera, J. *Dalton Trans.* **2019**, *48*, 15036-15048.
[205] Martin, R.; Buchwald, S. L. *Acc. Chem. Res.* **2008**, *41*, 1461-1473.
[206] Ackermann, M.; Pascariu, A.; Höcher, T.; Siehl, H.-U.; Berger, S. *J. Am. Chem. Soc.* **2006**, *128*, 8434-8440.
[207] Surry, D. S.; Buchwald, S. L. *Angew. Chem. Int. Ed.* **2008**, *47*, 6338-6361.
[208] Old, D. W.; Wolfe, J. P.; Buchwald, S. L. *J. Am. Chem. Soc.* **1998**, *120*, 9722-9723.
[209] Crawford, S. M.; Lavery, C. B.; Stradiotto, M. *Chem. Eur. J.* **2013**, *19*, 16760-16771.
[210] Issleib, K.; Müller, D.-W. *Chem. Ber.* **1959**, *92*, 3175-3182.
[211] Tatsuno, Y.; Yoshida, T.; Otsuka, S.; Al-Salem, N.; Shaw, B. L. *Inorg. Synth.* **1990**, 342-345.
[212] Amatore, C.; Carré, E.; Jutand, A.; Amine M'Barki, M.; Meyer, G. *Organometallics* **1995**, *14*, 5605-5614.
[213] Goossen, L. J.; Koley, D.; Hermann, H. L.; Thiel, W. *J. Am. Chem. Soc.* **2005**, *127*, 11102-11114.
[214] Vertesaljai, P.; Navaratne, P. V.; Grenning, A. J. *Angew. Chem., Int. Ed.* **2016**, *55*, 317-320.
[215] Kurotobi, K.; Murata, Y. *Science* **2011**, *333*, 613-616.
[216] Baskin, J. M.; Wang, Z. *Tetrahedron Lett.* **2002**, *43*, 8479-8483.
[217] Thirupathi, N.; Amoroso, D.; Bell, A.; Protasiewicz, J. D. *Organometallics* **2007**, *26*, 3157-3166.
[218] Ackermann, L.; Potukuchi, H. K.; Kapdi, A. R.; Schulzke, C. *Chem. Eur. J.* **2010**, *16*, 3300-3303.
[219] Agrawal, T.; Cook, S. P. *Org. Lett.* **2014**, *16*, 5080-5083.
[220] Yuan, B.; Pan, Y.; Li, Y.; Yin, B.; Jiang, H. *Angew. Chem., Int. Ed.* **2010**, *49*, 4054-4058.
[221] Yu, J.; Liu, J.; Shi, G.; Shao, C.; Zhang, Y. *Angew. Chem., Int. Ed.* **2015**, *54*, 4079-4082.
[222] Cosier, J.; Glazer, A. M. *J. Appl. Cryst.* **1986**, *19*, 105-107.
[223] Oxford Diffraction Ltd., Oxford Diffraction Ltd., 2011.
[224] Sheldrick, G. M. *Acta Cryst. A* **2015**, *71*, 3-8.
[225] Sheldrick, G. M. *Acta. Cryst.* **2015**, *A71*, 3-8.
[226] Sheldrick, G. M. *Acta. Cryst.* **2015**, *C71*, 3-8.
[227] Dolomanov, O. V.; Bourhis, L. J.; Gildea, R. J.; Howard, J. A. K.; Puschmann, H. *J. Appl. Cryst.* **2009**, *42*, 339-341.
[228] Kratzert, D.; Holstein, J. J.; Krossing, I. *J. Appl. Cryst.* **2015**, *48*, 933-938.

[229] Kratzert, D.; Krossing, I. *J. Appl. Cryst.* **2018**, *51*, 928-934.
[230] Chawla, R.; Yadav, L. D. S. *Org. Biomol. Chem.* **2019**, *17*, 4761-4766.
[231] Bandgar, B. P.; Bettigeri, S. V.; Phopase, J. *Org. Lett.* **2004**, *6*, 2105-2108.
[232] Forgione, P.; Chen, F.; Chacón-Huete, F.; El-Husseini, H. *Synthesis* **2018**, *50*, 1914-1920.
[233] Torregrosa, R. R. P. *Encyclopedia of Reagents for Organic Synthesis* **2013**, 10.1002/047084289x.rn01566.
[234] Yao, X.; Jin, L.; Rao, Y. *Asian J. Org. Chem.* **2017**, *6*, 825-830.
[235] Carpino, L. A.; Xia, J.; Zhang, C.; El-Faham, A. *J. Org. Chem.* **2004**, *69*, 62-71.
[236] Yang, G.-H.; Zheng, H.; Li, X.; Cheng, J.-P. *ACS Catal.* **2020**, *10*, 2324-2333.
[237] Borowski, P.; Stankevič, M.; Strzelecka, D.; Bąk, O. *Synthesis* **2018**, *50*, 4922-4932.
[238] Beaud, R.; Phipps, R. J.; Gaunt, M. J. **2016**, *138*, 13183-13186.
[239] Qi, N.; Zhang, N.; Allu, S. R.; Gao, J.; Guo, J.; He, Y. *Org. Lett.* **2016**, *18*, 6204-6207.
[240] Chiu, G.; Li, S.; Connolly, P. J.; Pulito, V.; Liu, J.; Middleton, S. A. *Bioorg. Med. Chem.* **2007**, *17*, 3930-3934.
[241] Wang, Y.; Zhang, P.; Di, X.; Dai, Q.; Zhang, Z.-M.; Zhang, J. *Angew. Chem. Int. Ed.* **2017**, *56*, 15905-15909.

9. NMR Spectra

Table of Contents

9.1. Compounds of Chapter 2 **277**

9.1.1. Biaryl Products 277

9.1.2. Palladium Complexes 282

9.1.3. Sulfinate Salts 305

9.2. Compounds of Chapter 3 **321**

9.2.1. Sulfone Products 321

9.2.2. Cationic Phosphine Ligands 325

9.3. Compounds of Chapter 4 **341**

9.3.1. Oxidative Addition Complex **19** 341

9.3.2. Novel Phosphinic Acids 343

9.3.3. (5-Iodo-9,9-dimethyl-9*H*-xanthen-4-yl)diphenylphosphane 349

9.3.4. Ligands **L1**-**L13** 350

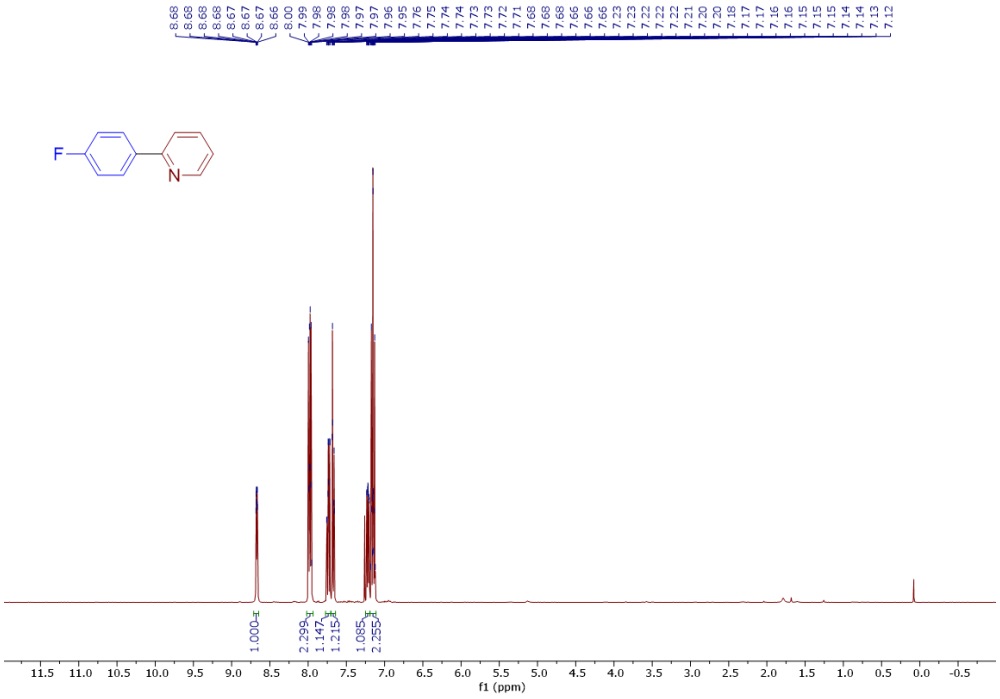
9.3.5. Other Novel Phosphine Ligands 370

9.1. Compounds of Chapter 2

9.1.1. Biaryl Products

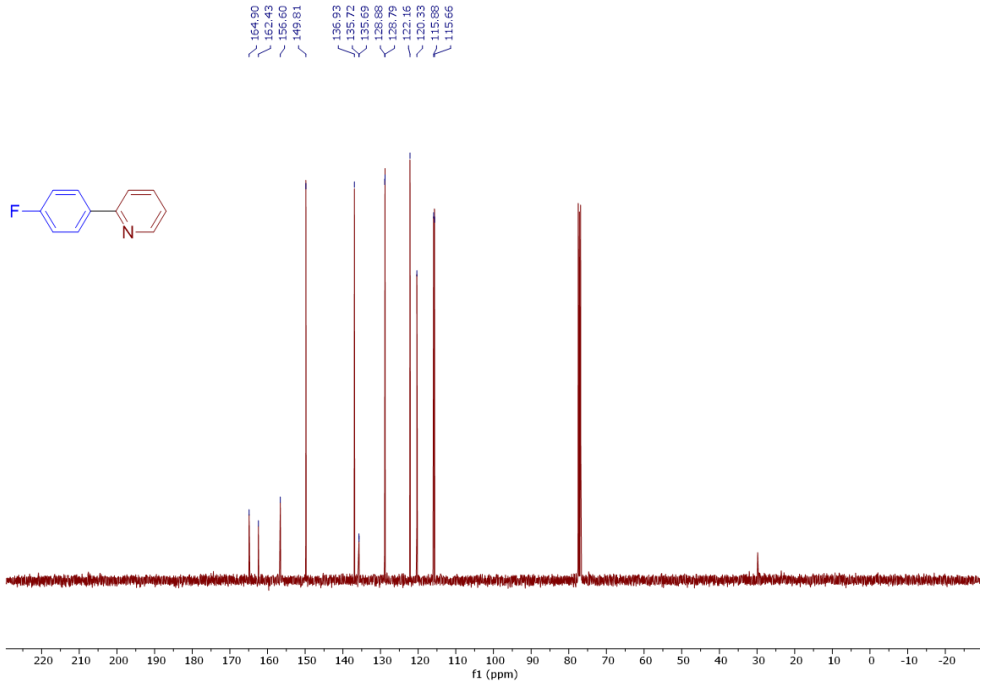
2-(4-fluorophenyl)pyridine (3)

^{1}H NMR (400 MHz, $CDCl_3$)



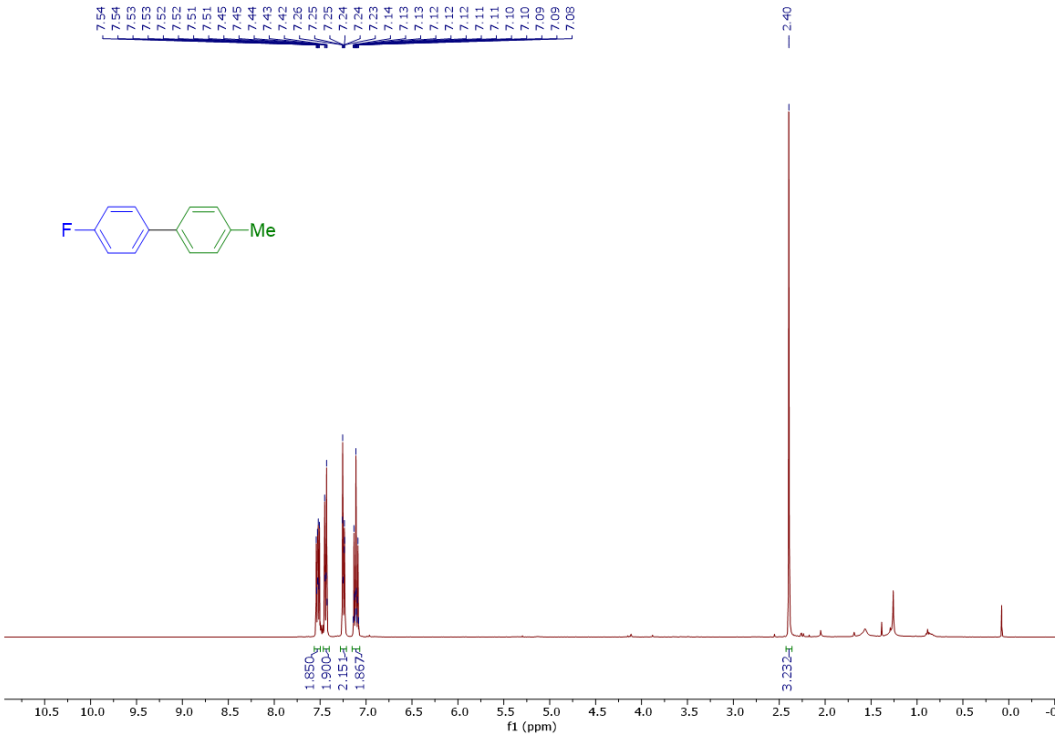
2-(4-fluorophenyl)pyridine (3)

^{13}C{^{1}H} NMR (101 MHz, $CDCl_3$)



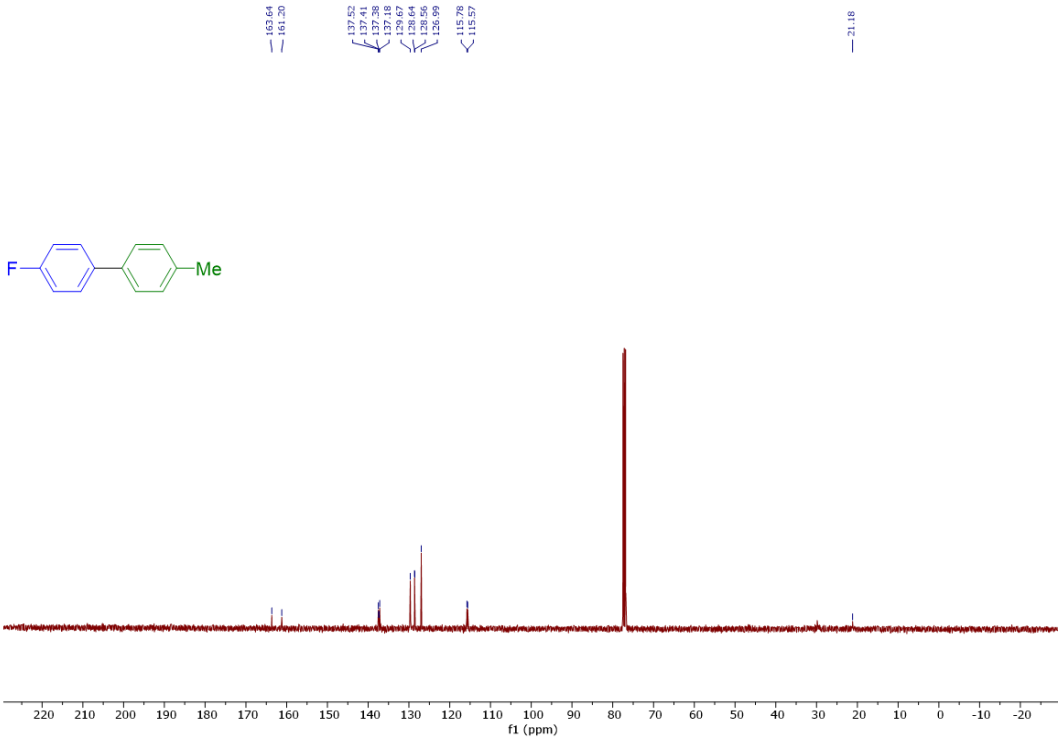
4-fluoro-4'-methyl-1,1'-biphenyl (5)

^{1}H NMR (400 MHz, $CDCl_3$)



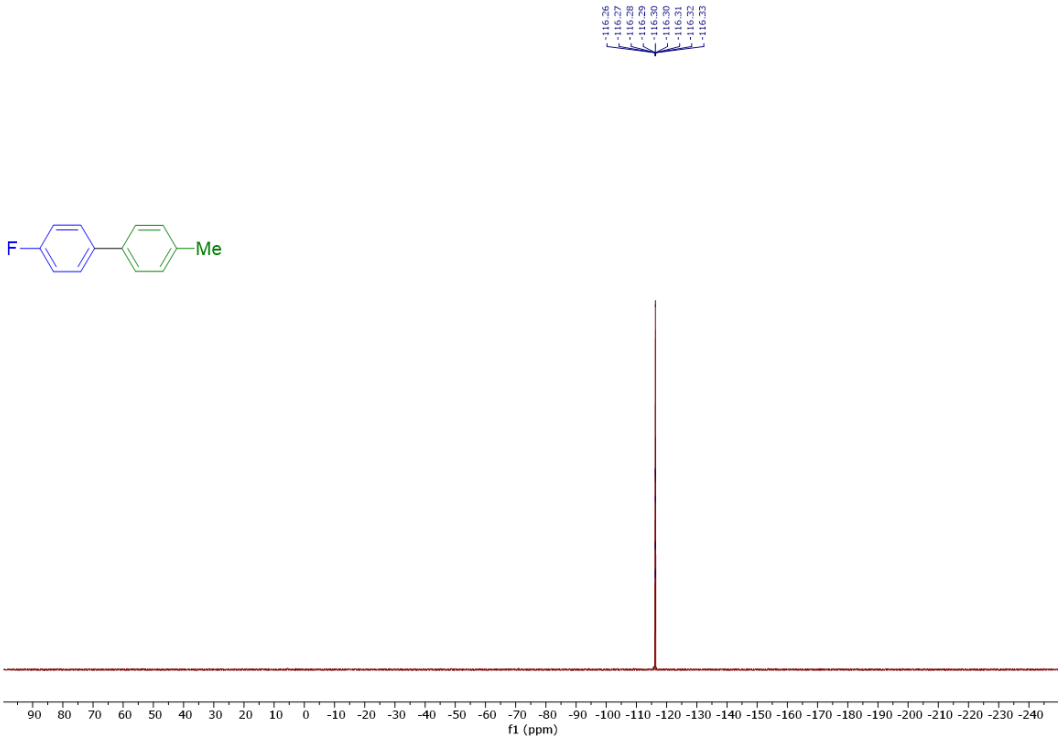
4-fluoro-4'-methyl-1,1'-biphenyl (5)

^{13}C{^{1}H} NMR (101 MHz, $CDCl_3$)



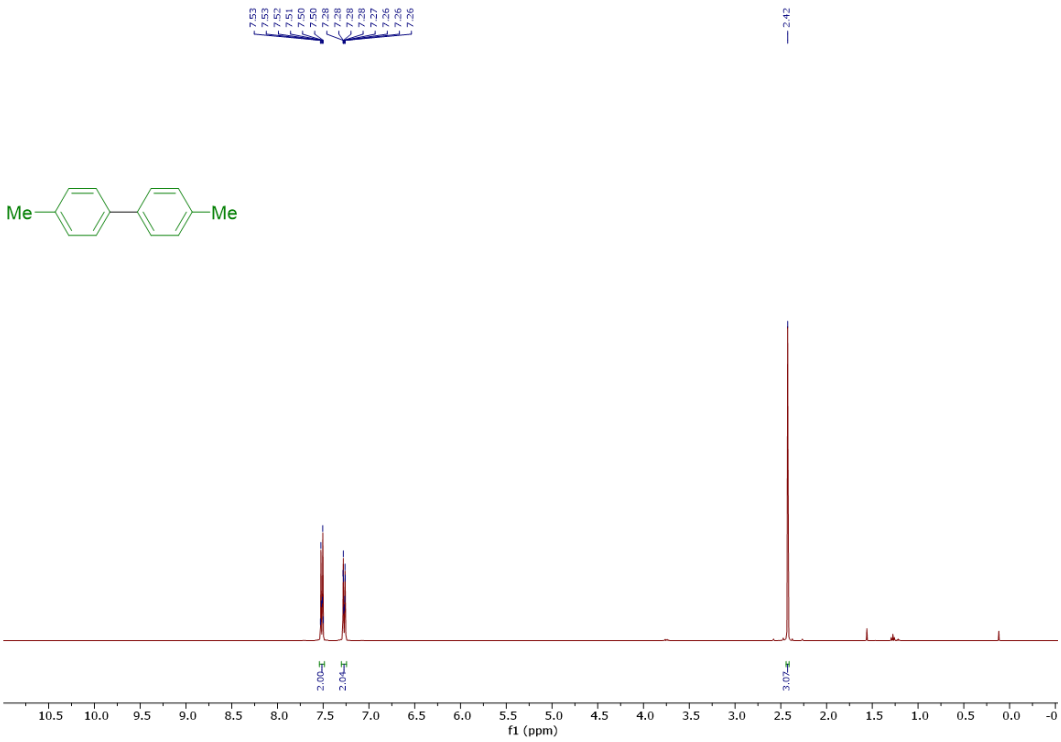
4-fluoro-4'-methyl-1,1'-biphenyl (5)

^{19}F NMR (377 MHz, $CDCl_3$)



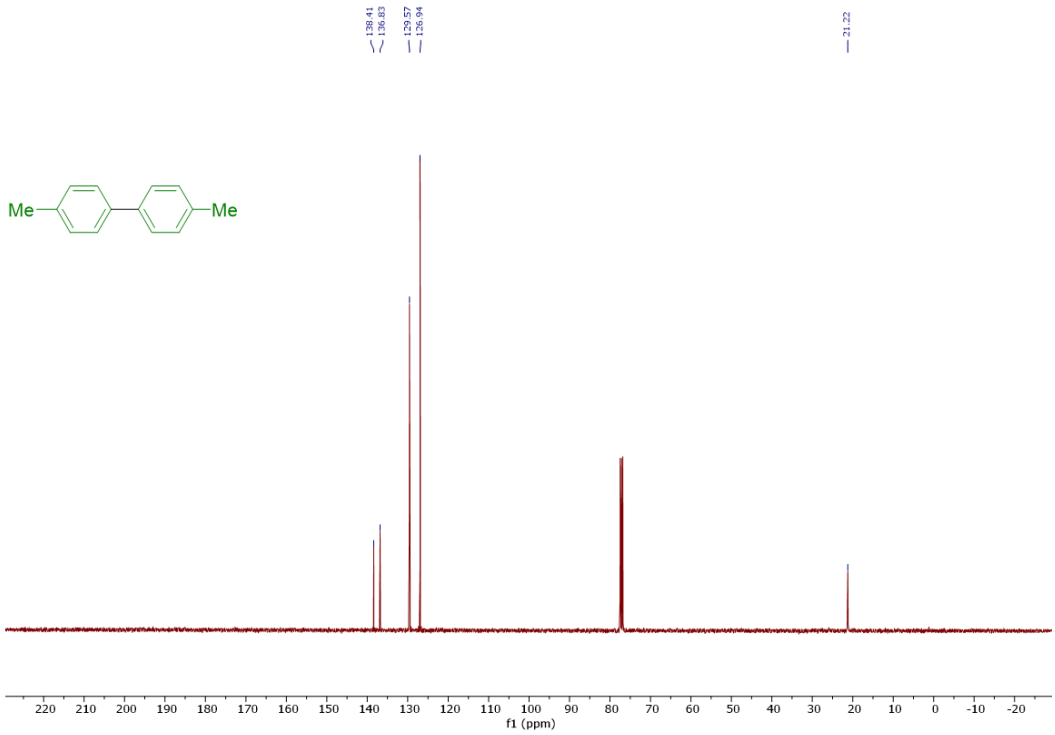
4,4'-dimethyl-1,1'-biphenyl (5b)

^{1}H NMR (400 MHz, $CDCl_3$)



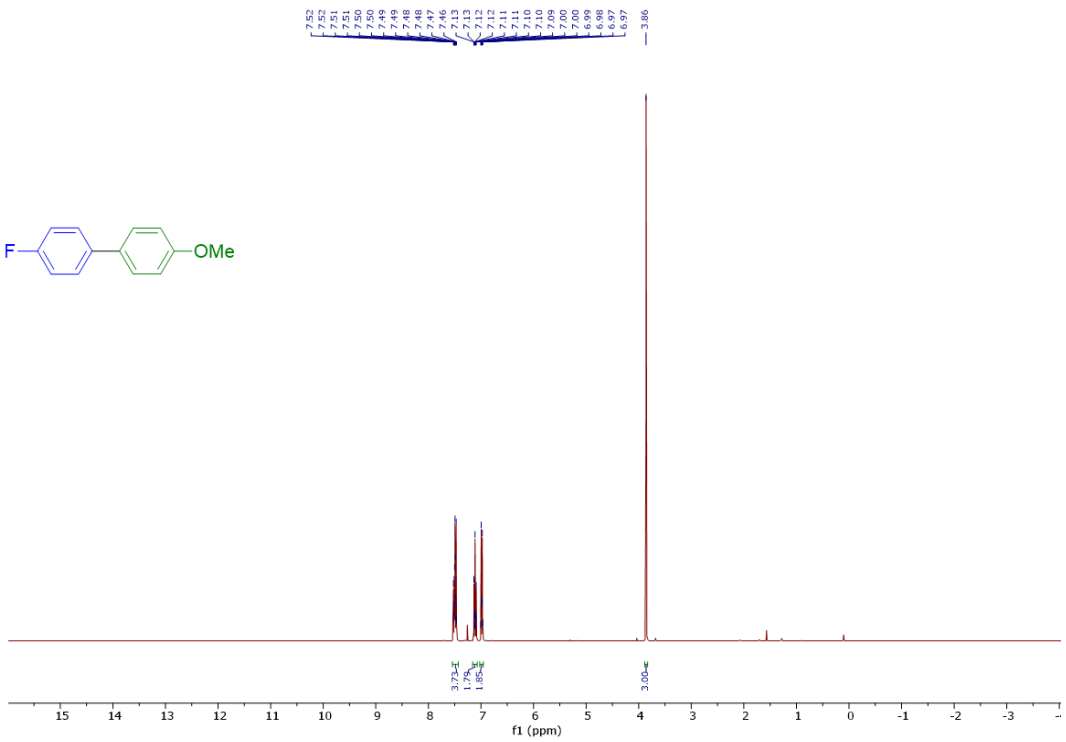
4,4'-dimethyl-1,1'-biphenyl (5b)

$^{13}C\{^{1}H\}$ NMR (101 MHz, $CDCl_3$)



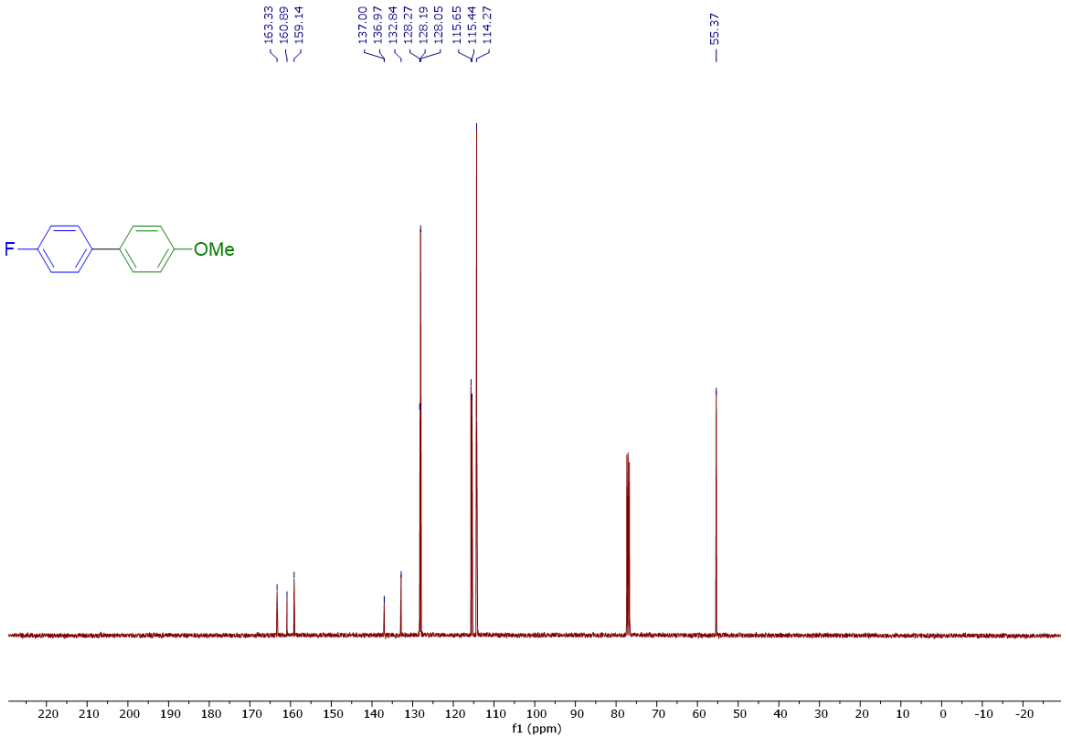
4-Fluoro-4'-methoxy-1,1'-biphenyl (5-OMe)

^{1}H NMR (400 MHz, $CDCl_3$)



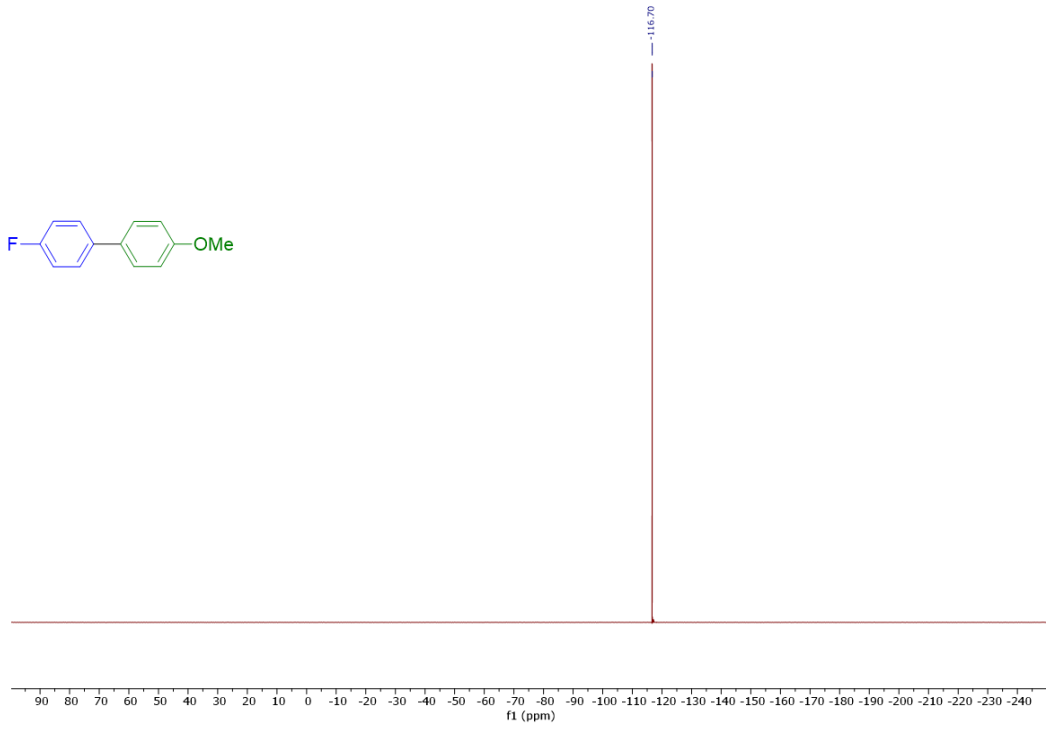
4-Fluoro-4'-methoxy-1,1'-biphenyl (5-OMe)

$^{13}C\{^{1}H\}$ NMR (101 MHz, $CDCl_3$)



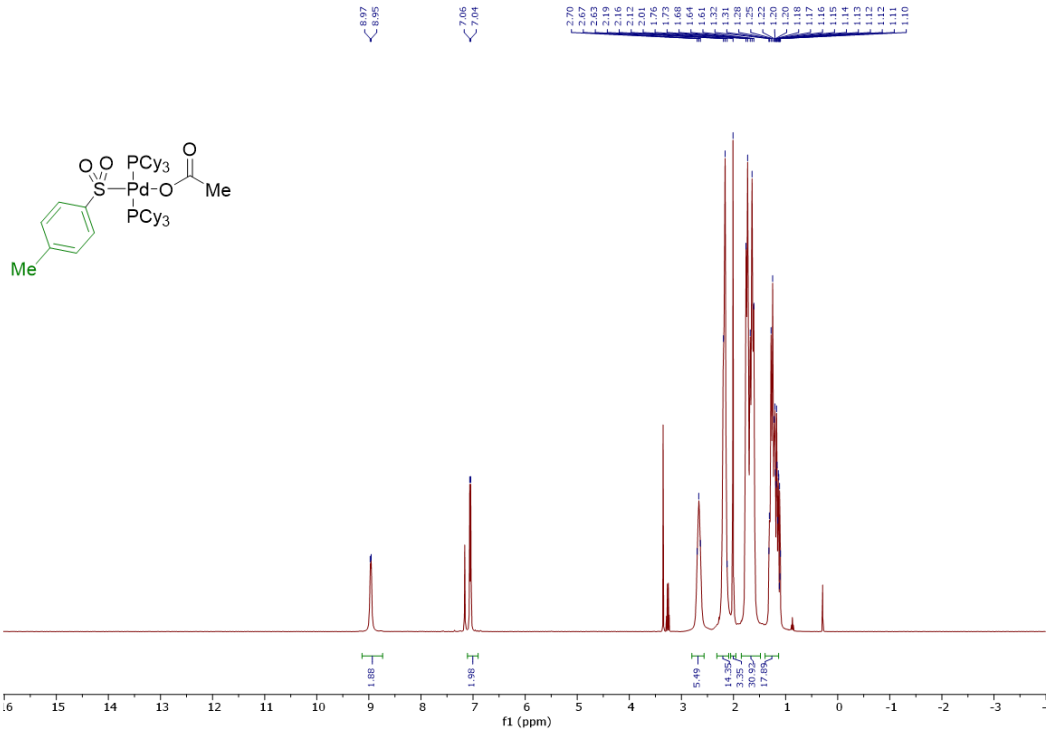
4-Fluoro-4'-methoxy-1,1'-biphenyl (5-OMe)

$^{19}F\{^{1}H\}$ NMR (377 MHz, $CDCl_3$)

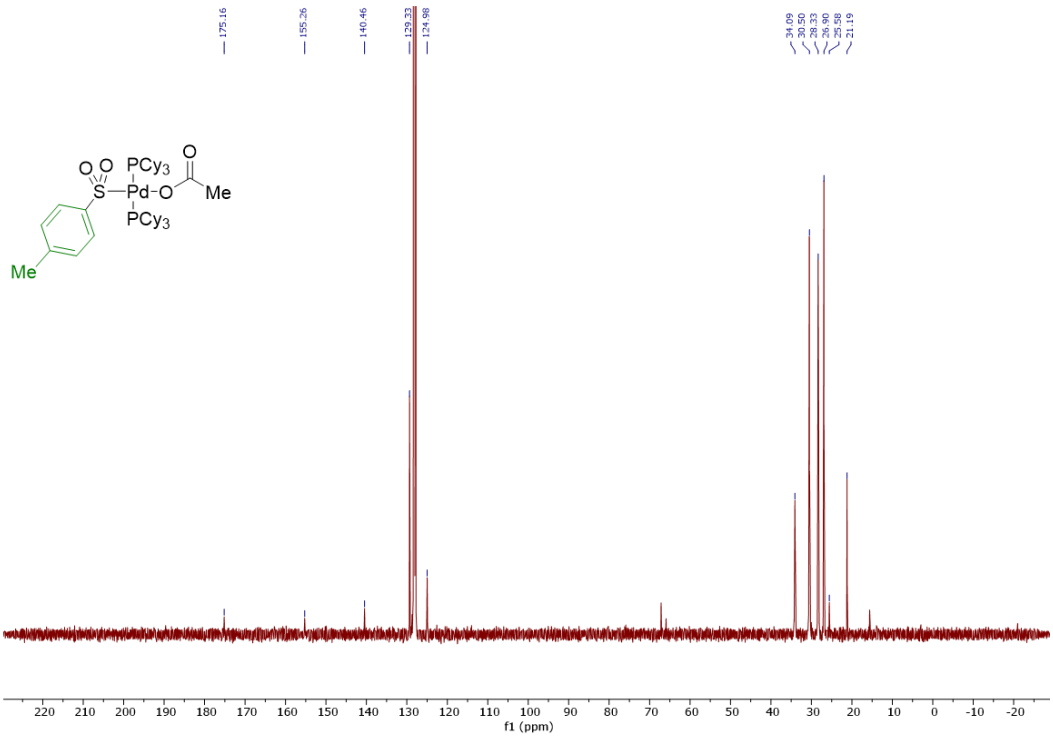


9.1.2. Palladium Complexes

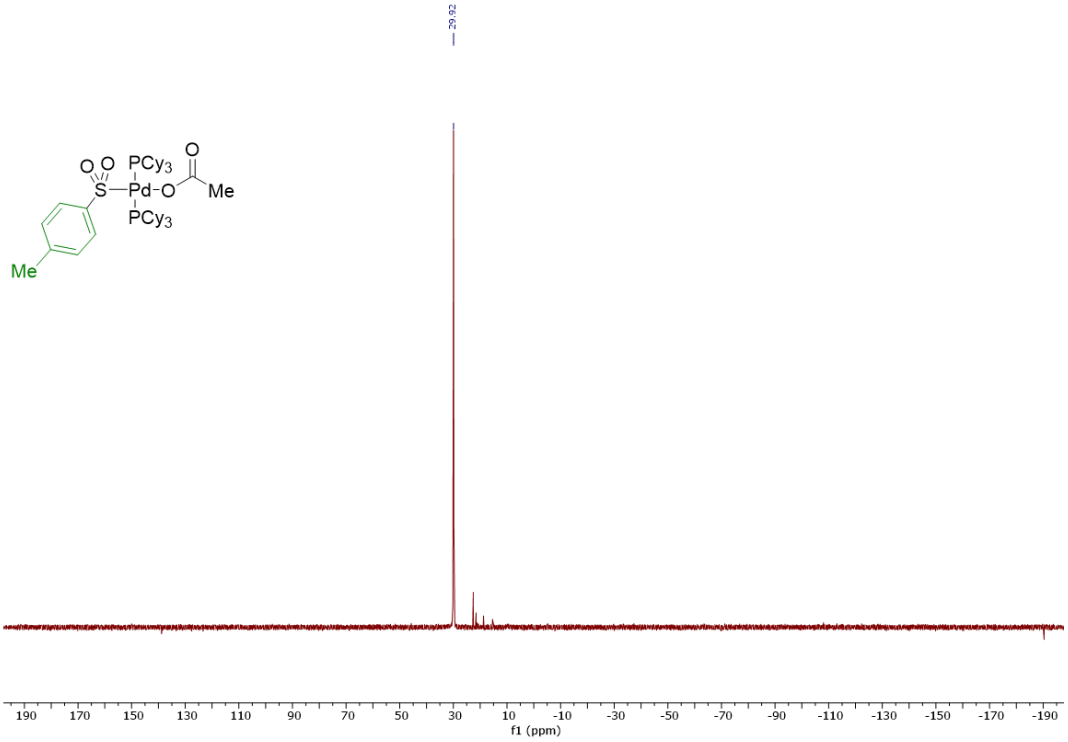
[Pd(OAc)(PCy$_3$)$_2$)(κ$_S$-4-CH$_3$-C$_6$H$_4$-SO$_2$)] (7)
^{1}H NMR (400 MHz, C_6D_6)



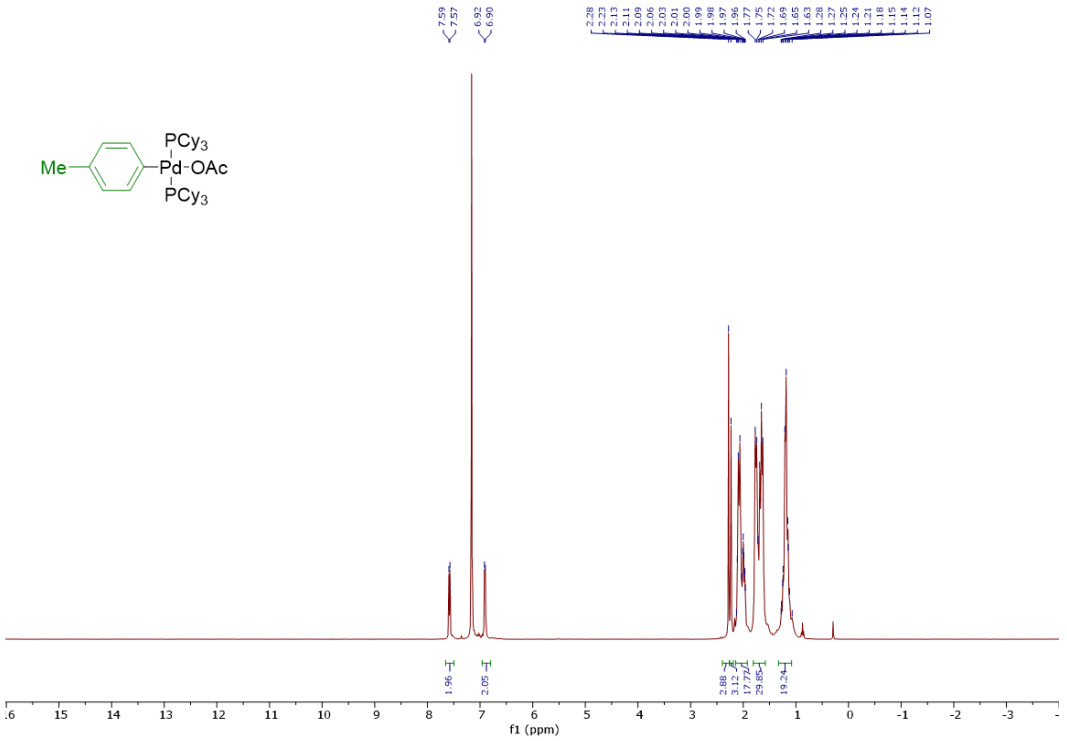
[Pd(OAc)(PCy$_3$)$_2$)(κ$_S$-4-CH$_3$-C$_6$H$_4$-SO$_2$)] (7)
^{13}C{^{1}H} NMR (101 MHz, C_6D_6)



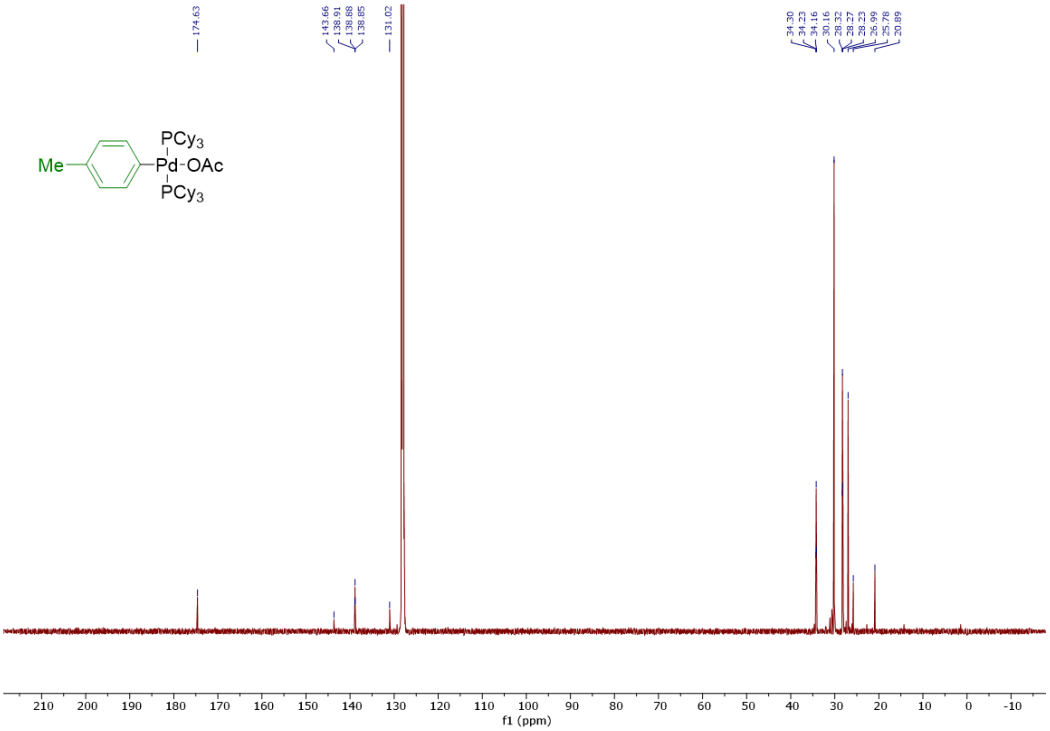
[Pd(OAc)(PCy$_3$)$_2$)(κ$_S$-4-CH$_3$-C$_6$H$_4$-SO$_2$)] (7)
^{31}P{^{1}H} NMR (162 MHz, C_6D_6)



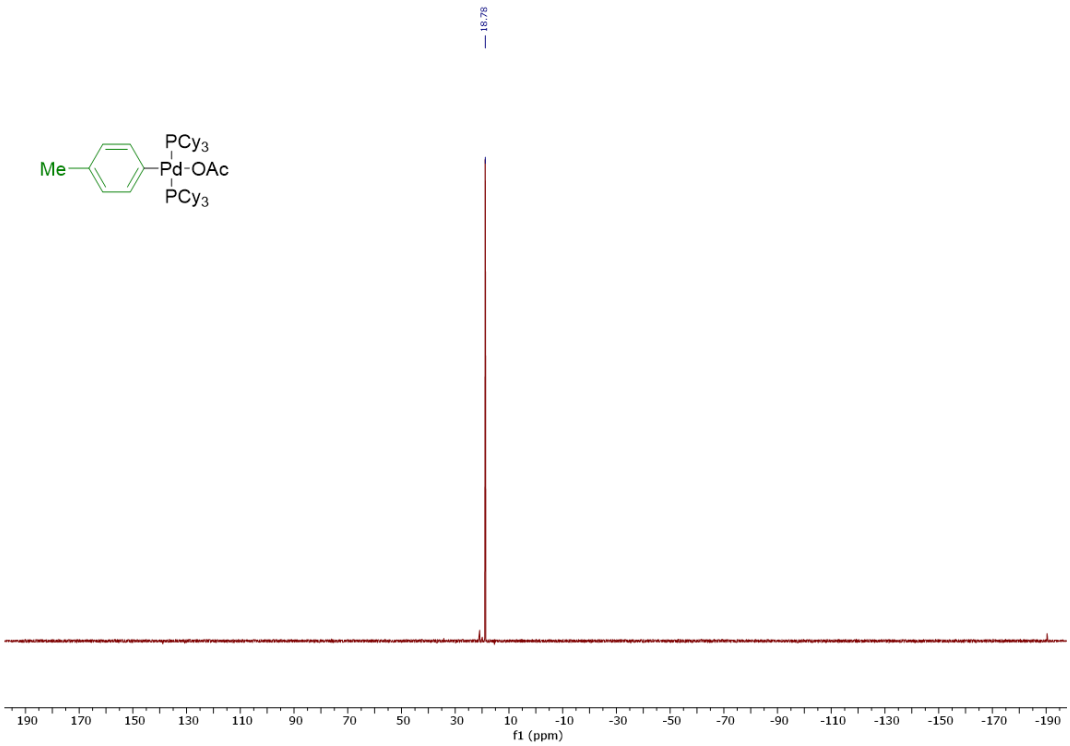
[(4-Me-C$_6$H$_4$)Pd(PCy$_3$)$_2$(OAc)] (8)
^{1}H NMR (400 MHz, C_6D_6)



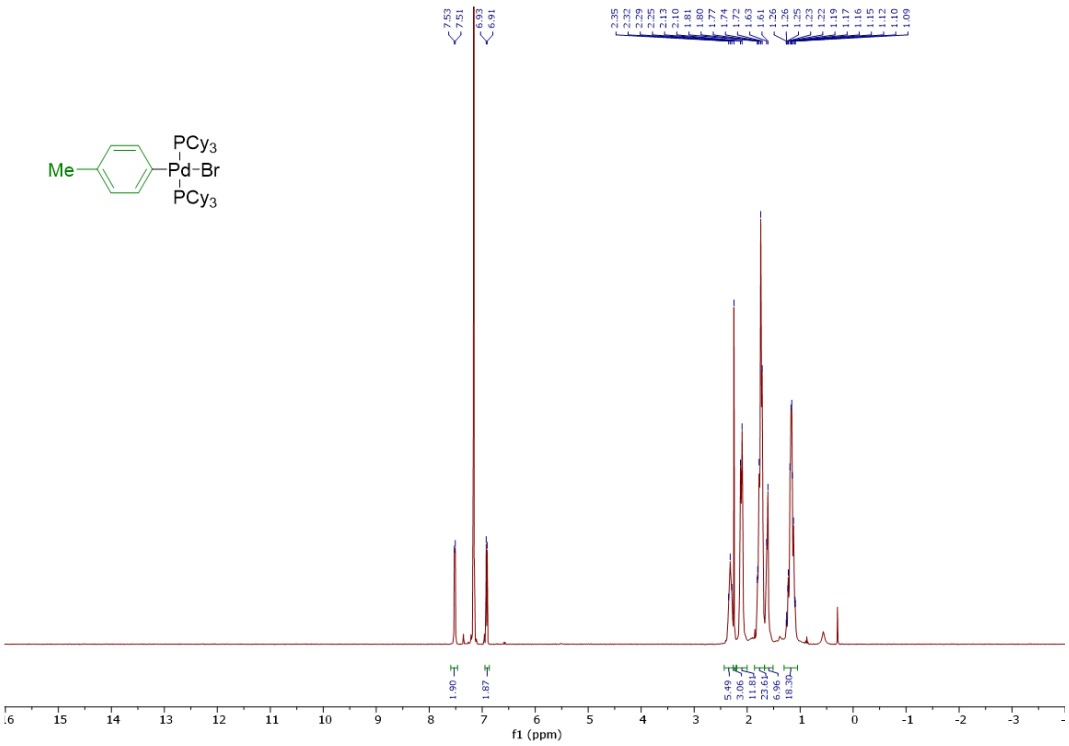
[(4-Me-C_6H_4)Pd(PCy_3)$_2$(OAc)] (8)
$^{13}C\{^1H\}$ NMR (126 MHz, C_6D_6)



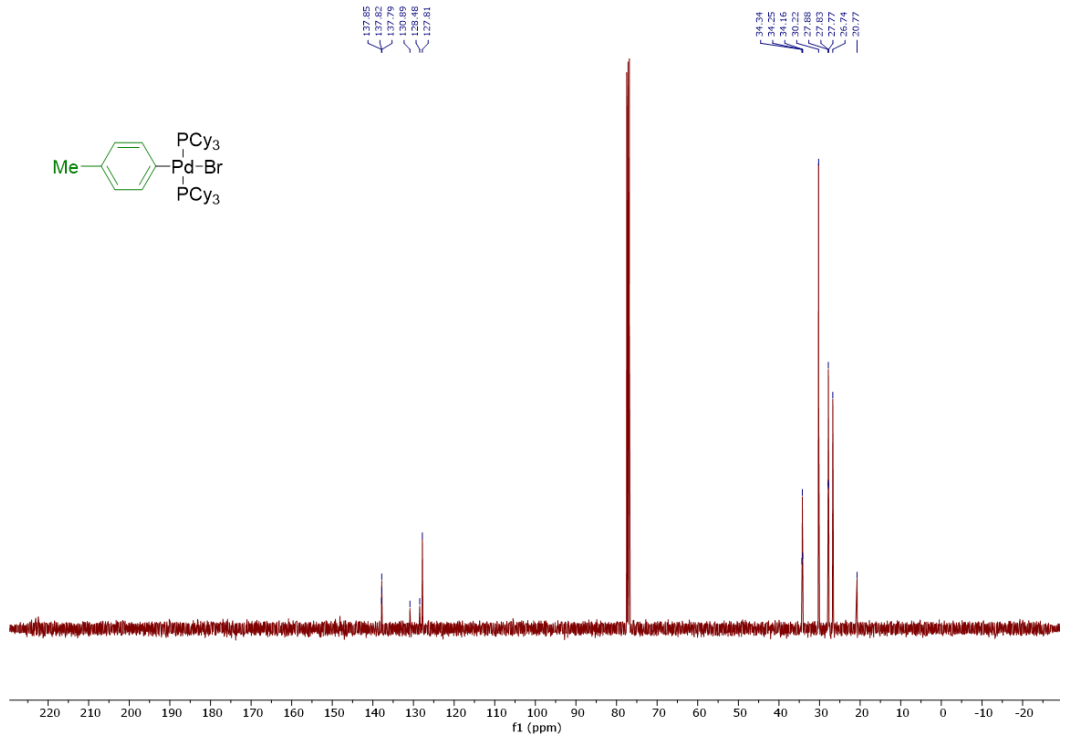
[(4-Me-C_6H_4)Pd(PCy_3)$_2$(OAc)] (8)
$^{31}P\{^1H\}$ NMR (162 MHz, C_6D_6)



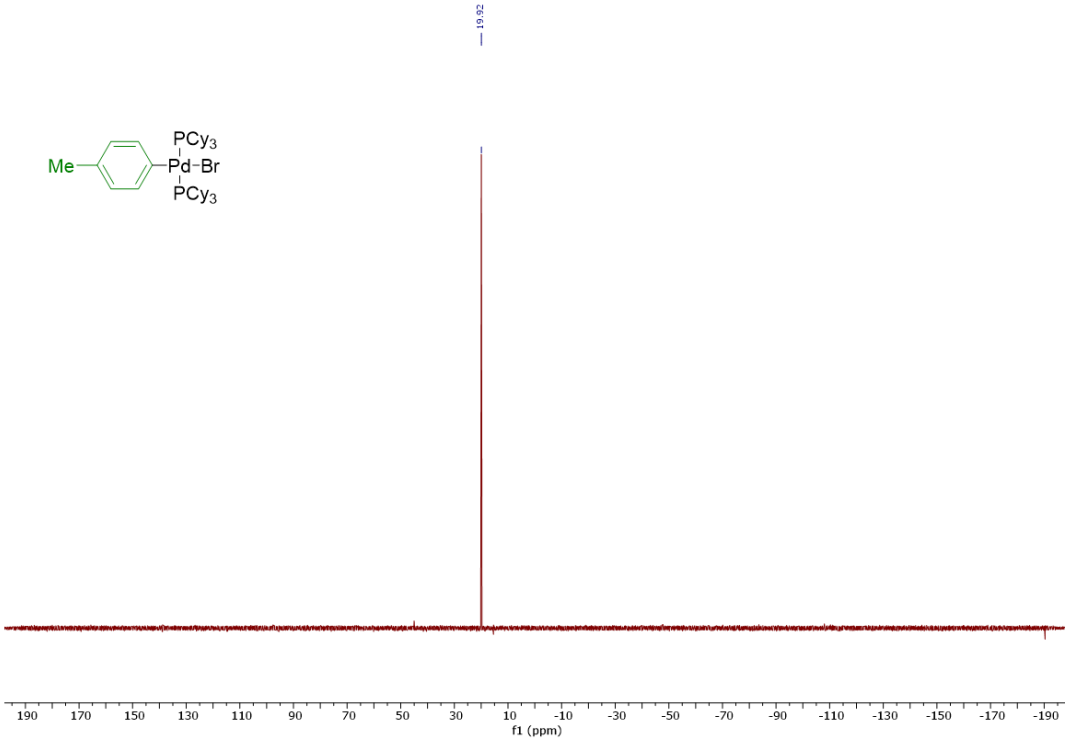
[(4-Me-C_6H_4)Pd(PCy_3)$_2$(Br)] (8b)
^{1}H NMR (400 MHz, C_6D_6)



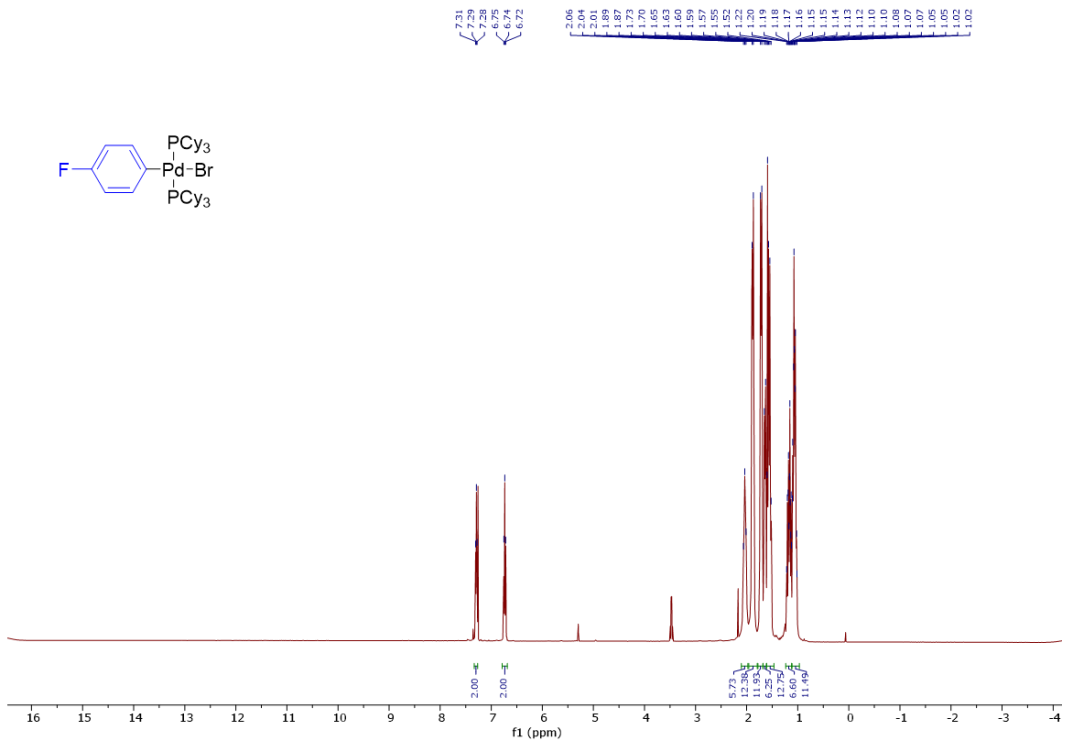
[(4-Me-C_6H_4)Pd(PCy_3)$_2$(Br)] (8b)
^{13}C{^{1}H} NMR (101 MHz, $CDCl_3$)



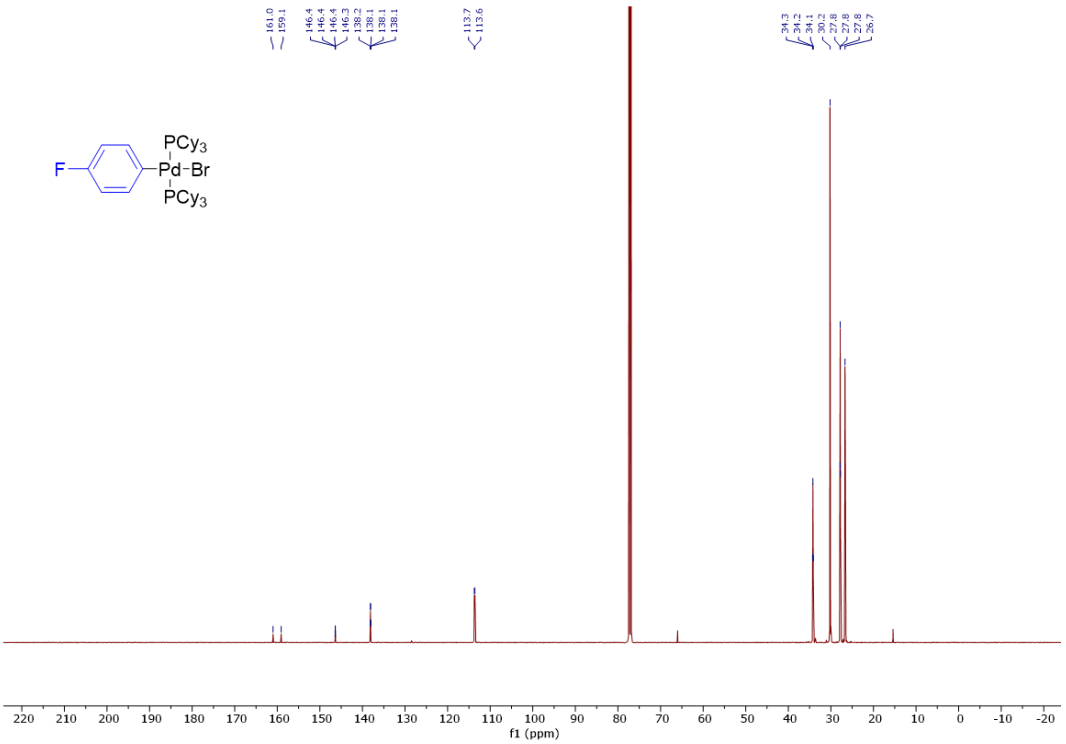
[(4-Me-C_6H_4)Pd(PCy_3)$_2$(Br)] (8b)
$^{31}P\{^1H\}$ NMR (162 MHz, C_6D_6)



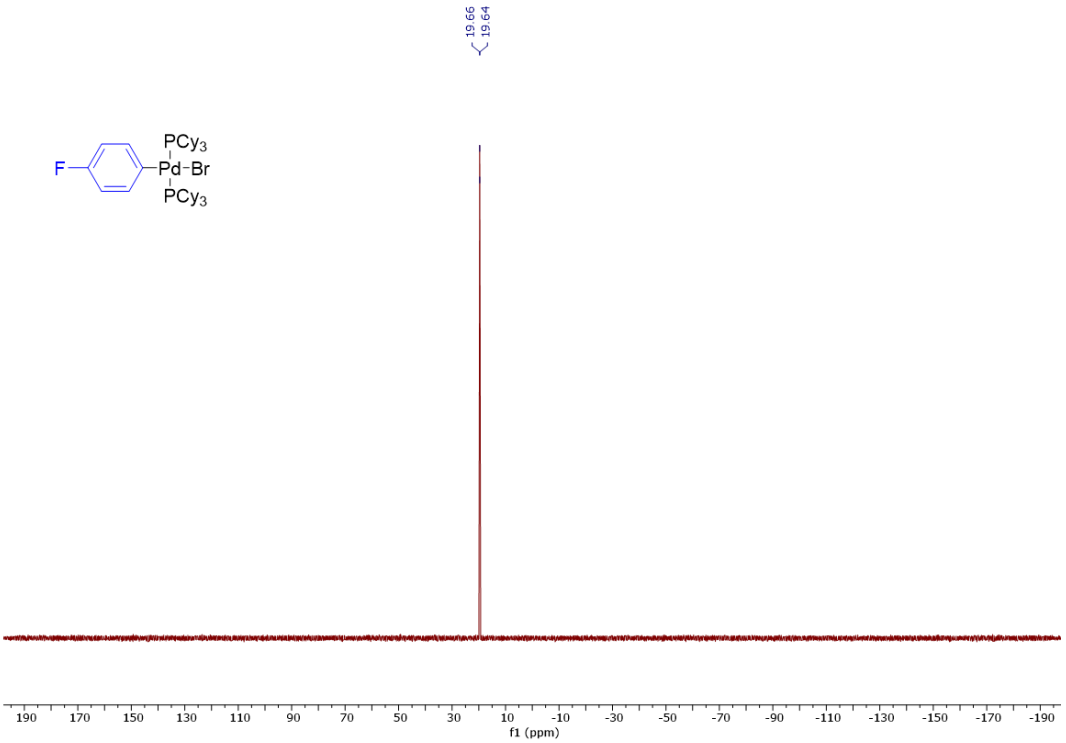
[(PCy_3)$_2$Pd(4-F-C_6H_4)(Br)] (9)
^1H NMR (500 MHz, $CDCl_3$)



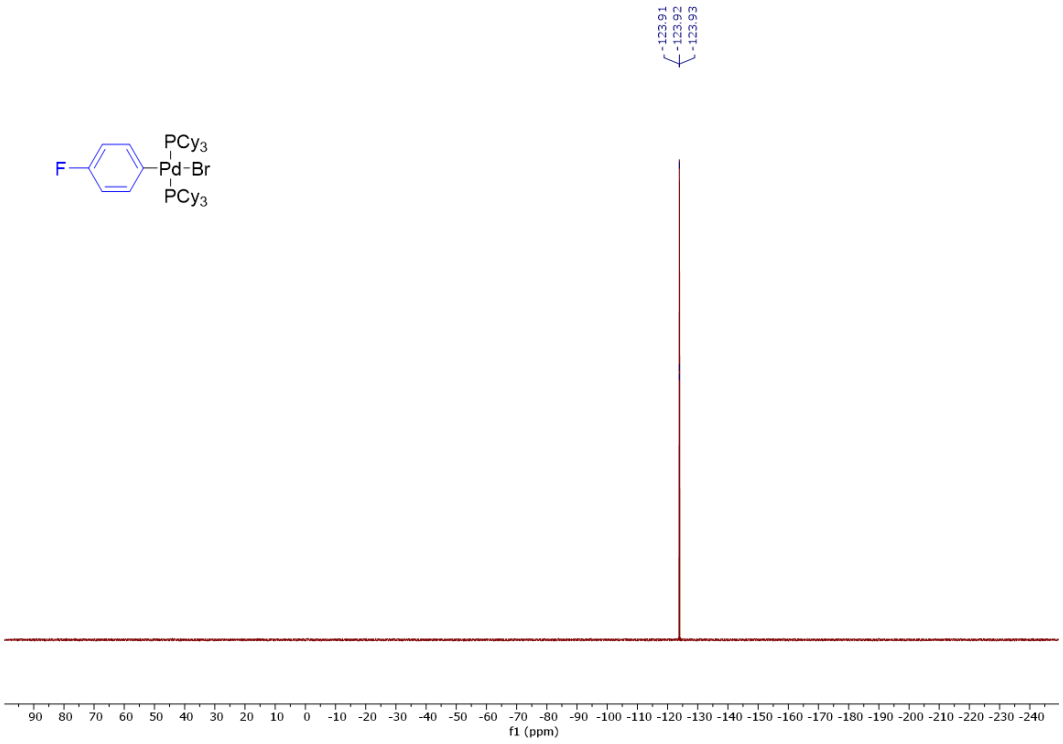
[$(PCy_3)_2Pd(4\text{-}F\text{-}C_6H_4)(Br)$] (9)
$^{13}C\{^1H\}$ NMR (126 MHz, $CDCl_3$)



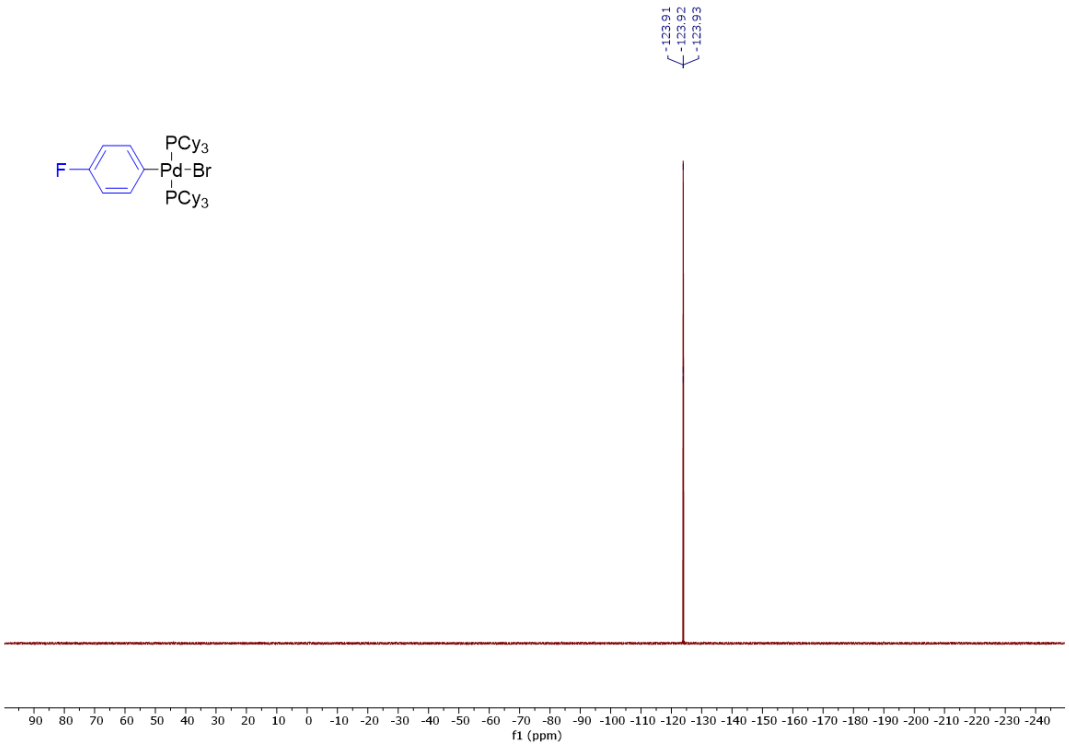
[$(PCy_3)_2Pd(4\text{-}F\text{-}C_6H_4)(Br)$] (9)
$^{31}P\{^1H\}$ NMR (162 MHz, $CDCl_3$)



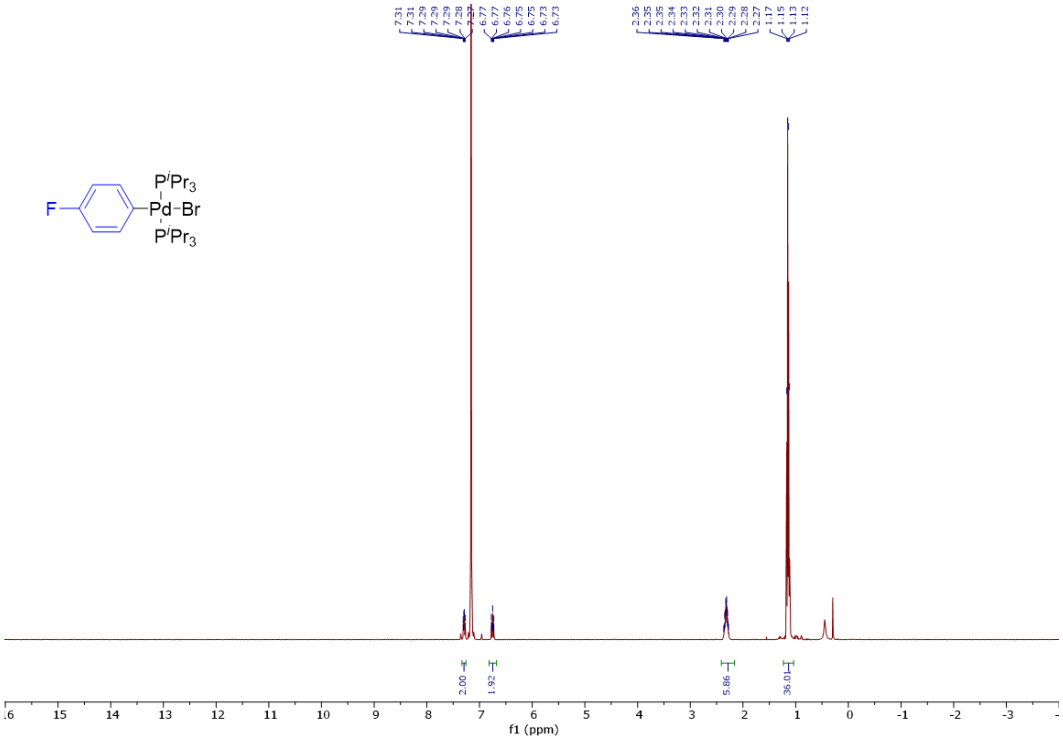
[(PCy$_3$)$_2$Pd(4-F-C$_6$H$_4$)(Br)] (9)
^{19}F{^{1}H} NMR (377 MHz, CDCl$_3$)



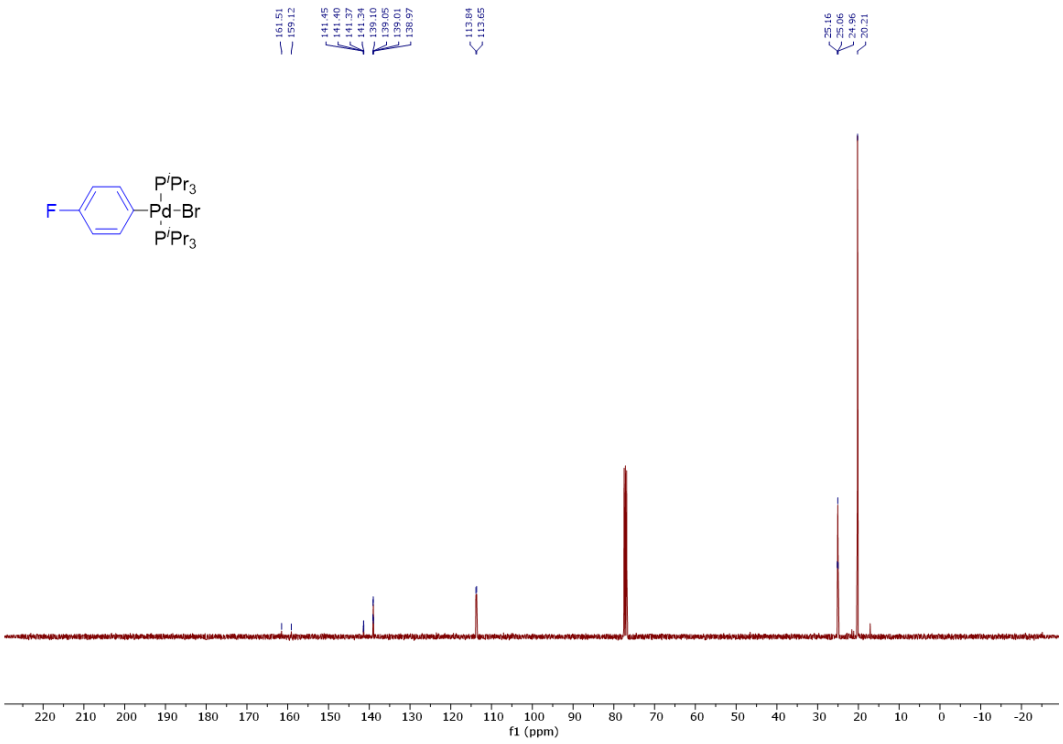
[(PCy$_3$)$_2$Pd(4-F-C$_6$H$_4$)(Br)] (9)
^{19}F{^{1}H} NMR (377 MHz, CDCl$_3$)



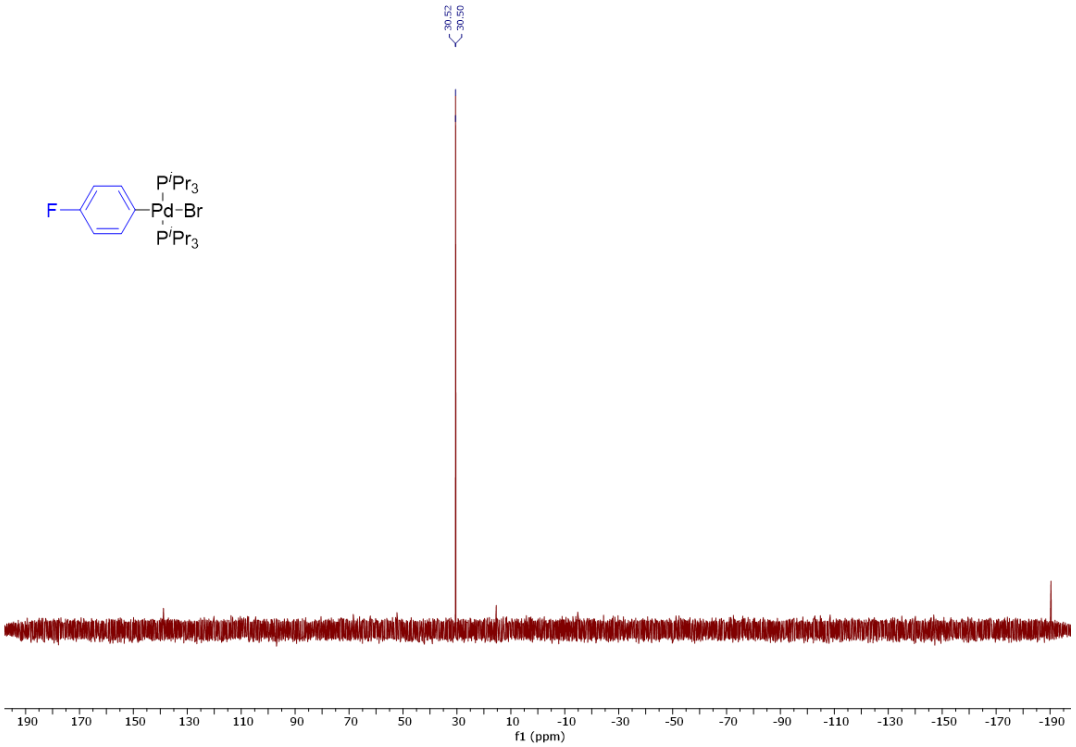
[(P*i*Pr$_3$)$_2$Pd(4-F-C$_6$H$_4$)(Br)] (9-*i*-Pr)
^{1}H NMR (400 MHz, C_6D_6)



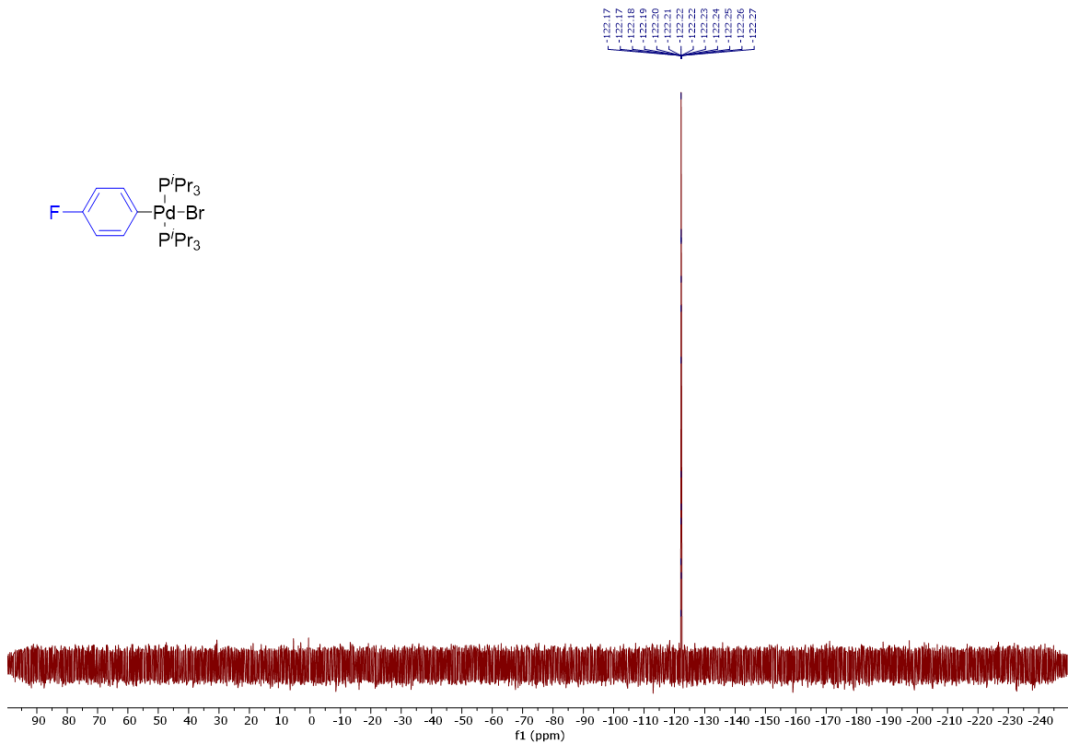
[(P*i*Pr$_3$)$_2$Pd(4-F-C$_6$H$_4$)(Br)] (9-*i*-Pr)
^{13}C{^{1}H} NMR (101 MHz, $CDCl_3$)



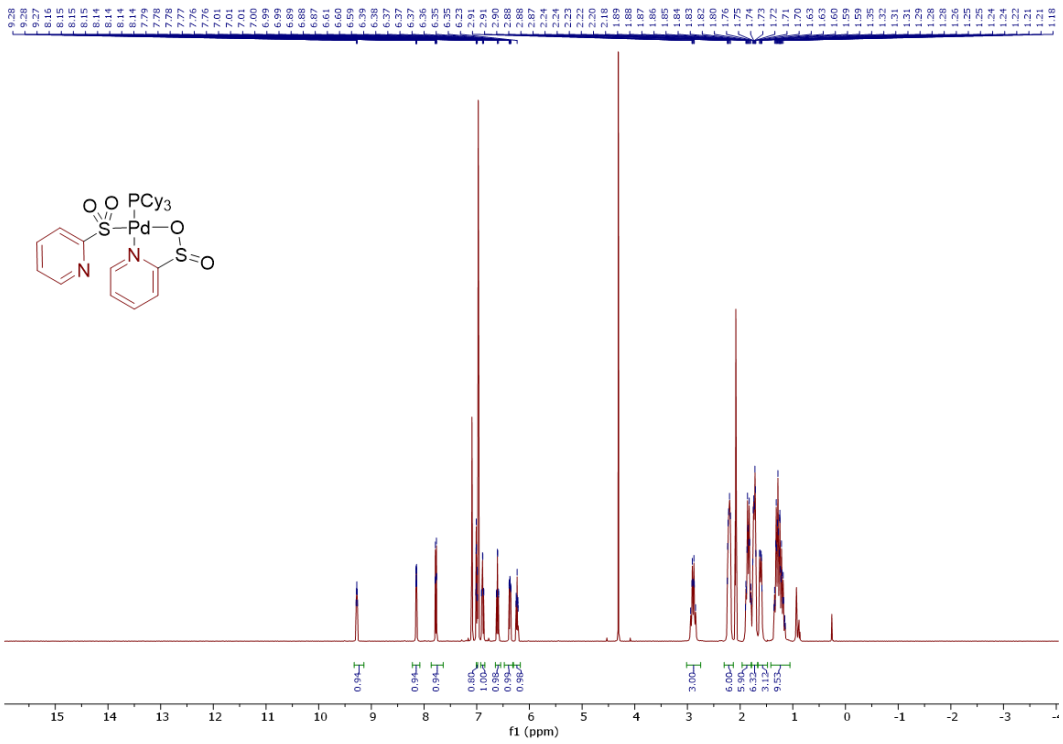
[(P*i*Pr$_3$)$_2$Pd(4-F-C$_6$H$_4$)(Br)] (9-*i*-Pr)
^{31}P{^{1}H} NMR (162 MHz, C_6D_6)



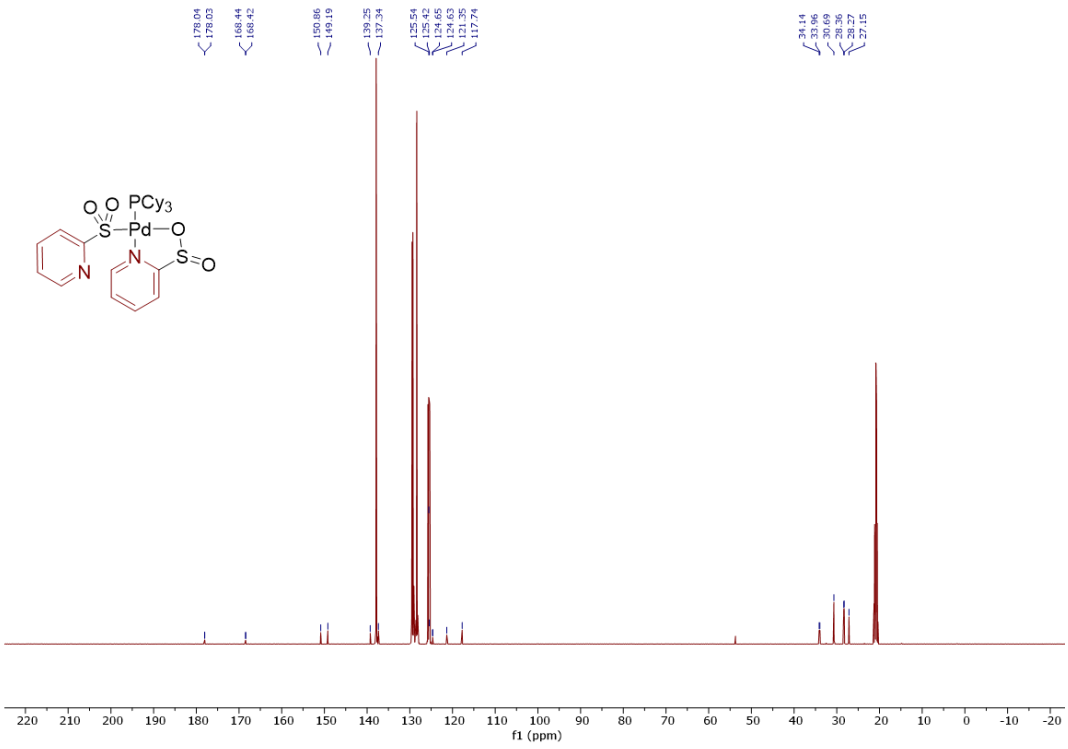
[(P*i*Pr$_3$)$_2$Pd(4-F-C$_6$H$_4$)(Br)] (9-*i*-Pr)
^{19}F NMR (377 MHz, C_6D_6)



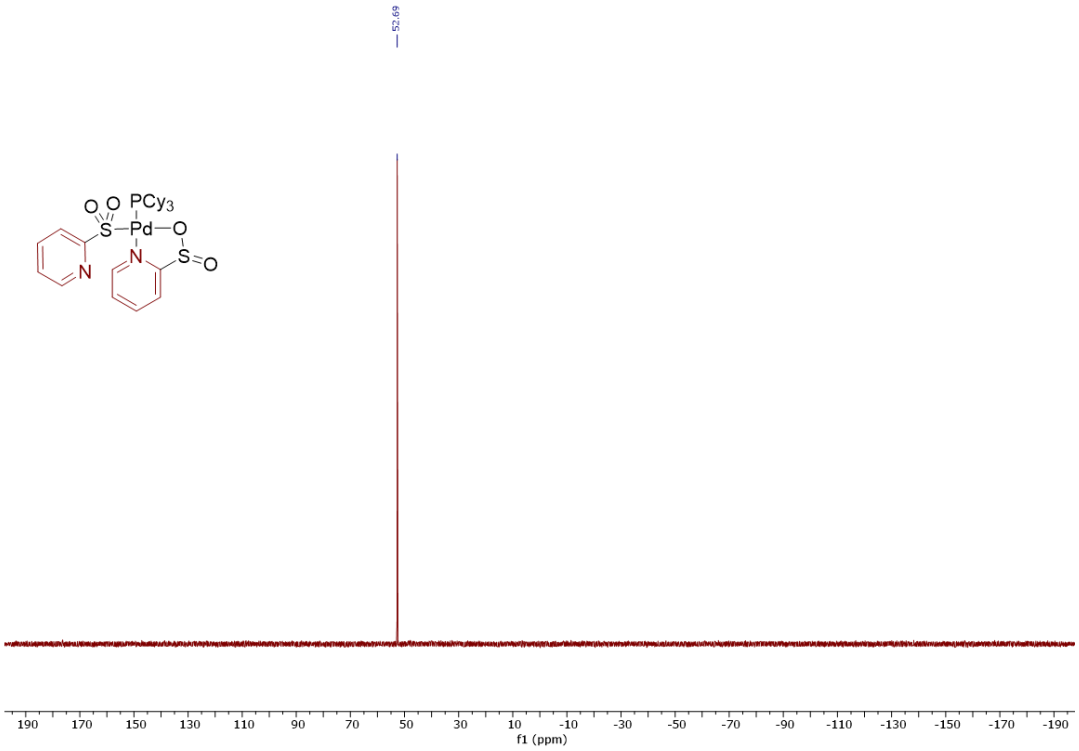
[(κ_S-2-pyridyl-SO_2)Pd(PCy_3)($\kappa^2_{N,O}$-pyridine-2-SO_2)] (10)
^{1}H NMR (400 MHz, Toluene-d_8)



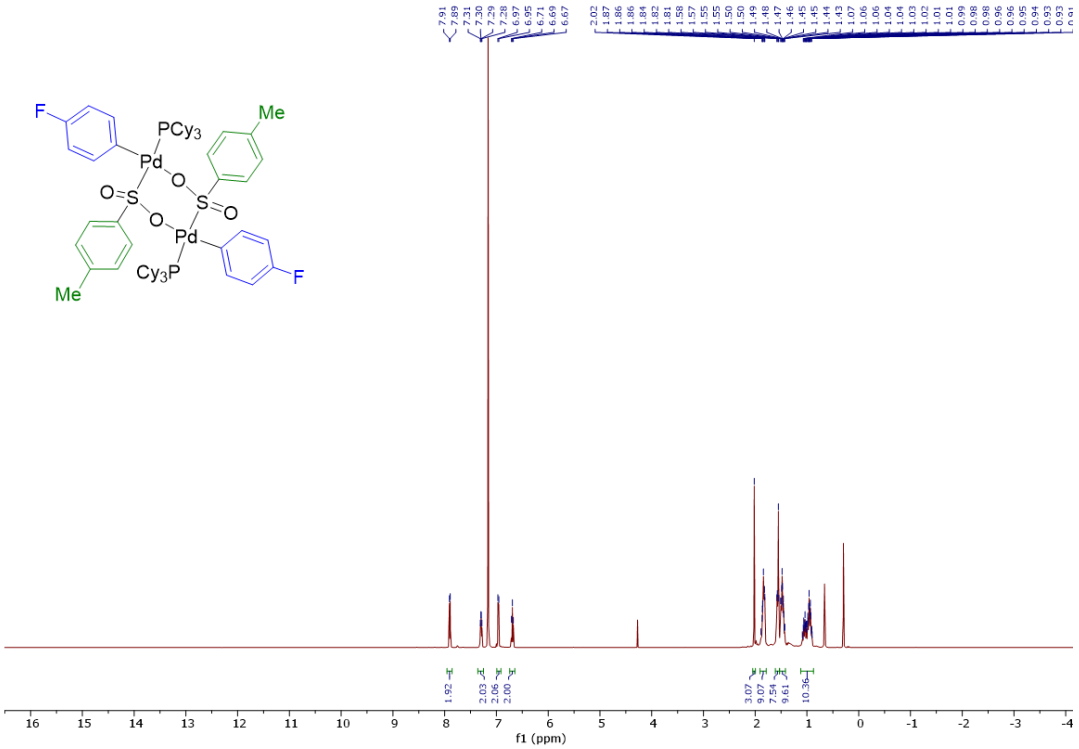
[(κ_S-2-pyridyl-SO_2)Pd(PCy_3)($\kappa^2_{N,O}$-pyridine-2-SO_2)] (10)
^{13}C{^{1}H} NMR (126 MHz, Toluene-d_8)



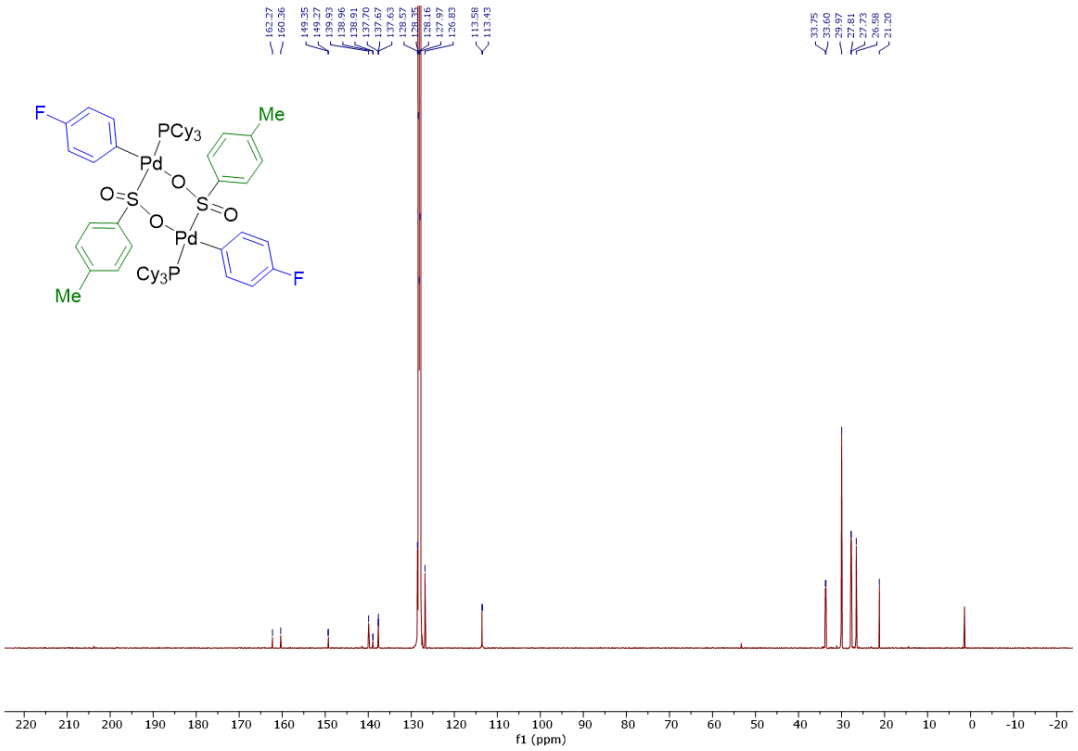
[(κ$_S$-2-pyridyl-SO$_2$)Pd(PCy$_3$))(κ$^2_{N,O}$-pyridine-2-SO$_2$)] (10)
^{31}P{^{1}H} NMR (162 MHz, Toluene-d_8)



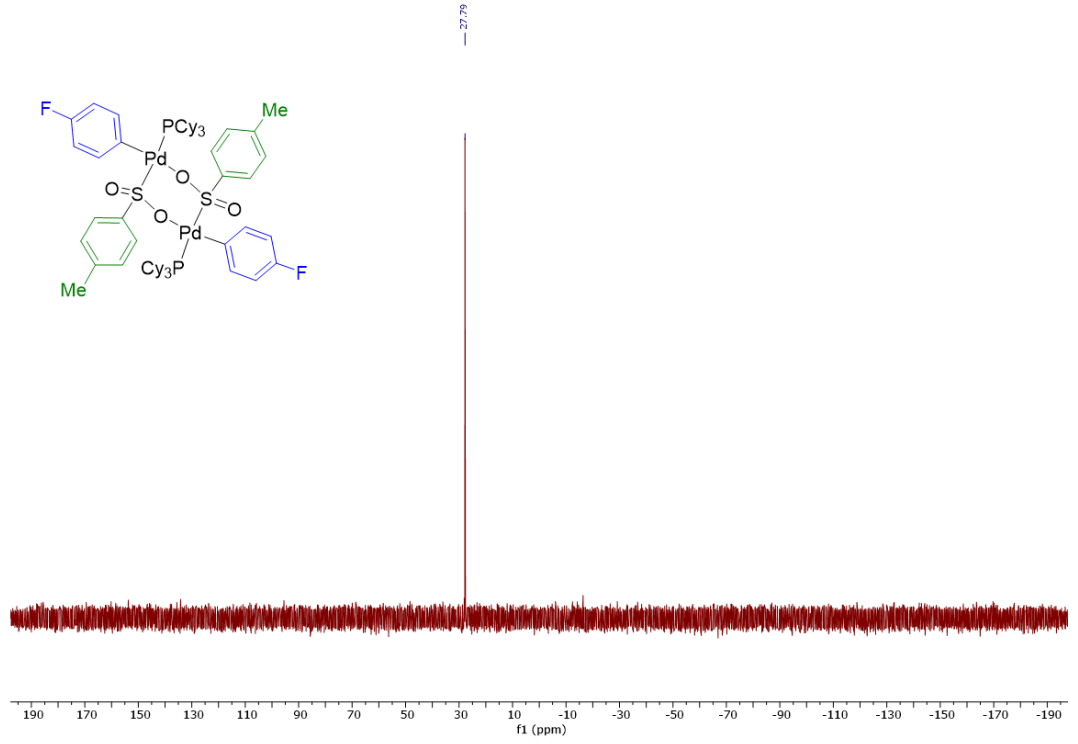
[(PCy$_3$)Pd(4-F-C$_6$H$_4$)(κ$_S$-κ$_{O'}$-4-Me-C$_6$H$_4$-SO$_2$)]$_2$ (11)
^{1}H NMR (500 MHz, C_6D_6)



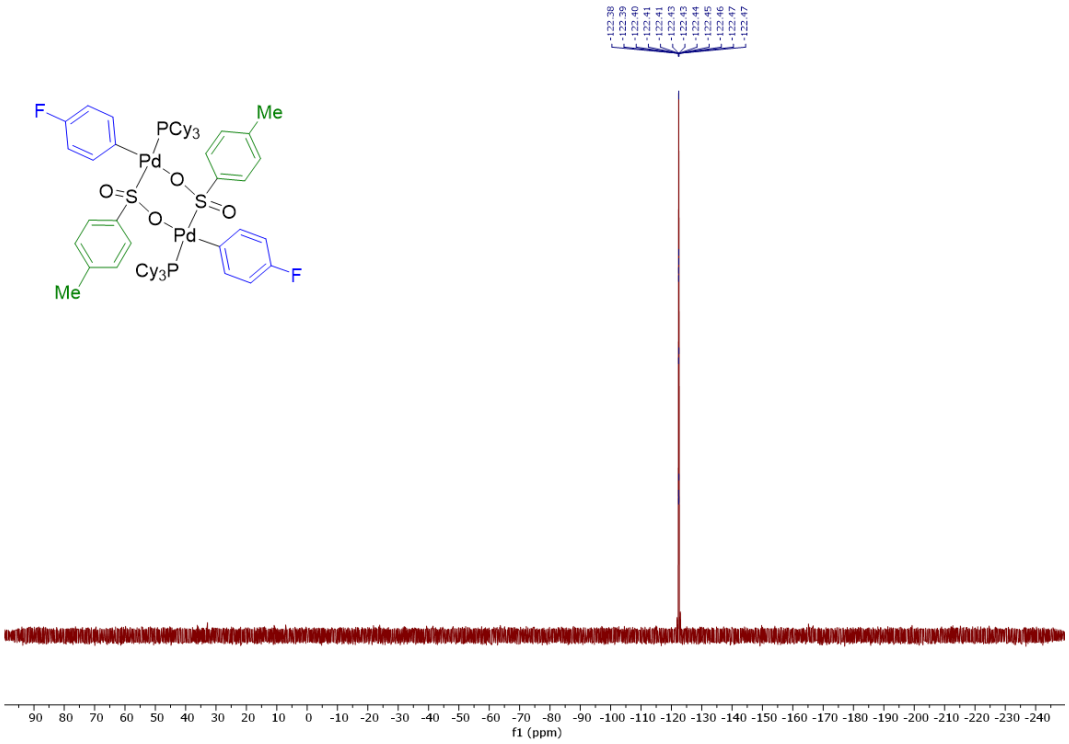
[(PCy$_3$)Pd(4-F-C$_6$H$_4$)(κ$_S$-κ$_O$'-4-Me-C$_6$H$_4$-SO$_2$)]$_2$ (11)
^{13}C{^{1}H} NMR (126 MHz, C$_6$D$_6$)



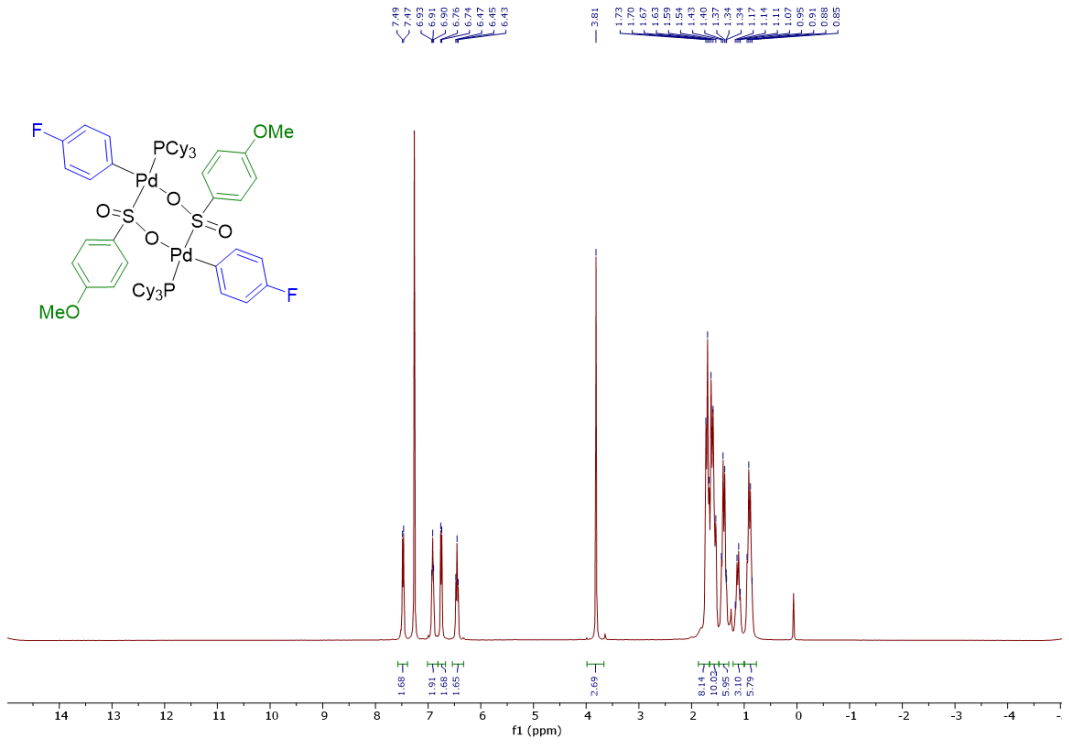
[(PCy$_3$)Pd(4-F-C$_6$H$_4$)(κ$_S$-κ$_O$'-4-Me-C$_6$H$_4$-SO$_2$)]$_2$ (11)
^{31}P{^{1}H} NMR (162 MHz, C$_6$D$_6$)



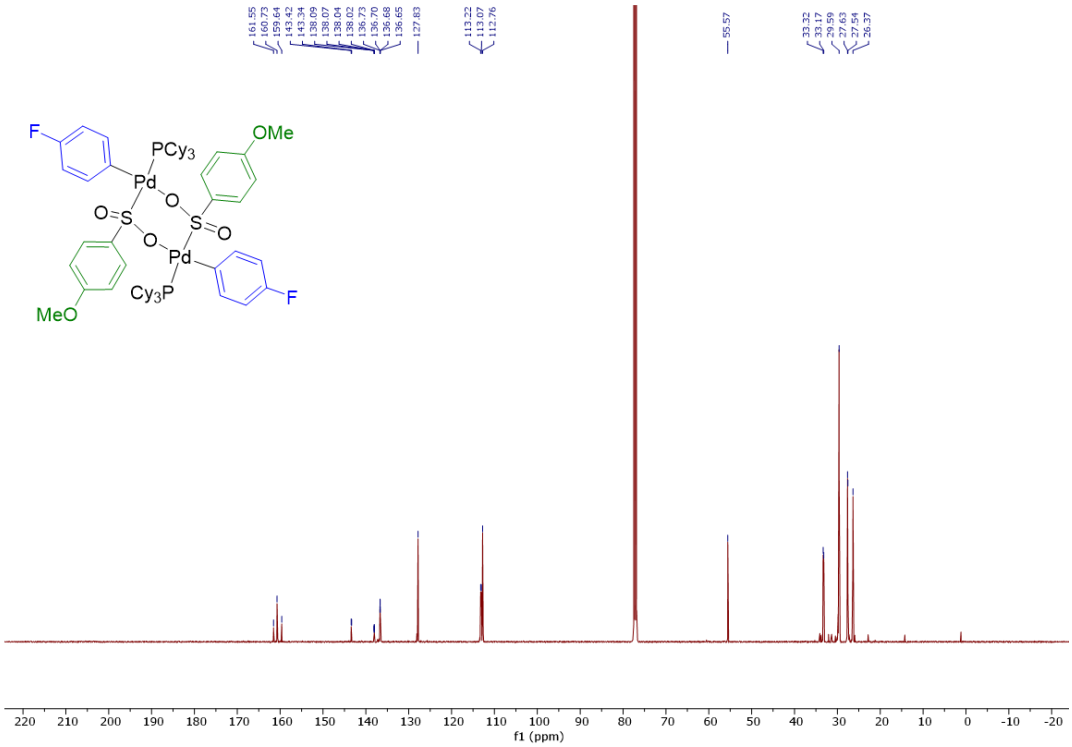
[(PCy$_3$)Pd(4-F-C$_6$H$_4$)(κ$_S$-κ$_O$'-4-Me-C$_6$H$_4$-SO$_2$)]$_2$ (11)
^{19}F NMR (377 MHz, C_6D_6)



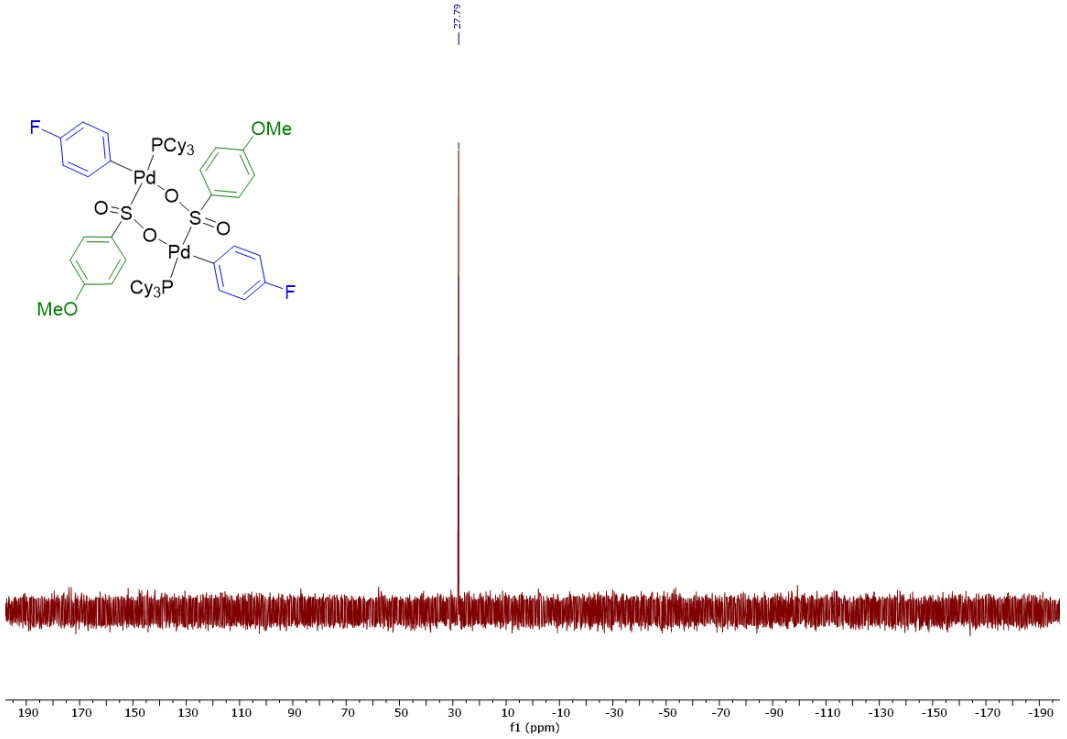
[(PCy$_3$)Pd(4-F-C$_6$H$_4$)(κ$_S$-κ$_O$'-4-MeO-C$_6$H$_4$-SO$_2$)]$_2$ (17)
^{1}H NMR (400 MHz, $CDCl_3$)



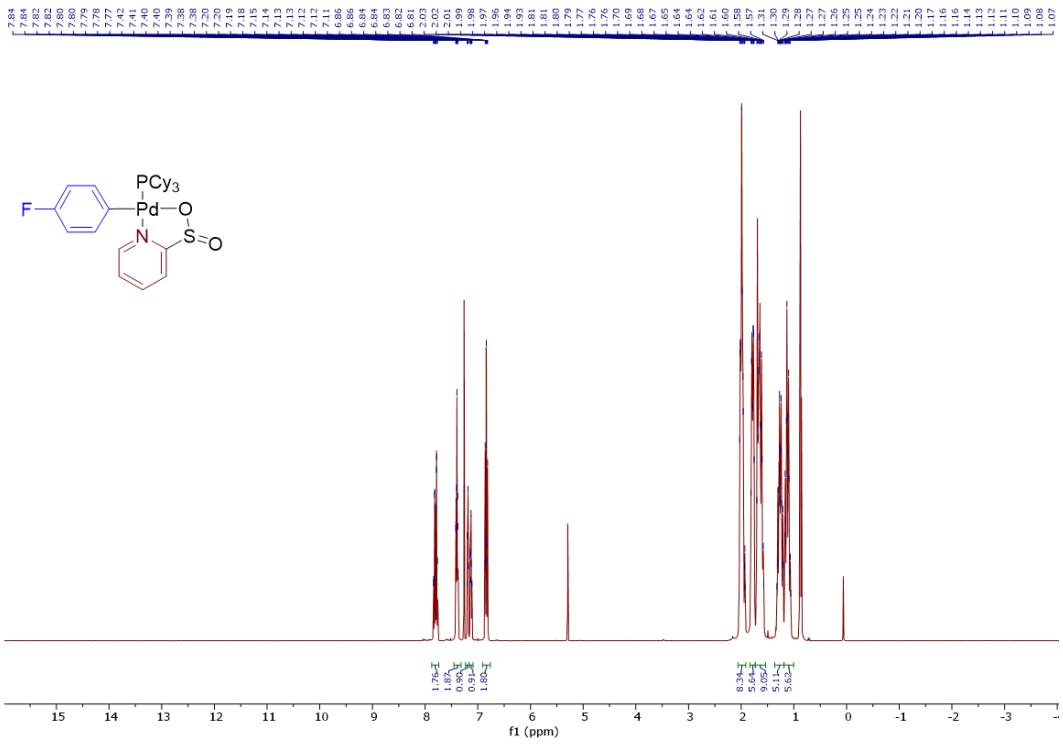
[(PCy$_3$)Pd(4-F-C$_6$H$_4$)(κ$_S$-κ$_{O'}$-4-MeO-C$_6$H$_4$-SO$_2$)]$_2$ (17)
^{13}C{^{1}H} NMR (101 MHz, CDCl$_3$)



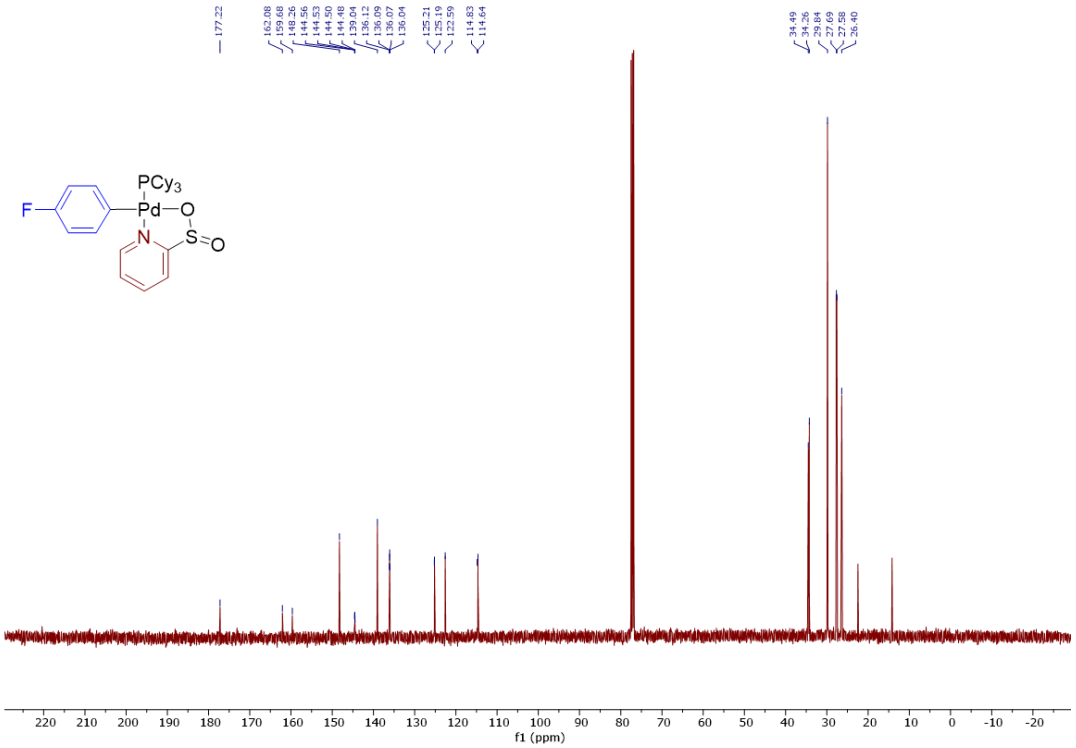
[(PCy$_3$)Pd(4-F-C$_6$H$_4$)(κ$_S$-κ$_{O'}$-4-MeO-C$_6$H$_4$-SO$_2$)]$_2$ (17)
^{31}P NMR (162 MHz, CDCl$_3$)



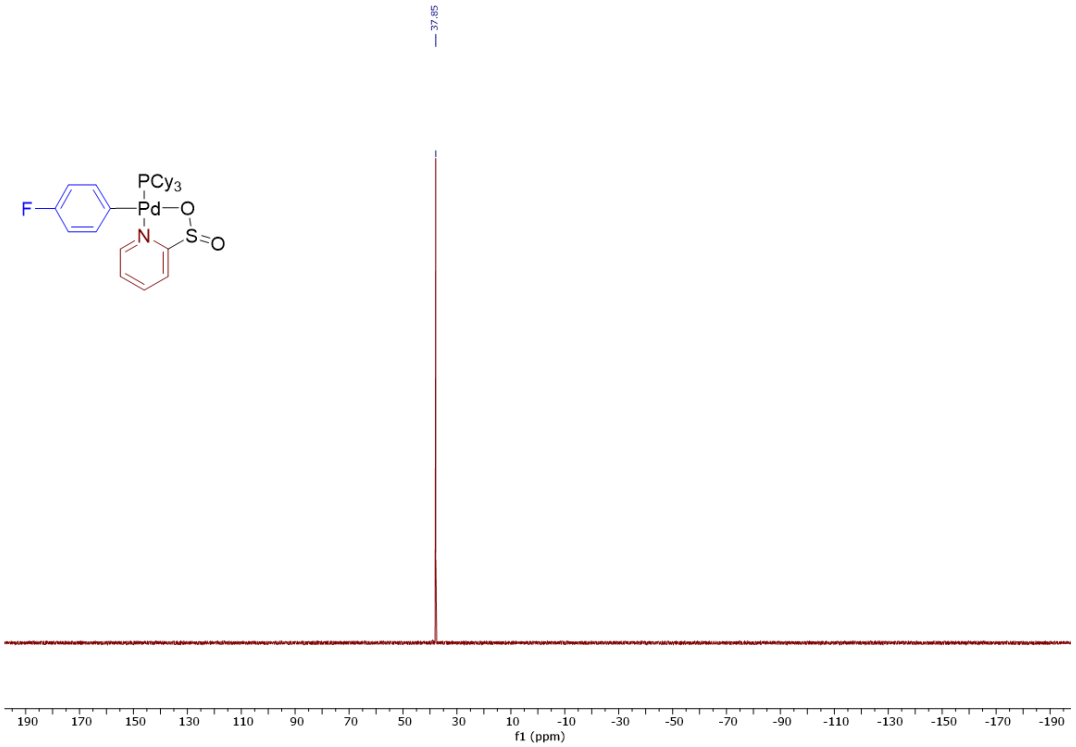
[(PCy_3)Pd(4-F-C_6H_4)($\kappa^2_{N,O}$-pyridine-2-SO_2)] (12)
^{1}H NMR (400 MHz, $CDCl_3$)



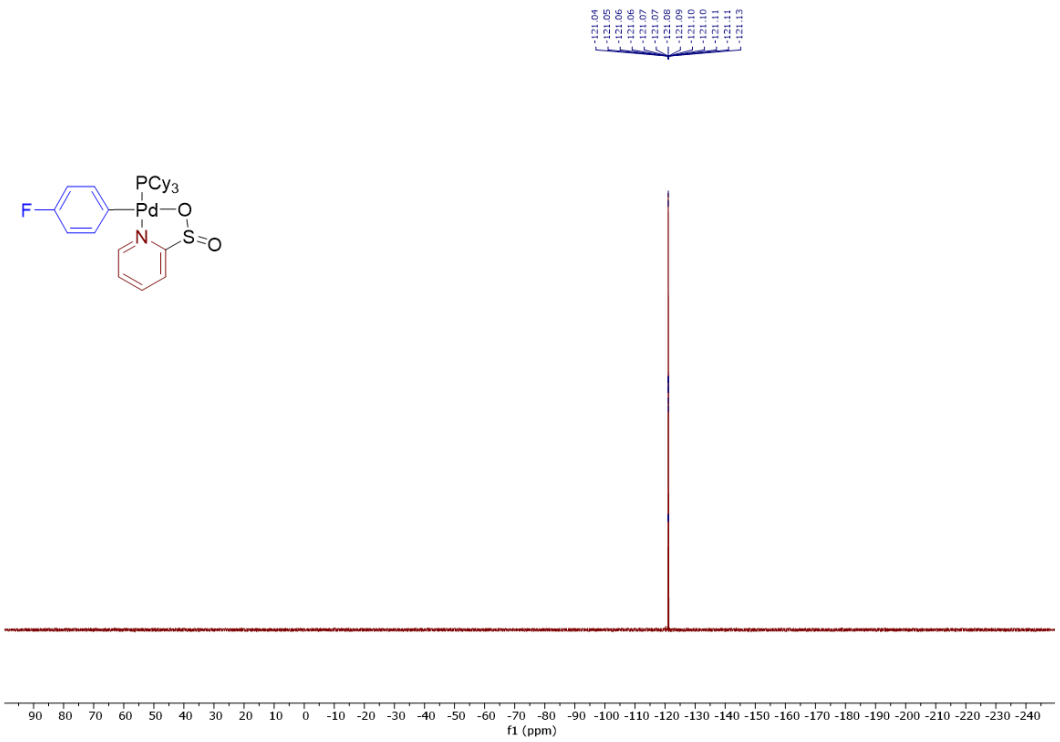
[(PCy_3)Pd(4-F-C_6H_4)($\kappa^2_{N,O}$-pyridine-2-SO_2)] (12)
^{13}C{^{1}H} NMR (101 MHz, $CDCl_3$)



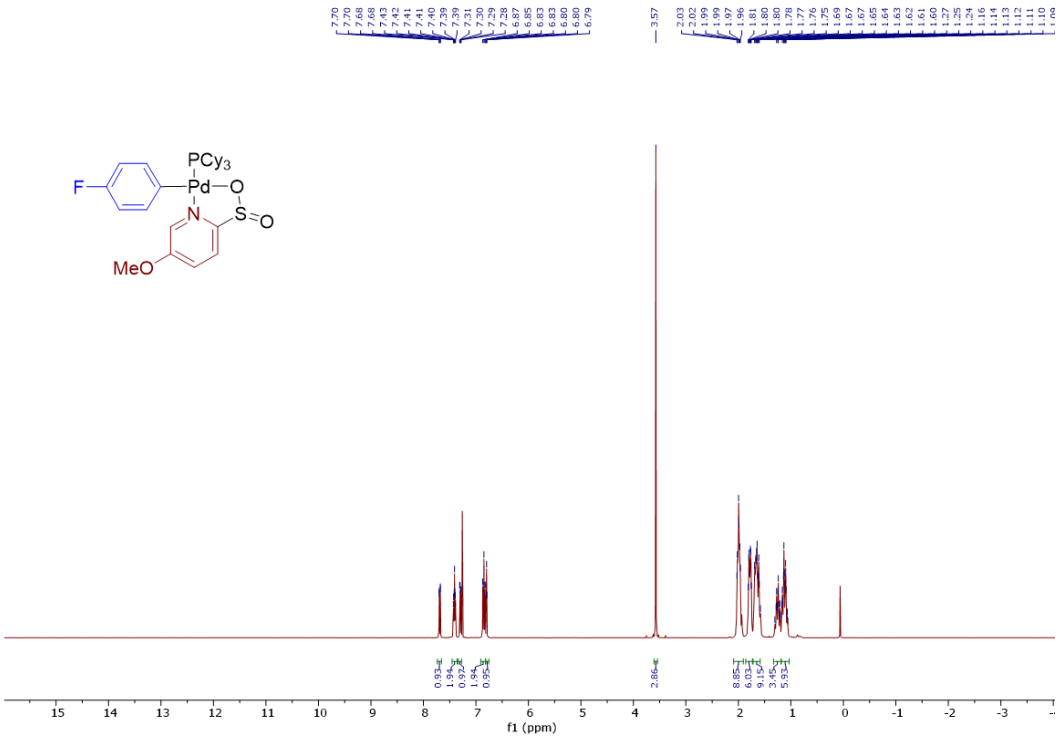
[(PCy_3)Pd(4-F-C_6H_4)($\kappa^2_{N,O}$-pyridine-2-SO_2)] (12)
$^{31}P\{^1H\}$ NMR (162 MHz, $CDCl_3$)



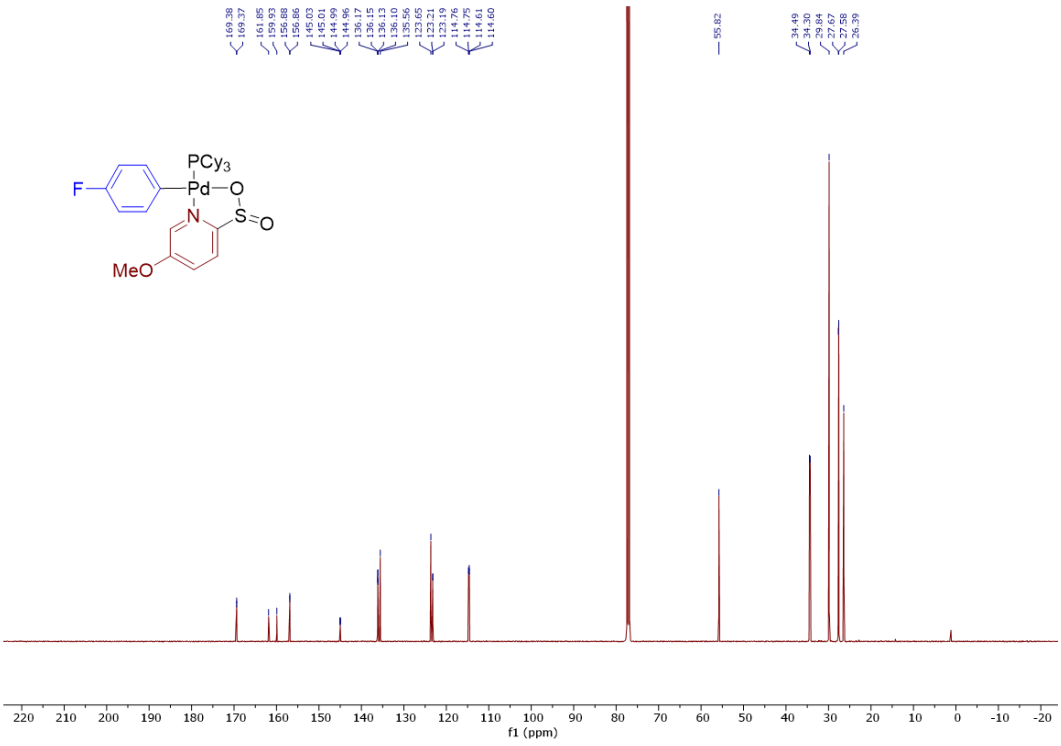
[(PCy_3)Pd(4-F-C_6H_4)($\kappa^2_{N,O}$-pyridine-2-SO_2)] (12)
^{19}F NMR (377 MHz, $CDCl_3$)



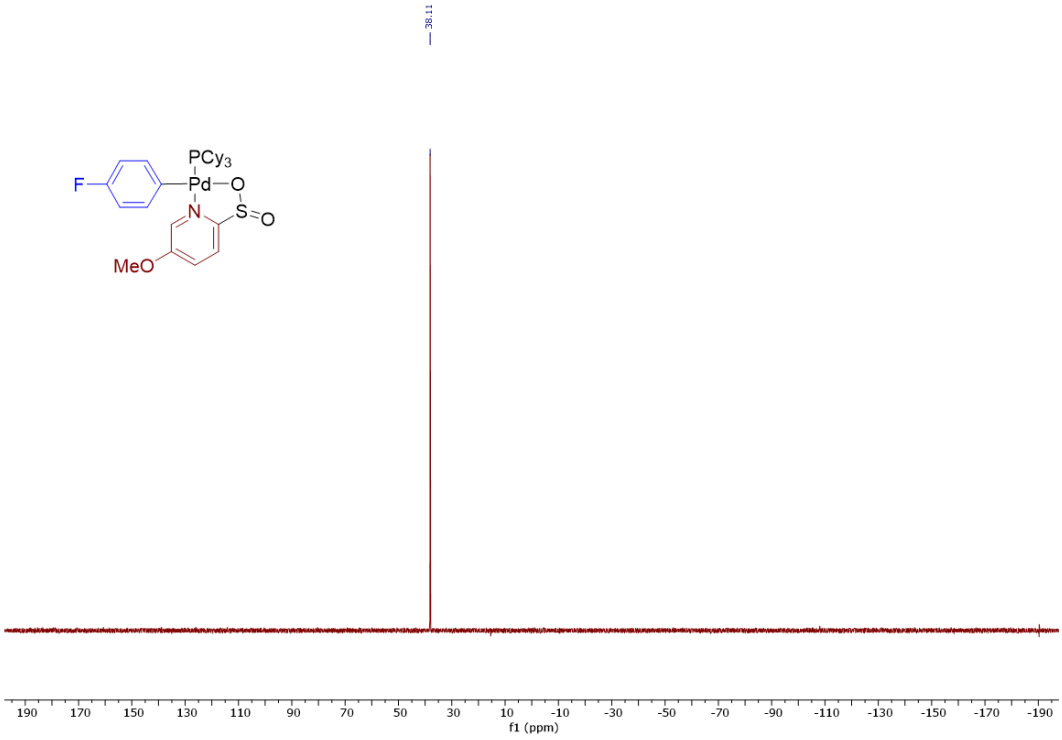
[(PCy_3)Pd(4-F-C_6H_4)($\kappa^2_{N,O}$-5-MeO-pyridine-2-SO_2)] (12-OMe)
^{1}H NMR (400 MHz, $CDCl_3$)



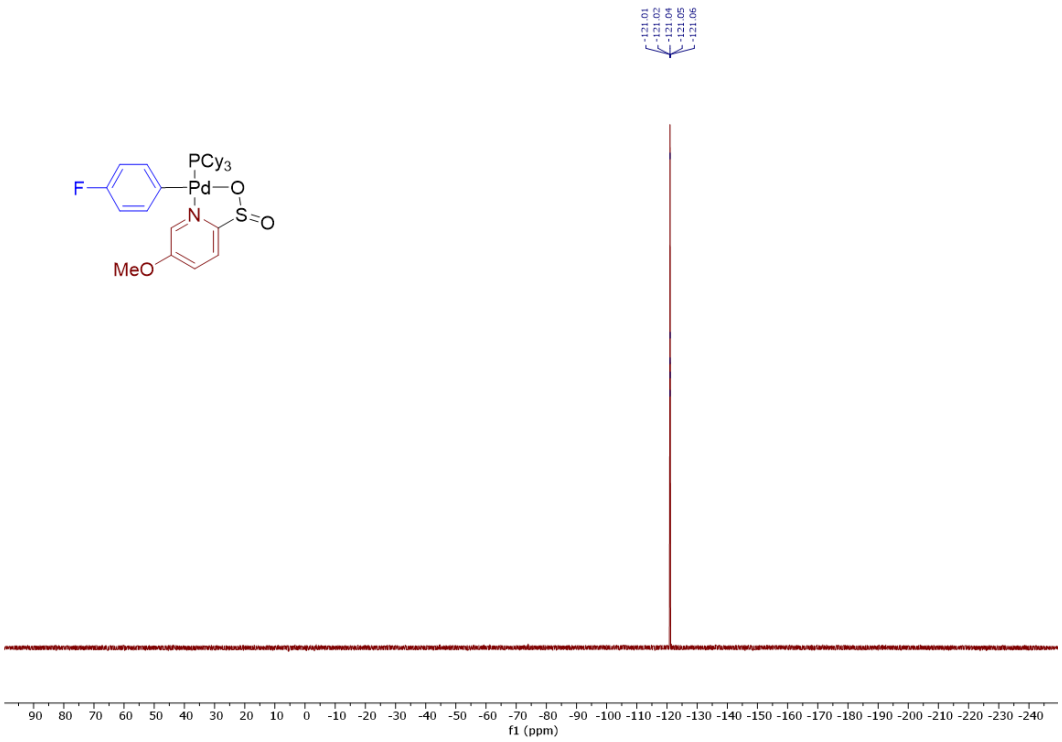
[(PCy_3)Pd(4-F-C_6H_4)($\kappa^2_{N,O}$-5-MeO-pyridine-2-SO_2)] (12-OMe)
^{13}C{^{1}H} NMR (126 MHz, $CDCl_3$)



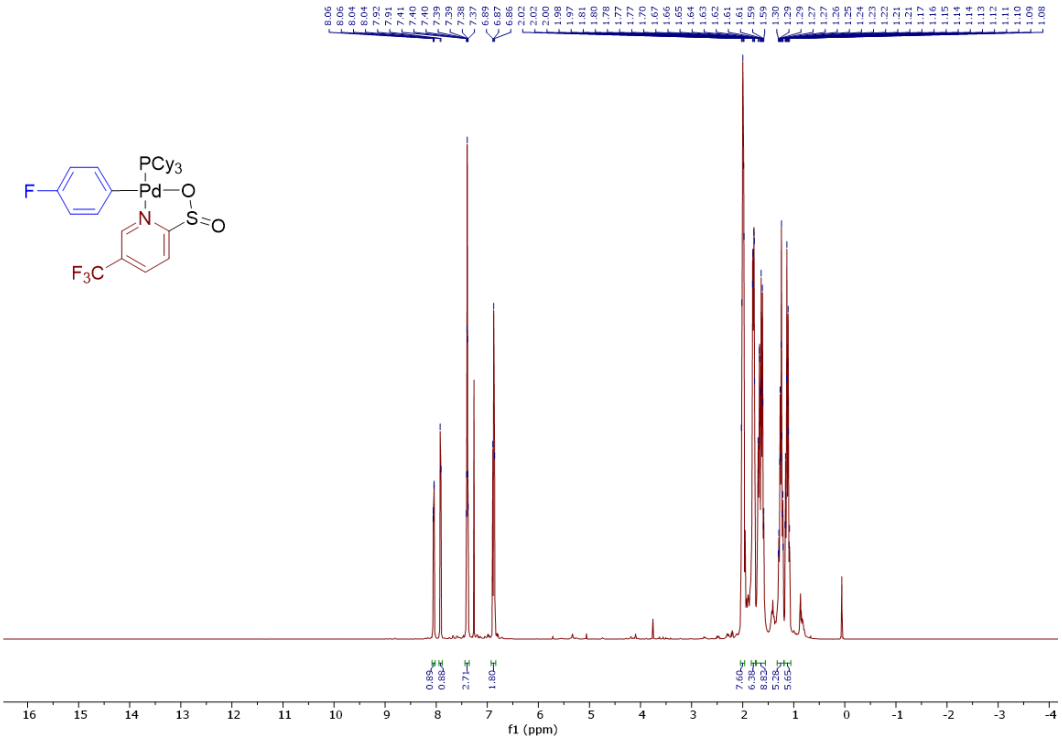
[(PCy_3)Pd(4-F-C_6H_4)($\kappa^2_{N,O}$-5-MeO-pyridine-2-SO_2)] (12-OMe)
$^{31}P\{^1H\}$ NMR (162 MHz, $CDCl_3$)



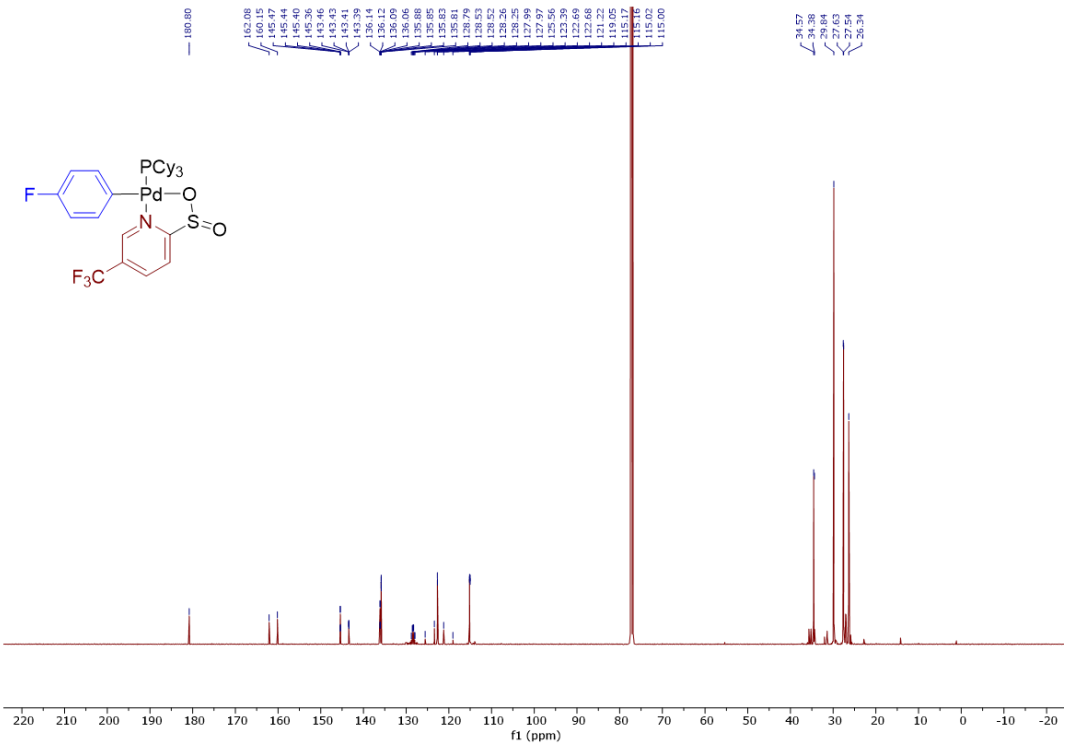
[(PCy_3)Pd(4-F-C_6H_4)($\kappa^2_{N,O}$-5-MeO-pyridine-2-SO_2)] (12-OMe)
^{19}F NMR (377 MHz, $CDCl_3$)



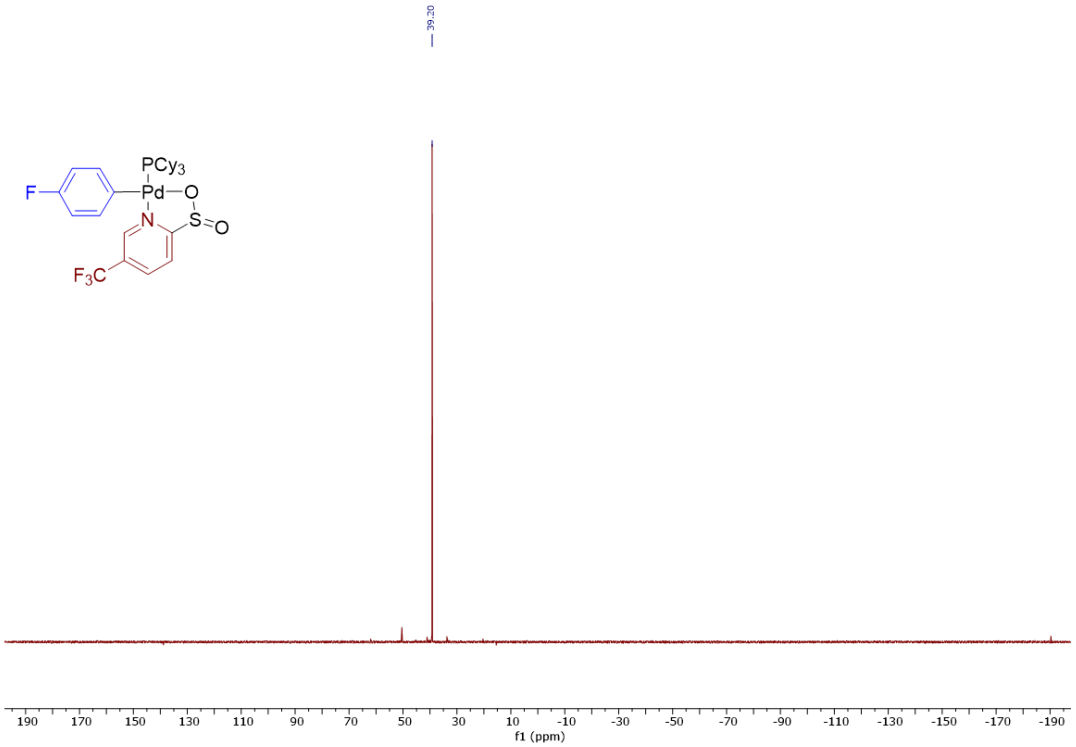
[(PCy_3)Pd(4-F-C_6H_4)($\kappa^2_{N,O}$-5-CF_3-pyridine-2-SO_2)] (12-CF_3)
^{1}H NMR (500 MHz, $CDCl_3$)



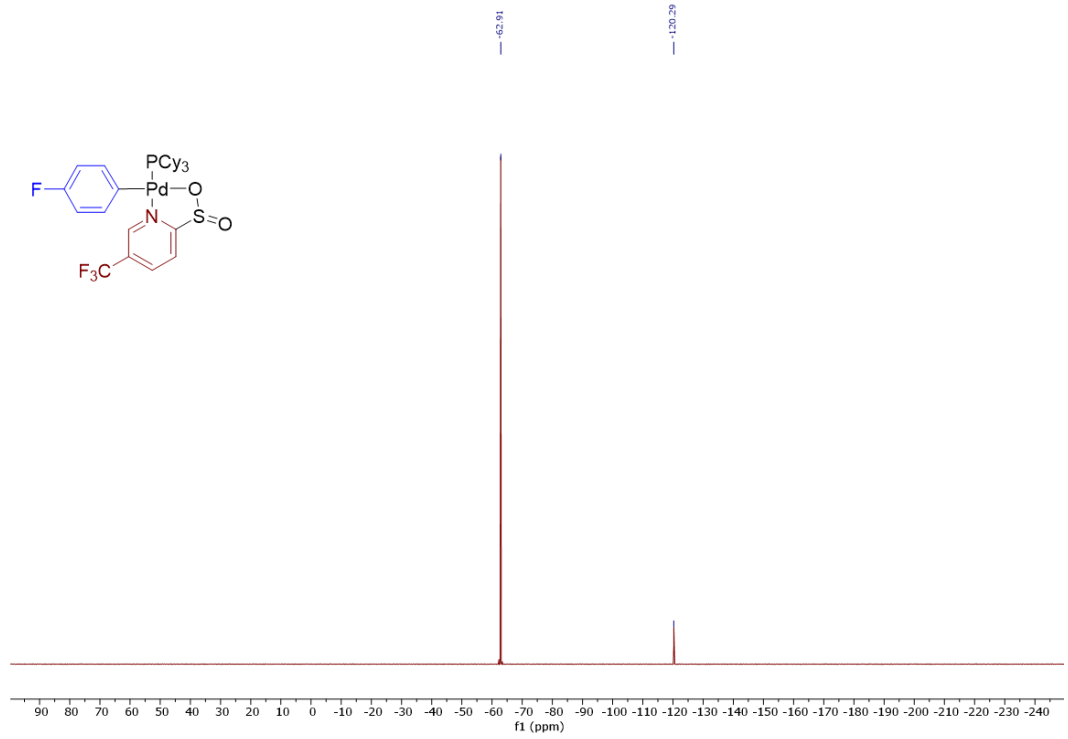
[(PCy_3)Pd(4-F-C_6H_4)($\kappa^2_{N,O}$-5-CF_3-pyridine-2-SO_2)] (12-CF_3)
^{13}C{^{1}H} NMR (126 MHz, $CDCl_3$)



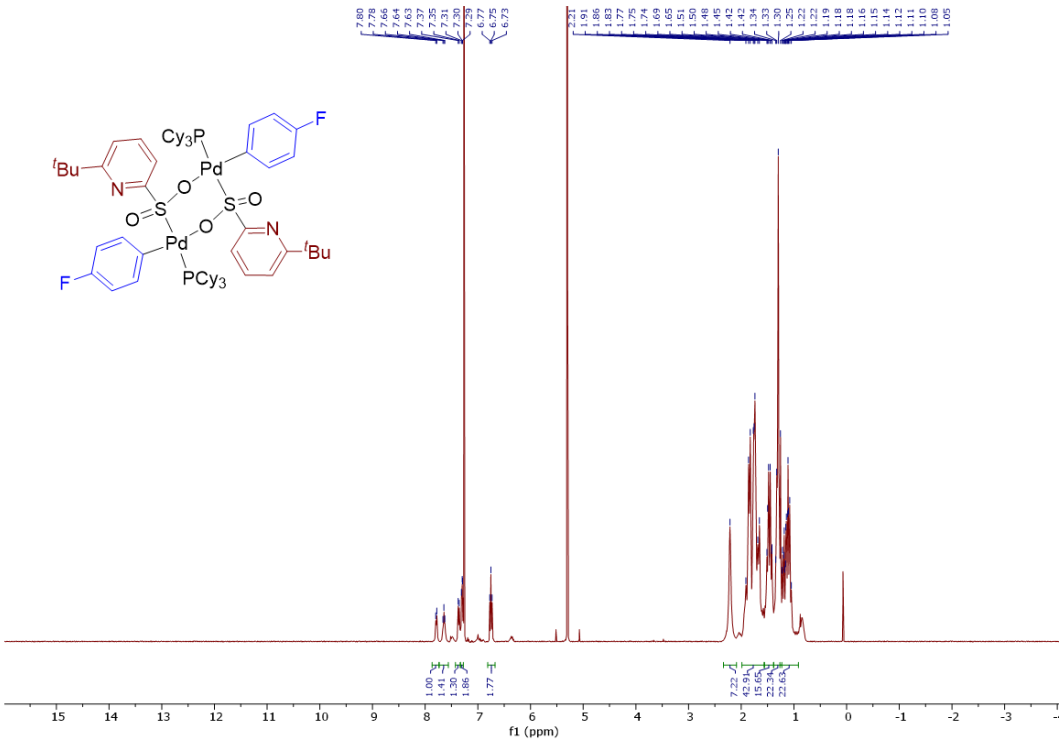
[(PCy_3)Pd(4-F-C_6H_4)($\kappa^2_{N,O}$-5-CF_3-pyridine-2-SO_2)] (12-CF_3)
$^{31}P\{^1H\}$ NMR (162 MHz, $CDCl_3$)



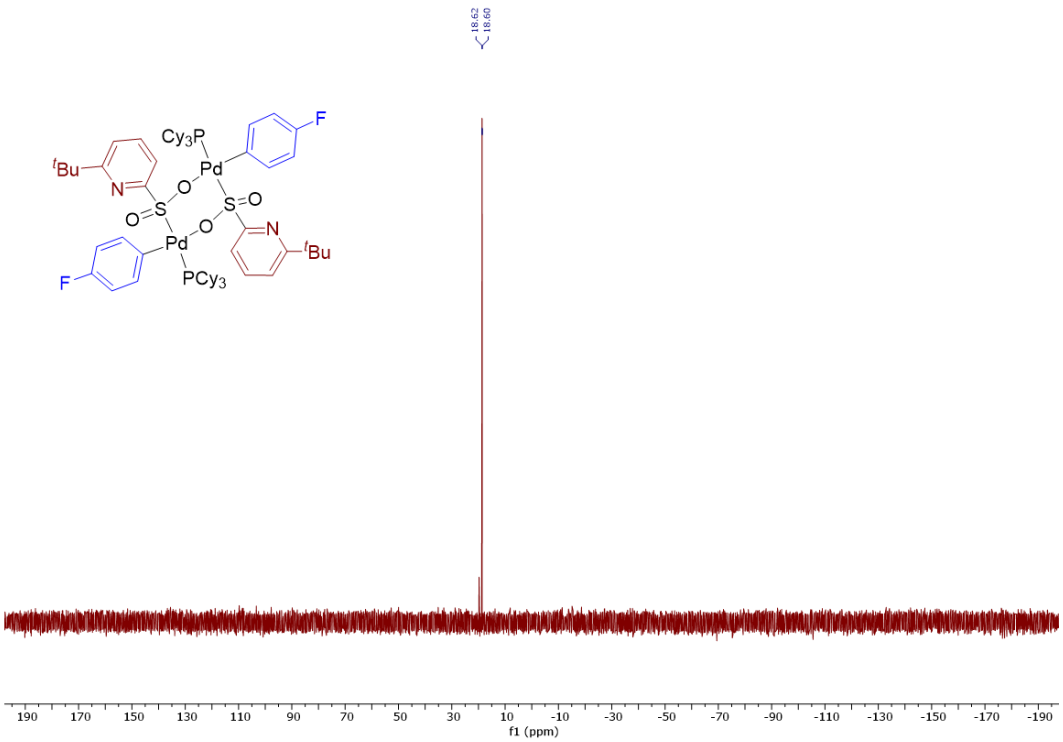
[(PCy_3)Pd(4-F-C_6H_4)($\kappa^2_{N,O}$-5-CF_3-pyridine-2-SO_2)] (12-CF_3)
^{19}F NMR (377 MHz, $CDCl_3$)



[(PCy$_3$)Pd(4-F-C$_6$H$_4$)(κ$_S$-κ$_O$,-6-*t*Bu-pyridine-2-SO$_2$)]$_2$ (13)
^{1}H NMR (400 MHz, $CDCl_3$)

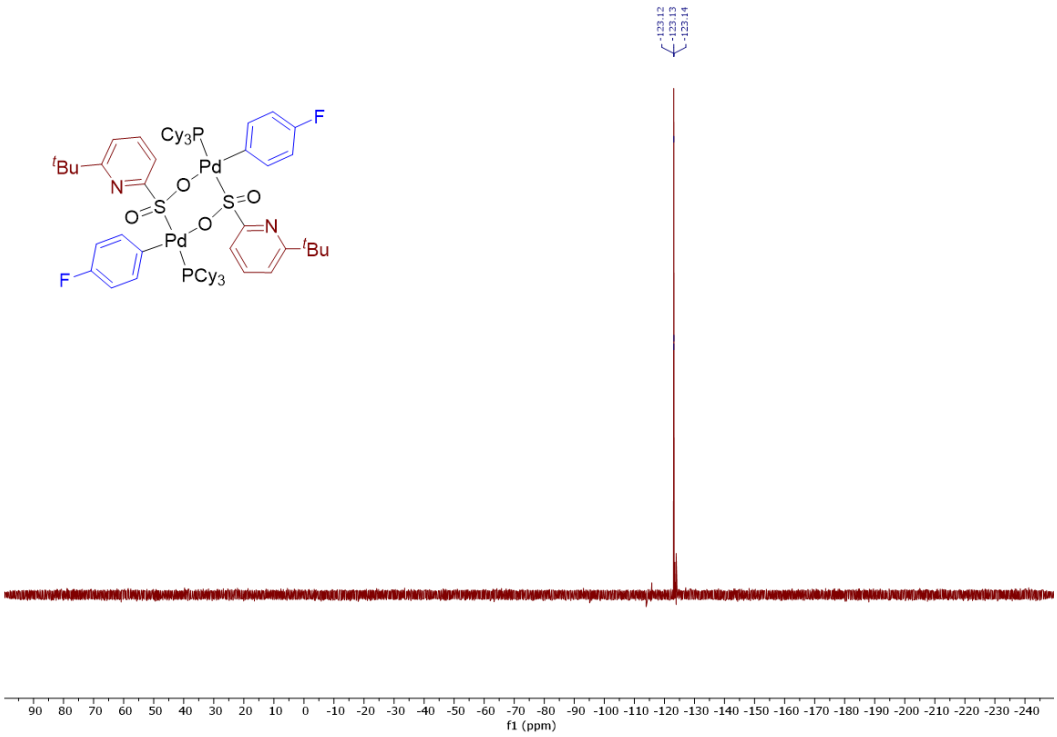


[(PCy$_3$)Pd(4-F-C$_6$H$_4$)(κ$_S$-κ$_O$,-6-*t*Bu-pyridine-2-SO$_2$)]$_2$ (13)
^{31}P{^{1}H} NMR (162 MHz, $CDCl_3$)



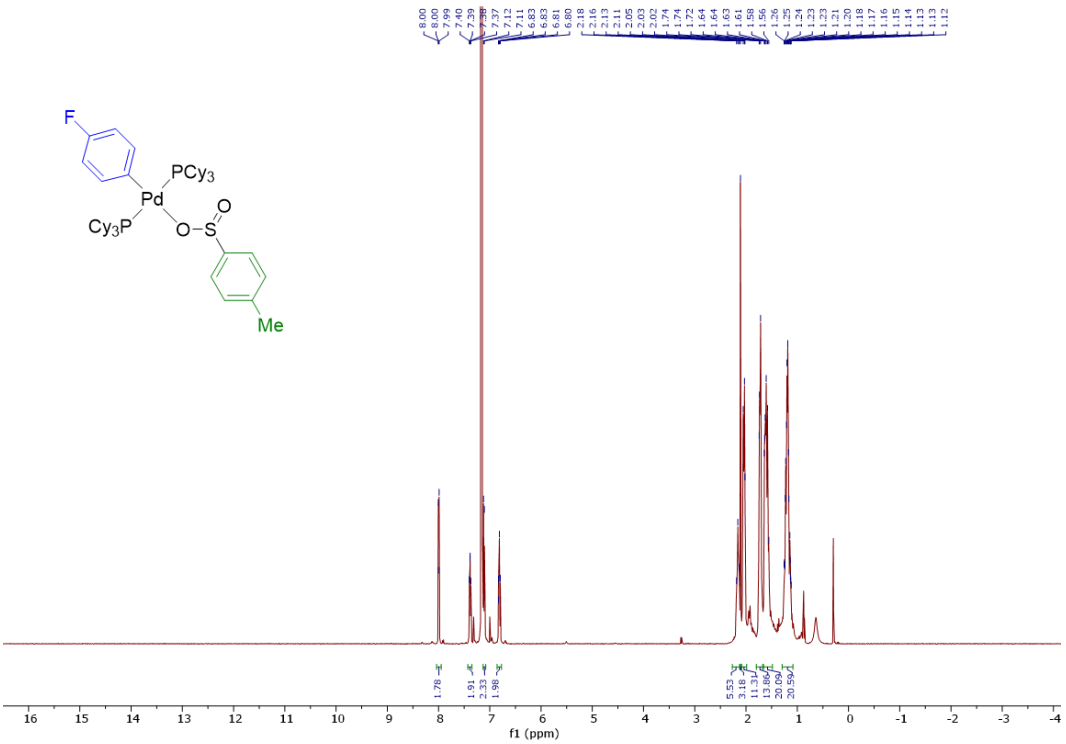
[(PCy_3)Pd(4-F-C_6H_4)(κ_S-$\kappa_{O'}$-6-*t*Bu-pyridine-2-SO_2)]$_2$ (13)

$^{19}F\{^1H\}$ NMR (377 MHz, $CDCl_3$)

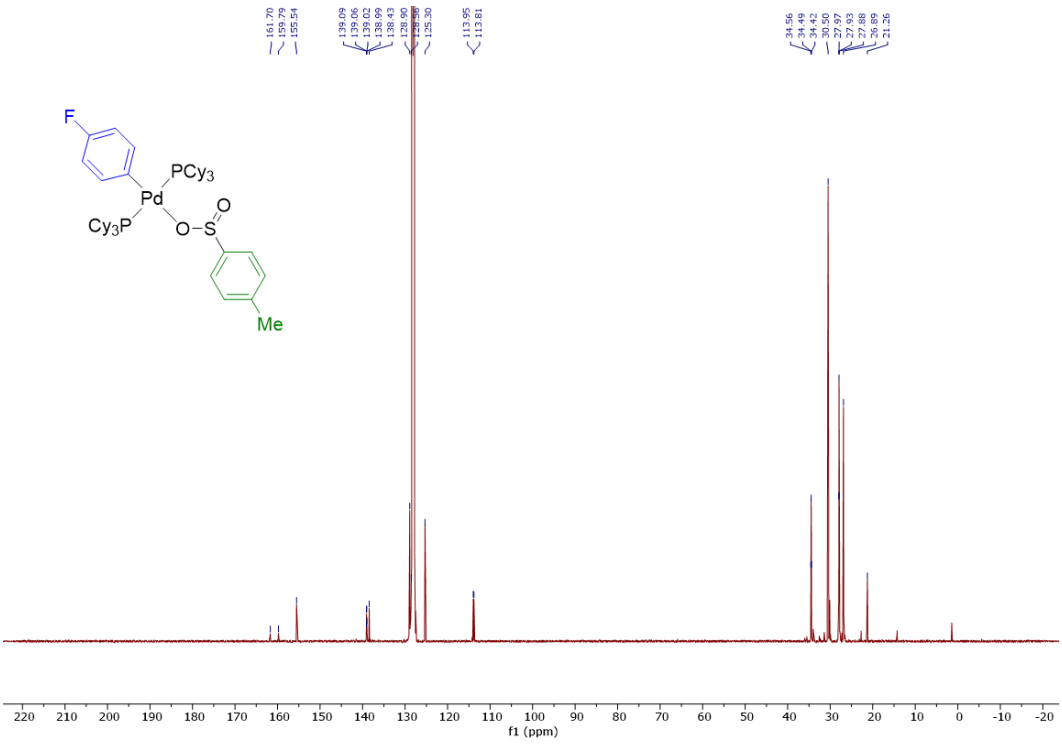


[Pd(4-F-C_6H_4) (PCy_3)$_2$(κ_O-4-Me-C_6H_4-SO_2)] (14)

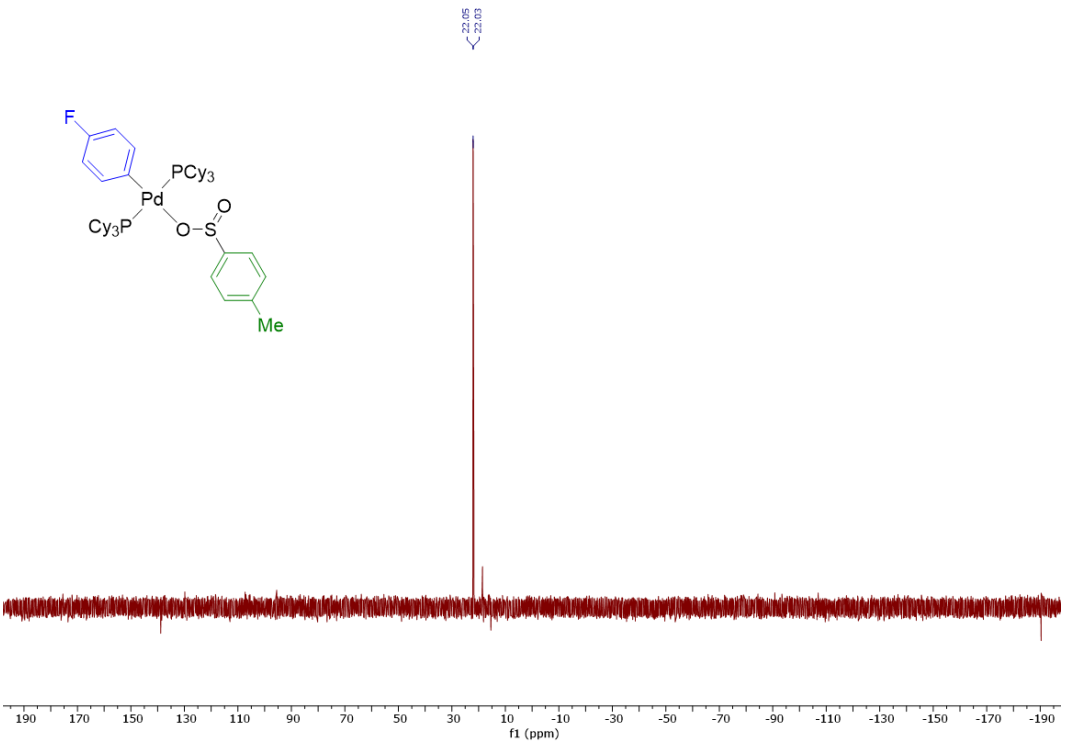
^1H NMR (500 MHz, C_6D_6)



[Pd(4-F-C_6H_4) (PCy_3)$_2$(κ_O-4-Me-C_6H_4-SO_2)] (14)
$^{13}C\{^1H\}$ NMR (126 MHz, C_6D_6)

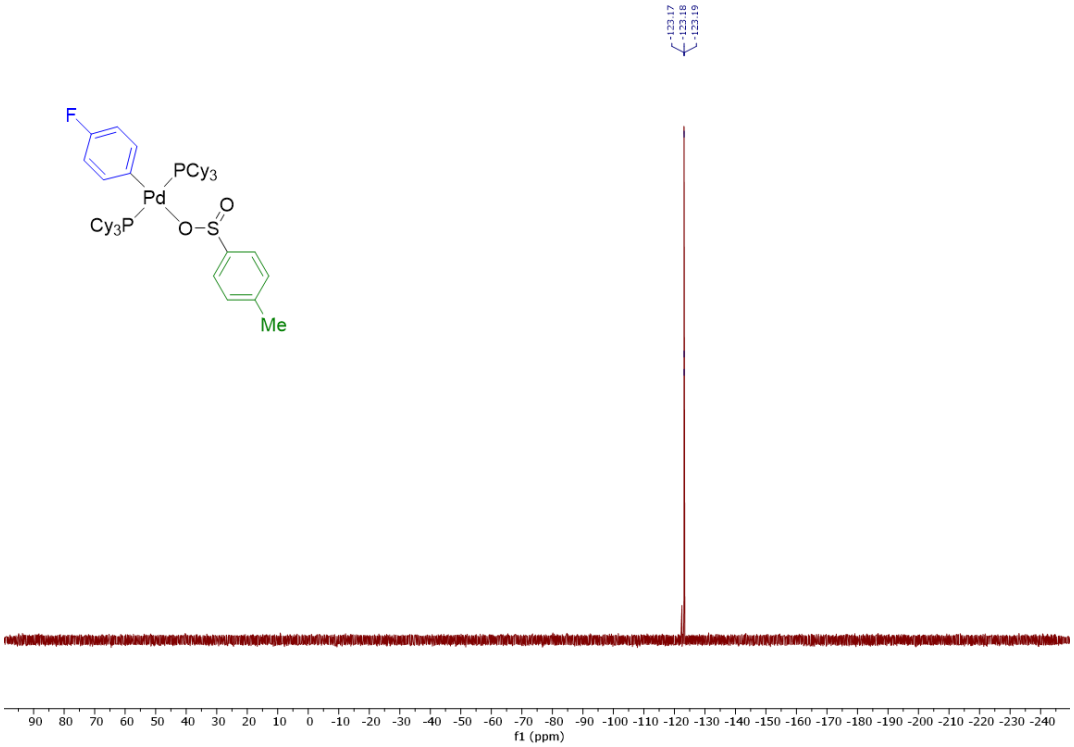


[Pd(4-F-C_6H_4) (PCy_3)$_2$(κ_O-4-Me-C_6H_4-SO_2)] (14)
$^{31}P\{^1H\}$ NMR (162 MHz, C_6D_6)



[Pd(4-F-C_6H_4) (PCy_3)$_2$(κ_O-4-Me-C_6H_4-SO_2)] (14)

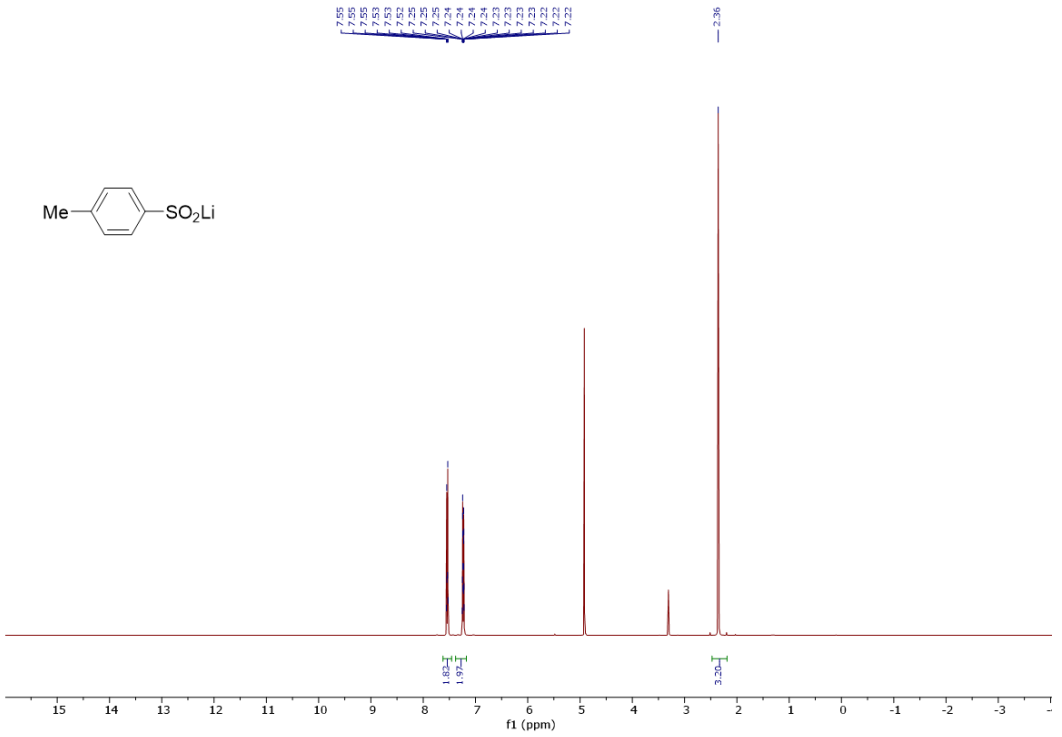
$^{19}F\{^1H\}$ NMR (377 MHz, C_6D_6)



9.1.3. Sulfinate Salts

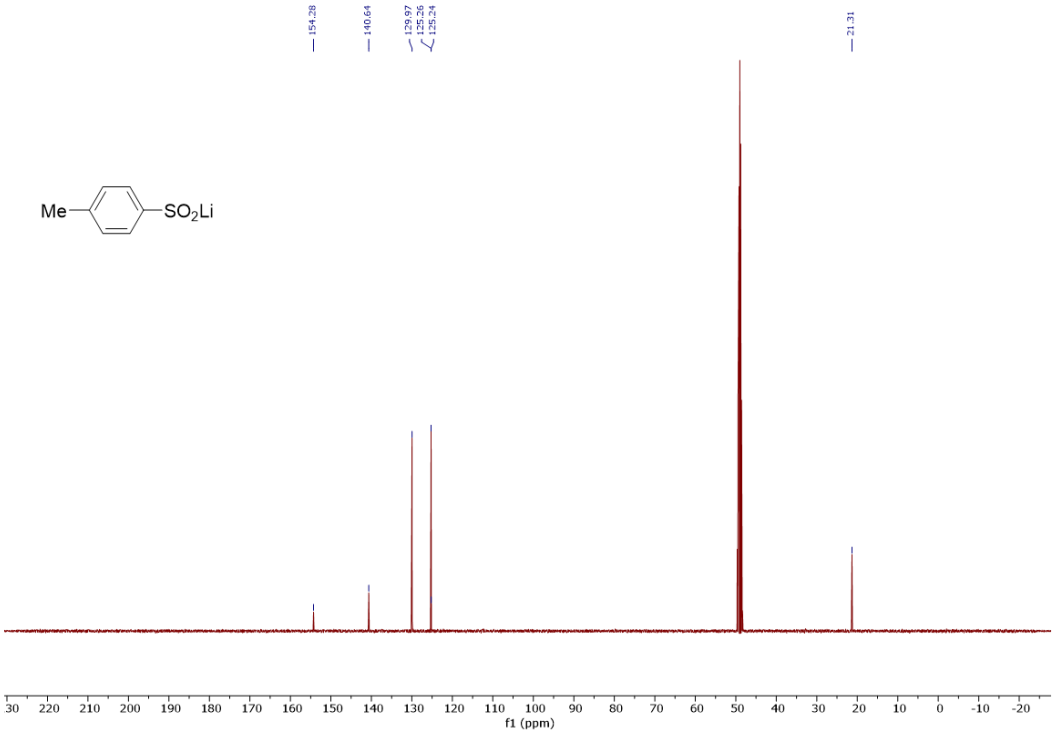
Lithium 4-methylbenzenesulfinate (4-Li)

^1H NMR (400 MHz, CD_3OD)



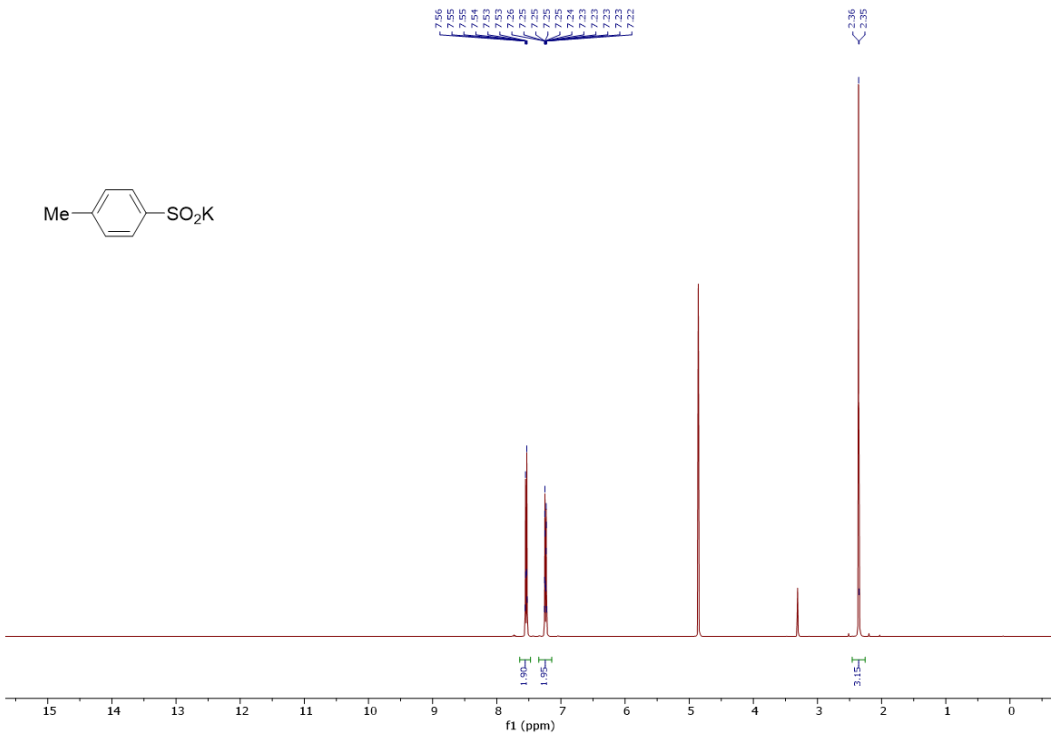
Lithium 4-methylbenzenesulfinate (4-Li)

$^{13}C\{^{1}H\}$ NMR (101 MHz, CD_3OD)



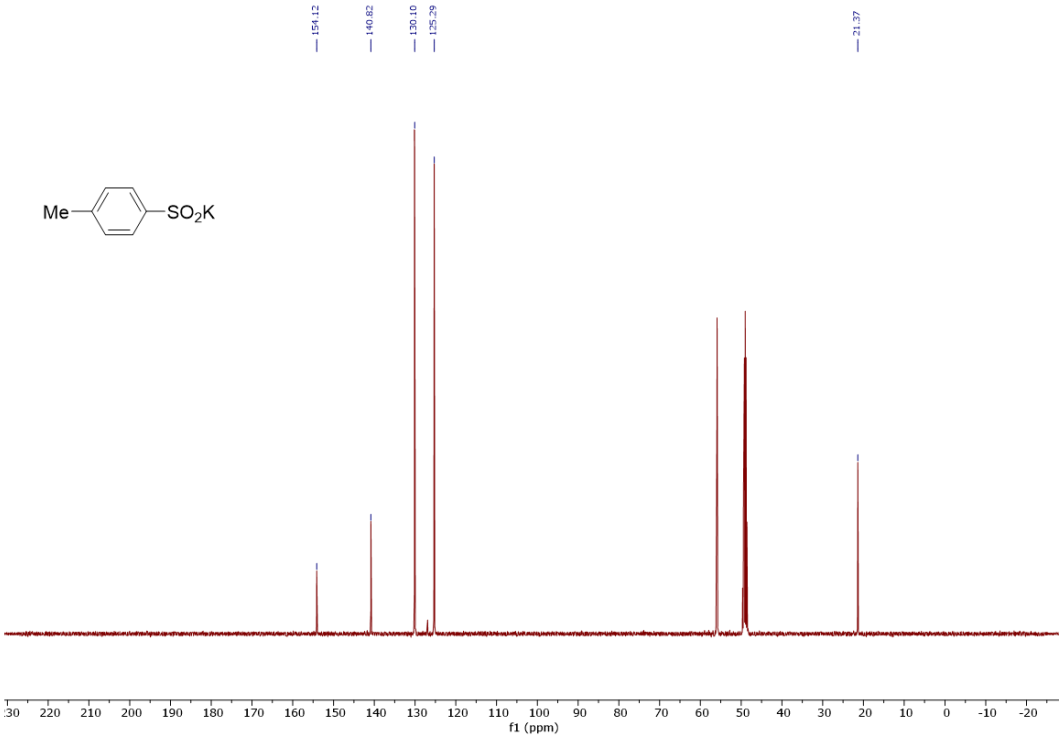
Potassium 4-methylbenzenesulfinate (4-K)

^{1}H NMR (400 MHz, CD_3OD)



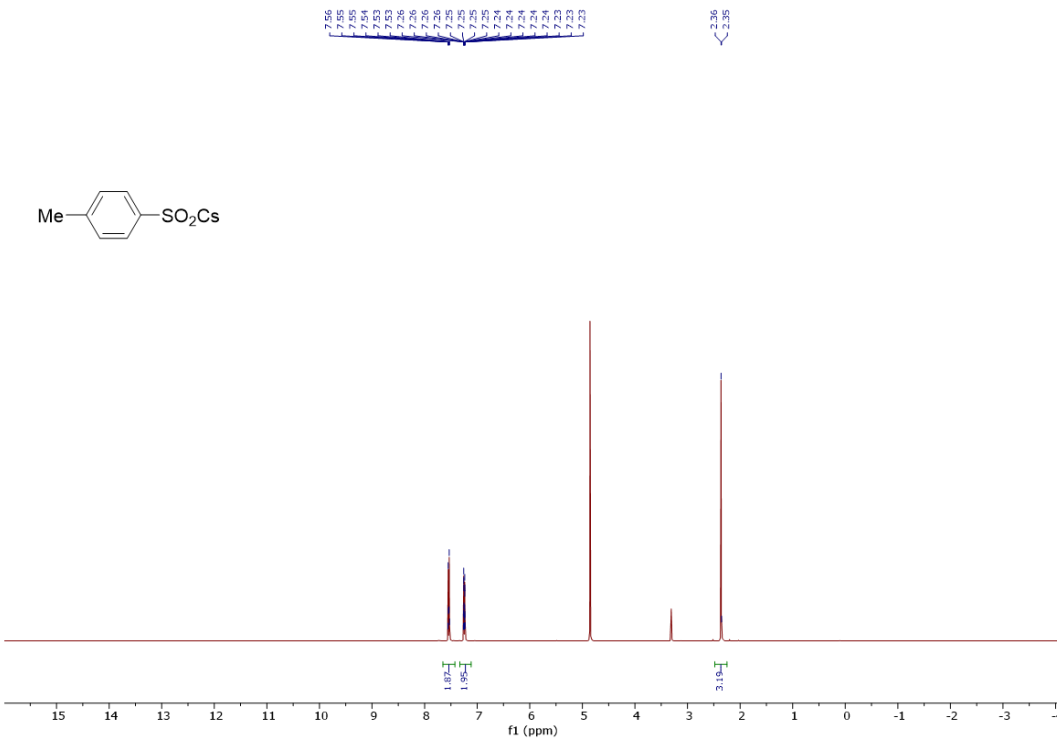
Potassium 4-methylbenzenesulfinate (4-K)

$^{13}C\{^{1}H\}$ NMR (101 MHz, CD_3OD)



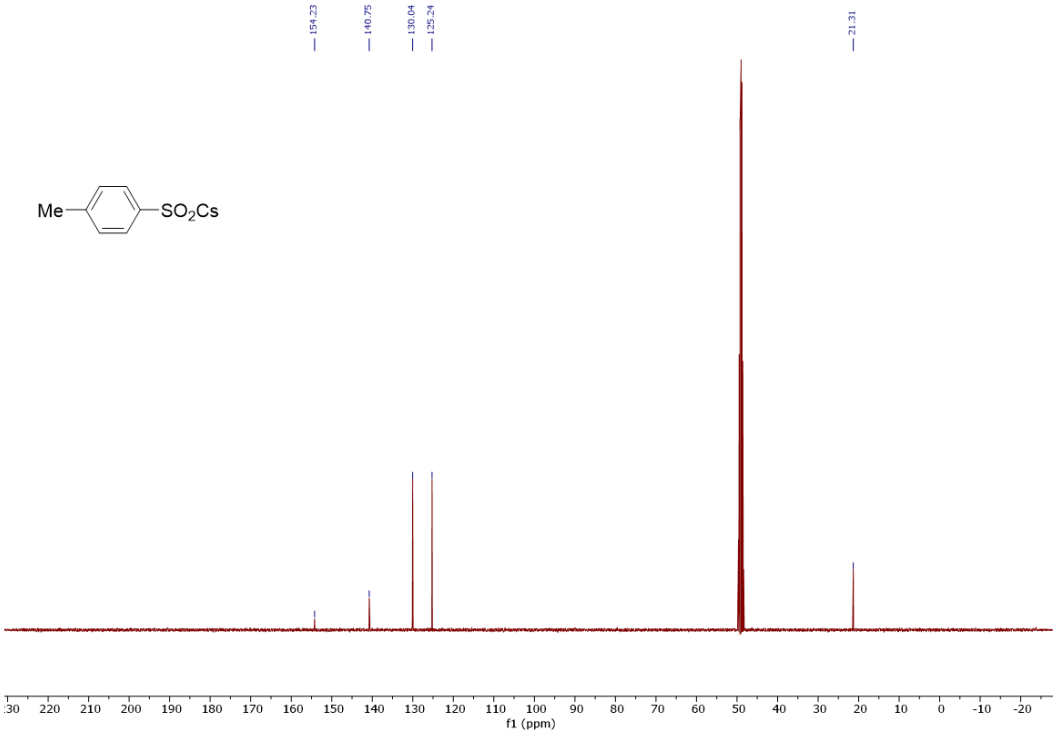
Caesium 4-methylbenzenesulfinate (4-Cs)

^{1}H NMR (400 MHz, CD_3OD)



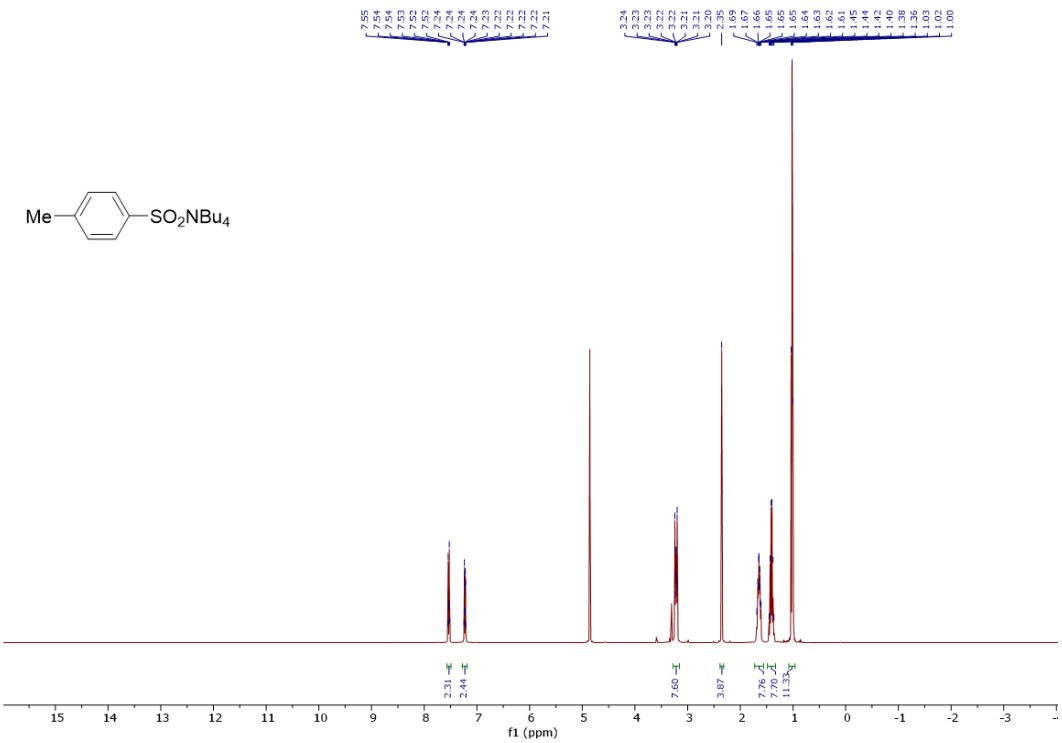
Caesium 4-methylbenzenesulfinate (4-Cs)

$^{13}C\{^{1}H\}$ NMR (101 MHz, CD_3OD)



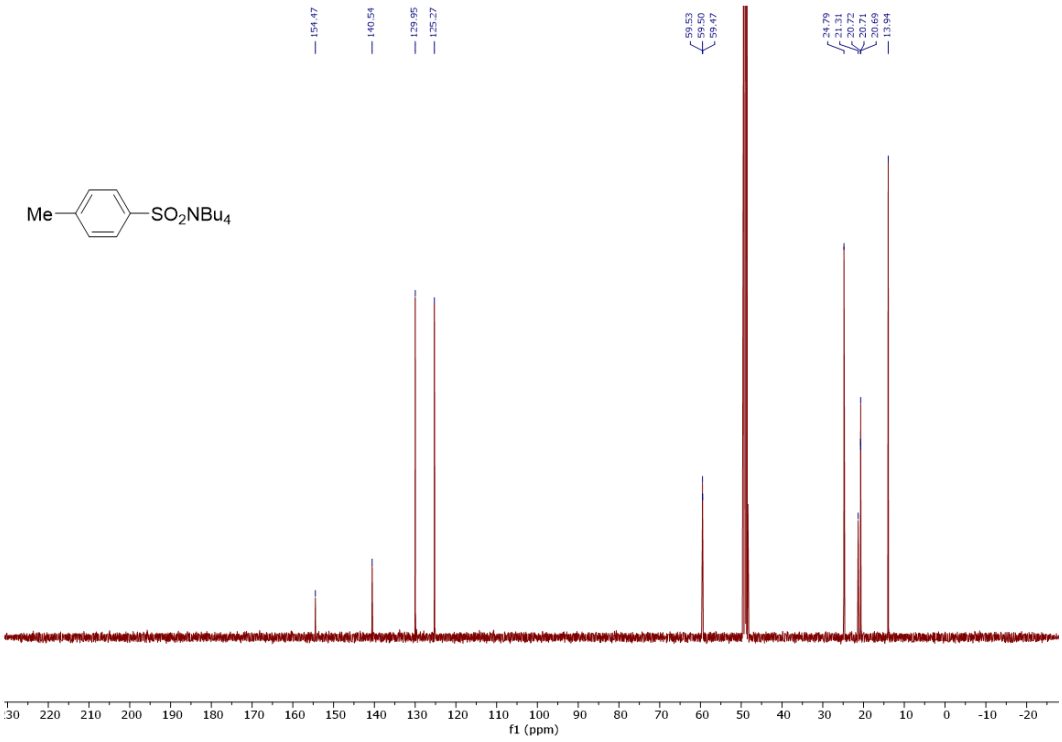
Tetrabutylammonium 4-methylbenzenesulfinate (4-TBA)

^{1}H NMR (400 MHz, CD_3OD)



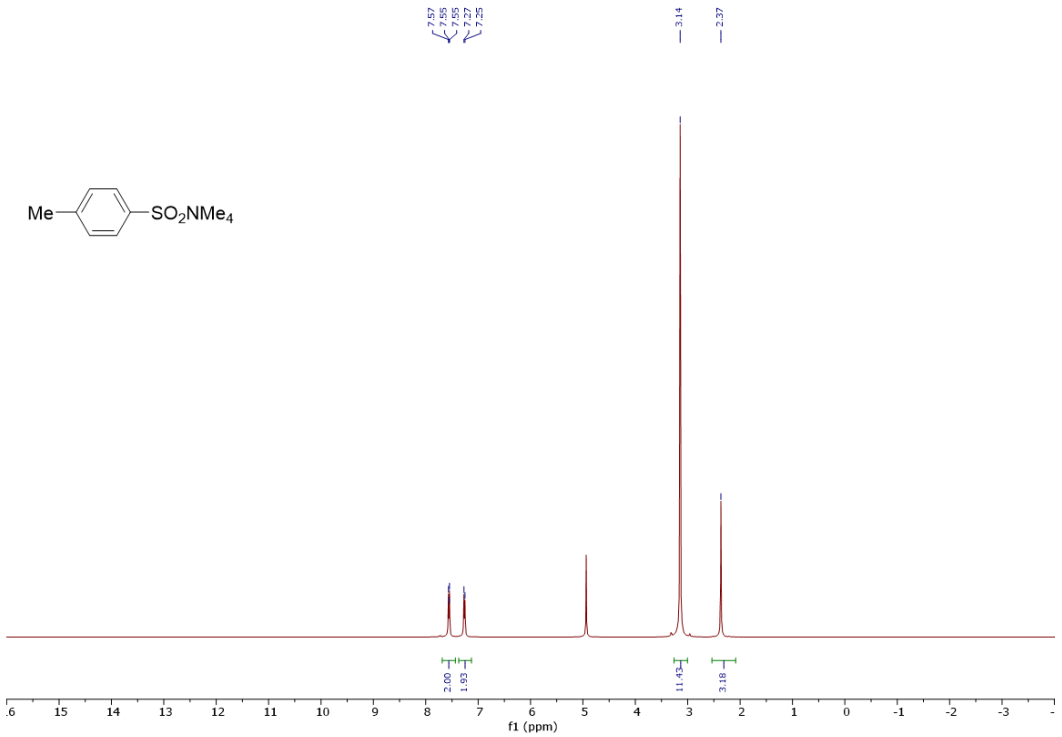
Tetrabutylammonium 4-methylbenzenesulfinate (4-TBA)

$^{13}C\{^{1}H\}$ NMR (101 MHz, CD_3OD)

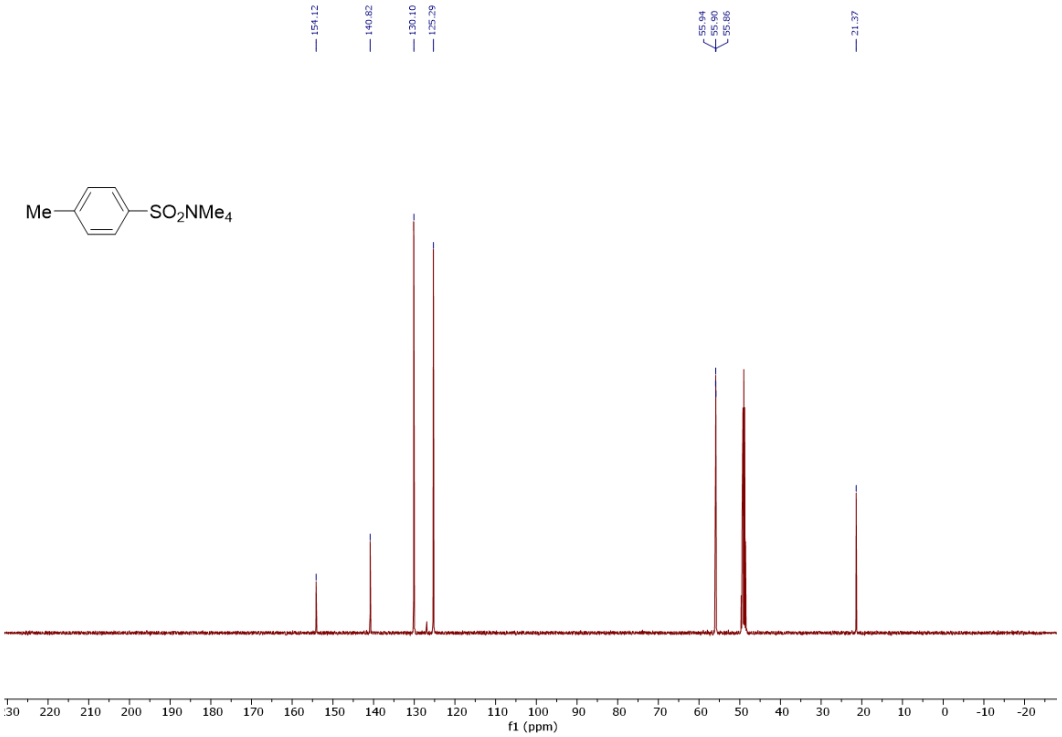


Tetramethylammonium 4-methylbenzenesulfinate (4-TMA)

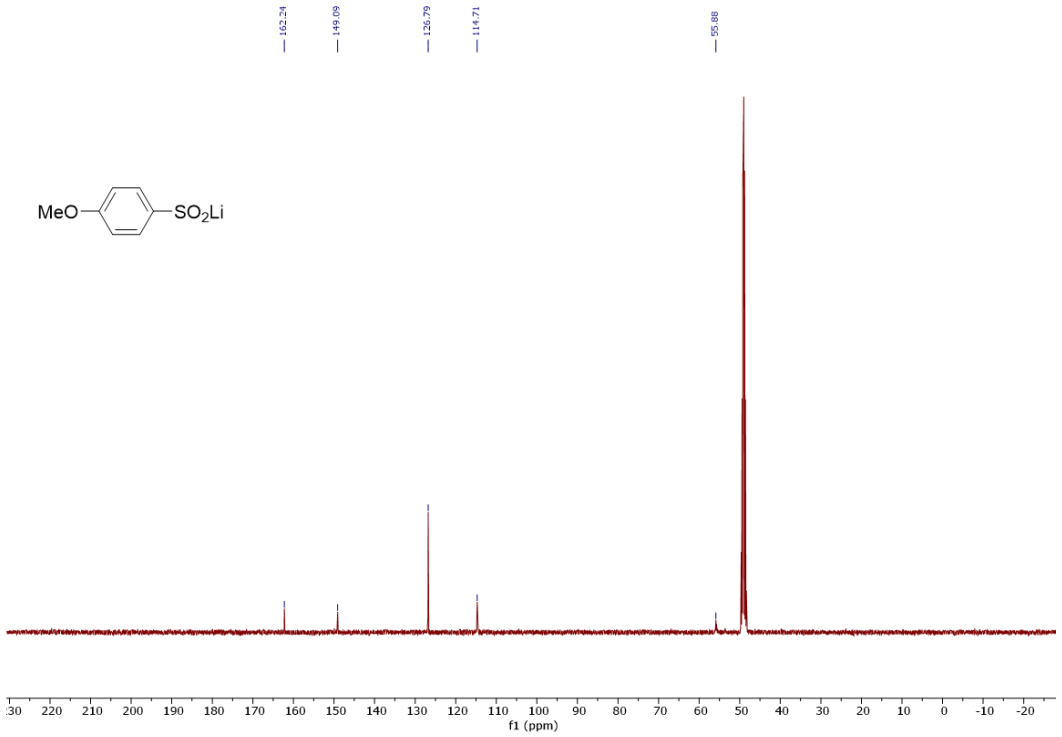
^{1}H NMR (400 MHz, CD_3OD)



Tetramethylammonium 4-methylbenzenesulfinate (4-TMA)
$^{13}C\{^{1}H\}$ NMR (101 MHz, CD_3OD)

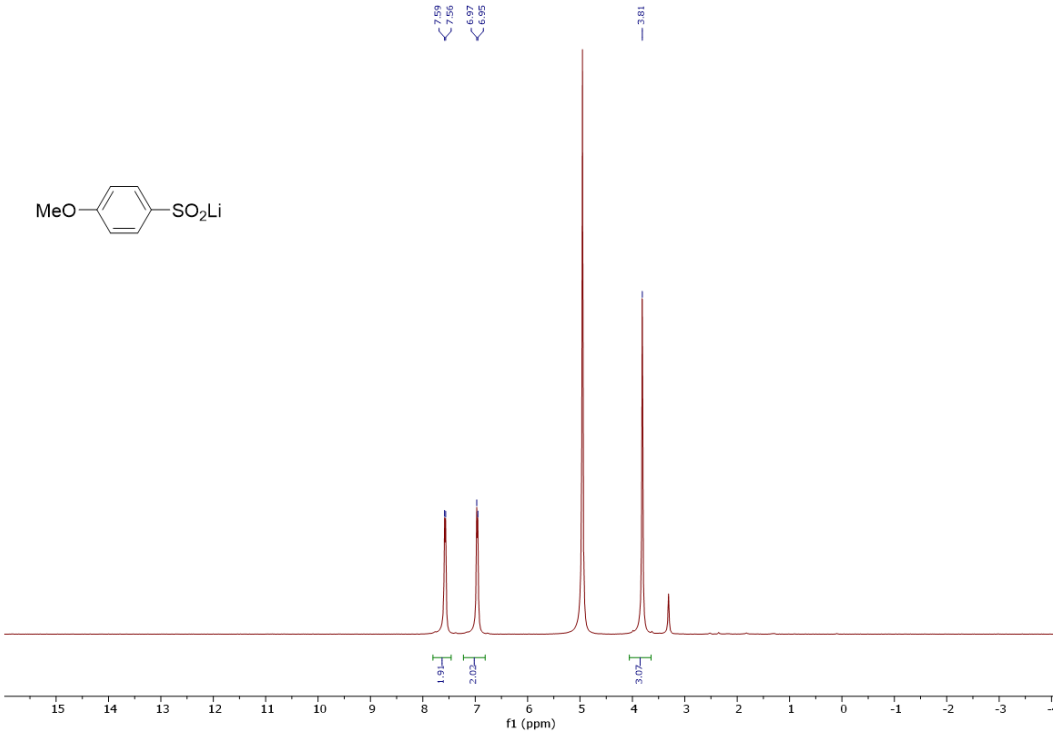


Lithium 4-methoxybenzenesulfinate (4-OMe)
$^{13}C\{^{1}H\}$ NMR (101 MHz, CD_3OD)



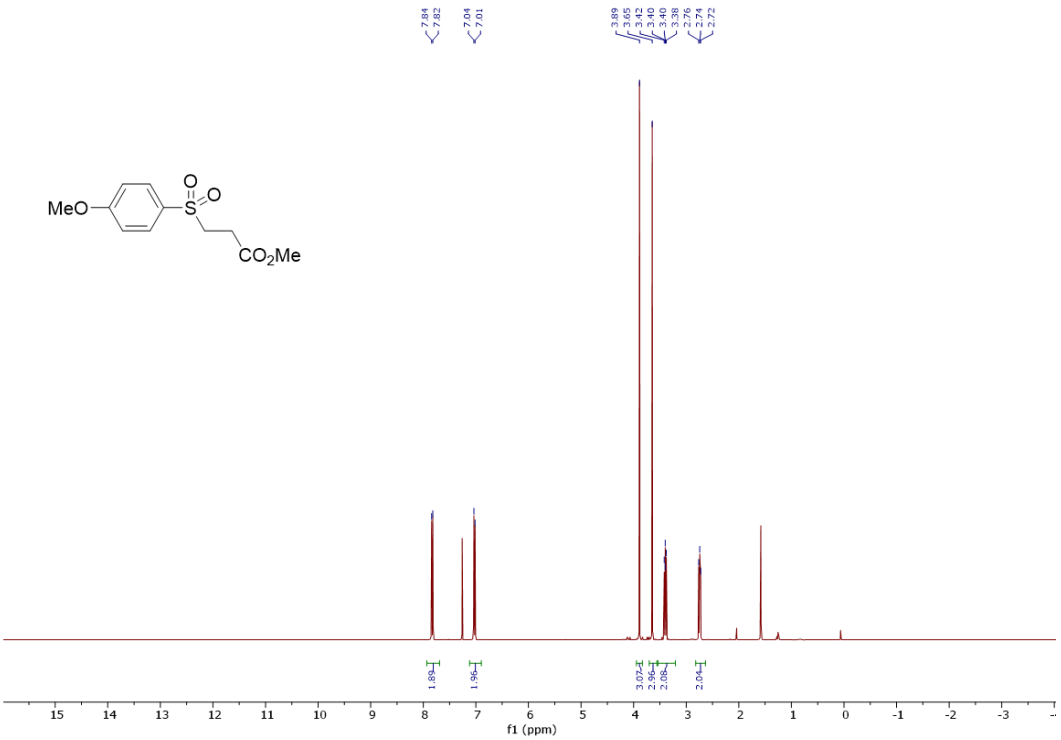
Lithium 4-methoxybenzenesulfinate (4-OMe)

^{1}H NMR (400 MHz, CD_3OD)



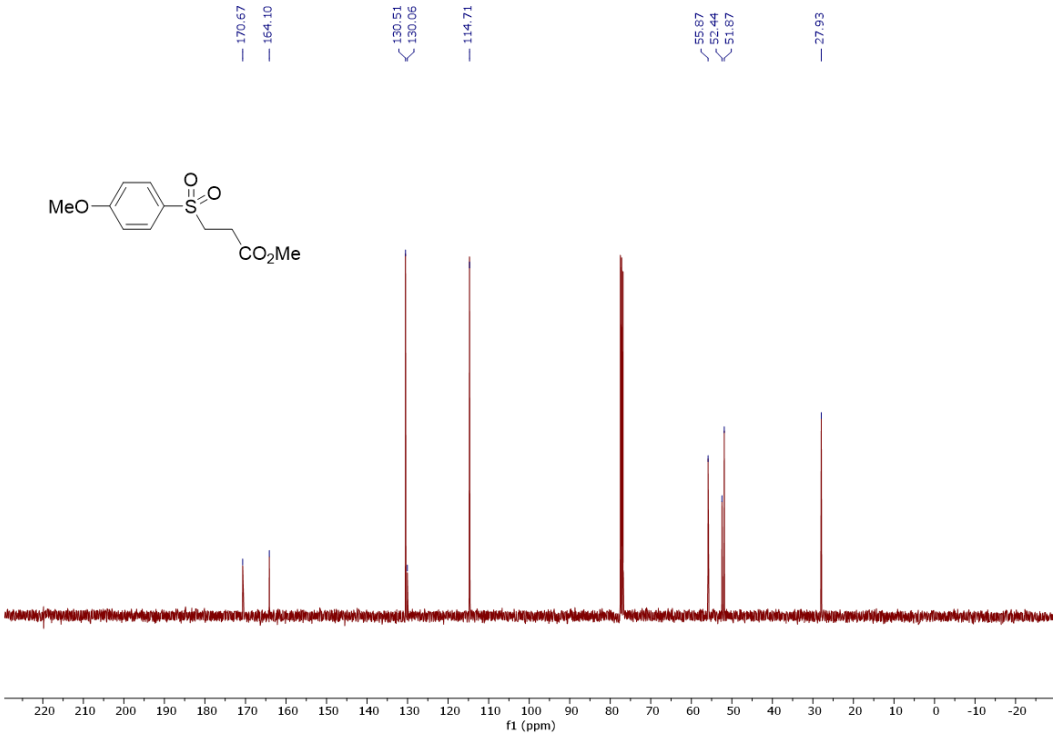
3-((4-methoxyphenyl)sulfonyl)propanoate

^{1}H NMR (400 MHz, $CDCl_3$)



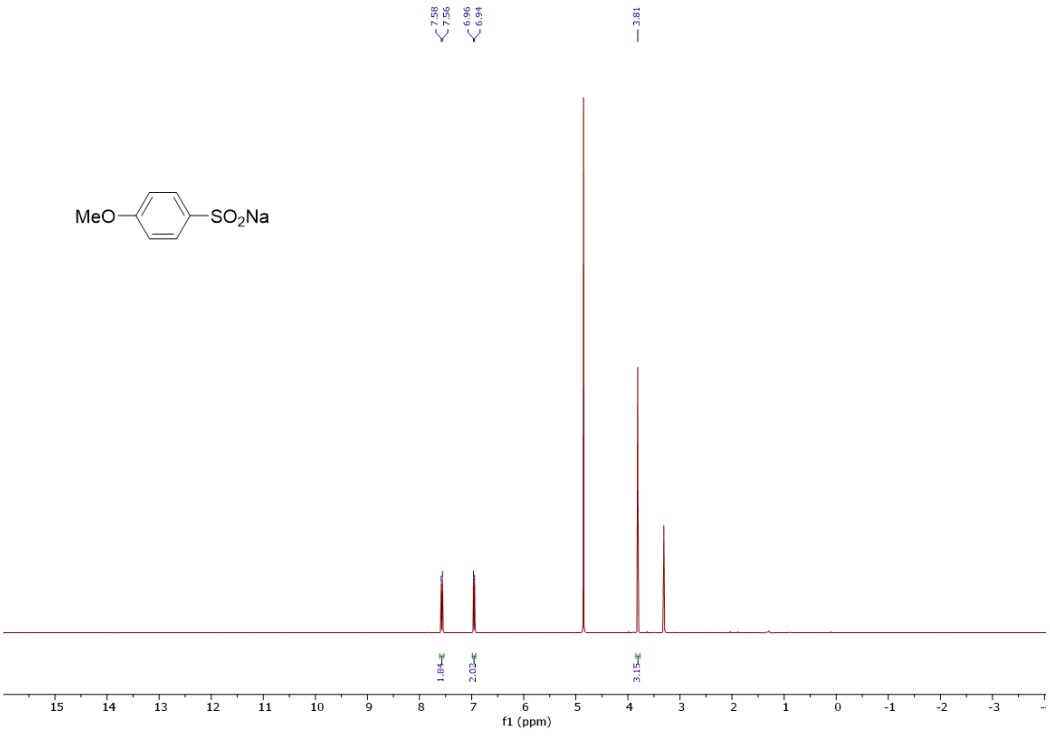
3-((4-methoxyphenyl)sulfonyl)propanoate

$^{13}C\{^{1}H\}$ NMR (101 MHz, $CDCl_3$)



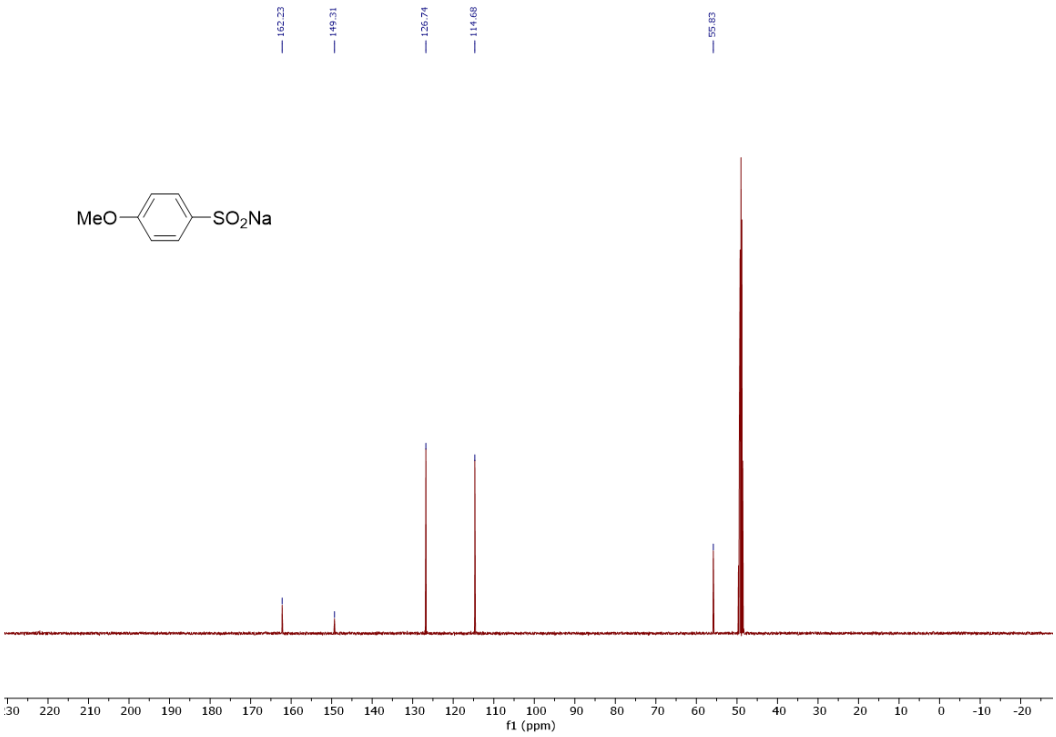
Sodium 4-methoxybenzenesulfinate (4-OMe-Na)

^{1}H NMR (400 MHz, CD_3OD)



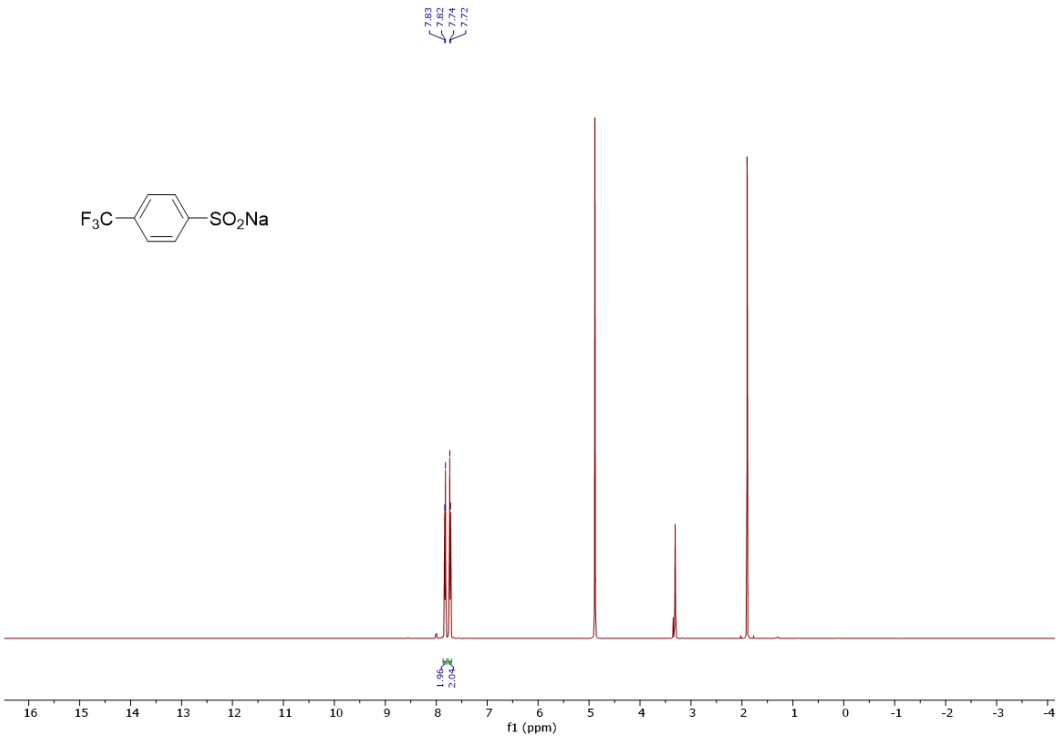
Sodium 4-methoxybenzenesulfinate (4-OMe-Na)

$^{13}C\{^{1}H\}$ NMR (101 MHz, CD_3OD)

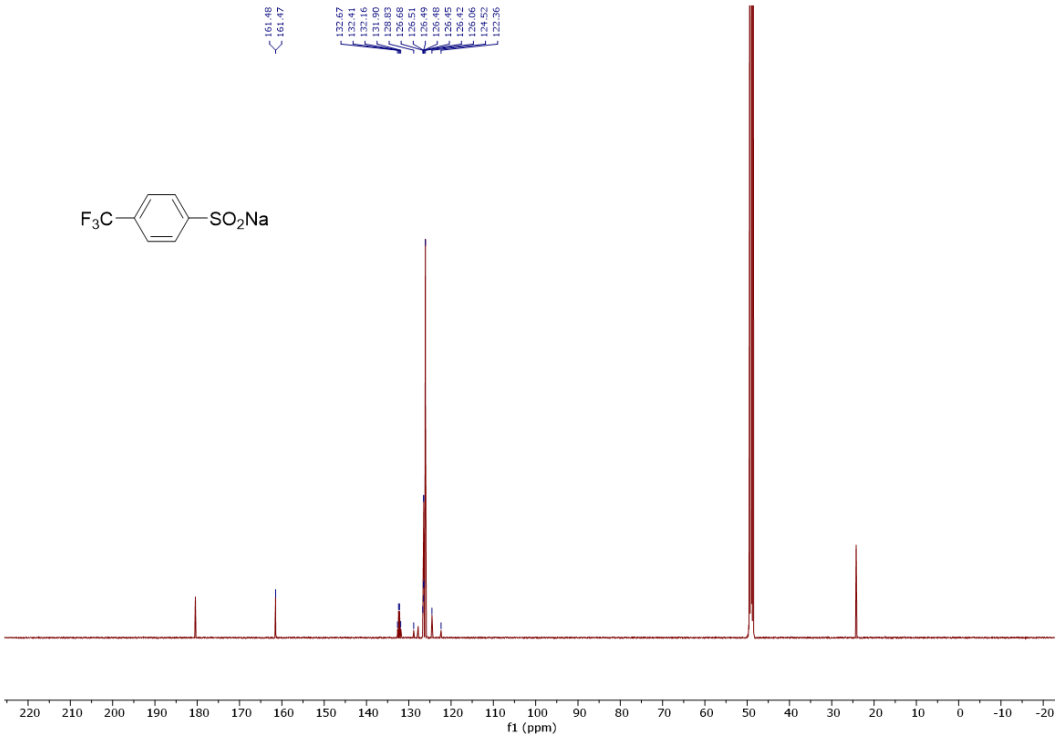


Sodium 4-(trifluoromethyl)benzenesulfinate (4-CF_3)

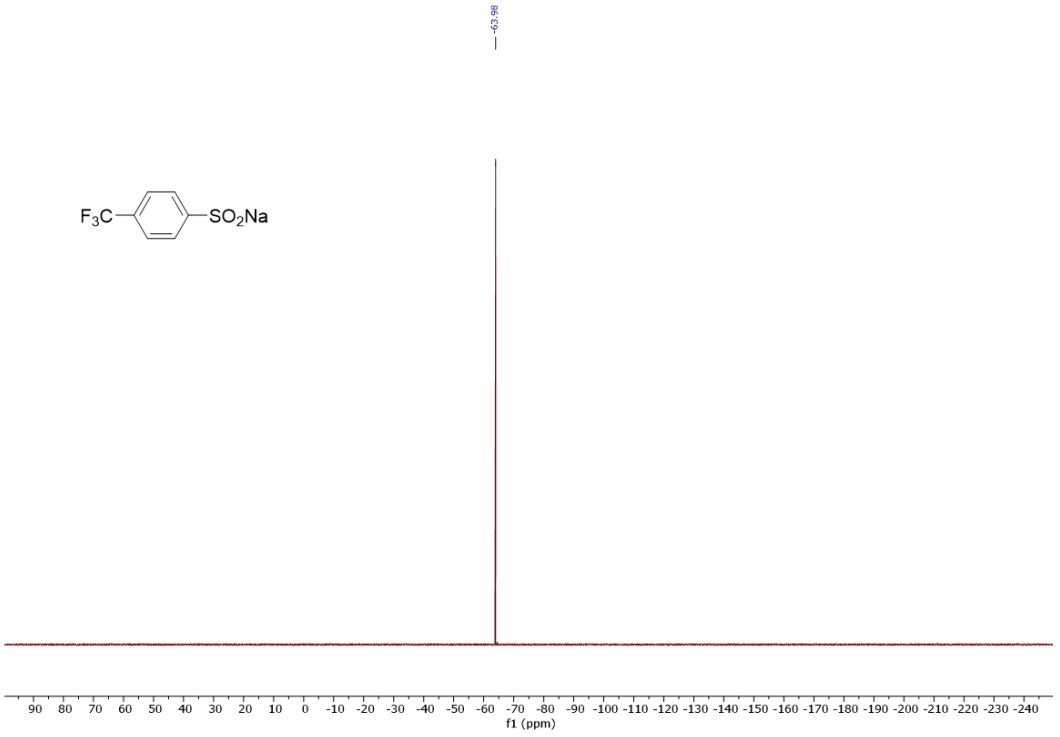
^{1}H NMR (500 MHz, CD_3OD)



Sodium 4-(trifluoromethyl)benzenesulfinate (4-CF_3)
$^{13}C\{^1H\}$ NMR (126 MHz, CD_3OD)

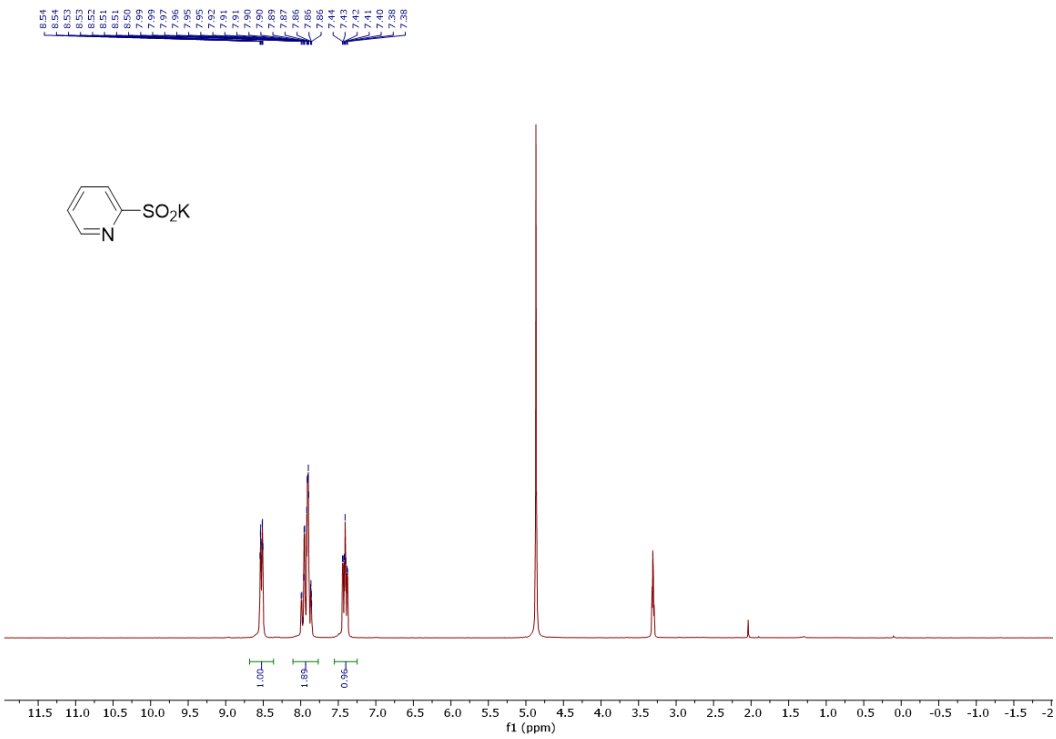


Sodium 4-(trifluoromethyl)benzenesulfinate (4-CF_3)
^{19}F NMR (377 MHz, CD_3OD)



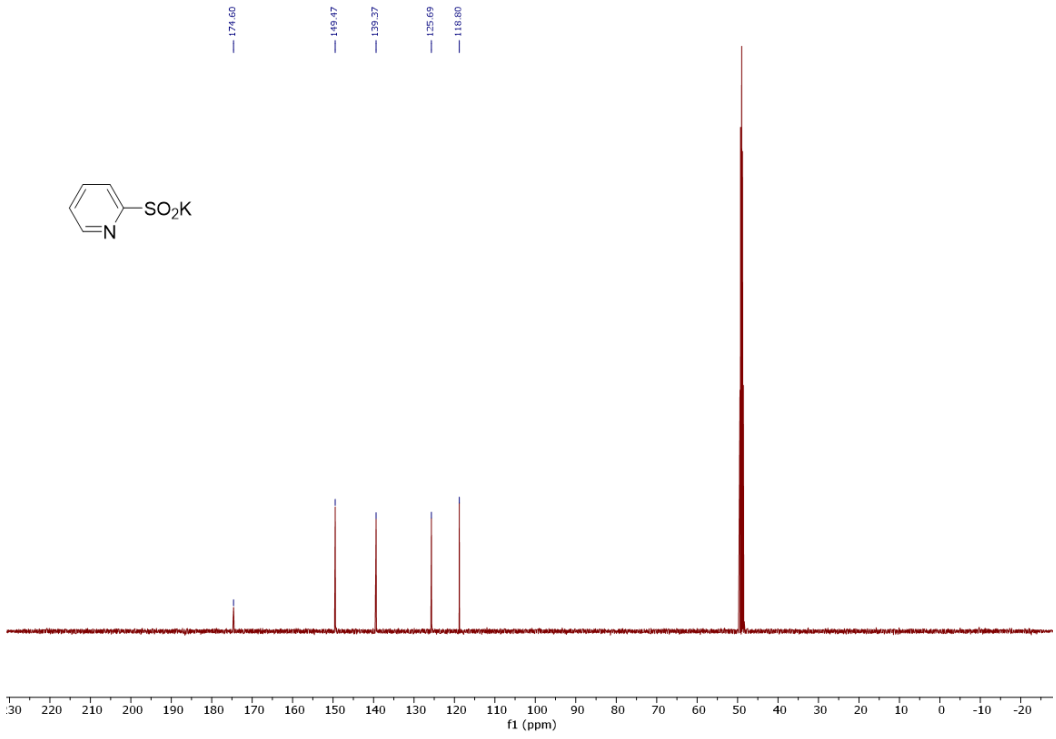
Potassium pyridine-2-sulfinate (1-K)

^{1}H NMR (200 MHz, CD_3OD)

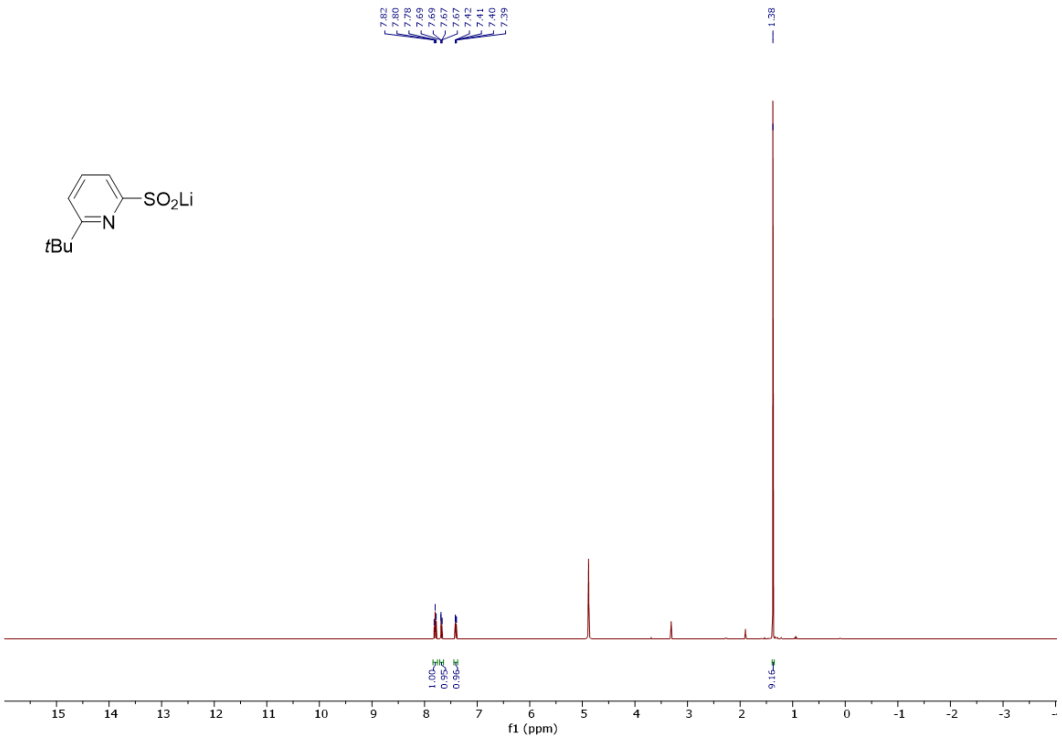


Potassium pyridine-2-sulfinate (1-K)

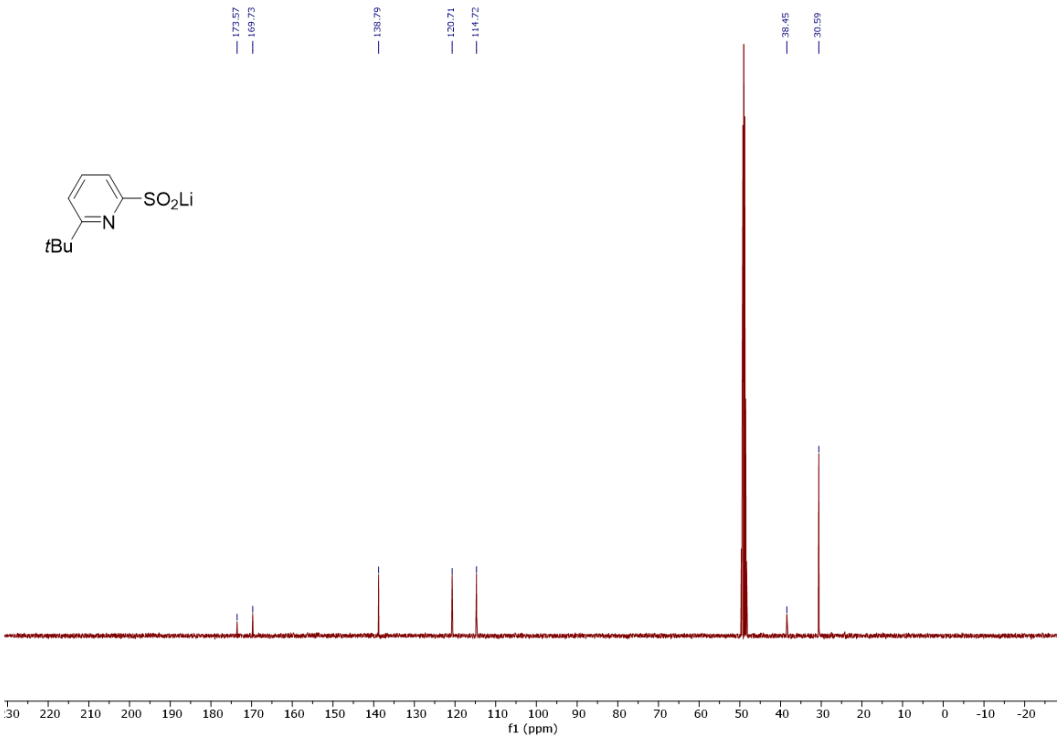
^{13}C{^{1}H} NMR (101 MHz, CD_3OD)



Lithium 6-(tert-butyl)pyridine-2-sulfinate (1-*t*-Bu)
^{1}H NMR (400 MHz, CD_3OD)

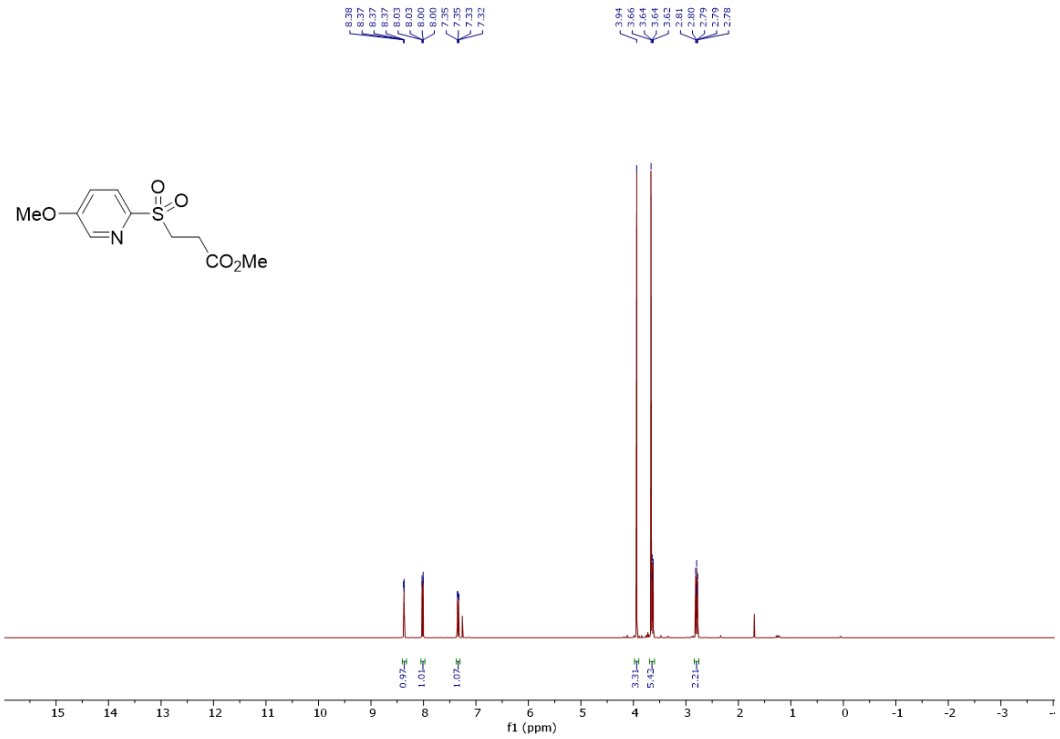


Lithium 6-(tert-butyl)pyridine-2-sulfinate (1-*t*-Bu)
^{13}C{^{1}H} NMR (101 MHz, CD_3OD)



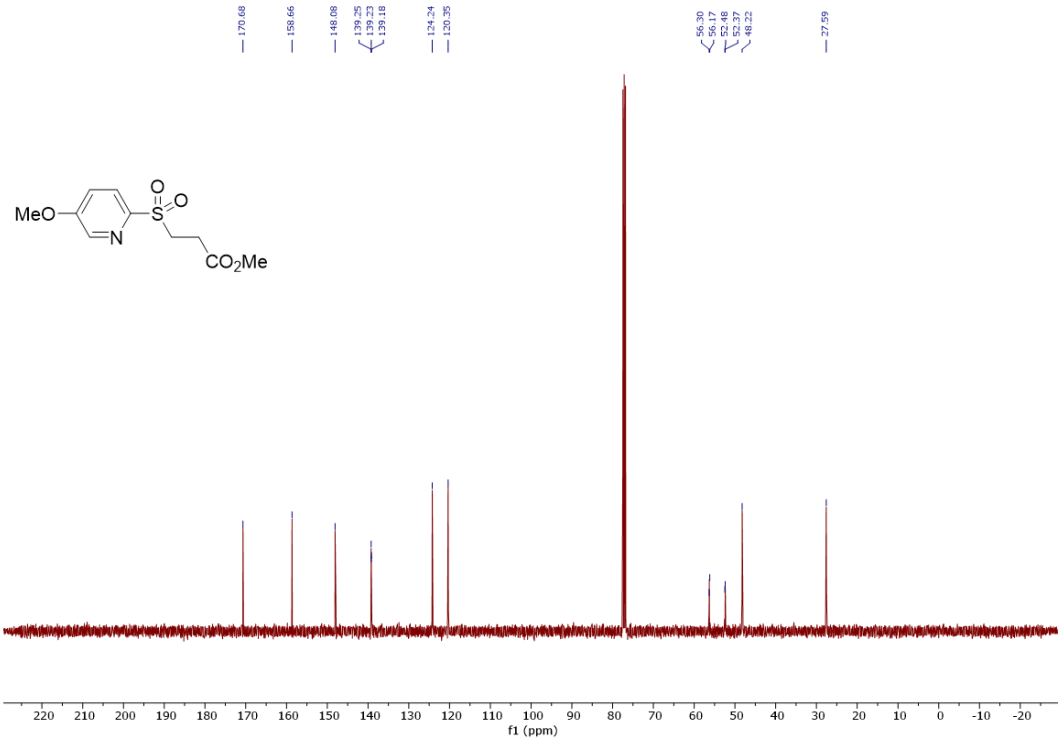
methyl 3-((5-methoxypyridin-2-yl)sulfonyl)propanoate

^{1}H NMR (400 MHz, $CDCl_3$)

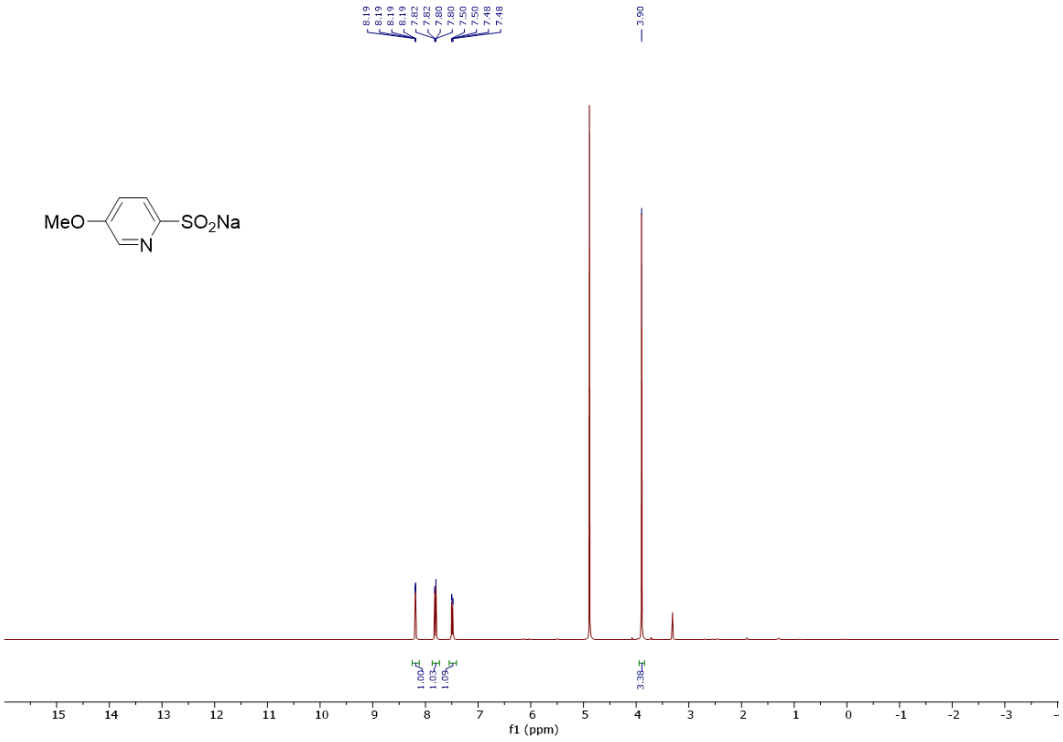


methyl 3-((5-methoxypyridin-2-yl)sulfonyl)propanoate

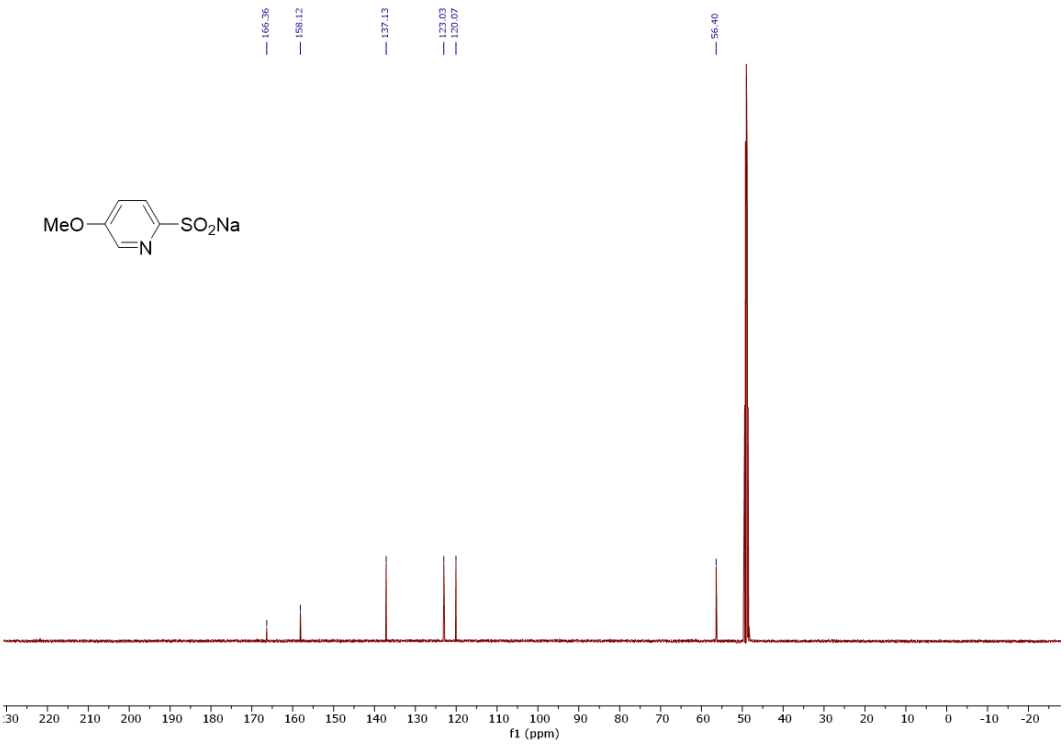
^{13}C{^{1}H} NMR (101 MHz, $CDCl_3$)



Sodium 5-methoxypyridine-2-sulfinate
^{1}H NMR (400 MHz, CD_3OD)

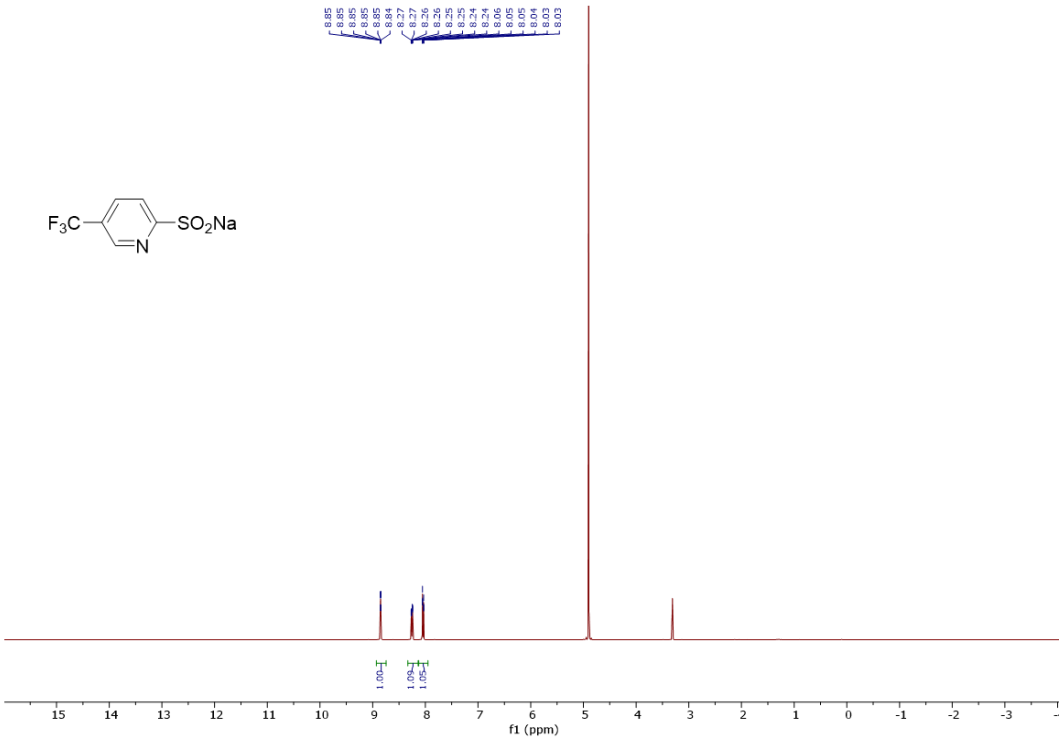


Sodium 5-methoxypyridine-2-sulfinate
^{13}C{^{1}H} NMR (101 MHz, CD_3OD)



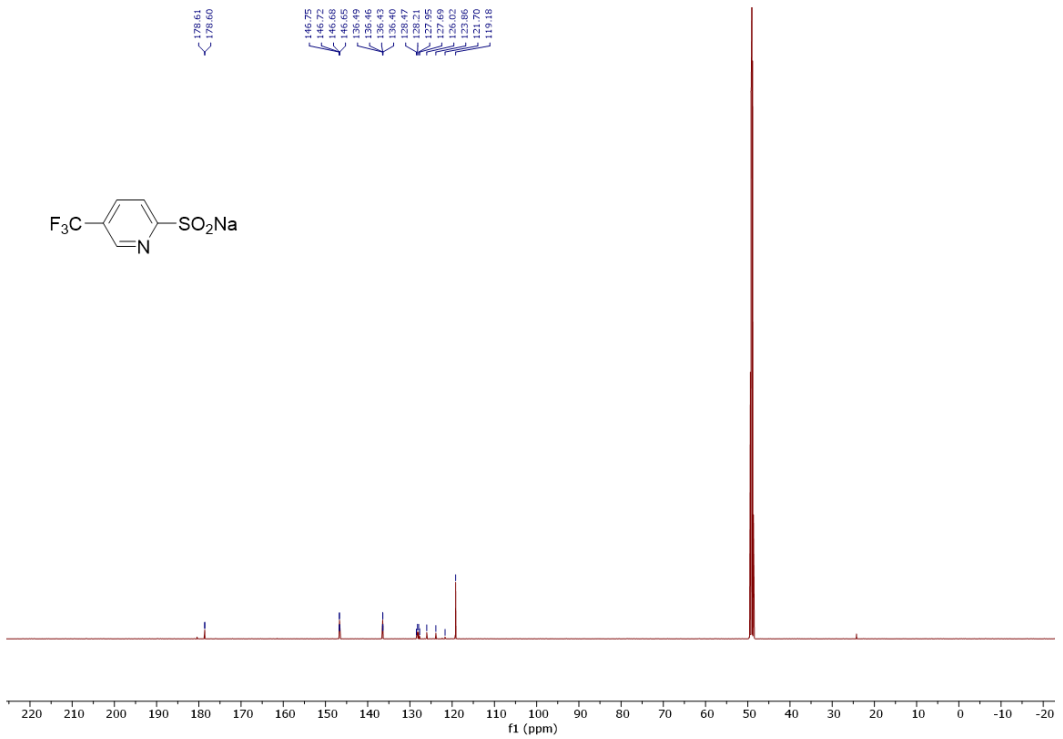
Sodium 5-(trifluoromethyl)pyridine-2-sulfinate

^{1}H NMR (400 MHz, CD_3OD)



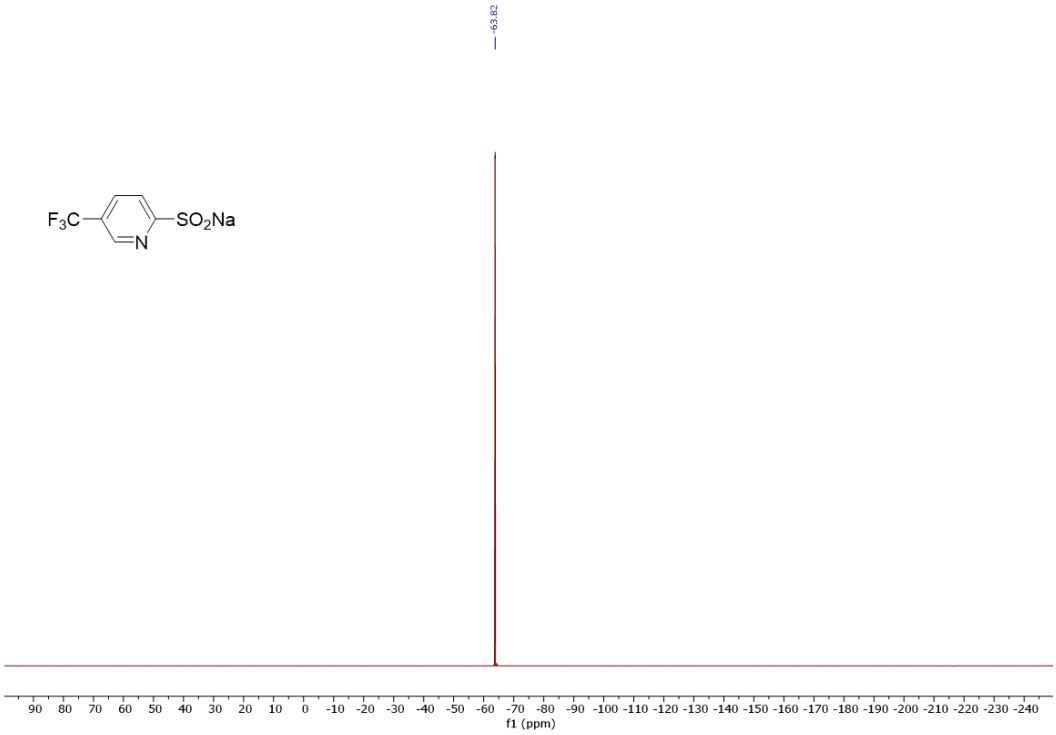
Sodium 5-(trifluoromethyl)pyridine-2-sulfinate

^{13}C{^{1}H} NMR (126 MHz, CD_3OD)



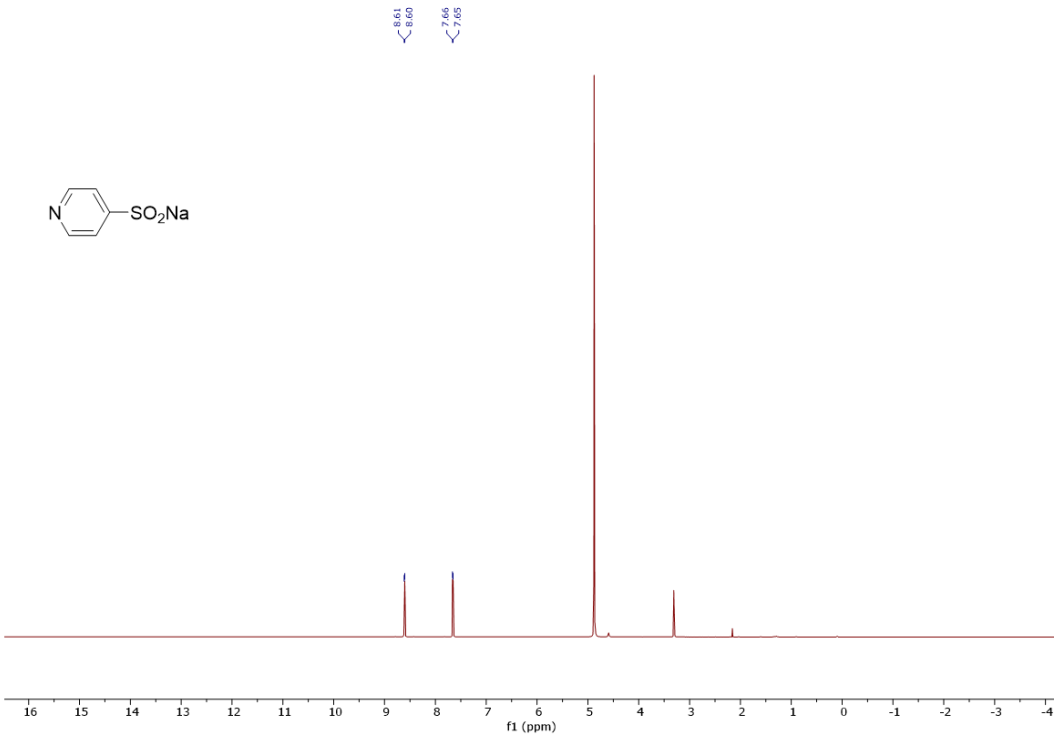
Sodium 5-(trifluoromethyl)pyridine-2-sulfinate

^{19}F NMR (377 MHz, CD_3OD)



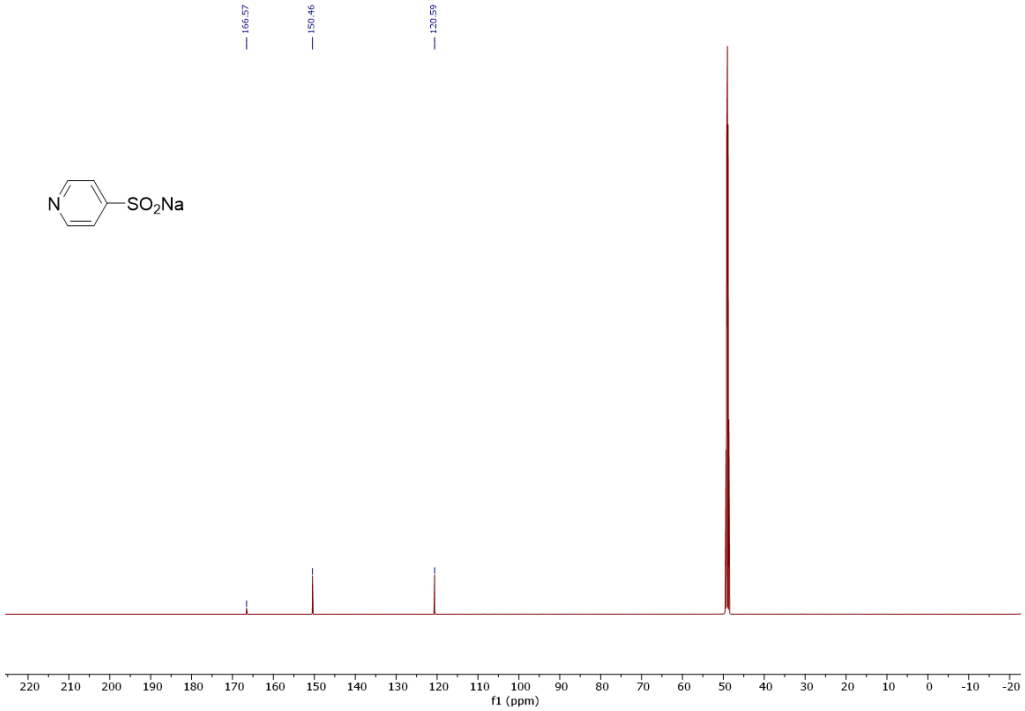
Sodium pyridine-4-sulfinate

^{1}H NMR (500 MHz, CD_3OD)



Sodium pyridine-4-sulfinate

$^{13}C\{^{1}H\}$ NMR (126 MHz, CD_3OD)

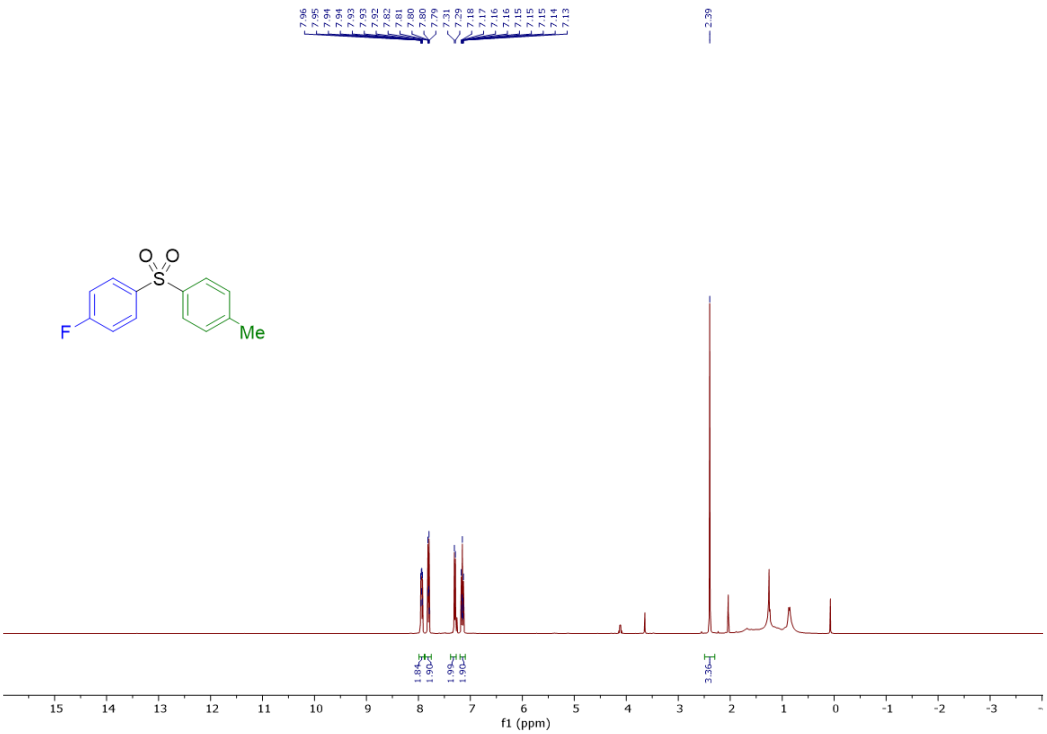


9.2. Compounds of Chapter 3

9.2.1. Sulfone Products

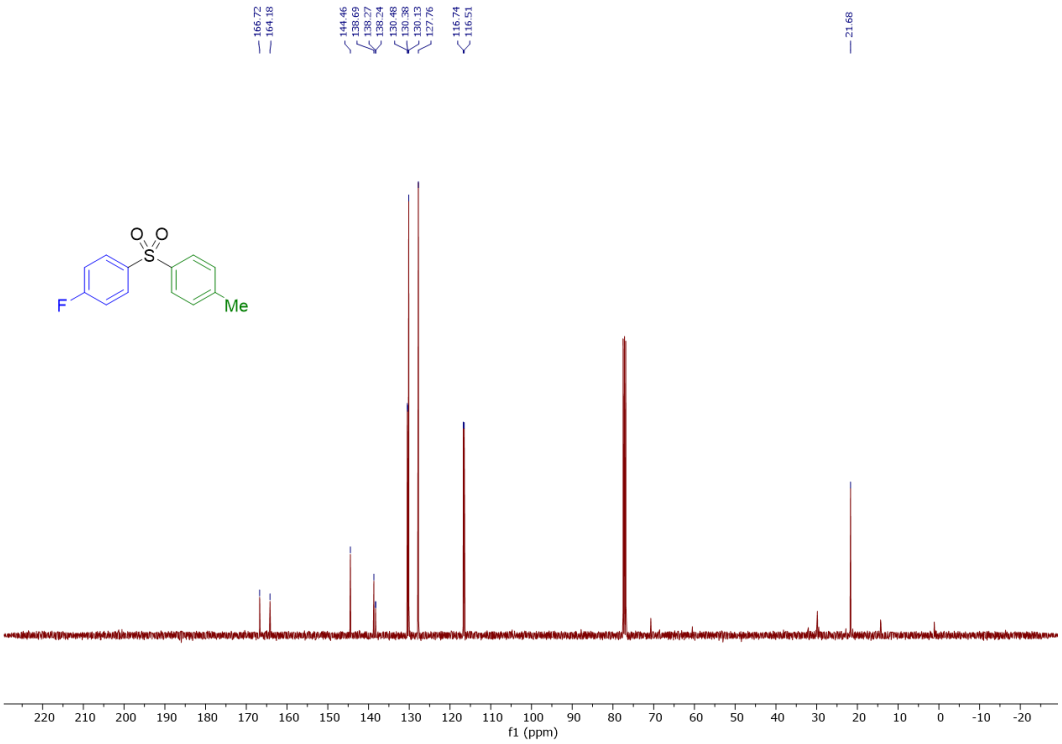
1-fluoro-4-tosylbenzene (17)

^{1}H NMR (400 MHz, $CDCl_3$)



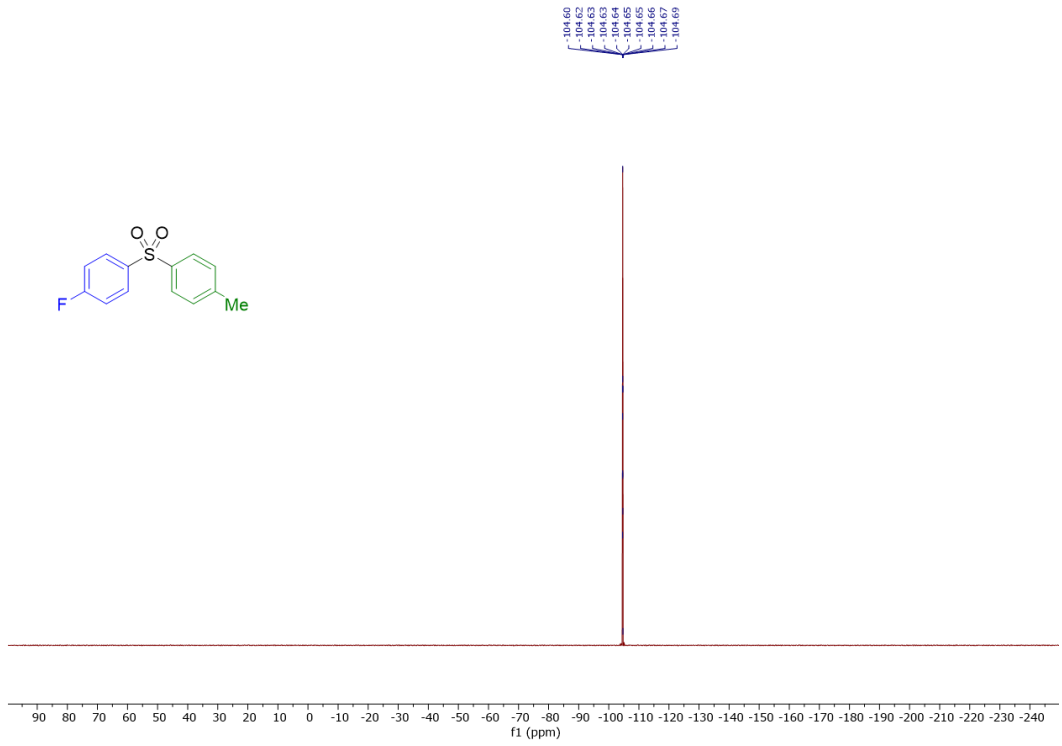
1-fluoro-4-tosylbenzene (17)

$^{13}C\{^{1}H\}$ NMR (101 MHz, $CDCl_3$)



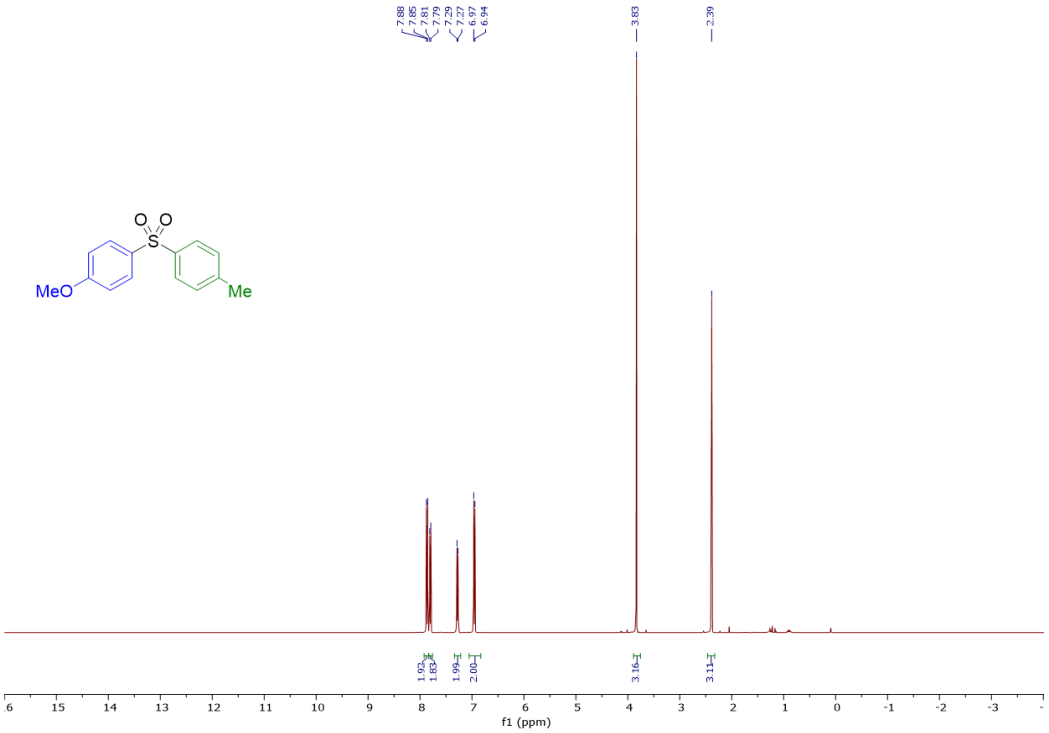
1-fluoro-4-tosylbenzene (17)

^{19}F NMR$\{^{1}H\}$ (376 MHz, $CDCl_3$)



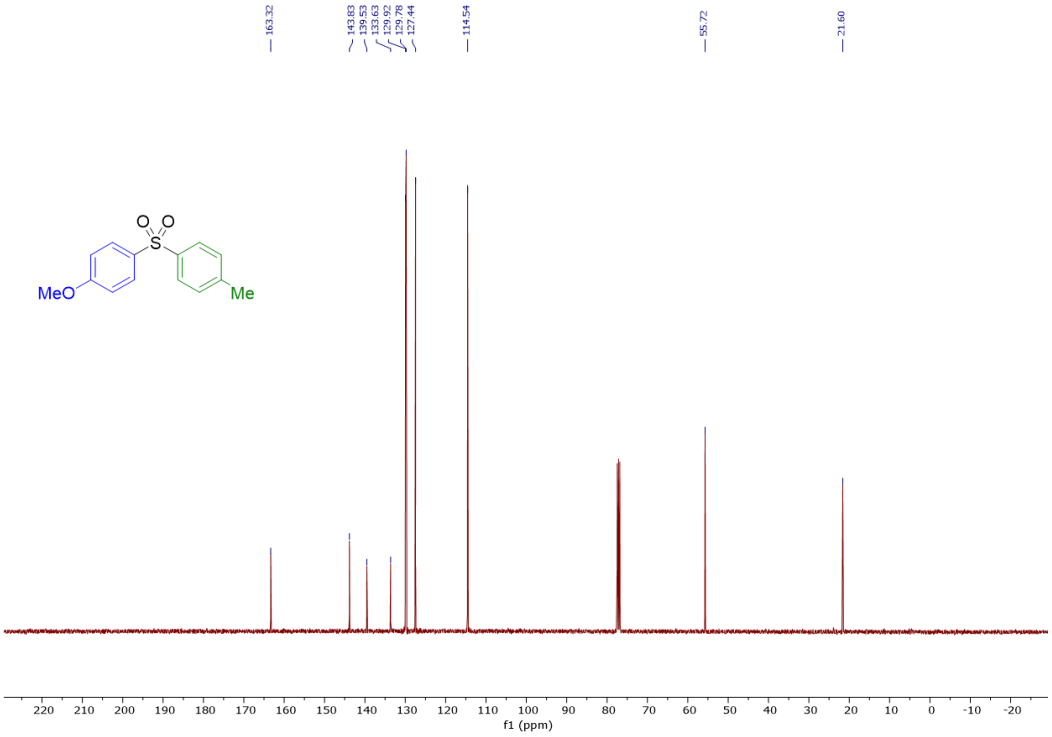
1-methoxy-4-tosylbenzene (17-OMe)

^{1}H NMR (400 MHz, $CDCl_3$)

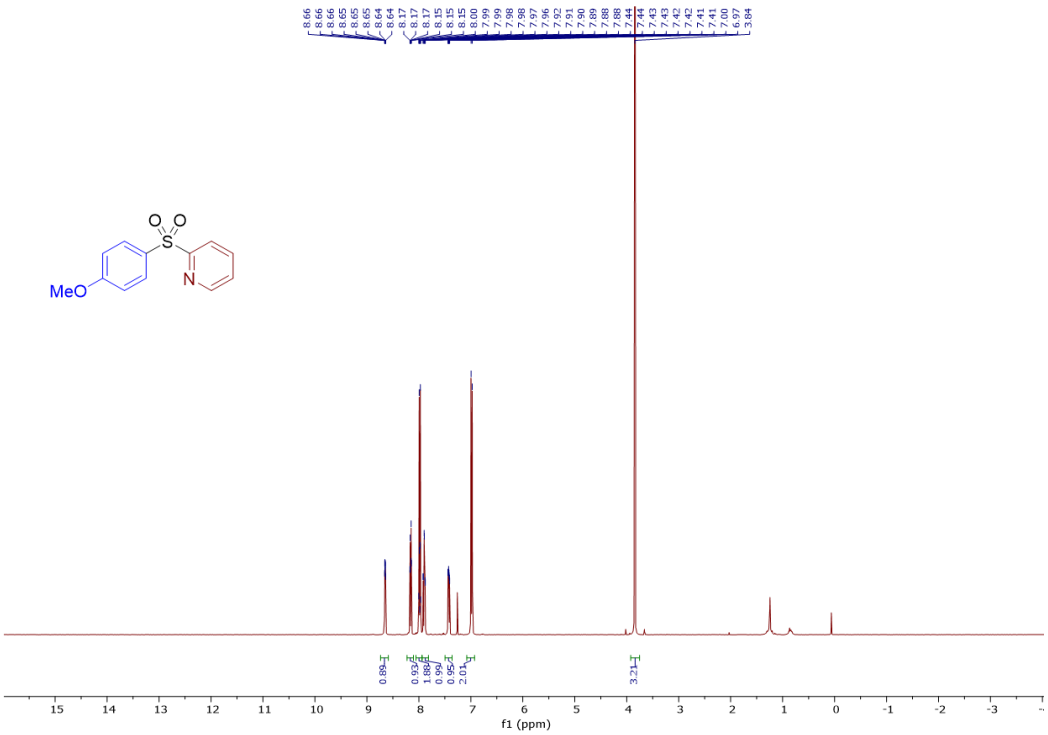


1-methoxy-4-tosylbenzene (17-OMe)

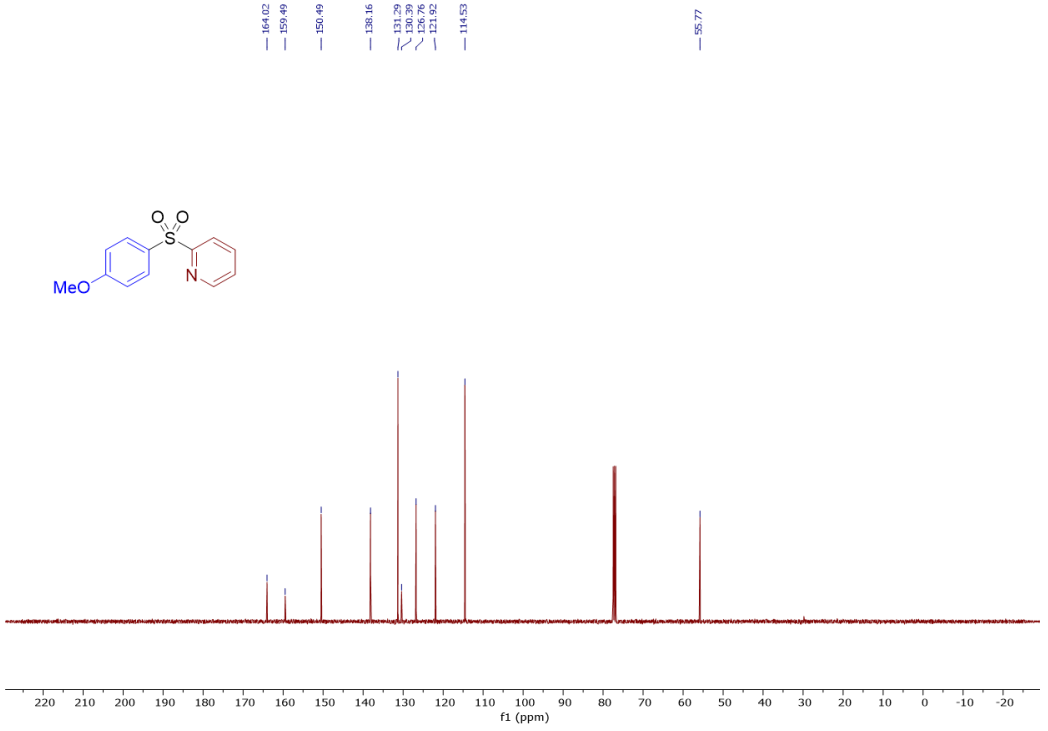
^{13}C{^{1}H} NMR (101 MHz, $CDCl_3$)



2-((4-methoxyphenyl)sulfonyl)pyridine (17-OMe-2-pyr)
^{1}H NMR (400 MHz, $CDCl_3$)



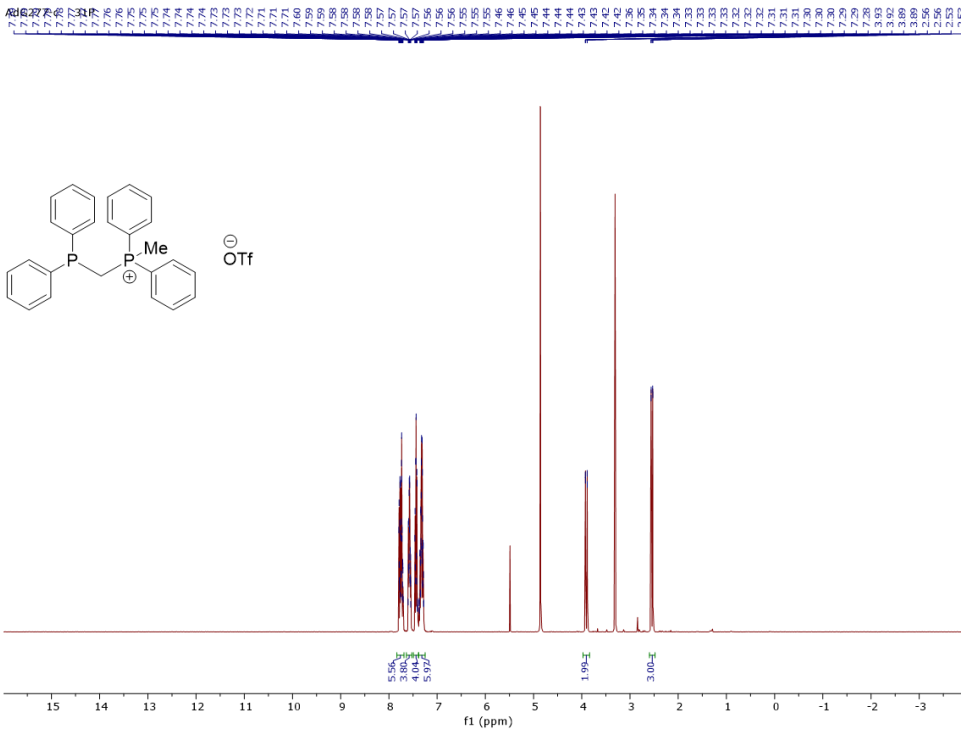
2-((4-methoxyphenyl)sulfonyl)pyridine (17-OMe-2-pyr)
^{13}C{^{1}H} NMR (101 MHz, $CDCl_3$)



9.2.2. Cationic Phosphine Ligands

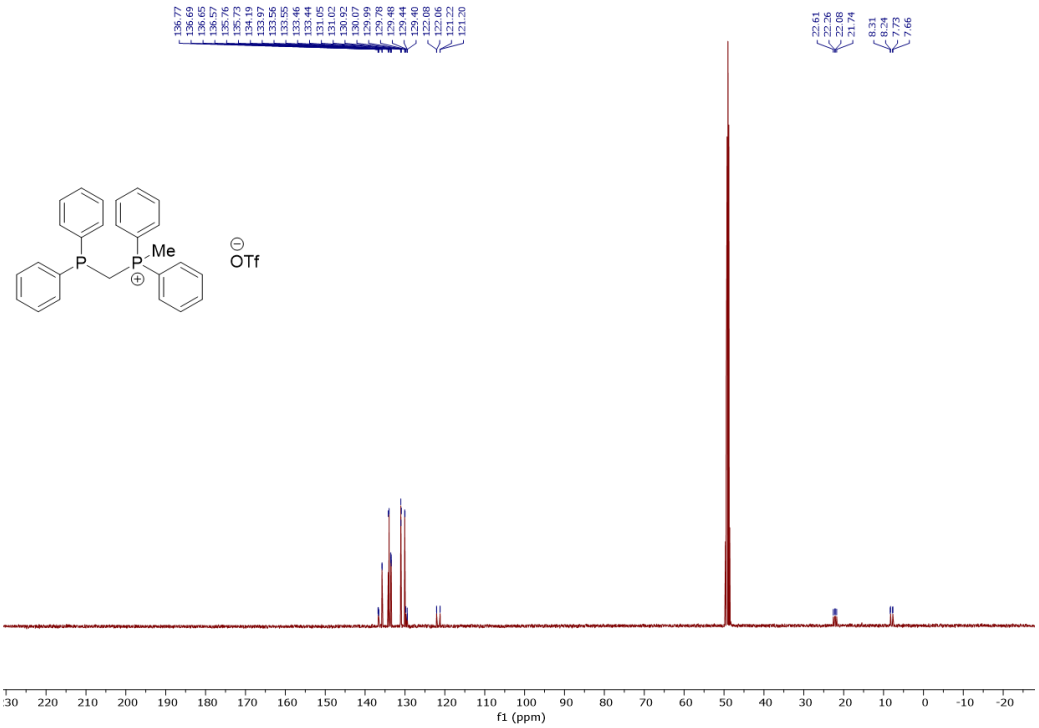
((Diphenylphosphaneyl)methyl)(methyl)diphenylphosphonium trifluoromethanesulfonate PP^{+}1

^{1}H NMR (400 MHz, CD_3OD)



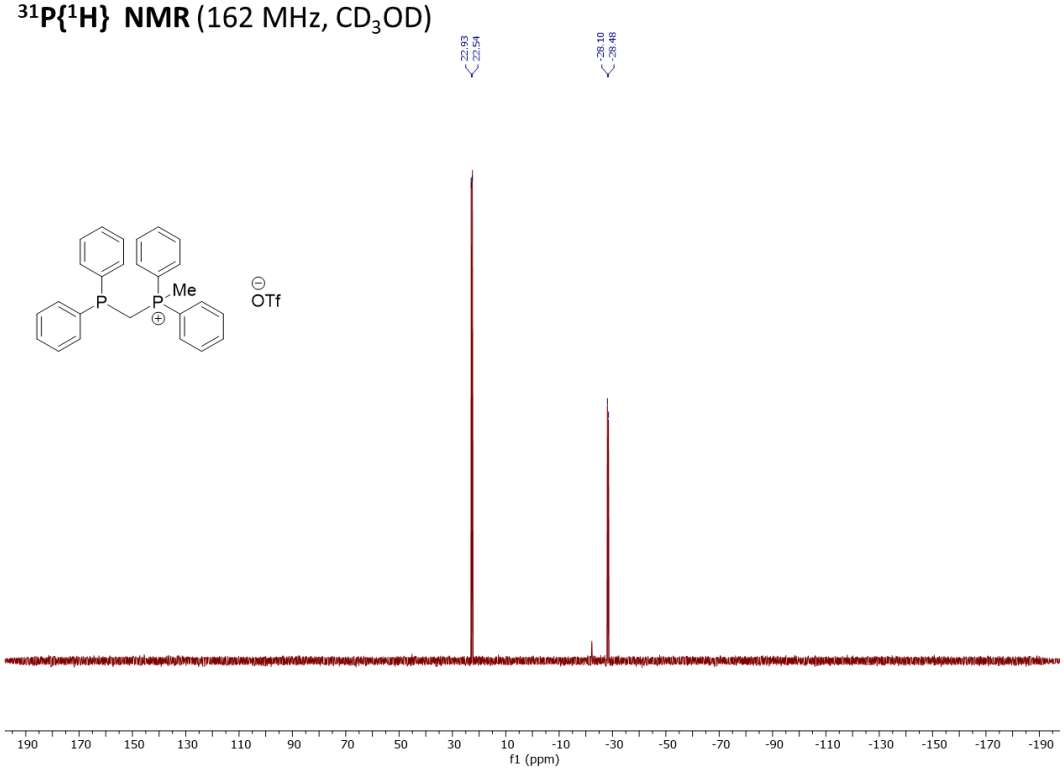
((Diphenylphosphaneyl)methyl)(methyl)diphenylphosphonium trifluoromethanesulfonate PP^{+}1

^{13}C{^{1}H} NMR (101 MHz, CD_3OD)



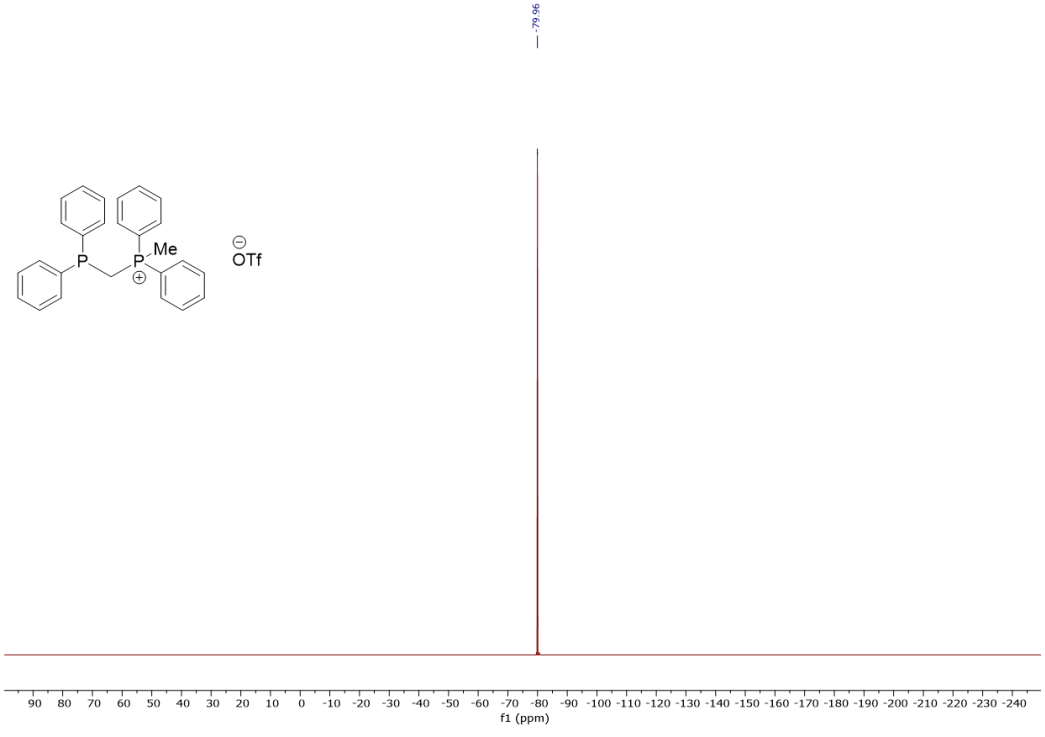
((Diphenylphosphaneyl)methyl)(methyl)diphenylphosphonium trifluoromethanesulfonate PP^{+}1

^{31}P{^{1}H} NMR (162 MHz, CD_3OD)



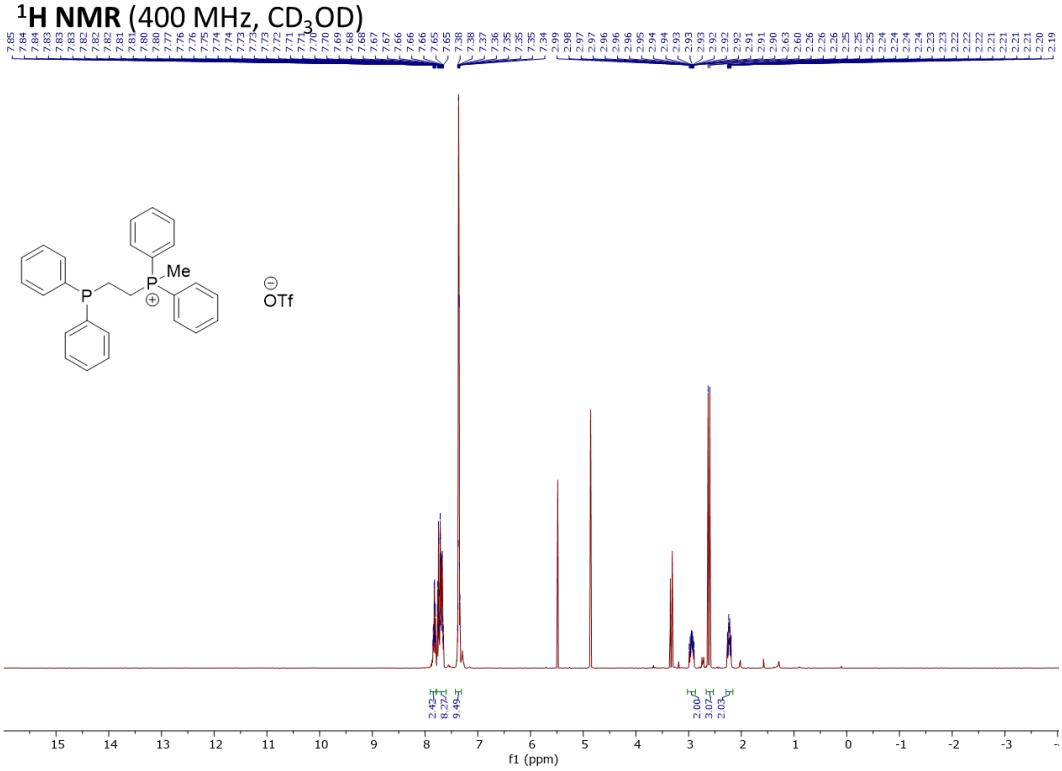
((Diphenylphosphaneyl)methyl)(methyl)diphenylphosphonium trifluoromethanesulfonate PP^{+}1

^{19}F{^{1}H} NMR (377 MHz, CD_3OD)



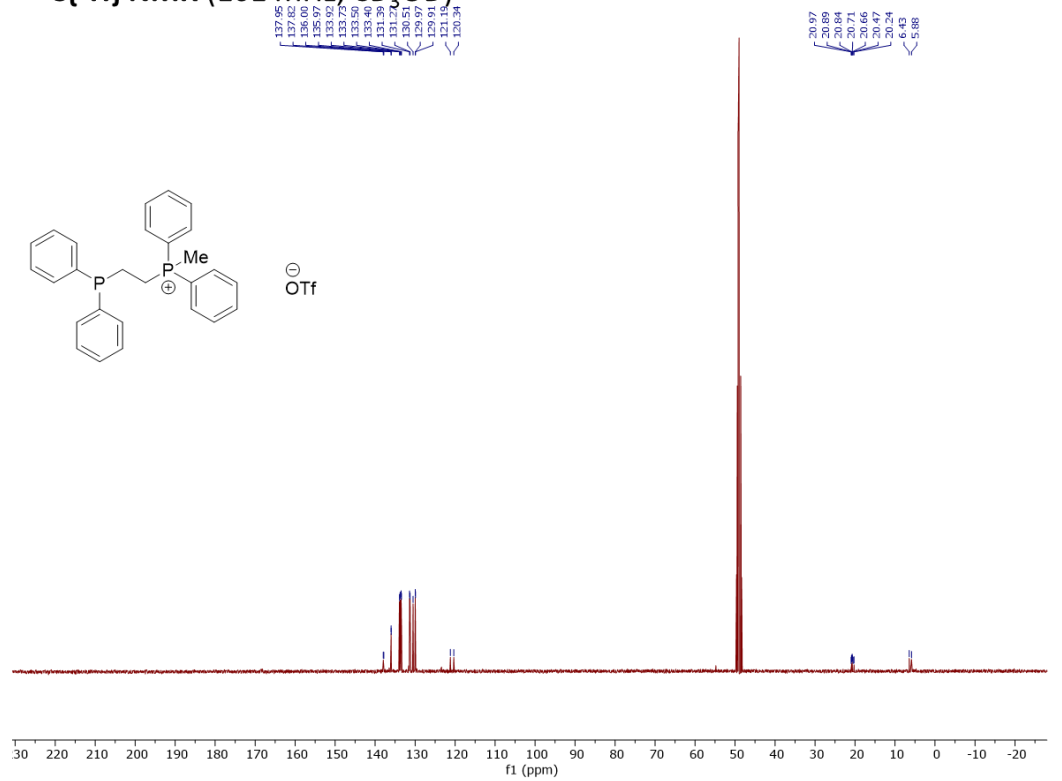
(2-(Diphenylphosphaneyl)ethyl)(methyl)diphenylphosphonium trifluoromethanesulfonate PP+2

^{1}H NMR (400 MHz, CD_3OD)



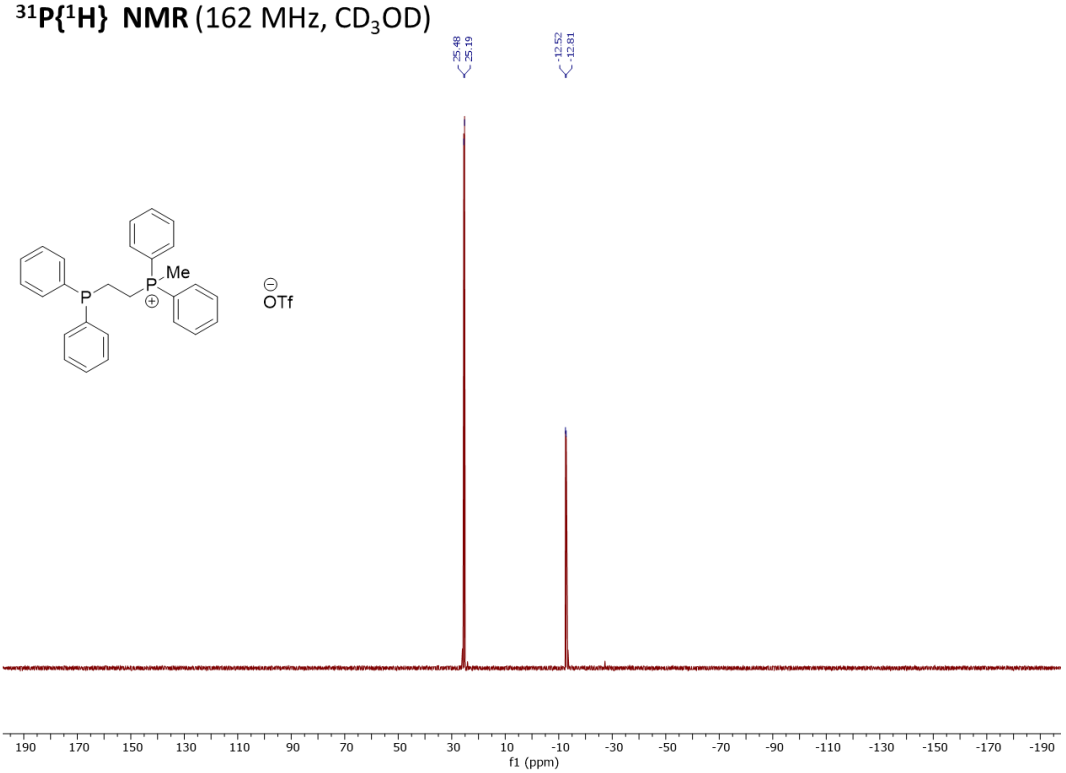
(2-(Diphenylphosphaneyl)ethyl)(methyl)diphenylphosphonium trifluoromethanesulfonate PP+2

^{13}C{^{1}H} NMR (101 MHz, CD_3OD)



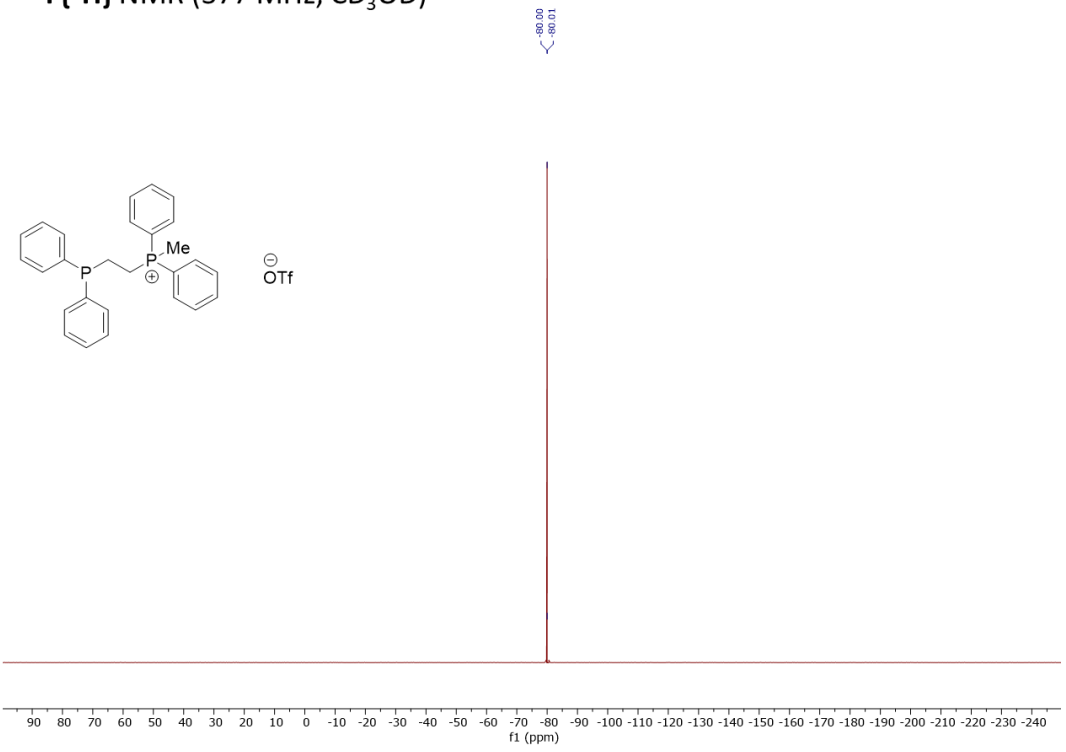
(2-(Diphenylphosphaneyl)ethyl)(methyl)diphenylphosphonium trifluoromethanesulfonate PP$^+$2

^{31}P{^{1}H} NMR (162 MHz, CD_3OD)



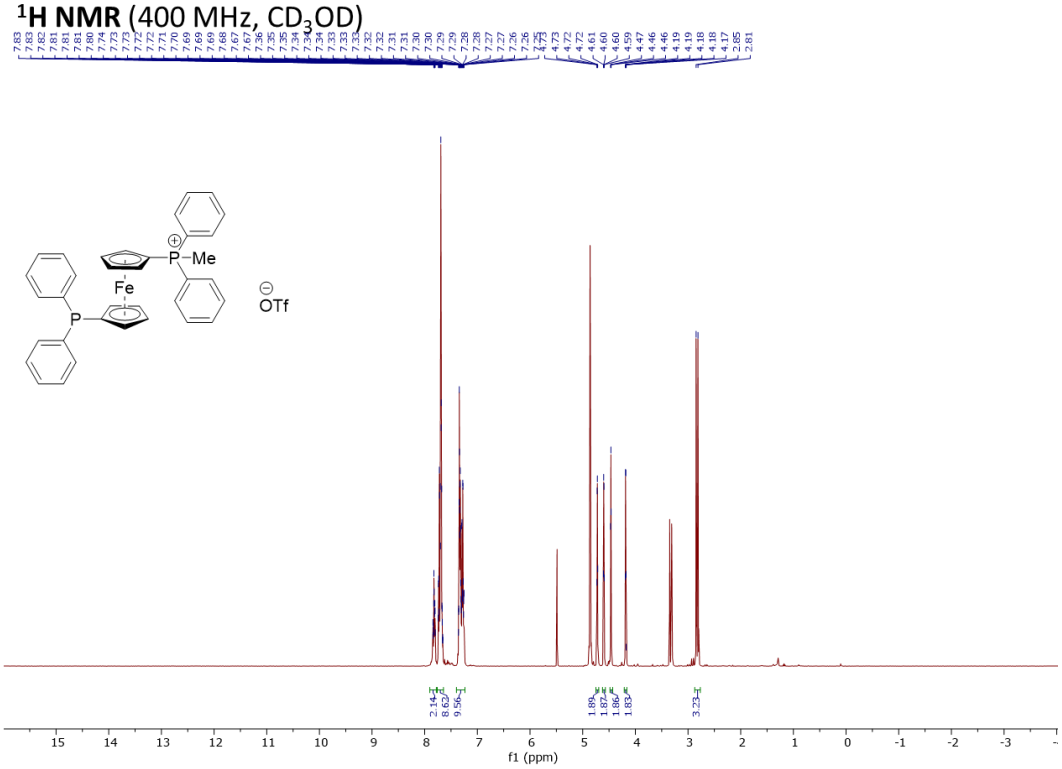
(2-(Diphenylphosphaneyl)ethyl)(methyl)diphenylphosphonium trifluoromethanesulfonate PP$^+$2

^{19}F{^{1}H} NMR (377 MHz, CD_3OD)



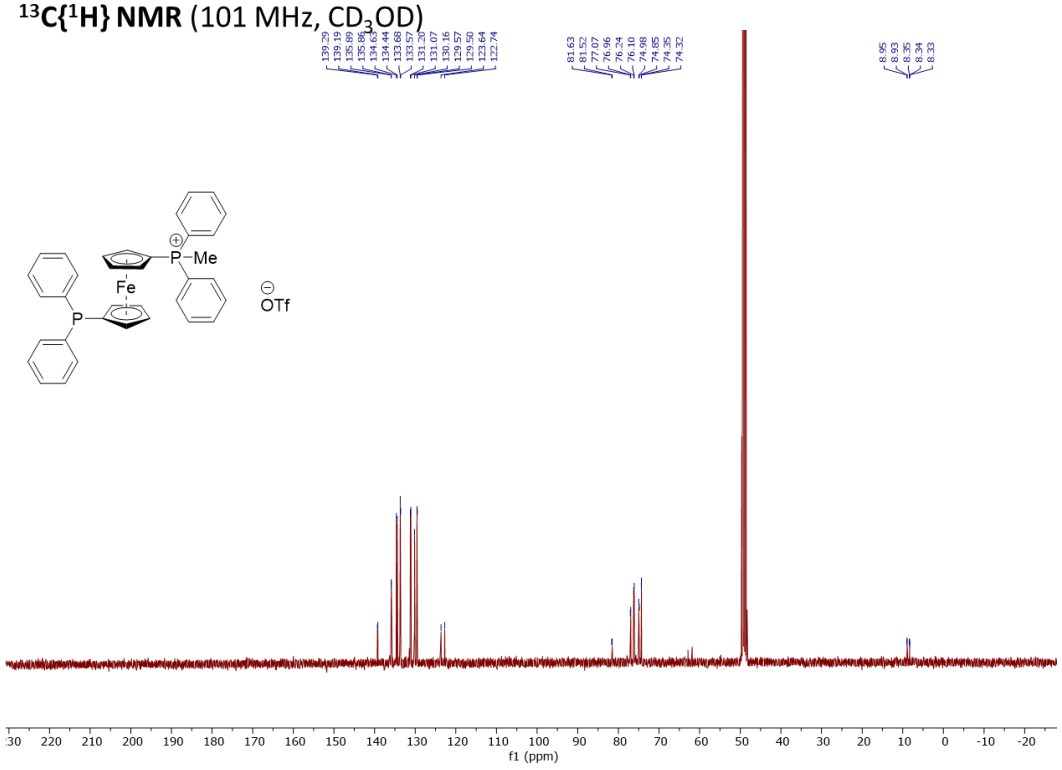
(1'-(Diphenylphosphaneyl)ferrocenyl)(methyl)diphenylphosphonium trifluoromethanesulfonate PP$^+$3

^{1}H NMR (400 MHz, CD_3OD)



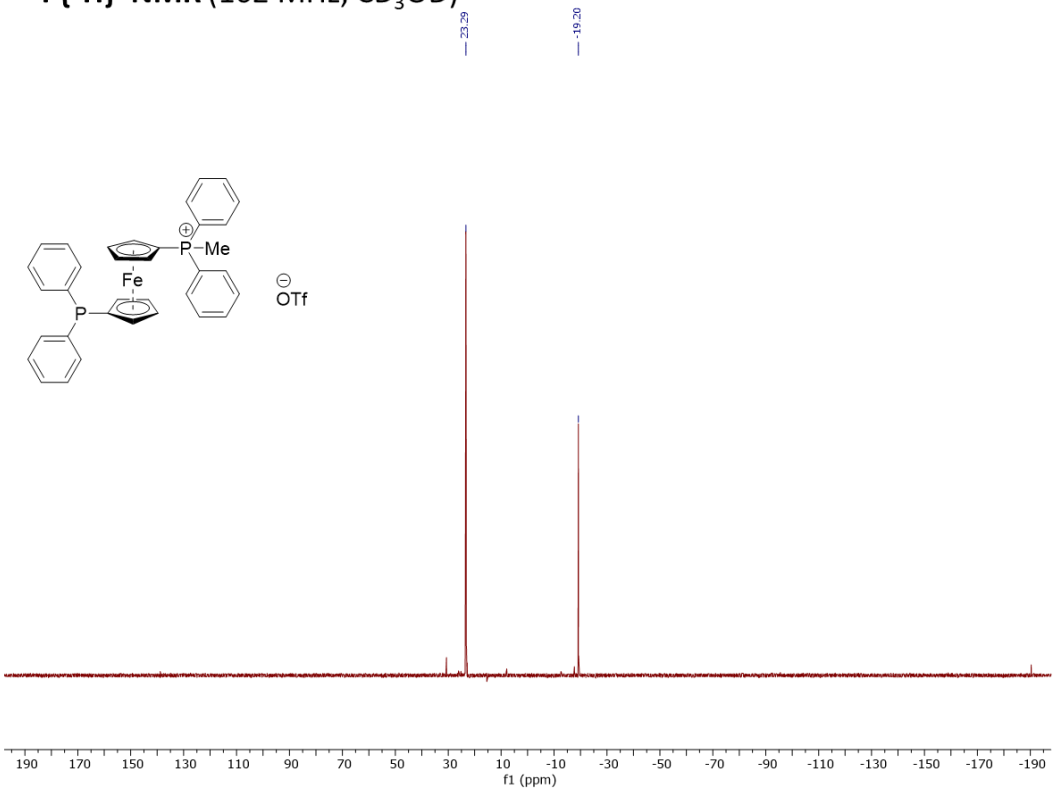
(1'-(Diphenylphosphaneyl)ferrocenyl)(methyl)diphenylphosphonium trifluoromethanesulfonate PP$^+$3

^{13}C{^{1}H} NMR (101 MHz, CD_3OD)



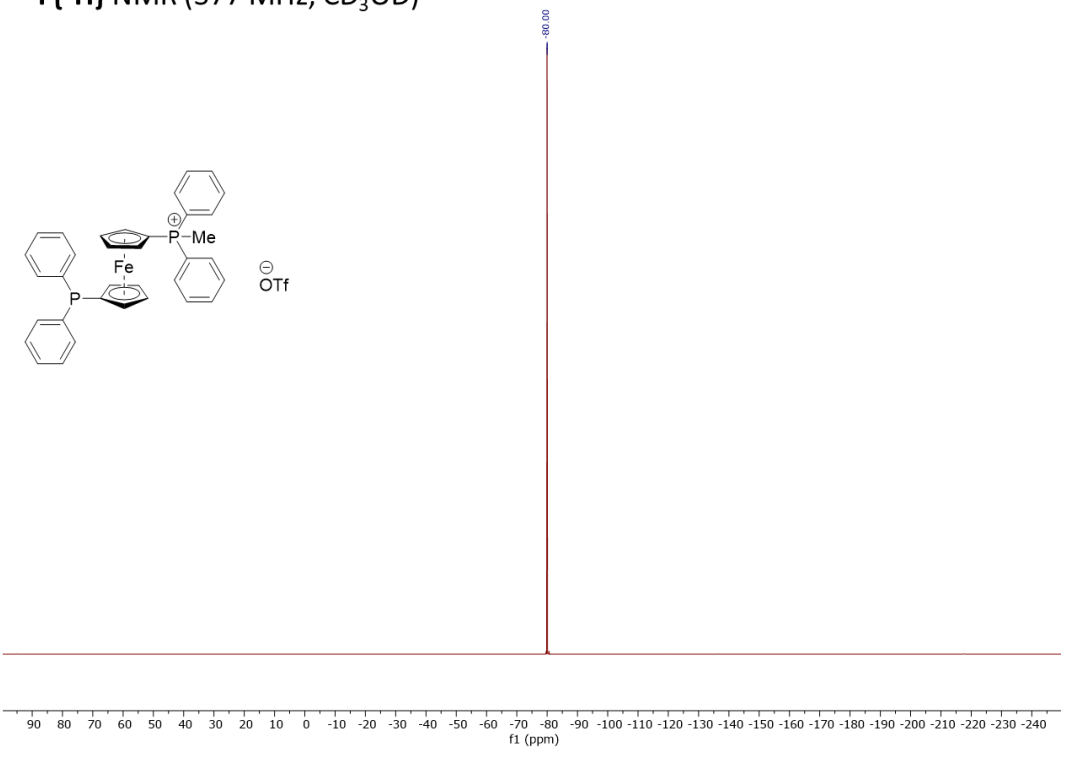
(1'-(Diphenylphosphaneyl)ferrocenyl)(methyl)diphenylphosphonium trifluoromethanesulfonate PP$^+$3

^{31}P{^{1}H} NMR (162 MHz, CD_3OD)



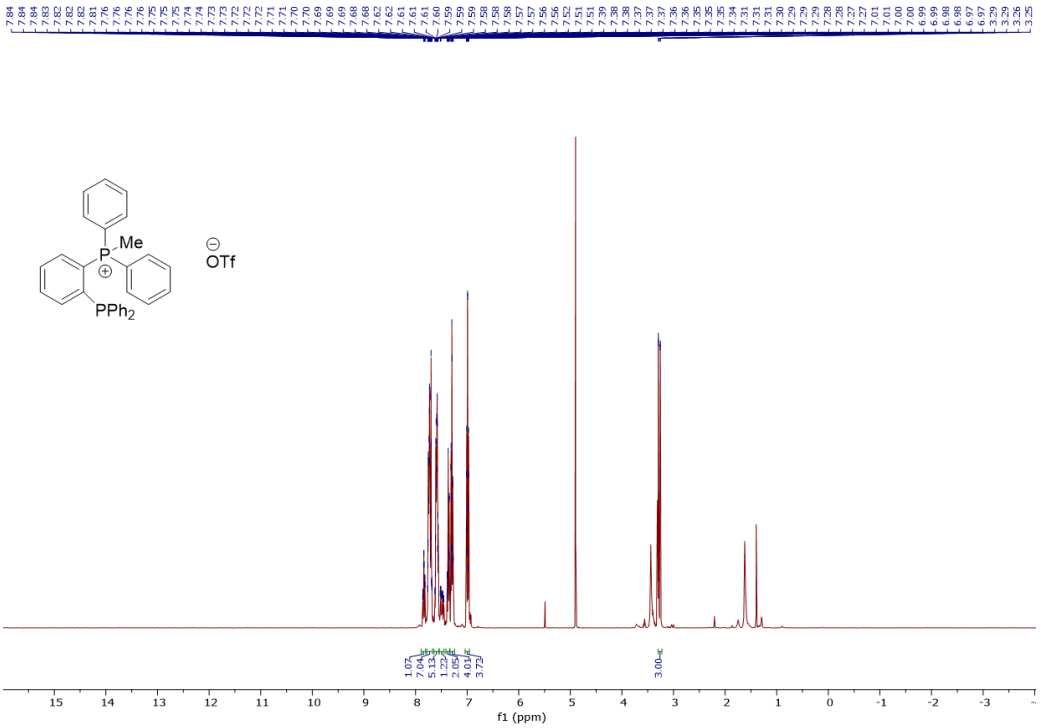
(1'-(Diphenylphosphaneyl)ferrocenyl)(methyl)diphenylphosphonium trifluoromethanesulfonate PP$^+$3

^{19}F{^{1}H} NMR (377 MHz, CD_3OD)



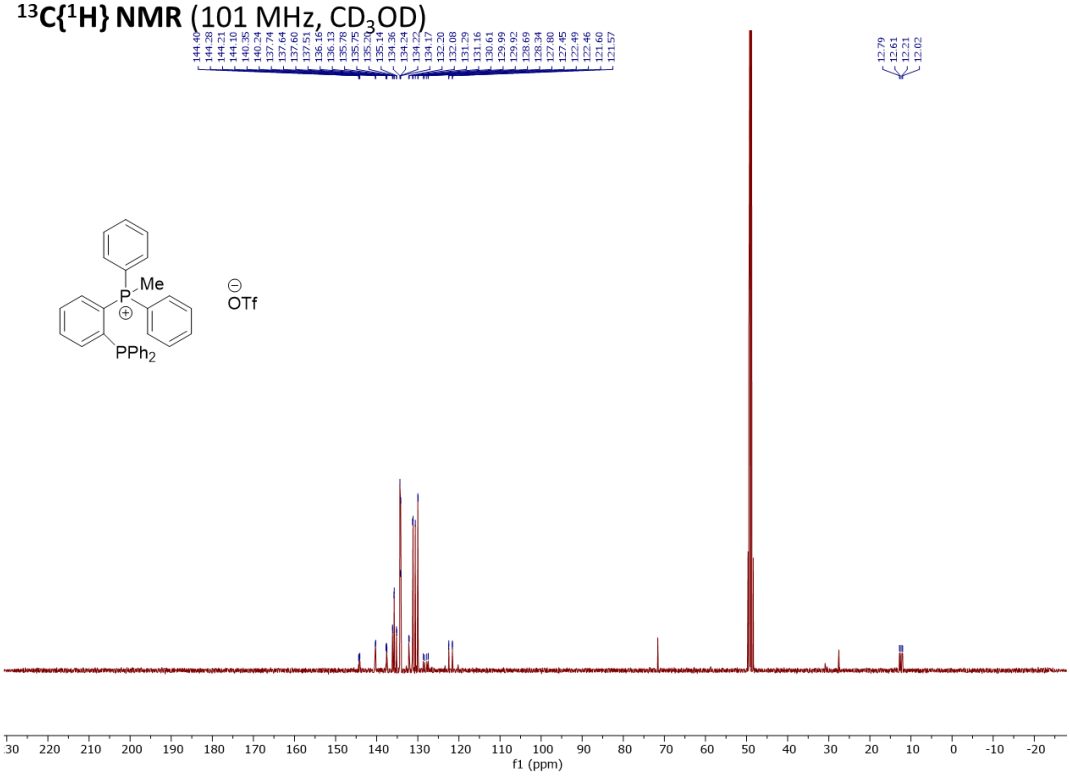
(2-(Diphenylphosphaneyl)phenyl)(methyl)diphenylphosphonium trifluoromethanesulfonate PP+4

^{1}H NMR (400 MHz, CD_3OD)



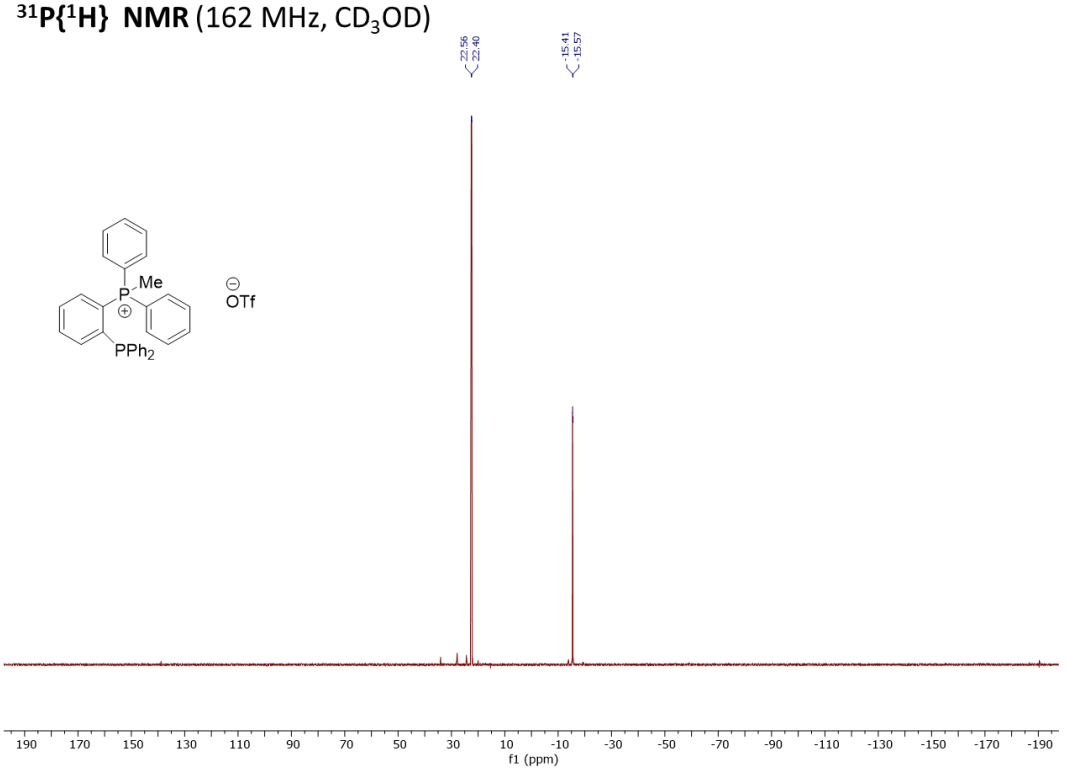
(2-(Diphenylphosphaneyl)phenyl)(methyl)diphenylphosphonium trifluoromethanesulfonate PP+4

^{13}C{^{1}H} NMR (101 MHz, CD_3OD)



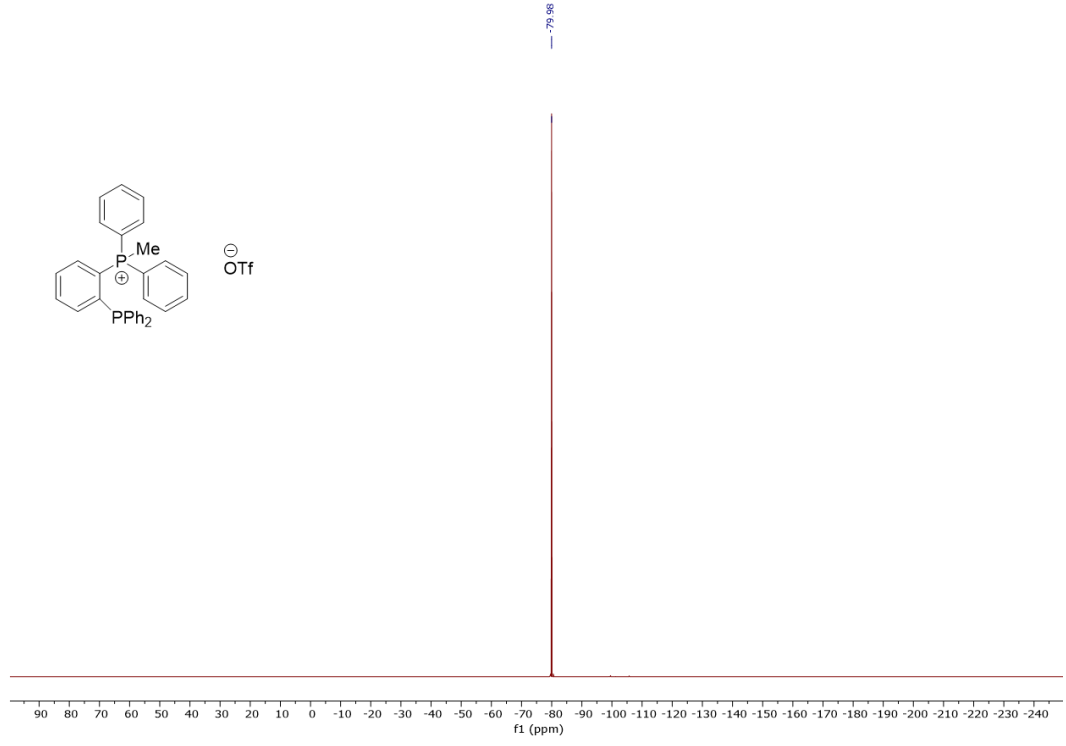
(2-(Diphenylphosphaneyl)phenyl)(methyl)diphenylphosphonium trifluoromethanesulfonate PP^{+}4

^{31}P{^{1}H} NMR (162 MHz, CD_3OD)



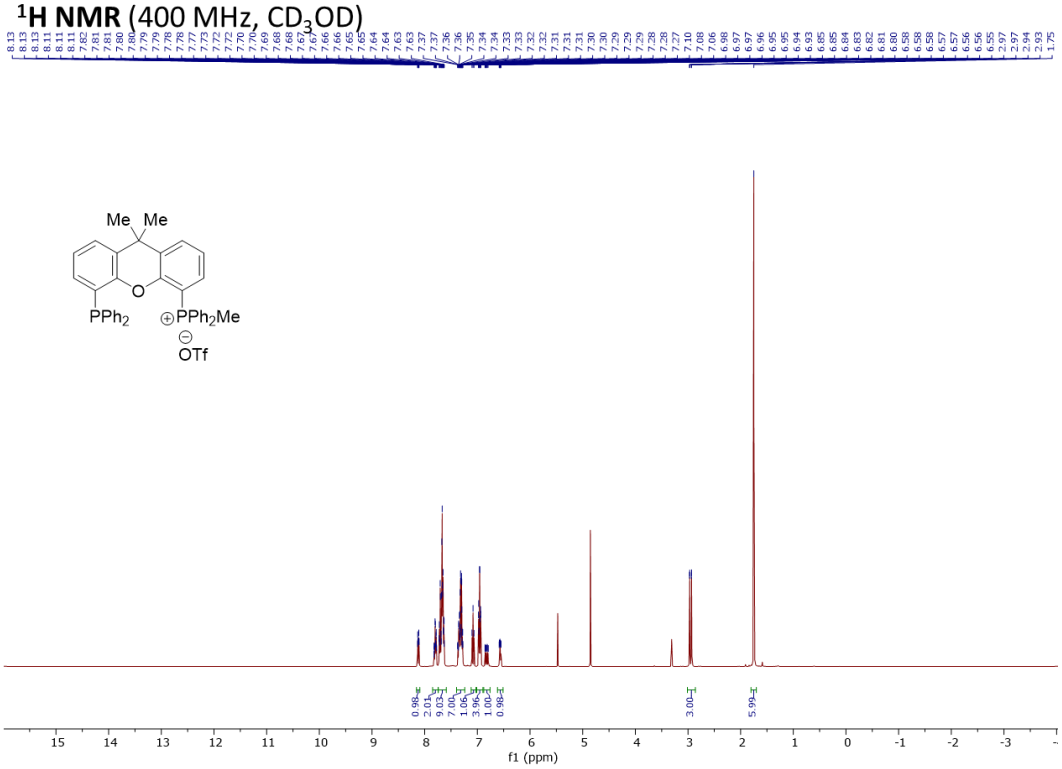
(2-(Diphenylphosphaneyl)phenyl)(methyl)diphenylphosphonium trifluoromethanesulfonate PP^{+}4

^{19}F{^{1}H} NMR (377 MHz, CD_3OD)



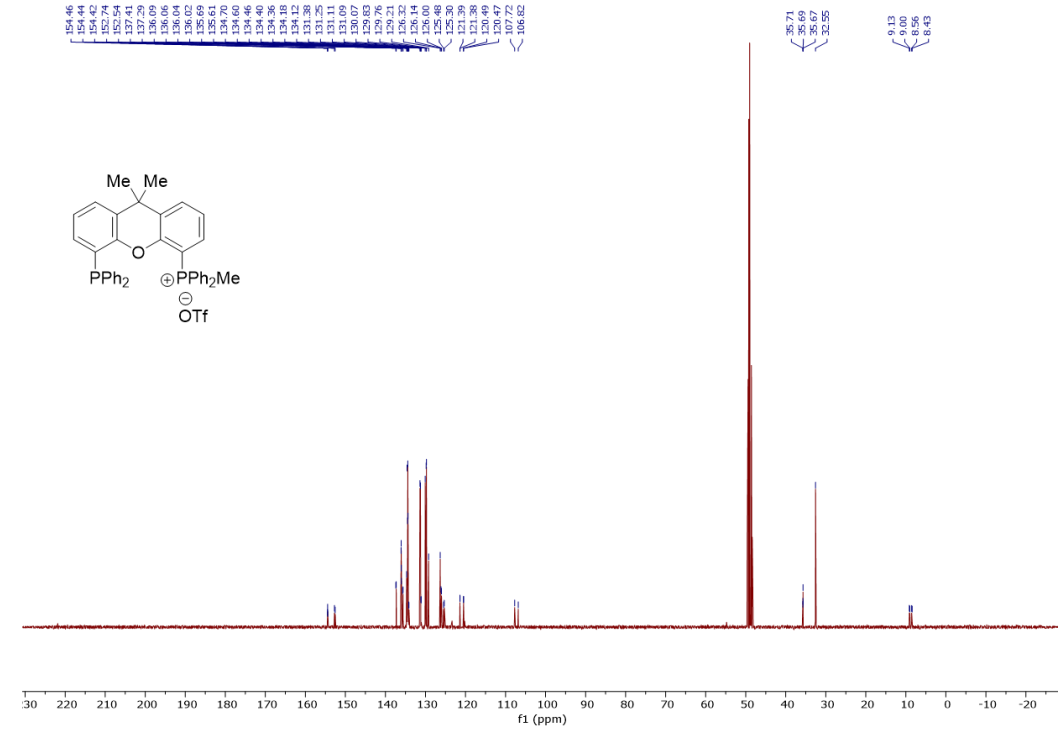
(5-(Diphenylphosphaneyl)-9,9-dimethyl-9H-xanthen-4-yl)(methyl)diphenylphosphonium trifluoromethanesulfonate PP+5

^{1}H NMR (400 MHz, CD_3OD)



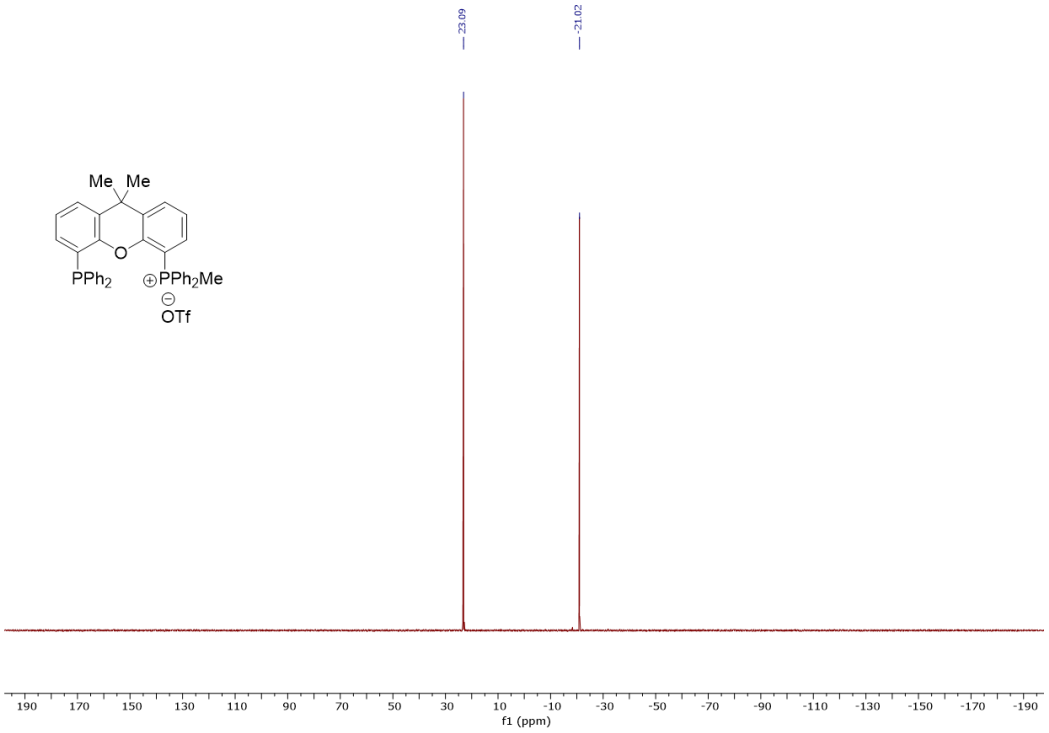
(5-(Diphenylphosphaneyl)-9,9-dimethyl-9H-xanthen-4-yl)(methyl)diphenylphosphonium trifluoromethanesulfonate PP+5

^{13}C{^{1}H} NMR (101 MHz, CD_3OD)



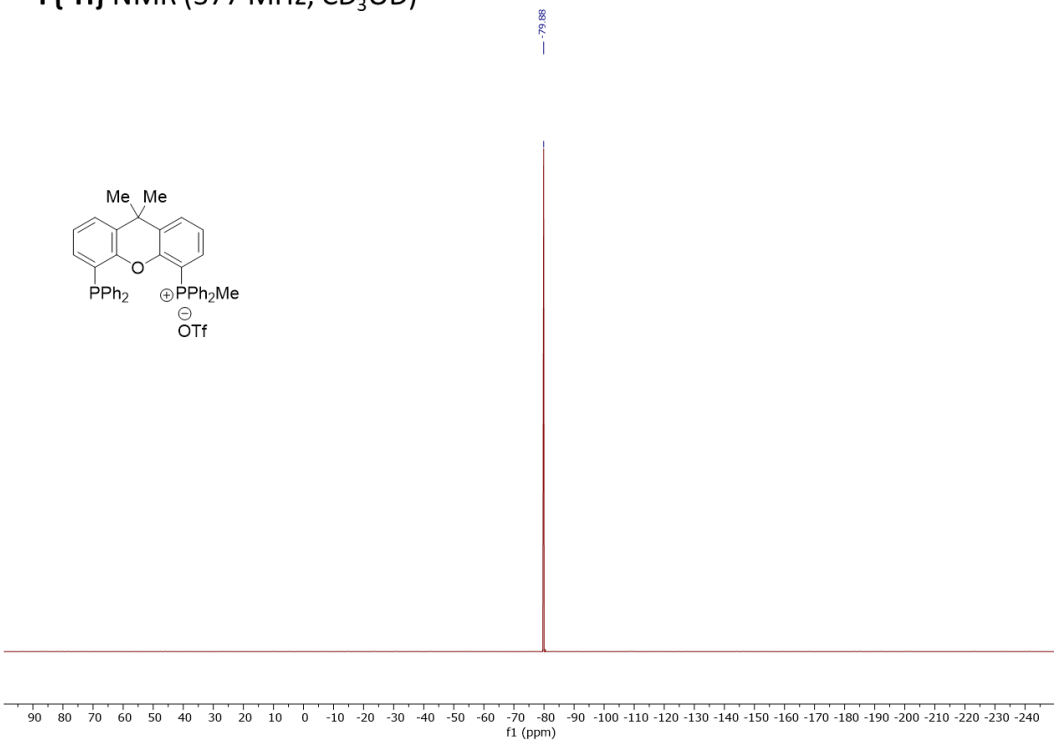
(5-(Diphenylphosphaneyl)-9,9-dimethyl-9H-xanthen-4-yl)(methyl)diphenylphosphonium trifluoromethanesulfonate PP^{+}5

^{31}P{^{1}H} NMR (162 MHz, CD_3OD)



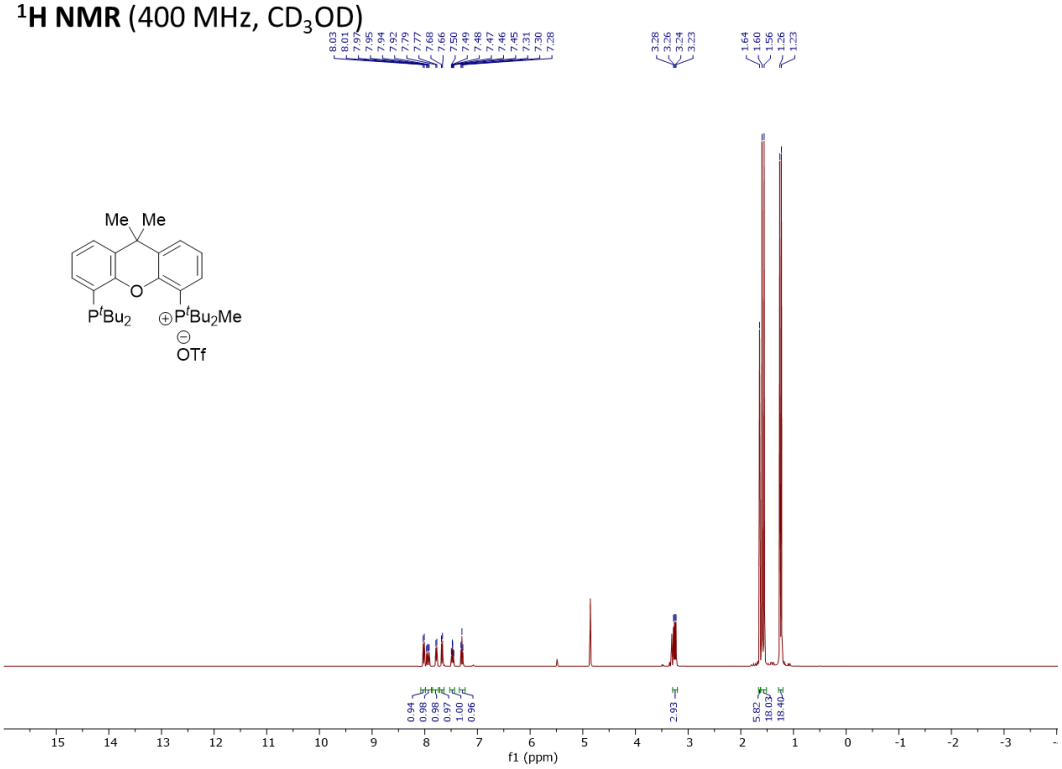
(5-(Diphenylphosphaneyl)-9,9-dimethyl-9H-xanthen-4-yl)(methyl)diphenylphosphonium trifluoromethanesulfonate PP^{+}5

^{19}F{^{1}H} NMR (377 MHz, CD_3OD)



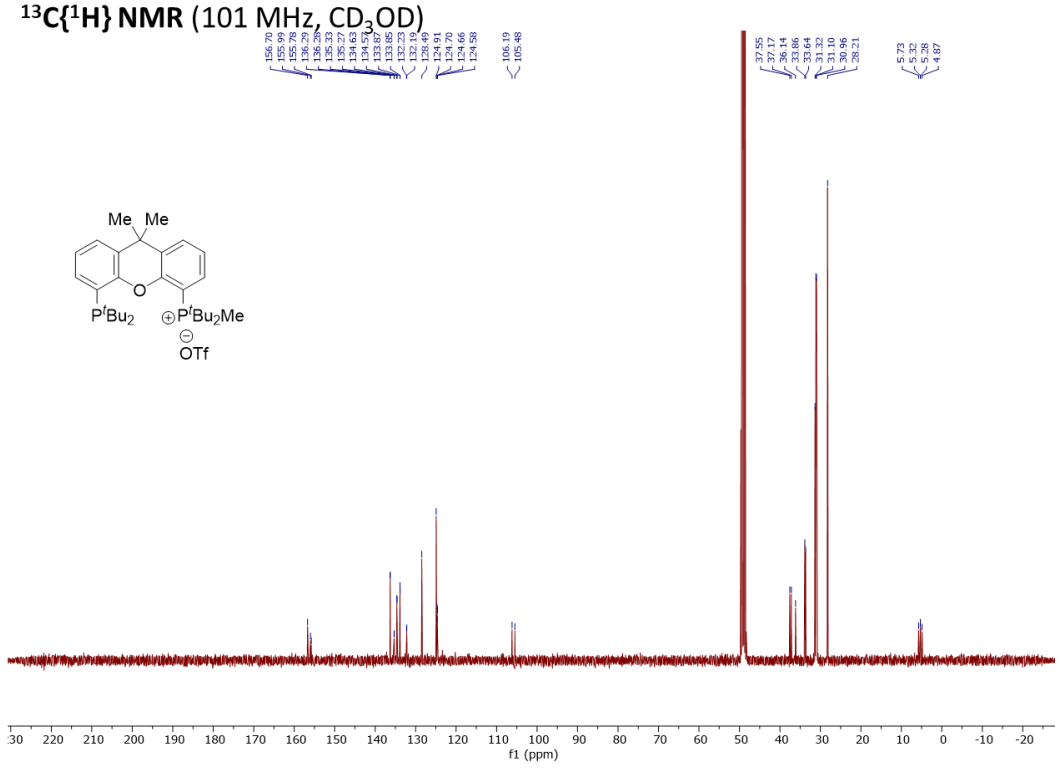
Di-tert-butyl(5-(di-tert-butylphosphaneyl)-9,9-dimethyl-9H-xanthen-4-yl)(methyl)phosphonium trifluoromethanesulfonate PP^{+}6

^{1}H NMR (400 MHz, CD_3OD)



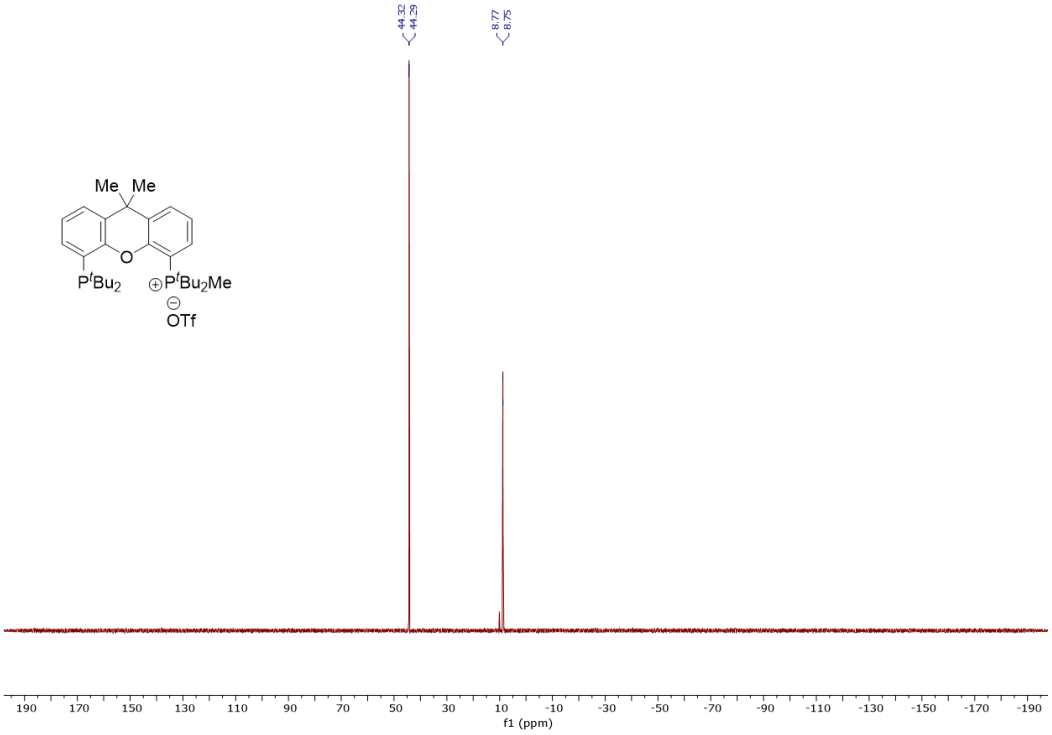
Di-tert-butyl(5-(di-tert-butylphosphaneyl)-9,9-dimethyl-9H-xanthen-4-yl)(methyl)phosphonium trifluoromethanesulfonate PP^{+}6

^{13}C{^{1}H} NMR (101 MHz, CD_3OD)



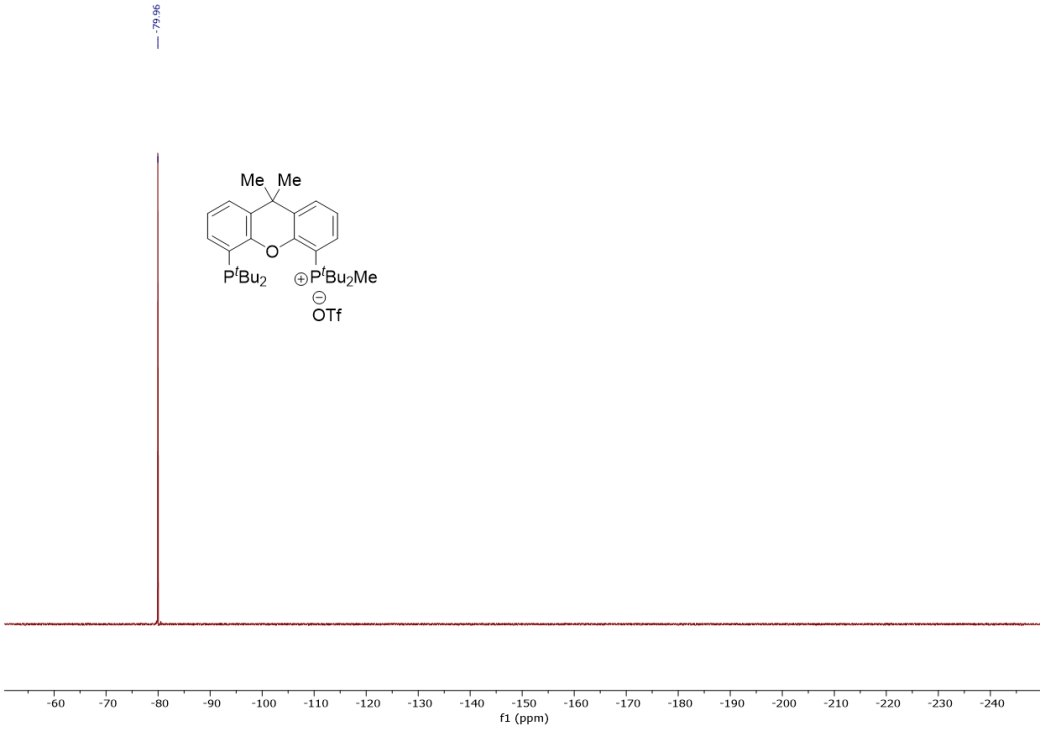
Di-tert-butyl(5-(di-tert-butylphosphaneyl)-9,9-dimethyl-9H-xanthen-4-yl)(methyl)phosphonium trifluoromethanesulfonate PP^{+}6

^{31}P{^{1}H} NMR (162 MHz, CD_3OD)



Di-tert-butyl(5-(di-tert-butylphosphaneyl)-9,9-dimethyl-9H-xanthen-4-yl)(methyl)phosphonium trifluoromethanesulfonate PP^{+}6

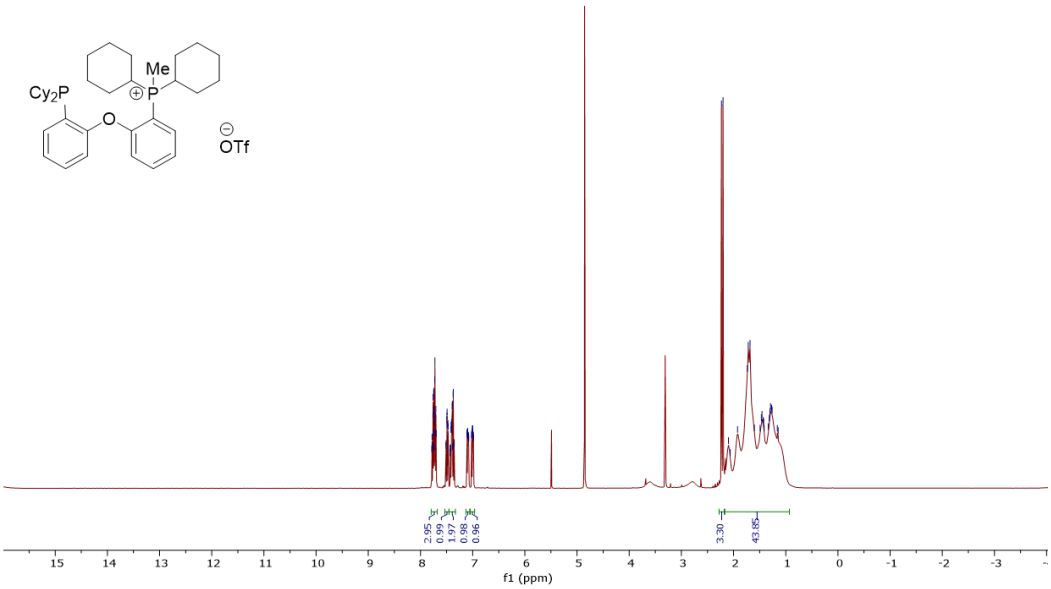
^{19}F{^{1}H} NMR (377 MHz, CD_3OD)



Dicyclohexyl(2-(2-(dicyclohexylphosphaneyl)phenoxy)phenyl)(methyl)phosphonium trifluoromethanesulfonate PP^{+}7

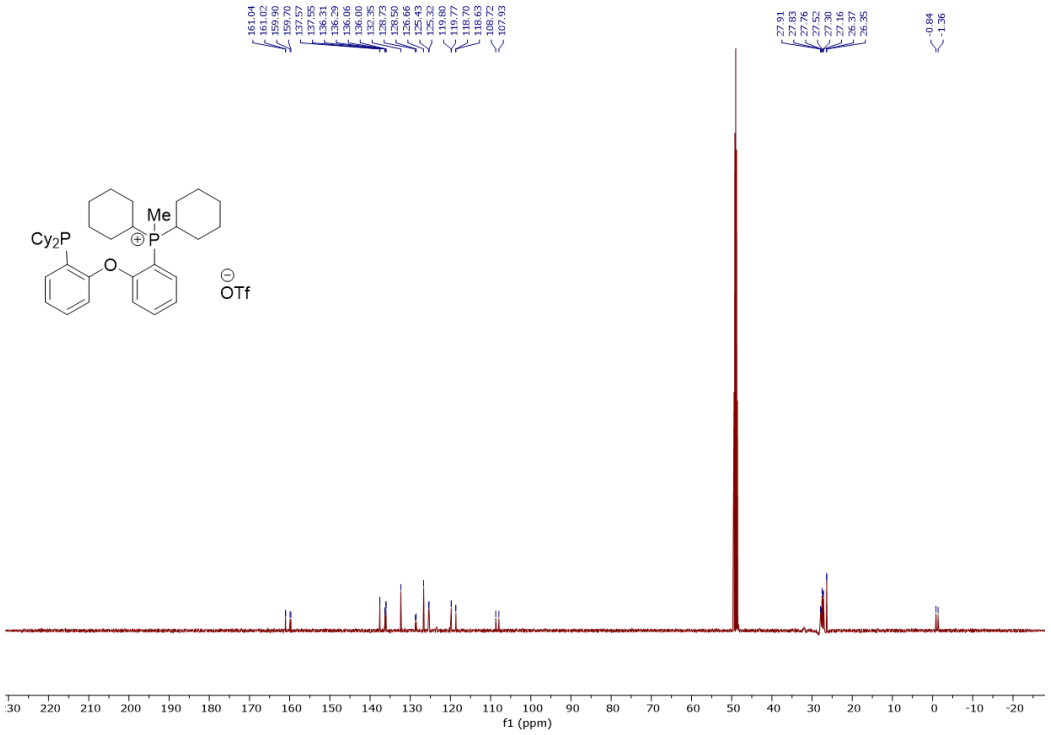
^{1}H NMR (400 MHz, CD_3OD)





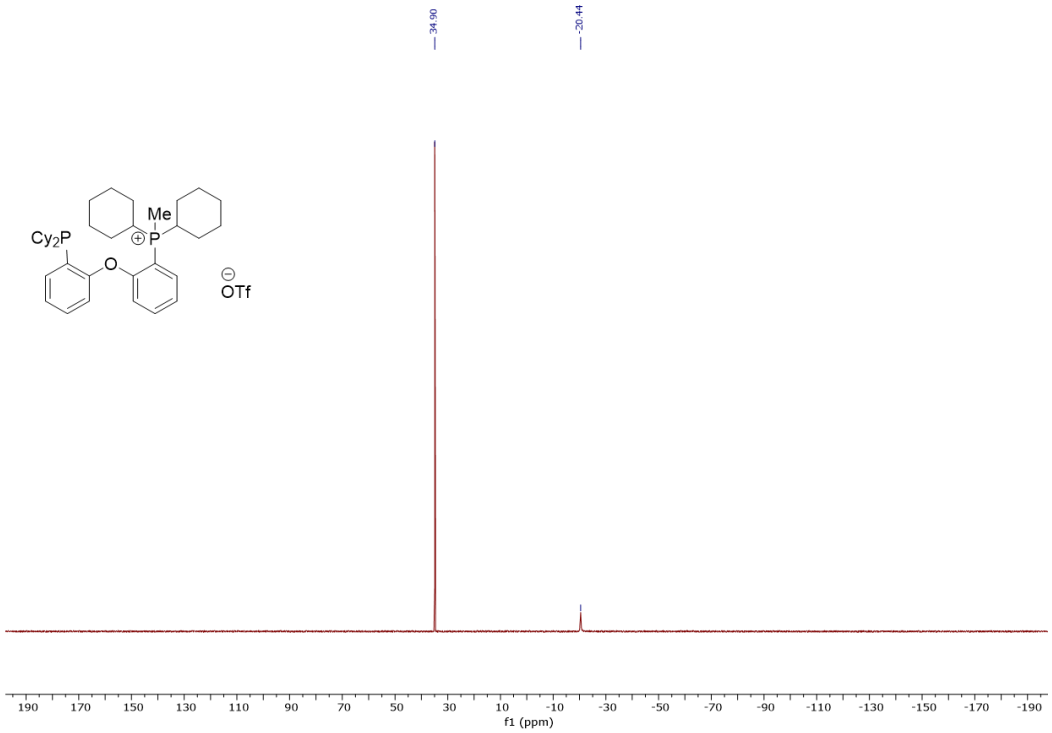
Dicyclohexyl(2-(2-(dicyclohexylphosphaneyl)phenoxy)phenyl)(methyl)phosphonium trifluoromethanesulfonate PP^{+}7

^{13}C{^{1}H} NMR (101 MHz, CD_3OD)



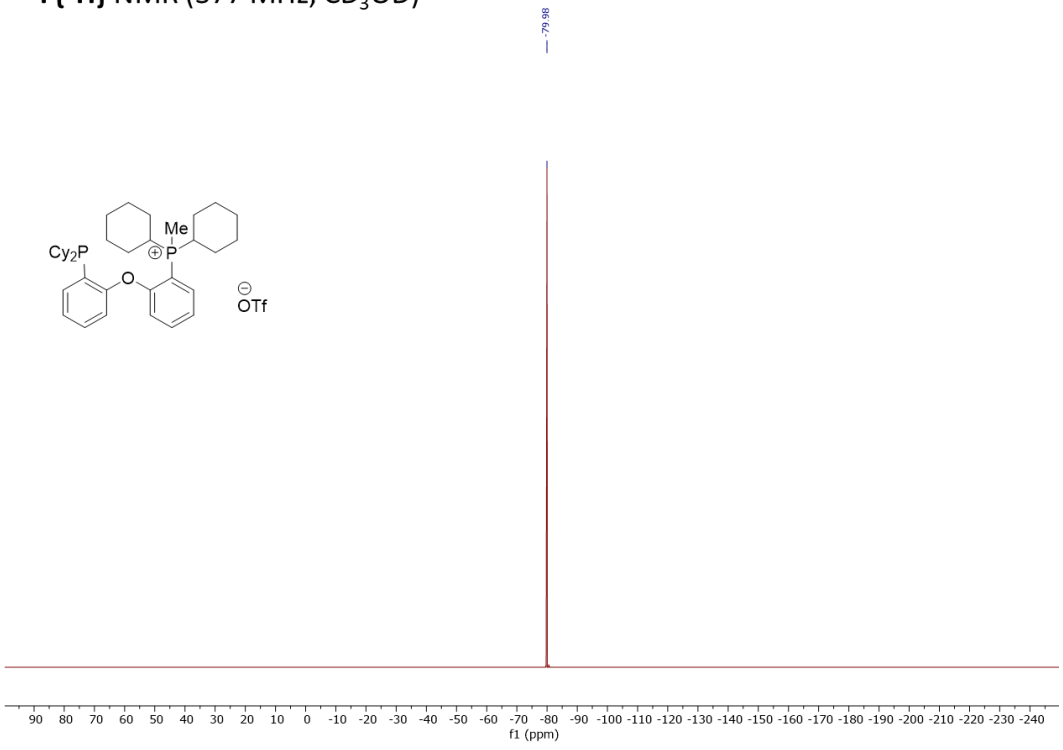
Dicyclohexyl(2-(2-(dicyclohexylphosphaneyl)phenoxy)phenyl)(methyl)phosphonium trifluoromethanesulfonate PP^{+}7

^{31}P{^{1}H} NMR (162 MHz, CD_3OD)



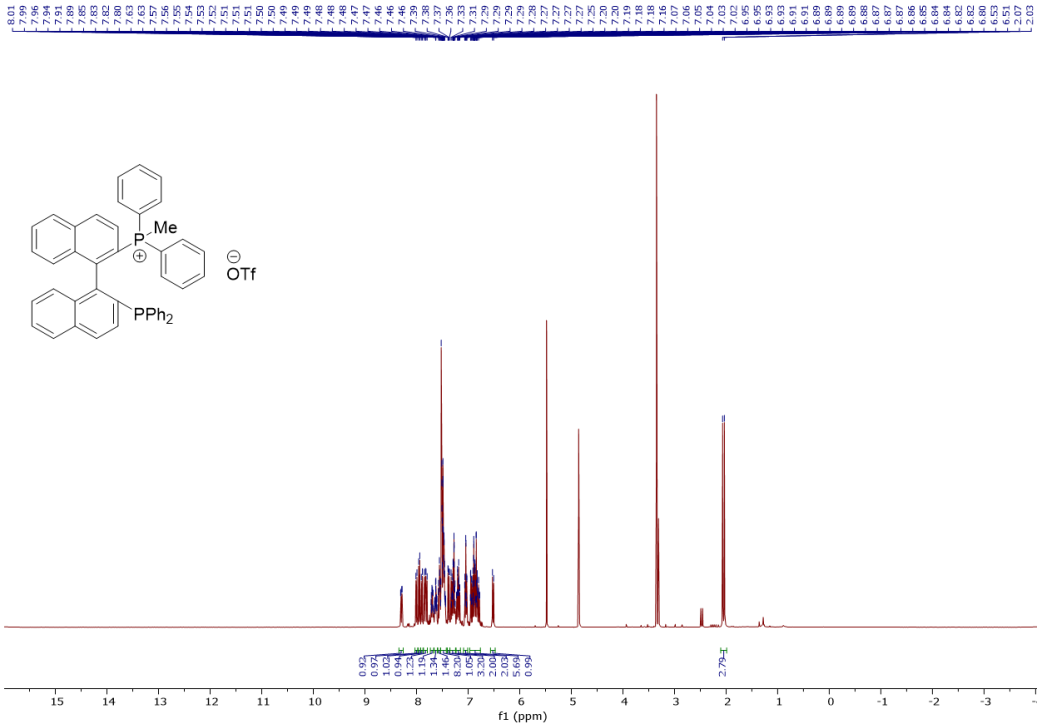
Dicyclohexyl(2-(2-(dicyclohexylphosphaneyl)phenoxy)phenyl)(methyl)phosphonium trifluoromethanesulfonate PP^{+}7

^{19}F{^{1}H} NMR (377 MHz, CD_3OD)



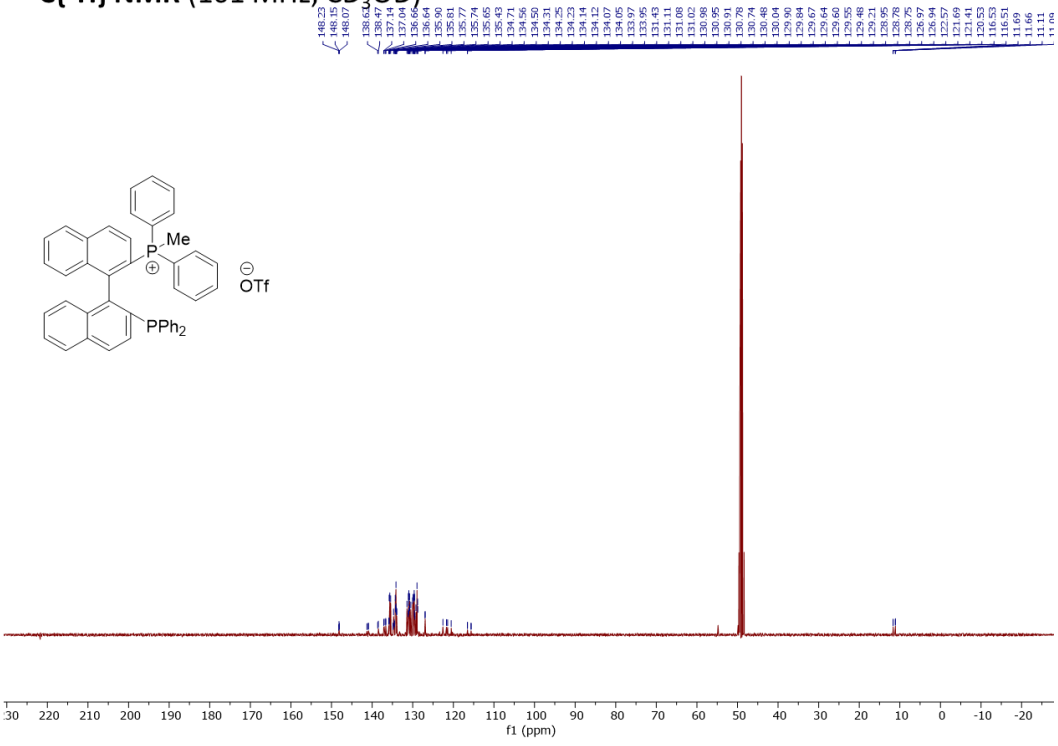
(2'-(Diphenylphosphaneyl)-[1,1'-binaphthalen]-2-yl)(methyl) diphenylphosphonium trifluoromethanesulfonate PP⁺8

^{1}H NMR (400 MHz, CD_3OD)



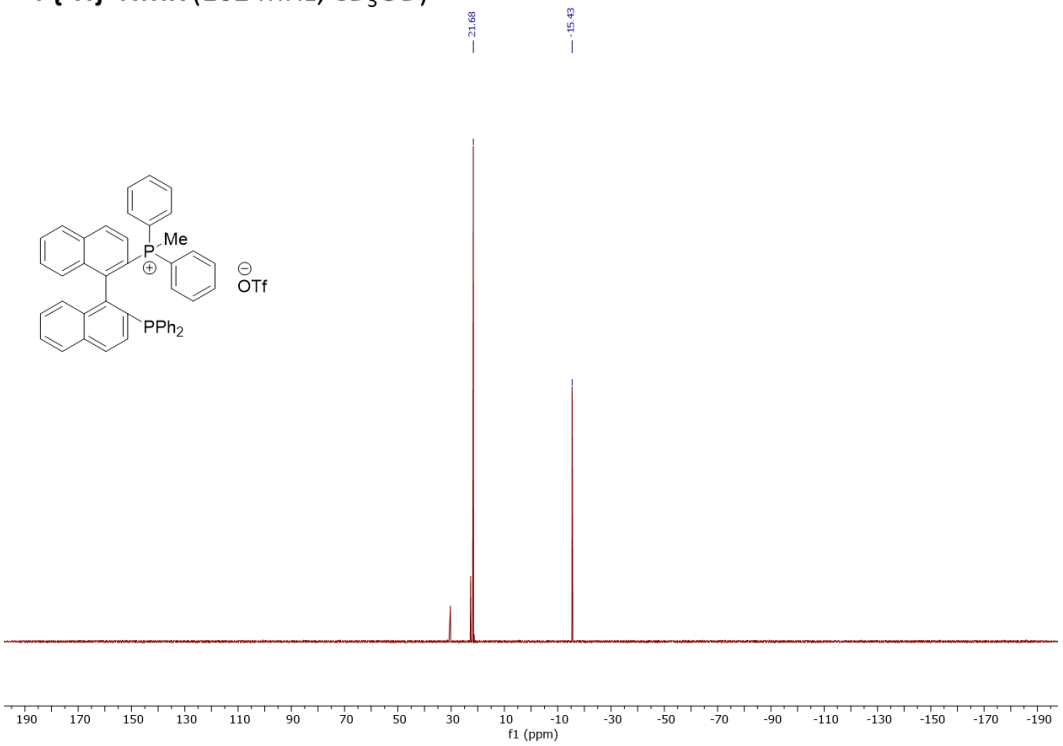
(2'-(Diphenylphosphaneyl)-[1,1'-binaphthalen]-2-yl)(methyl) diphenylphosphonium trifluoromethanesulfonate PP⁺8

^{13}C{^{1}H} NMR (101 MHz, CD_3OD)



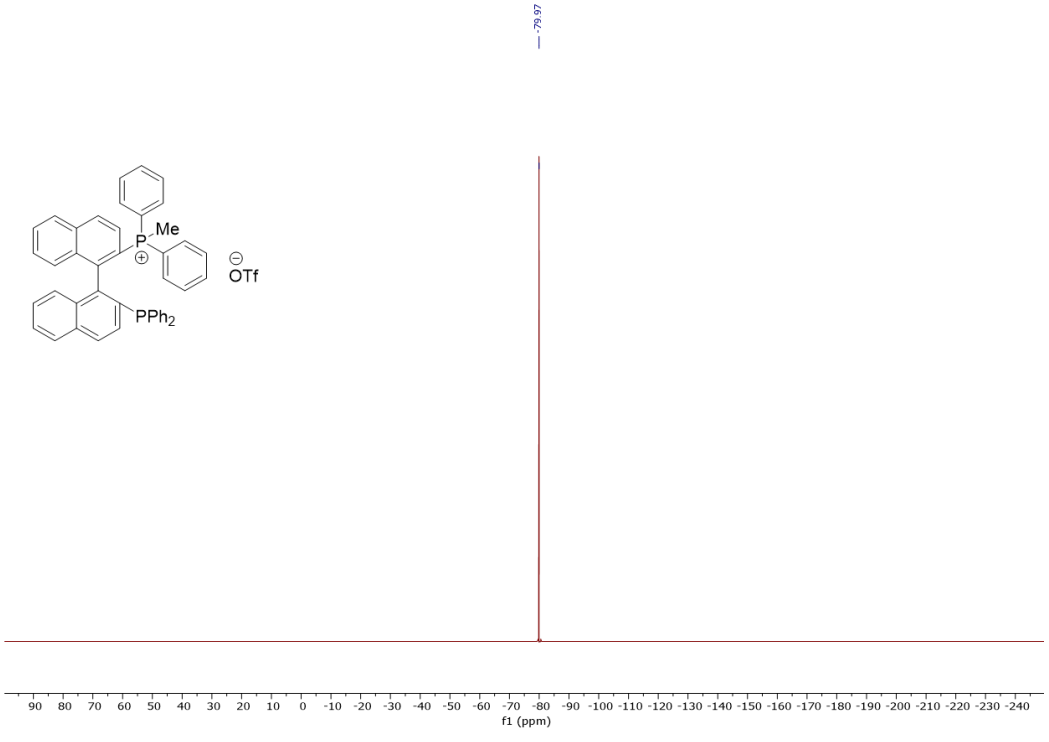
(2'-(Diphenylphosphaneyl)-[1,1'-binaphthalen]-2-yl)(methyl) diphenylphosphonium trifluoromethanesulfonate PP+8

$^{31}P\{^{1}H\}$ NMR (162 MHz, CD_3OD)



(2'-(Diphenylphosphaneyl)-[1,1'-binaphthalen]-2-yl)(methyl) diphenylphosphonium trifluoromethanesulfonate PP+8

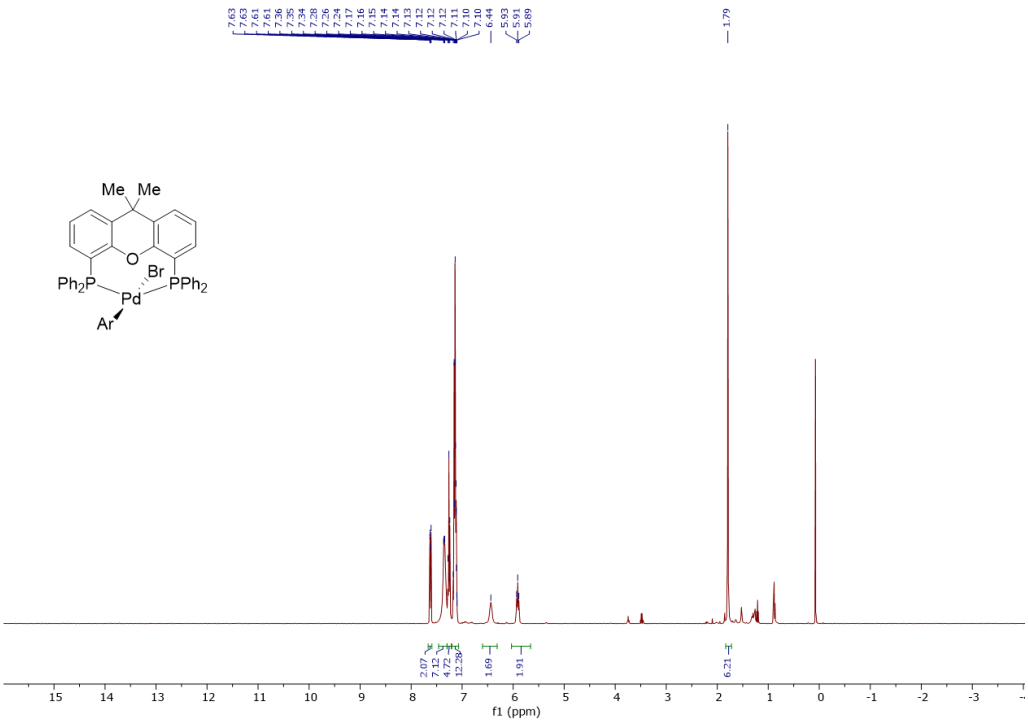
$^{19}F\{^{1}H\}$ NMR (377 MHz, CD_3OD)



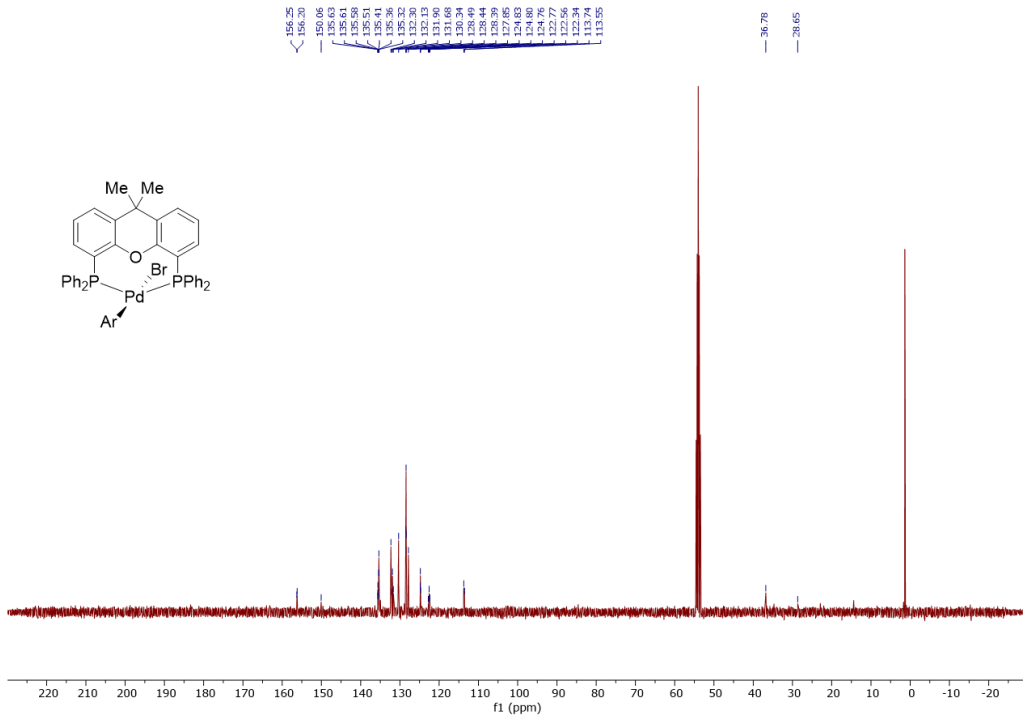
9.3. Compounds of Chapter 4

9.3.1. Oxidative Addition Complex 19

[(Xantphos)Pd(4-F-C_6H_4)(Br)] 19
^{1}H NMR (400 MHz, $CDCl_3$)

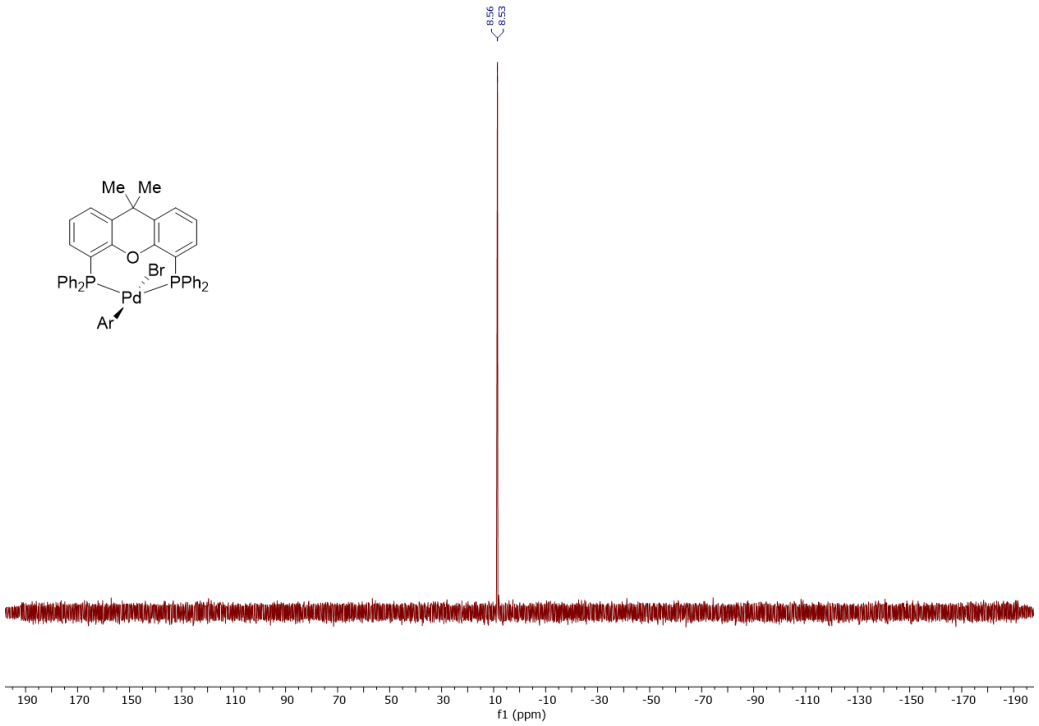


[(Xantphos)Pd(4-F-C_6H_4)(Br)] 19
^{13}C{^{1}H} NMR (101 MHz, CD_2Cl_2)



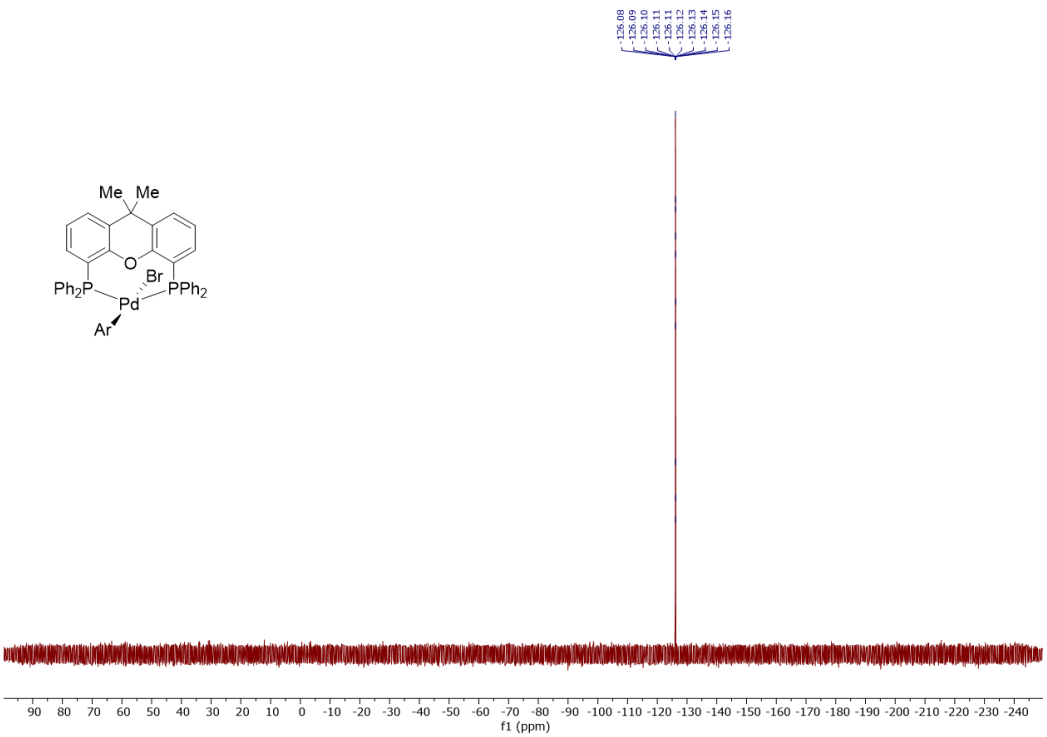
[(Xantphos)Pd(4-F-C_6H_4)(Br)] 19

$^{31}P\{^1H\}$ NMR (162 MHz, $CDCl_3$)



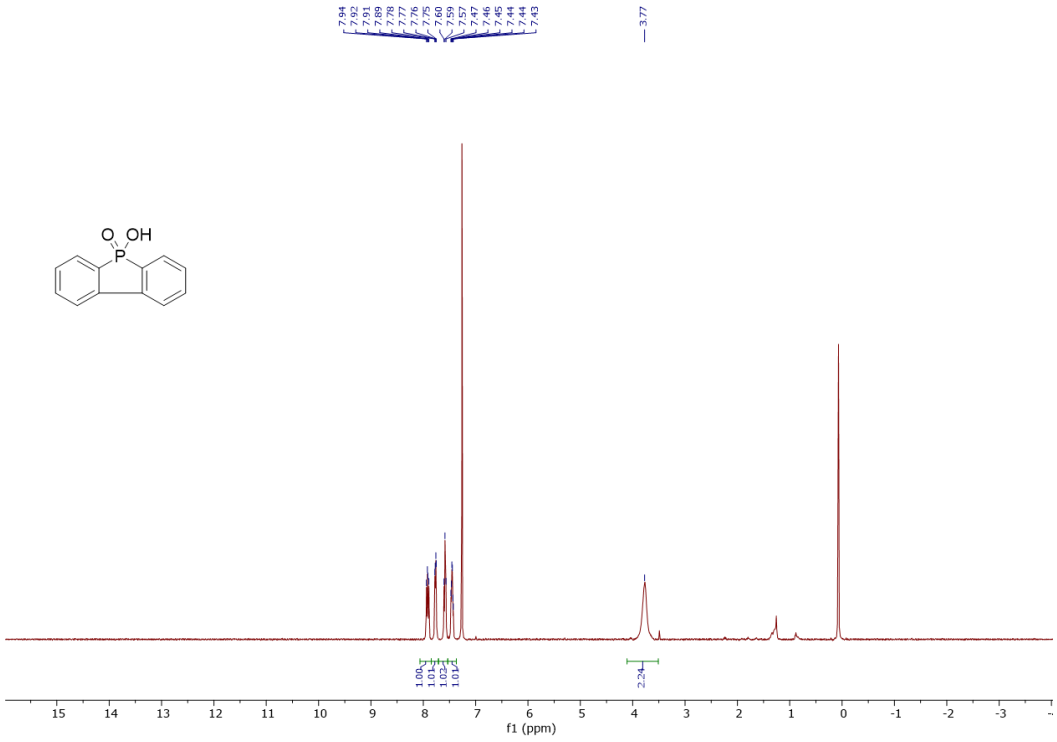
[(Xantphos)Pd(4-F-C_6H_4)(Br)] 19

$^{19}F\{^1H\}$ NMR (377 MHz, $CDCl_3$)

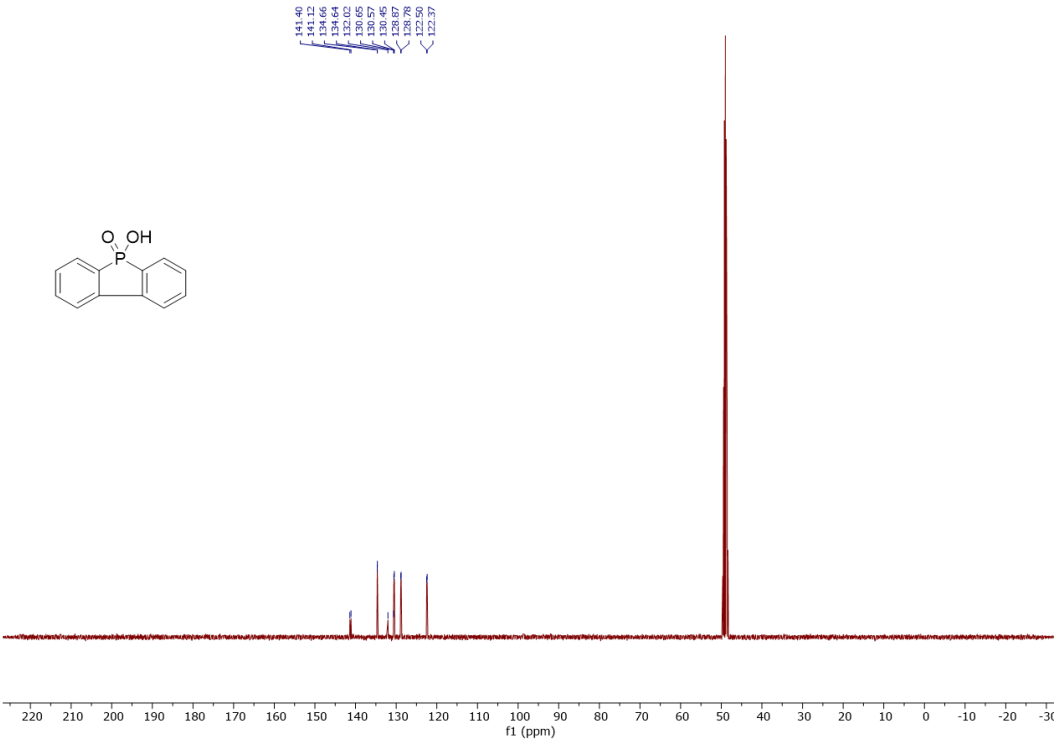


9.3.2. Novel Phosphinic Acids

5-Hydroxybenzo[*b*]phosphindole 5-oxide
^{1}H NMR (400 MHz, $CDCl_3$)

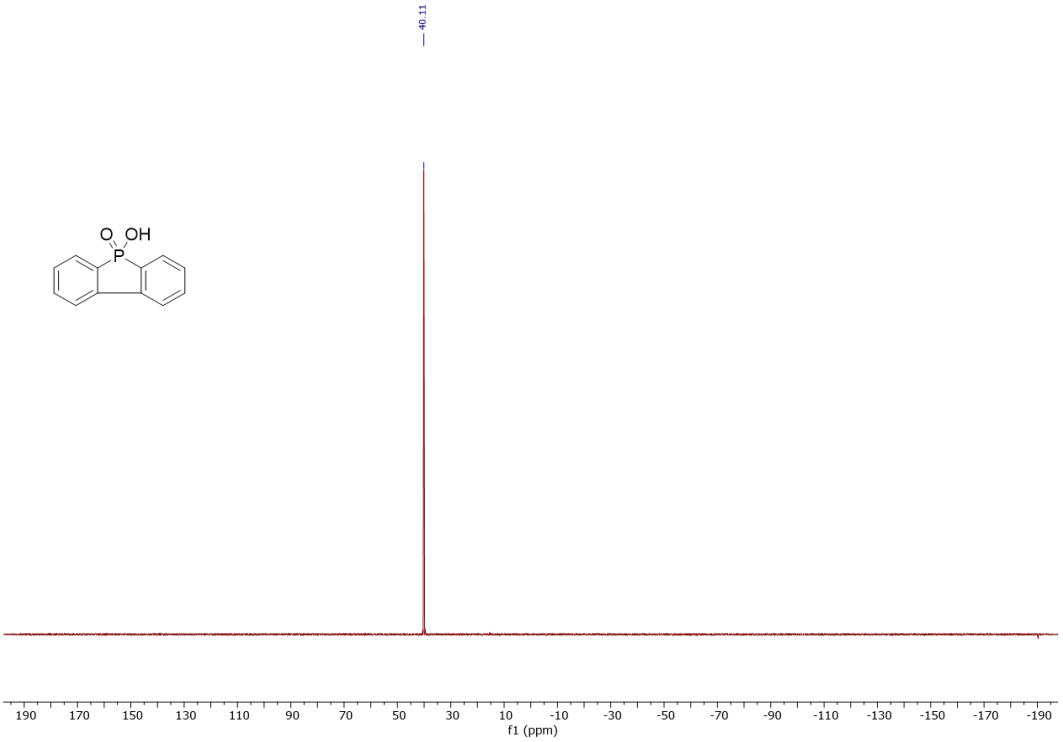


5-Hydroxybenzo[*b*]phosphindole 5-oxide
^{13}C{^{1}H} NMR (101 MHz, CD_3OD)



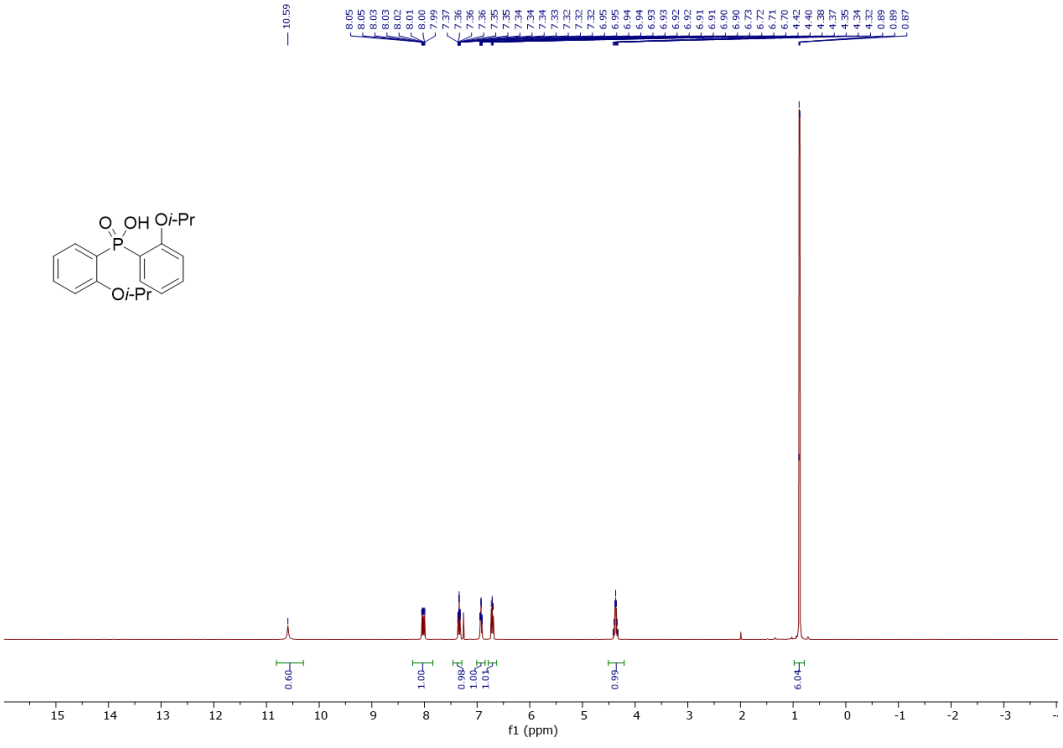
5-Hydroxybenzo[*b*]phosphindole 5-oxide

$^{31}P\{^{1}H\}$ NMR (162 MHz, CD_3OD)

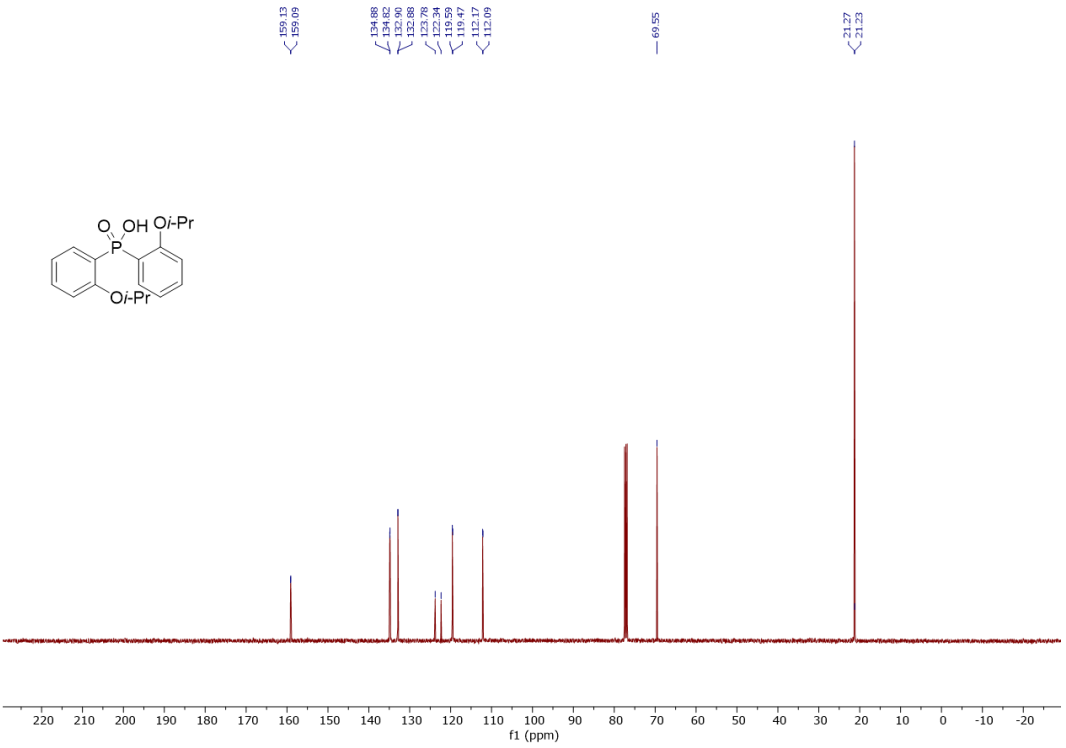


Bis(2-isopropoxyphenyl)phosphinic acid

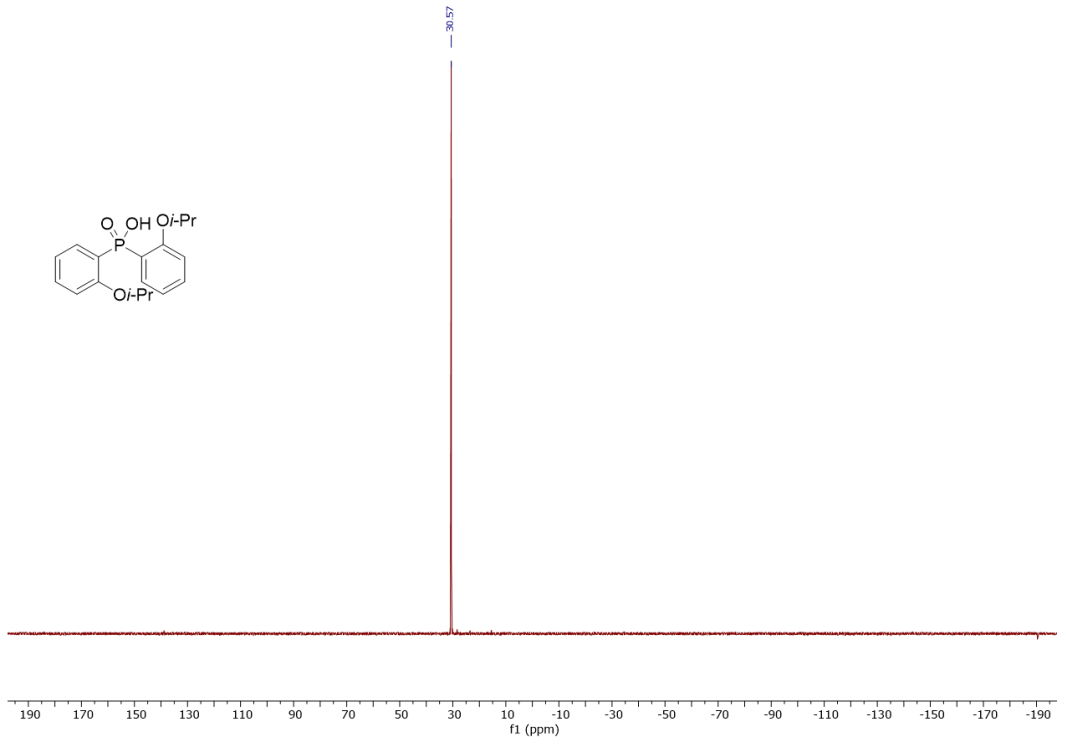
^{1}H NMR (400 MHz, $CDCl_3$)



Bis(2-isopropoxyphenyl)phosphinic acid
$^{13}C\{^{1}H\}$ NMR (101 MHz, $CDCl_3$)

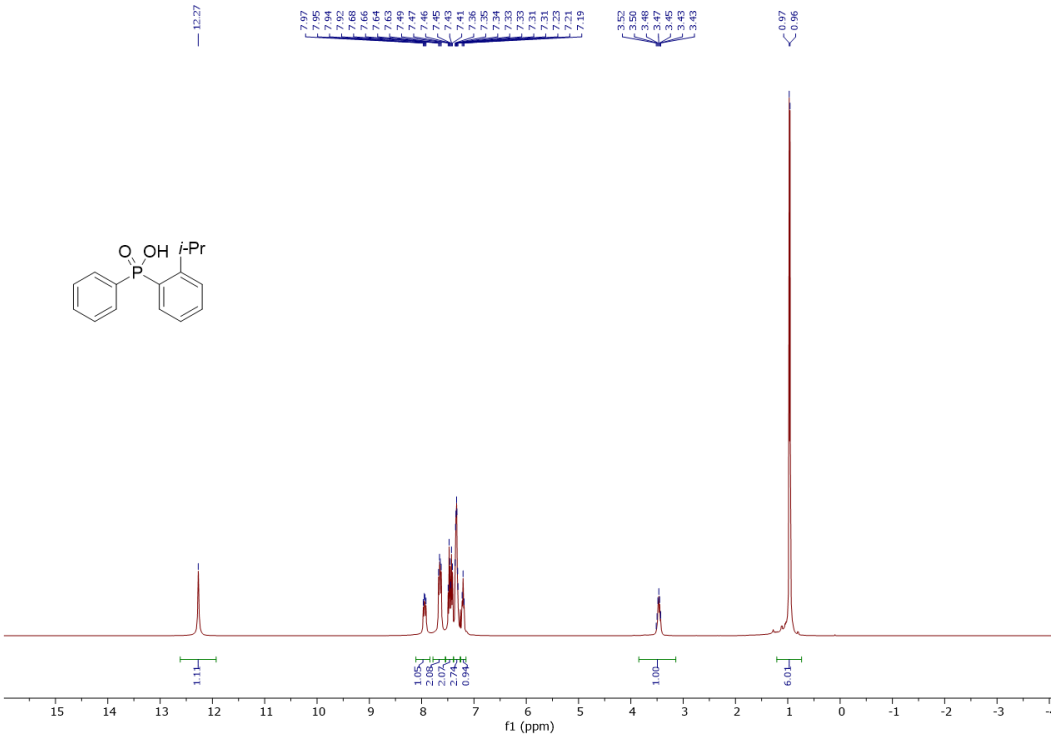


Bis(2-isopropoxyphenyl)phosphinic acid
$^{31}P\{^{1}H\}$ NMR (162 MHz, $CDCl_3$)



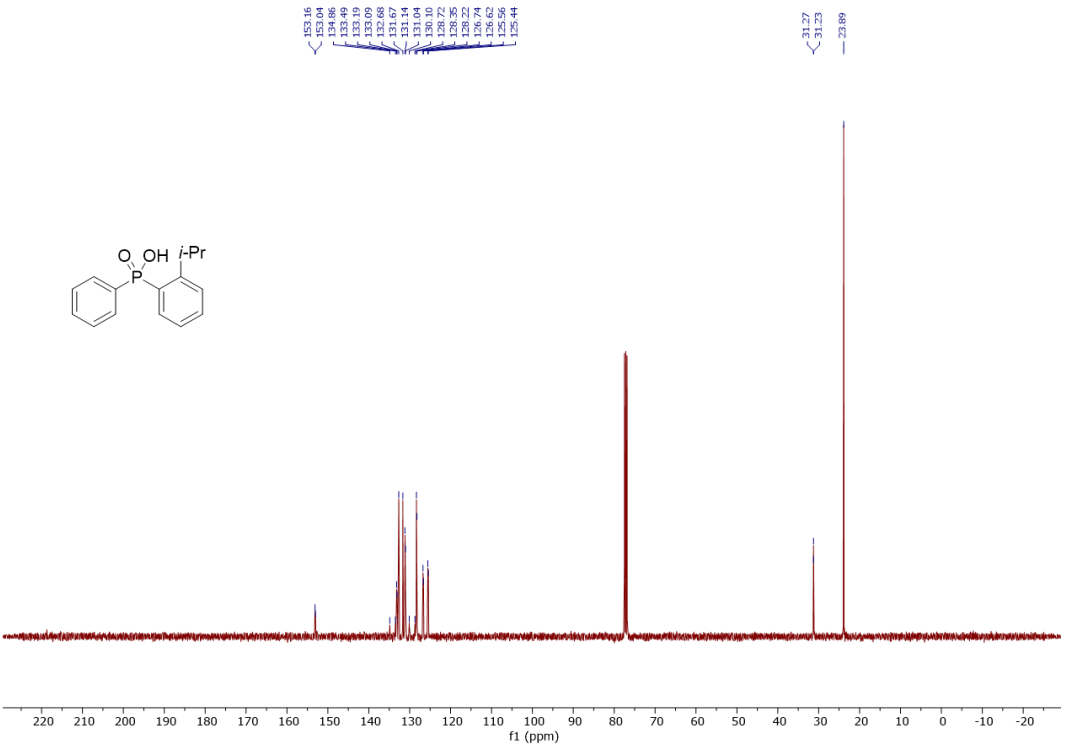
(2-Isopropylphenyl)(phenyl)phosphinic acid

^{1}H NMR (400 MHz, $CDCl_3$)



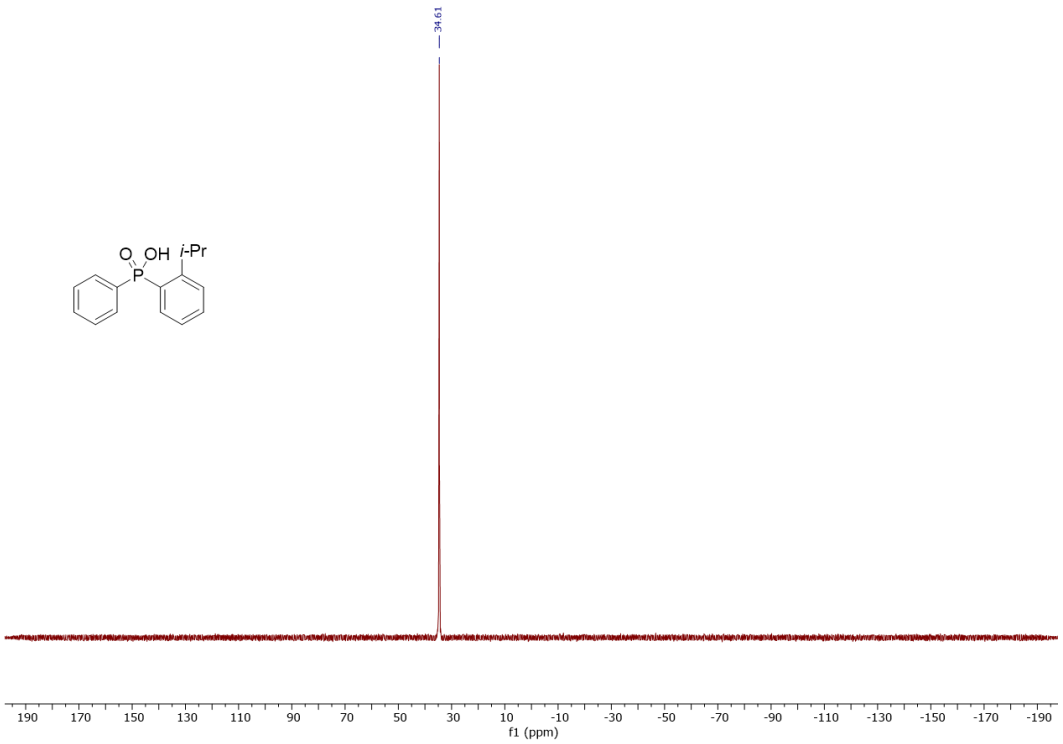
(2-Isopropylphenyl)(phenyl)phosphinic acid

^{13}C{^{1}H} NMR (101 MHz, $CDCl_3$)



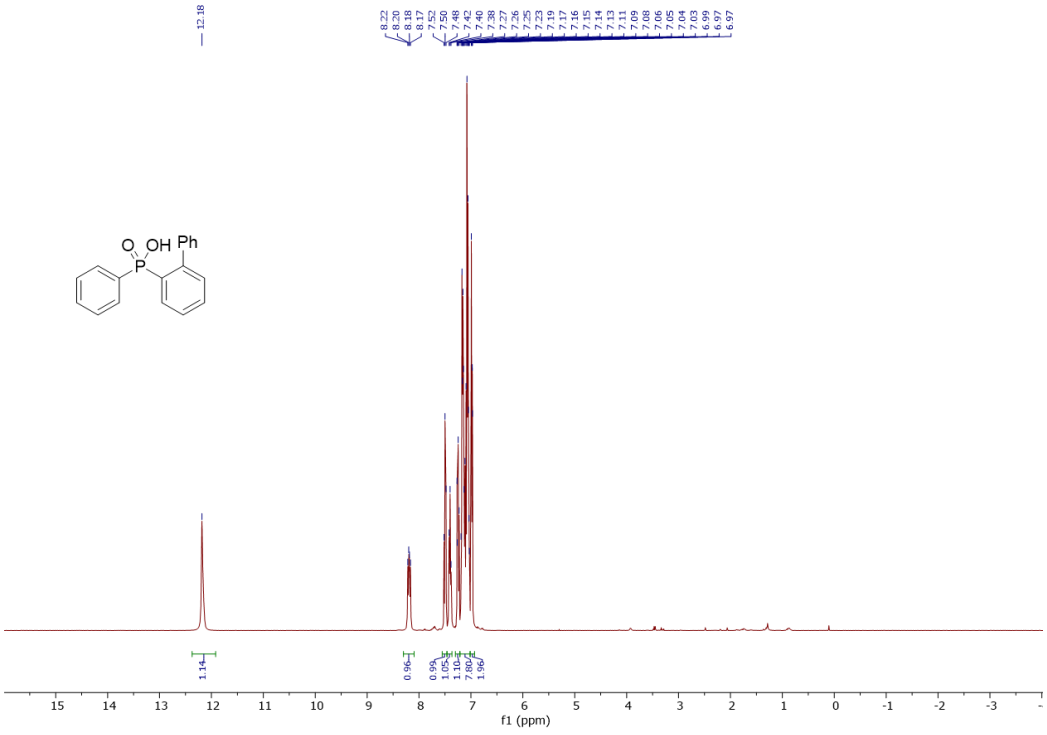
(2-Isopropylphenyl)(phenyl)phosphinic acid

$^{31}P\{^{1}H\}$ NMR (162 MHz, $CDCl_3$)

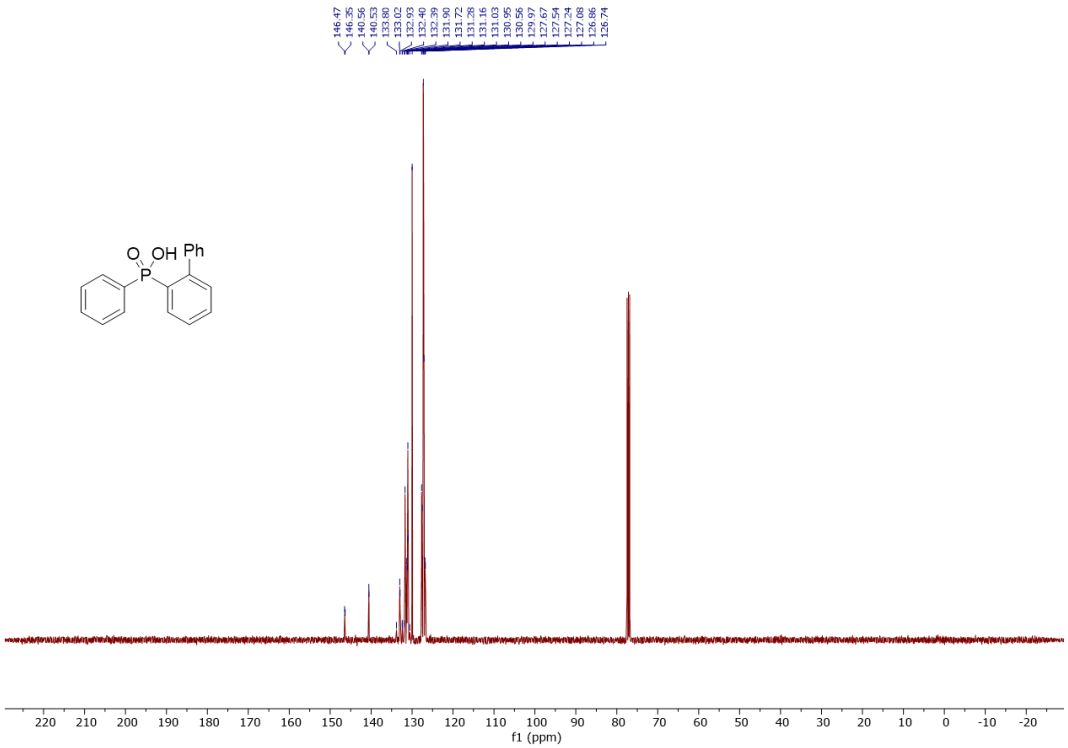


[1,1'-Biphenyl]-2-yl(phenyl)phosphinic acid

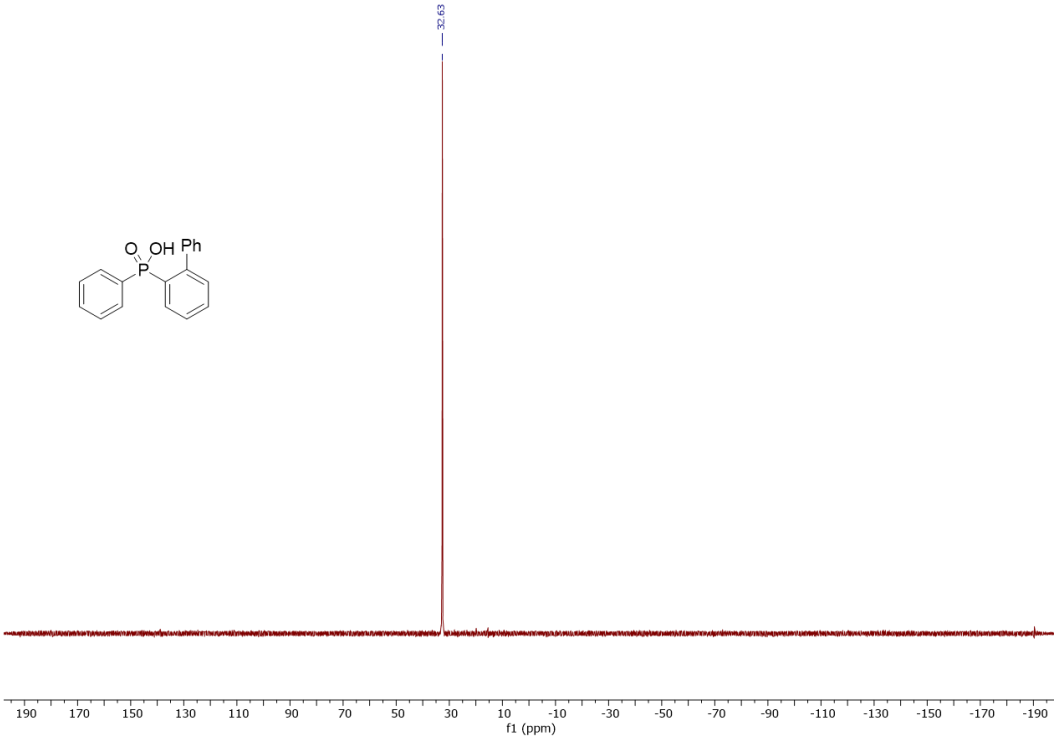
^{1}H NMR (400 MHz, $CDCl_3$)



[1,1'-Biphenyl]-2-yl(phenyl)phosphinic acid
$^{13}C\{^{1}H\}$ NMR (101 MHz, $CDCl_3$)

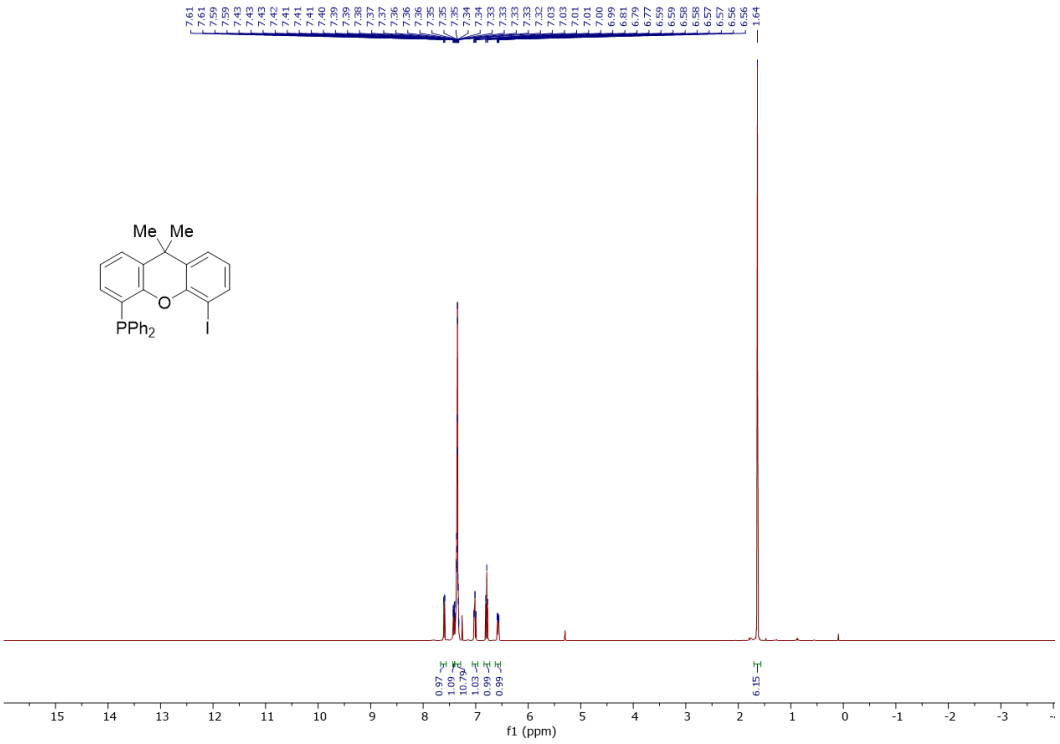


[1,1'-Biphenyl]-2-yl(phenyl)phosphinic acid
$^{31}P\{^{1}H\}$ NMR (162 MHz, $CDCl_3$)

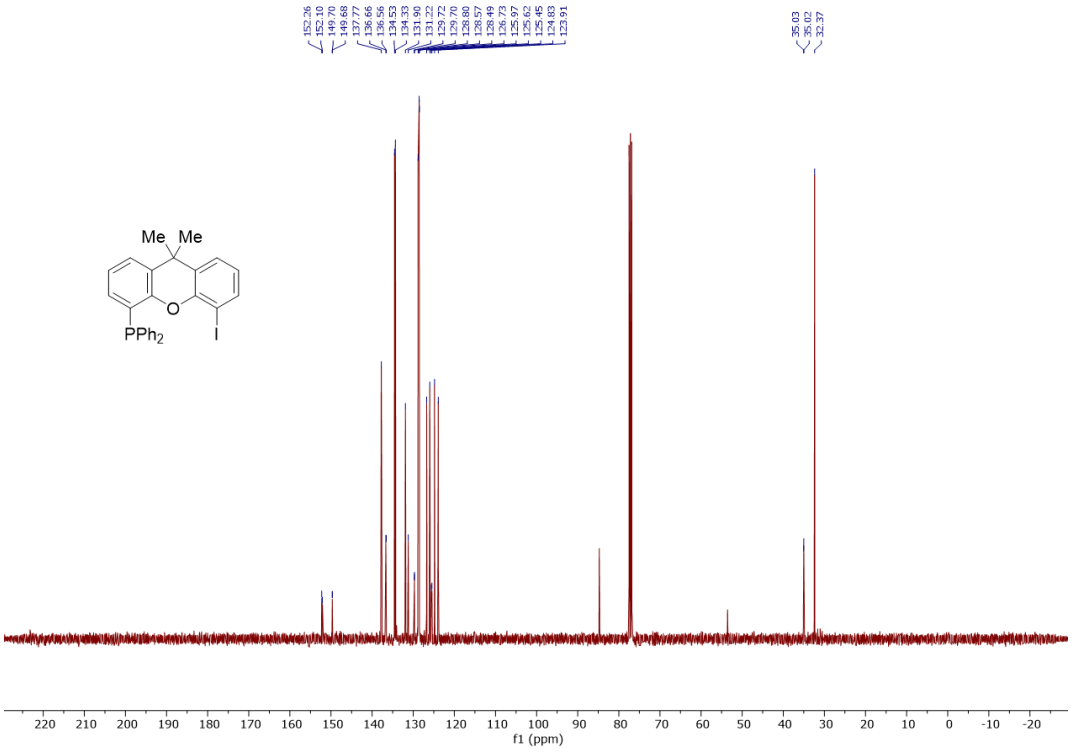


9.3.3. (5-Iodo-9,9-dimethyl-9H-xanthen-4-yl)diphenylphosphane

(5-Iodo-9,9-dimethyl-9*H*-xanthen-4-yl)diphenylphosphane
^{1}H NMR (400 MHz, $CDCl_3$)

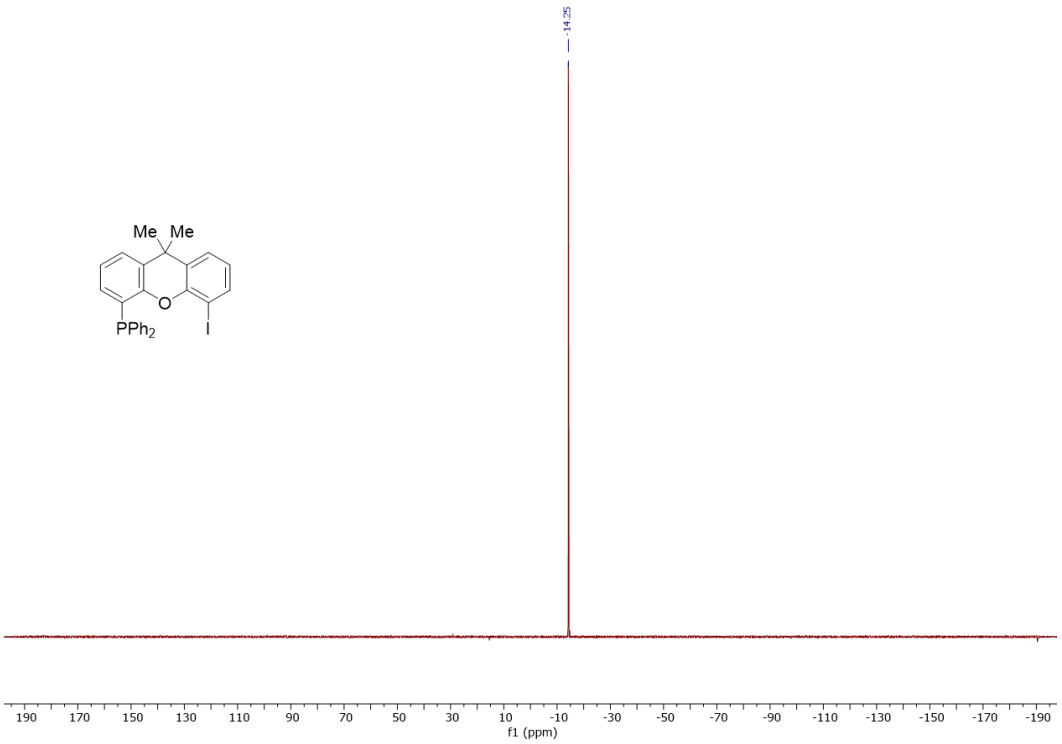


(5-Iodo-9,9-dimethyl-9*H*-xanthen-4-yl)diphenylphosphane
^{13}C{^{1}H} NMR (101 MHz, $CDCl_3$)



(5-Iodo-9,9-dimethyl-9*H*-xanthen-4-yl)diphenylphosphane

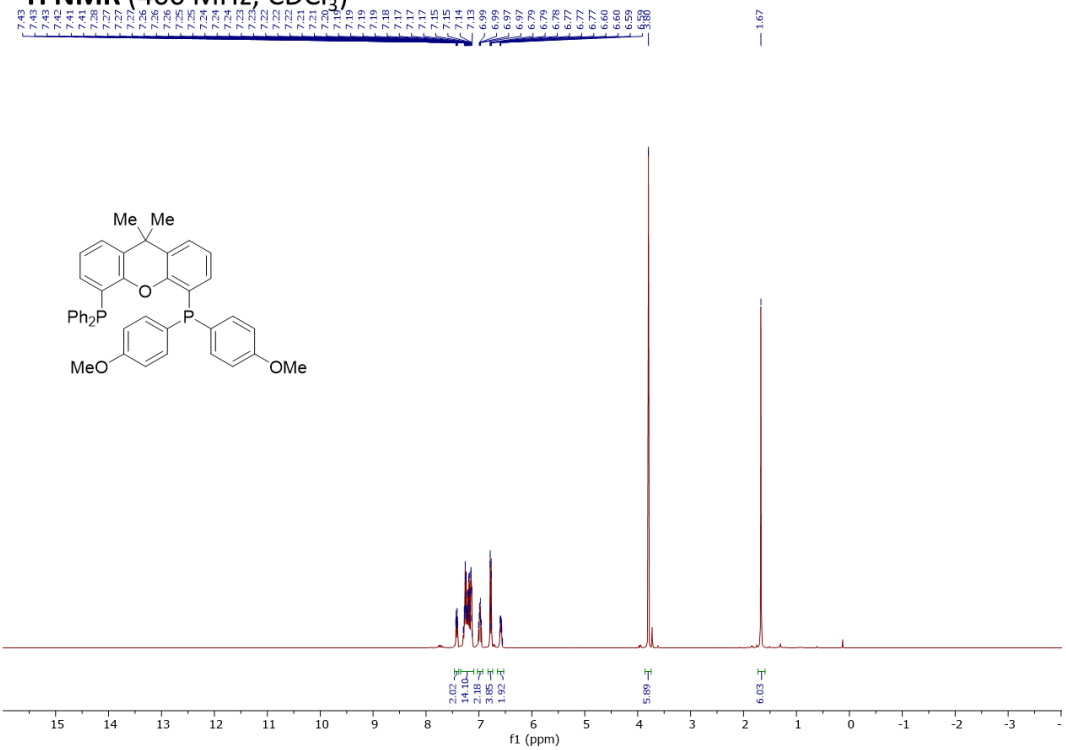
$^{31}P\{^{1}H\}$ NMR (162 MHz, $CDCl_3$)



9.3.4. Ligands L1-L13

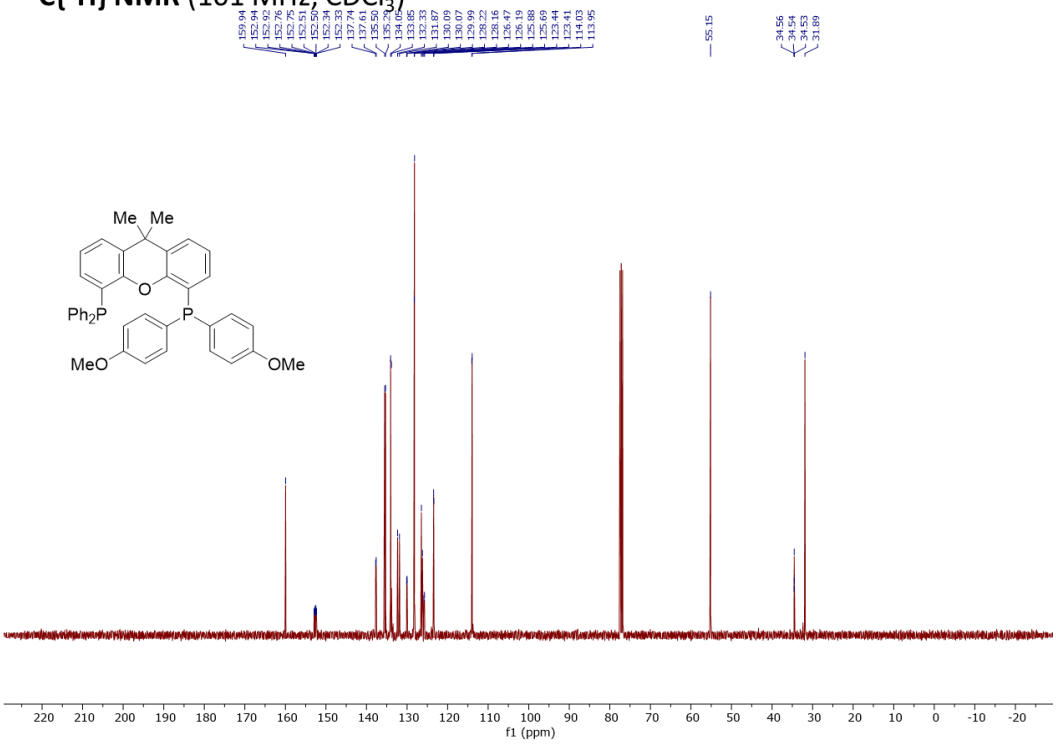
(5-(Bis(4-methoxyphenyl)phosphaneyl)-9,9-dimethyl-9*H*-xanthen-4-yl)diphenylphosphane L1

^{1}H NMR (400 MHz, $CDCl_3$)



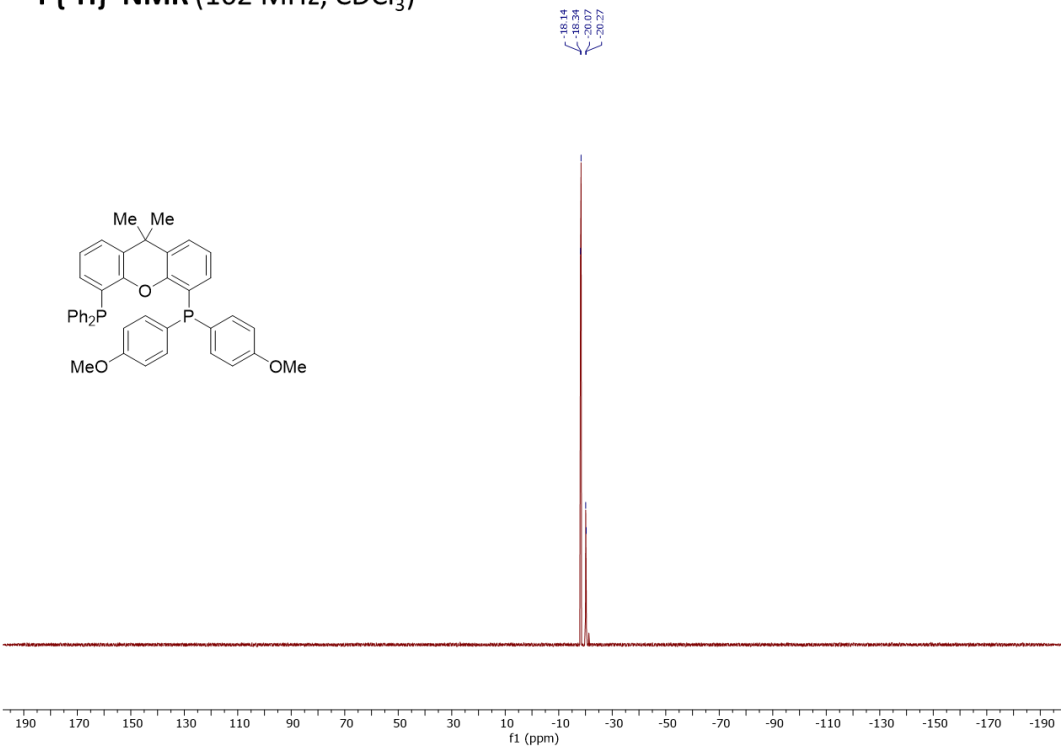
(5-(Bis(4-methoxyphenyl)phosphaneyl)-9,9-dimethyl-9*H*-xanthen-4-yl)diphenylphosphane L1

$^{13}C\{^{1}H\}$ NMR (101 MHz, $CDCl_3$)



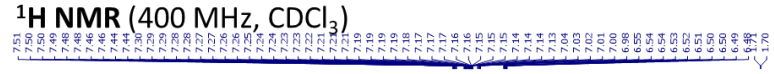
(5-(Bis(4-methoxyphenyl)phosphaneyl)-9,9-dimethyl-9*H*-xanthen-4-yl)diphenylphosphane L1

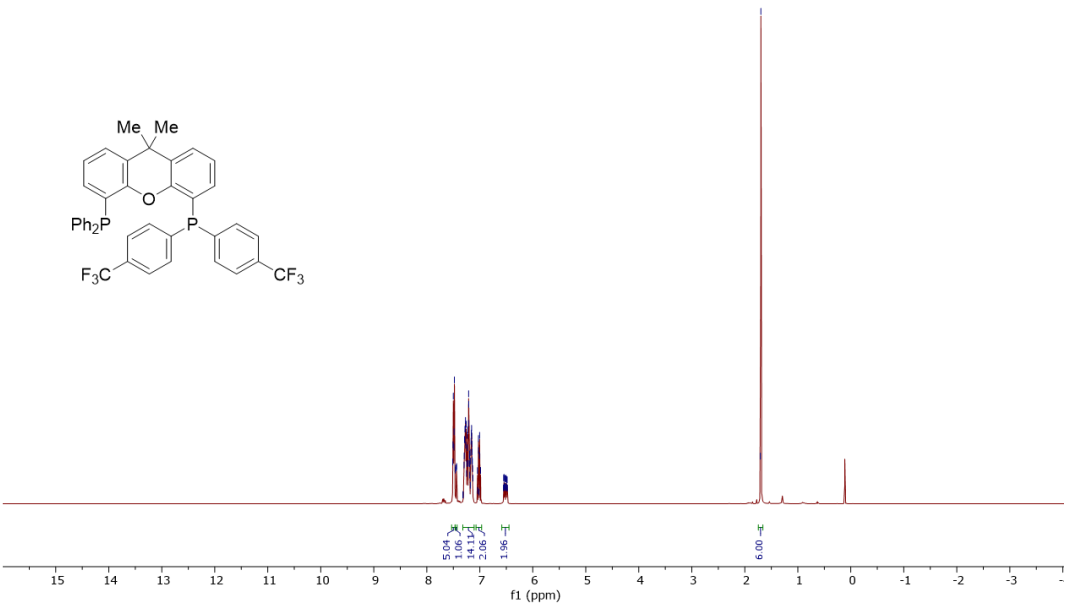
$^{31}P\{^{1}H\}$ NMR (162 MHz, $CDCl_3$)



(5-(Bis(4-(trifluoromethyl)phenyl)phosphaneyl)-9,9-dimethyl-9*H*-xanthen-4-yl)diphenylphosphane L2

^{1}H NMR (400 MHz, $CDCl_3$)

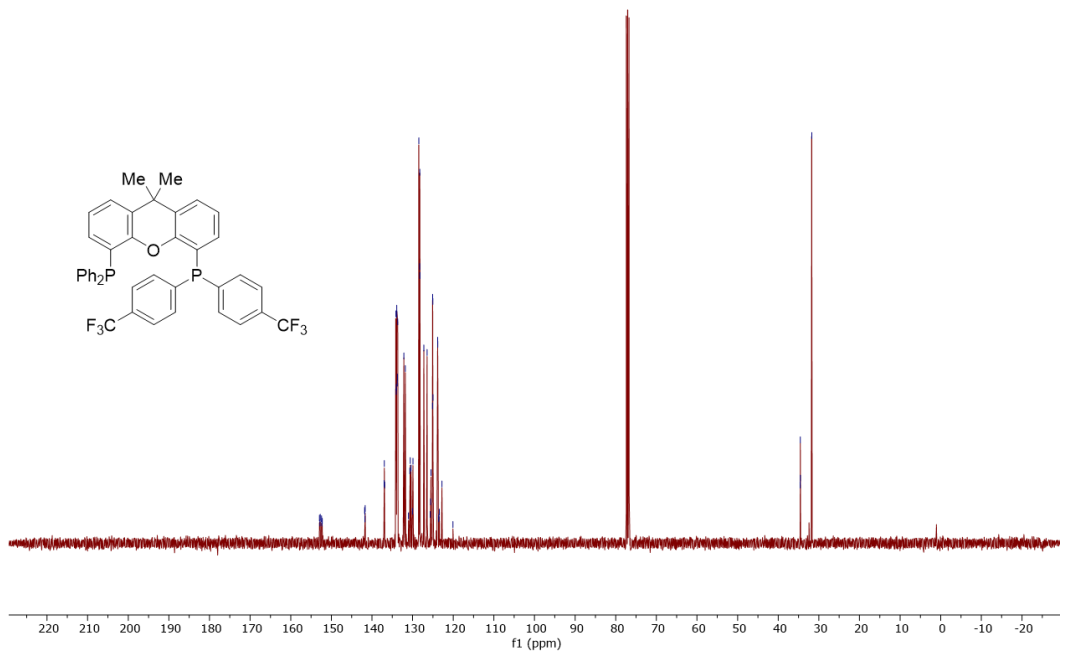




(5-(Bis(4-(trifluoromethyl)phenyl)phosphaneyl)-9,9-dimethyl-9*H*-xanthen-4-yl)diphenylphosphane L2

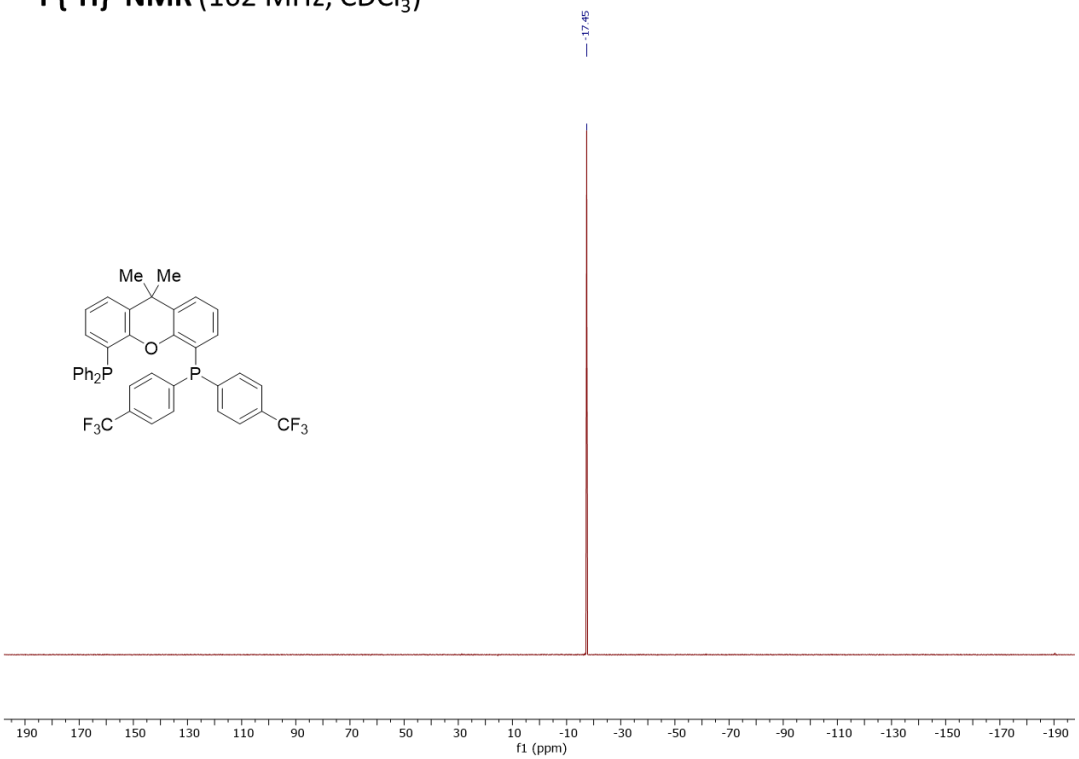
^{13}C{^{1}H} NMR (101 MHz, $CDCl_3$)





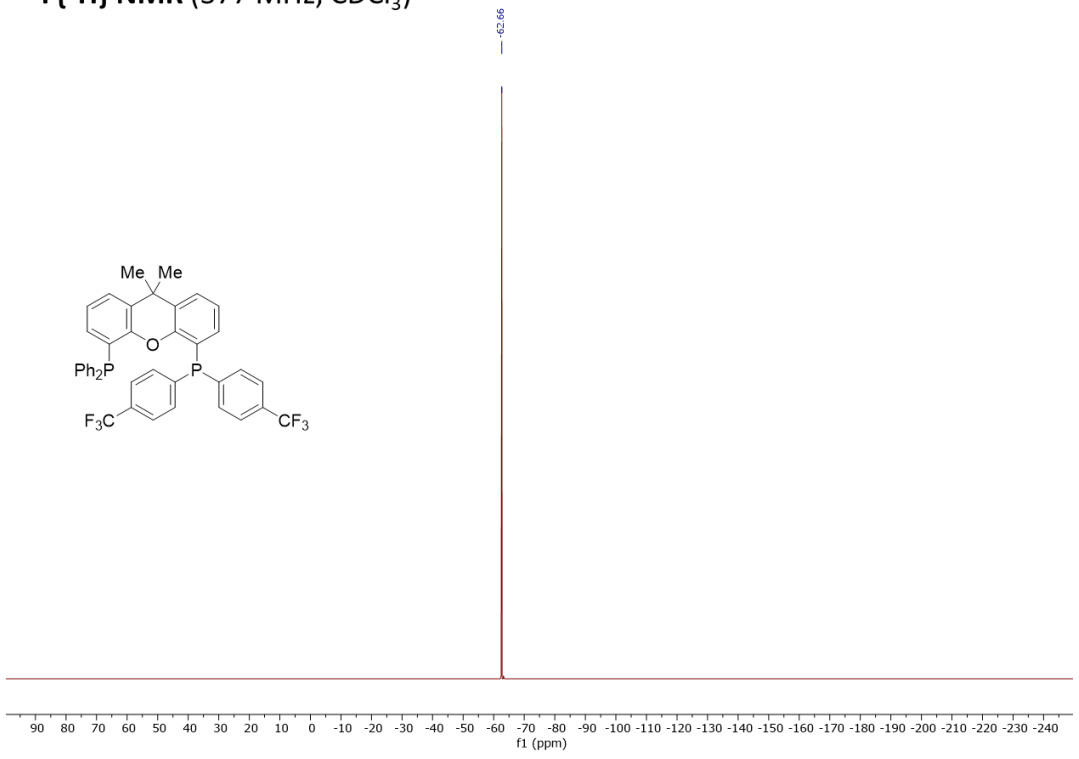
(5-(Bis(4-(trifluoromethyl)phenyl)phosphaneyl)-9,9-dimethyl-9*H*-xanthen-4-yl)diphenylphosphane L2

$^{31}P\{^{1}H\}$ NMR (162 MHz, $CDCl_3$)



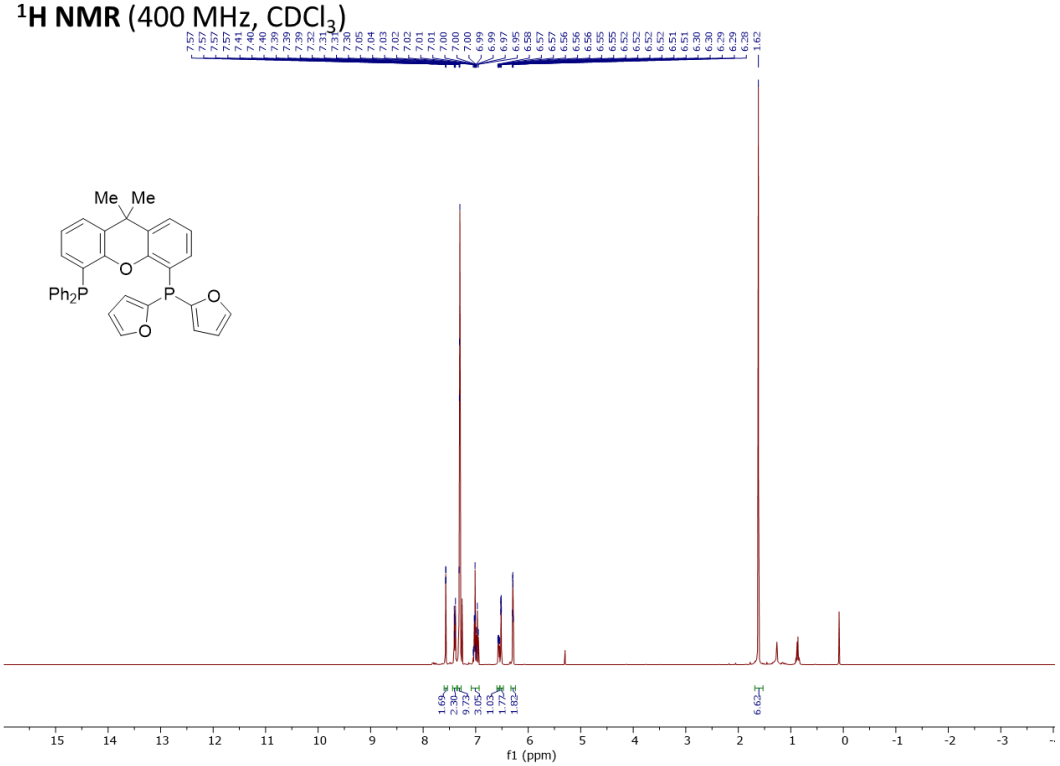
(5-(Bis(4-(trifluoromethyl)phenyl)phosphaneyl)-9,9-dimethyl-9*H*-xanthen-4-yl)diphenylphosphane L2

$^{19}F\{^{1}H\}$ NMR (377 MHz, $CDCl_3$)



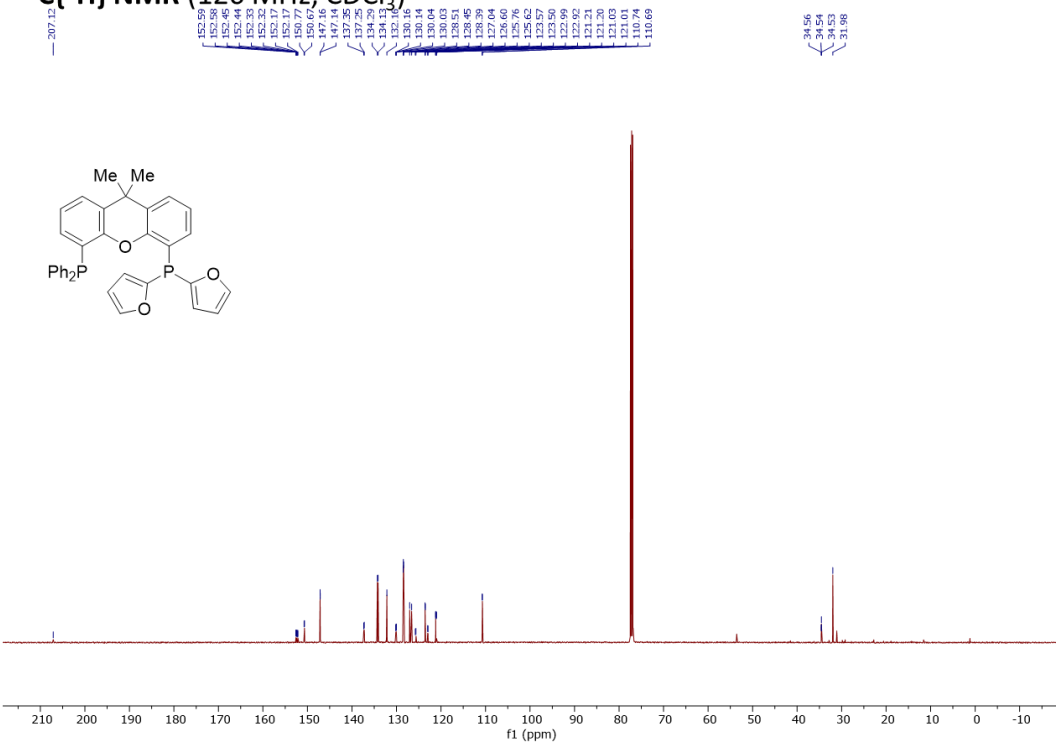
(5-(Di(furan-2-yl)phosphaneyl)-9,9-dimethyl-9*H*-xanthen-4-yl)diphenylphosphane L3

^{1}H NMR (400 MHz, $CDCl_3$)



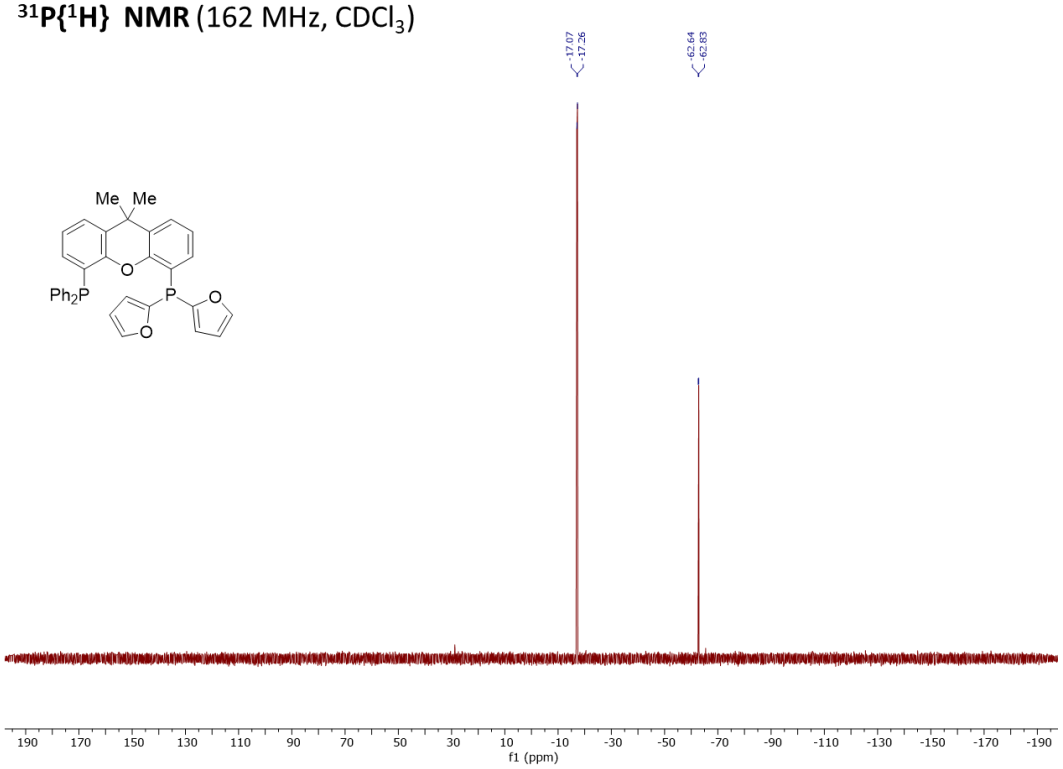
(5-(Di(furan-2-yl)phosphaneyl)-9,9-dimethyl-9*H*-xanthen-4-yl)diphenylphosphane L3

^{13}C{^{1}H} NMR (126 MHz, $CDCl_3$)



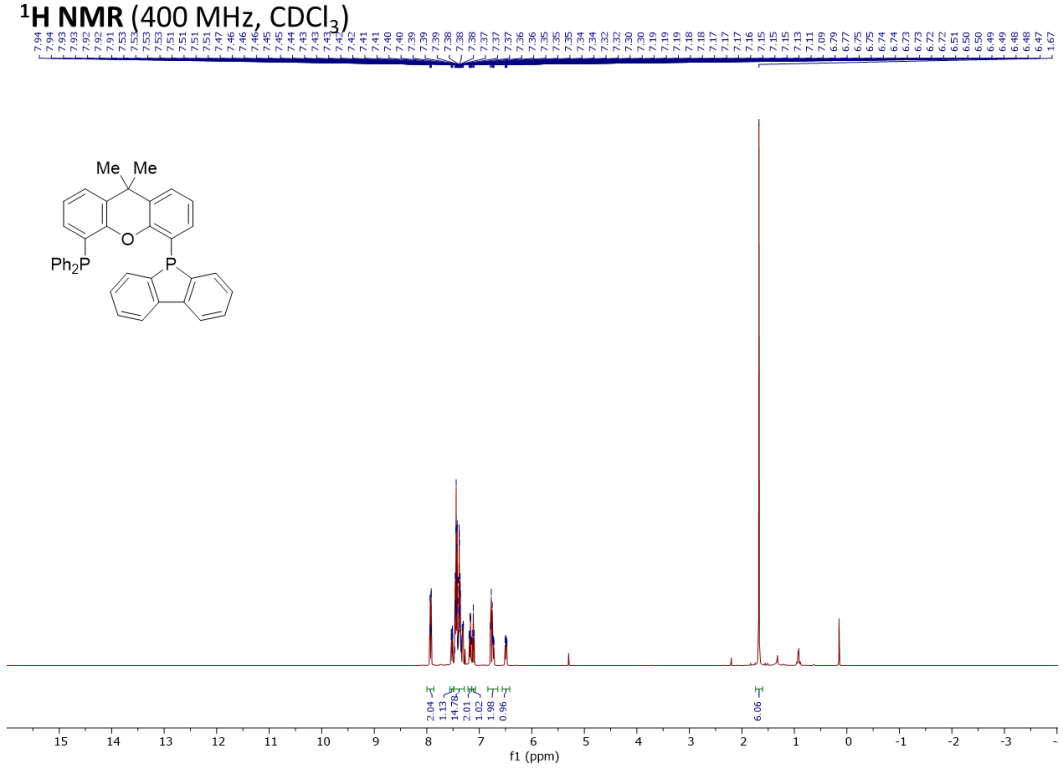
(5-(Di(furan-2-yl)phosphaneyl)-9,9-dimethyl-9*H*-xanthen-4-yl)diphenylphosphane L3

$^{31}P\{^{1}H\}$ NMR (162 MHz, $CDCl_3$)



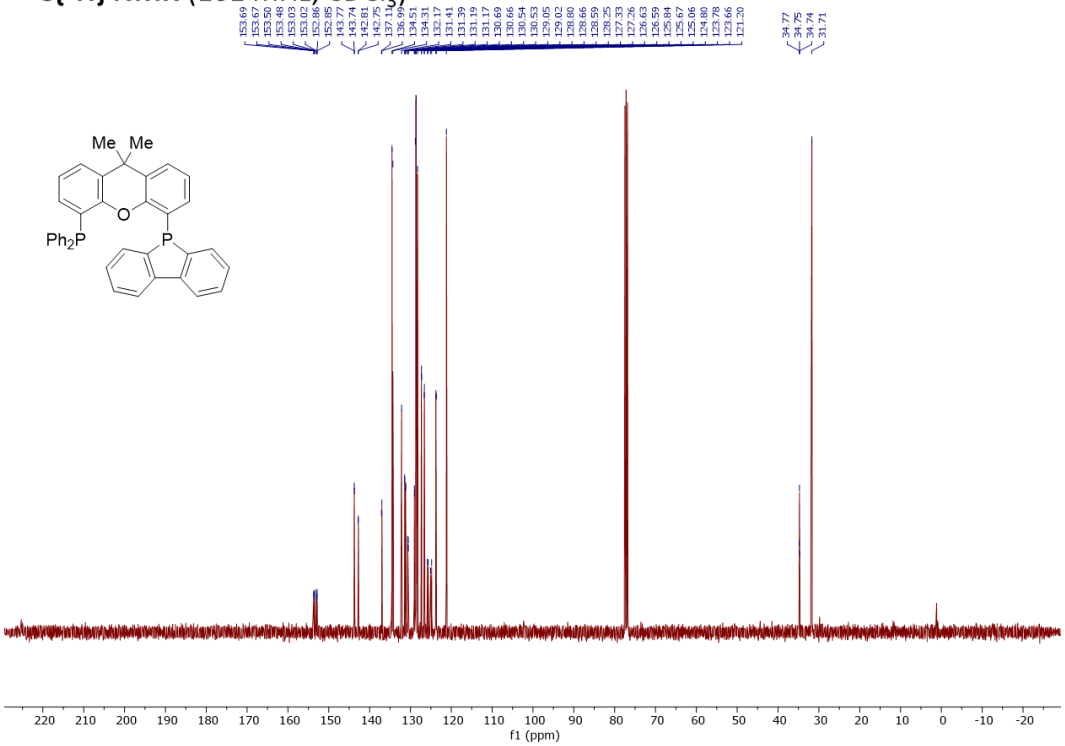
5-(5-(Diphenylphosphaneyl)-9,9-dimethyl-9*H*-xanthen-4-yl)-5*H*-benzo[*b*]phosphindole L4

^{1}H NMR (400 MHz, $CDCl_3$)



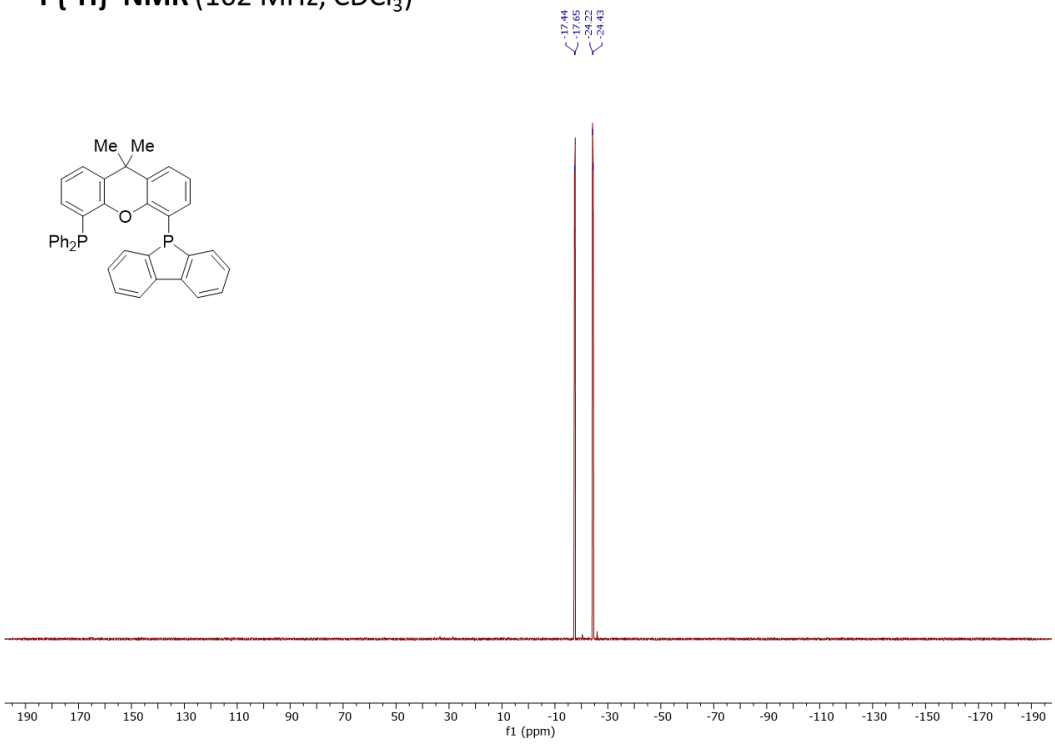
5-(5-(Diphenylphosphaneyl)-9,9-dimethyl-9*H*-xanthen-4-yl)-5*H*-benzo[*b*]phosphindole L4

$^{13}C\{^{1}H\}$ NMR (101 MHz, $CDCl_3$)



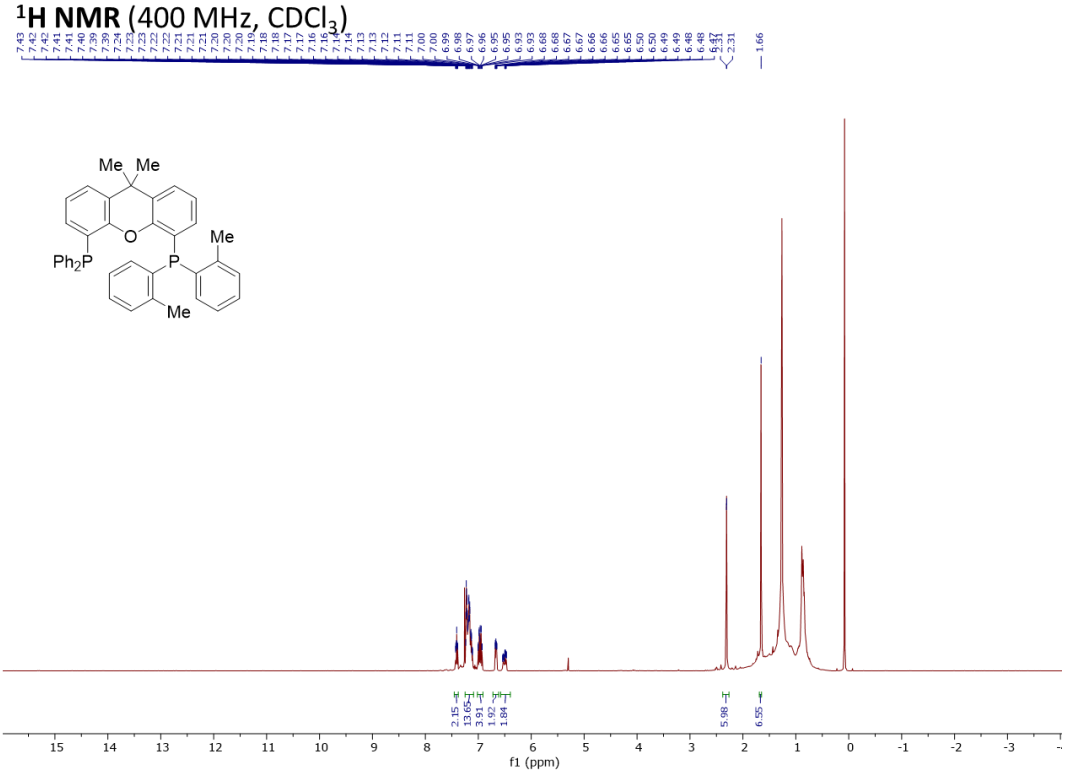
5-(5-(Diphenylphosphaneyl)-9,9-dimethyl-9*H*-xanthen-4-yl)-5*H*-benzo[*b*]phosphindole L4

$^{31}P\{^{1}H\}$ NMR (162 MHz, $CDCl_3$)



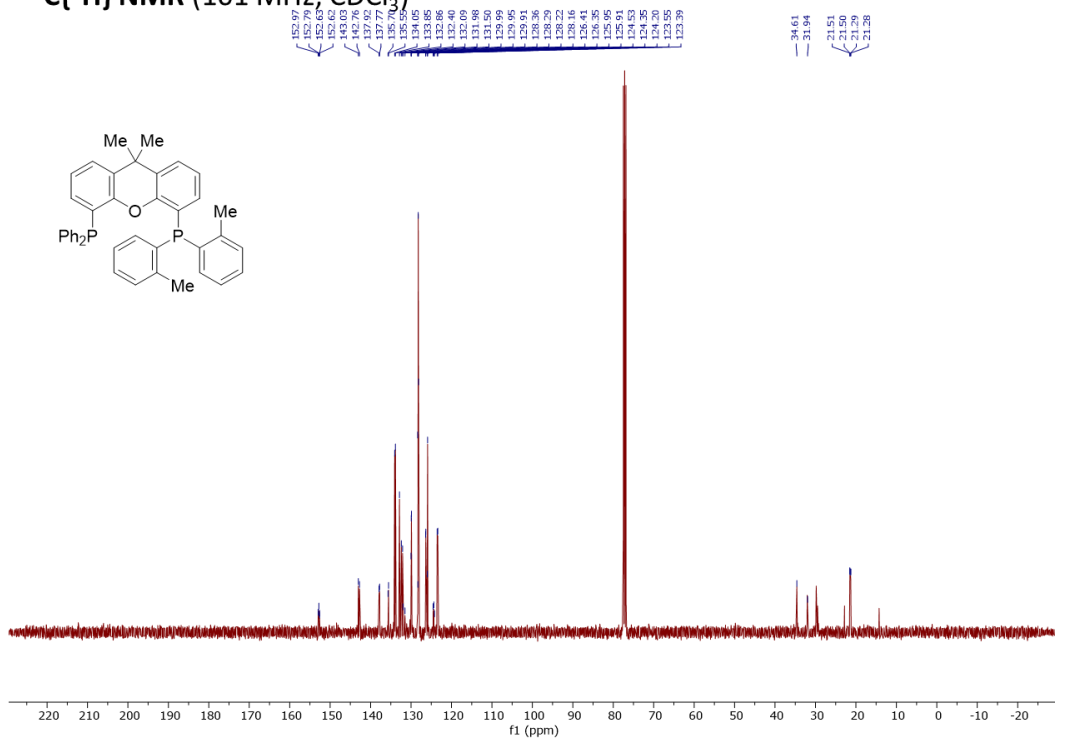
(5-(Di-*o*-tolylphosphaneyl)-9,9-dimethyl-9*H*-xanthen-4-yl)diphenylphosphane L5

^{1}H NMR (400 MHz, $CDCl_3$)



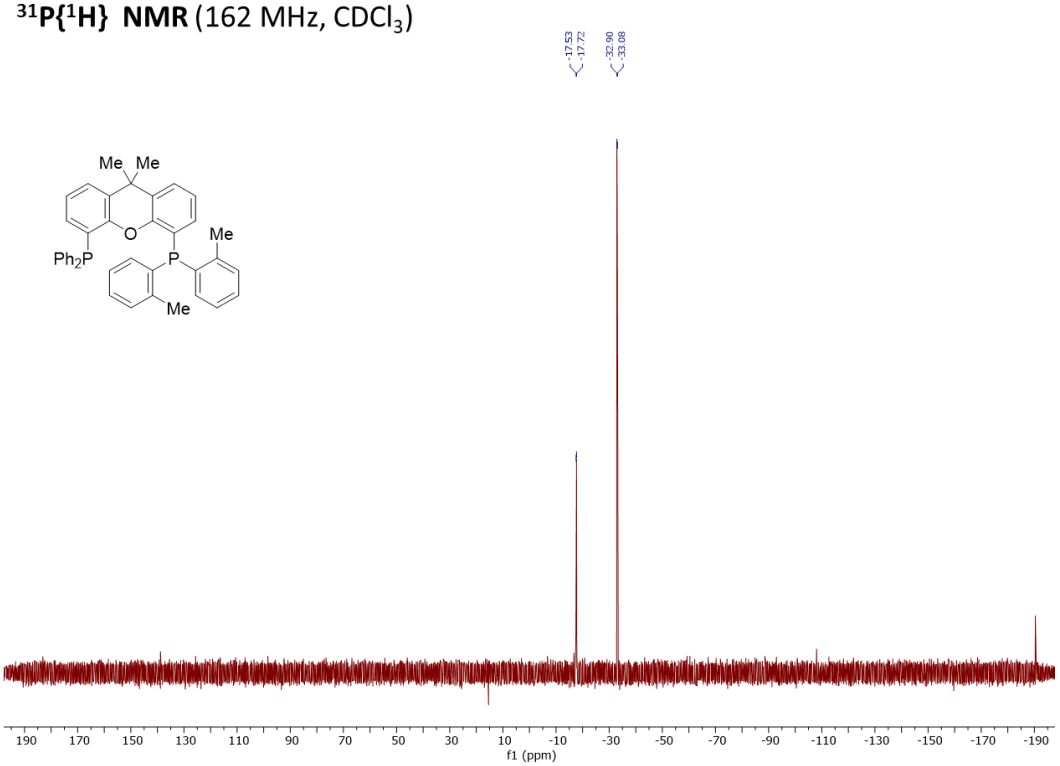
(5-(Di-*o*-tolylphosphaneyl)-9,9-dimethyl-9*H*-xanthen-4-yl)diphenylphosphane L5

^{13}C{^{1}H} NMR (101 MHz, $CDCl_3$)



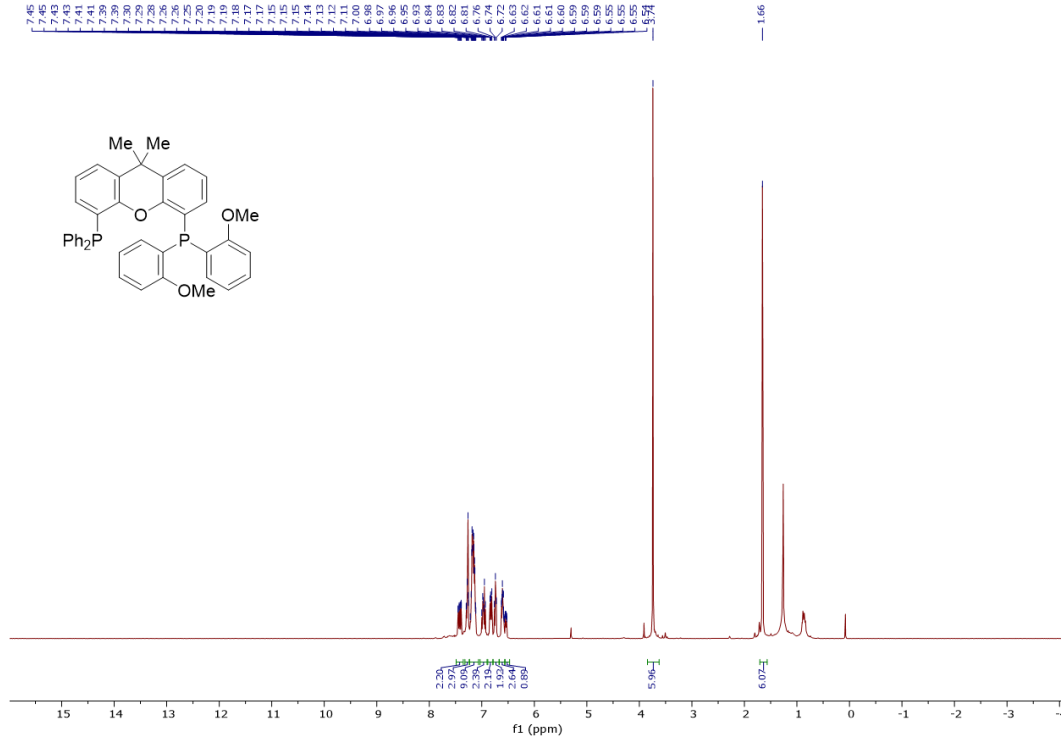
(5-(Di-*o*-tolylphosphaneyl)-9,9-dimethyl-9*H*-xanthen-4-yl)diphenylphosphane L5

$^{31}P\{^{1}H\}$ NMR (162 MHz, $CDCl_3$)



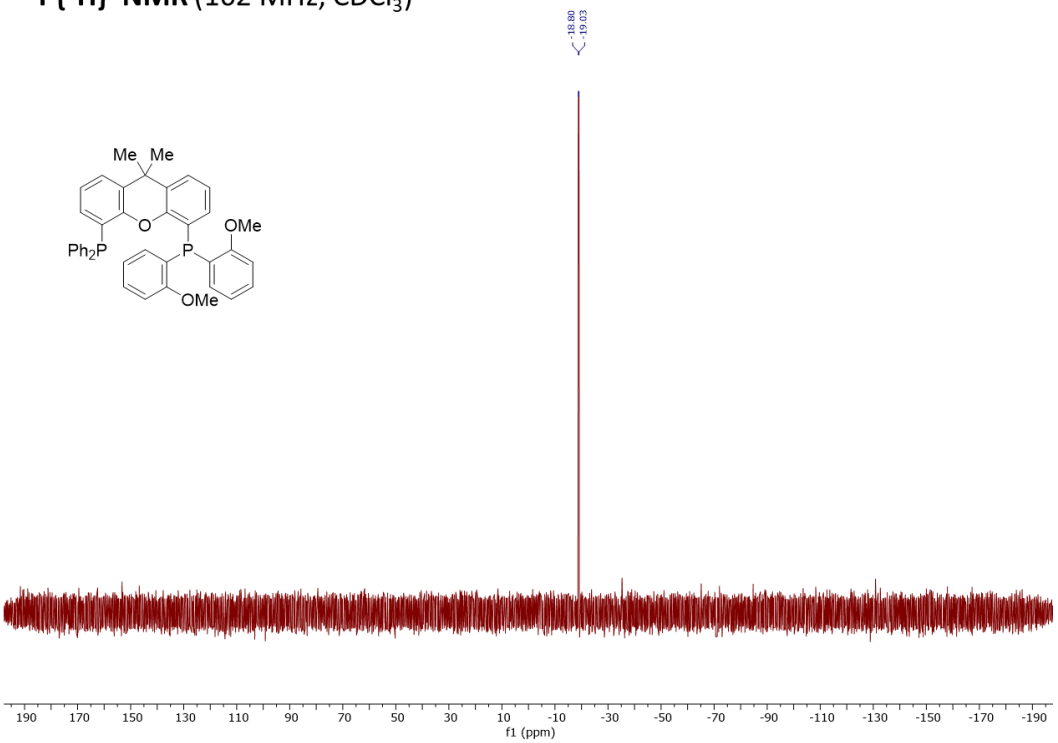
(5-(Bis(2-methoxyphenyl)phosphaneyl)-9,9-dimethyl-9*H*-xanthen-4-yl)diphenylphosphane L6

^{1}H NMR (400 MHz, $CDCl_3$)



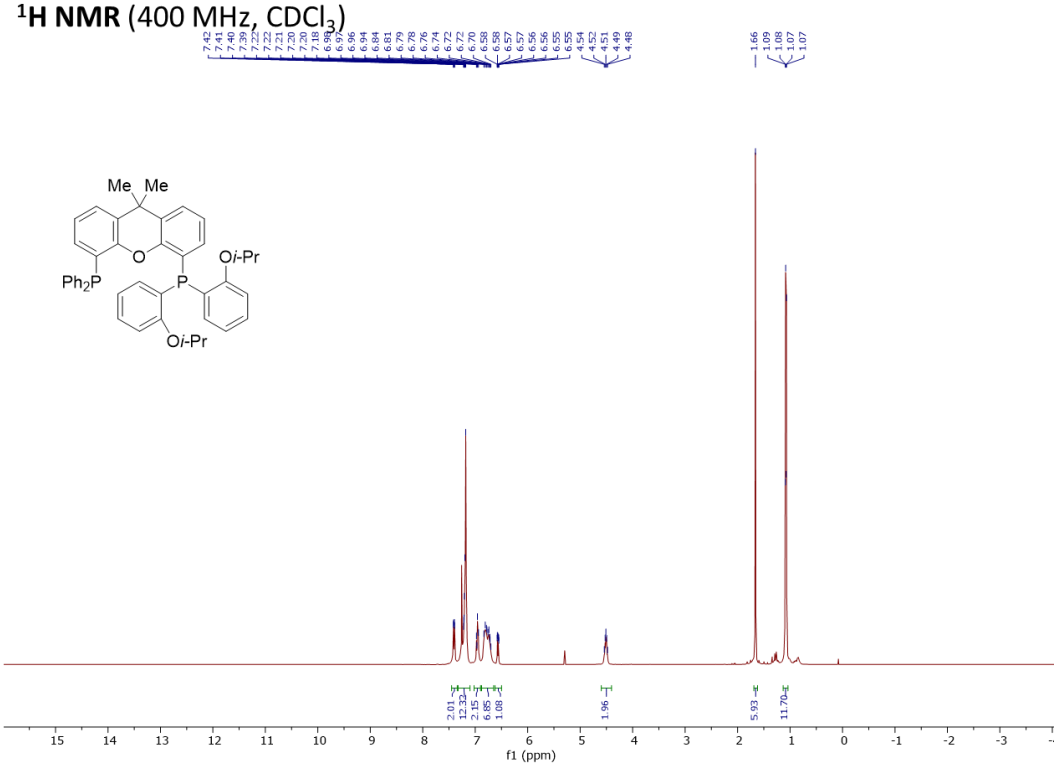
(5-(Bis(2-methoxyphenyl)phosphaneyl)-9,9-dimethyl-9*H*-xanthen-4-yl)diphenylphosphane L6

$^{31}P\{^{1}H\}$ NMR (162 MHz, $CDCl_3$)



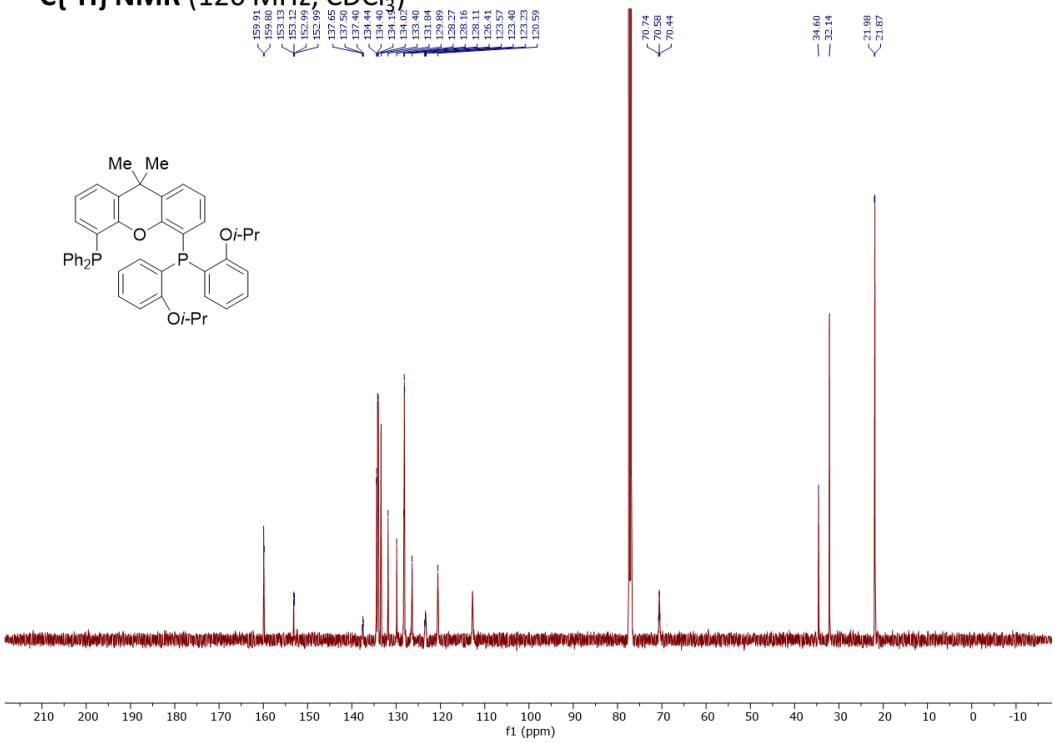
(5-(Bis(2-isopropoxyphenyl)phosphaneyl)-9,9-dimethyl-9*H*-xanthen-4-yl)diphenylphosphane L7

^{1}H NMR (400 MHz, $CDCl_3$)



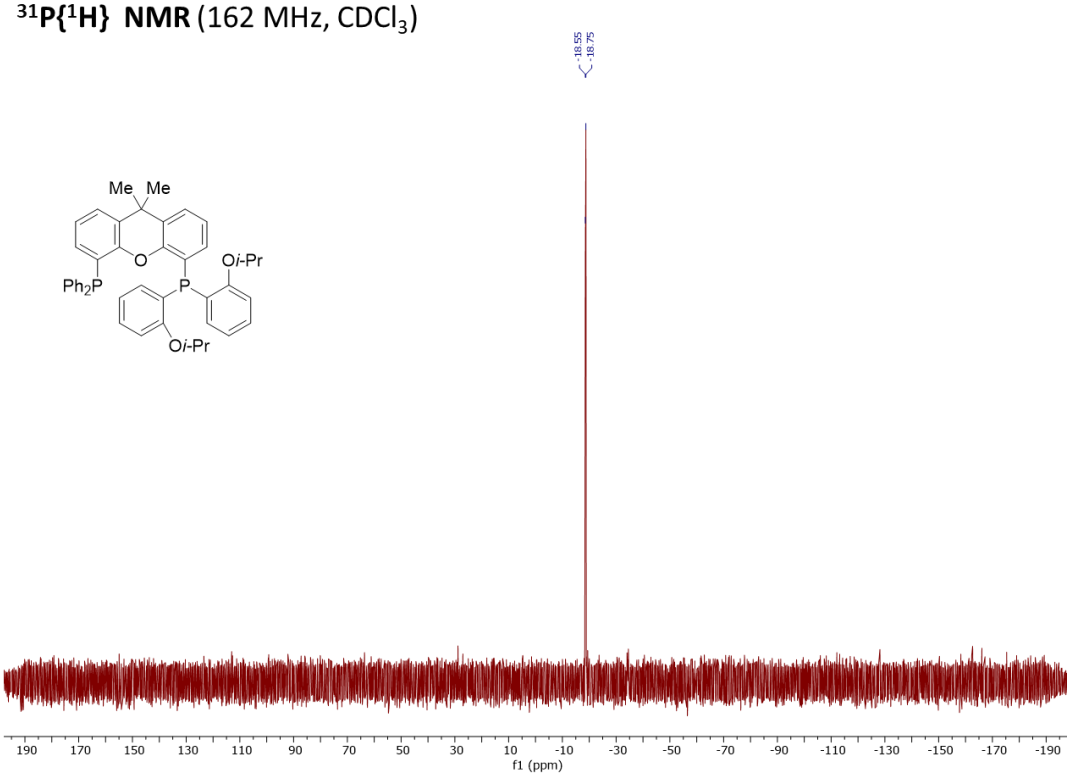
(5-(Bis(2-isopropoxyphenyl)phosphaneyl)-9,9-dimethyl-9*H*-xanthen-4-yl)diphenylphosphane L7

$^{13}C\{^{1}H\}$ NMR (126 MHz, $CDCl_3$)



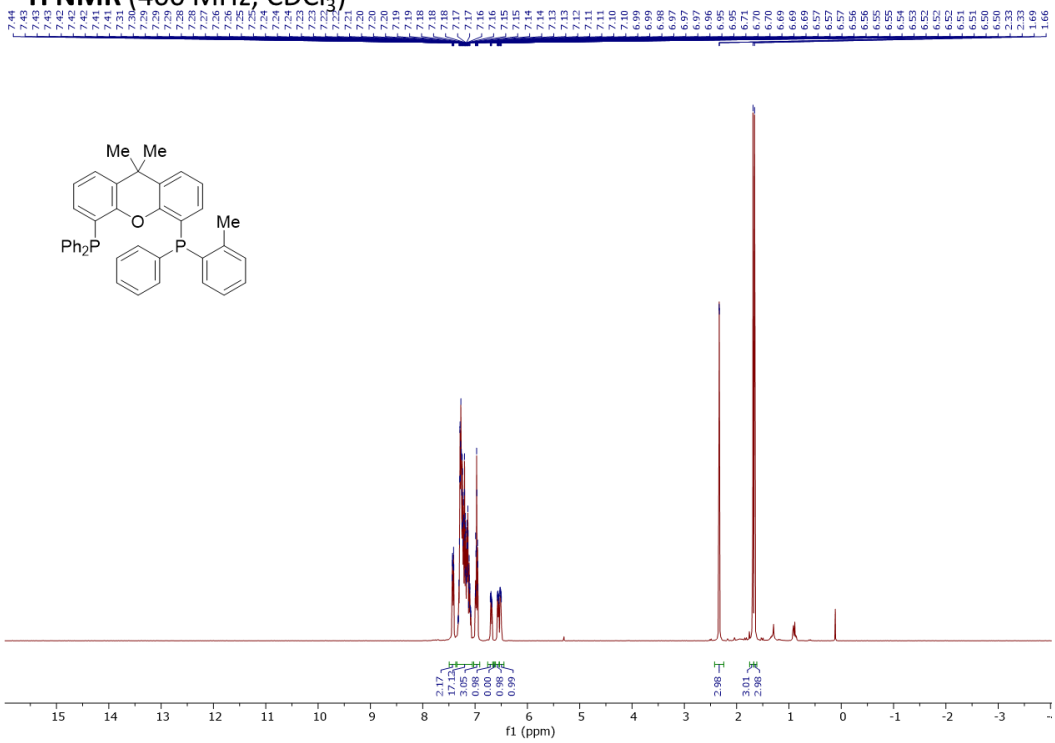
(5-(Bis(2-isopropoxyphenyl)phosphaneyl)-9,9-dimethyl-9*H*-xanthen-4-yl)diphenylphosphane L7

$^{31}P\{^{1}H\}$ NMR (162 MHz, $CDCl_3$)



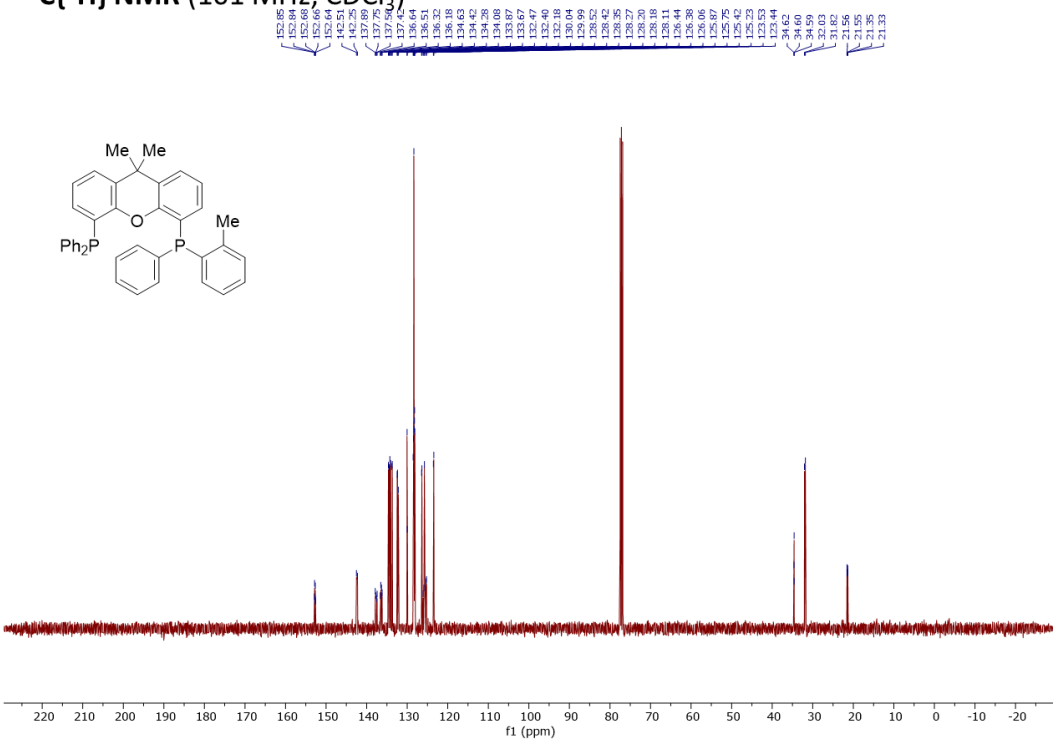
(9,9-Dimethyl-5-(phenyl(*o*-tolyl)phosphaneyl)-9*H*-xanthen-4-yl)diphenylphosphane L8

^{1}H NMR (400 MHz, $CDCl_3$)



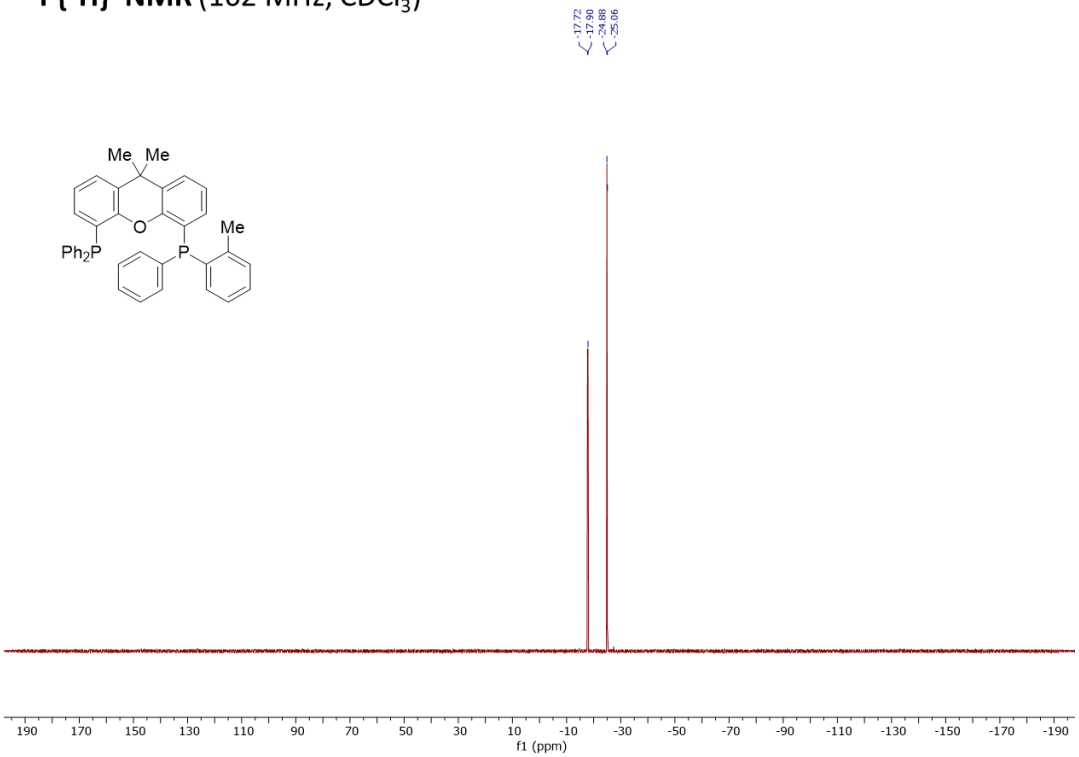
(9,9-Dimethyl-5-(phenyl(*o*-tolyl)phosphaneyl)-9*H*-xanthen-4-yl)diphenylphosphane L8

^{13}C{^{1}H} NMR (101 MHz, $CDCl_3$)



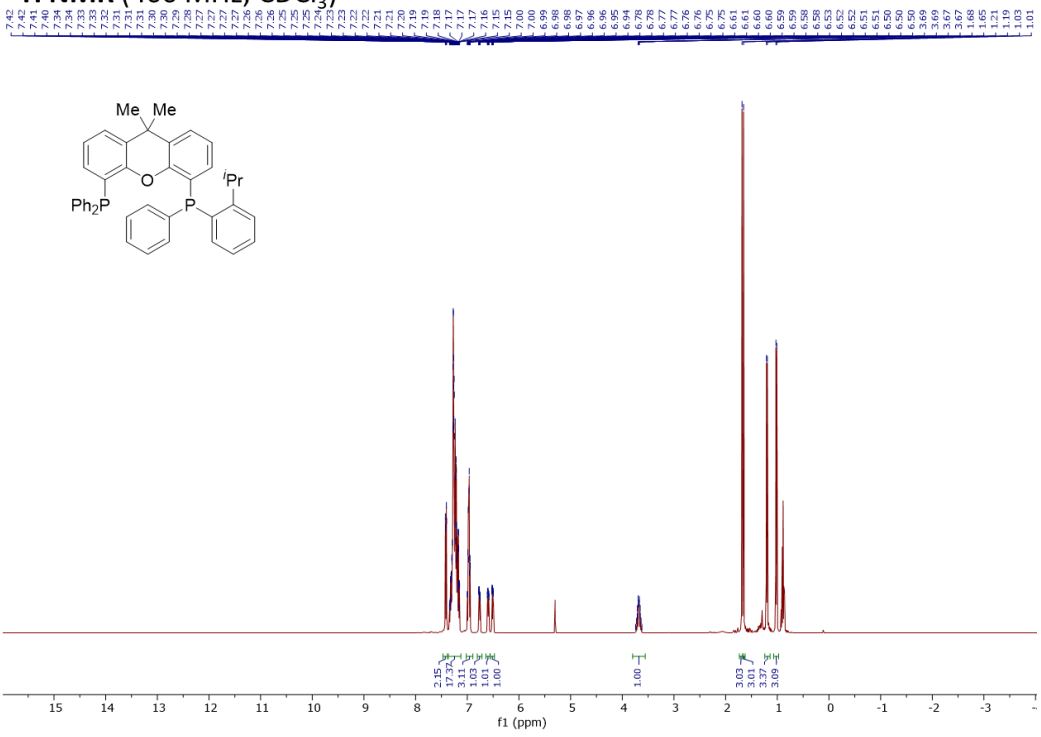
(9,9-Dimethyl-5-(phenyl(*o*-tolyl)phosphaneyl)-9*H*-xanthen-4-yl)diphenylphosphane L8

$^{31}P\{^{1}H\}$ NMR (162 MHz, $CDCl_3$)



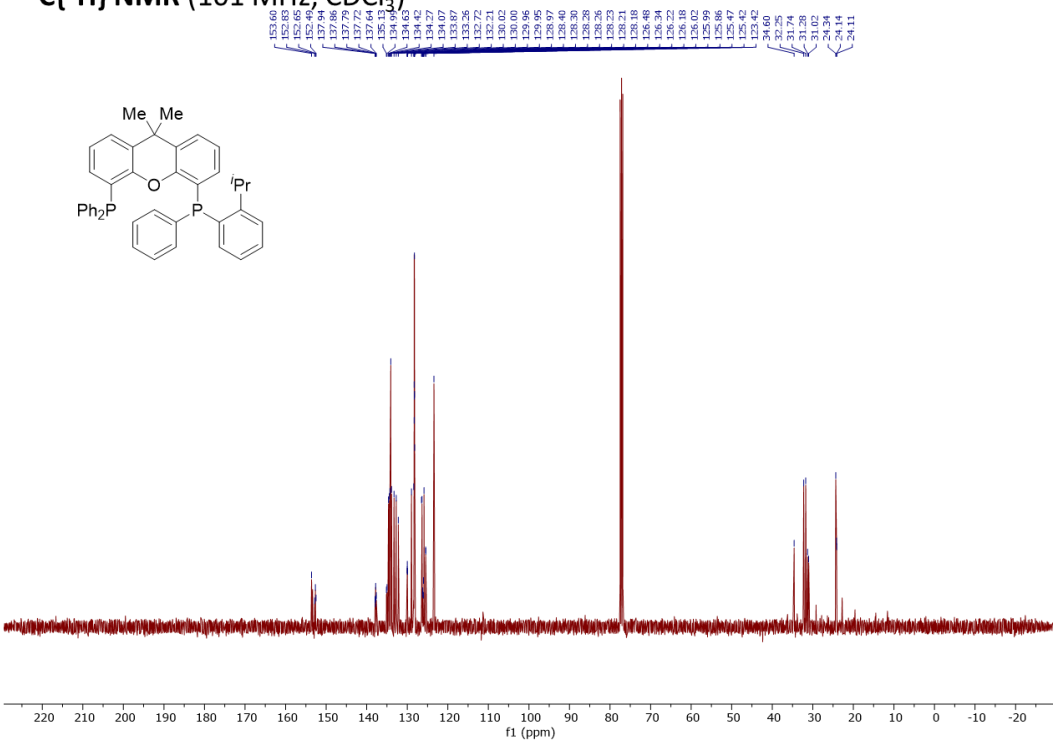
(5-(Diphenylphosphaneyl)-9,9-dimethyl-9*H*-xanthen-4-yl)(2-isopropylphenyl)(phenyl)phosphane L9

^{1}H NMR (400 MHz, $CDCl_3$)



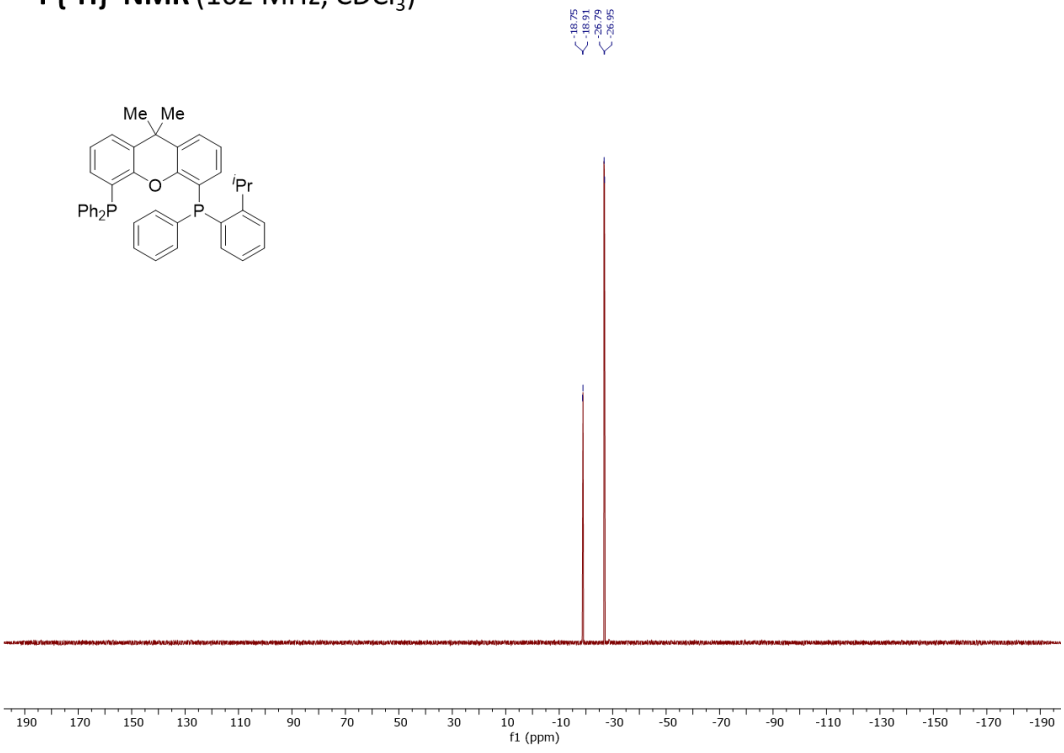
(5-(Diphenylphosphaneyl)-9,9-dimethyl-9*H*-xanthen-4-yl)(2-isopropylphenyl)(phenyl)phosphane L9

$^{13}C\{^{1}H\}$ NMR (101 MHz, $CDCl_3$)



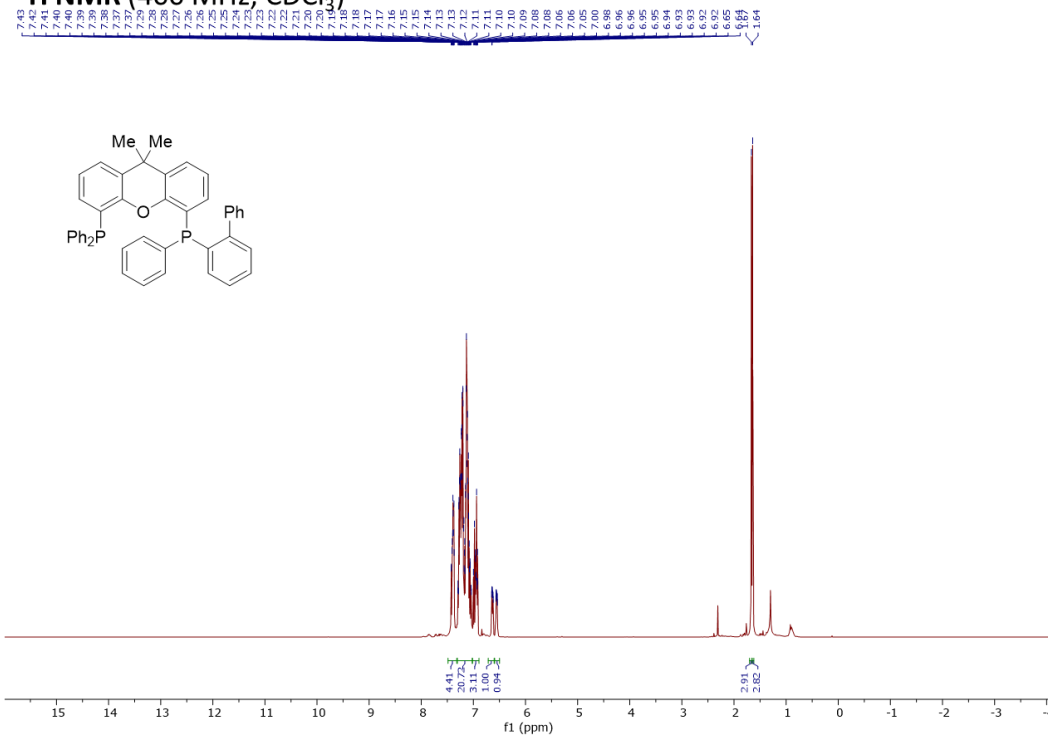
(5-(Diphenylphosphaneyl)-9,9-dimethyl-9*H*-xanthen-4-yl)(2-isopropylphenyl)(phenyl)phosphane L9

$^{31}P\{^{1}H\}$ NMR (162 MHz, $CDCl_3$)



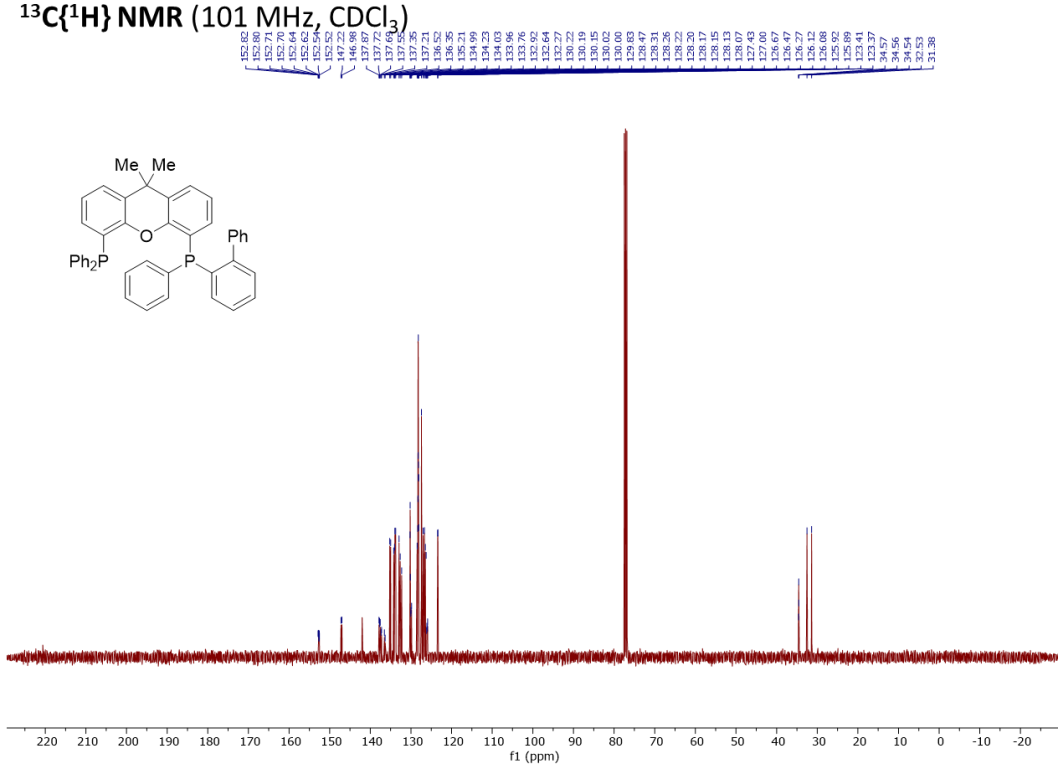
[1,1'-Biphenyl]-2-yl(5-(diphenylphosphaneyl)-9,9-dimethyl-9*H*-xanthen-4-yl)(phenyl)phosphane L10

^{1}H NMR (400 MHz, $CDCl_3$)



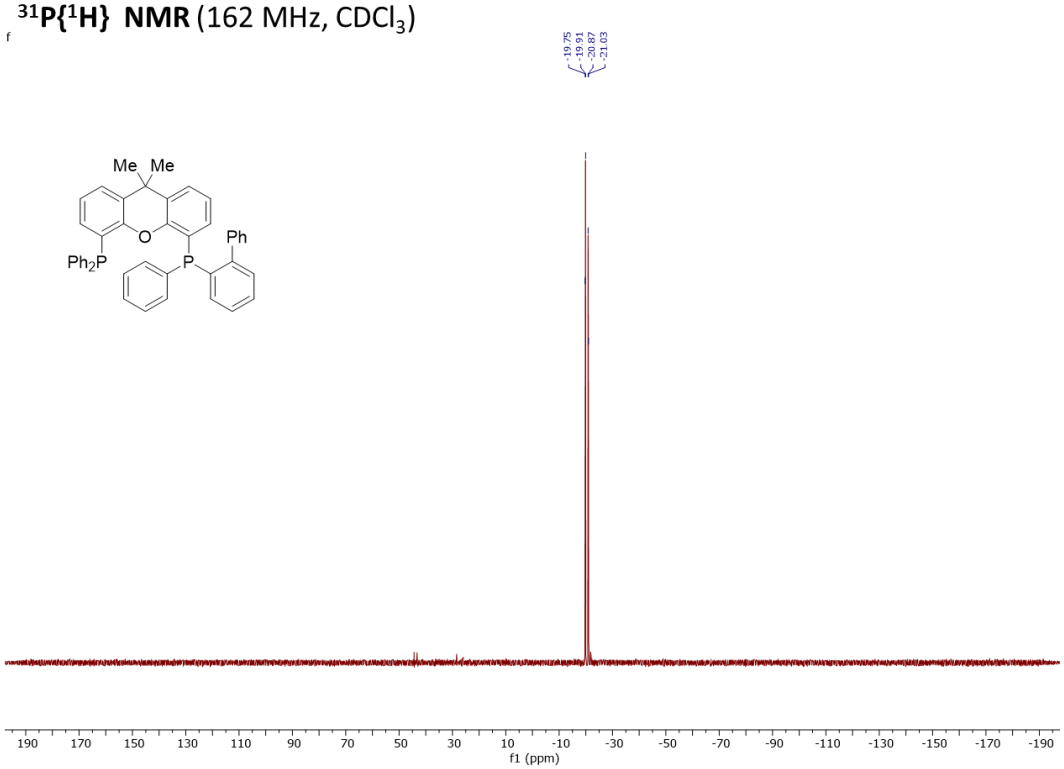
[1,1'-Biphenyl]-2-yl(5-(diphenylphosphaneyl)-9,9-dimethyl-9*H*-xanthen-4-yl)(phenyl)phosphane L10

^{13}C{^{1}H} NMR (101 MHz, $CDCl_3$)



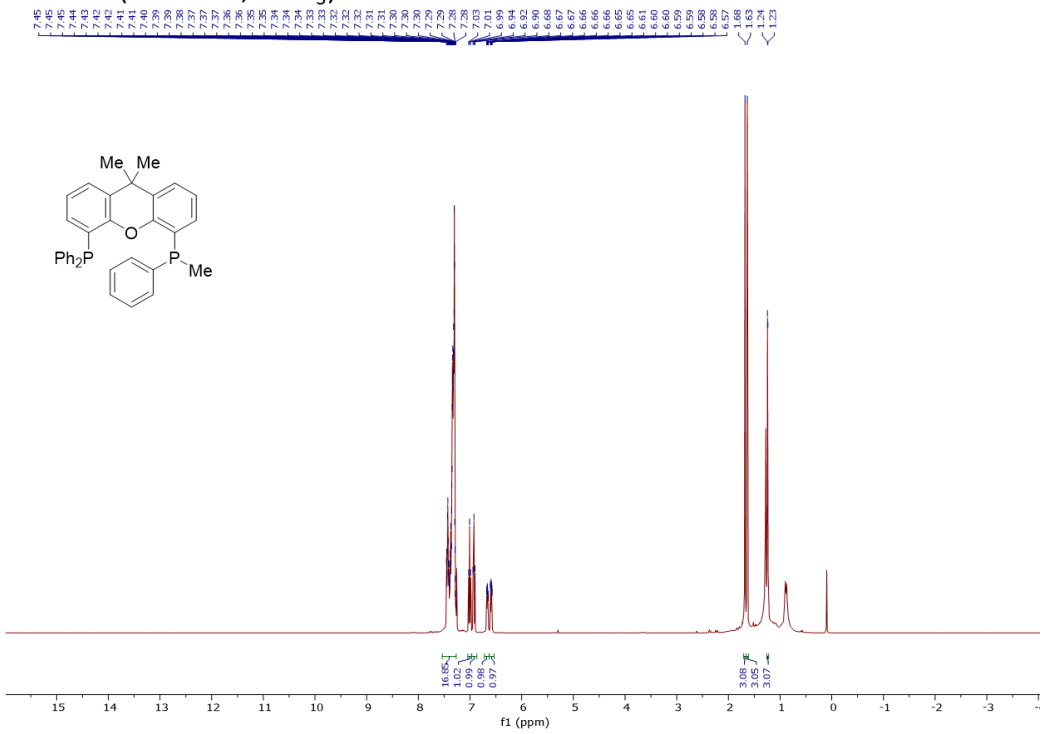
[1,1'-Biphenyl]-2-yl(5-(diphenylphosphaneyl)-9,9-dimethyl-9*H*-xanthen-4-yl)(phenyl)phosphane L10

$^{31}P\{^{1}H\}$ NMR (162 MHz, $CDCl_3$)



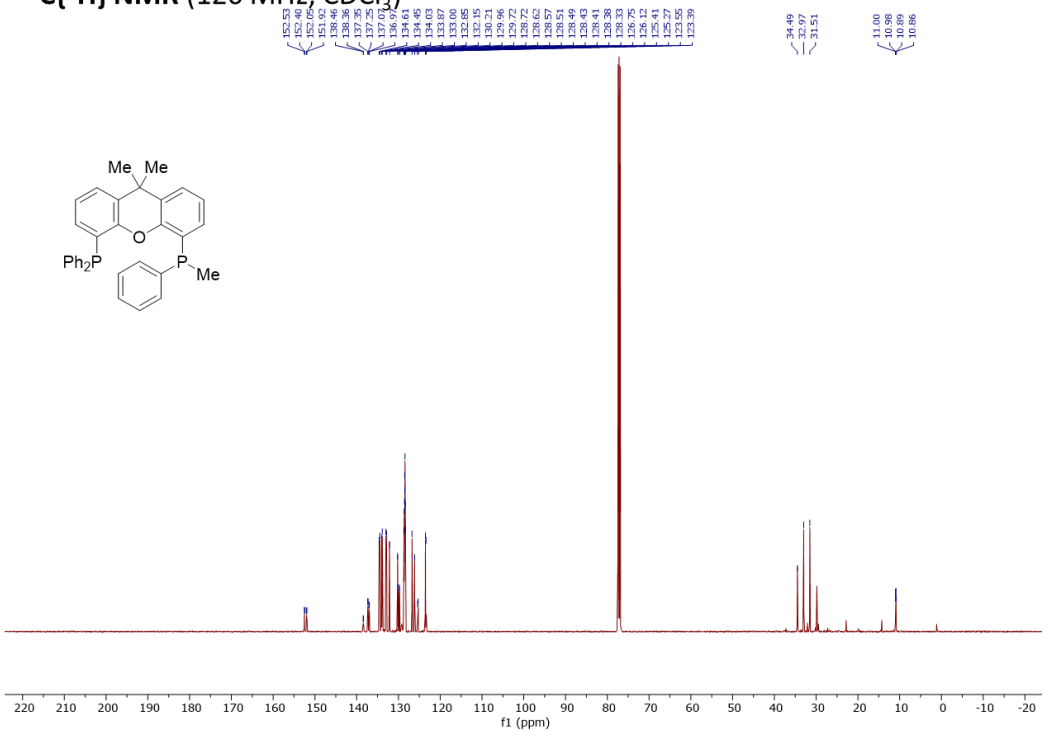
(9,9-Dimethyl-5-(methyl(phenyl)phosphaneyl)-9*H*-xanthen-4-yl)diphenylphosphane L11

^{1}H NMR (400 MHz, $CDCl_3$)



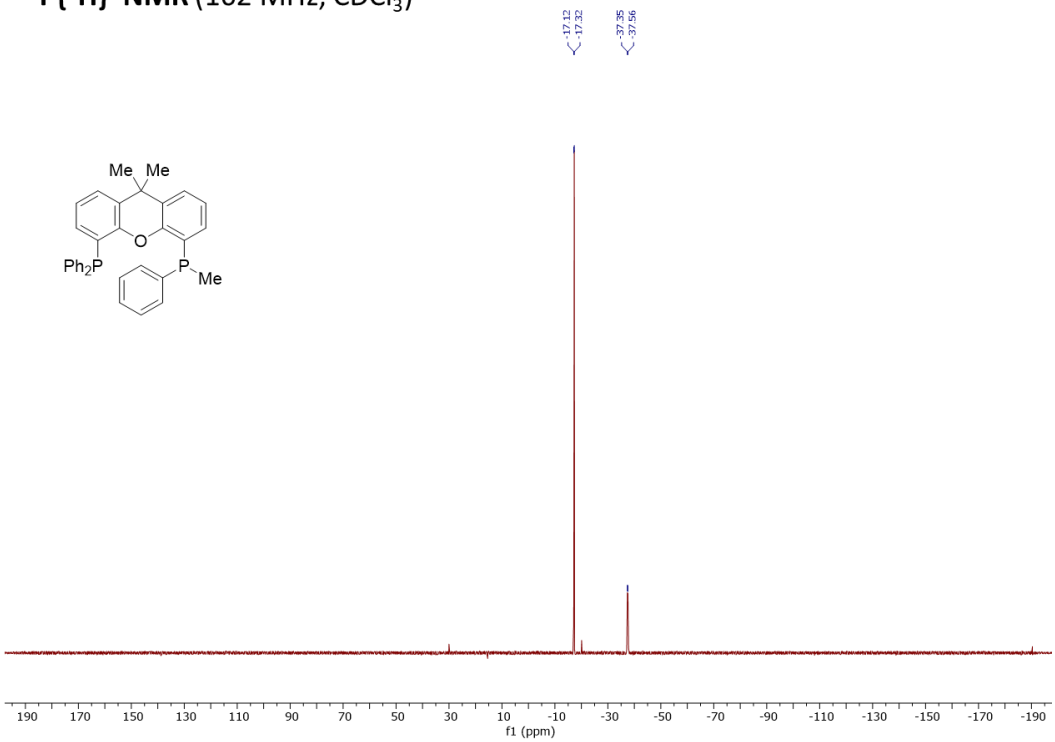
(9,9-Dimethyl-5-(methyl(phenyl)phosphaneyl)-9*H*-xanthen-4-yl)diphenylphosphane L11

$^{13}C\{^{1}H\}$ NMR (126 MHz, $CDCl_3$)



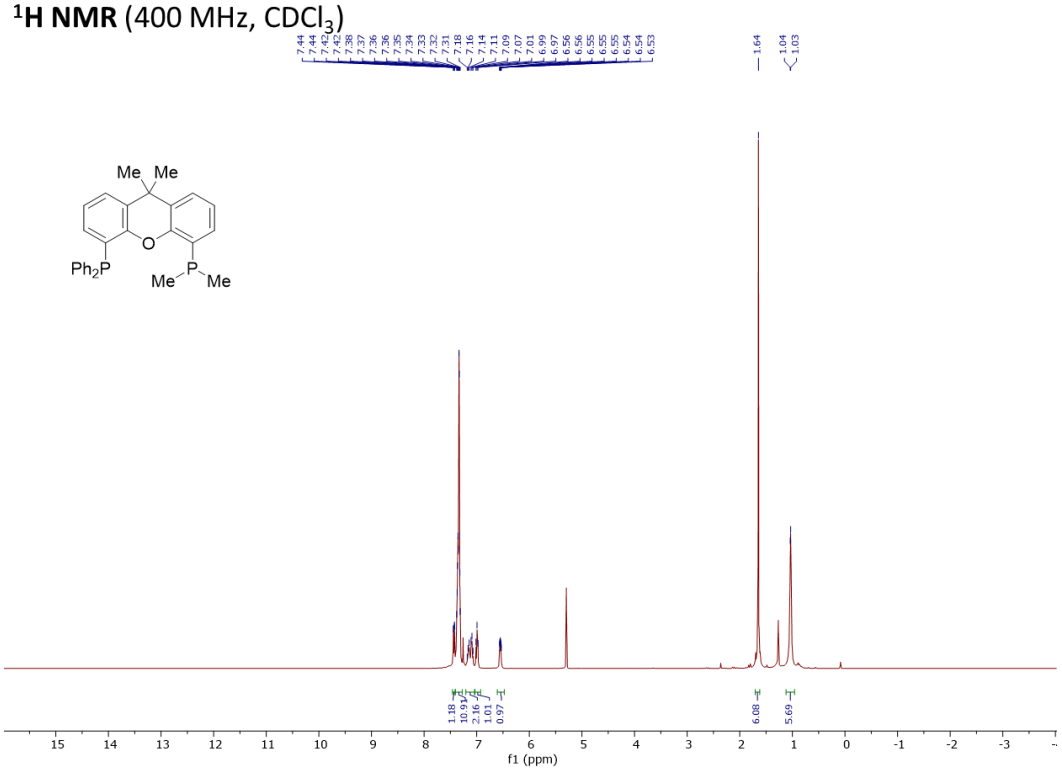
(9,9-Dimethyl-5-(methyl(phenyl)phosphaneyl)-9*H*-xanthen-4-yl)diphenylphosphane L11

$^{31}P\{^{1}H\}$ NMR (162 MHz, $CDCl_3$)



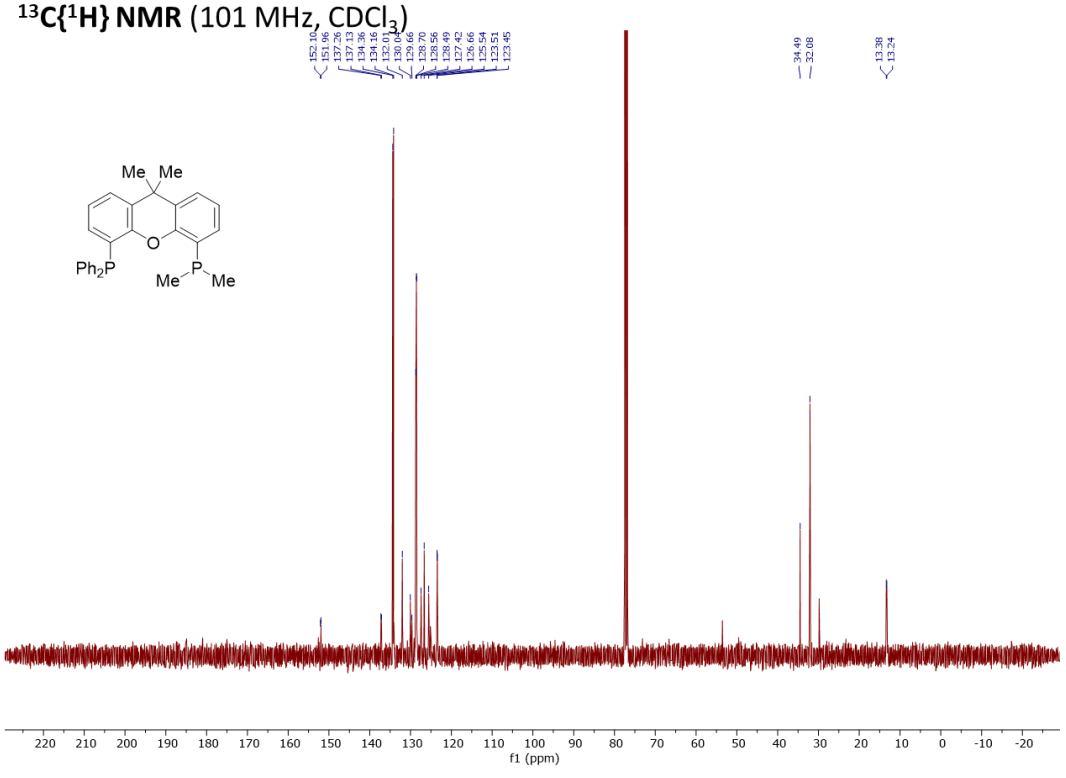
(5-(Dimethylphosphaneyl)-9,9-dimethyl-9*H*-xanthen-4-yl)diphenylphosphane L12

^{1}H NMR (400 MHz, $CDCl_3$)



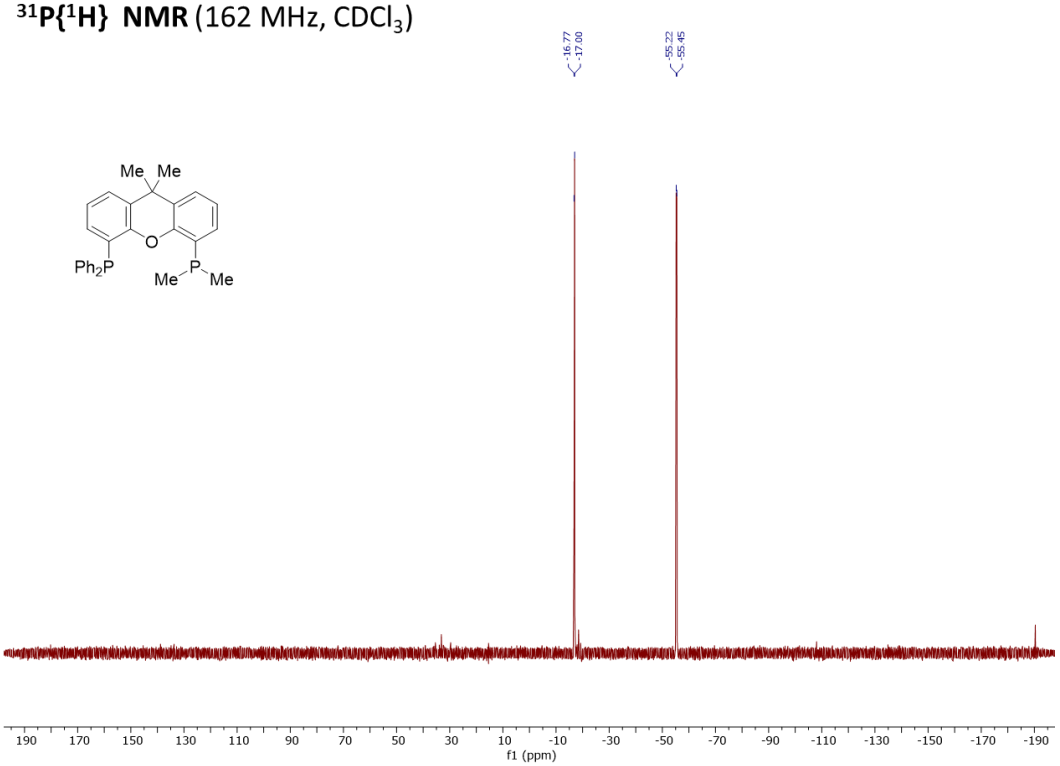
(5-(Dimethylphosphaneyl)-9,9-dimethyl-9*H*-xanthen-4-yl)diphenylphosphane L12

^{13}C{^{1}H} NMR (101 MHz, $CDCl_3$)



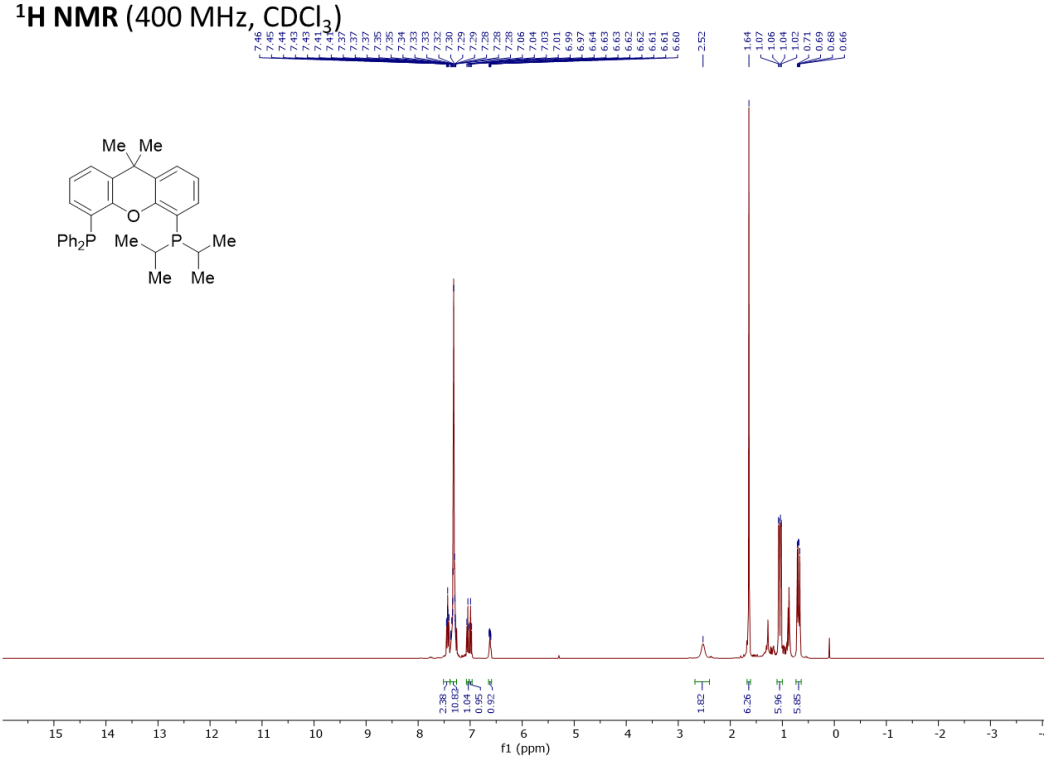
(5-(Dimethylphosphaneyl)-9,9-dimethyl-9*H*-xanthen-4-yl)diphenylphosphane L12

$^{31}P\{^{1}H\}$ NMR (162 MHz, $CDCl_3$)



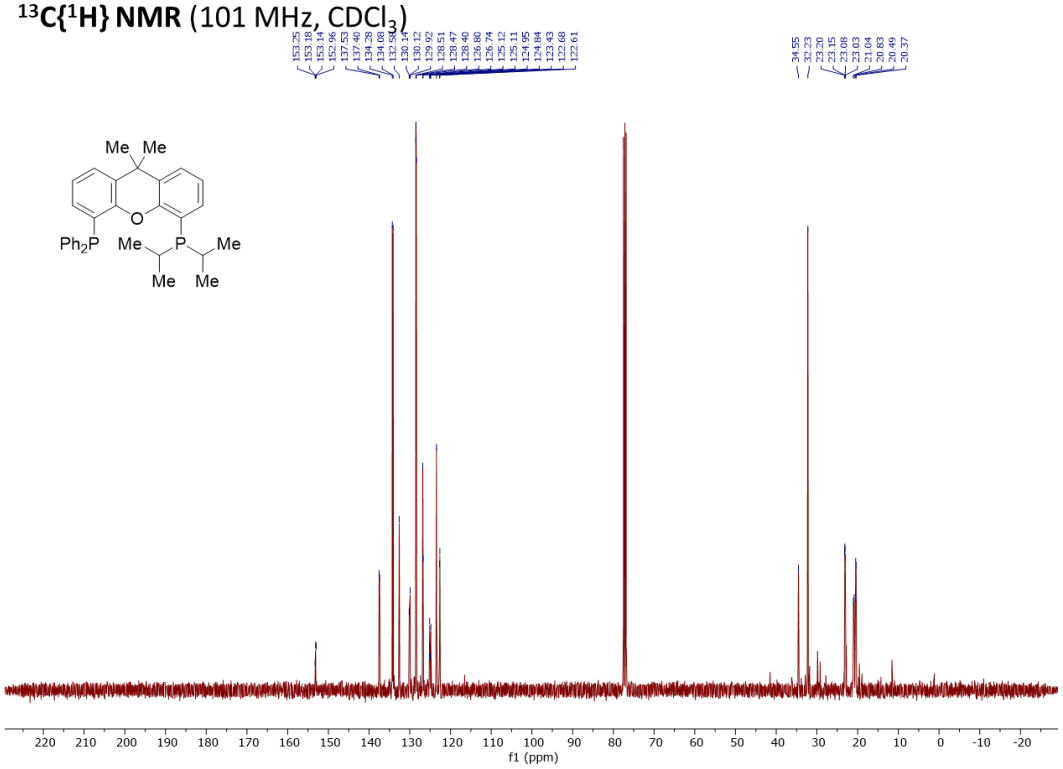
(5-(Diisopropylphosphaneyl)-9,9-dimethyl-9*H*-xanthen-4-yl)diphenylphosphane L13

^{1}H NMR (400 MHz, $CDCl_3$)



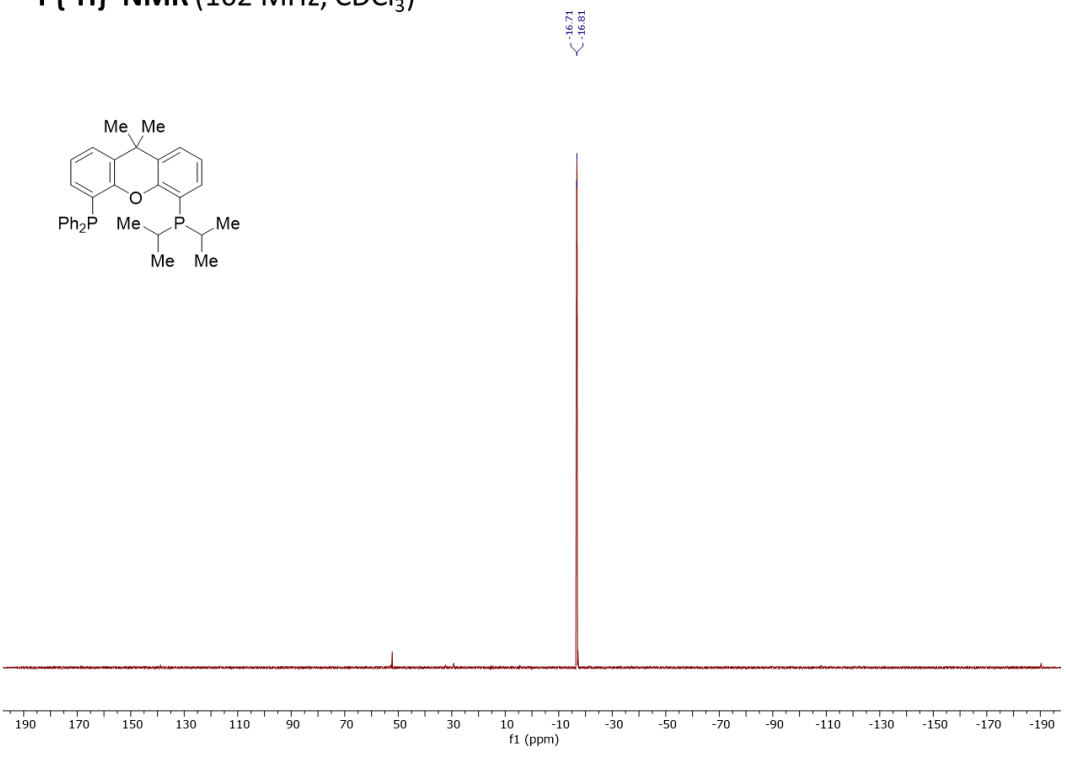
(5-(Diisopropylphosphaneyl)-9,9-dimethyl-9*H*-xanthen-4-yl)diphenylphosphane L13

$^{13}C\{^{1}H\}$ NMR (101 MHz, $CDCl_3$)



(5-(Diisopropylphosphaneyl)-9,9-dimethyl-9*H*-xanthen-4-yl)diphenylphosphane L13

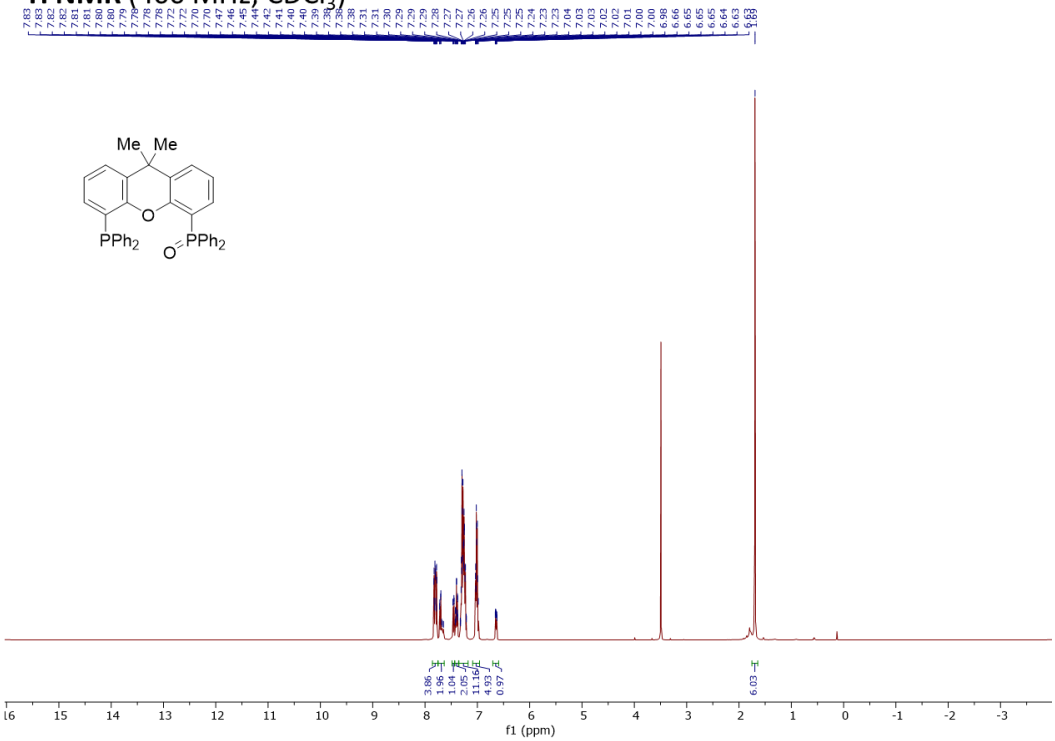
$^{31}P\{^{1}H\}$ NMR (162 MHz, $CDCl_3$)



9.3.5. Other Novel Phosphine Ligands

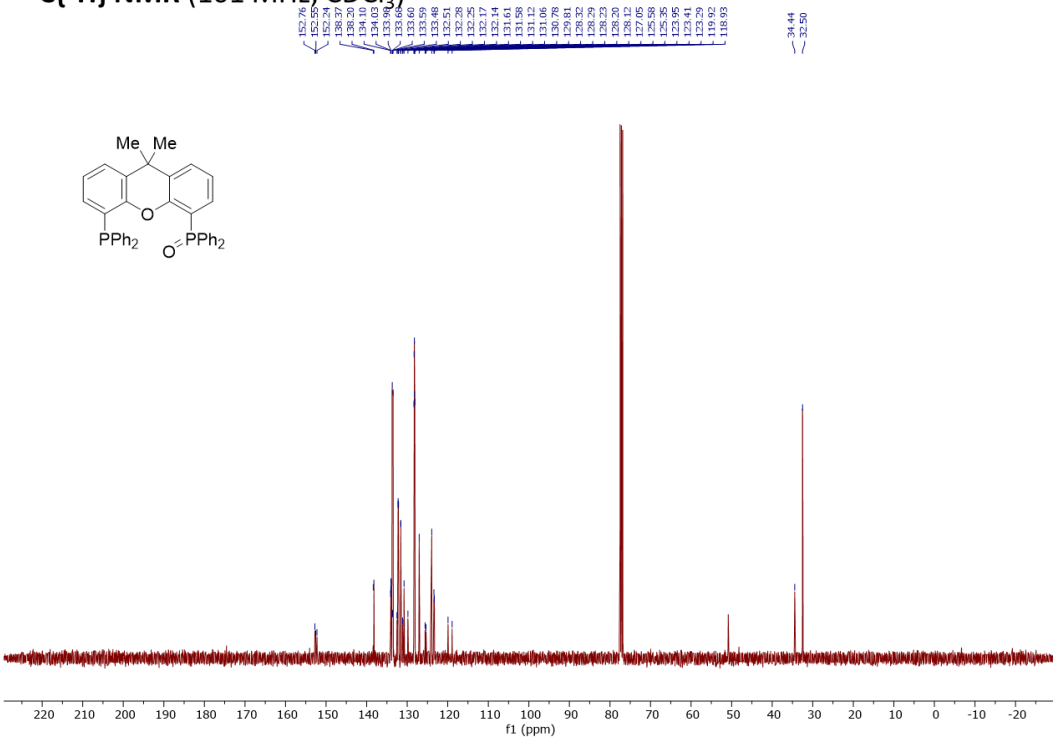
(5-(Diphenylphosphaneyl)-9,9-dimethyl-9*H*-xanthen-4-yl)diphenylphosphine oxide Ox-Xantphos

^{1}H NMR (400 MHz, $CDCl_3$)



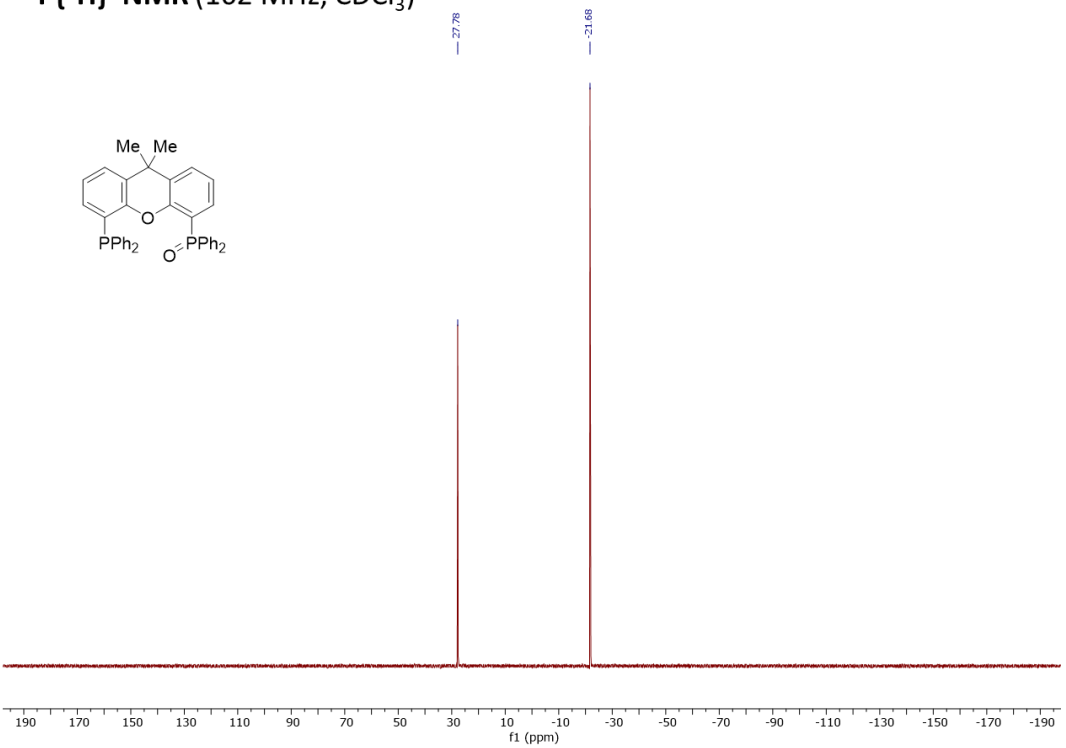
(5-(Diphenylphosphaneyl)-9,9-dimethyl-9*H*-xanthen-4-yl)diphenylphosphine oxide Ox-Xantphos

^{13}C{^{1}H} NMR (101 MHz, $CDCl_3$)

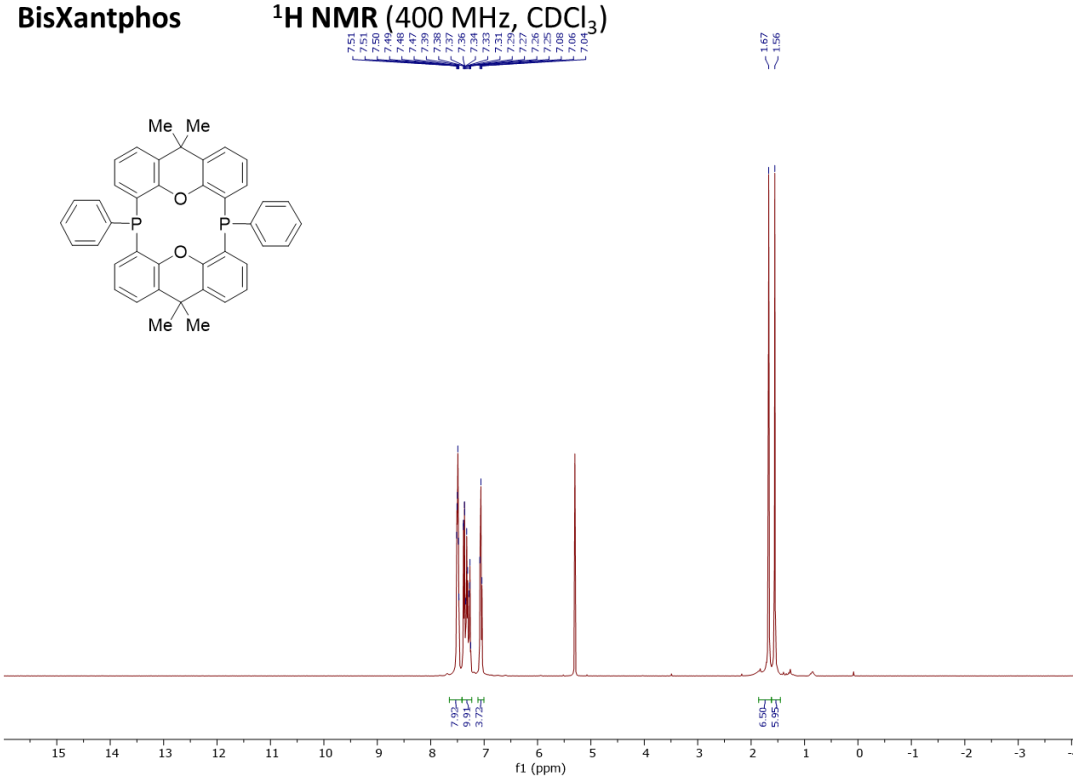


(5-(Diphenylphosphaneyl)-9,9-dimethyl-9*H*-xanthen-4-yl)diphenylphosphine oxide Ox-Xantphos

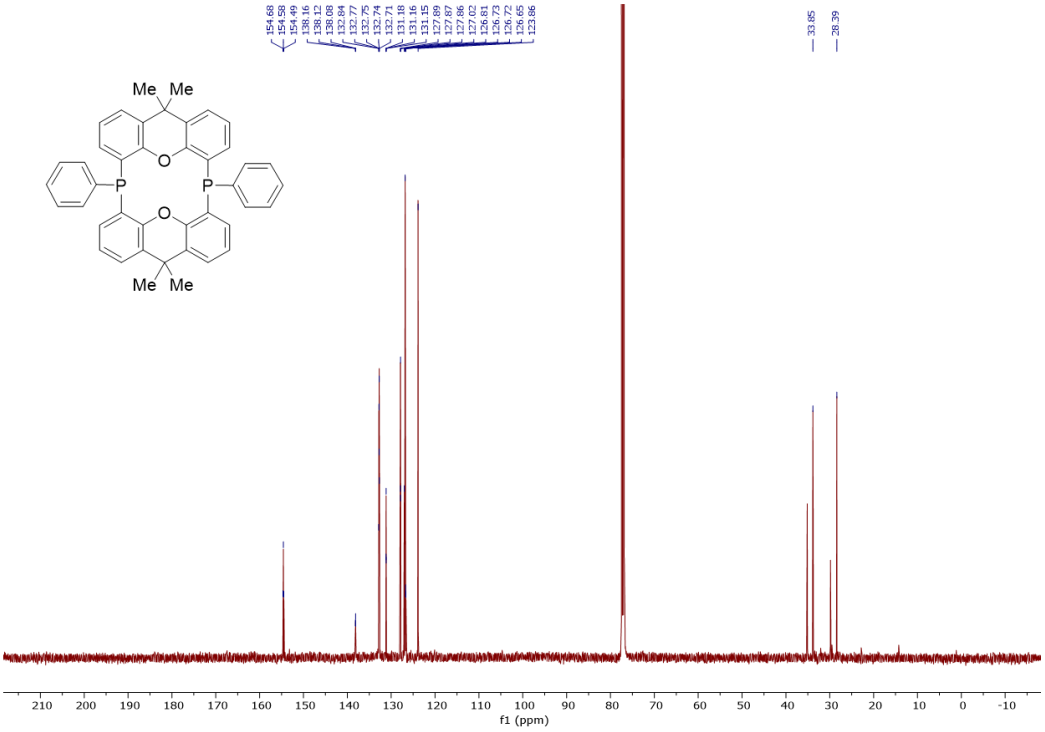
$^{31}P\{^{1}H\}$ NMR (162 MHz, $CDCl_3$)



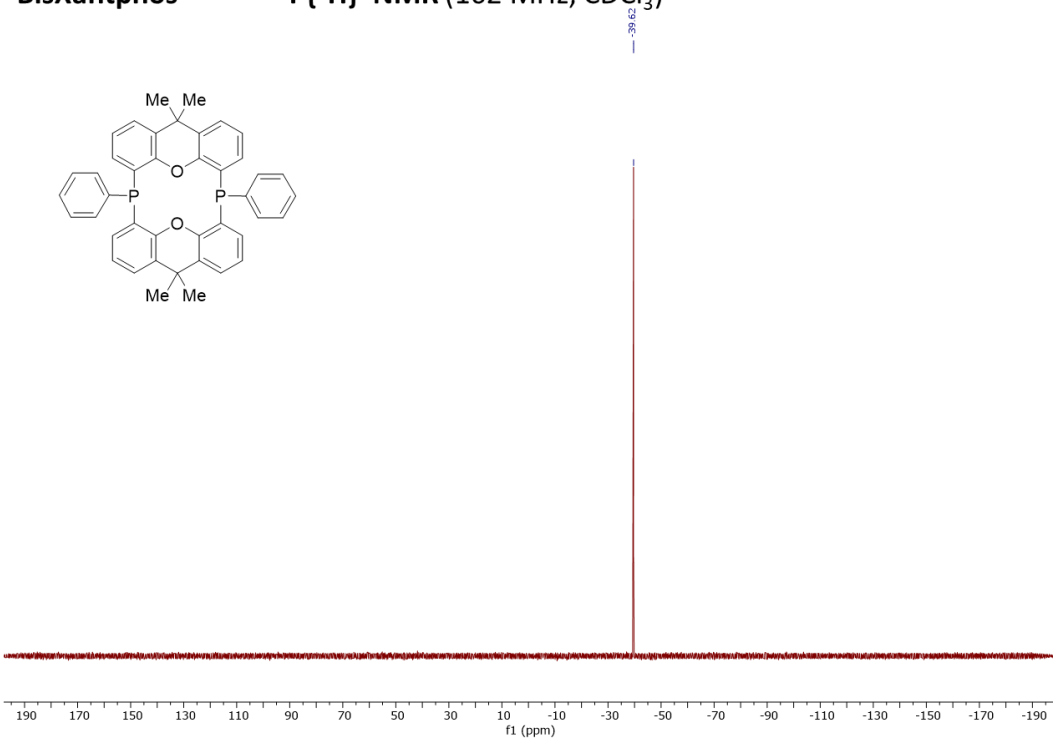
21,21,22,22-Tetramethyl-10,20-diphenyl-10*H*,20*H*-4,6:14,16-dimethanotetrabenzo[*b*,*e*,*h*,*k*][1,7]dioxa[4,10]diphosphacyclododecine BisXantphos **^{1}H NMR** (400 MHz, $CDCl_3$)



21,21,22,22-Tetramethyl-10,20-diphenyl-10*H*,20*H*-4,6:14,16-dimethanotetrabenzo[*b*,*e*,*h*,*k*][1,7]dioxa[4,10]diphosphacyclododecine BisXantphos **$^{13}C\{^{1}H\}$ NMR** (126 MHz, $CDCl_3$)

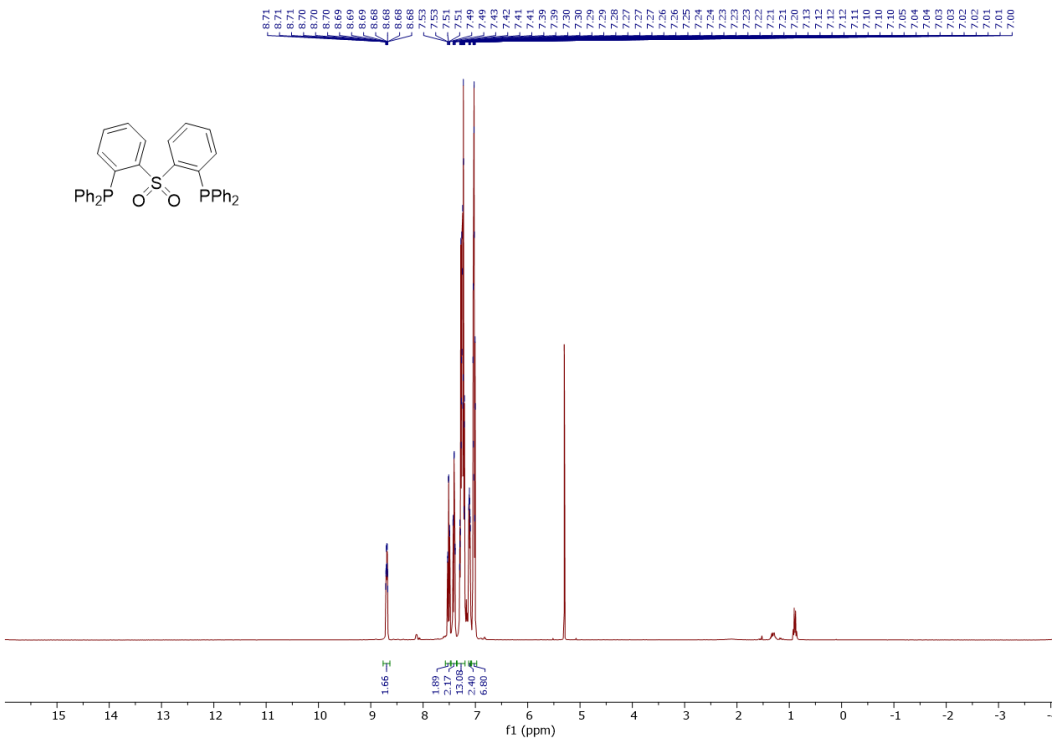


21,21,22,22-Tetramethyl-10,20-diphenyl-10*H*,20*H*-4,6:14,16-dimethanotetrabenzo[*b*,*e*,*h*,*k*][1,7]dioxa[4,10]diphosphacyclododecine BisXantphos **$^{31}P\{^{1}H\}$ NMR** (162 MHz, $CDCl_3$)



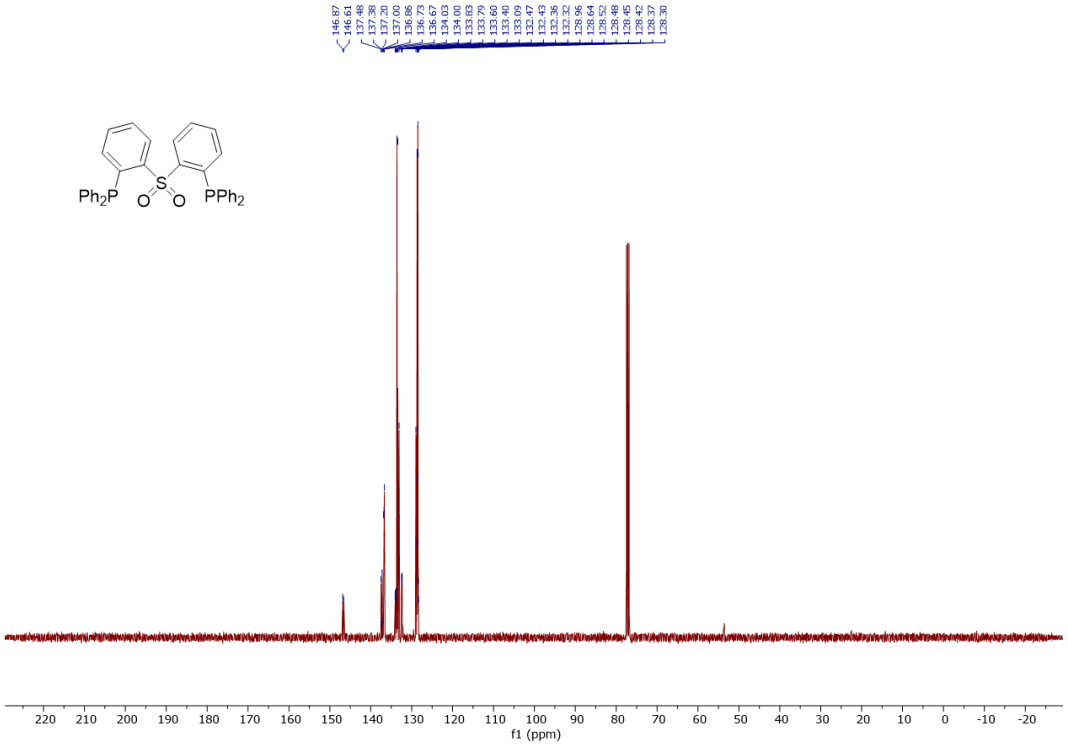
(Sulfonylbis(2,1-phenylene))bis(diphenylphosphane) SulfPhos

^{1}H NMR (400 MHz, $CDCl_3$)

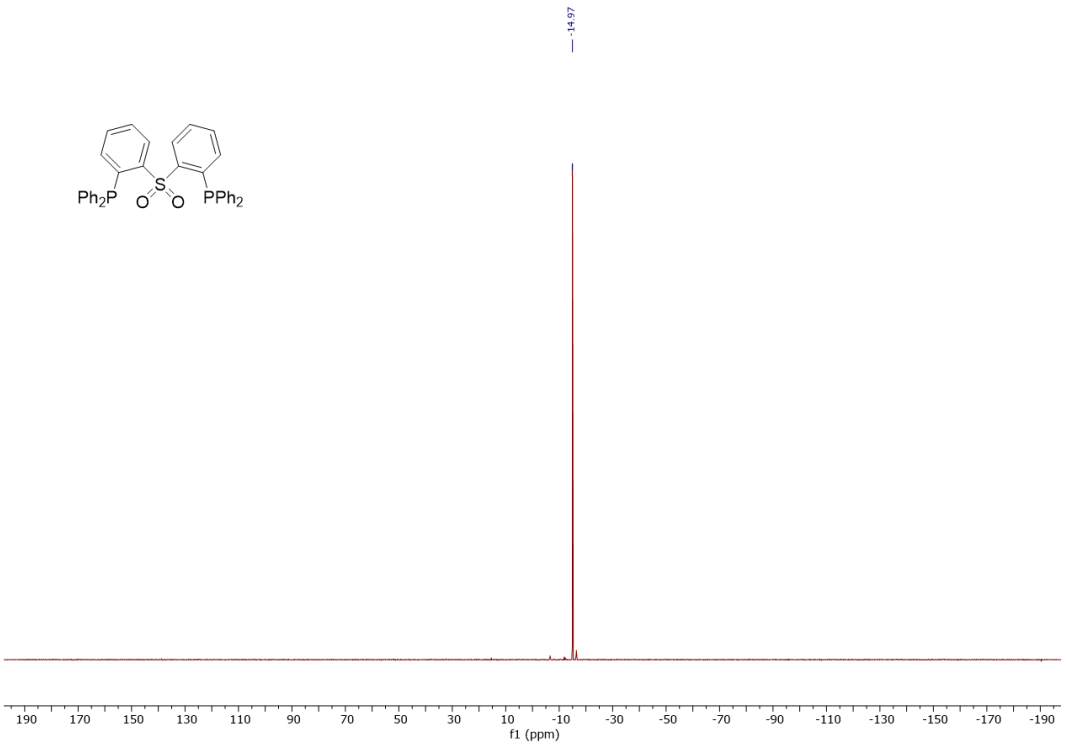


(Sulfonylbis(2,1-phenylene))bis(diphenylphosphane) SulfPhos

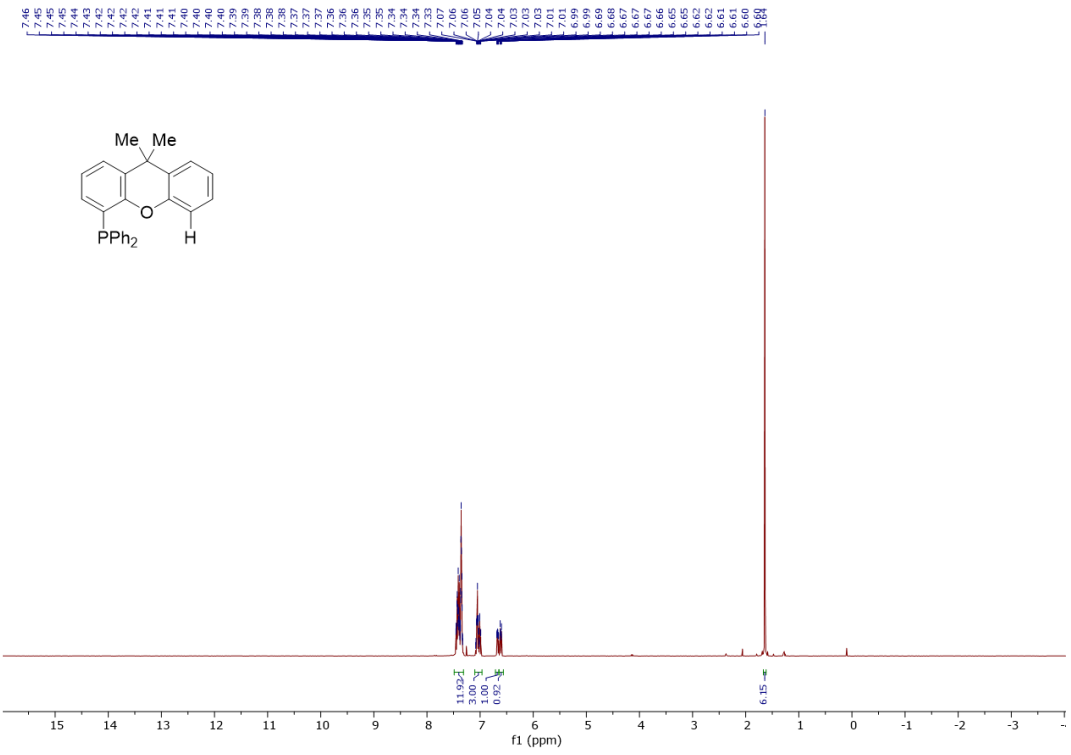
^{13}C{^{1}H} NMR (101 MHz, $CDCl_3$)



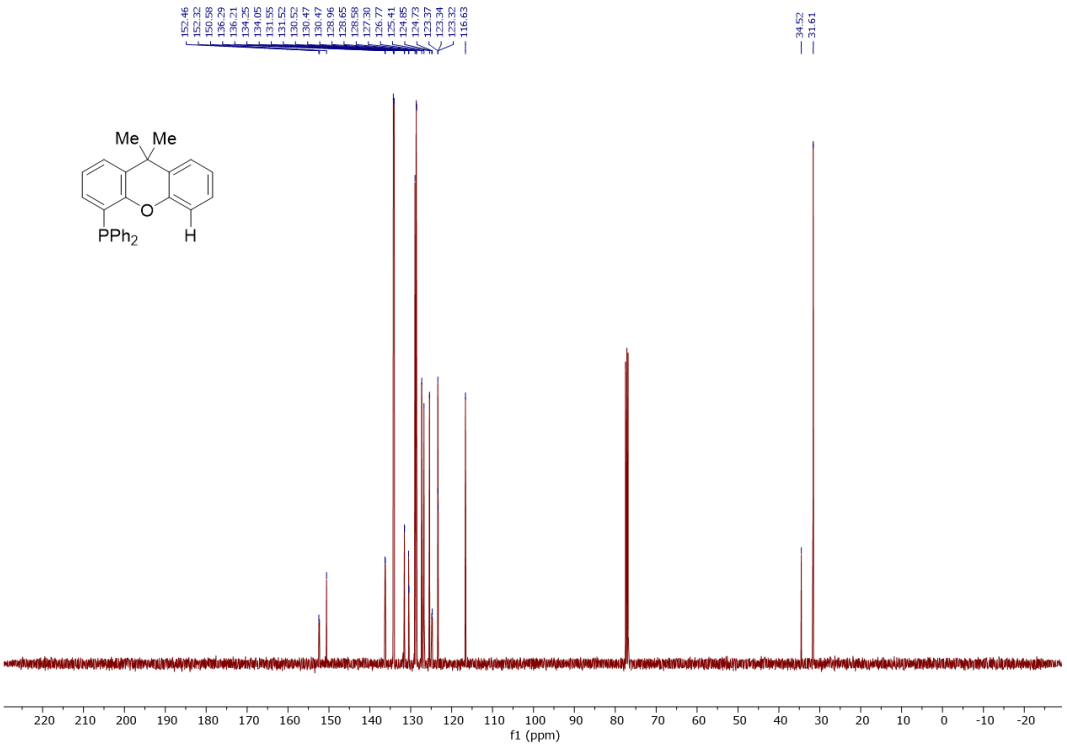
(Sulfonylbis(2,1-phenylene))bis(diphenylphosphane) SulfPhos
$^{31}P\{^{1}H\}$ NMR (162 MHz, $CDCl_3$)



(9,9-Dimethyl-9*H*-xanthen-4-yl)diphenylphosphane PPh_2-Xanthene
^{1}H NMR (400 MHz, $CDCl_3$)



(9,9-Dimethyl-9*H*-xanthen-4-yl)diphenylphosphane PPh_2-Xanthene
$^{13}C\{^1H\}$ NMR (101 MHz, $CDCl_3$)



(9,9-Dimethyl-9*H*-xanthen-4-yl)diphenylphosphane PPh_2-Xanthene
$^{31}P\{^1H\}$ NMR (162 MHz, $CDCl_3$)

